Impact of Timanian thrusts on the Phanerozoic tectonic history of Svalbard

Jean-Baptiste Koehl
jean-baptiste.koehl@uit.no

Impact of Timanian thrusts on the Phanerozoic tectonic history of Svalbard

Jean-Baptiste Koehl
jean-baptiste.koehl@uit.no

Impact of Timanian thrusts on the Phanerozoic tectonic history of Svalbard

Jean-Baptiste Koehl
jean-baptiste.koehl@uit.no

Impact of Timanian thrusts on the Phanerozoic tectonic history of Svalbard

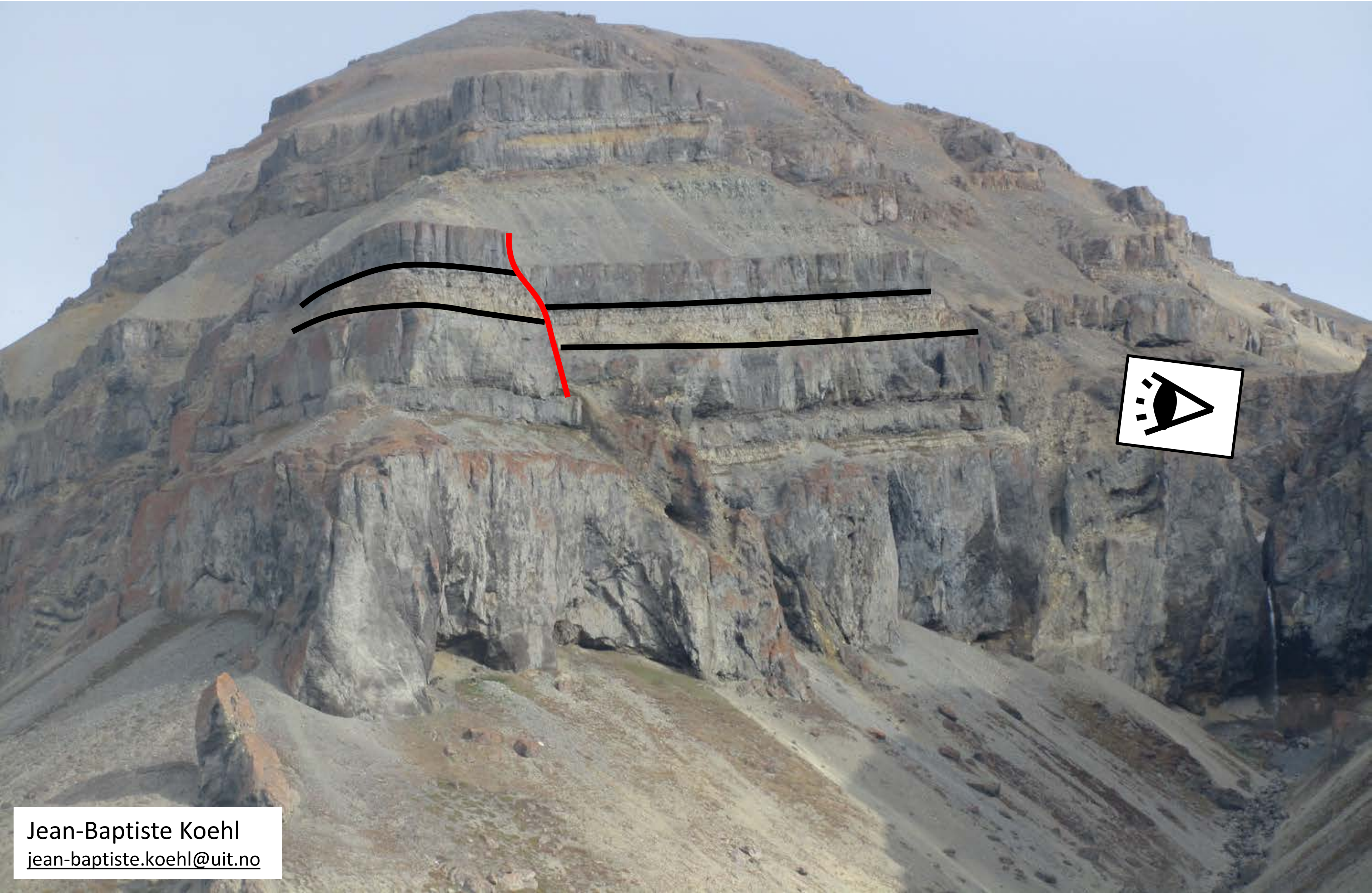

Jean-Baptiste Koehl
jean-baptiste.koehl@uit.no

Impact of Timanian thrusts on the Phanerozoic tectonic history of Svalbard

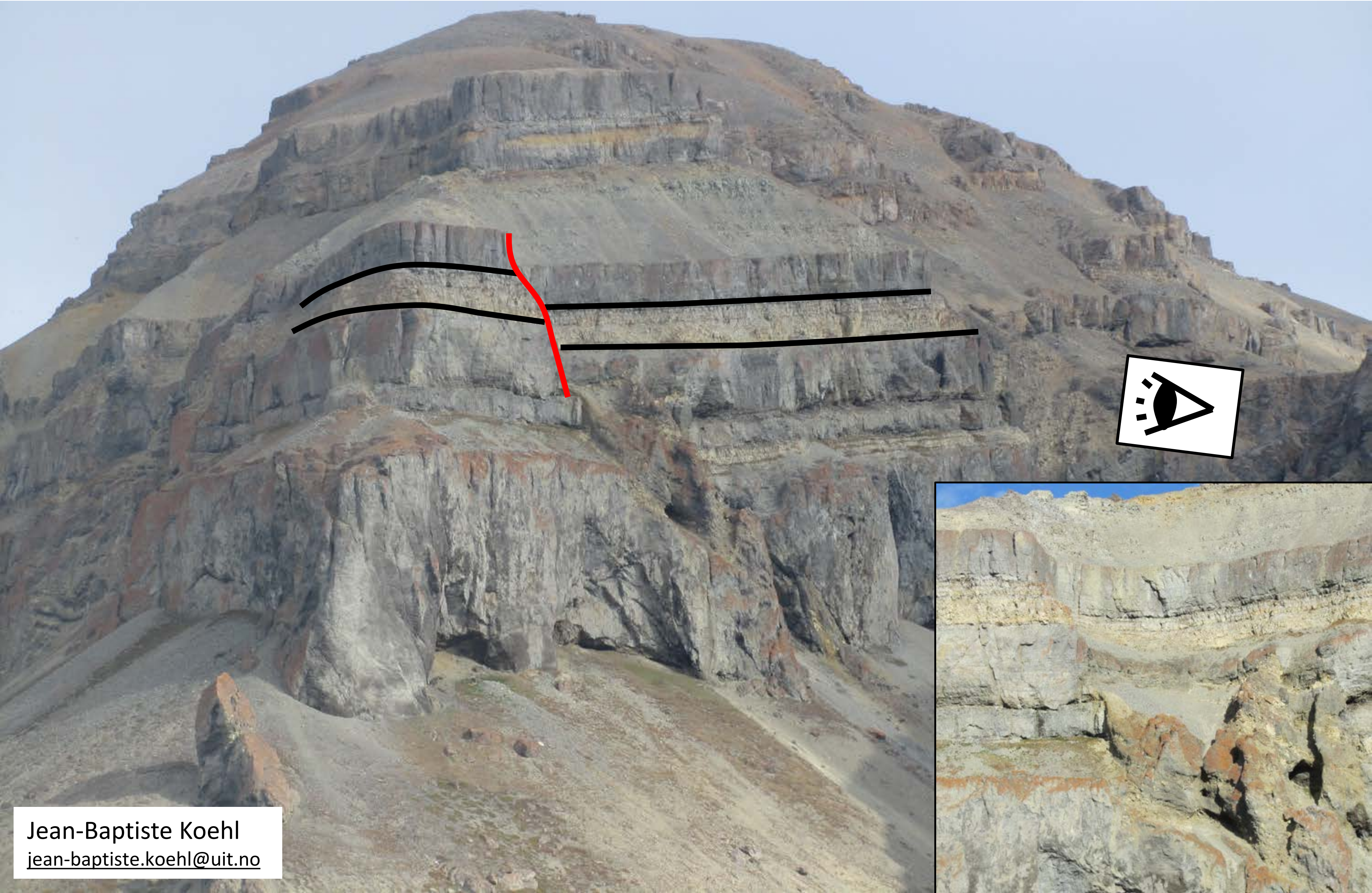

Jean-Baptiste Koehl
jean-baptiste.koehl@uit.no

Impact of Timanian thrusts on the Phanerozoic tectonic history of Svalbard

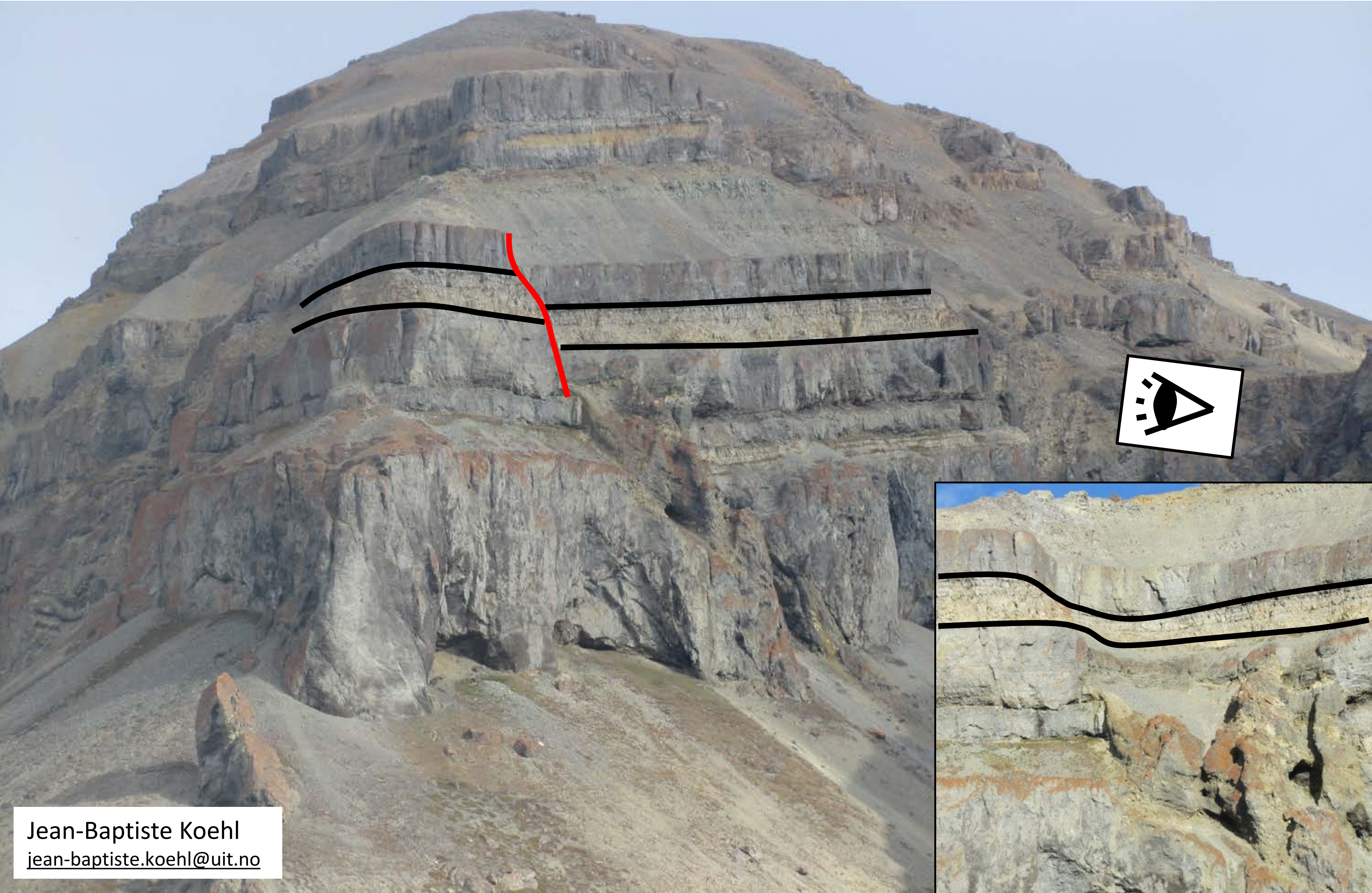

Jean-Baptiste Koehl
jean-baptiste.koehl@uit.no

Impact of Timanian thrusts on the Phanerozoic tectonic history of Svalbard

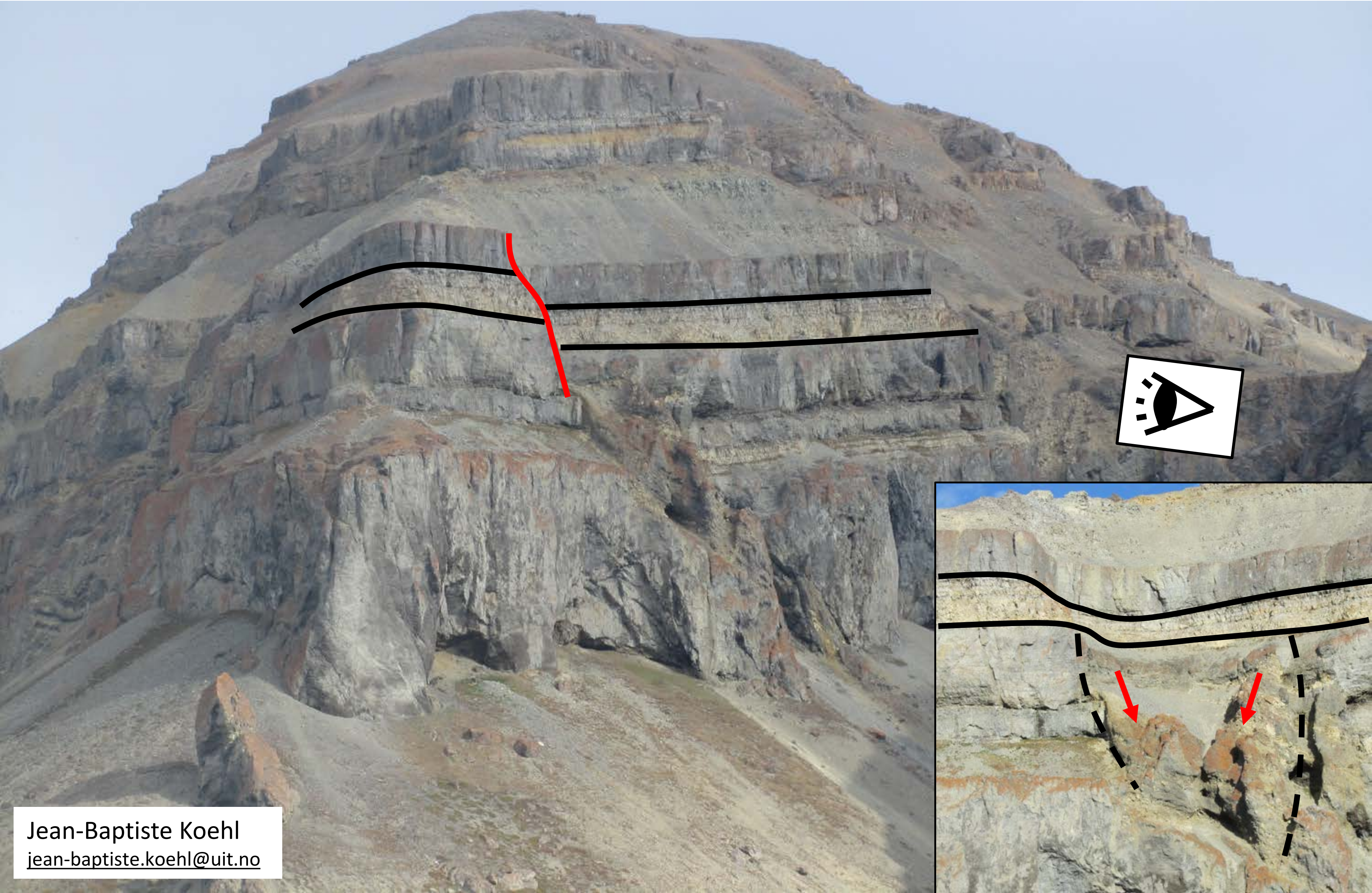

Jean-Baptiste Koehl
jean-baptiste.koehl@uit.no


THANK YOU

ARCEx
Research Centre for
Arctic Petroleum Exploration

CAGE
Centre for Arctic Gas Hydrate, Environment and Climate

UNIVERSITETET I TROMSØ

UNIVERSITAS OSLOENSIS
MDCCCXI


THANK YOU
ARCEx
Research Centre for
Arctic Petroleum Exploration
Centre for Arctic Gas Hydrate, Environment and Climate
CAGE
UNIVERSITETET I TROMSØ
UNIVERSITAS OSLOENSIS
MDCCCXI

Goals

Goals

Goals

+

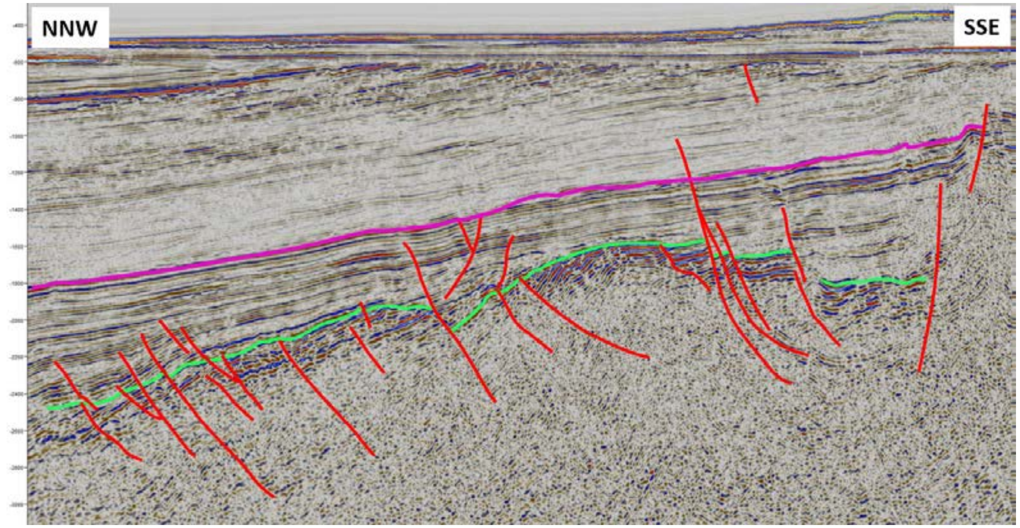

Goals

+

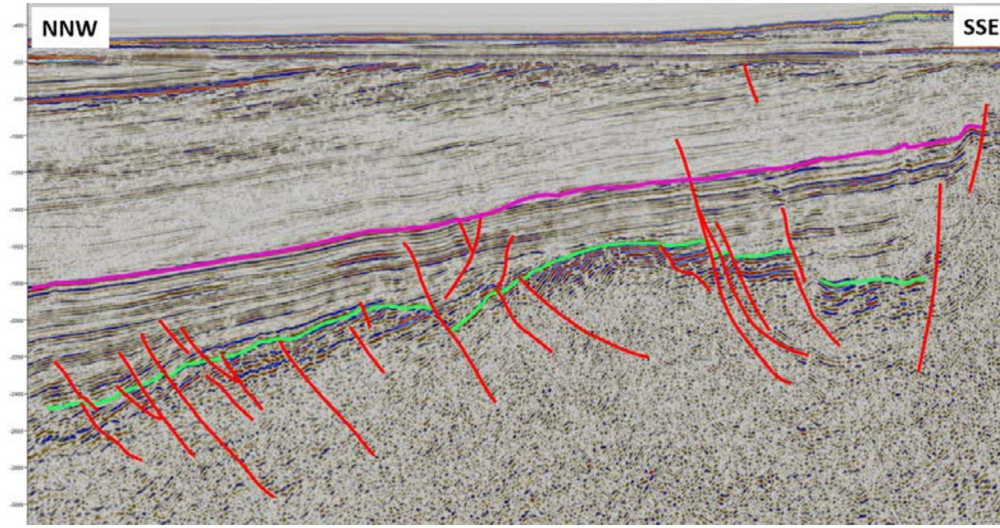
NNW
SSE

=

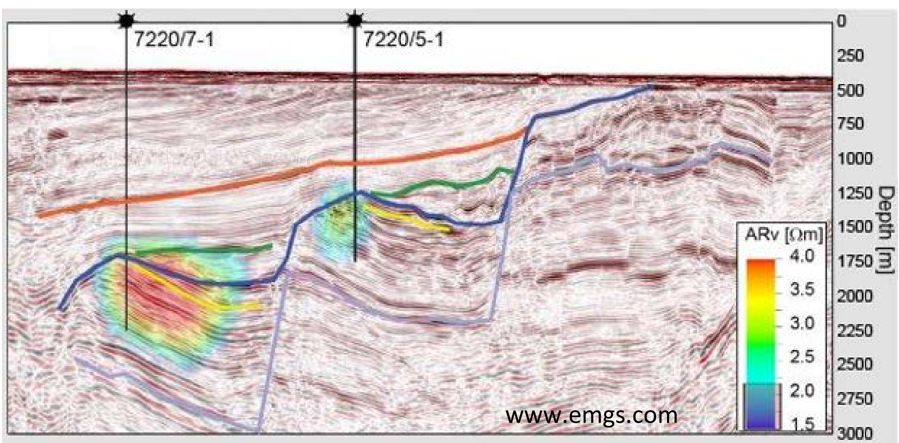
7220/7-1
7220/5-1
0
250
500
750
1000
1250
1500
1750
2000
2250
2500
2750
3000
Depth [m]
ARv [Ωm]
4.0
3.5
3.0
2.5
2.0
1.5
www.emgs.com

Goals

+

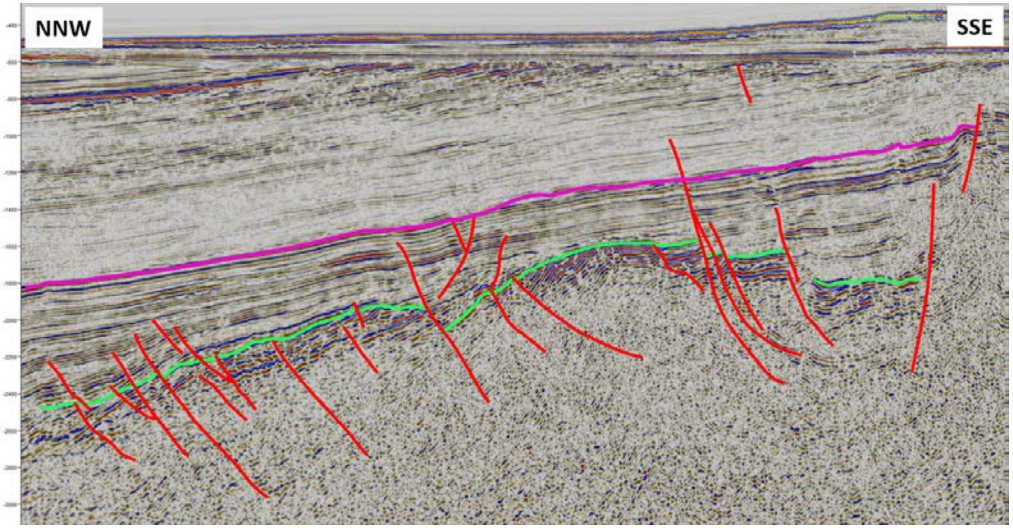
NNW
SSE

=

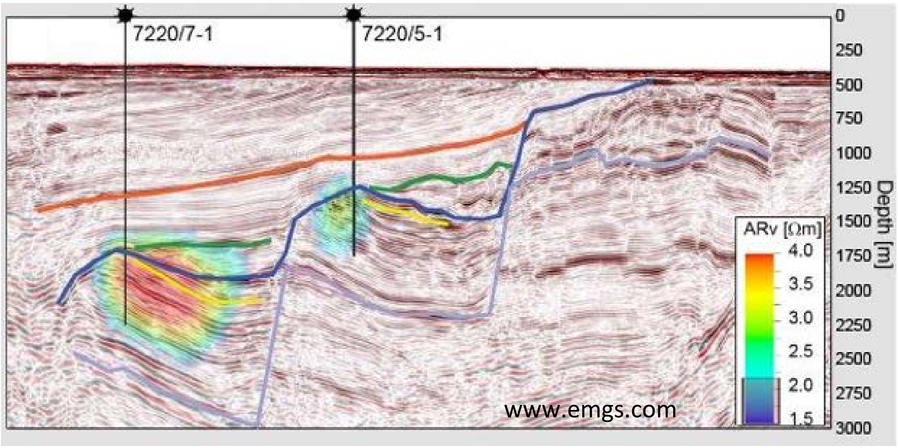
7220/7-1
7220/5-1
0
250
500
750
1000
1250
1500
1750
2000
2250
2500
2750
3000
Depth [m]
ARv [Ωm]
4.0
3.5
3.0
2.5
2.0
1.5
www.emgs.com

+

Goals

+

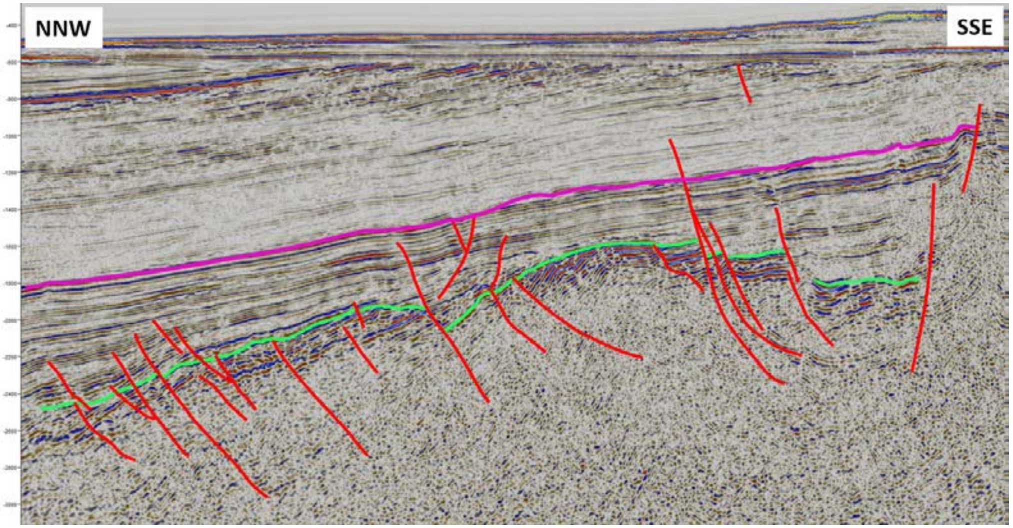

=

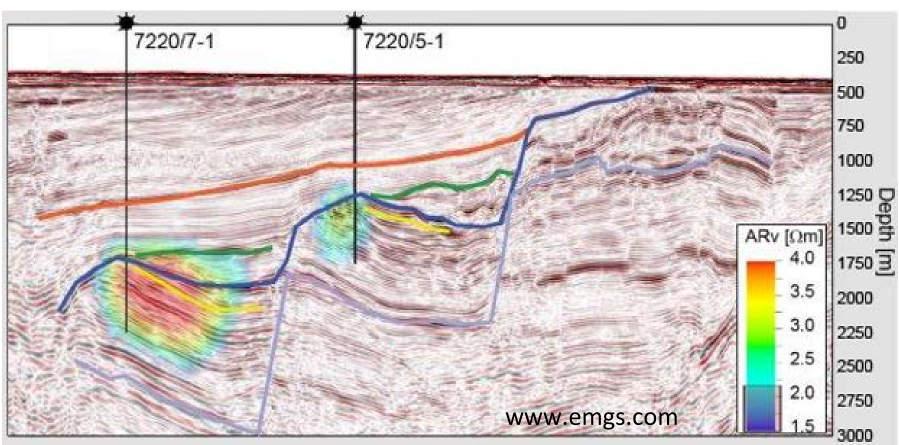

+

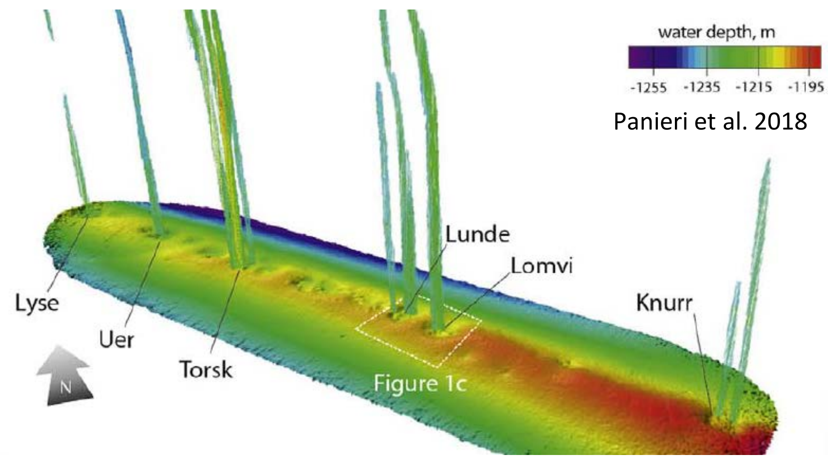

Panieri et al. 2018

Datasets

Datasets

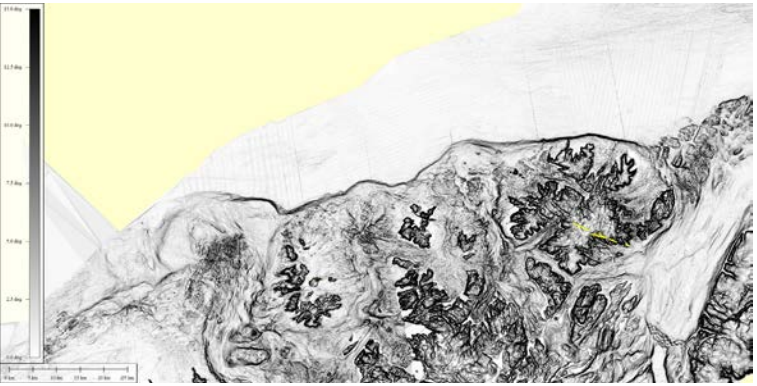

Datasets

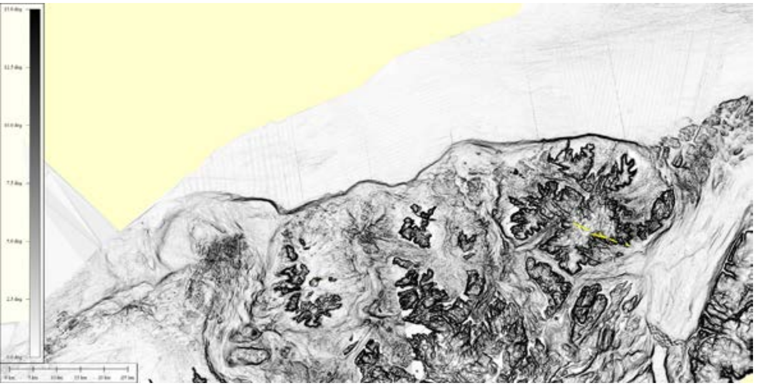

Datasets

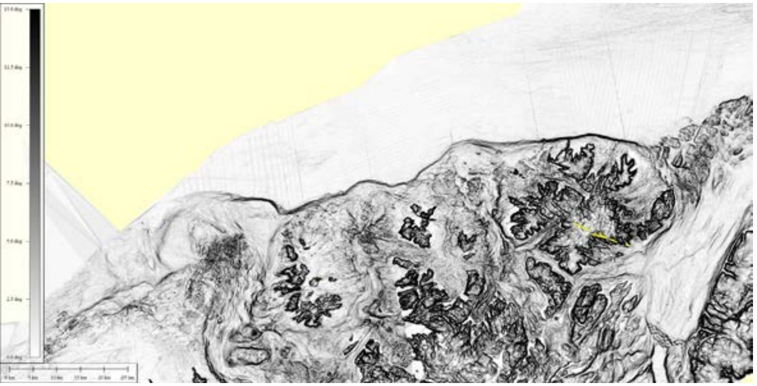

Datasets

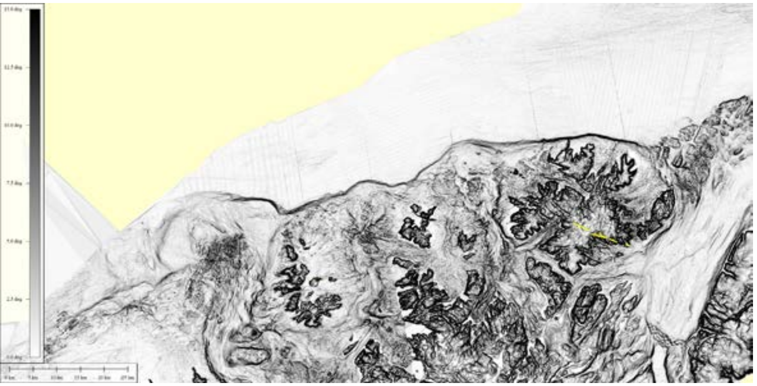

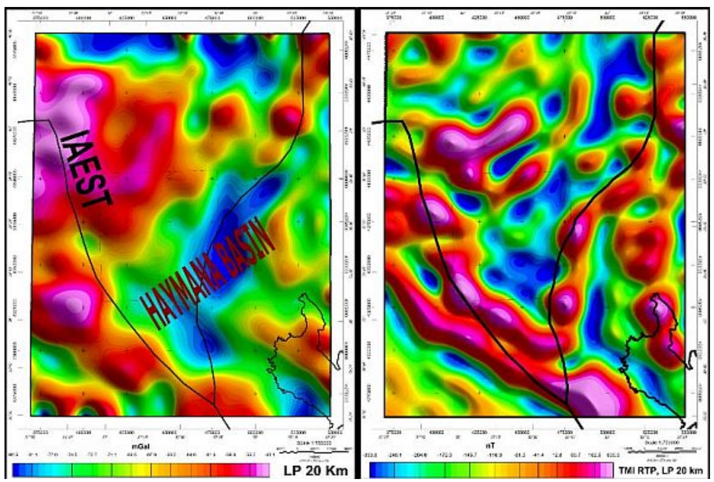

Datasets

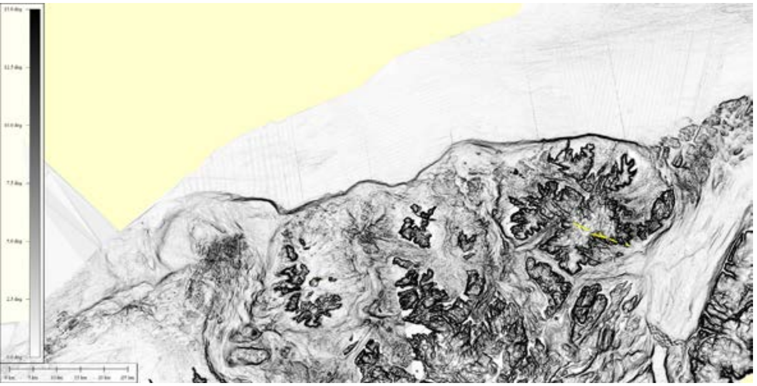

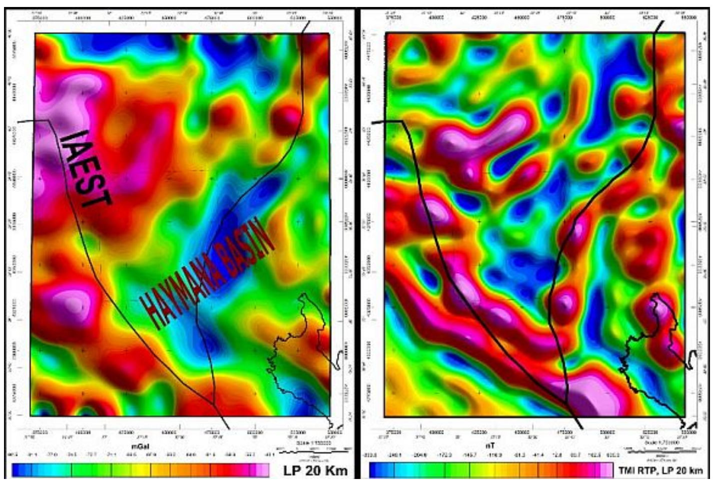

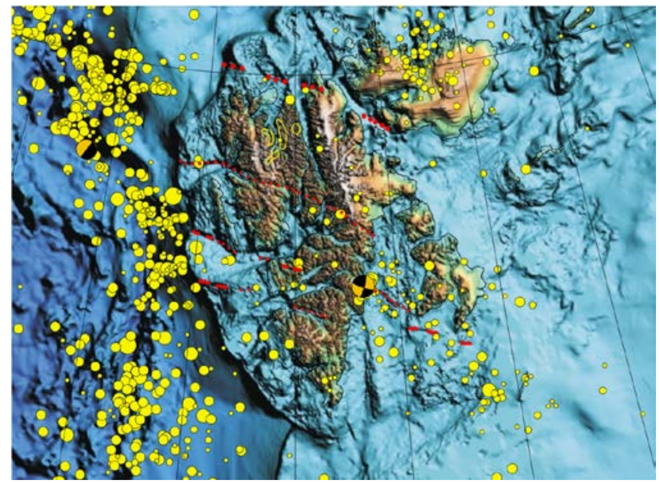

Datasets

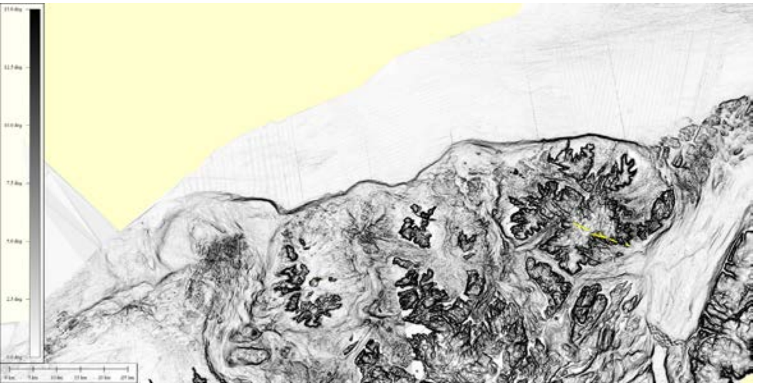

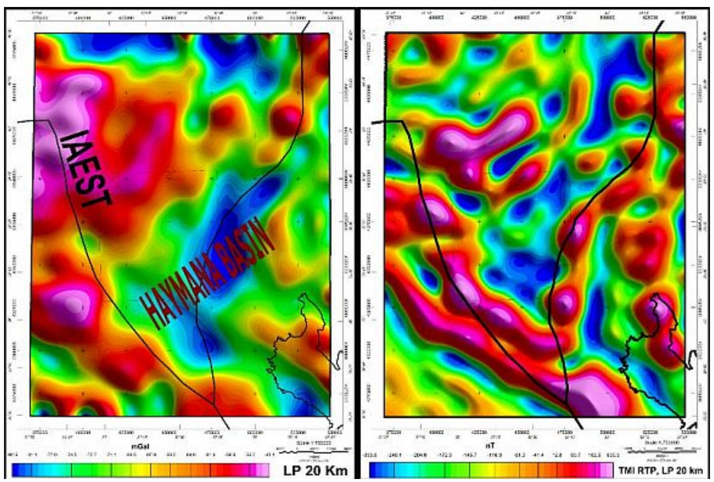

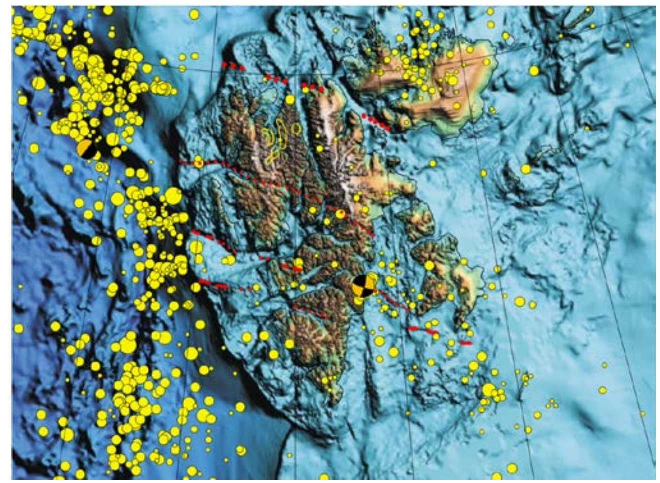

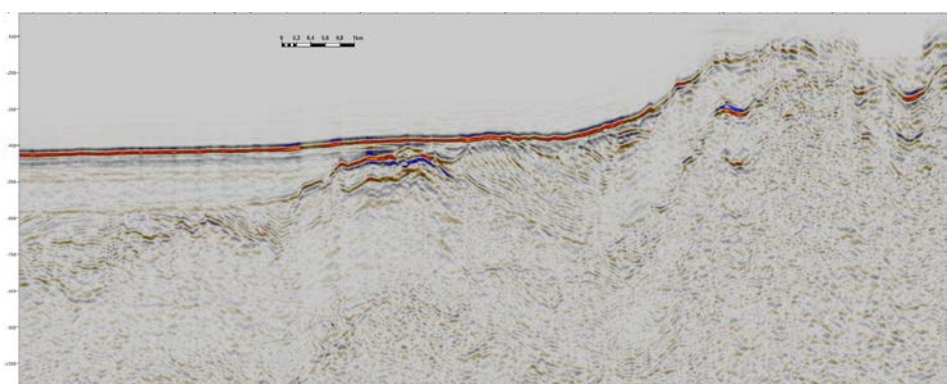

Outline

0

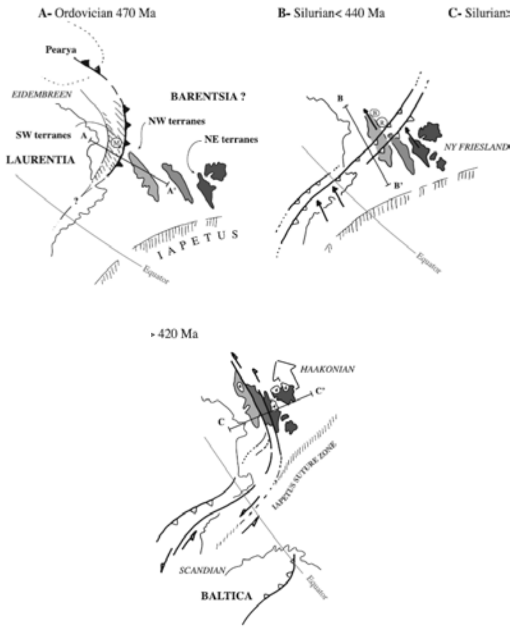
A- Ordovician 470 Ma
B- Silurian< 440 Ma
C- Silurian
420 Ma
Pearya
EIDEMBREEN
BARENTSIA ?
NW terranes
SW terranes
NE terranes
LAURENTIA
IAPETUS
Equator
NY FRIESLAND
HAAKONIAN
IAPETUS SUTURE ZONE
SCANDIAN
BALTICA

Outline

0

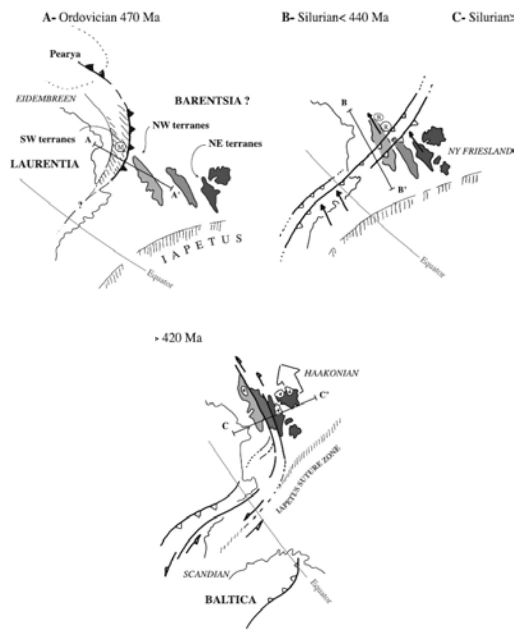

A- Ordovician 470 Ma
B- Silurian< 440 Ma
C- Silurian
Pearya
EIDEMBREEN
BARENTSIA ?
NW terranes
SW terranes
NE terranes
LAURENTIA
IAPETUS
NY FRIESLAND
420 Ma
HAAKONIAN
IAPETUS SUTURE ZONE
SCANDIAN
BALTICA

1

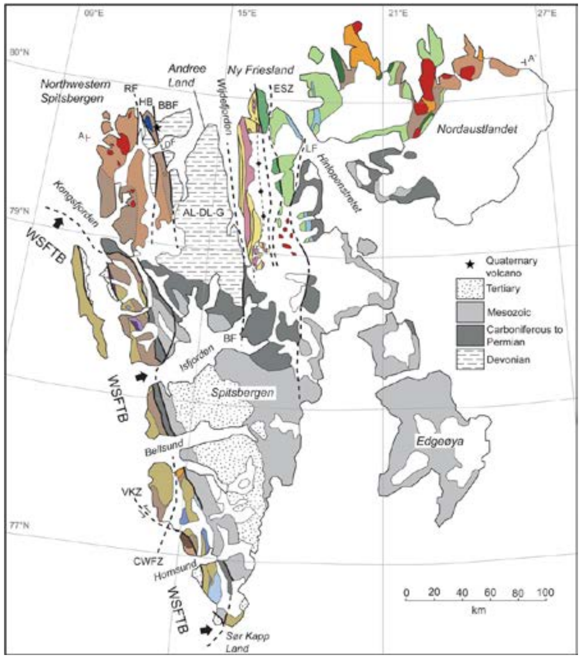

Northwestern Spitsbergen
Andree Land
Ny Friesland
Nordaustlandet
Kongsfjorden
WSFTB
AL-DL-G
Isfjorden
Spitsbergen
Bellsund
VKZ
CWFZ
Hornsund
Sør Kapp Land
Edgeøya
Hinlopenstretet
Wijdefjorden
Quaternary volcano
Tertiary
Mesozoic
Carboniferous to Permian
Devonian
0 20 40 60 80 100
km

Outline

0

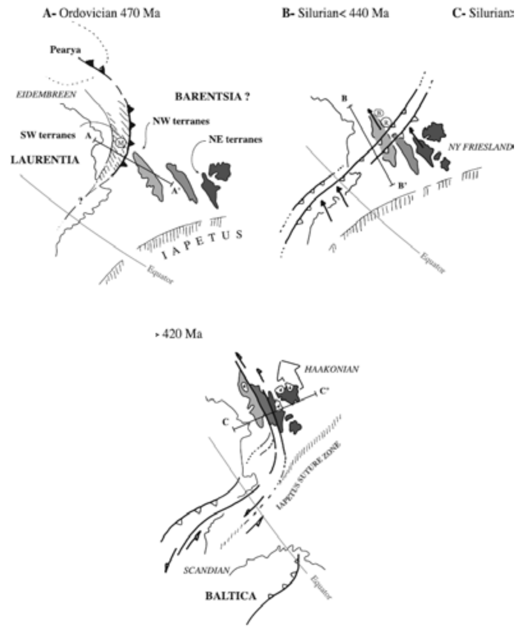

A- Ordovician 470 Ma
B- Silurian< 440 Ma
C- Silurian
420 Ma
Pearya
EIDEMBREEN
BARENTSIA ?
NW terranes
SW terranes
NE terranes
LAURENTIA
IAPETUS
NY FRIESLAND
HAAKONIAN
IAPETUS SUTURE ZONE
SCANDIAN
BALTICA
Equator

1

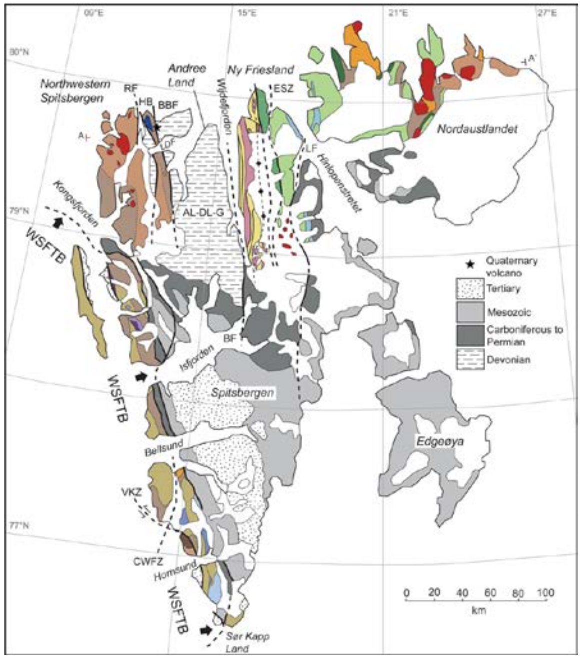

Northwestern Spitsbergen
Andree Land
Ny Friesland
RF
HB
BBF
ESZ
Wijdefjorden
Nordaustlandet
Kongsfjorden
WSFTB
AL-DL-G
Hinlopenstretet
LF
BFF
Isfjorden
Spitsbergen
Bellsund
VKZ
CWFZ
Hornsund
Sør Kapp Land
Edgeøya
Quaternary volcano
Tertiary
Mesozoic
Carboniferous to Permian
Devonian
0 20 40 60 80 100
km

2

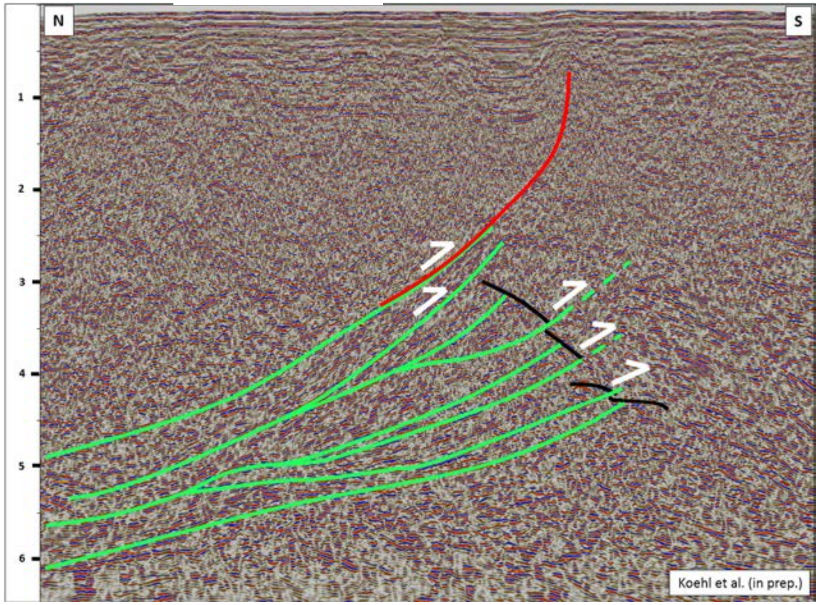

N
S
1
2
3
4
5
6
Koehl et al. (in prep.)

Outline

0

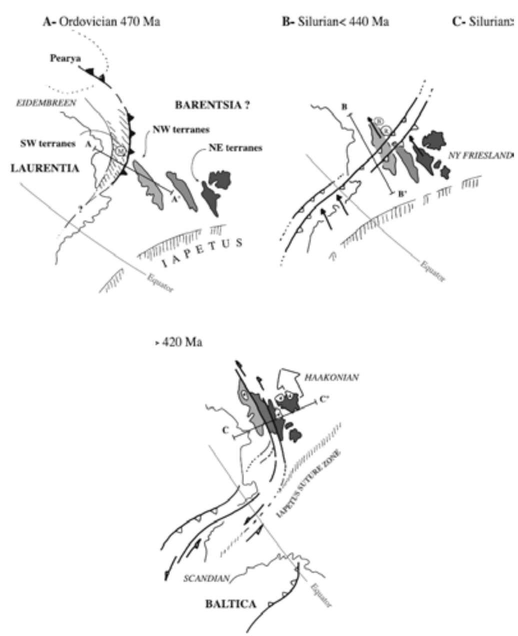

1

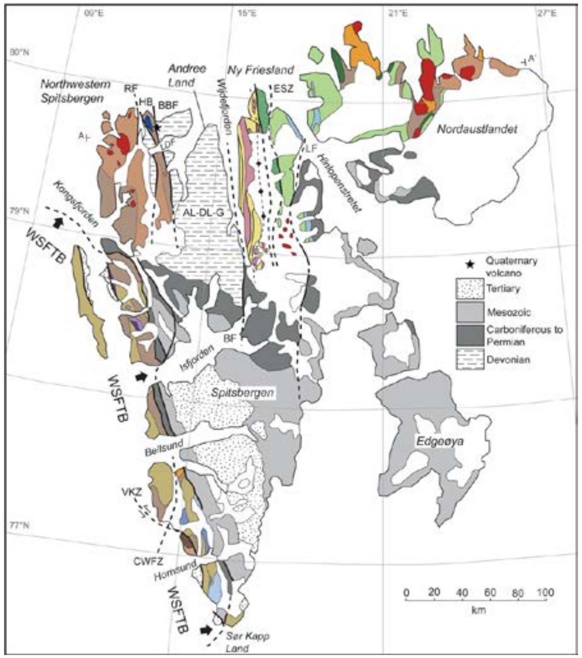

2

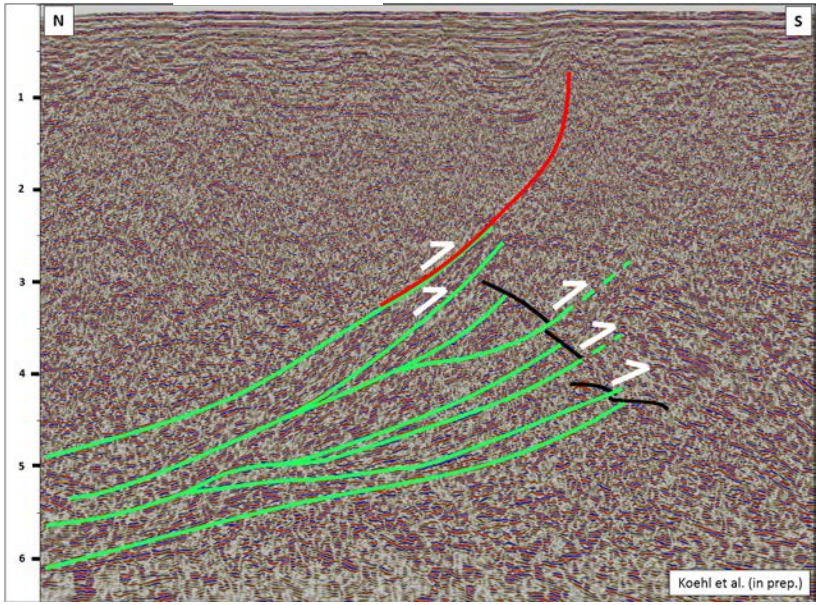

3

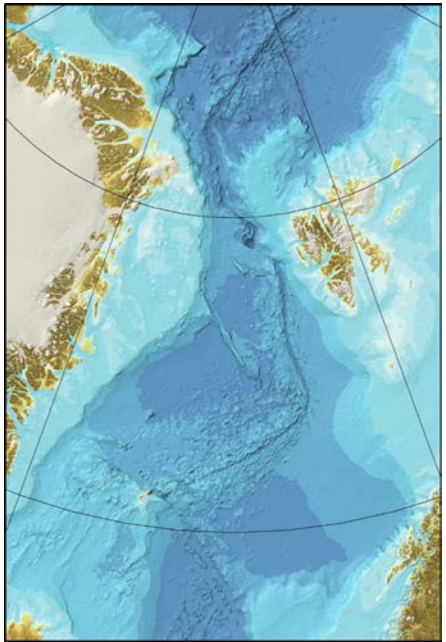

0

The Svalbard Archipelago is made of three terranes accreted together during the Caledonian Orogeny showing dominantly N–S-trending fabrics, folds and faults.

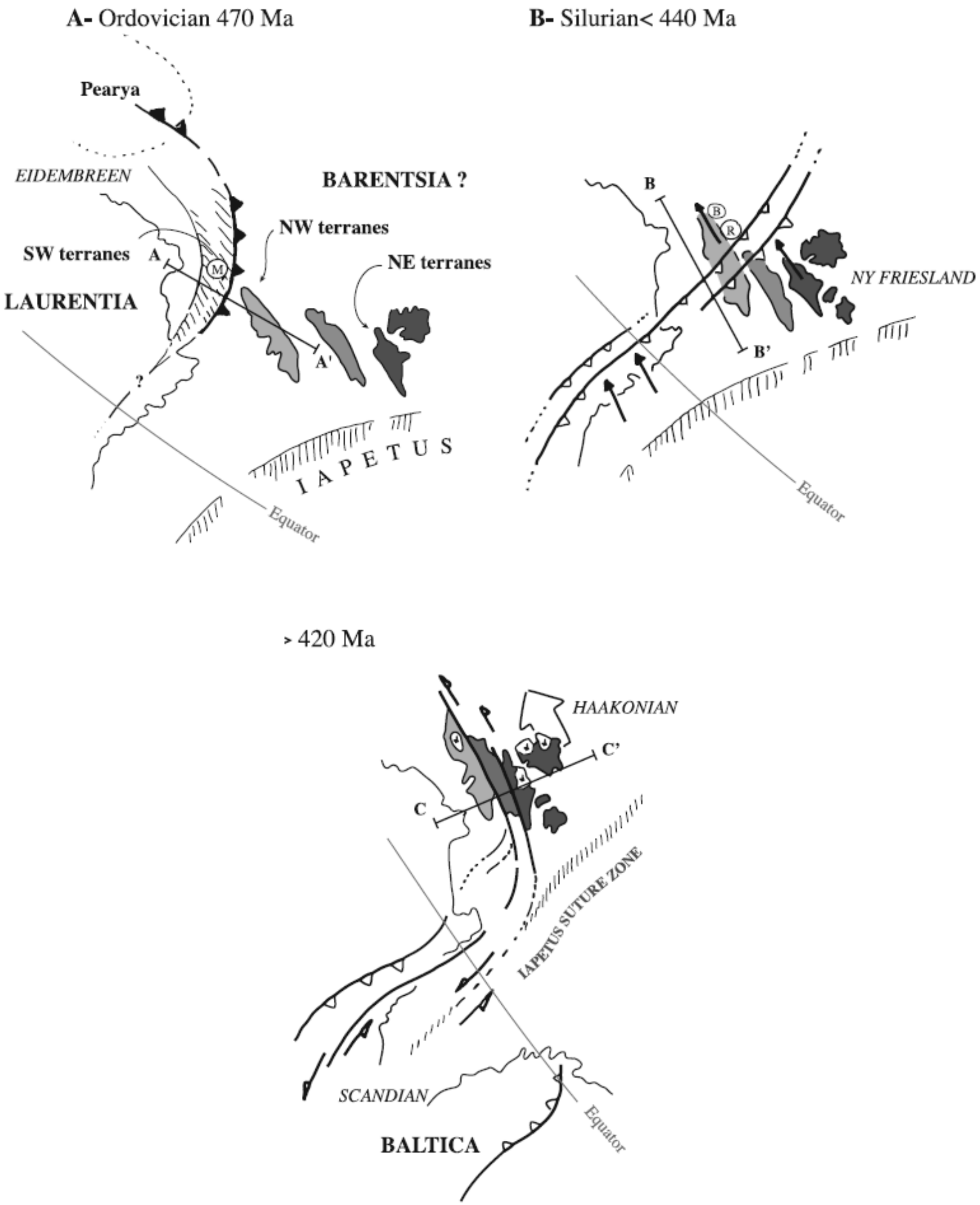

Labrousse et al. (2008)

0

The Svalbard Archipelago is made of three terranes accreted together during the Caledonian Orogeny showing dominantly N–S-trending fabrics, folds and faults.

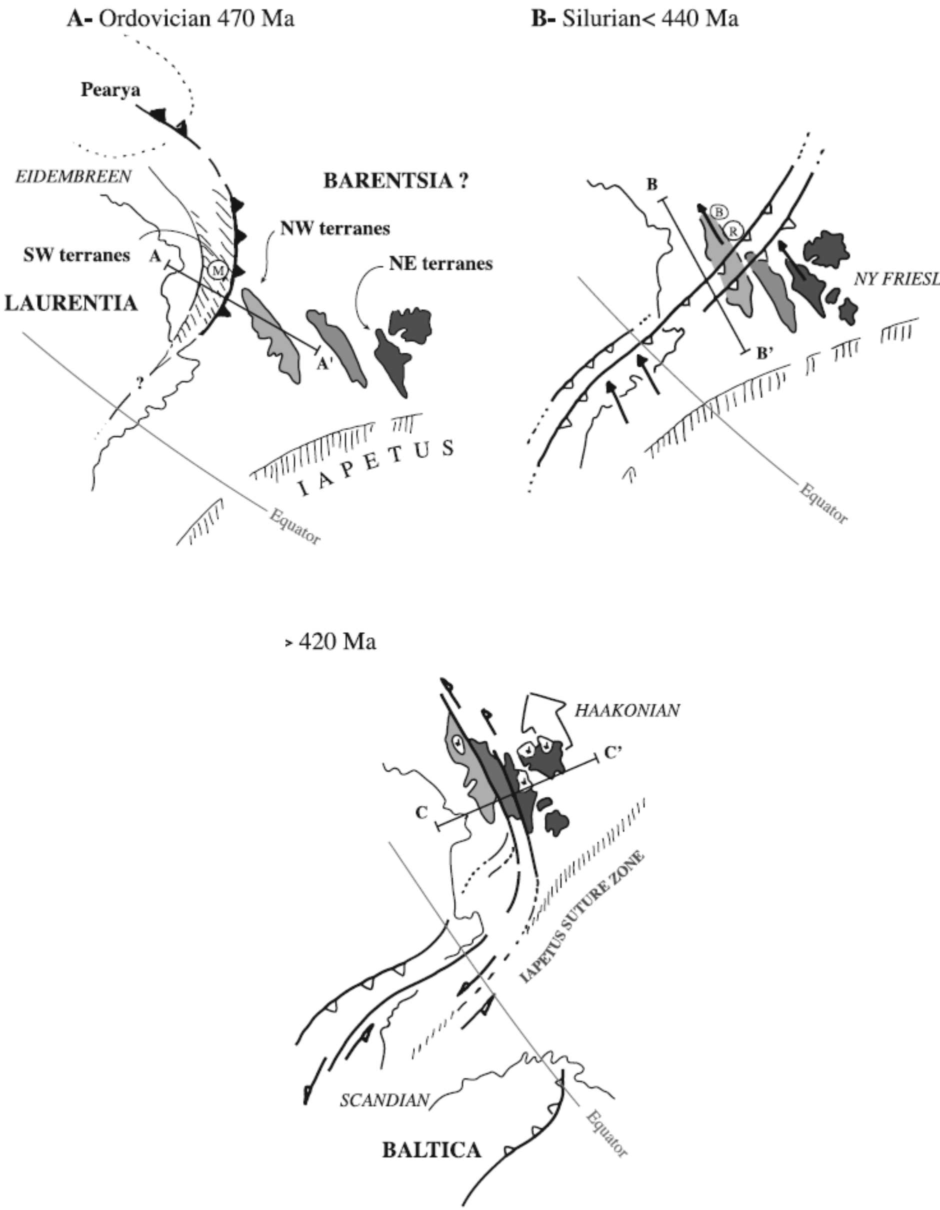

Labrousse et al. (2008)

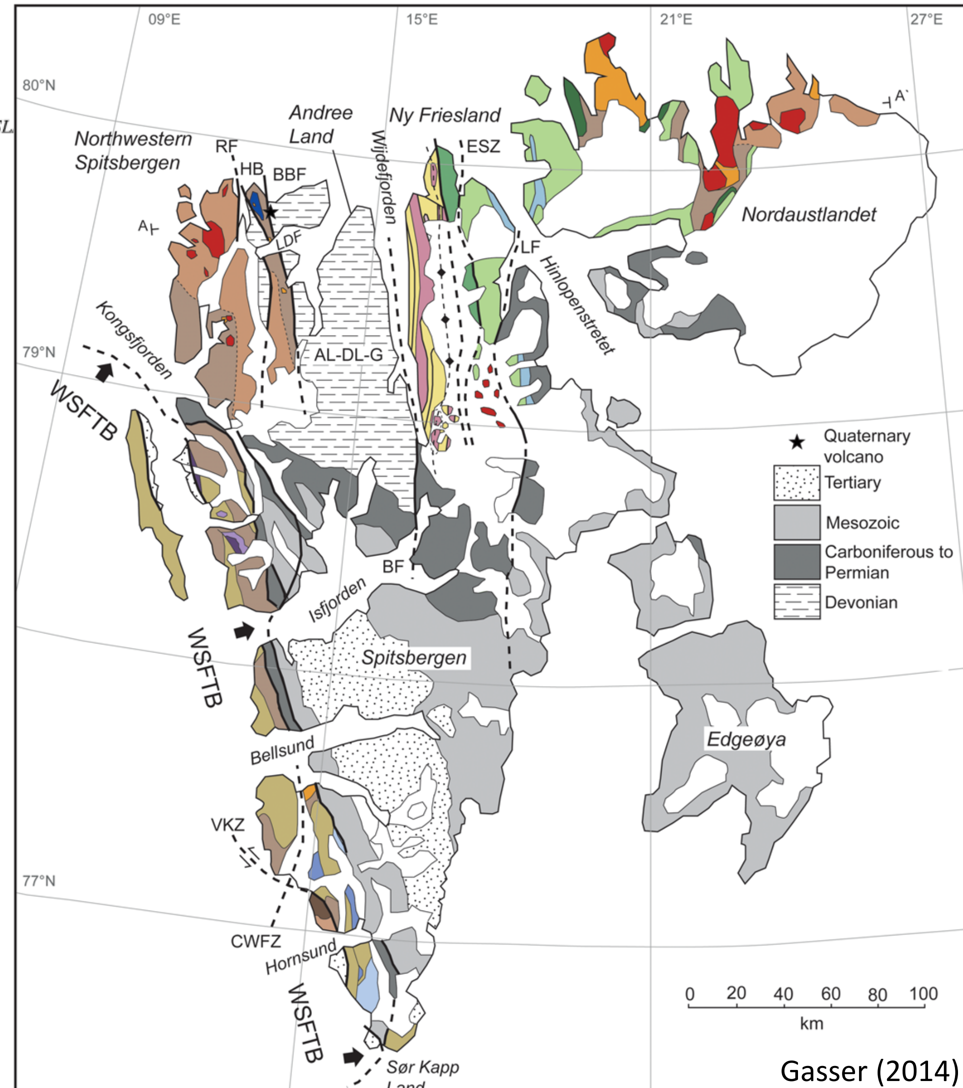

Gasser (2014)

0

The Svalbard Archipelago is made of three terranes accreted together during the Caledonian Orogeny showing dominantly N–S-trending fabrics, folds and faults.

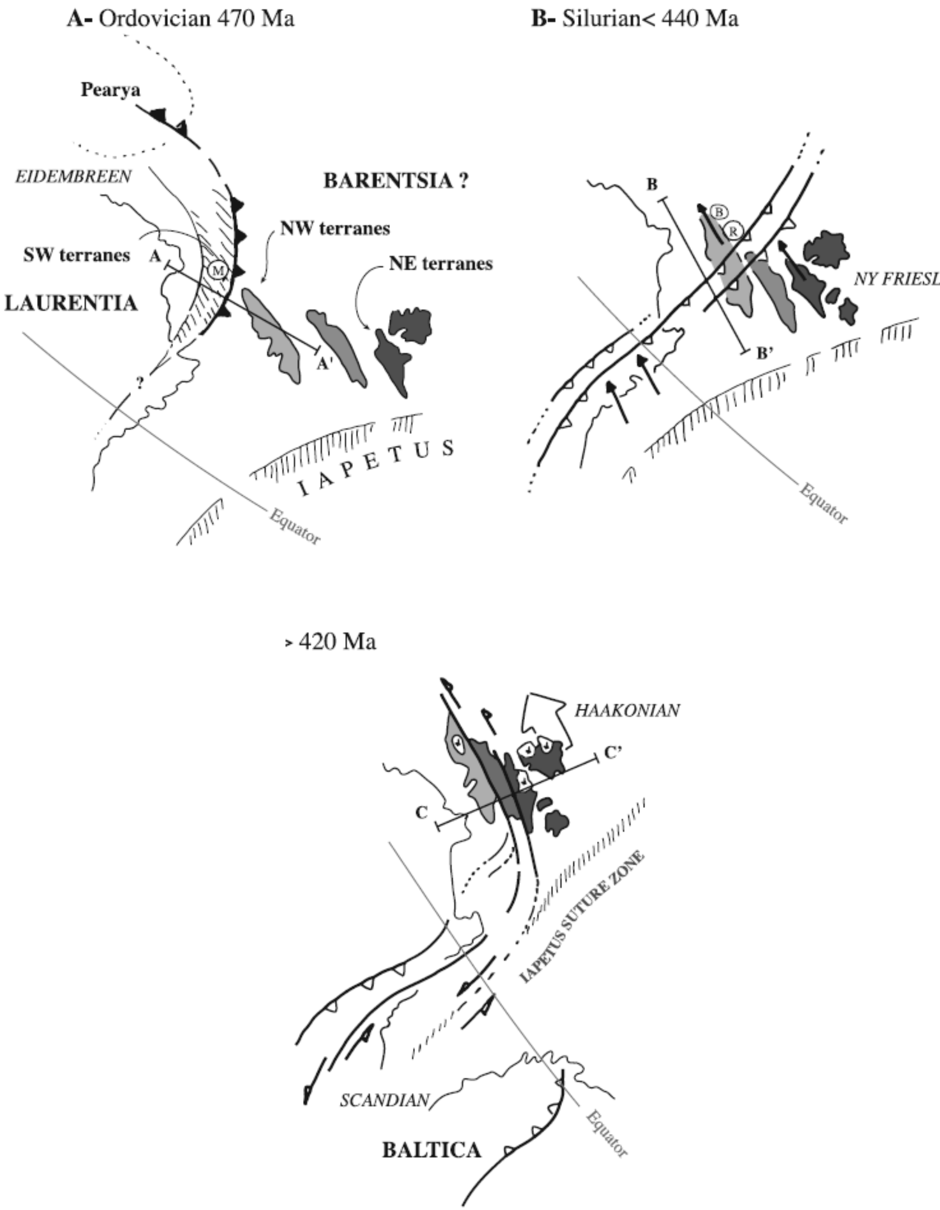

Labrousse et al. (2008)

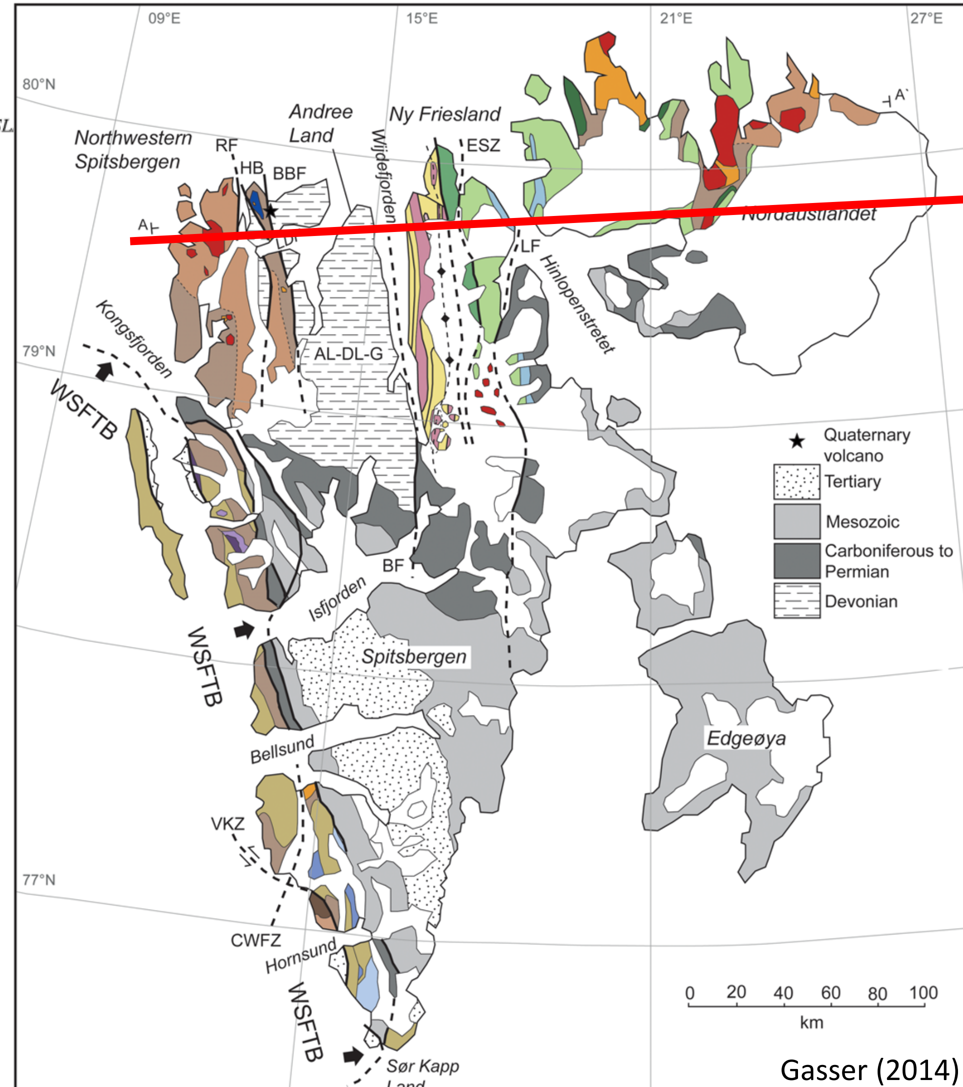

Gasser (2014)

0

The Svalbard Archipelago is made of three terranes accreted together during the Caledonian Orogeny showing dominantly N–S-trending fabrics, folds and faults.

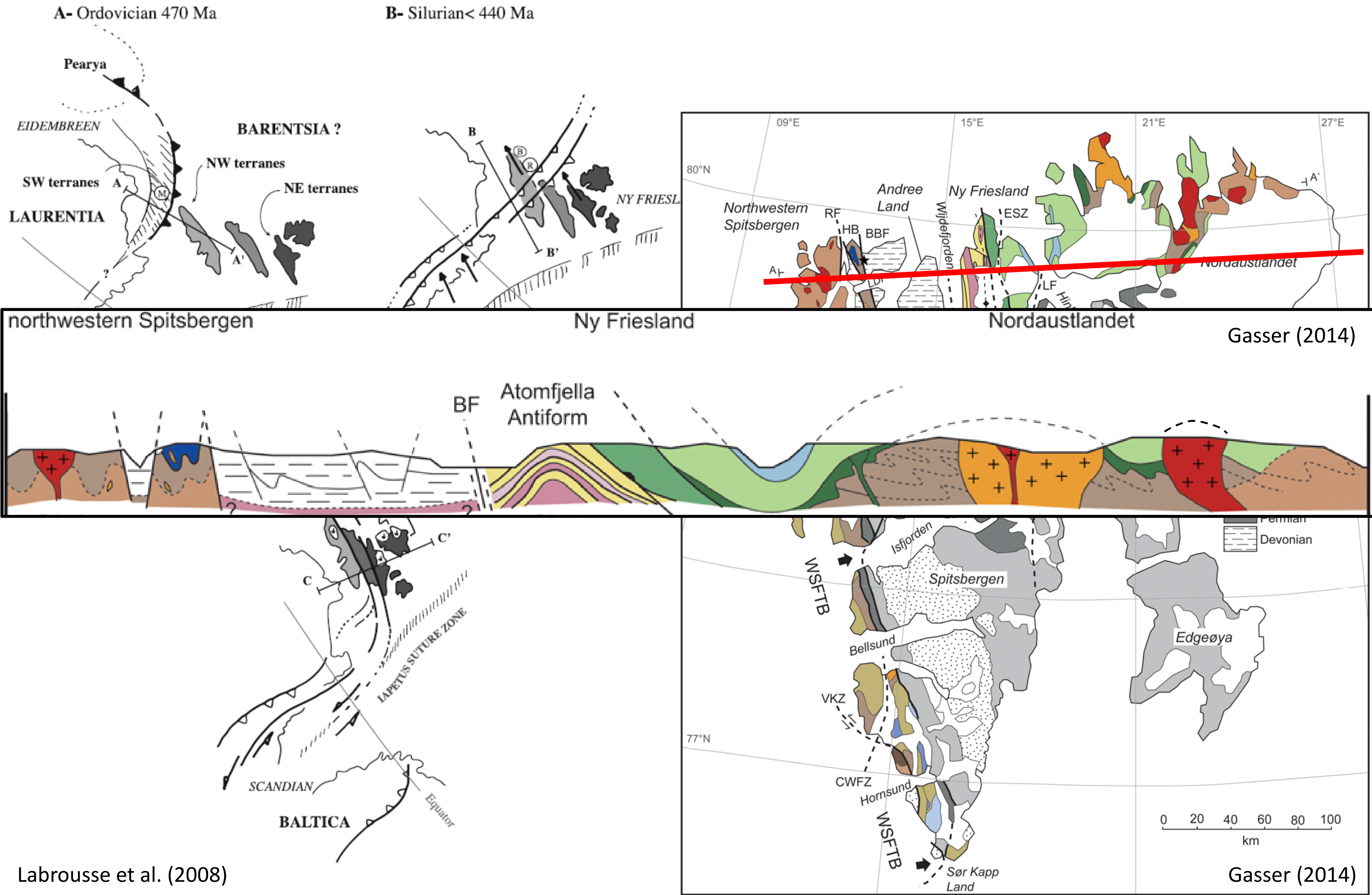

0

The Svalbard Archipelago is made of three terranes accreted together during the Caledonian Orogeny showing dominantly N–S-trending fabrics, folds and faults.

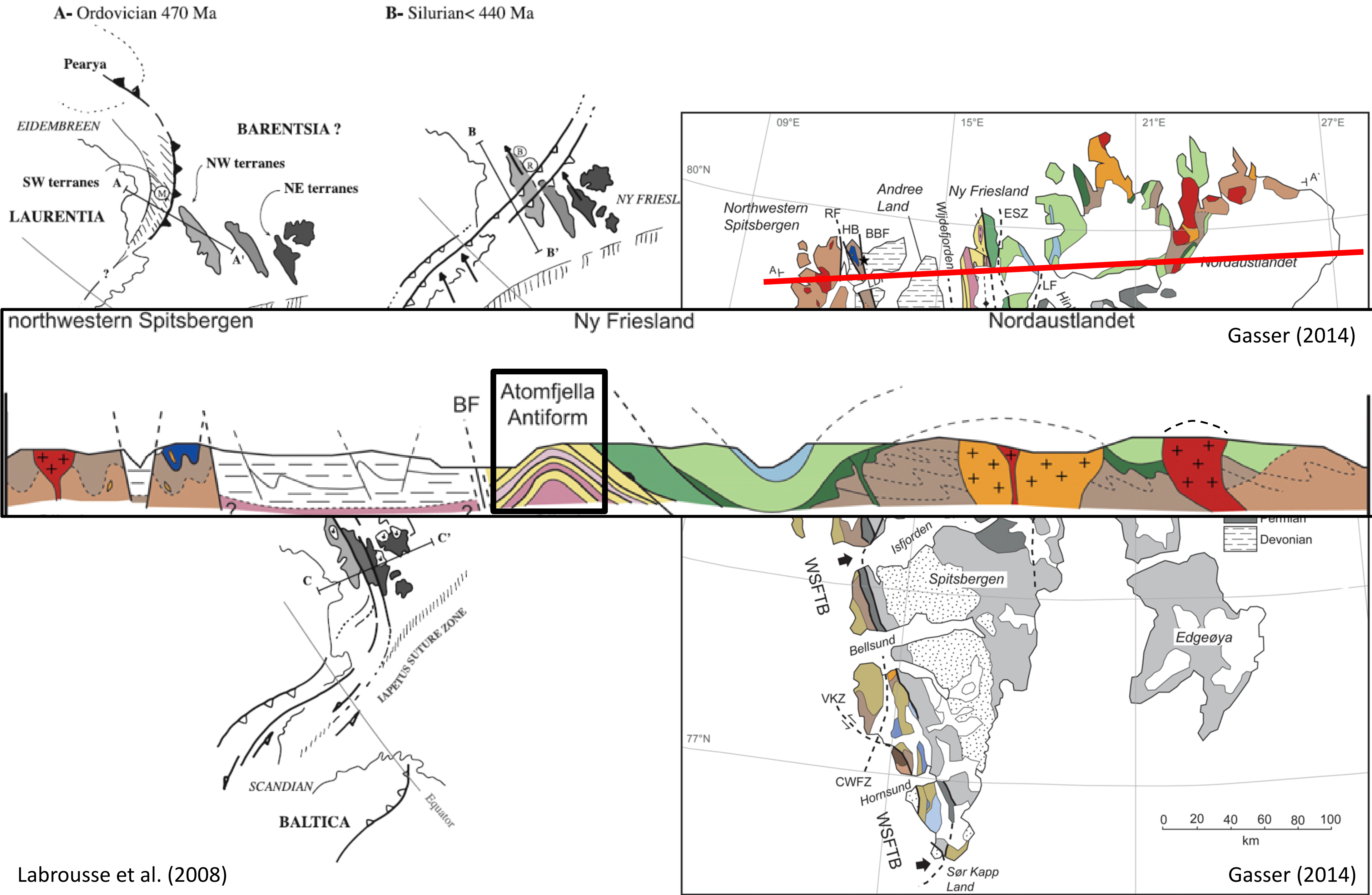

0

The Svalbard Archipelago is made of three terranes accreted together during the Caledonian Orogeny showing dominantly N–S-trending fabrics, folds and faults.

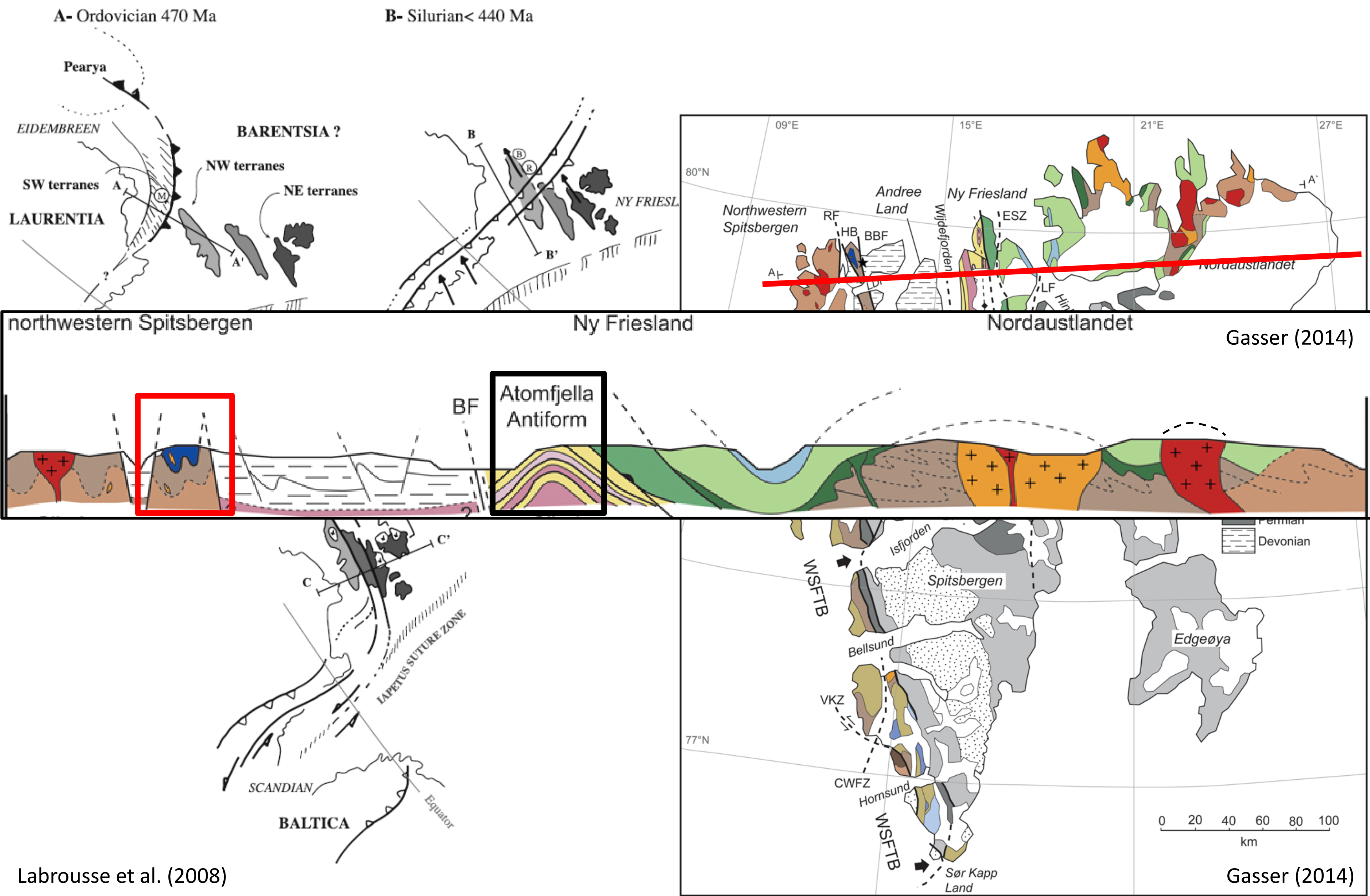

0

Core complexes exhumed in the late Silurian–Devonian due to normal top-north, top-west and top-east movements along bowed shear zones.

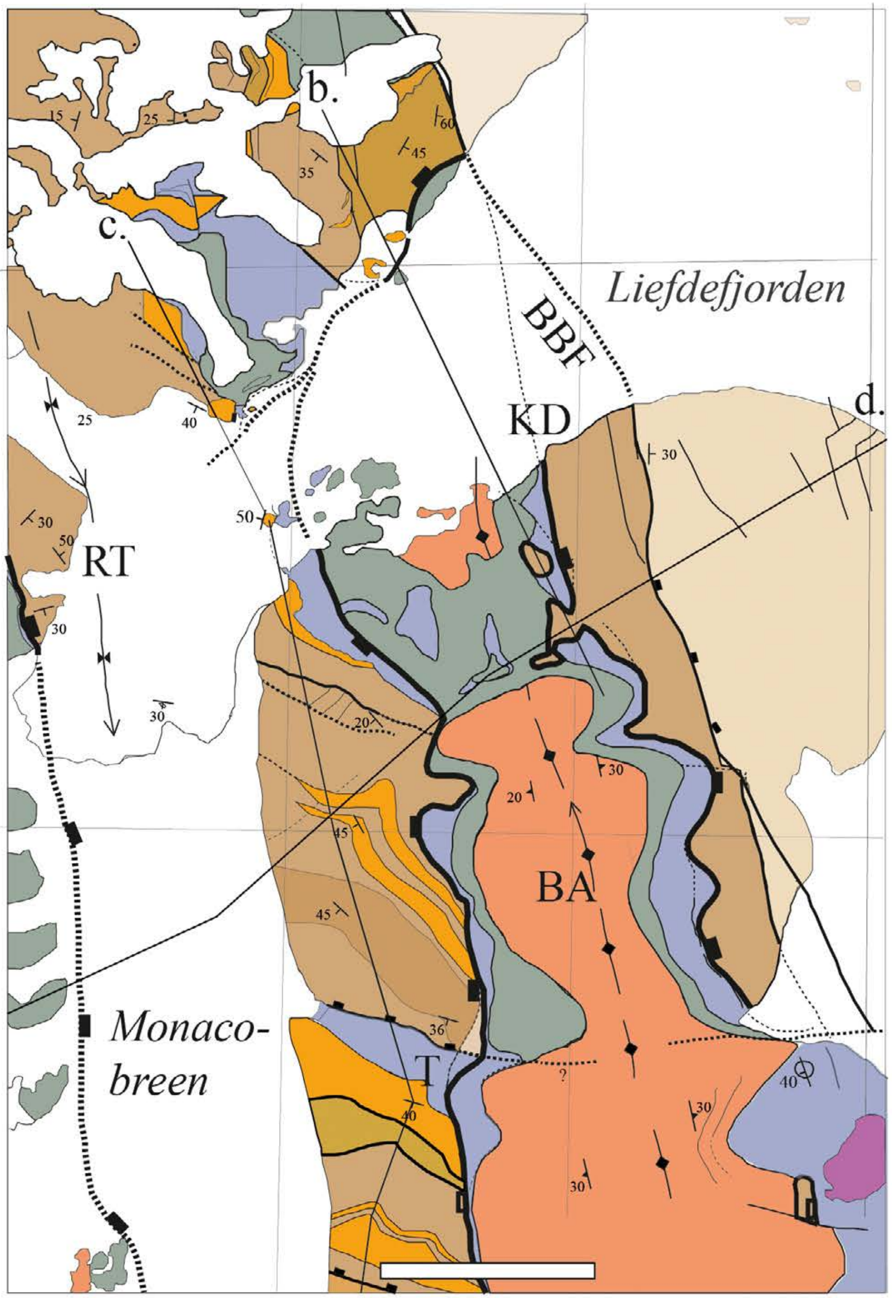

Braathen et al. (2018)

0

Core complexes exhumed in the late Silurian–Devonian due to normal top-north, top-west and top-east movements along bowed shear zones.

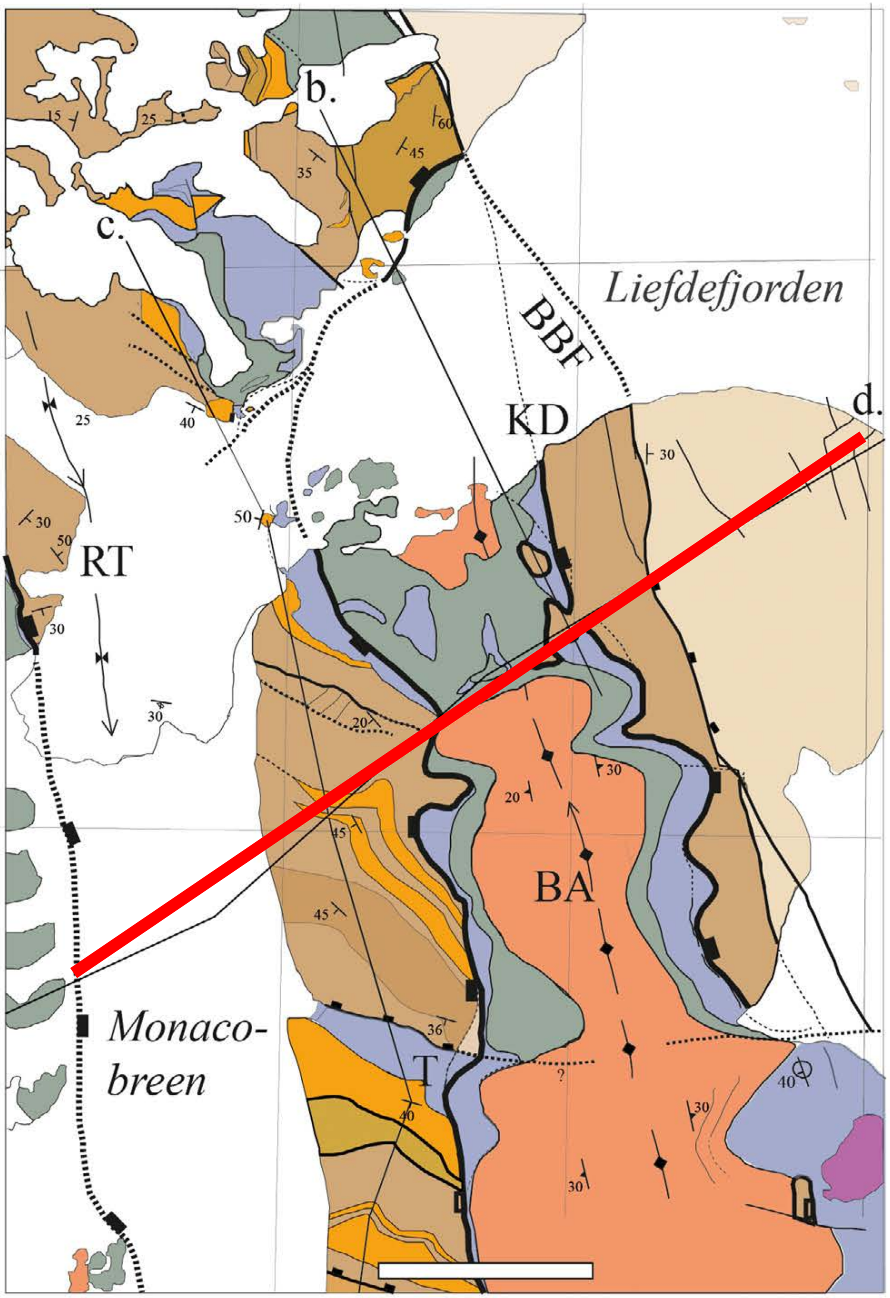

Braathen et al. (2018)

0

Core complexes exhumed in the late Silurian–Devonian due to normal top-north, top-west and top-east movements along bowed shear zones.

Braathen et al. (2018)

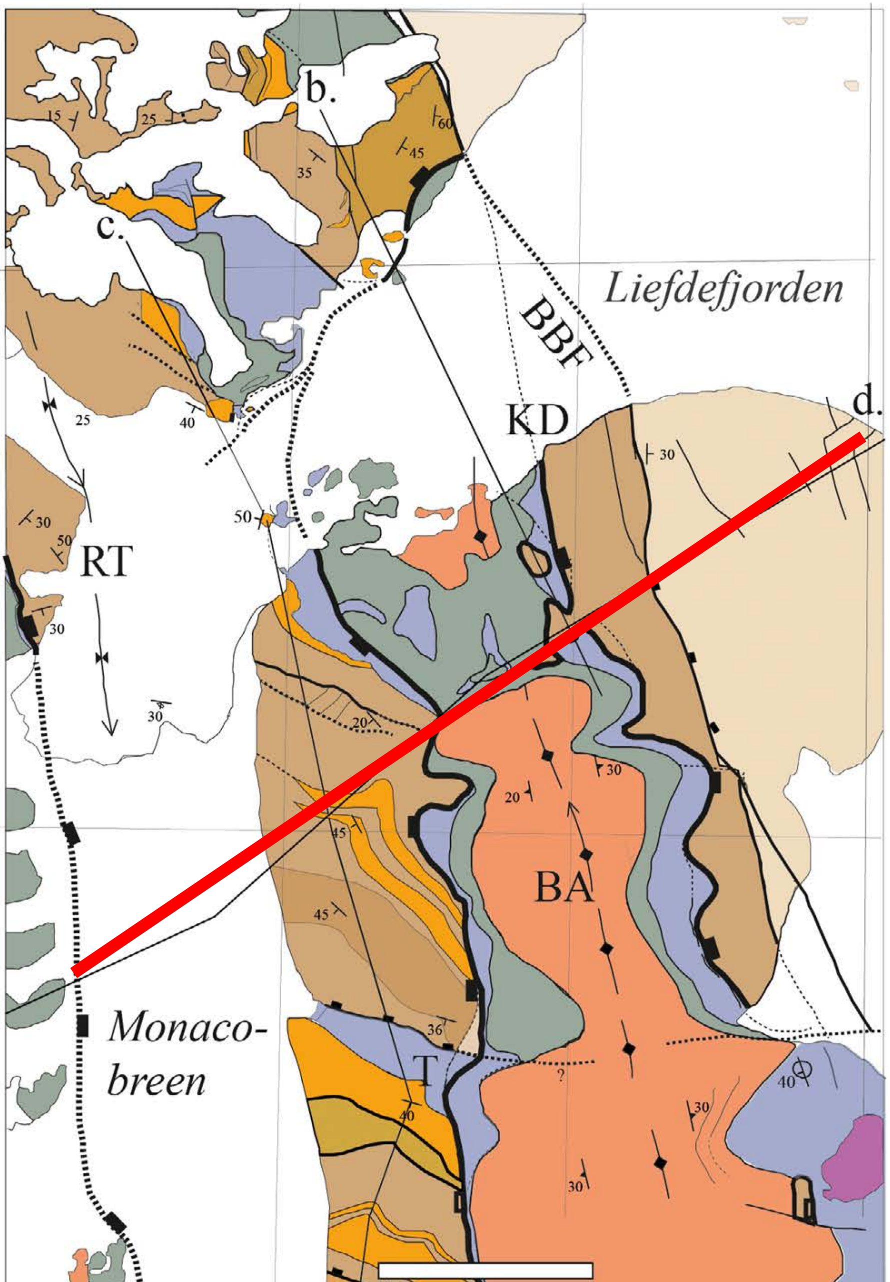

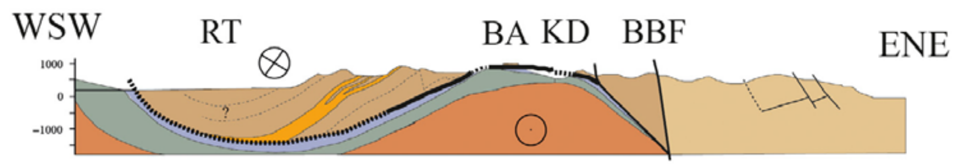

0

Core complexes exhumed in the late Silurian–Devonian due to normal top-north, top-west and top-east movements along bowed shear zones.

Braathen et al. (2018)

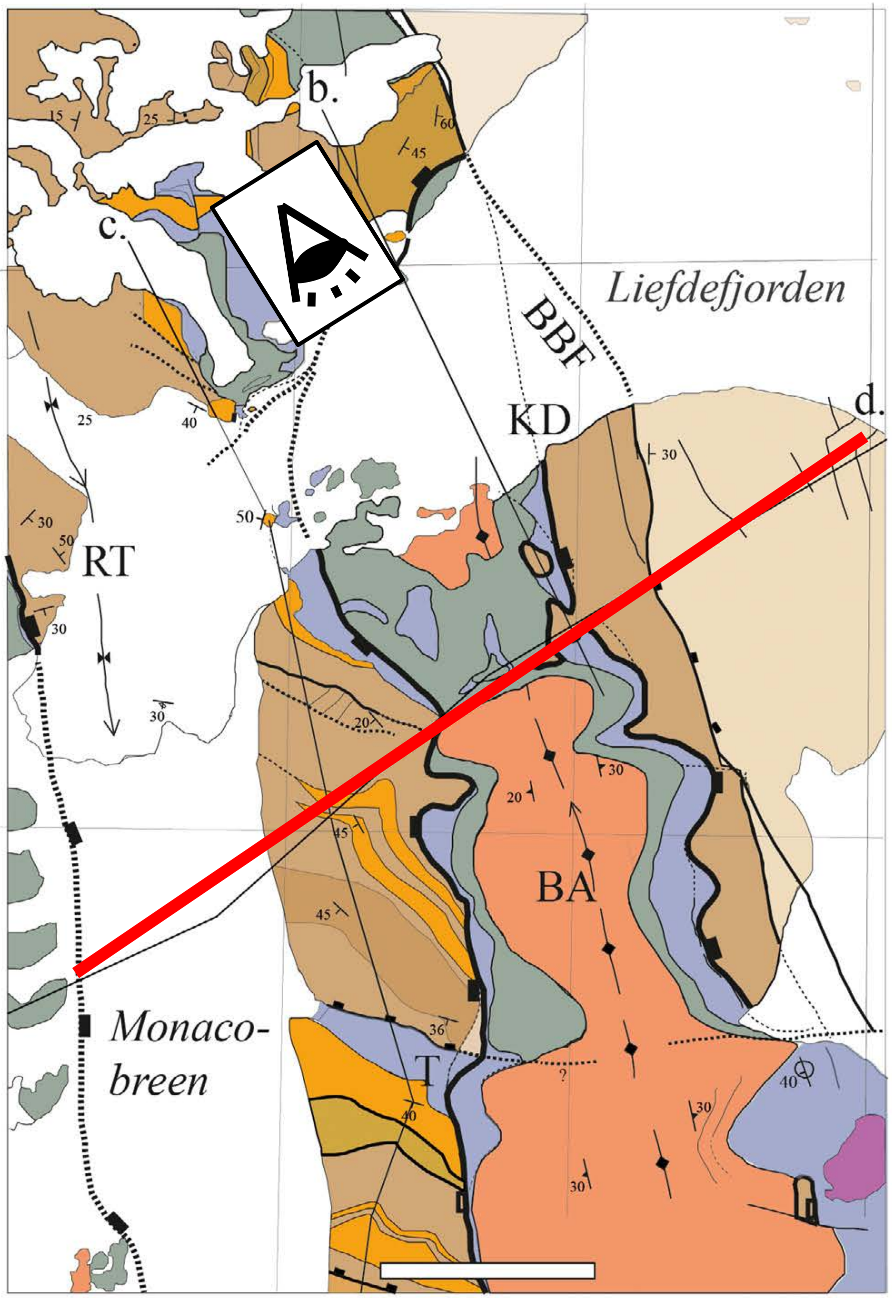

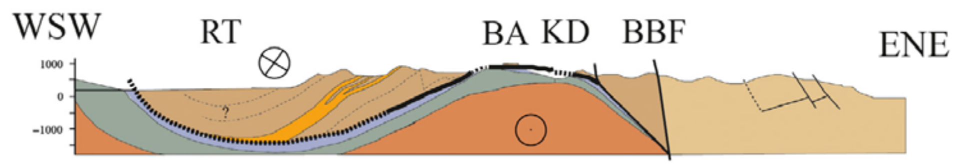

0

Core complexes exhumed in the late Silurian–Devonian due to normal top-north, top-west and top-east movements along bowed shear zones.

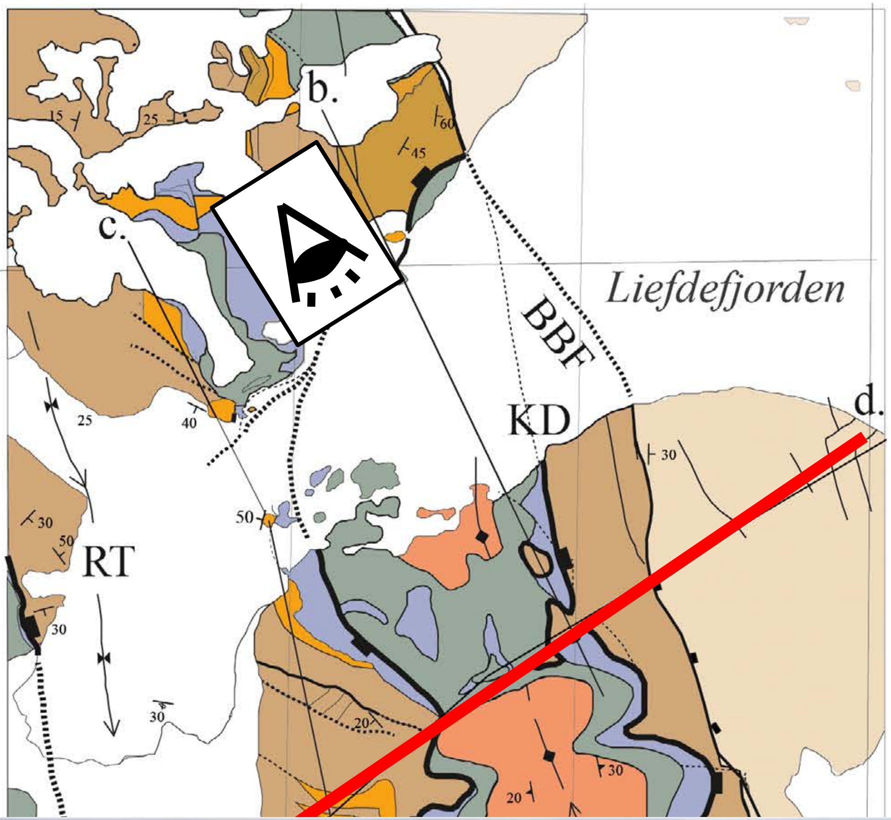

Braathen et al. (2018)

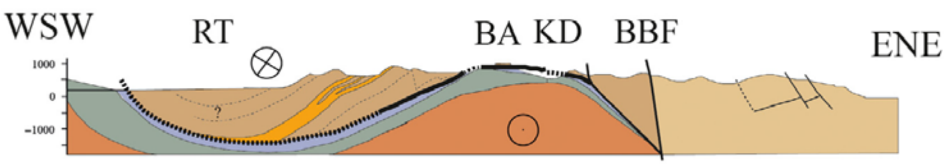

0

Core complexes exhumed in the late Silurian–Devonian due to normal top-north, top-west and top-east movements along bowed shear zones.

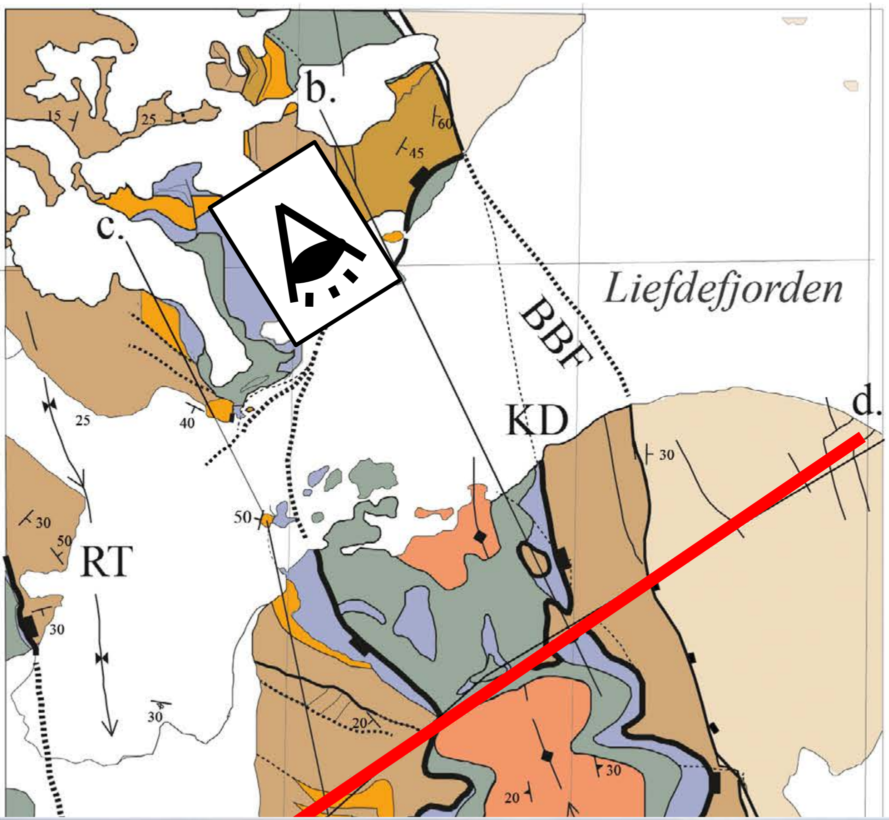

Braathen et al. (2018)

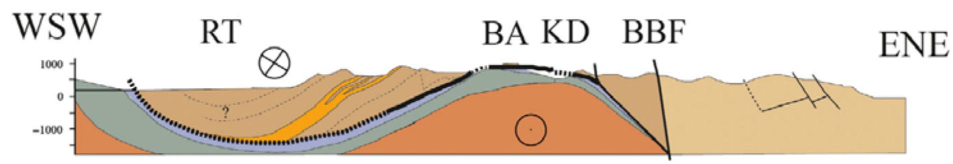

0

Core complexes exhumed in the late Silurian–Devonian due to normal top-north, top-west and top-east movements along bowed shear zones.

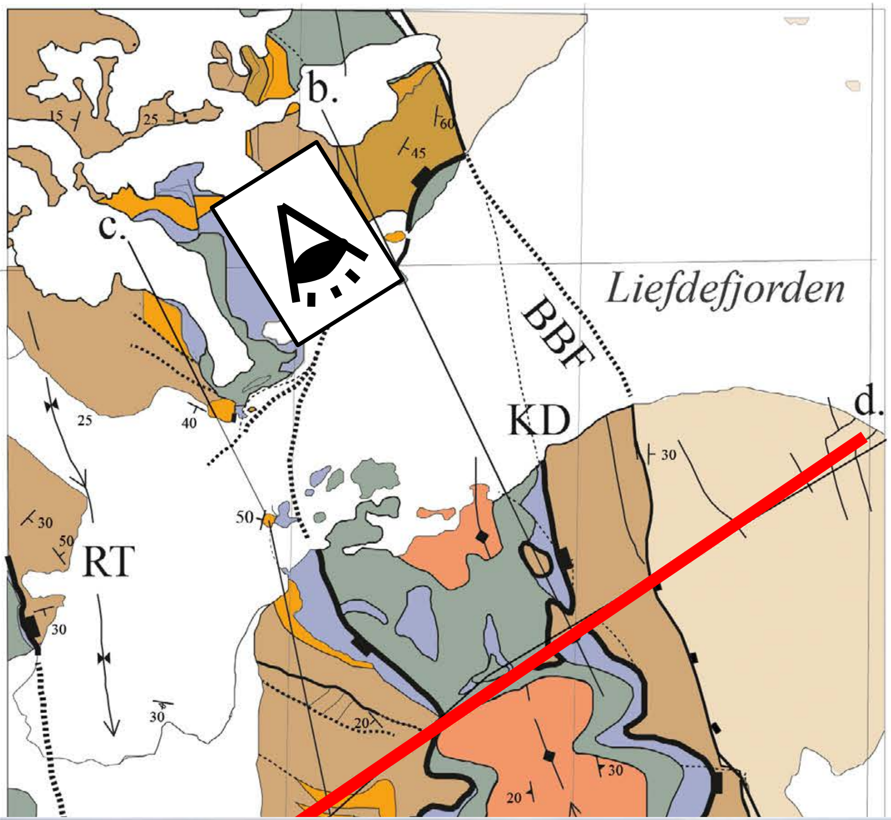

Braathen et al. (2018)

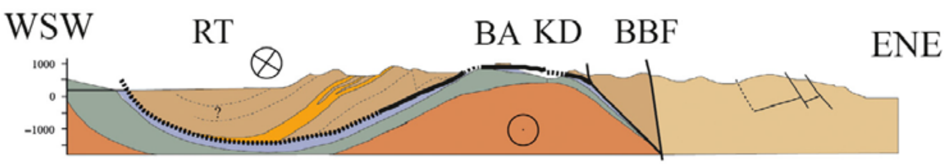

0

In Svalbard, Pennsylvanian rifting led to the formation of thick N–S-trending sedimentary basins like the Billefjorden Trough, which parallel dominant Caledonian fabrics.

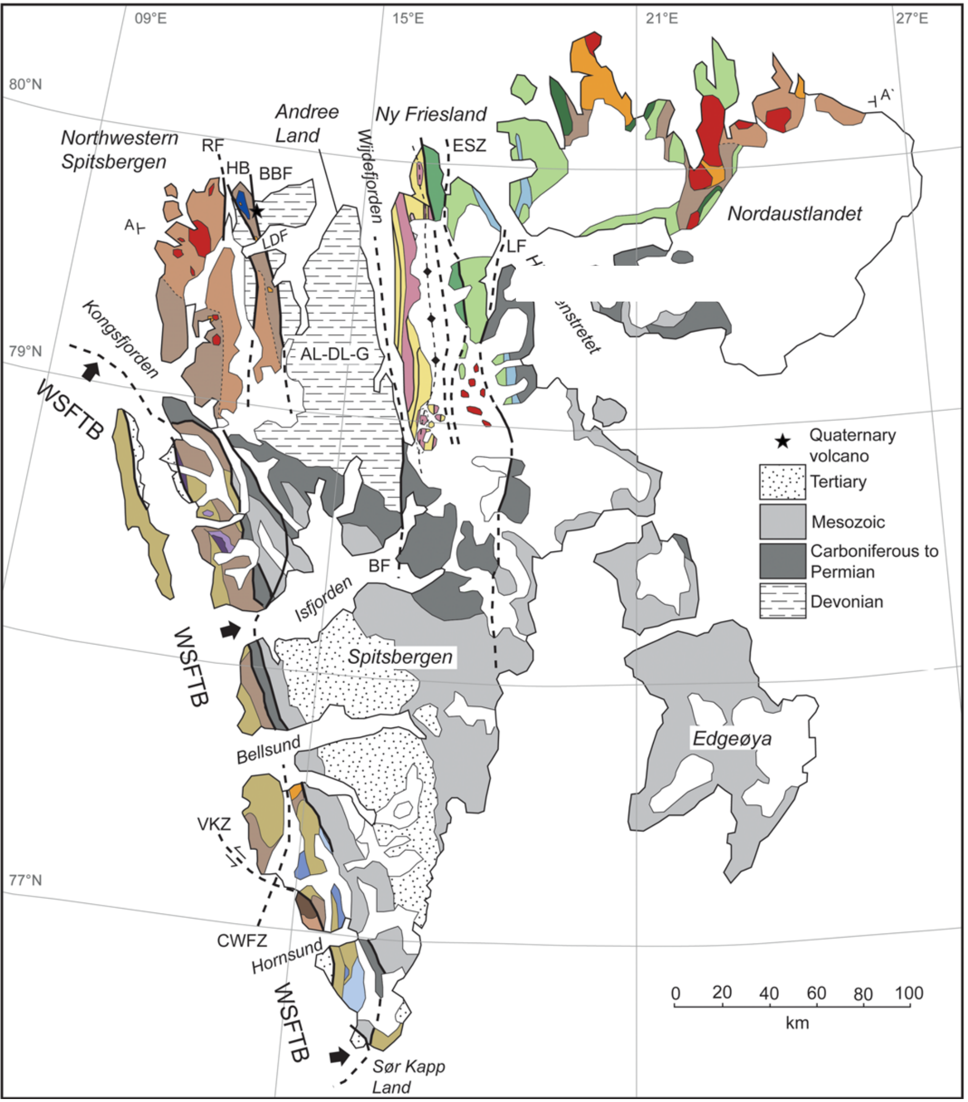

Gasser (2014)

0

In Svalbard, Pennsylvanian rifting led to the formation of thick N–S-trending sedimentary basins like the Billefjorden Trough, which parallel dominant Caledonian fabrics.

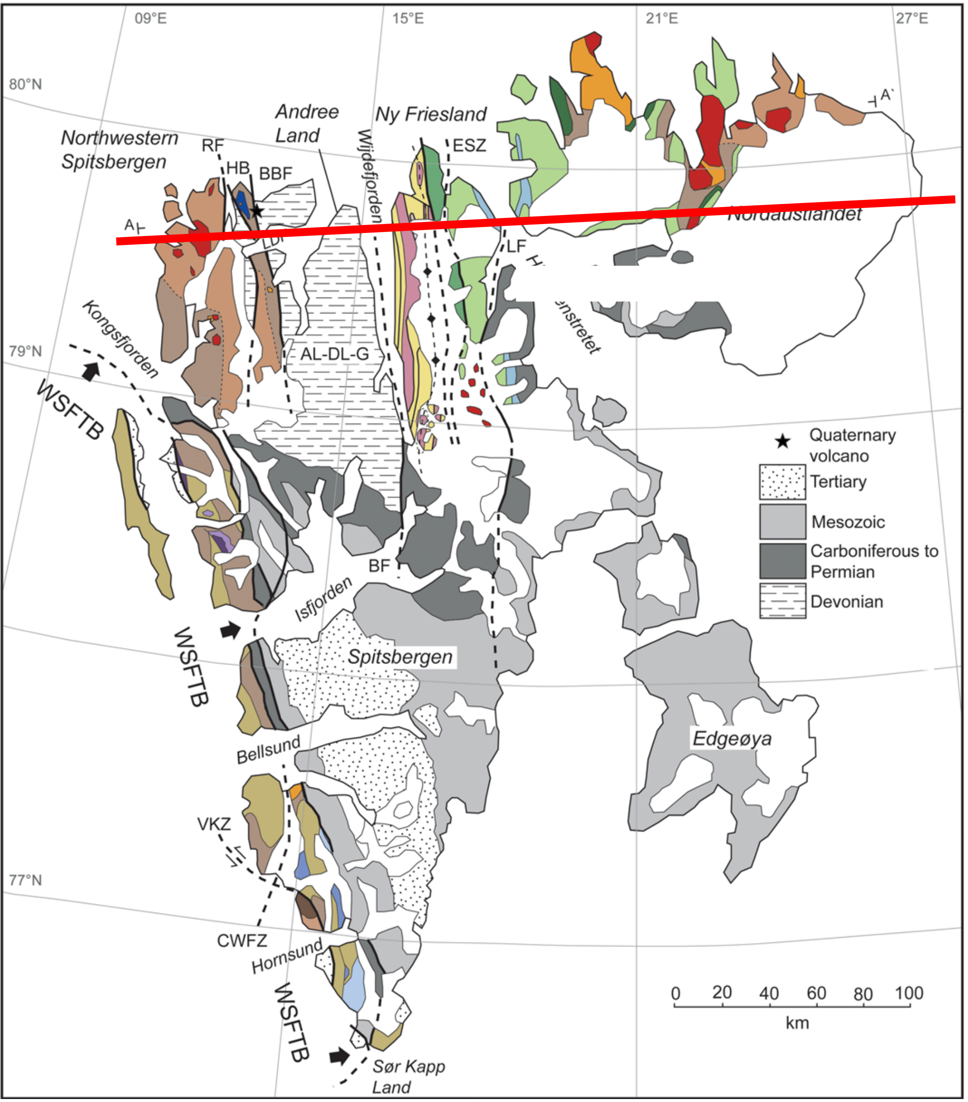

Gasser (2014)

0

In Svalbard, Pennsylvanian rifting led to the formation of thick N–S-trending sedimentary basins like the Billefjorden Trough, which parallel dominant Caledonian fabrics.

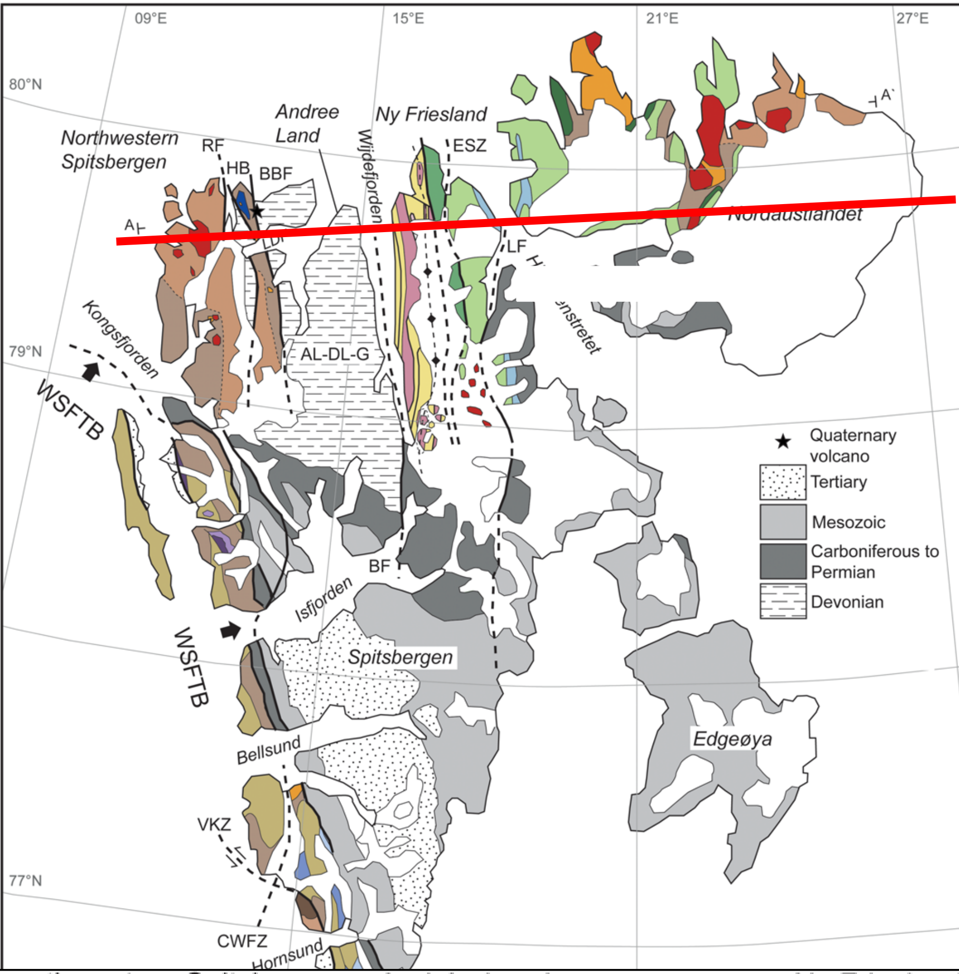

Gasser (2014)

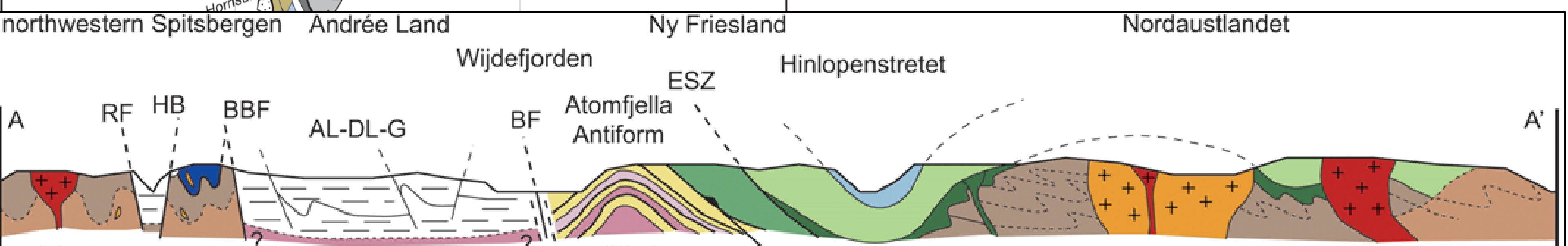

0

In Svalbard, Pennsylvanian rifting led to the formation of thick N–S-trending sedimentary basins like the Billefjorden Trough, which parallel dominant Caledonian fabrics.

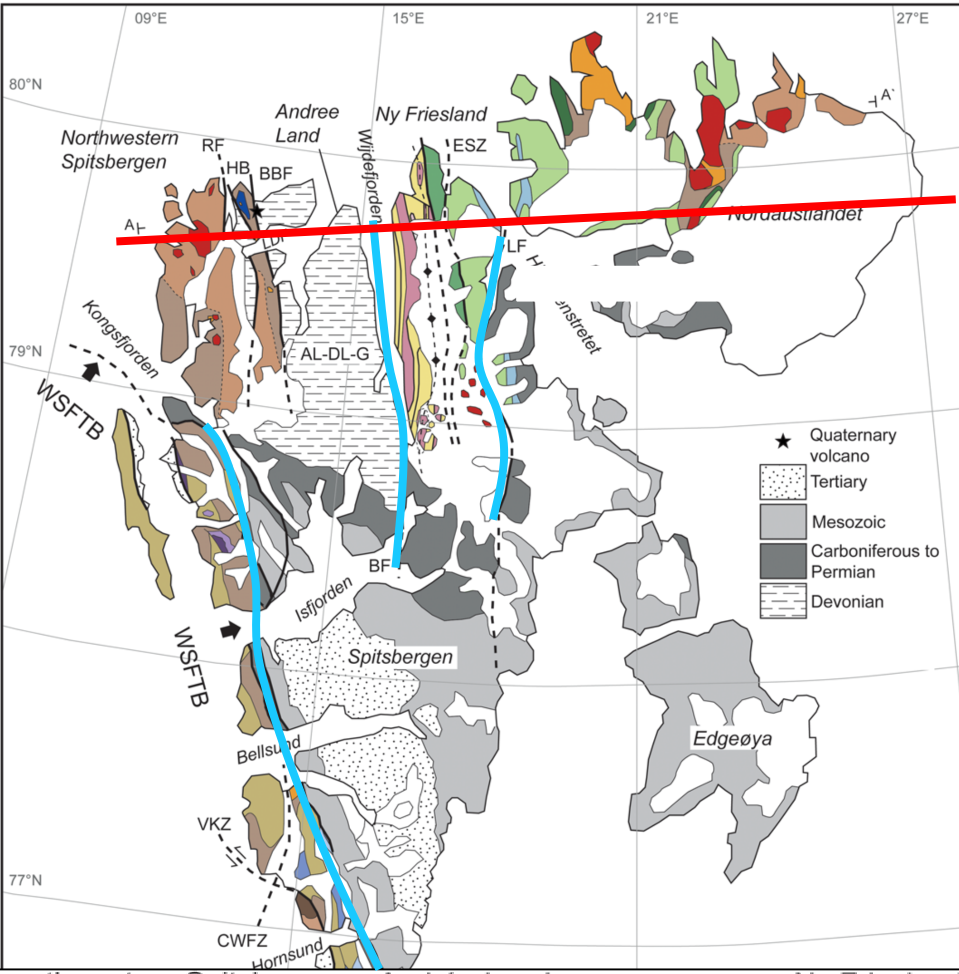

Gasser (2014)

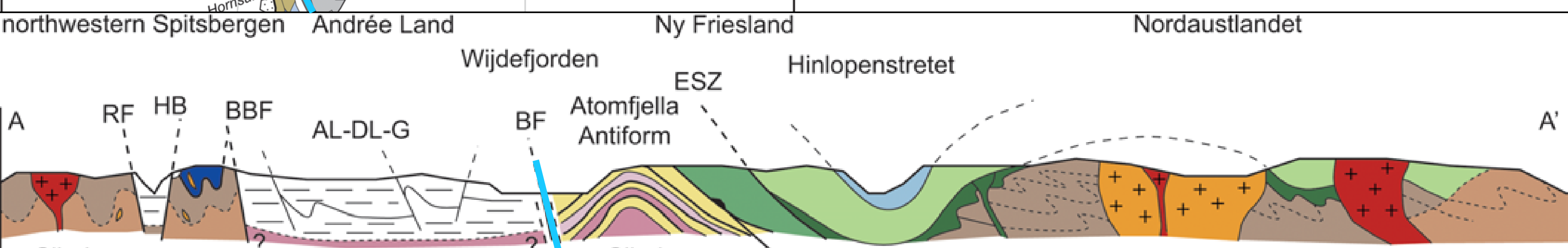

0

In Svalbard, Pennsylvanian rifting led to the formation of thick N–S-trending sedimentary basins like the Billefjorden Trough, which parallel dominant Caledonian fabrics.

Gasser (2014)

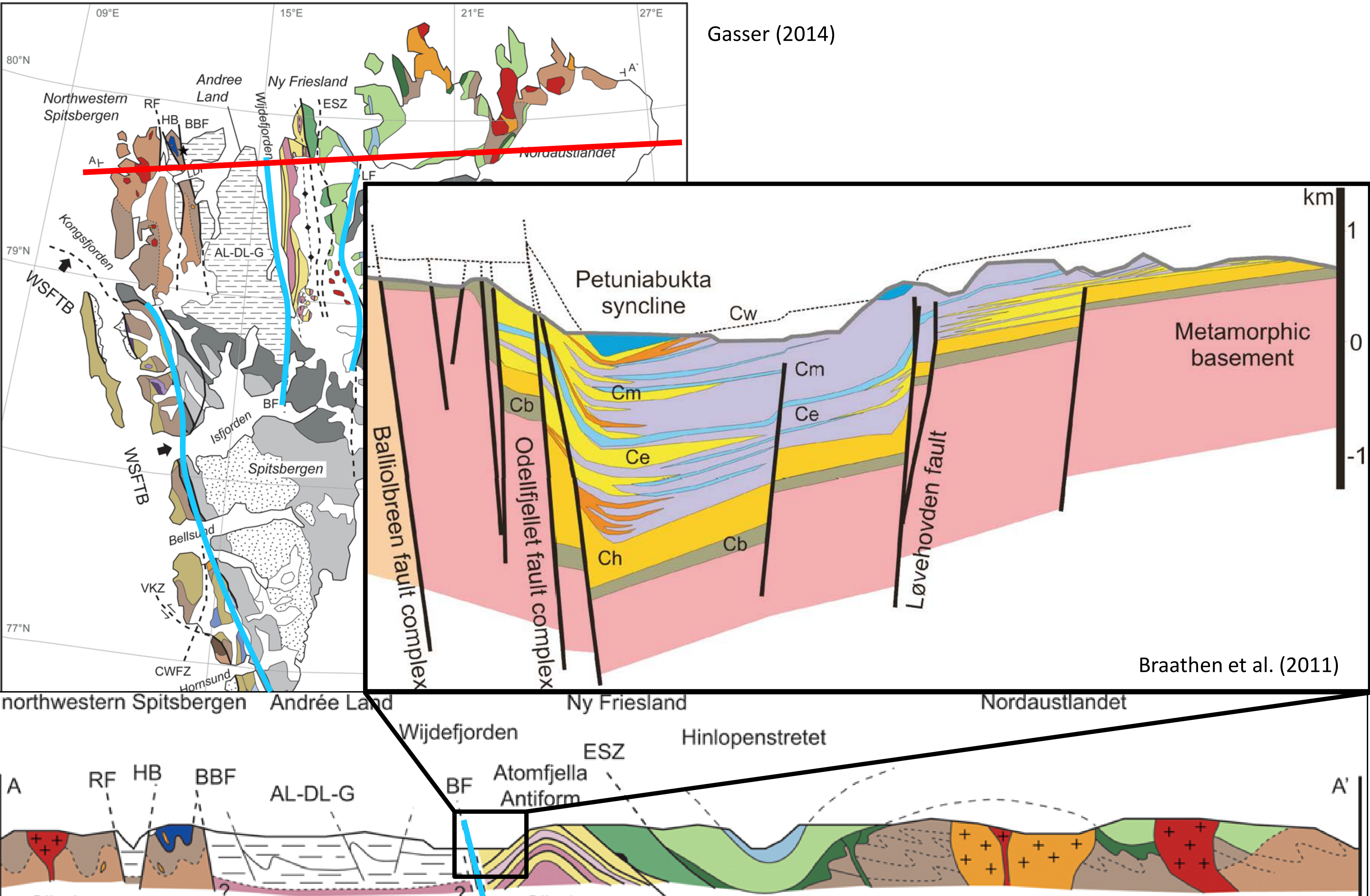

0

In the Cenozoic, opening of the Labrador Sea and Baffin Bay led to transpression and the formation of the West Spitsbergen Fold-and-Thrust Belt in western Svalbard.

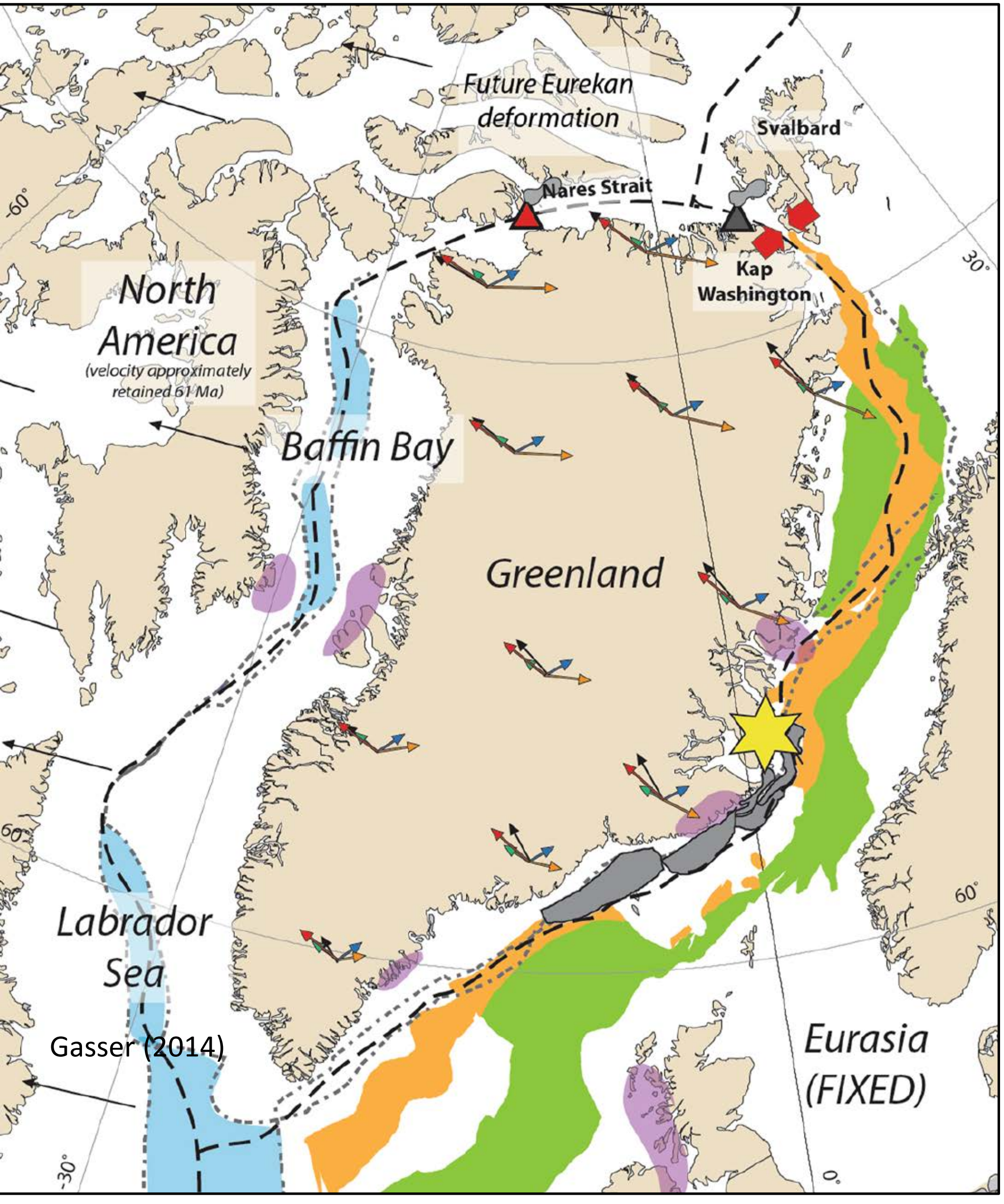

Gasser (2014)

0

In the Cenozoic, opening of the Labrador Sea and Baffin Bay led to transpression and the formation of the West Spitsbergen Fold-and-Thrust Belt in western Svalbard.

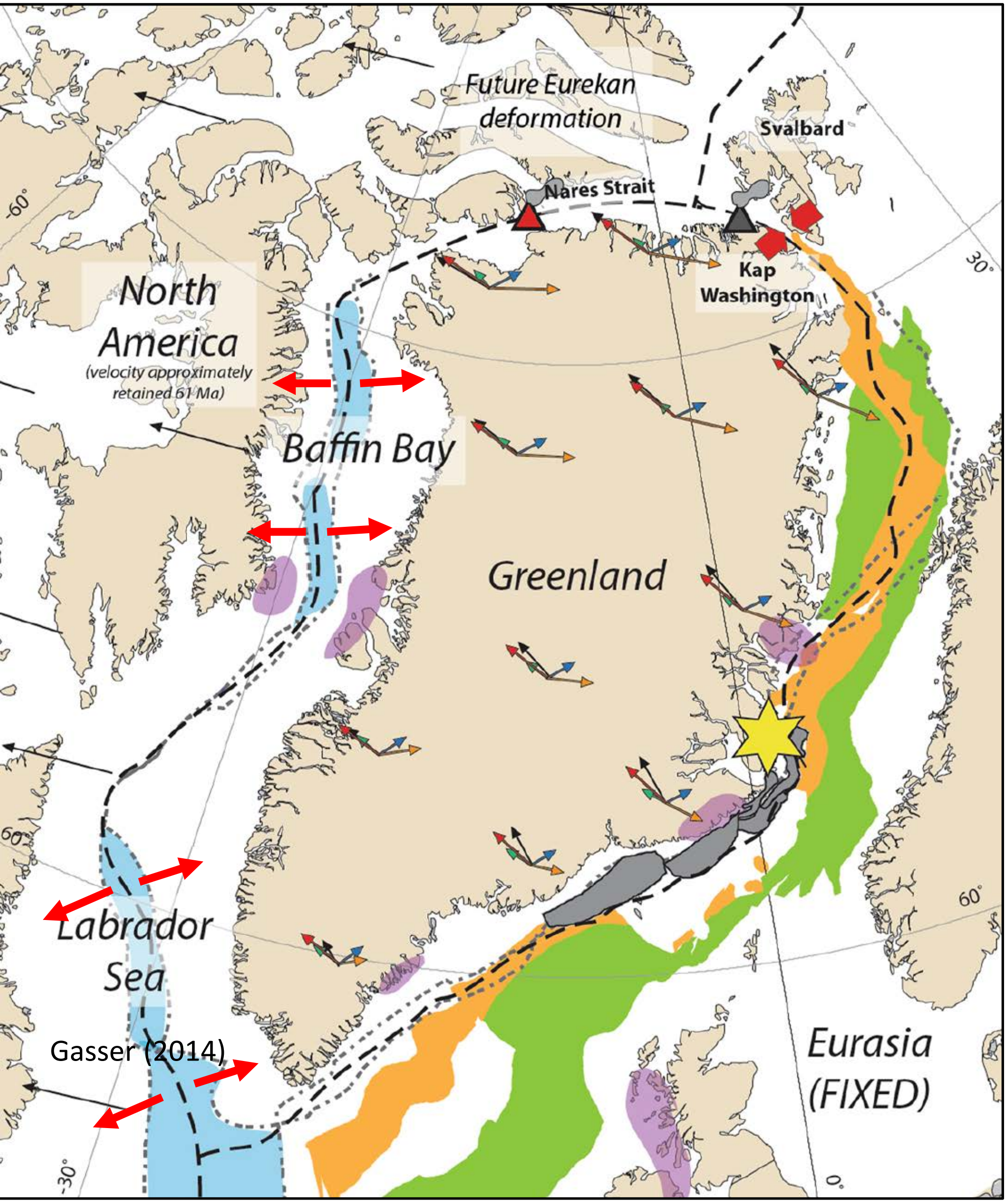

0

In the Cenozoic, opening of the Labrador Sea and Baffin Bay led to transpression and the formation of the West Spitsbergen Fold-and-Thrust Belt in western Svalbard.

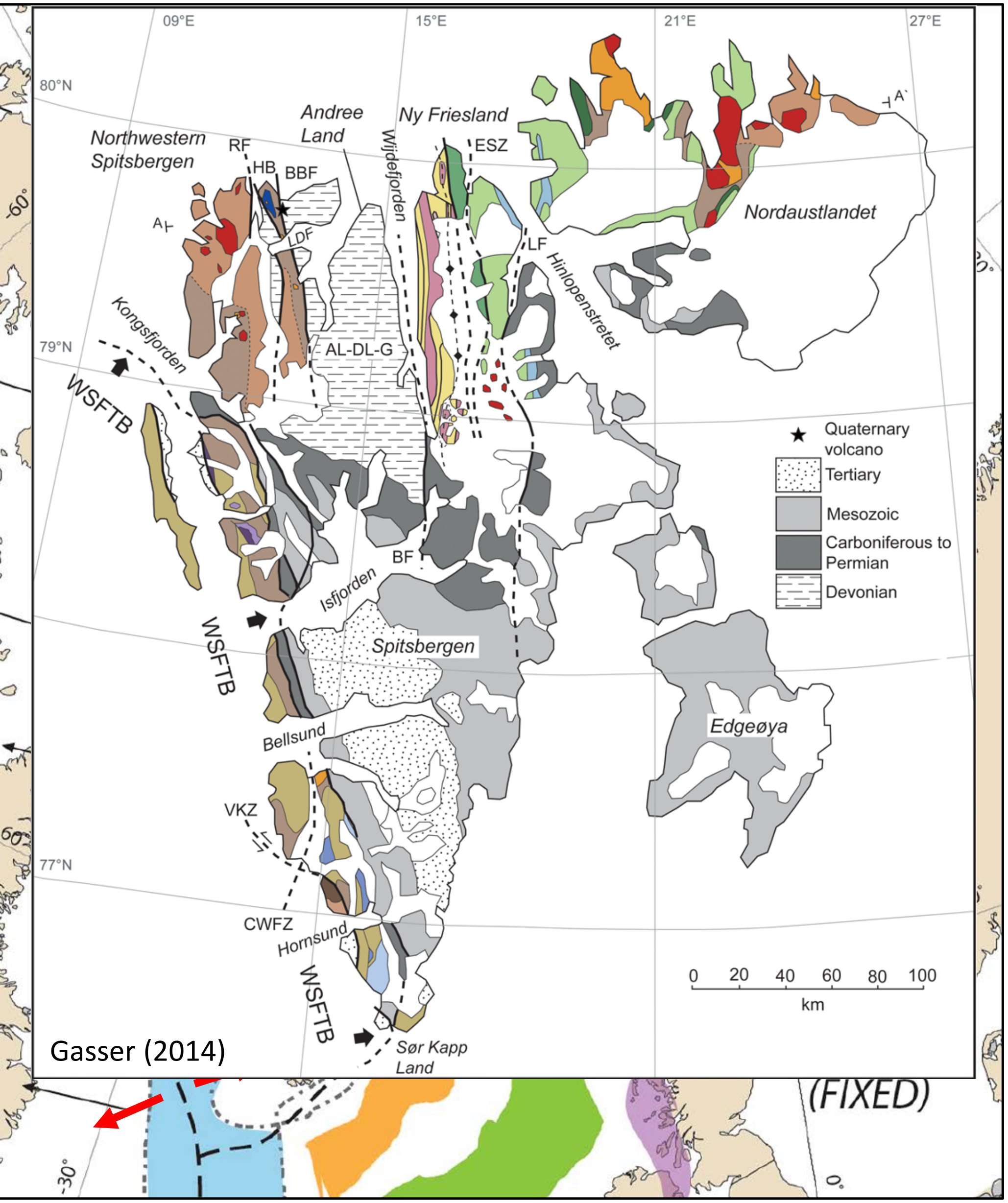

In the Cenozoic, opening of the Labrador Sea and Baffin Bay led to transpression and the formation of the West Spitsbergen Fold-and-Thrust Belt in western Svalbard.

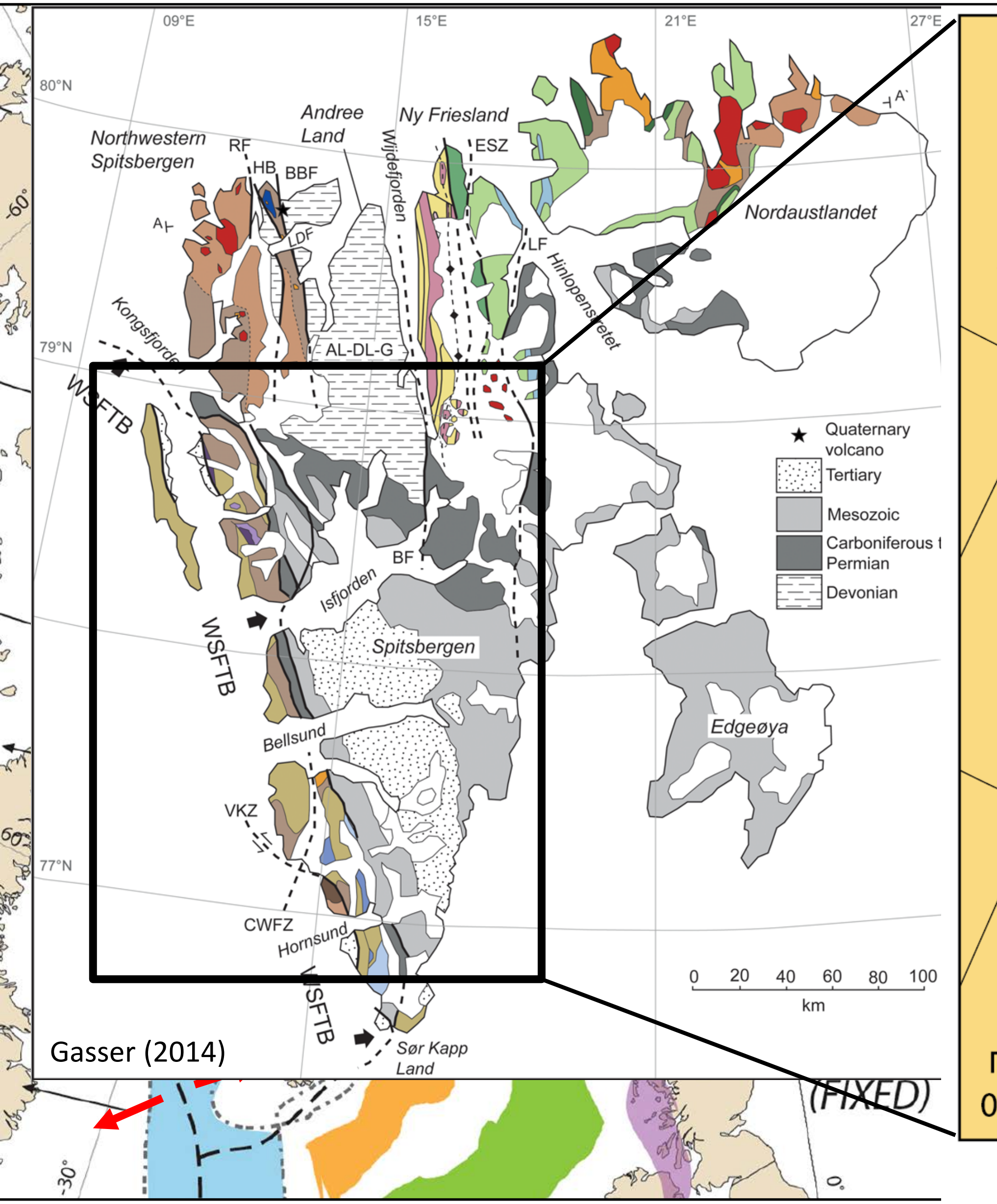

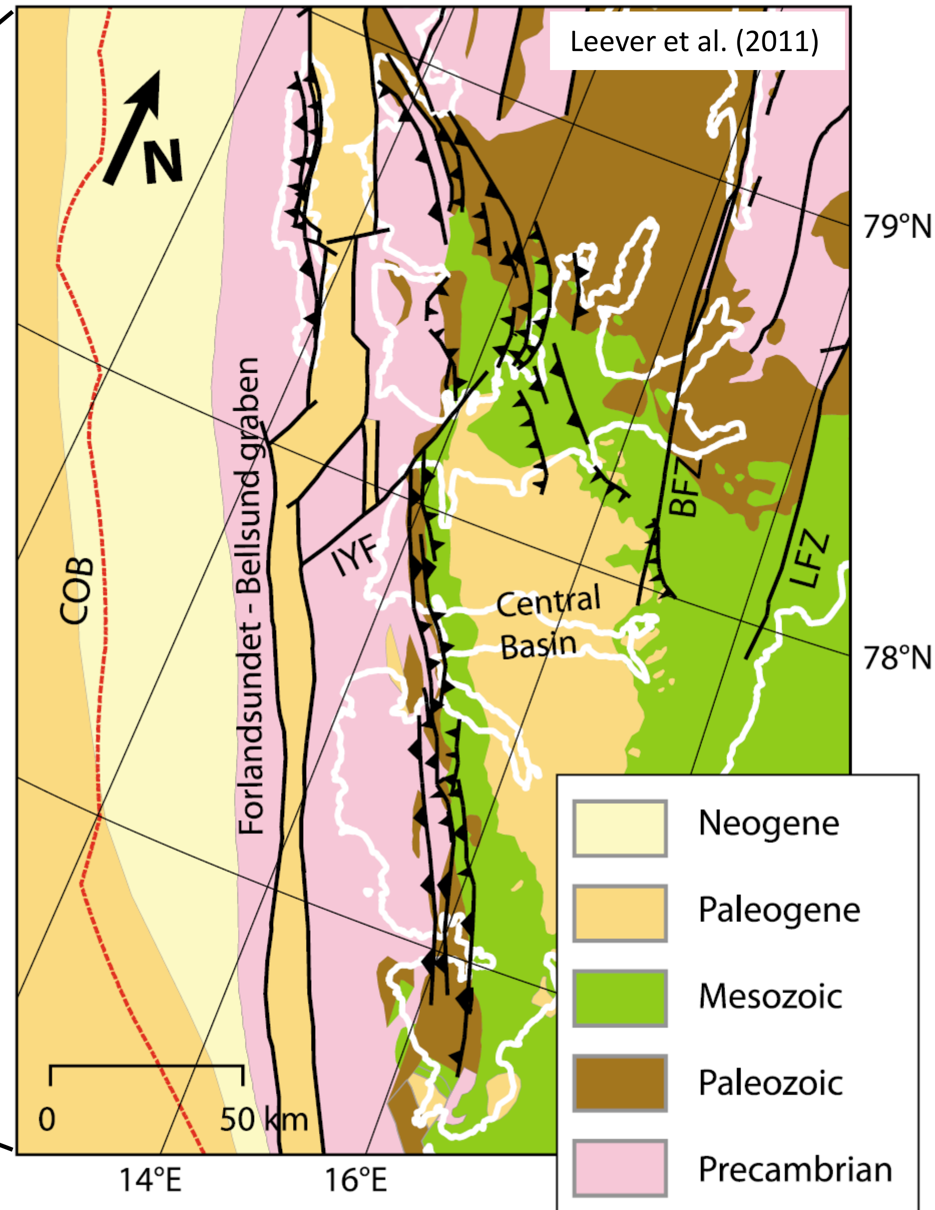

0

Subsequent Cenozoic extension led to the opening of the North Atlantic Ocean and movement of Svalbard c. 400 km to the south along dextral fault zones.

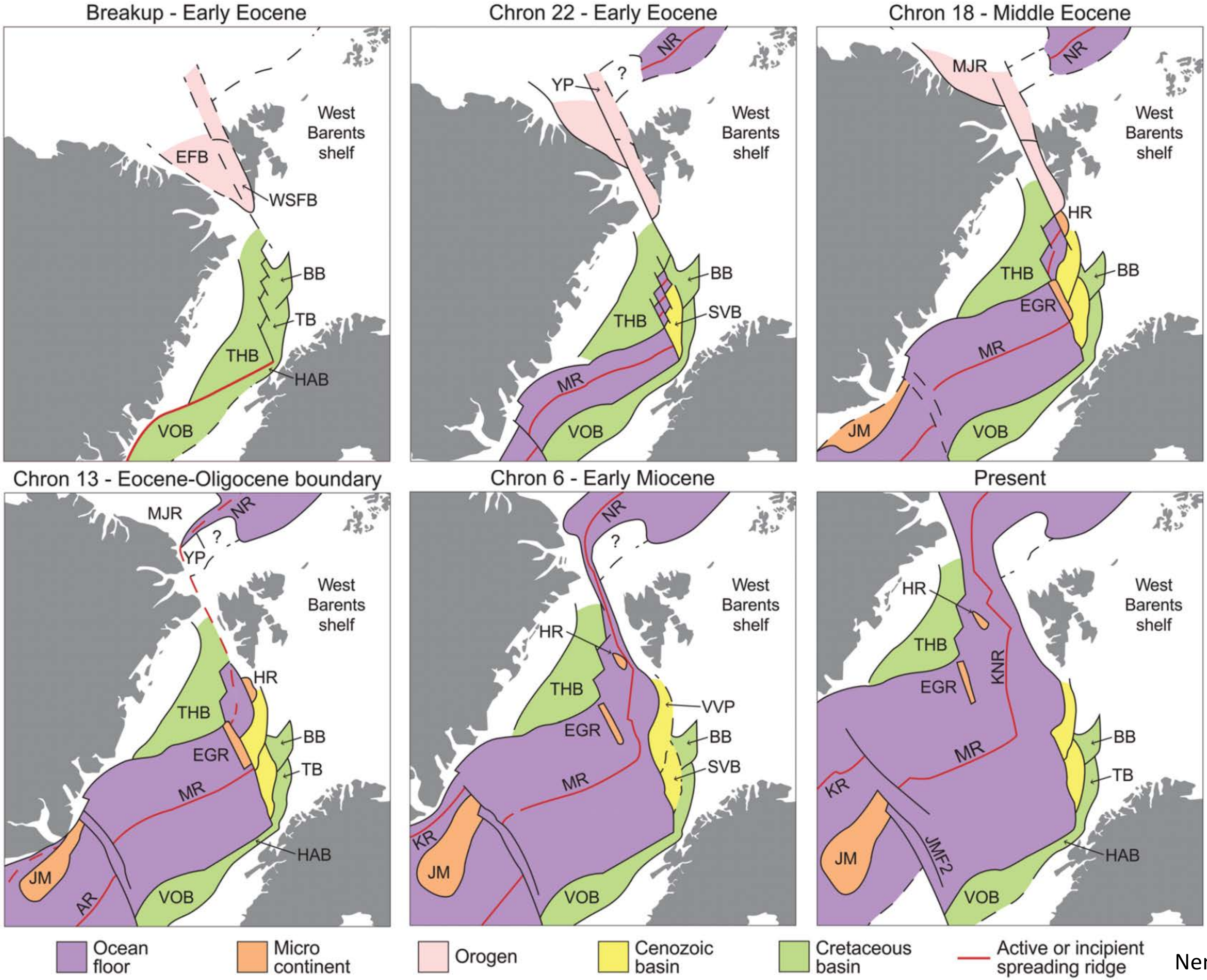

Nemcok et al. (2016)

0

Subsequent Cenozoic extension led to the opening of the North Atlantic Ocean and movement of Svalbard c. 400 km to the south along dextral fault zones.

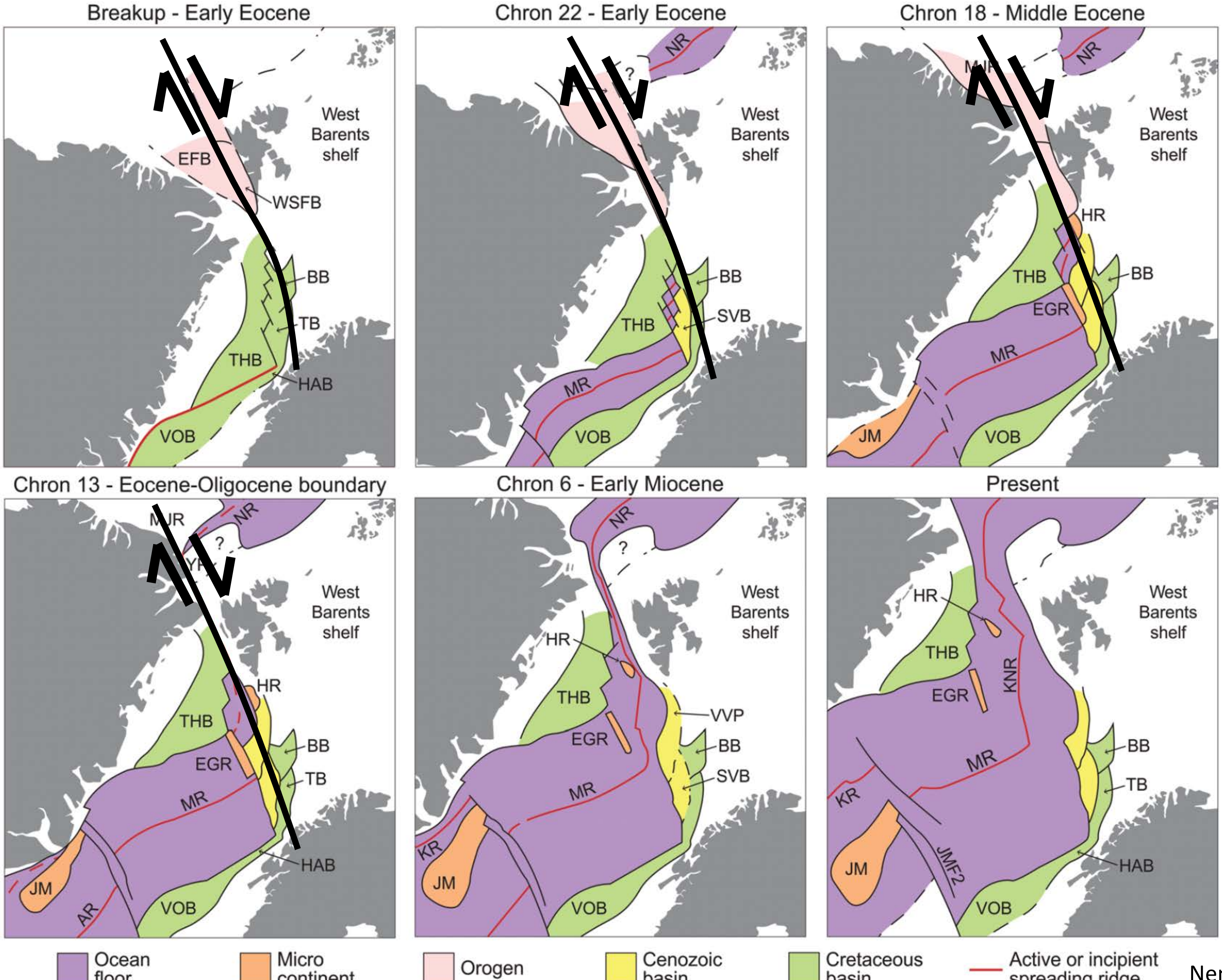

Nemcok et al. (2016)

0

Subsequent Cenozoic extension led to the opening of the North Atlantic Ocean and movement of Svalbard c. 400 km to the south along dextral fault zones.

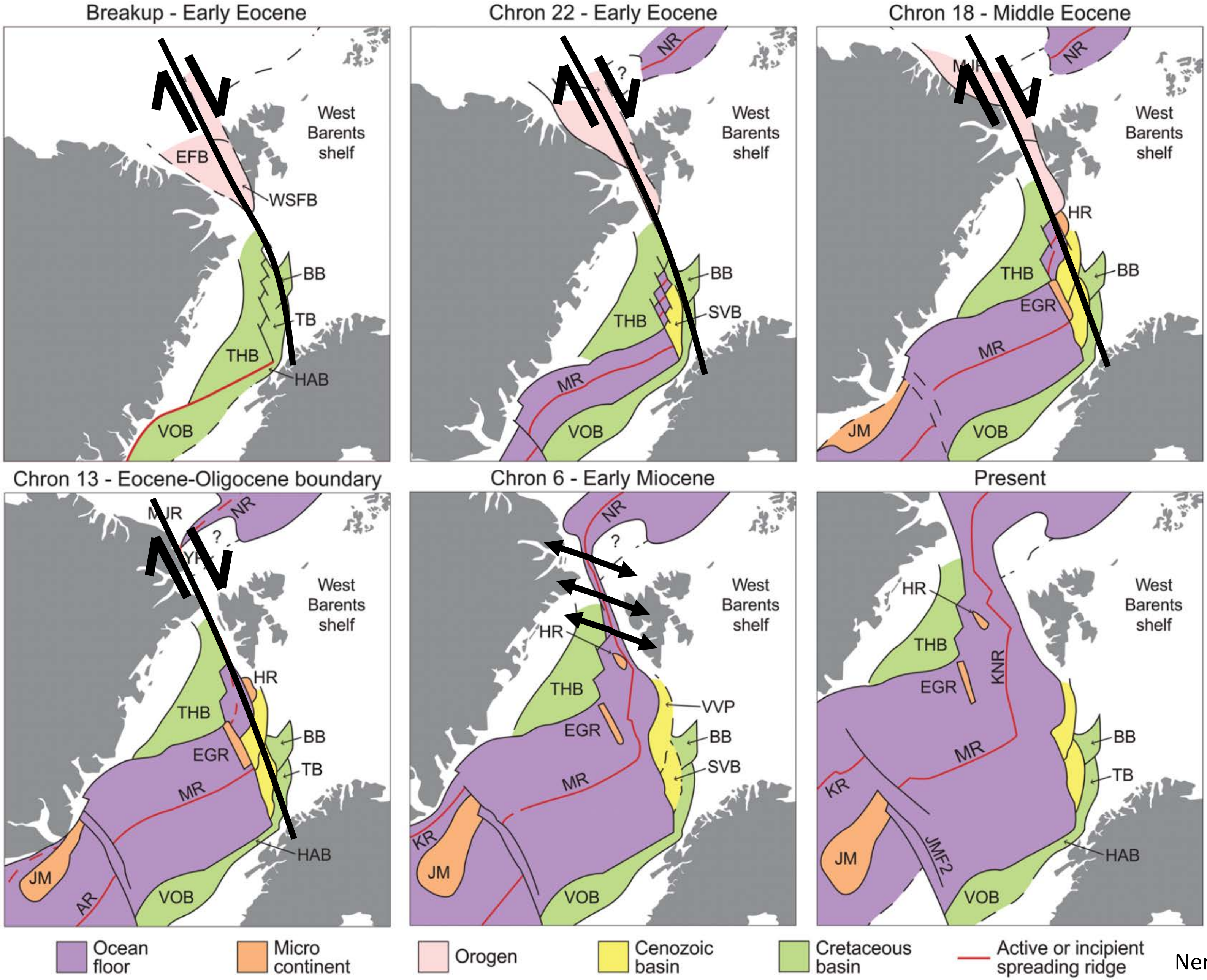

Nemcok et al. (2016)

1 **A major N–S-trending basement ridge in Isfjorden may represent the southwards continuation of the Bockfjorden Anticline core complex.**

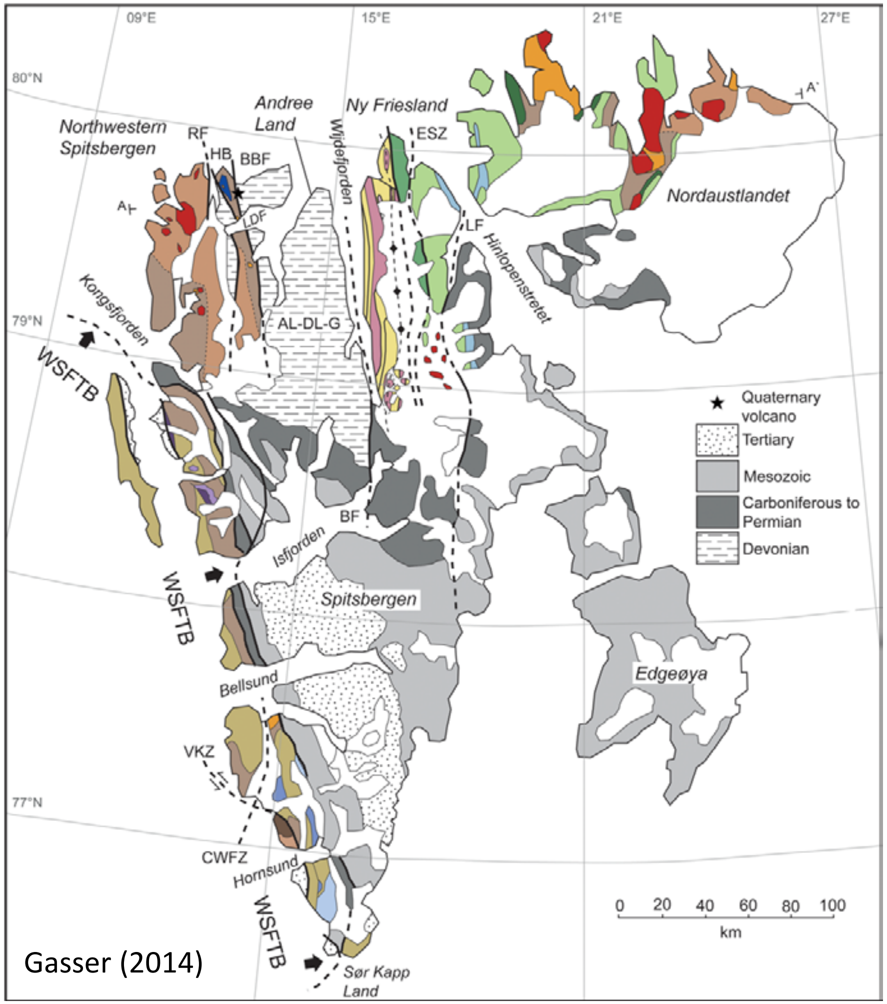

Gasser (2014)

1

A major N–S-trending basement ridge in Isfjorden may represent the southwards continuation of the Bockfjorden Anticline core complex.

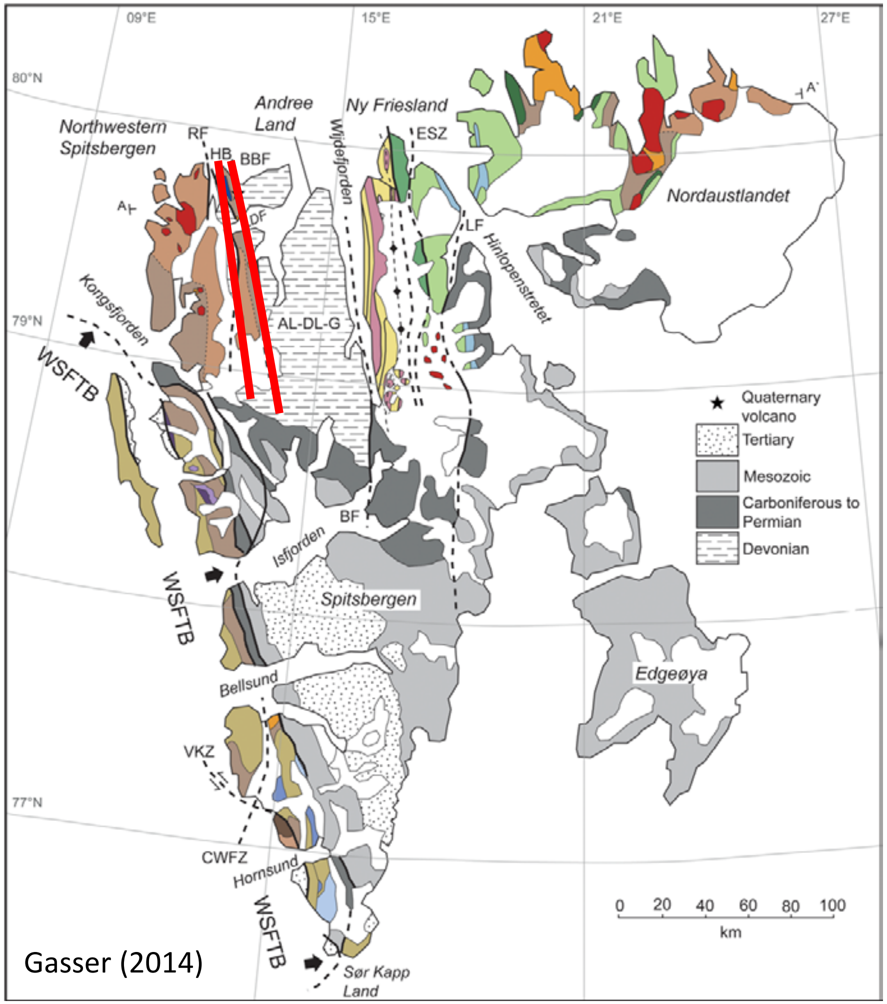

1

A major N–S-trending basement ridge in Isfjorden may represent the southwards continuation of the Bockfjorden Anticline core complex.

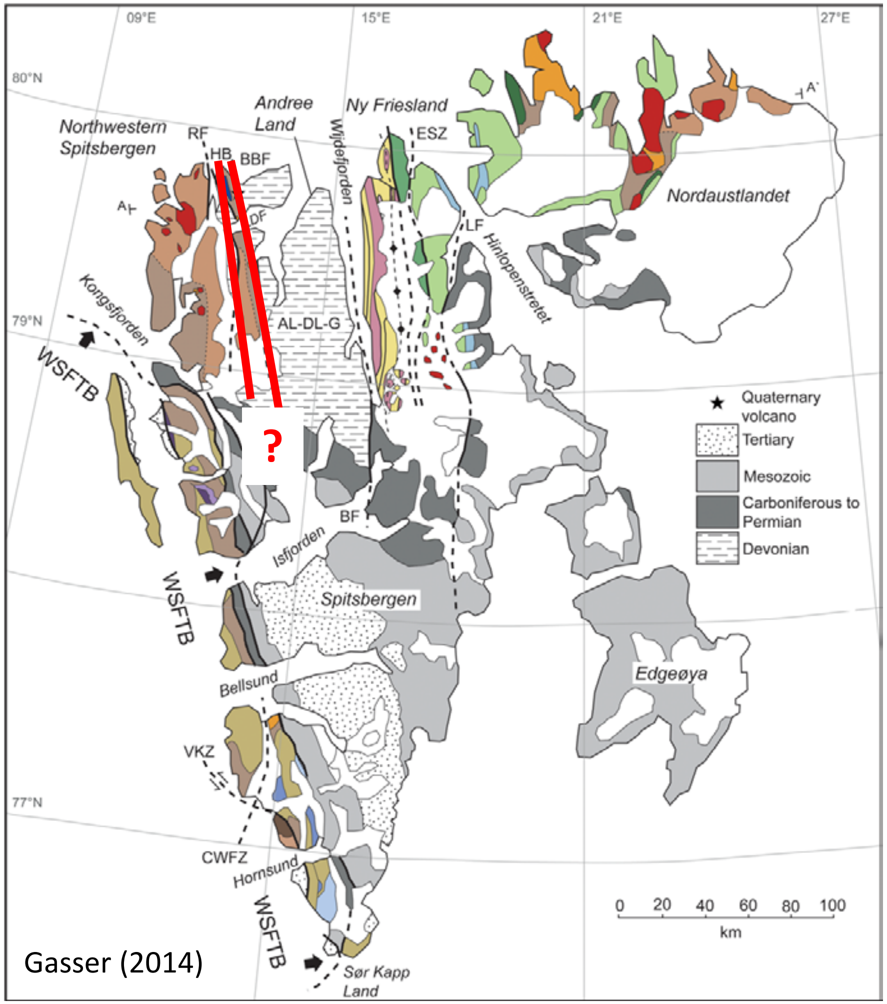

1

A major N–S-trending basement ridge in Isfjorden may represent the southwards continuation of the Bockfjorden Anticline core complex.

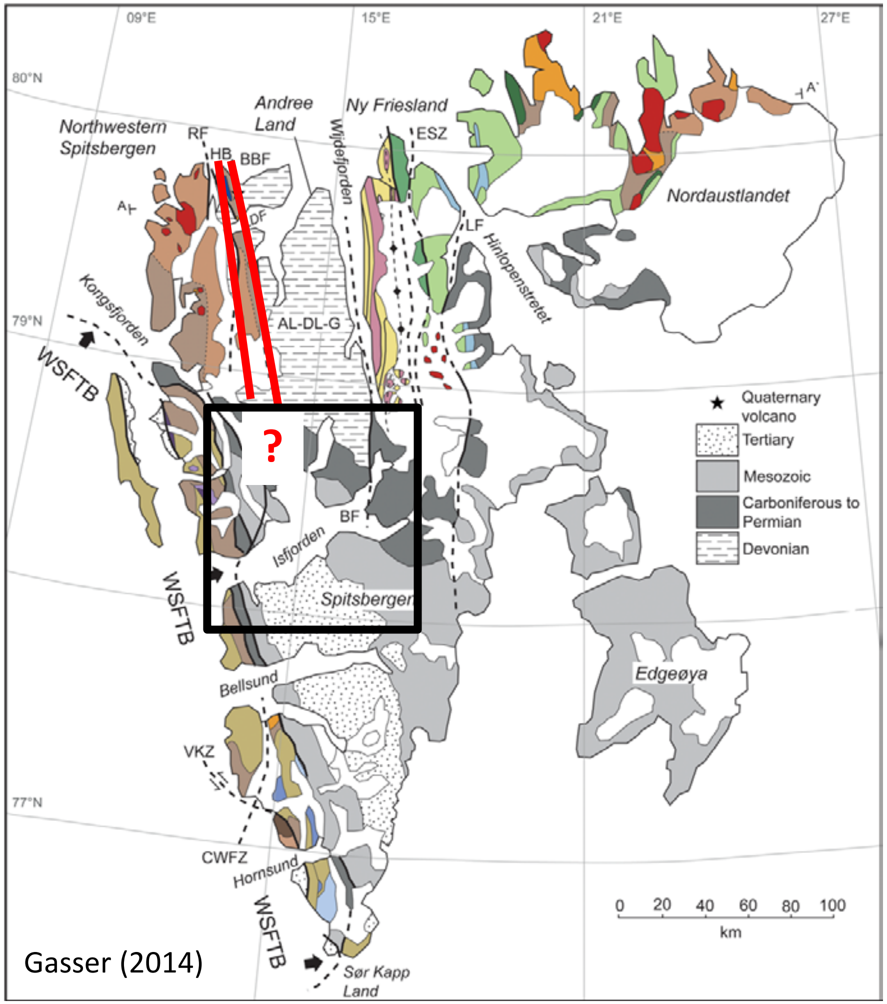

1 A major N–S-trending basement ridge in Isfjorden may represent the southwards continuation of the Bockfjorden Anticline core complex.

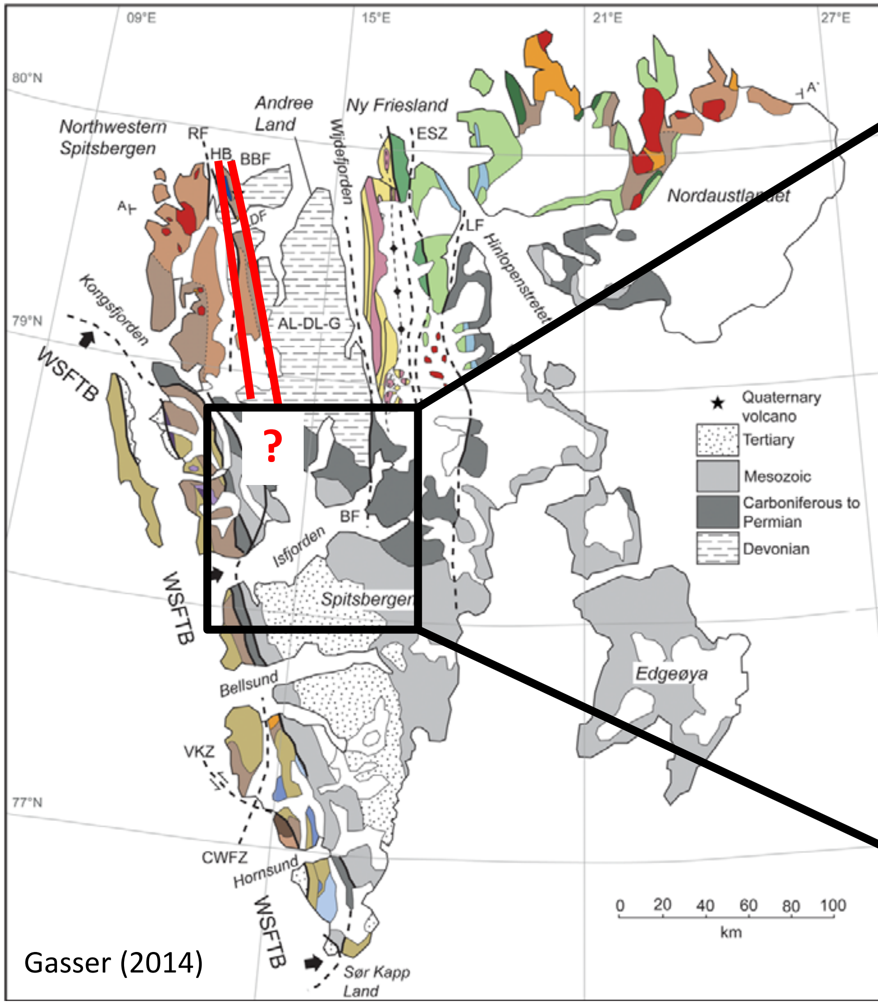

Gasser (2014)

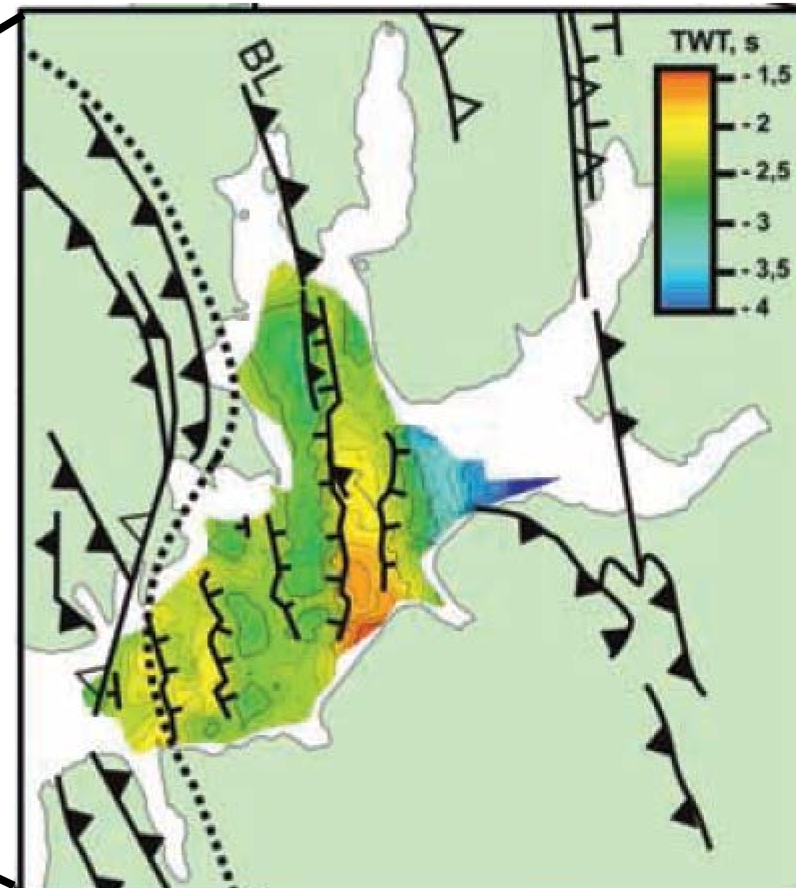

Blinova et al. (2013)

1

A major N–S-trending basement ridge in Isfjorden may represent the southwards continuation of the Bockfjorden Anticline core complex.

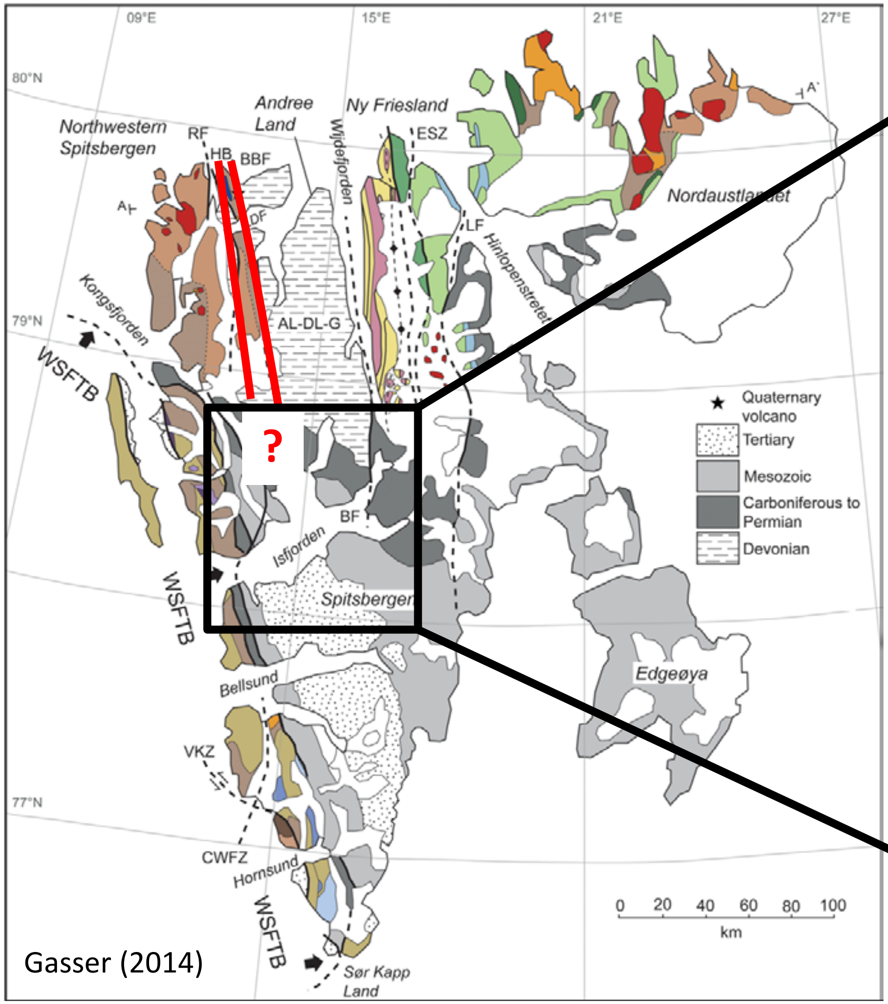

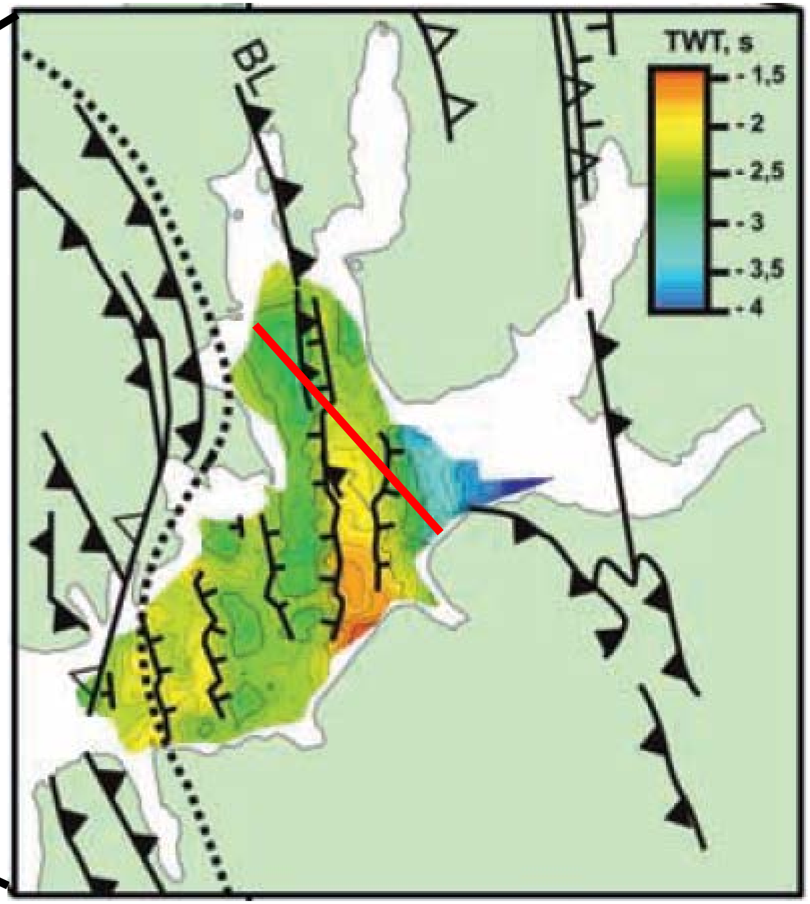

Blinova et al. (2013)

1 **In Isfjorden, lens-shaped reflections may represent incisement processes commonly related to core complex exhumation.**

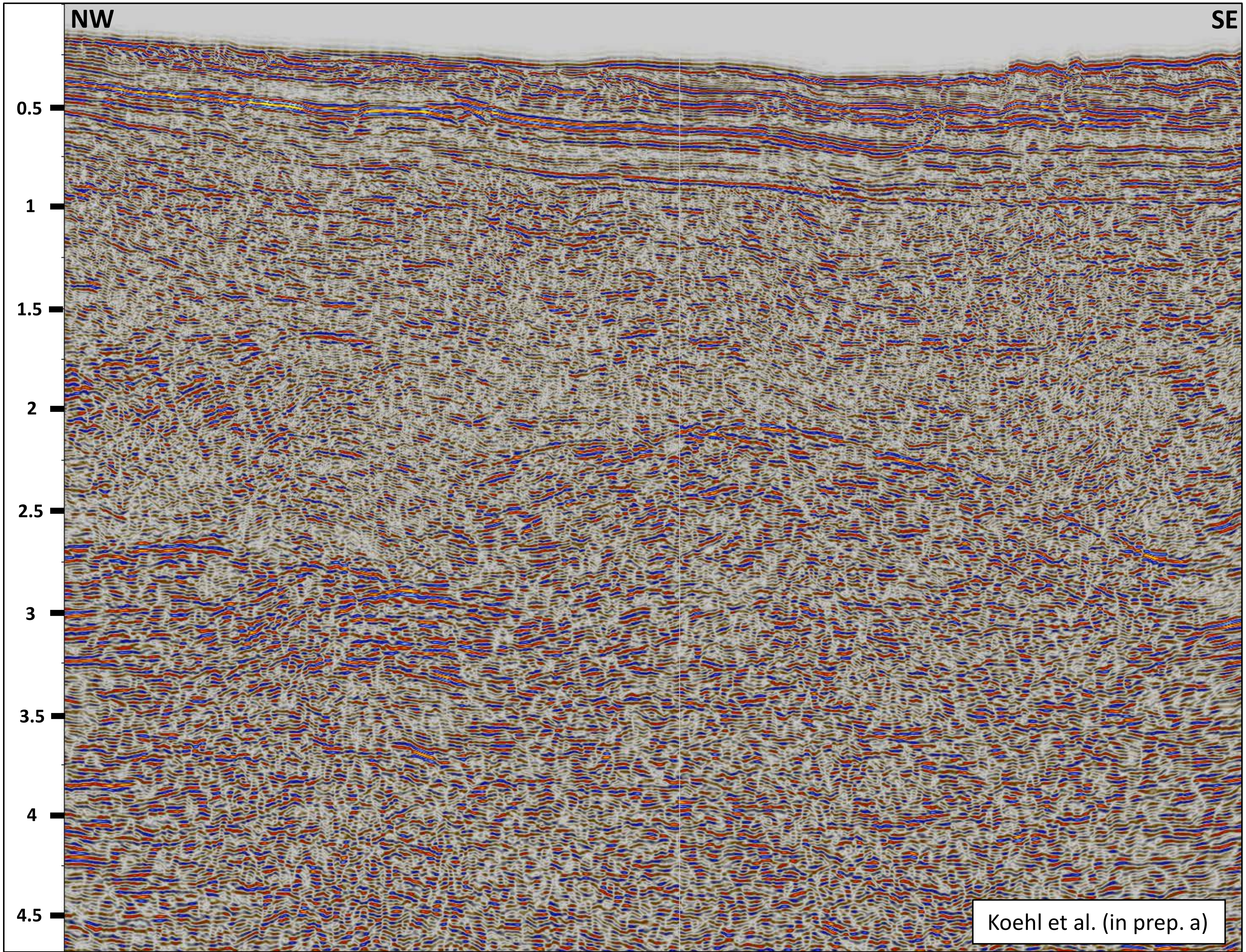

1

In Isfjorden, lens-shaped reflections may represent incisement processes commonly related to core complex exhumation.

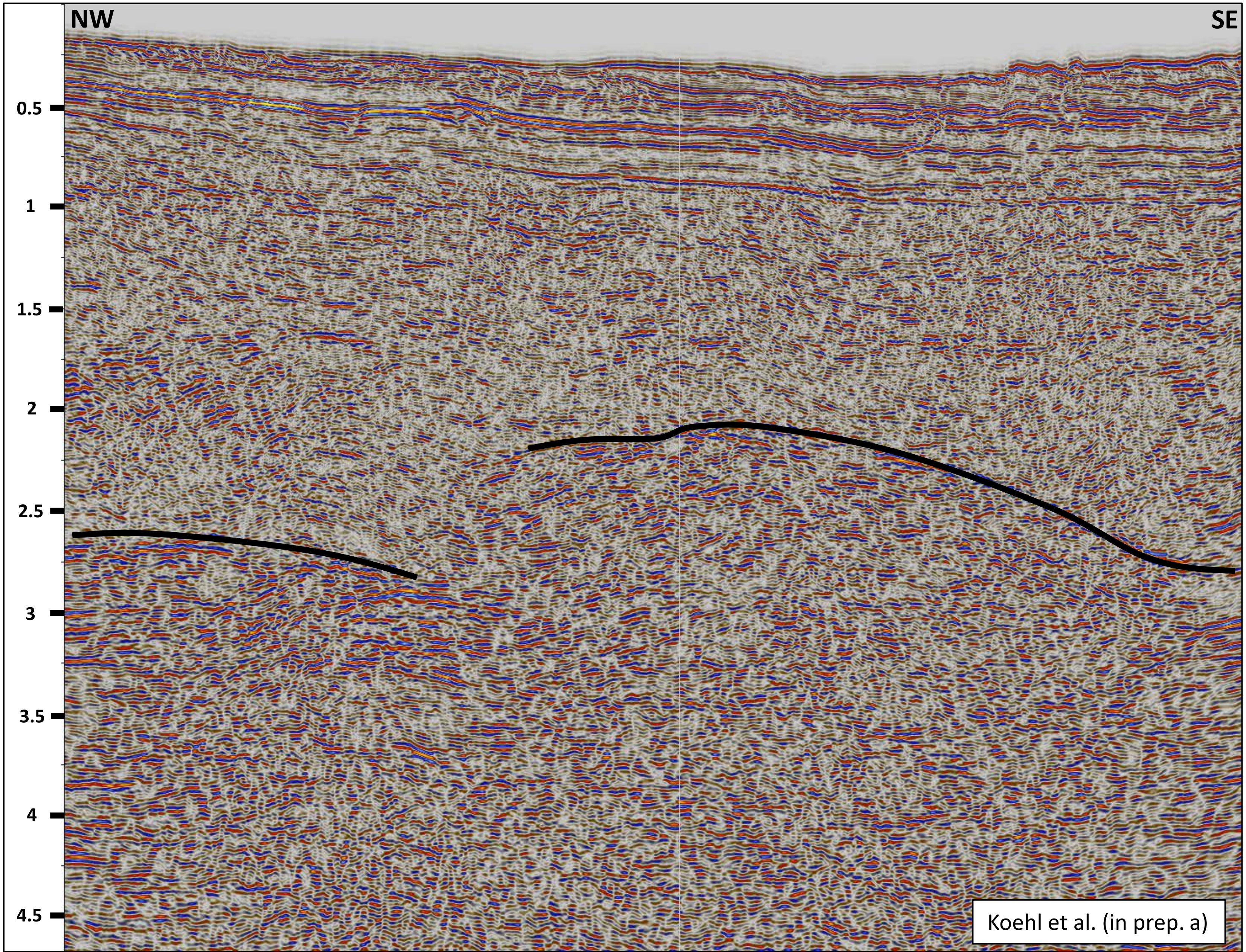

1 **In Isfjorden, lens-shaped reflections may represent incisement processes commonly related to core complex exhumation.**

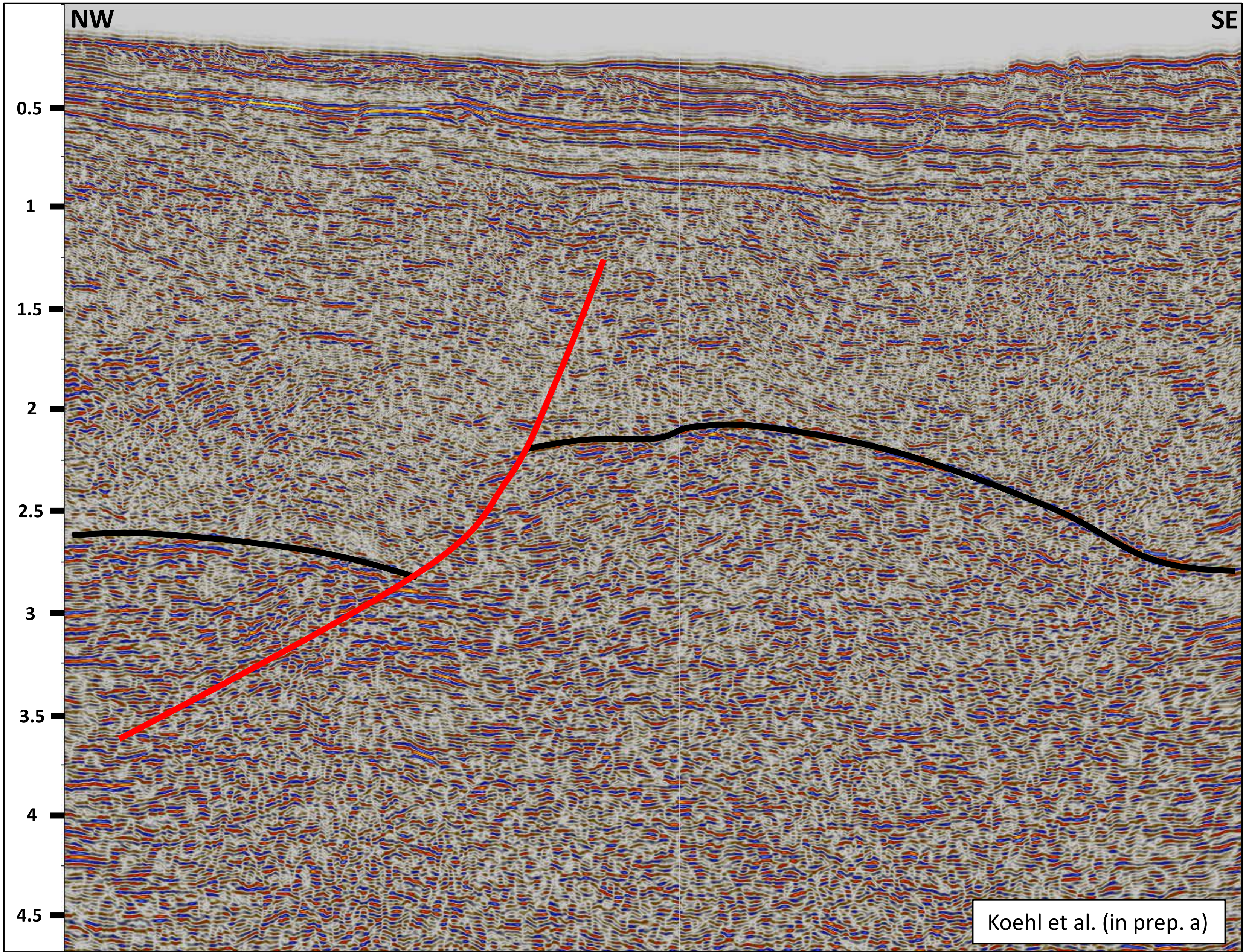

1 **In Isfjorden, lens-shaped reflections may represent incisement processes commonly related to core complex exhumation.**

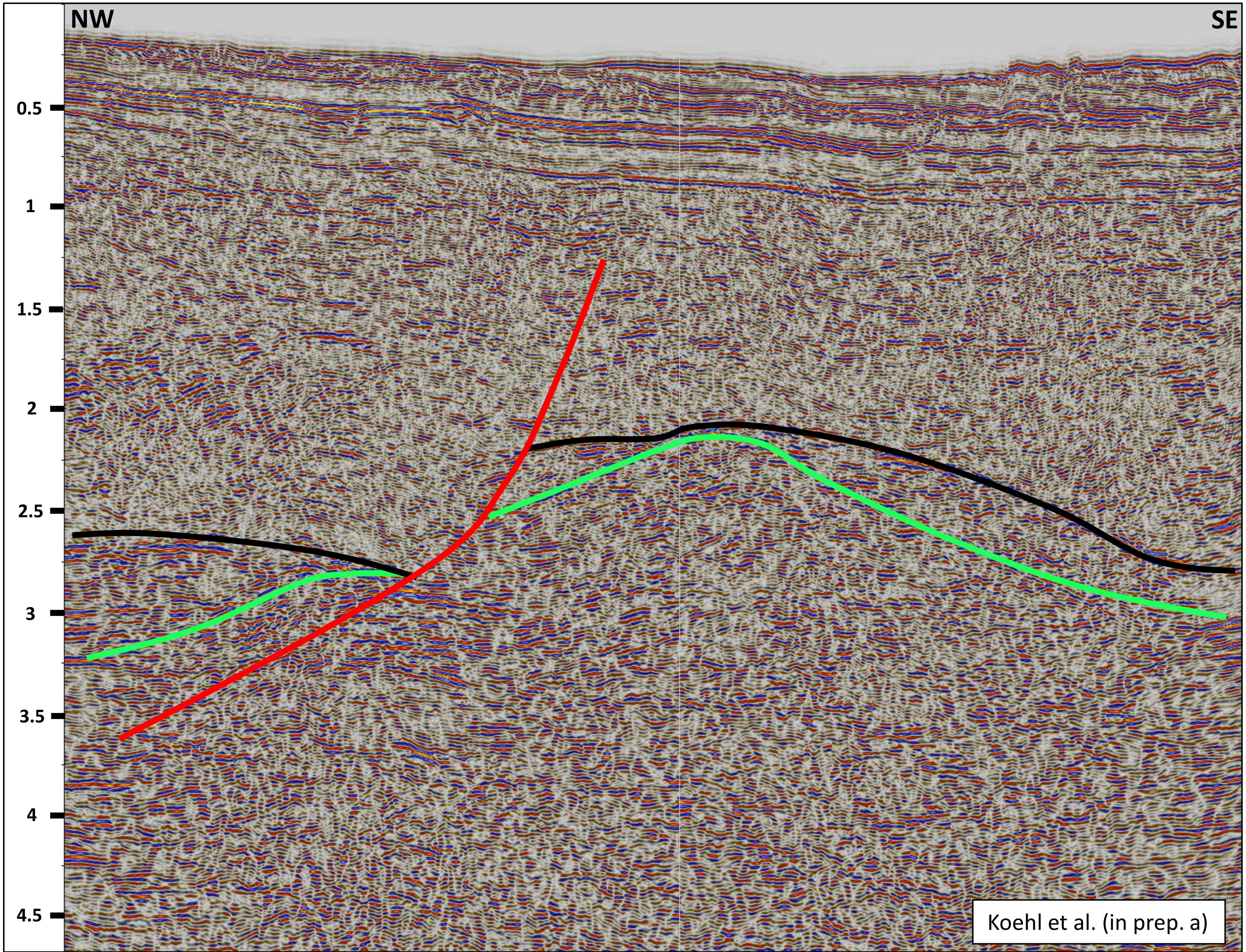

1 **In Isfjorden, lens-shaped reflections may represent incisement processes commonly related to core complex exhumation.**

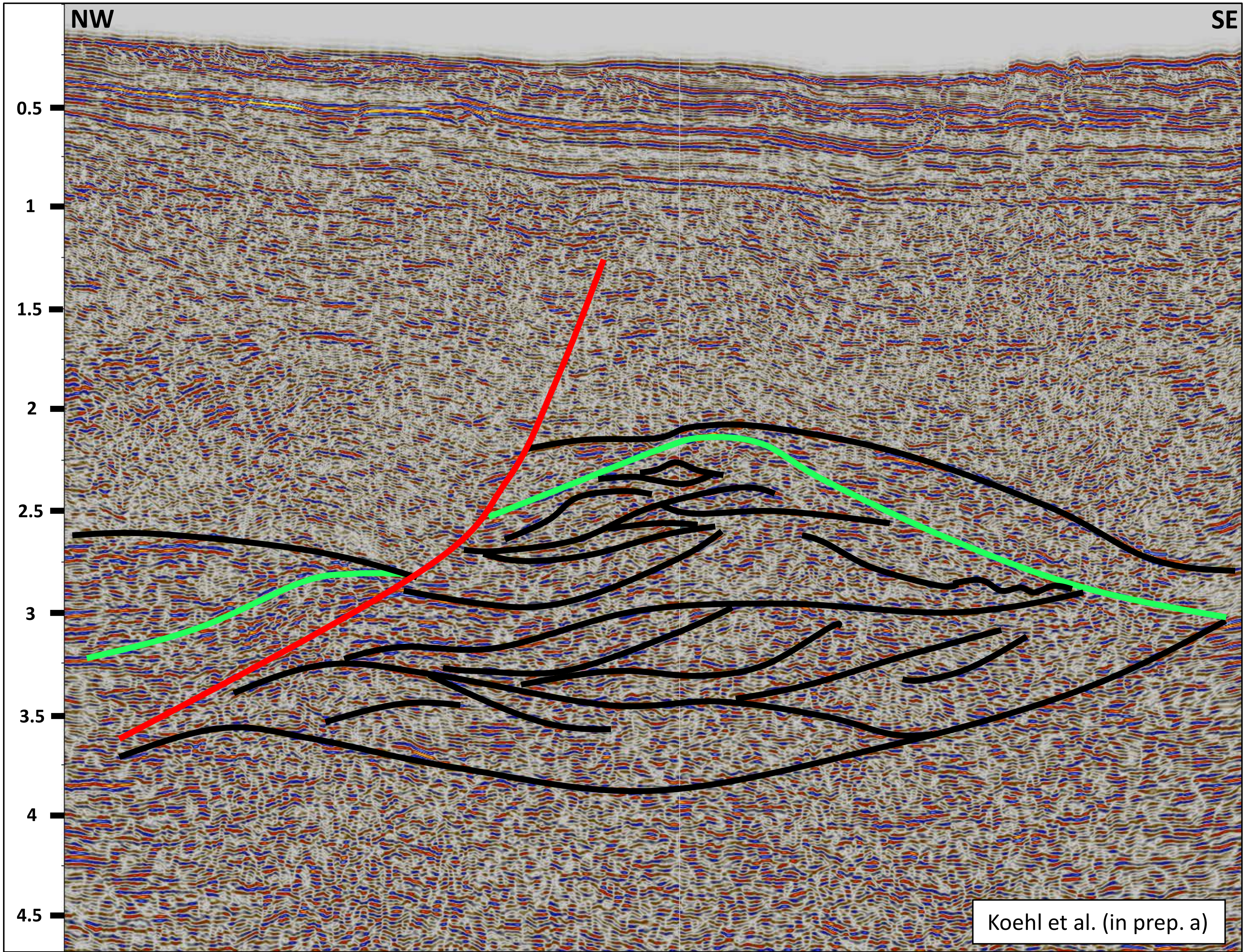

1

In Isfjorden, lens-shaped reflections may represent incisement processes commonly related to core complex exhumation.

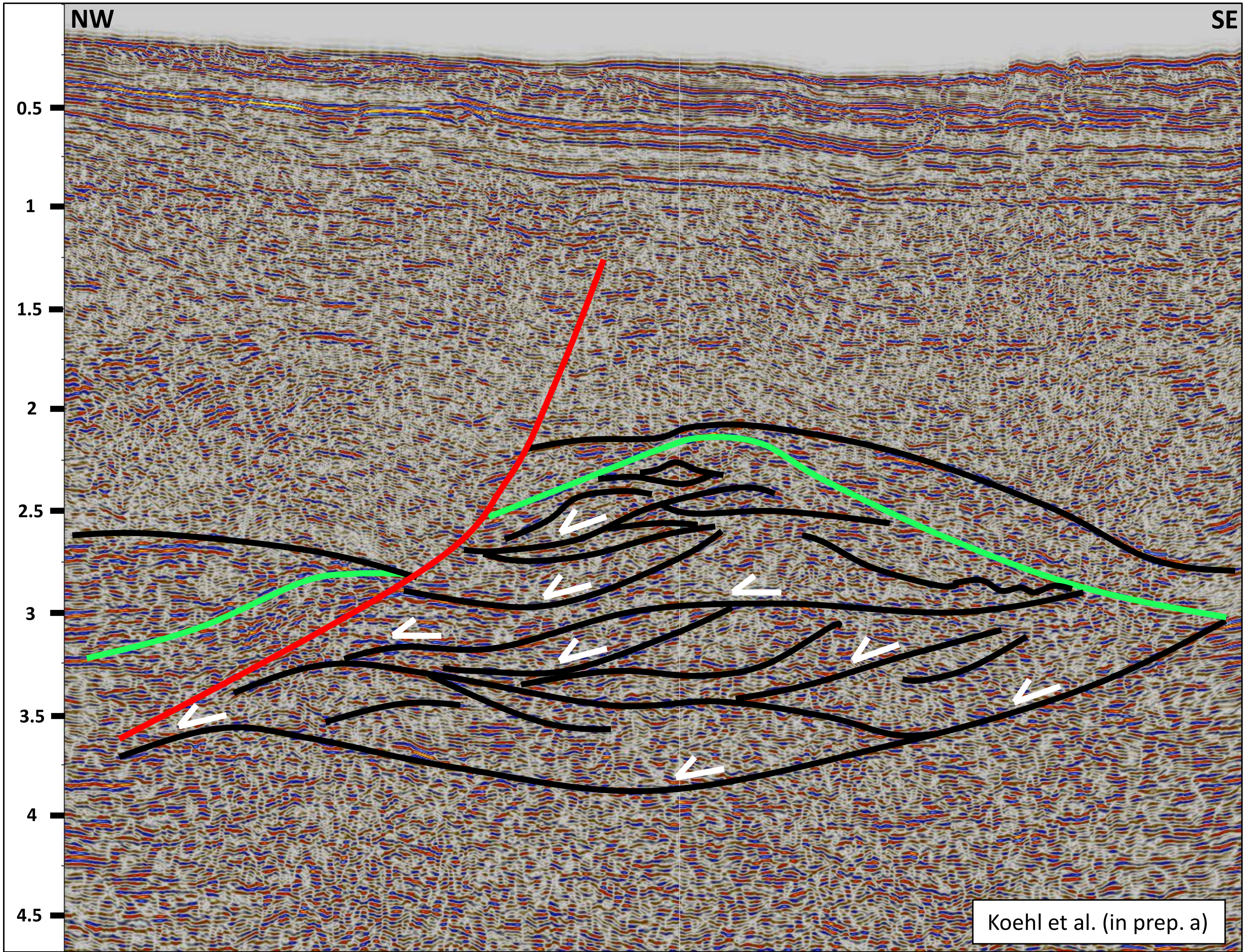

2 **The potential continuation of the Bockfjorden Anticline in Isfjorden appears offset by > 10 km left-laterally, and c. 5 km vertically down to the south.**

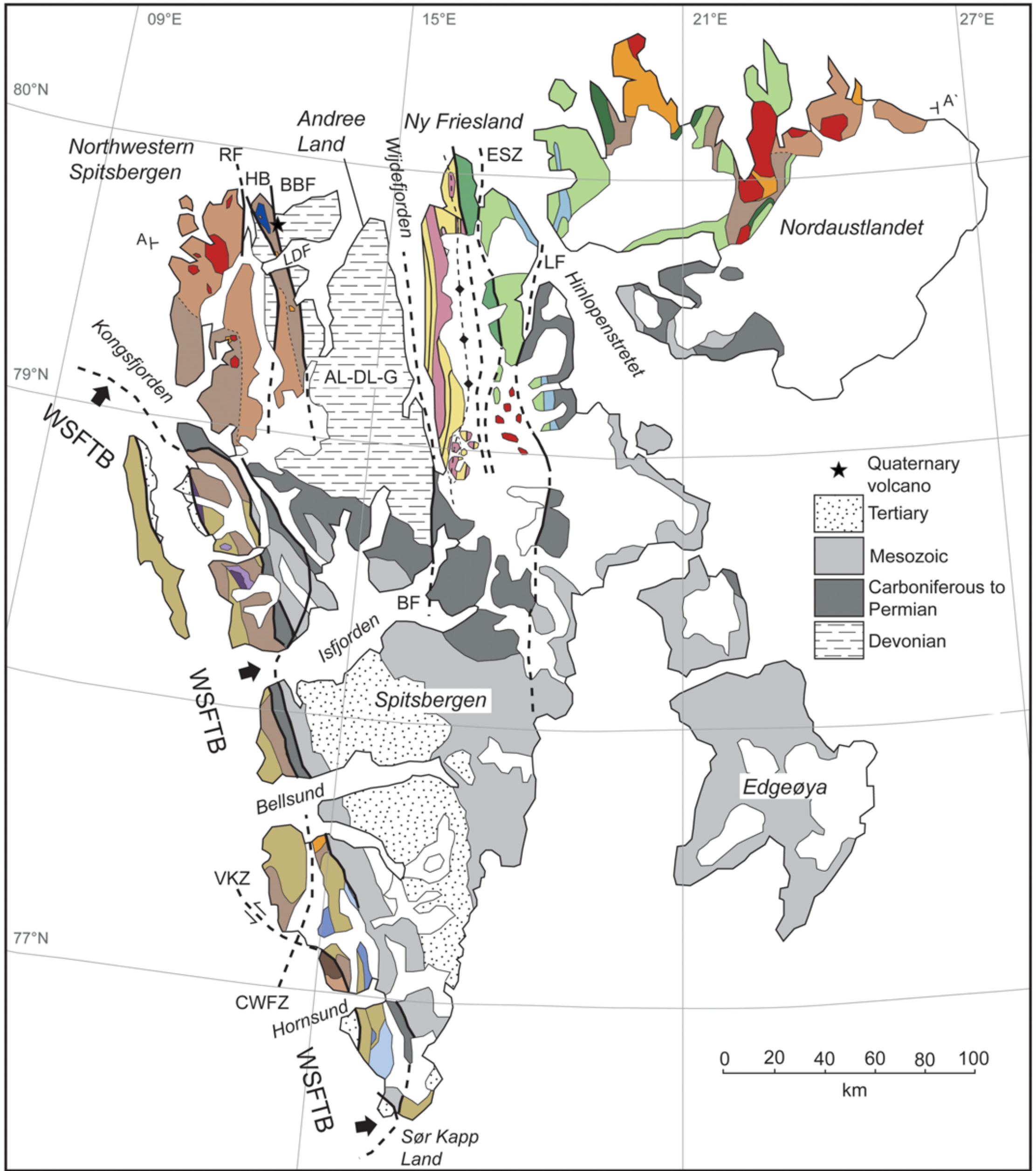

Gasser (2014)

2 **The potential continuation of the Bockfjorden Anticline in Isfjorden appears offset by > 10 km left-laterally, and c. 5 km vertically down to the south.**

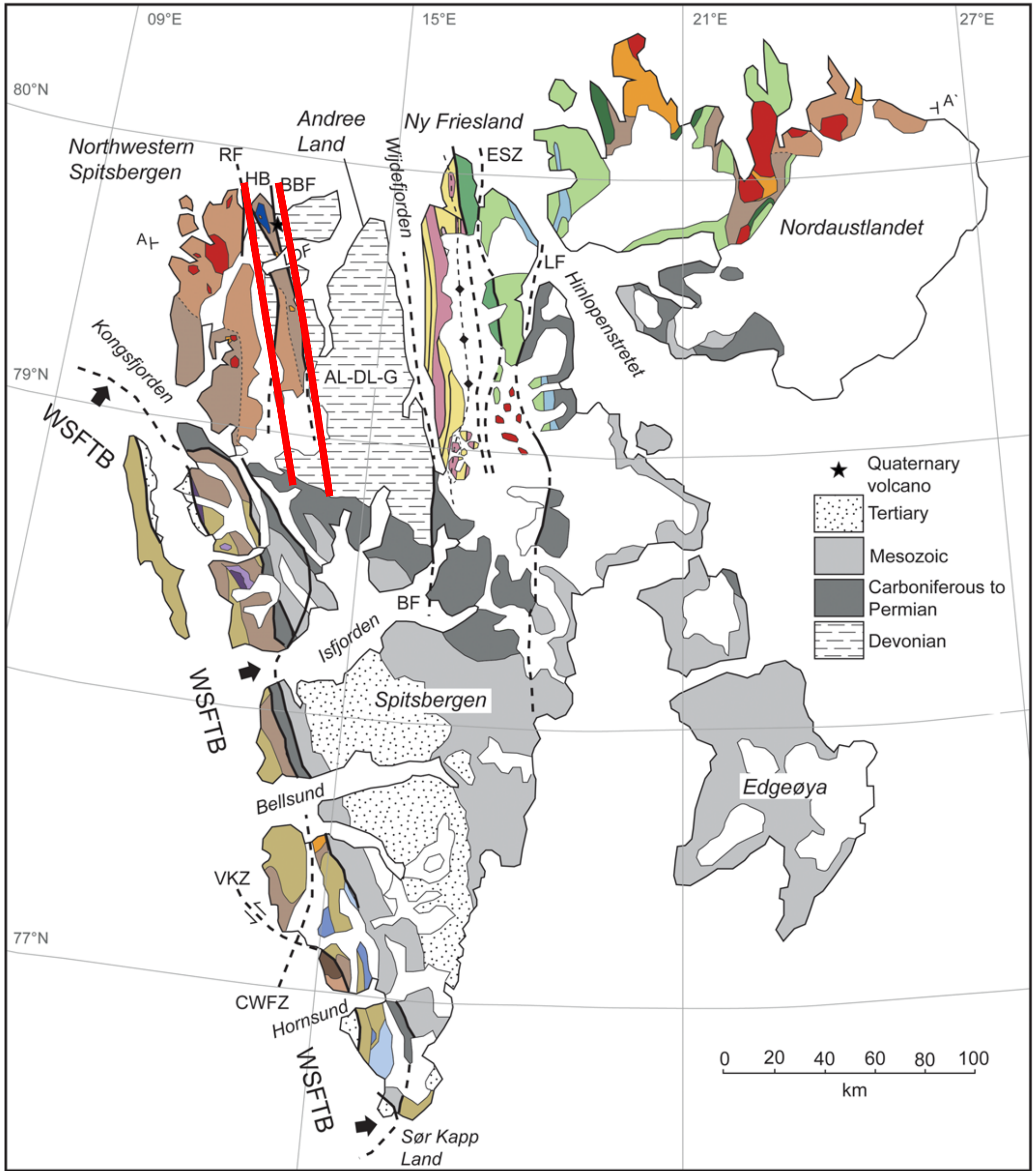

Gasser (2014)

2 **The potential continuation of the Bockfjorden Anticline in Isfjorden appears offset by > 10 km left-laterally, and c. 5 km vertically down to the south.**

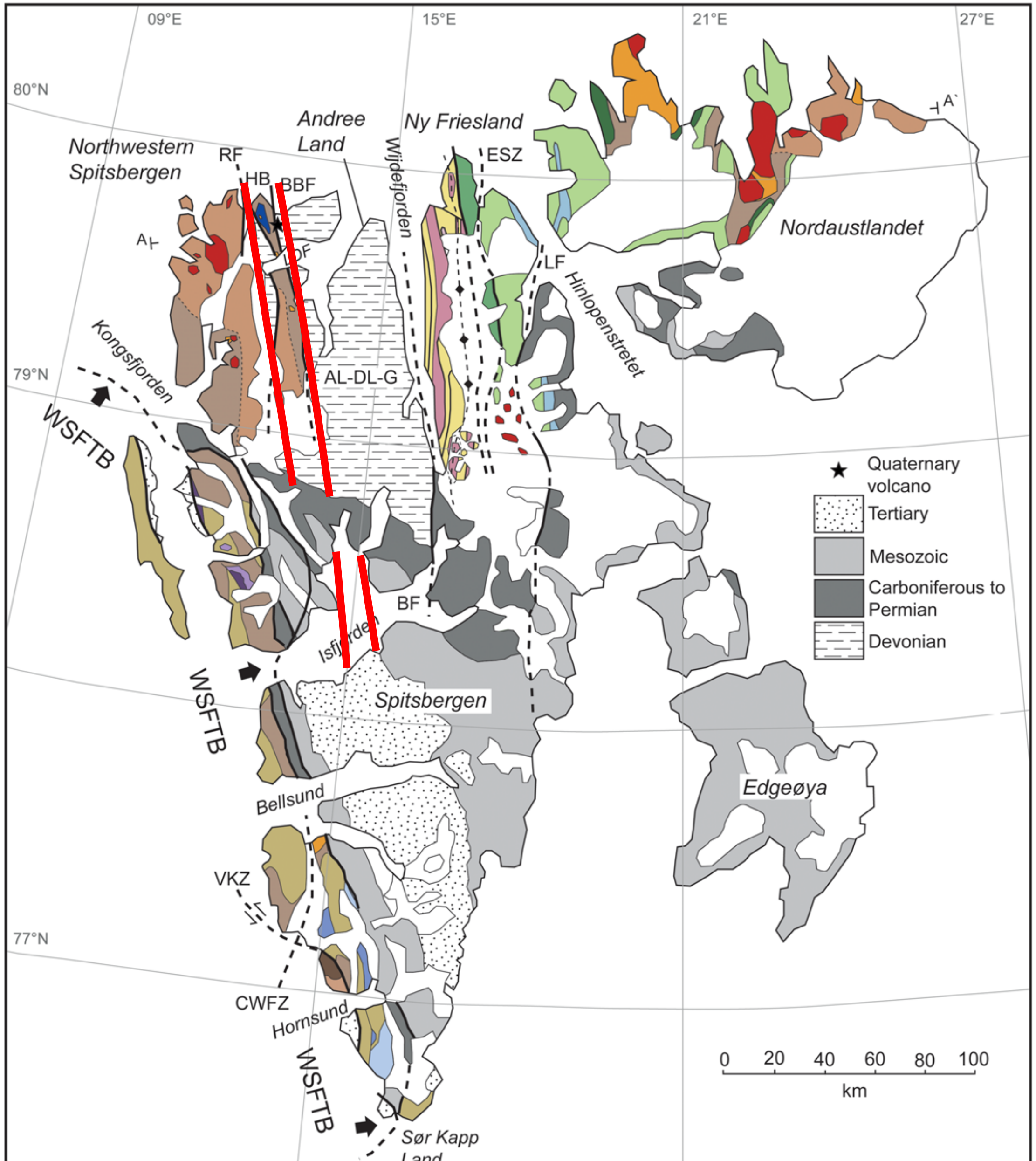

Gasser (2014)

2

The potential continuation of the Bockfjorden Anticline in Isfjorden appears offset by > 10 km left-laterally, and c. 5 km vertically down to the south.

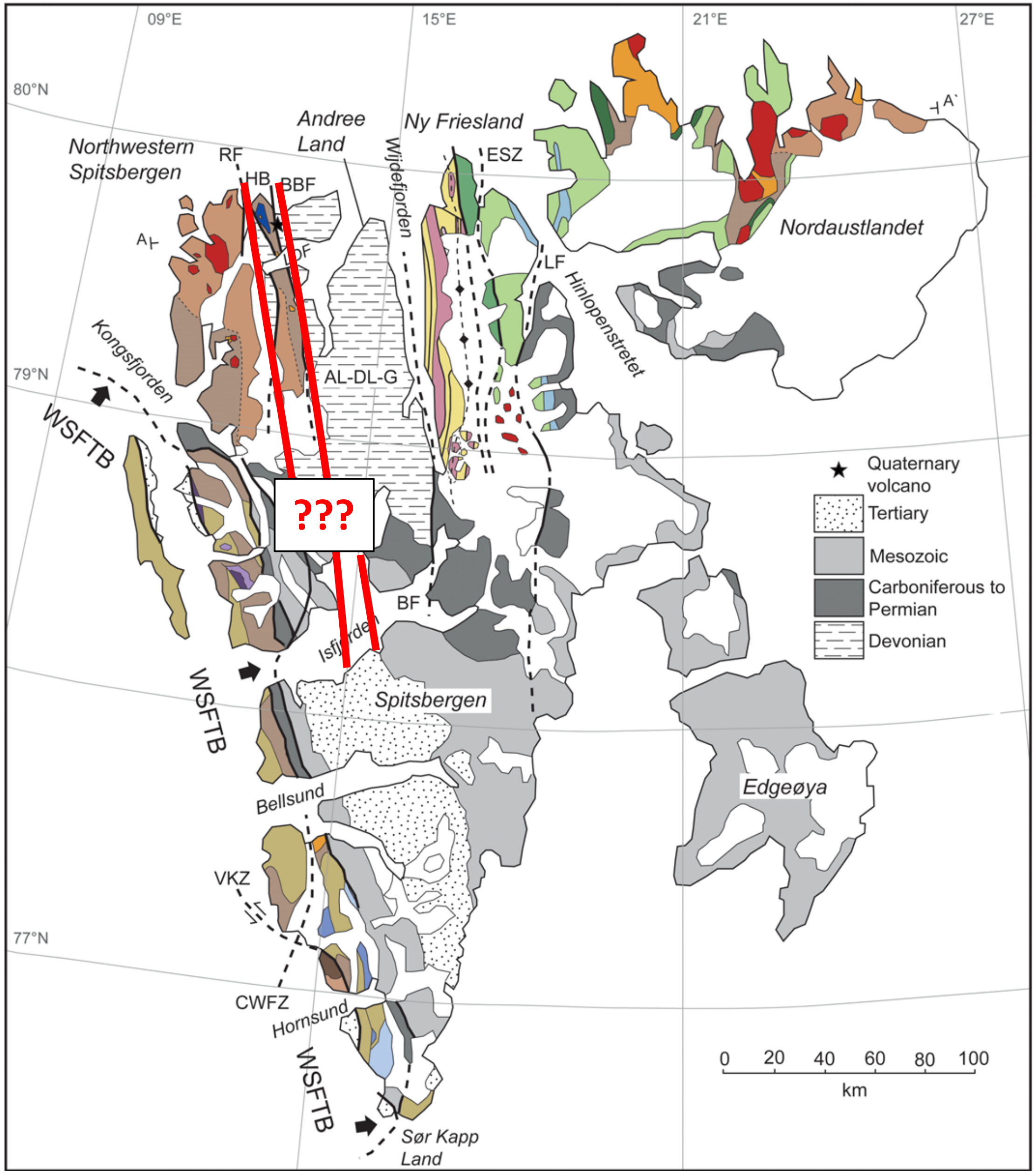

Gasser (2014)

2 **Gravimetric, aeromagnetic and seismic data in the Barents Sea show the existence of potentially inverted WNW–ESE- to NW–SE-striking Timamian thrusts.**

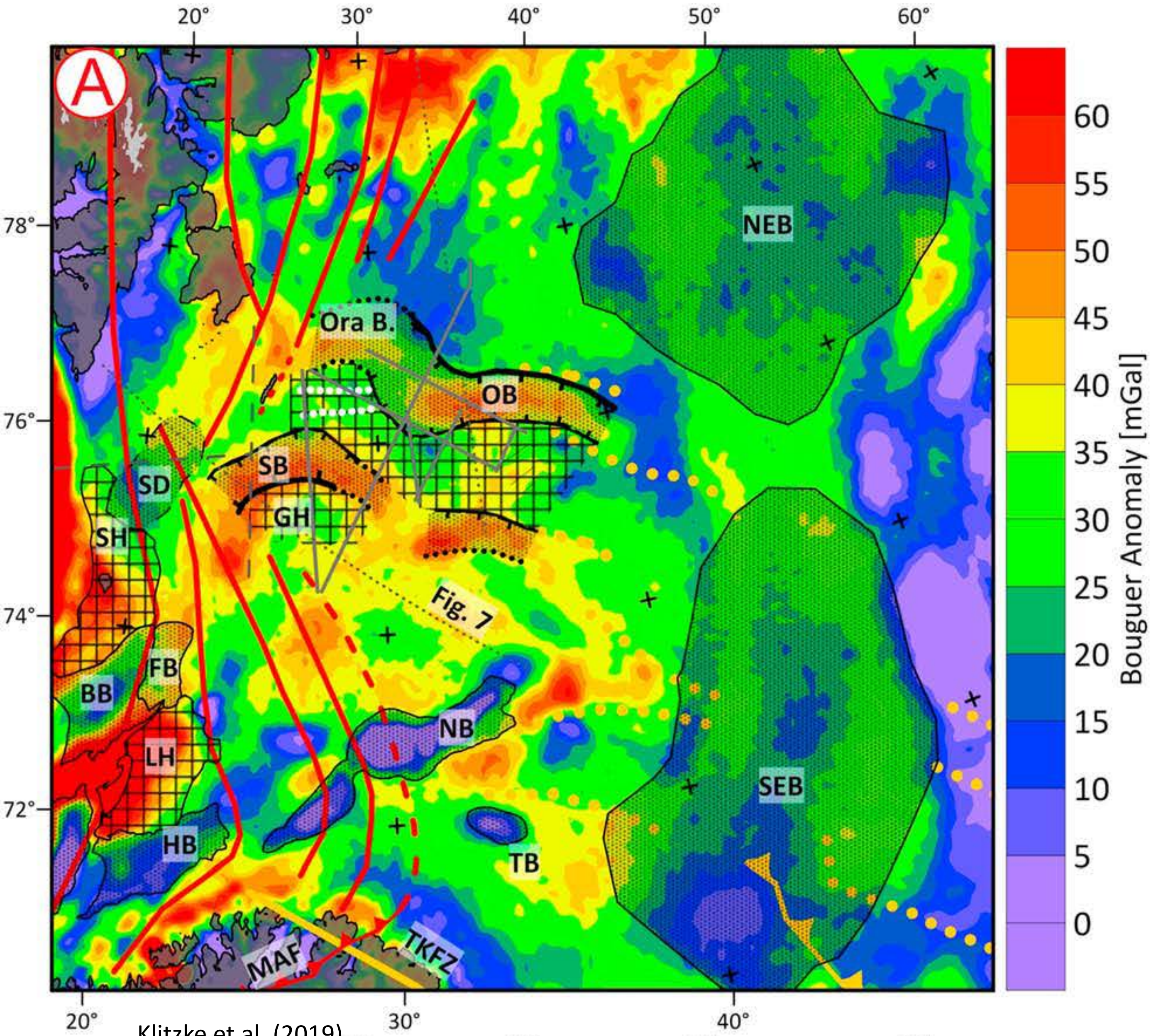

Klitzke et al. (2019)

2

Gravimetric, aeromagnetic and seismic data in the Barents Sea show the existence of potentially inverted WNW–ESE- to NW–SE-striking Timamian thrusts.

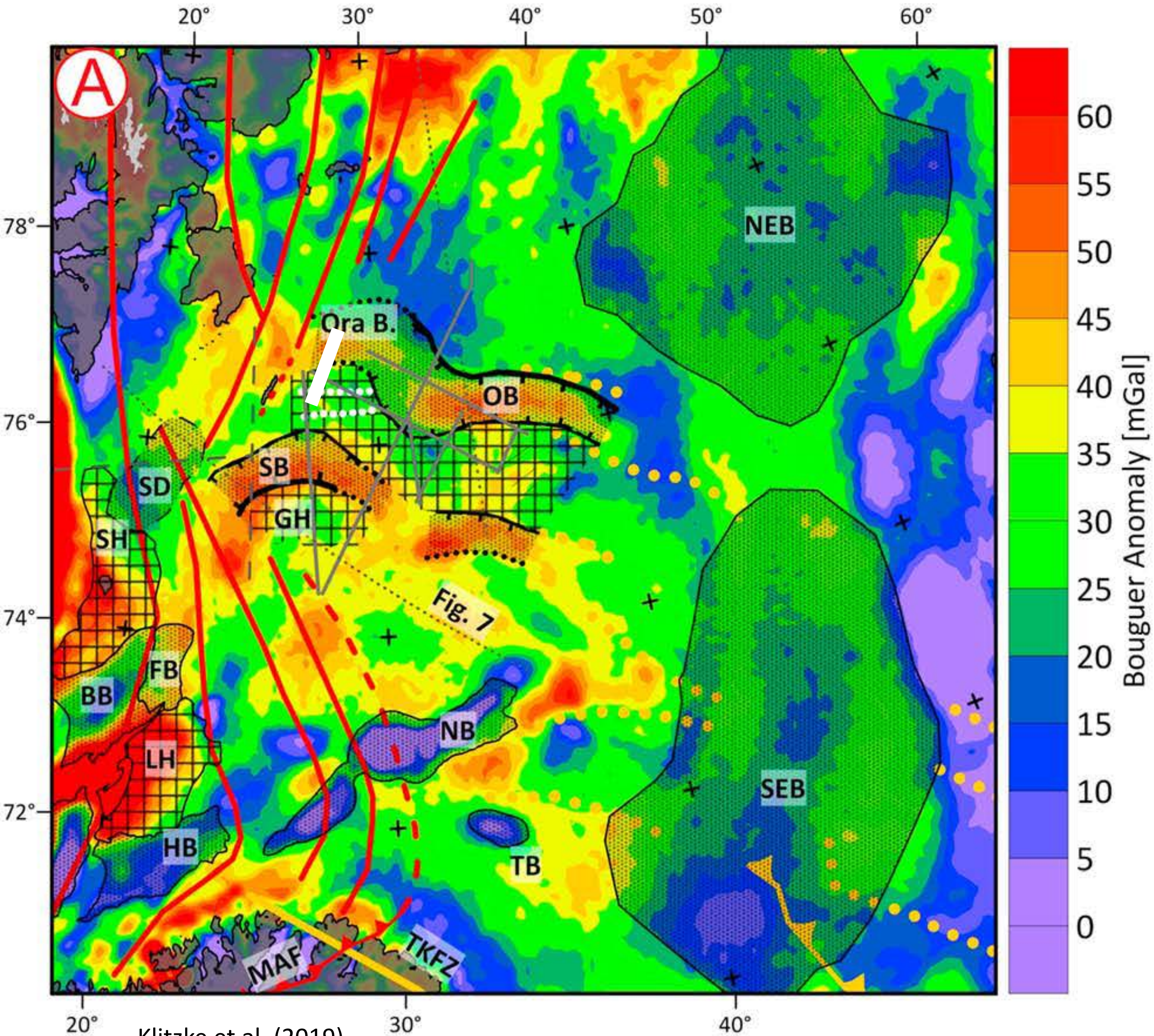

Klitzke et al. (2019)

2 **Gravimetric, aeromagnetic and seismic data in the Barents Sea show the existence of potentially inverted WNW–ESE- to NW–SE-striking Timamian thrusts.**

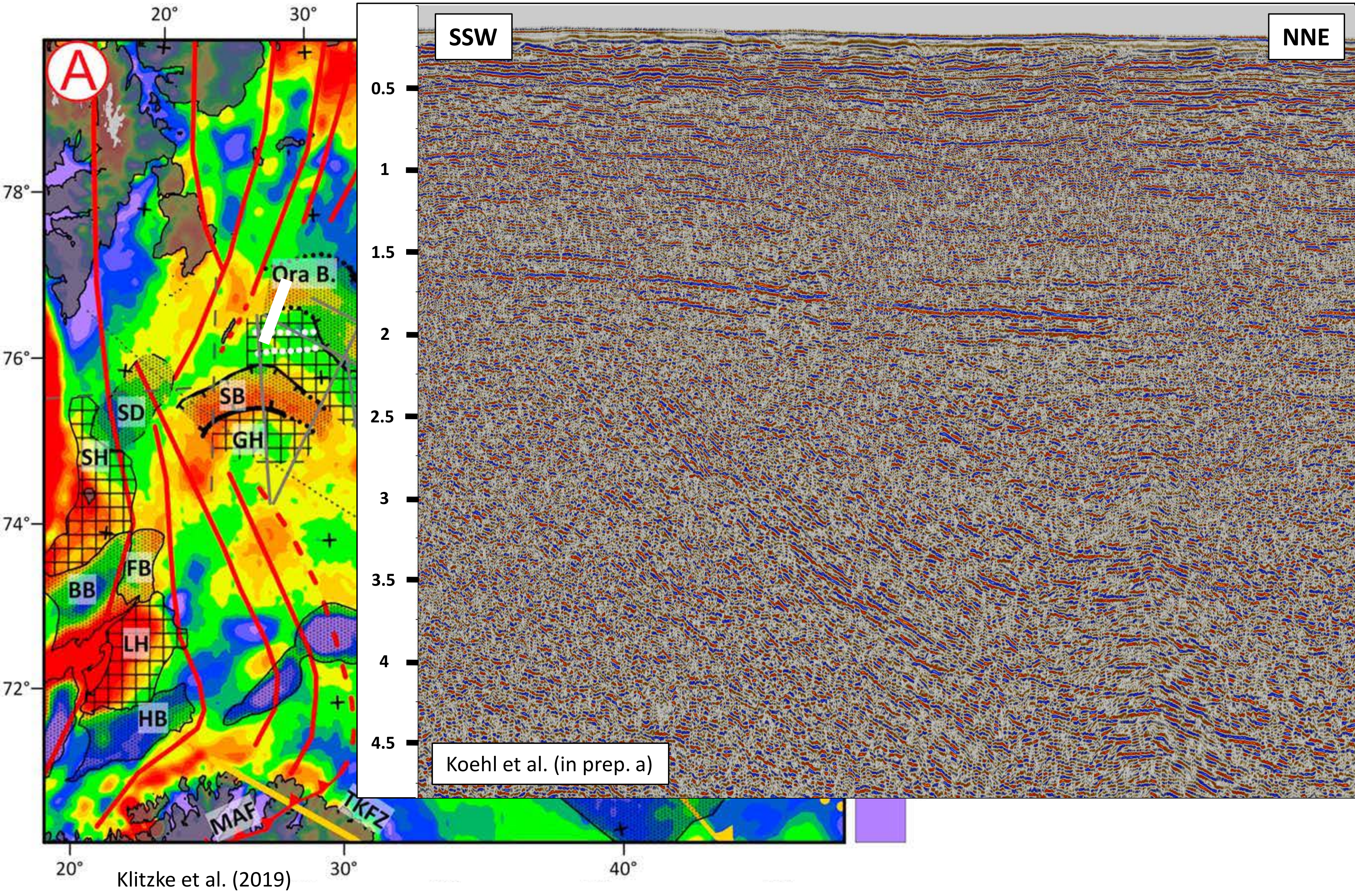

2 **Gravimetric, aeromagnetic and seismic data in the Barents Sea show the existence of potentially inverted WNW–ESE- to NW–SE-striking Timamian thrusts.**

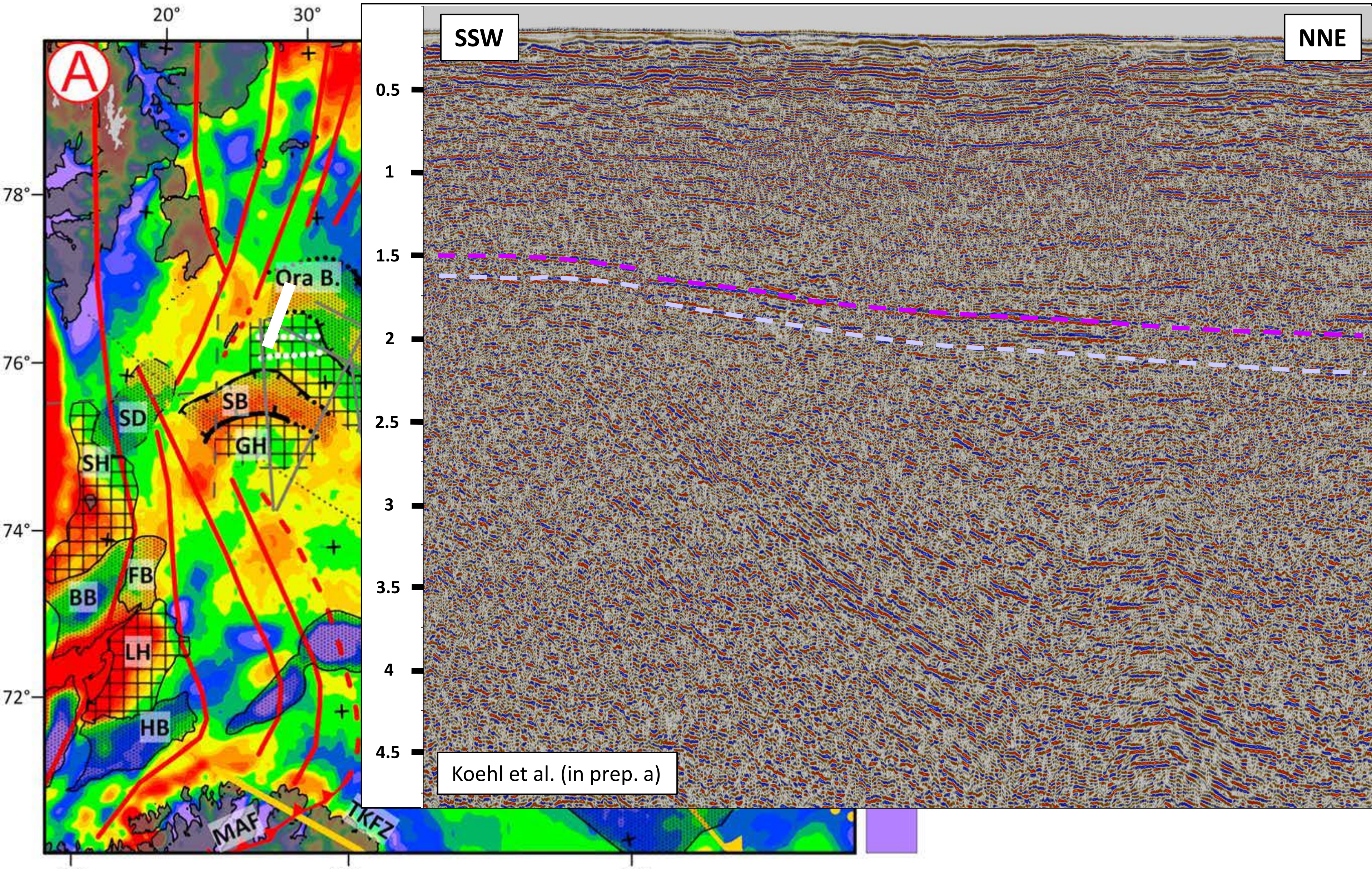

Klitzke et al. (2019)

2 **Gravimetric, aeromagnetic and seismic data in the Barents Sea show the existence of potentially inverted WNW–ESE- to NW–SE-striking Timamian thrusts.**

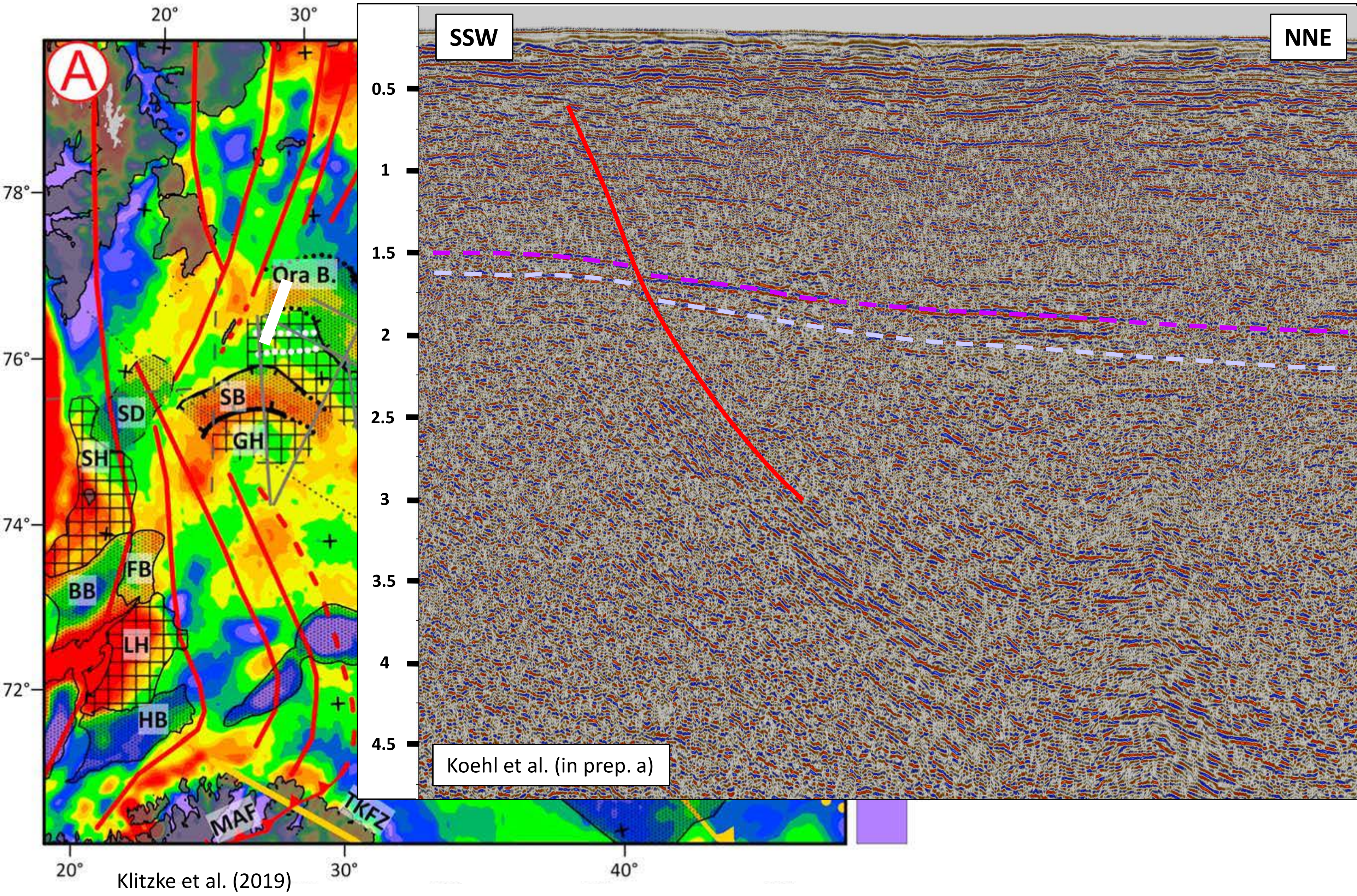

2 Gravimetric, aeromagnetic and seismic data in the Barents Sea show the existence of potentially inverted WNW–ESE- to NW–SE-striking Timamian thrusts.

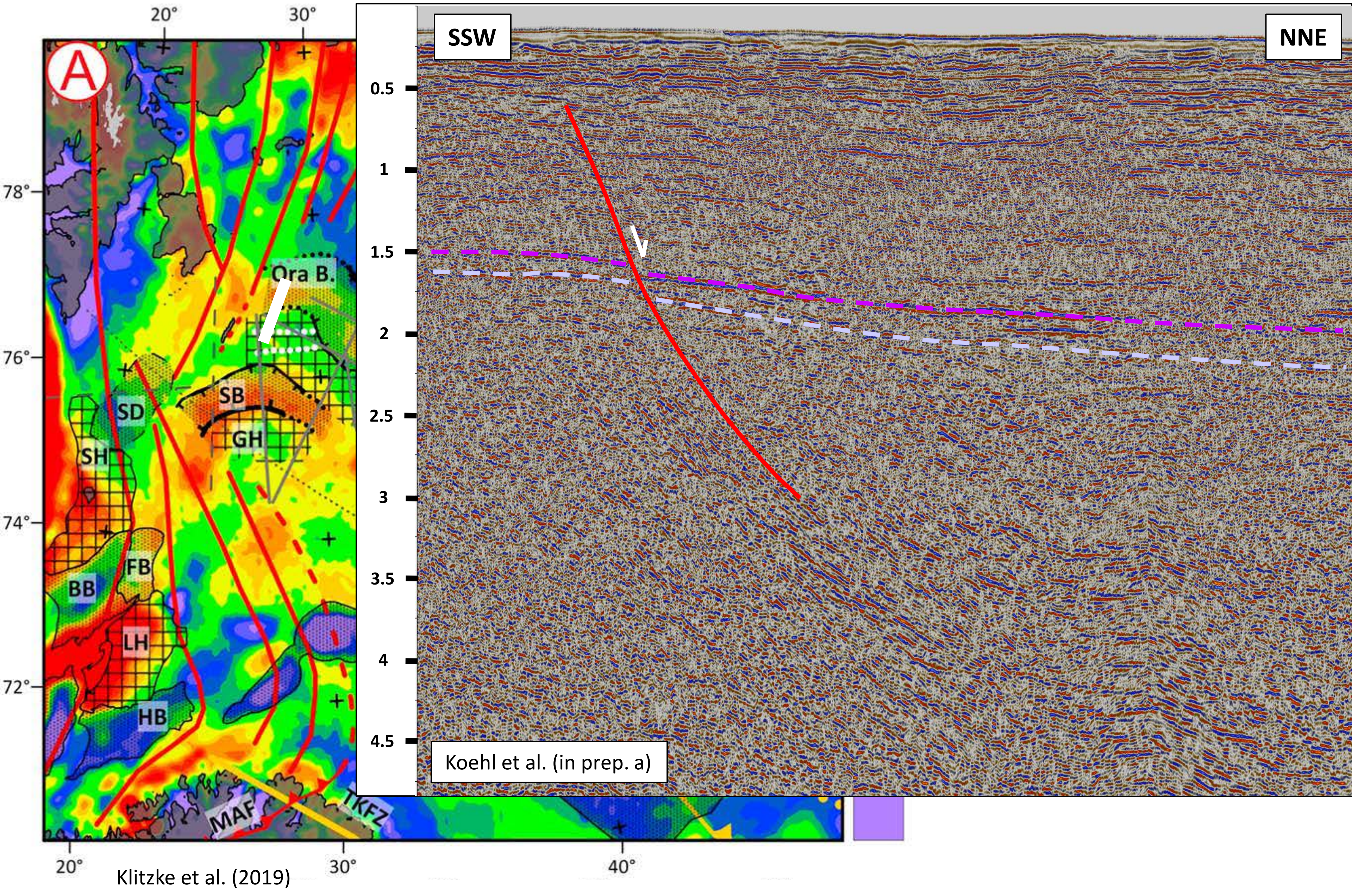

2 **Gravimetric, aeromagnetic and seismic data in the Barents Sea show the existence of potentially inverted WNW–ESE- to NW–SE-striking Timamian thrusts.**

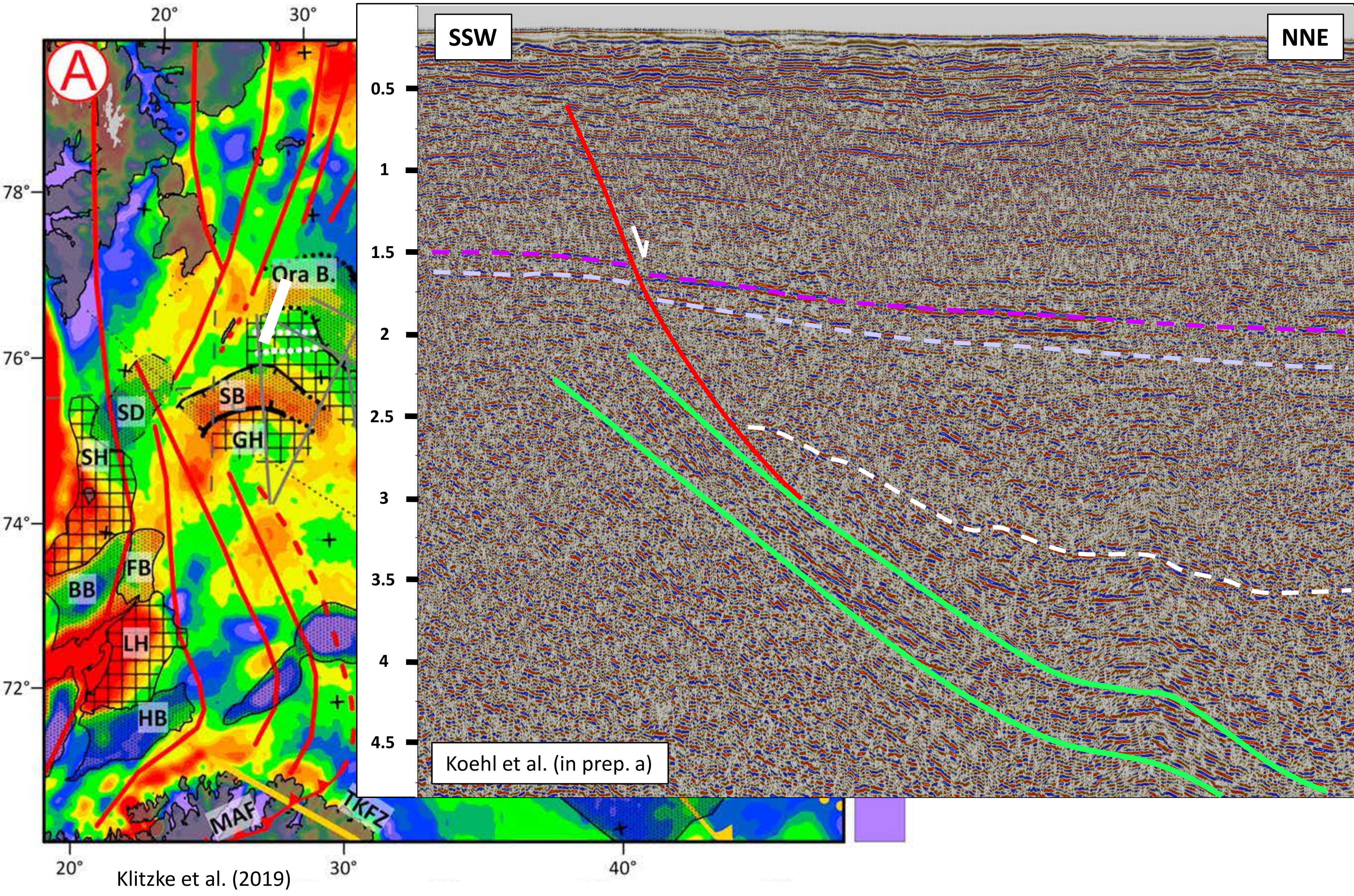

2 **Gravimetric, aeromagnetic and seismic data in the Barents Sea show the existence of potentially inverted WNW–ESE- to NW–SE-striking Timamian thrusts.**

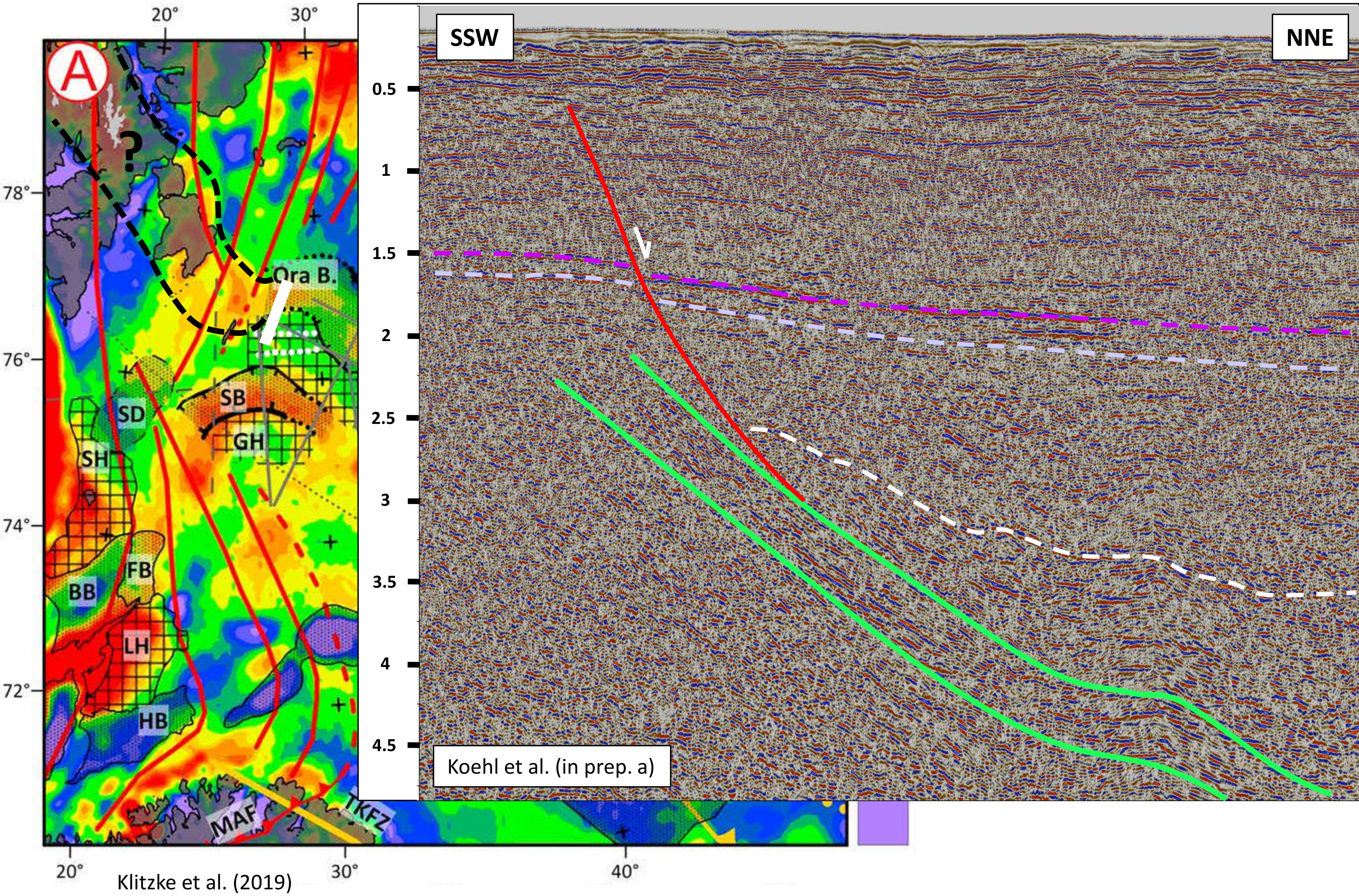

2 Gravimetric, aeromagnetic and seismic data in the Barents Sea show the existence of potentially inverted WNW–ESE- to NW–SE-striking Timamian thrusts.

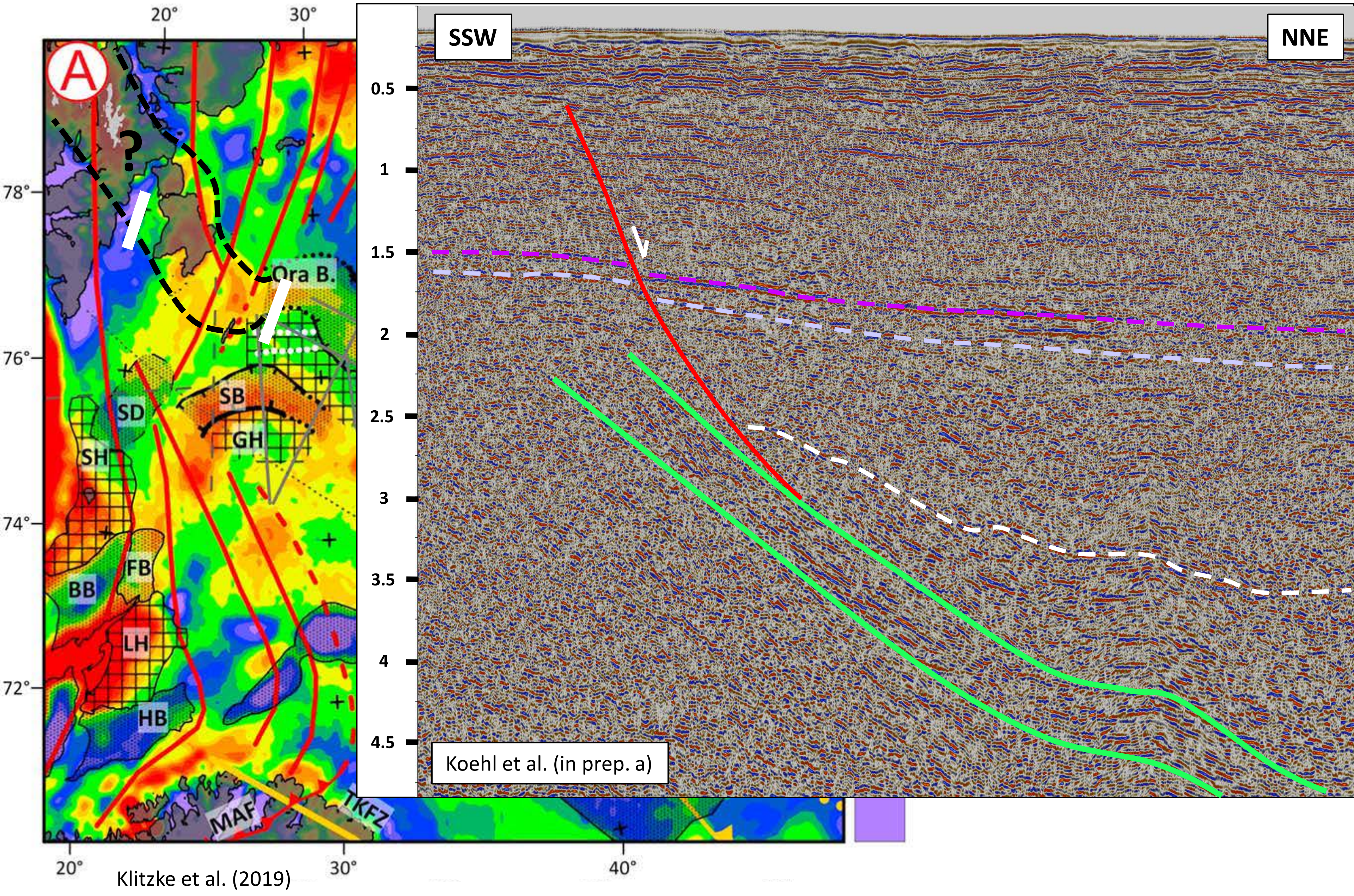

2 **In Storfjorden, a high-angle brittle fault folding the seafloor merges with a suite of moderate amplitude reflections possibly representing a major WNW–ESE-striking thrust.**

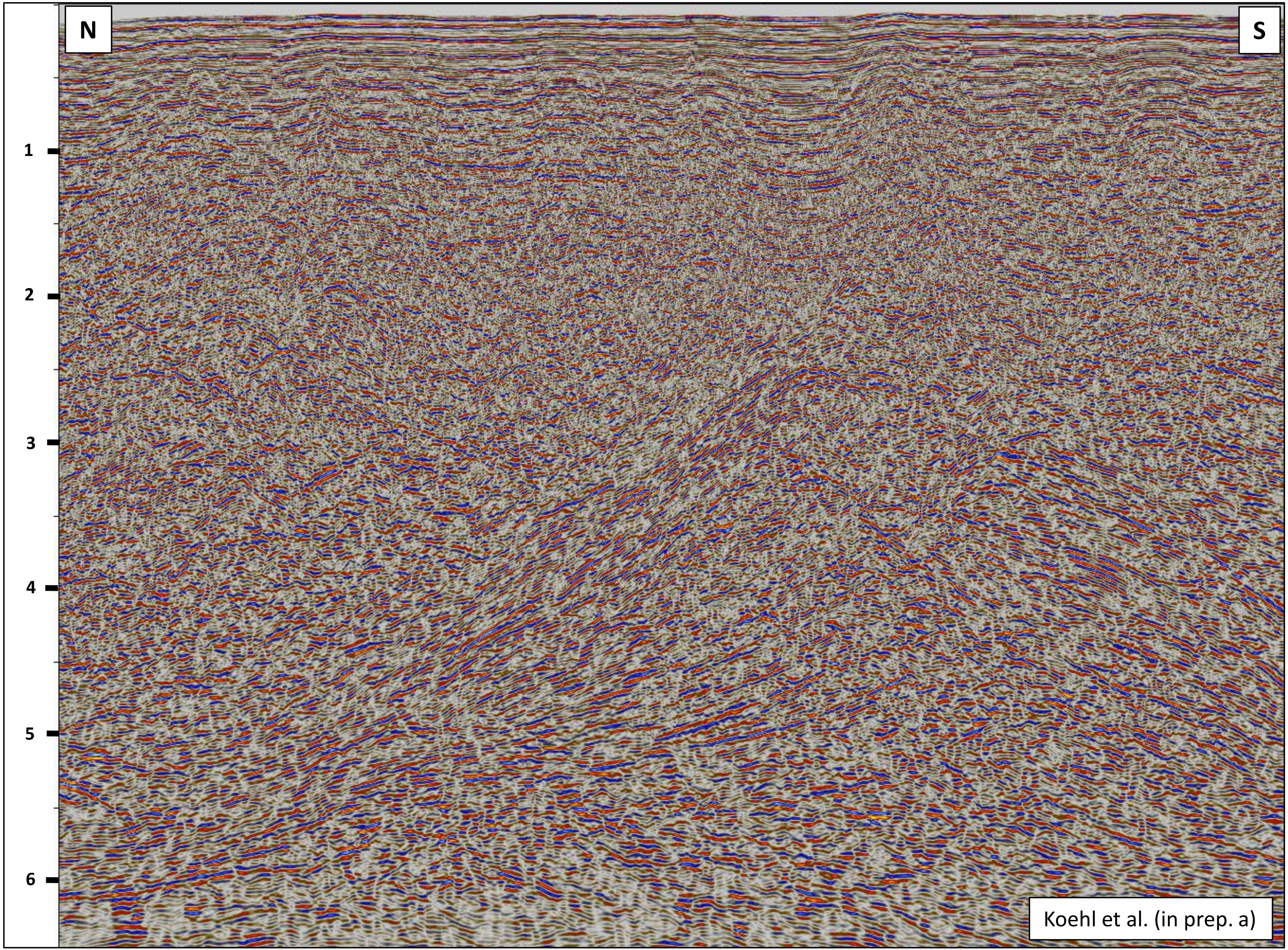

2 **In Storfjorden, a high-angle brittle fault folding the seafloor merges with a suite of moderate amplitude reflections possibly representing a major WNW–ESE-striking thrust.**

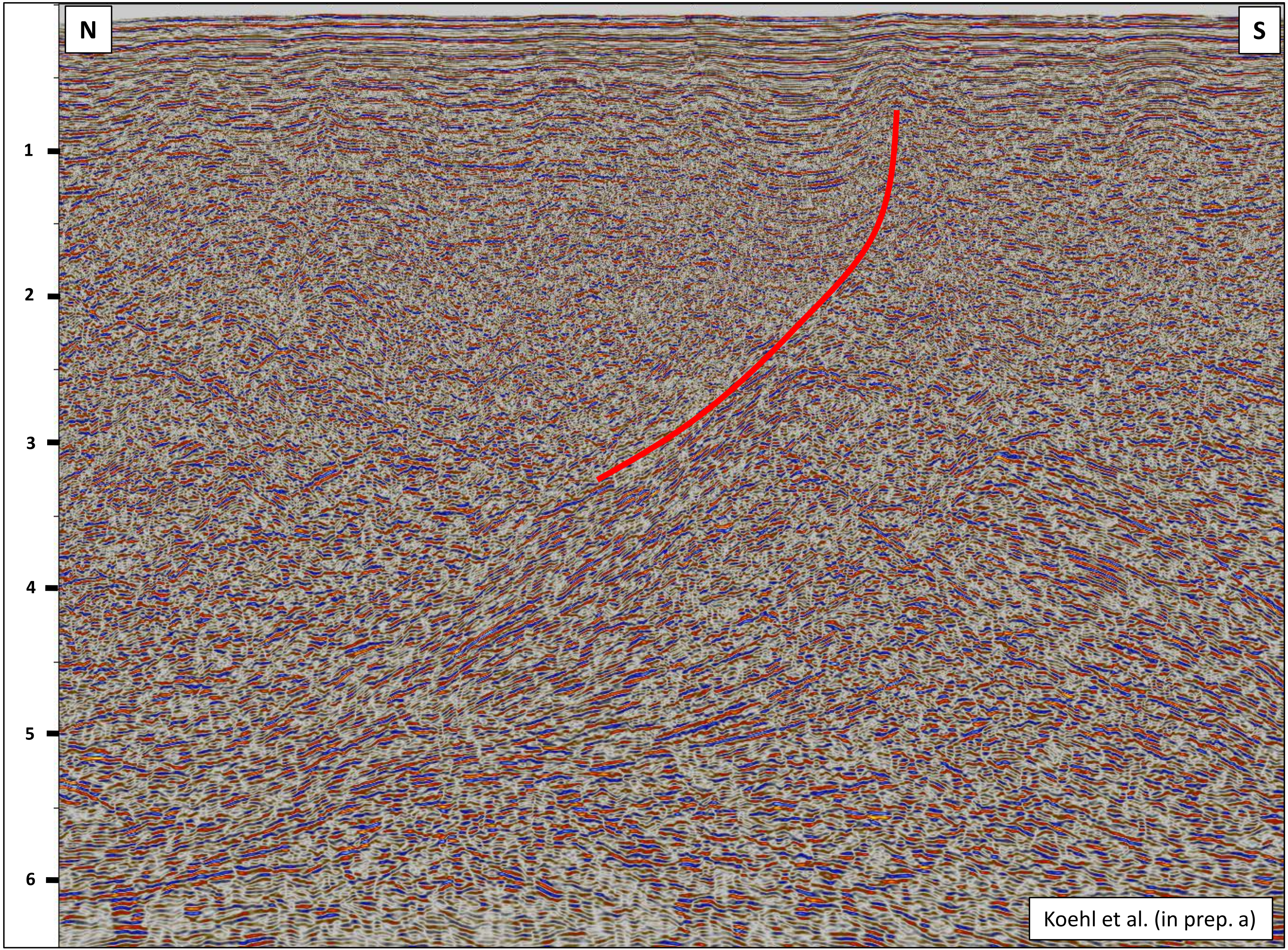

2

In Storfjorden, a high-angle brittle fault folding the seafloor merges with a suite of moderate amplitude reflections possibly representing a major WNW–ESE-striking thrust.

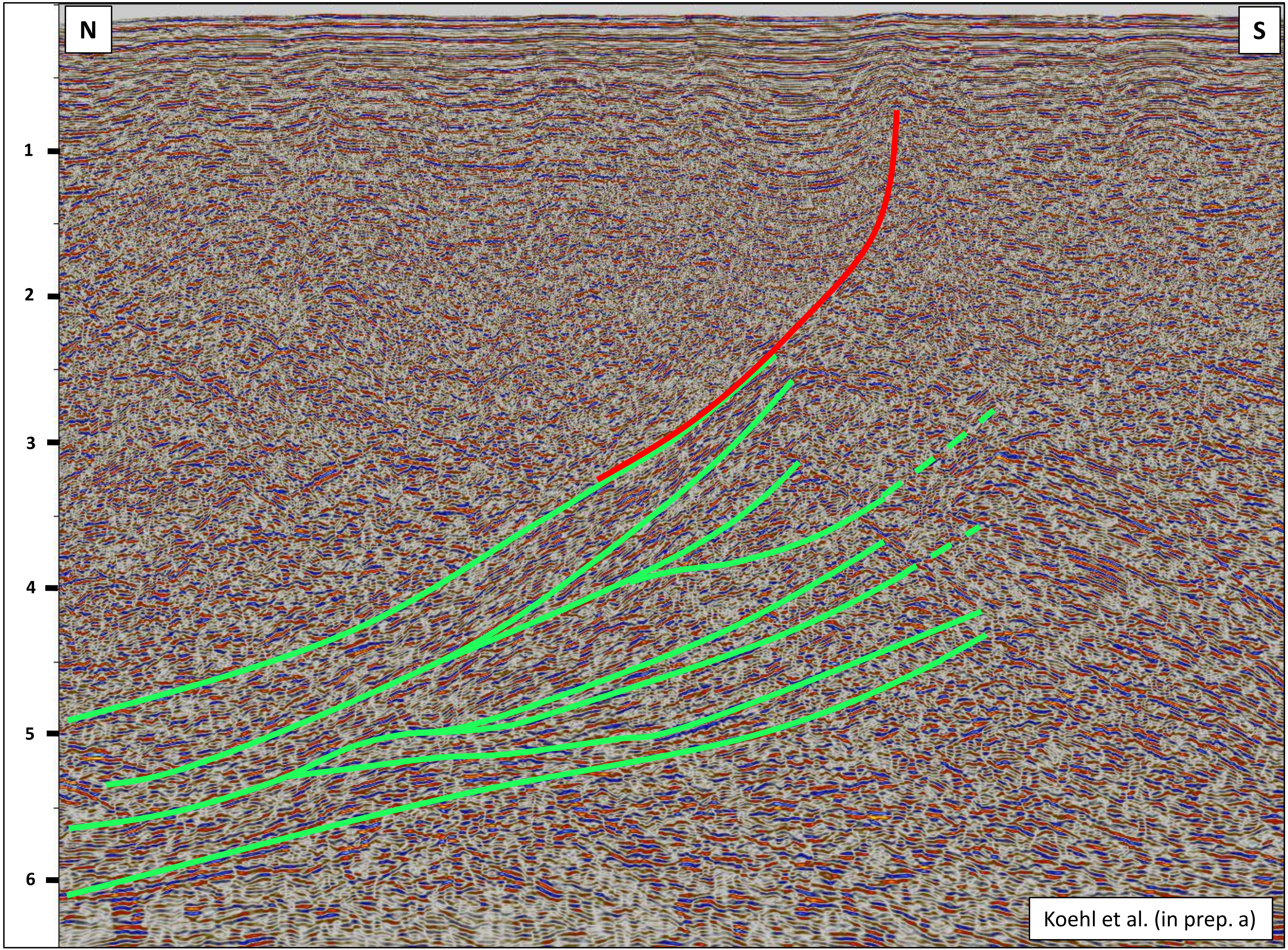

2 In Storfjorden, a high-angle brittle fault folding the seafloor merges with a suite of moderate amplitude reflections possibly representing a major WNW–ESE-striking thrust.

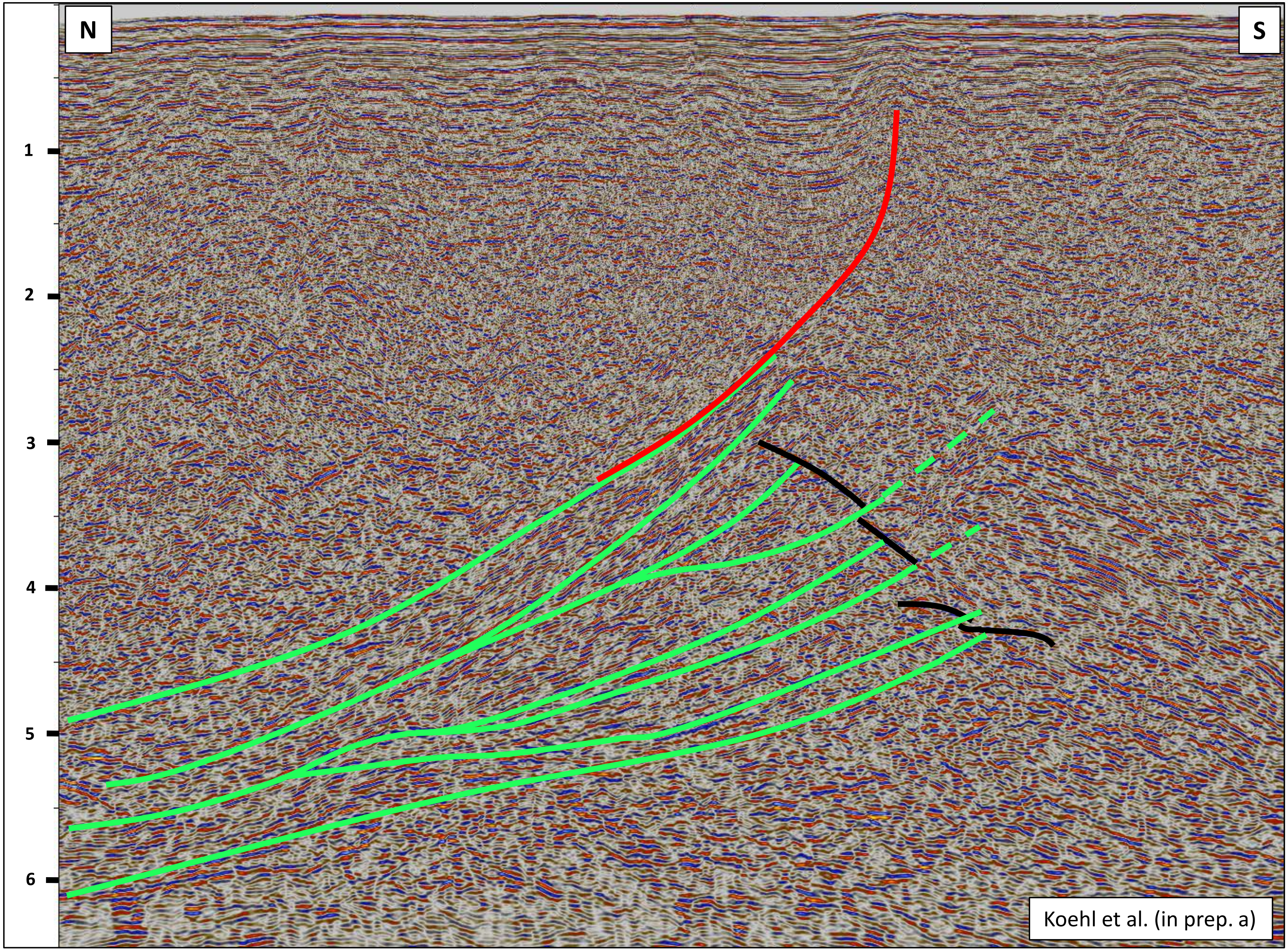

2 **In Storfjorden, a high-angle brittle fault folding the seafloor merges with a suite of moderate amplitude reflections possibly representing a major WNW–ESE-striking thrust.**

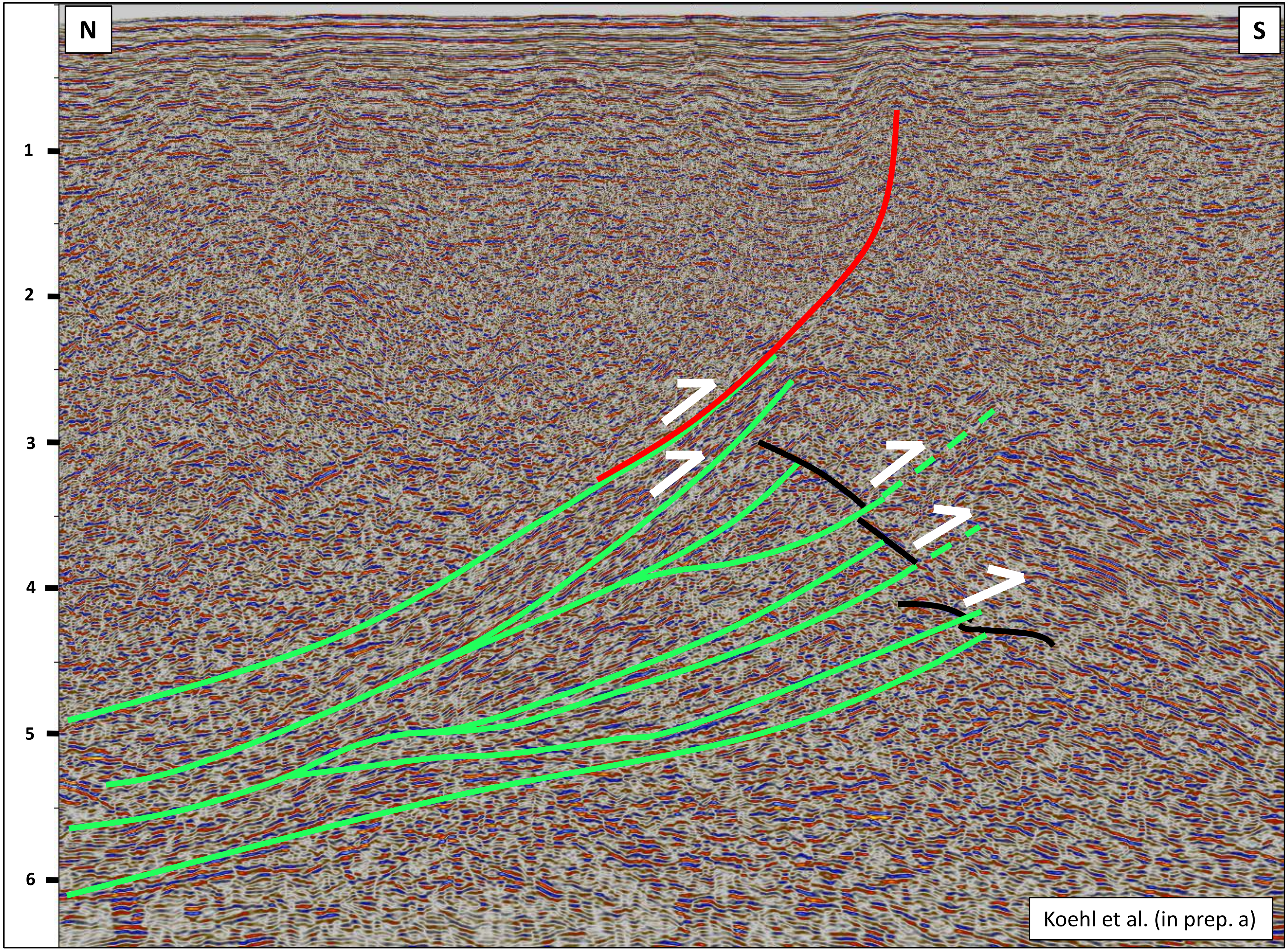

2 **In Storfjorden, a high-angle brittle fault folding the seafloor merges with a suite of moderate amplitude reflections possibly representing a major WNW–ESE-striking thrust.**

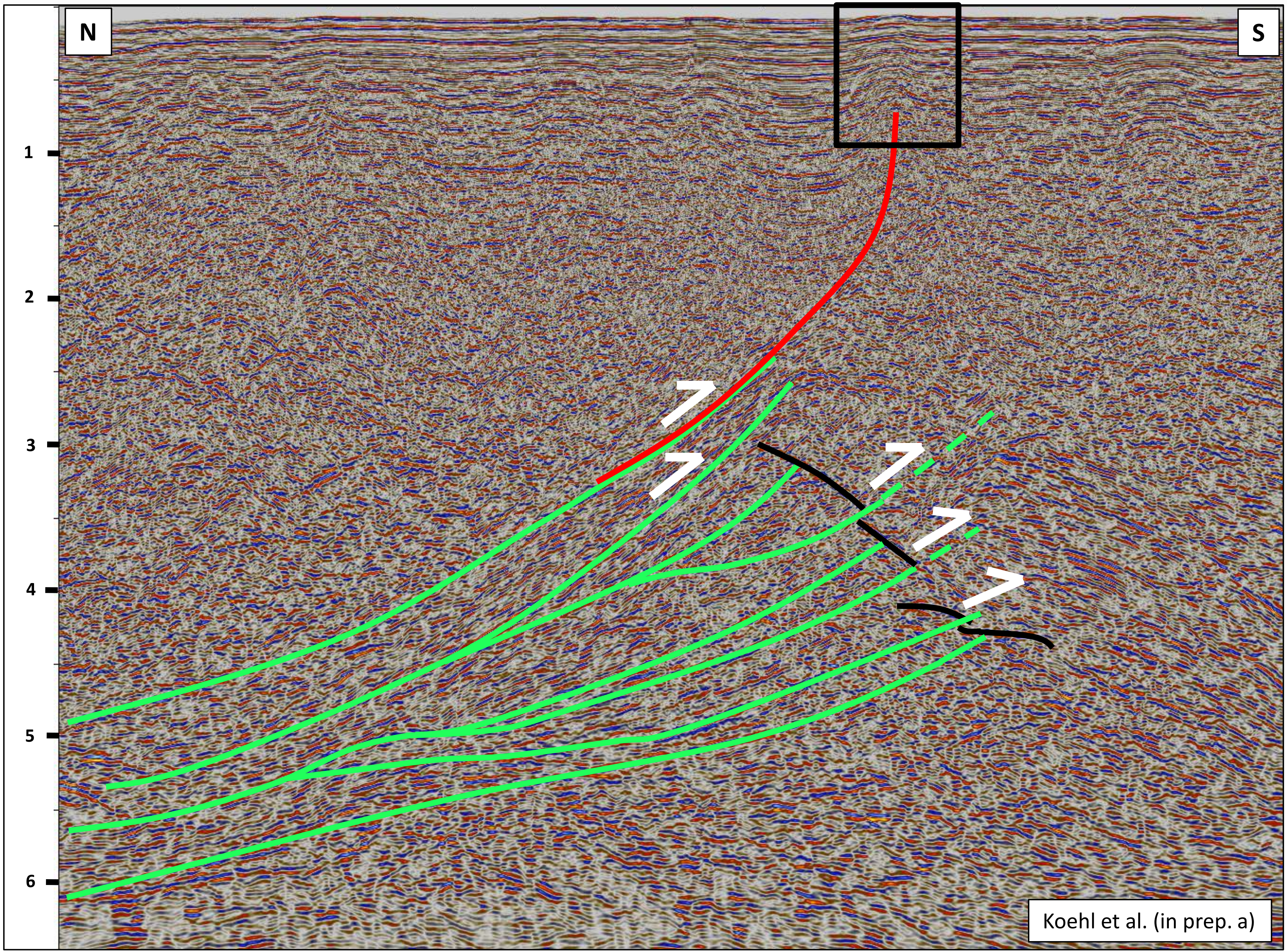

2 **In Storfjorden, a high-angle brittle fault folding the seafloor merges with a suite of moderate amplitude reflections possibly representing a major WNW–ESE-striking thrust.**

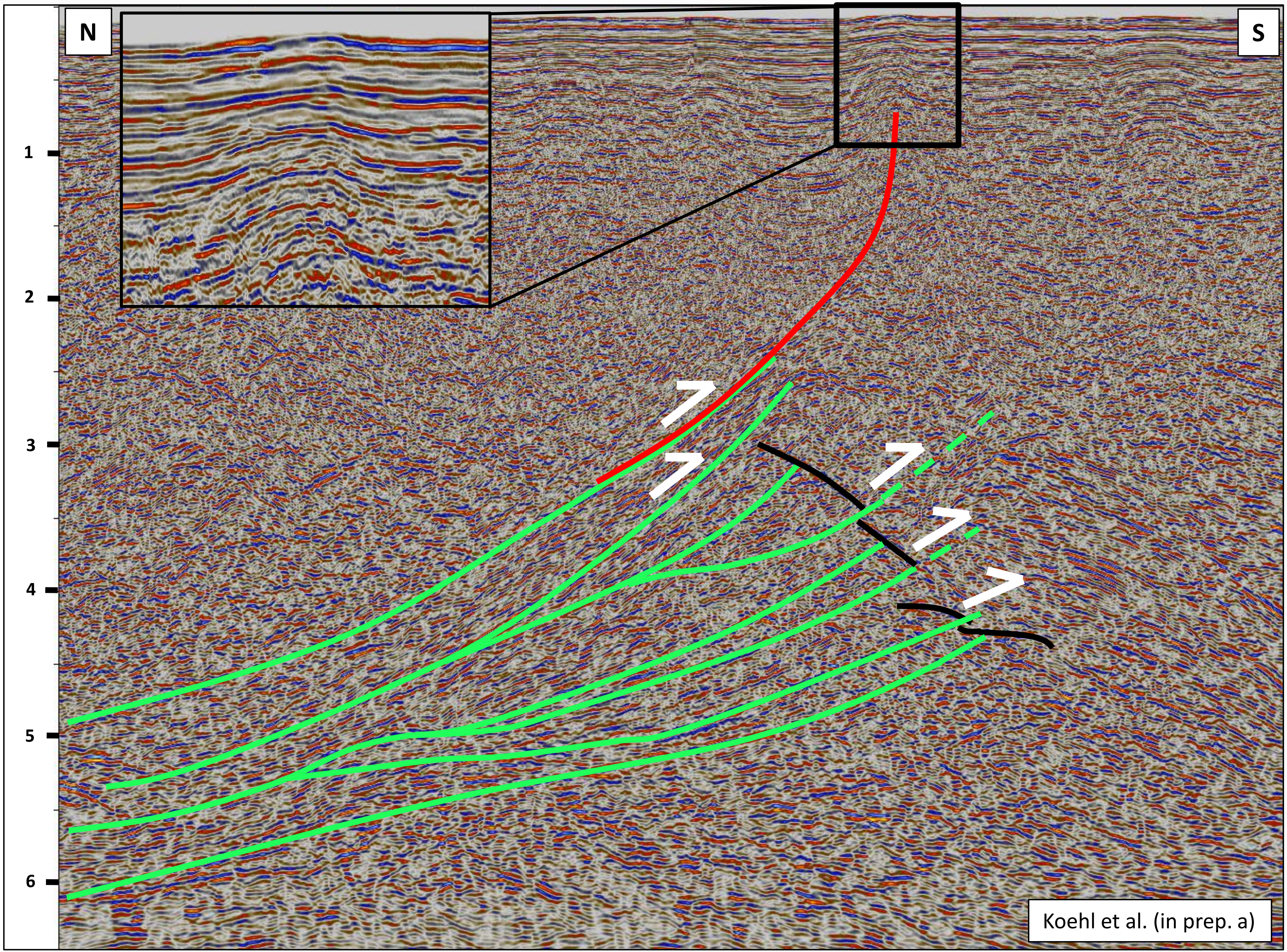

2 **In Storfjorden, a high-angle brittle fault folding the seafloor merges with a suite of moderate amplitude reflections possibly representing a major WNW–ESE-striking thrust.**

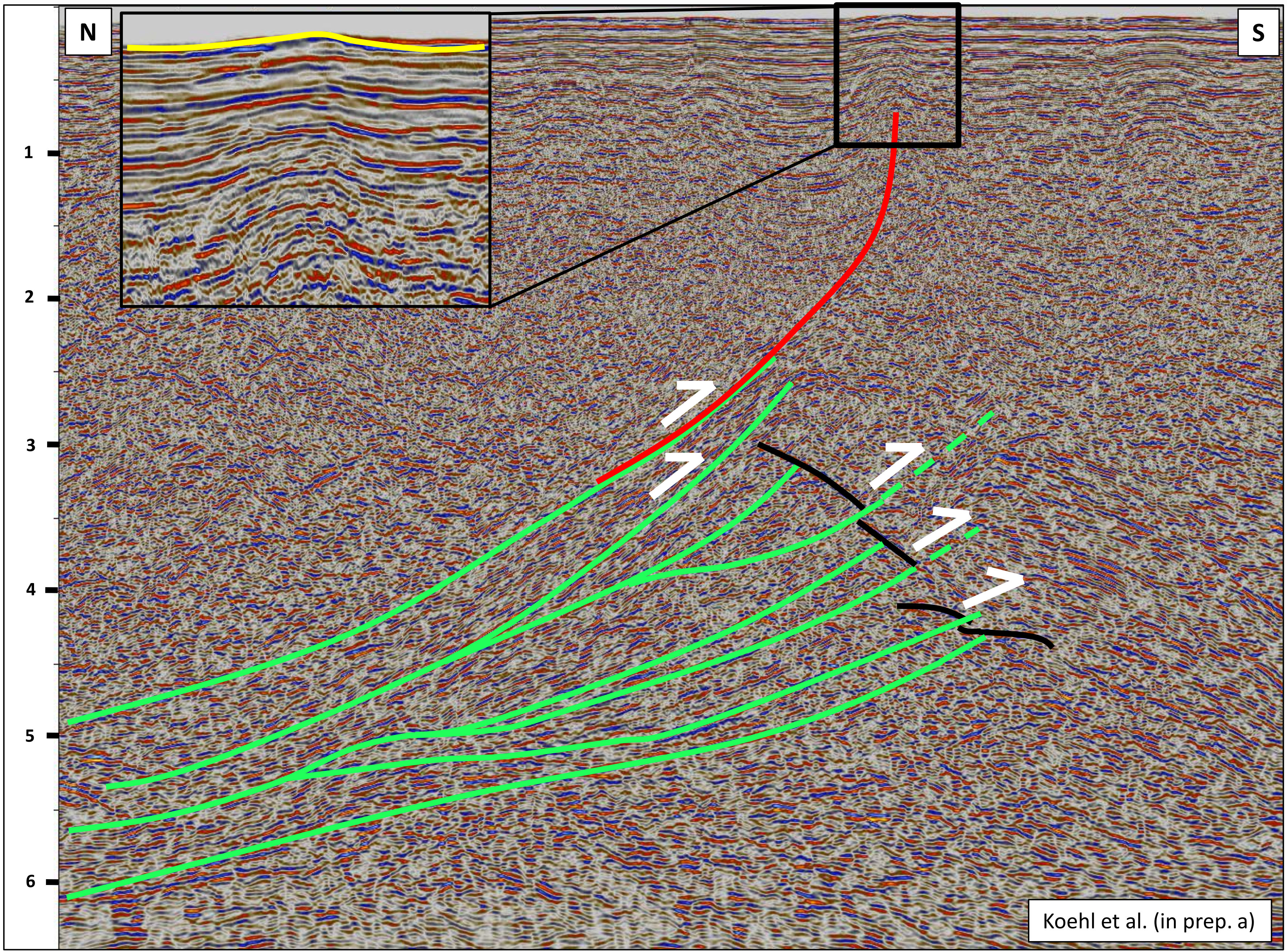

2

Bathymetry data in Billefjorden show that the N–S-striking Billefjorden Fault Zone is left-laterally offset by WNW–ESE-striking fault-related escarpments.

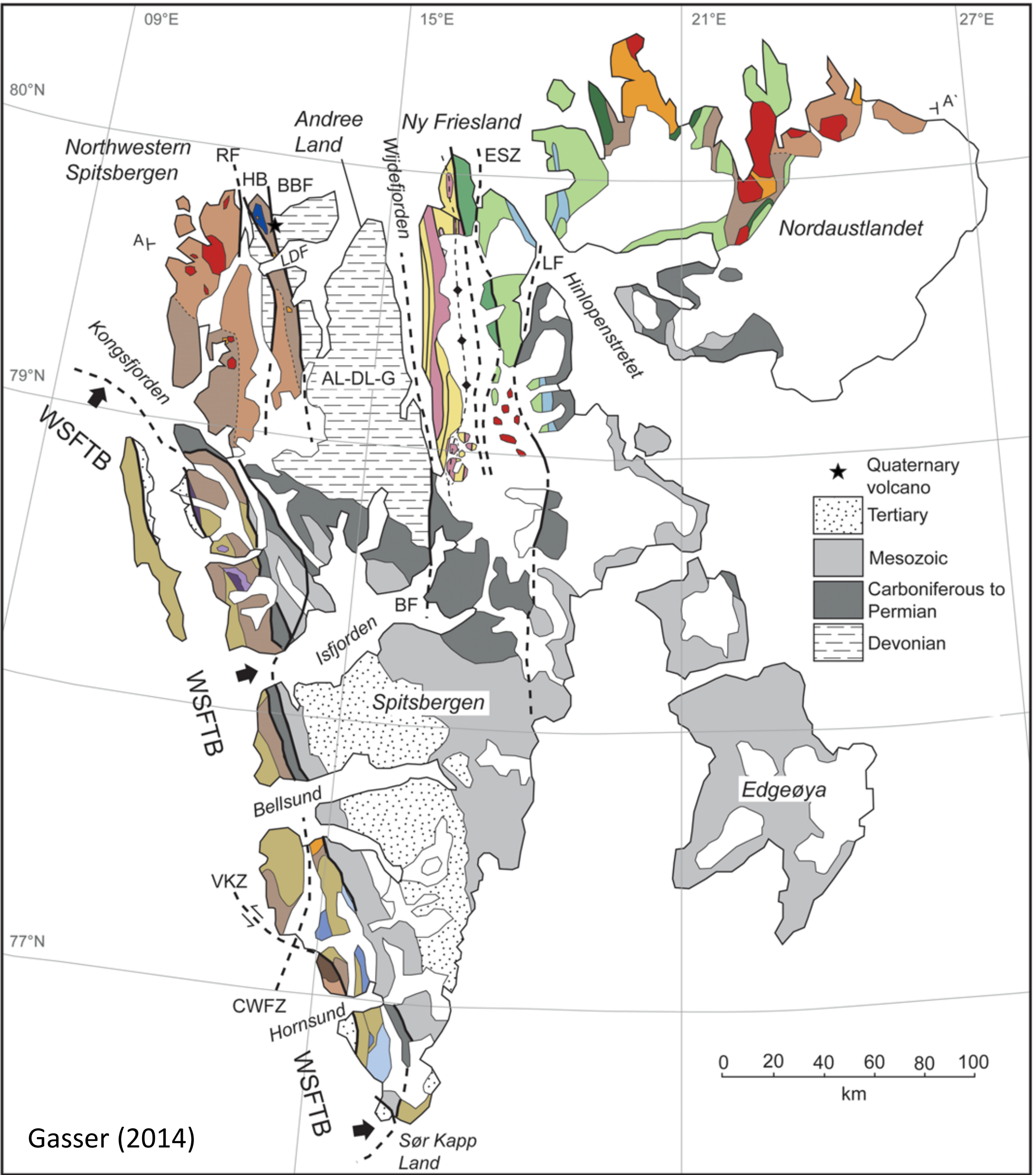

Gasser (2014)

2 **Bathymetry data in Billefjorden show that the N–S-striking Billefjorden Fault Zone is left-laterally offset by WNW–ESE-striking fault-related escarpments.**

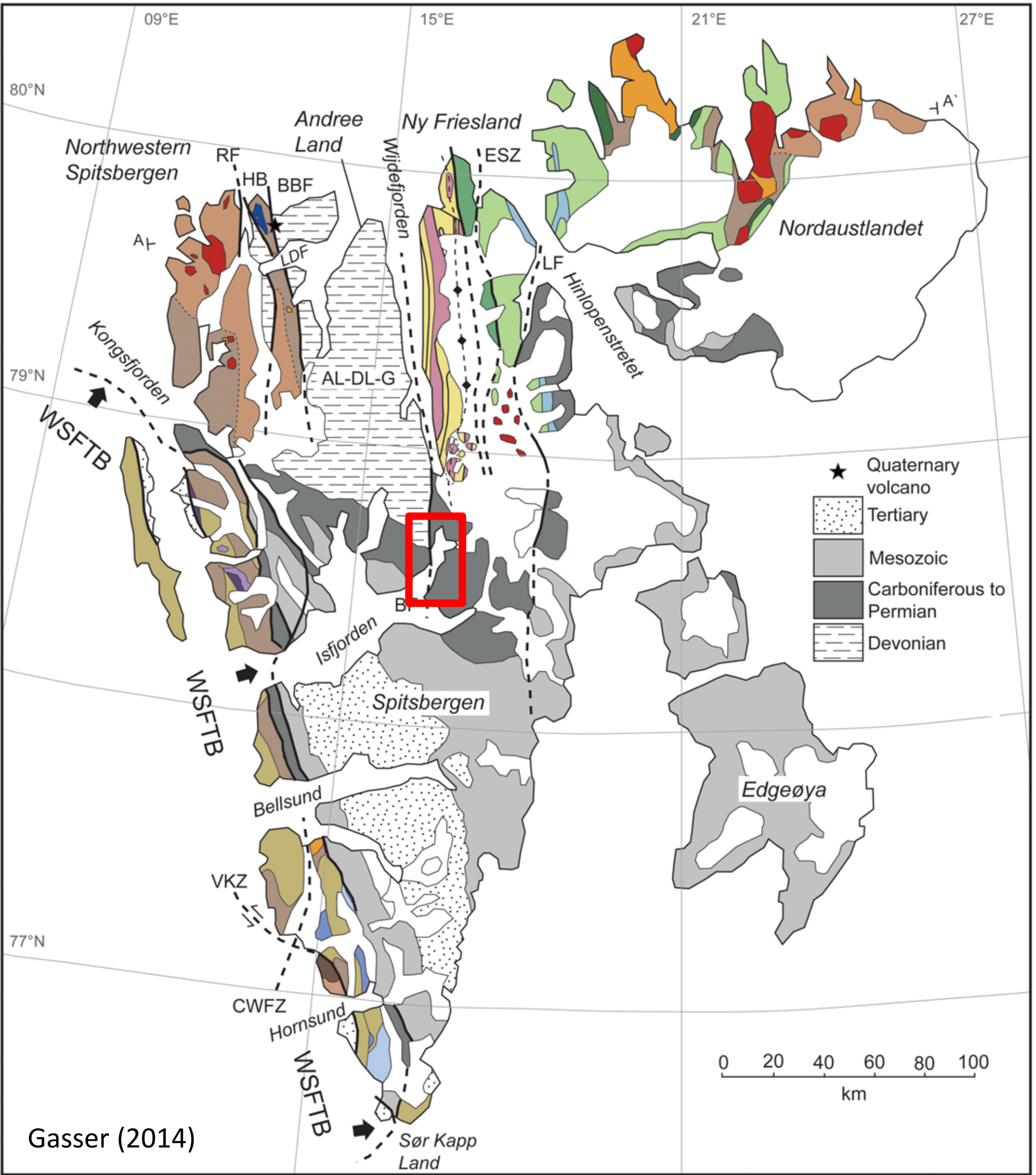

Gasser (2014)

2 **Bathymetry data in Billefjorden show that the N–S-striking Billefjorden Fault Zone is left-laterally offset by WNW–ESE-striking fault-related escarpments.**

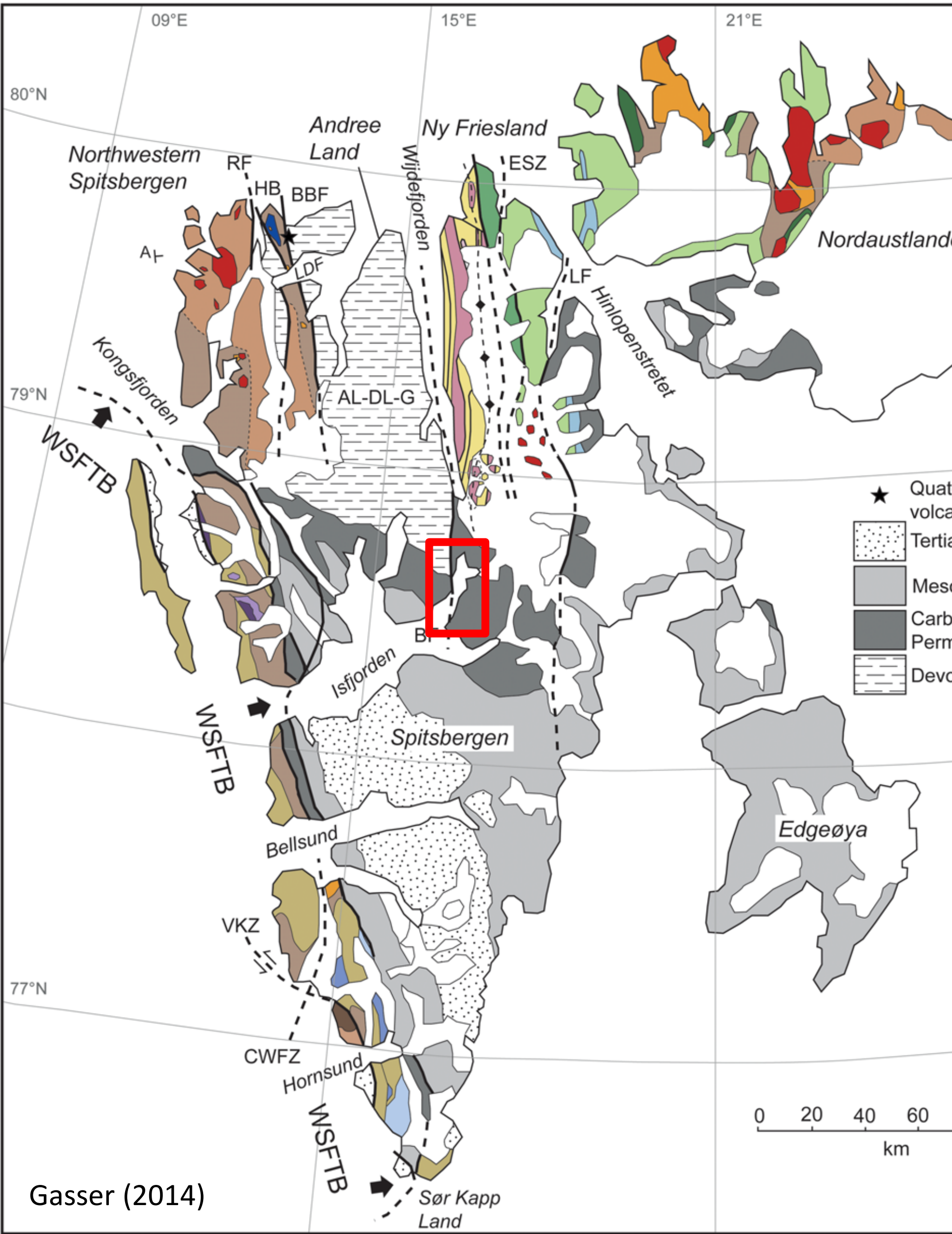

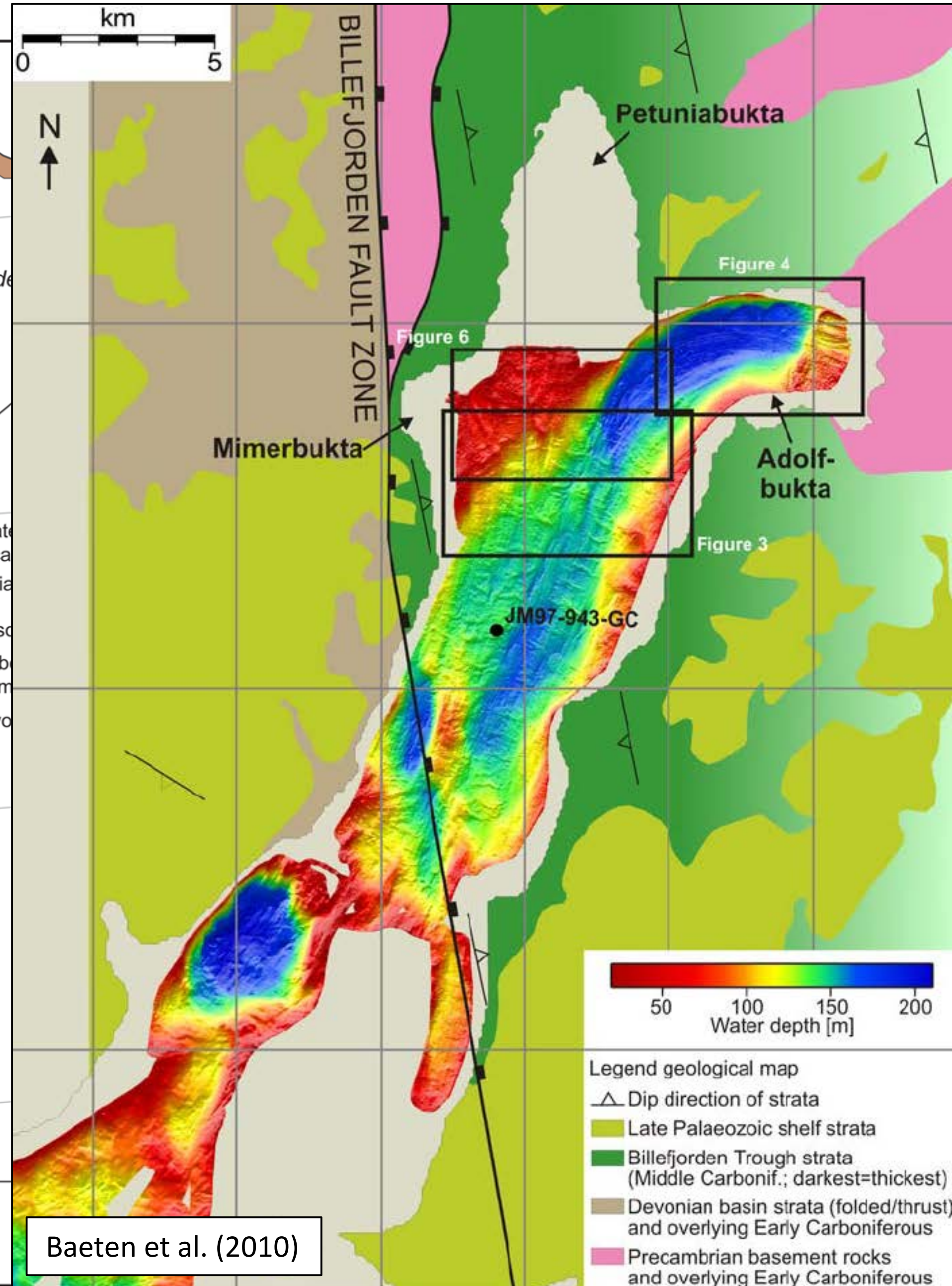

2 Bathymetry data in Billefjorden show that the N–S-striking Billefjorden Fault Zone is left-laterally offset by WNW–ESE-striking fault-related escarpments.

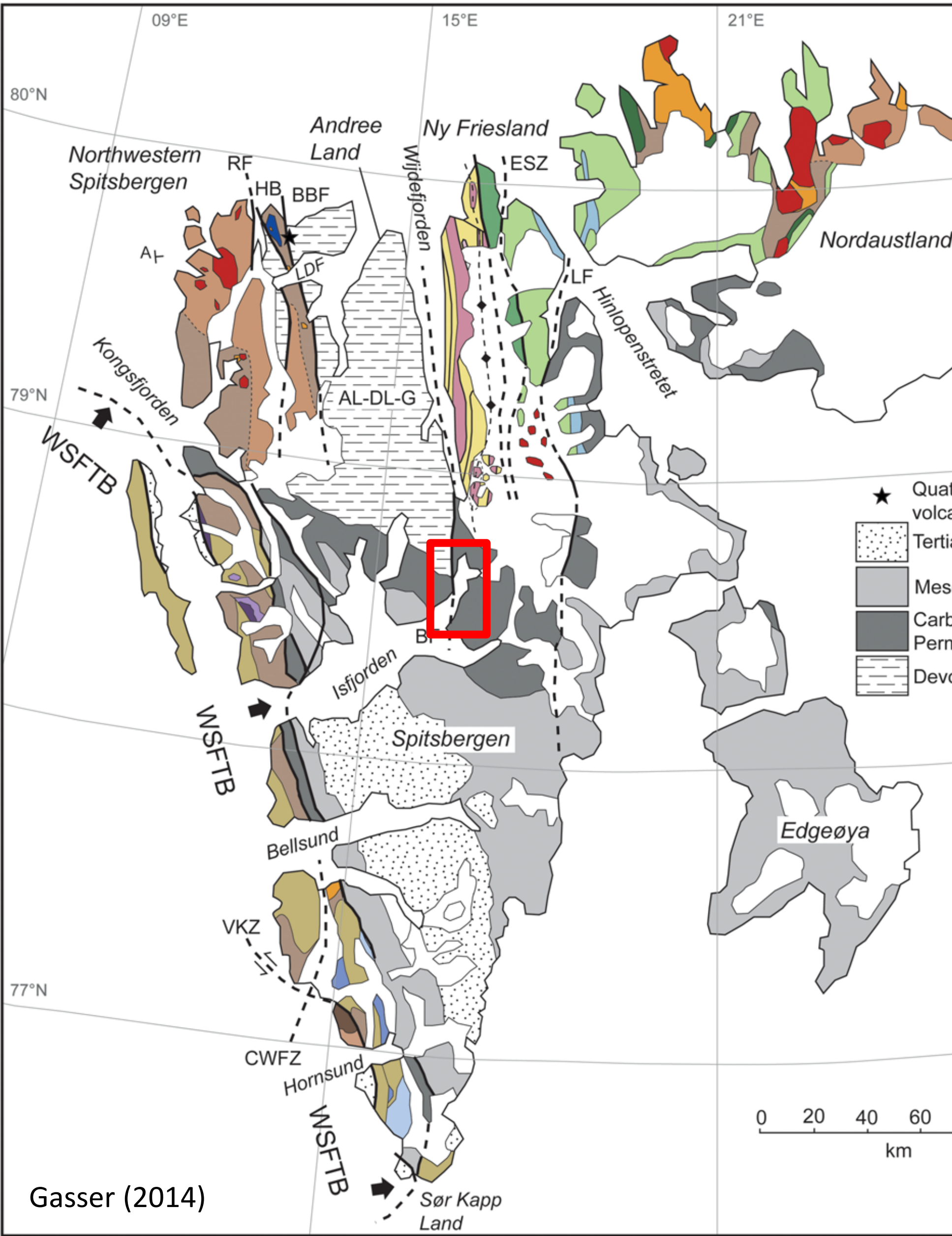

Gasser (2014)

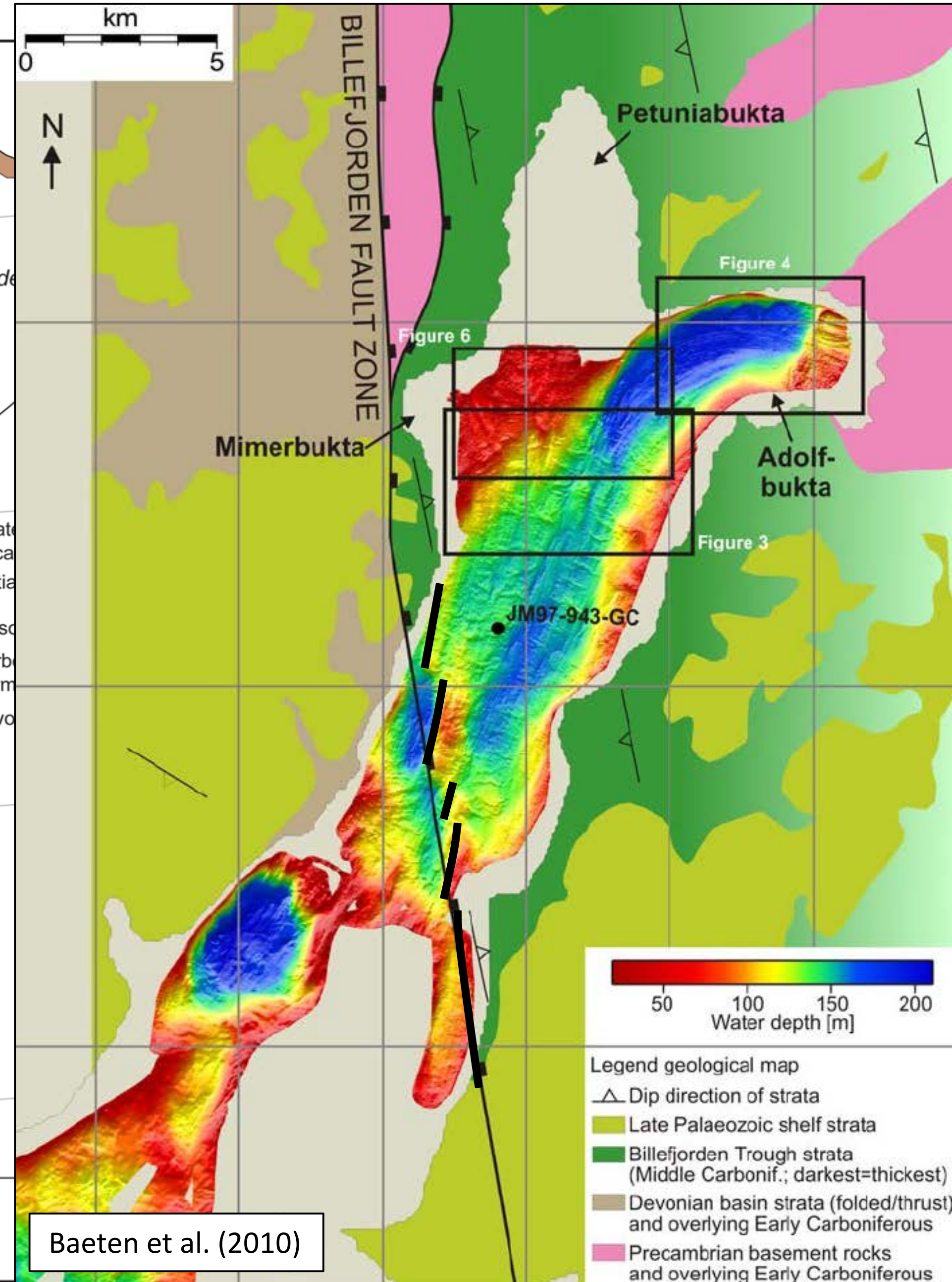

Baeten et al. (2010)

2 **Bathymetry data in Billefjorden show that the N–S-striking Billefjorden Fault Zone is left-laterally offset by WNW–ESE-striking fault-related escarpments.**

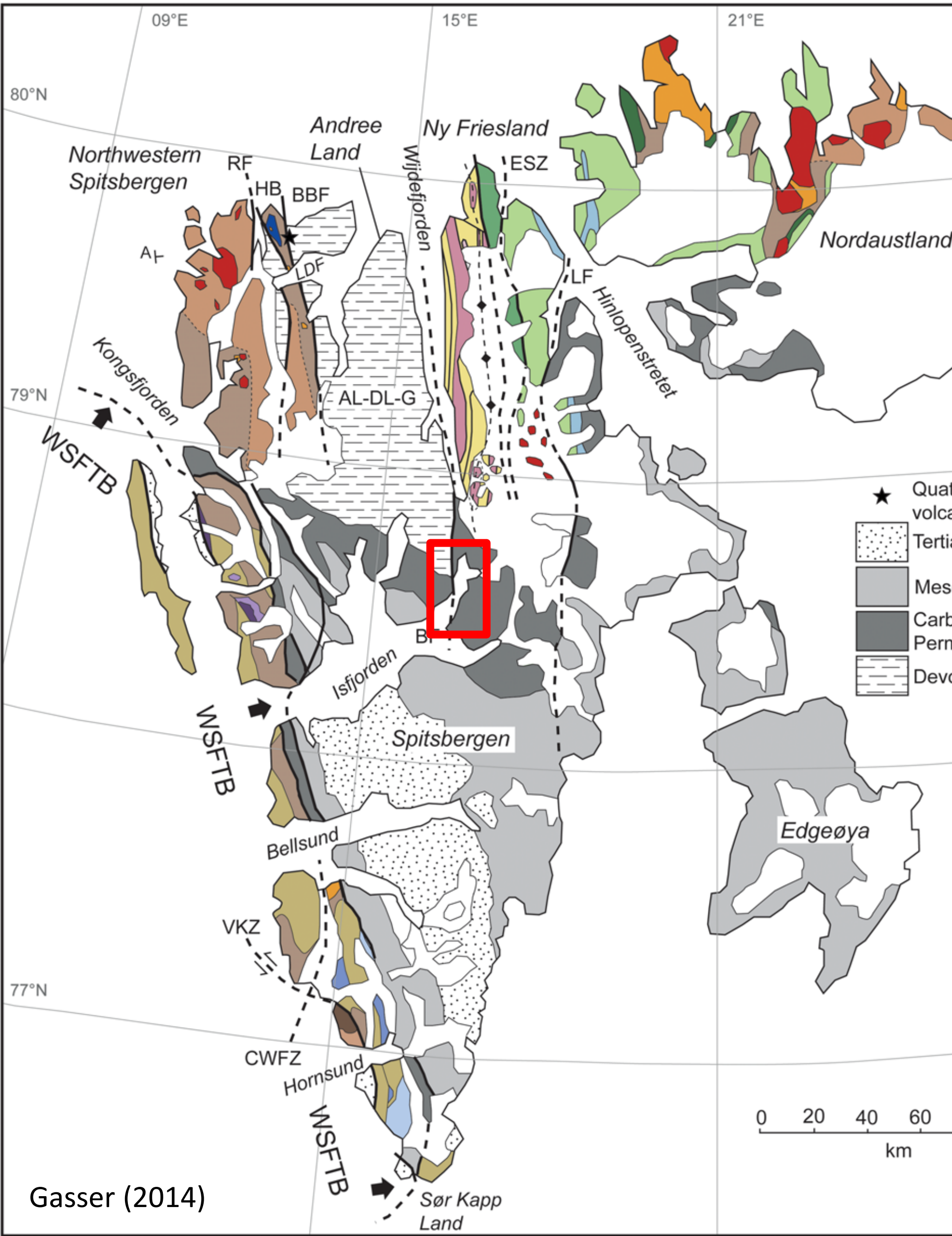

Gasser (2014)

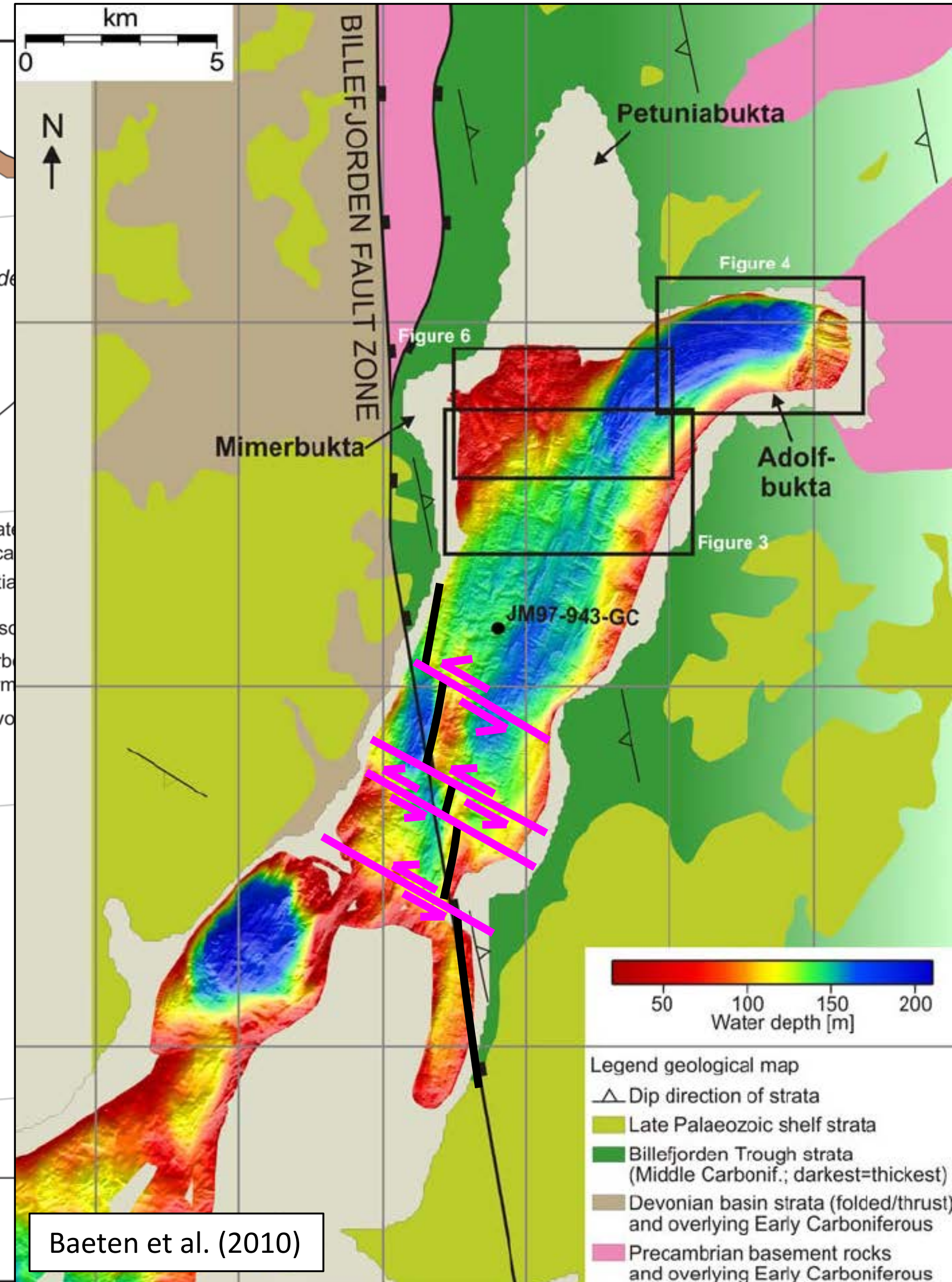

Baeten et al. (2010)

2

Bathymetry data in Billefjorden show that the N–S-striking Billefjorden Fault Zone is left-laterally offset by WNW–ESE-striking fault-related escarpments.

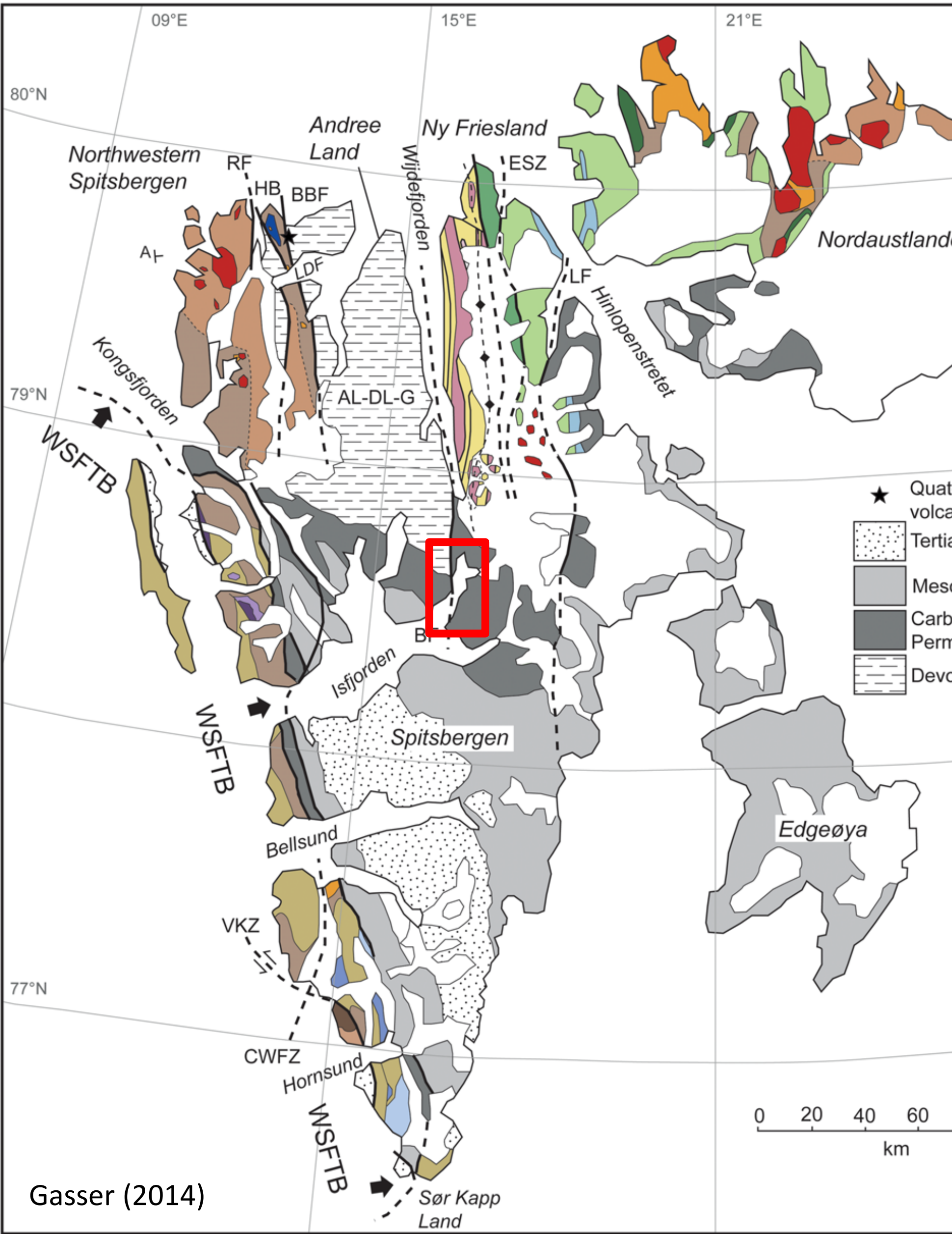

Gasser (2014)

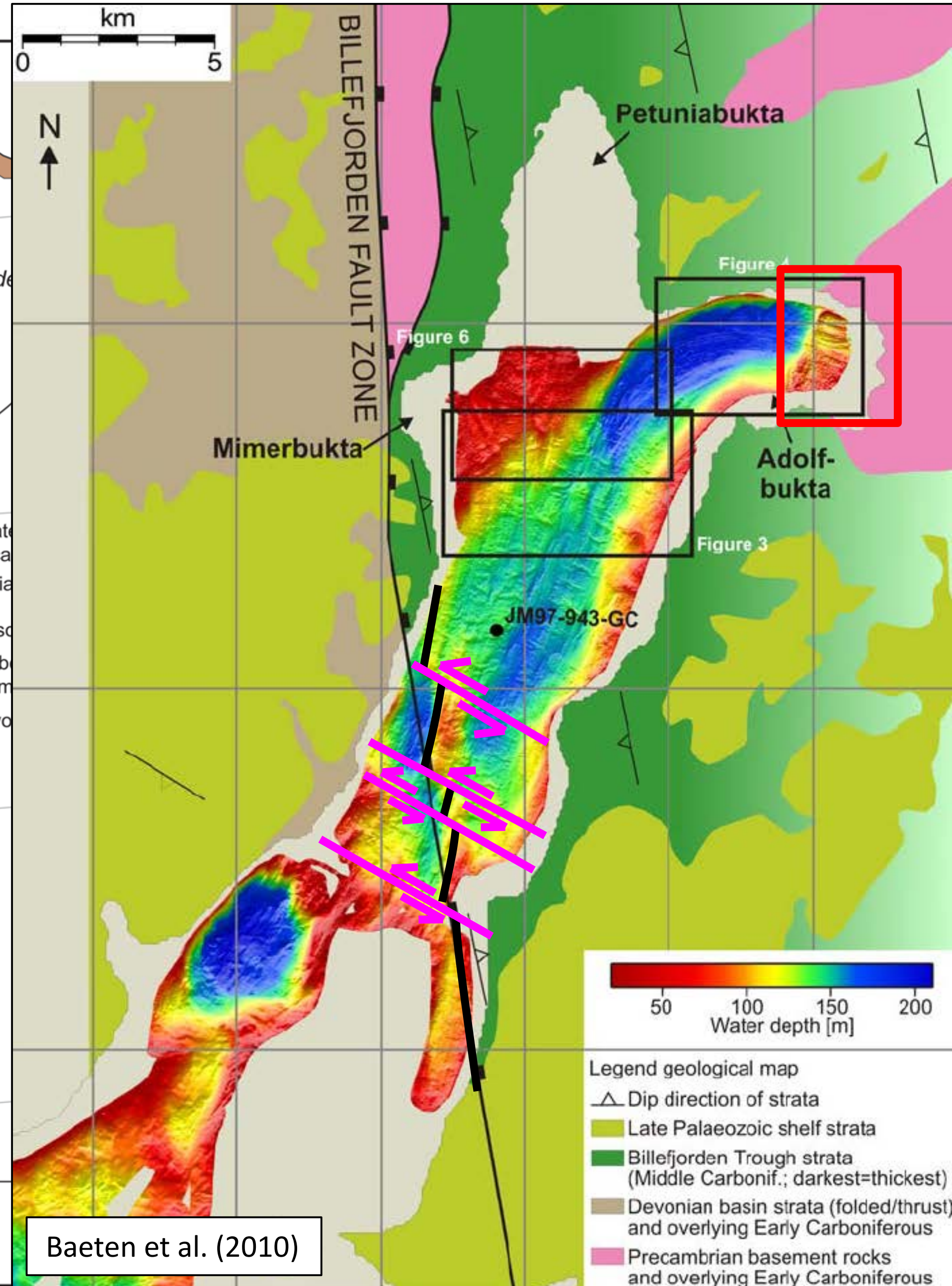

Baeten et al. (2010)

2 Bathymetry data in Billefjorden show that the N–S-striking Billefjorden Fault Zone is left-laterally offset by WNW–ESE-striking fault-related escarpments.

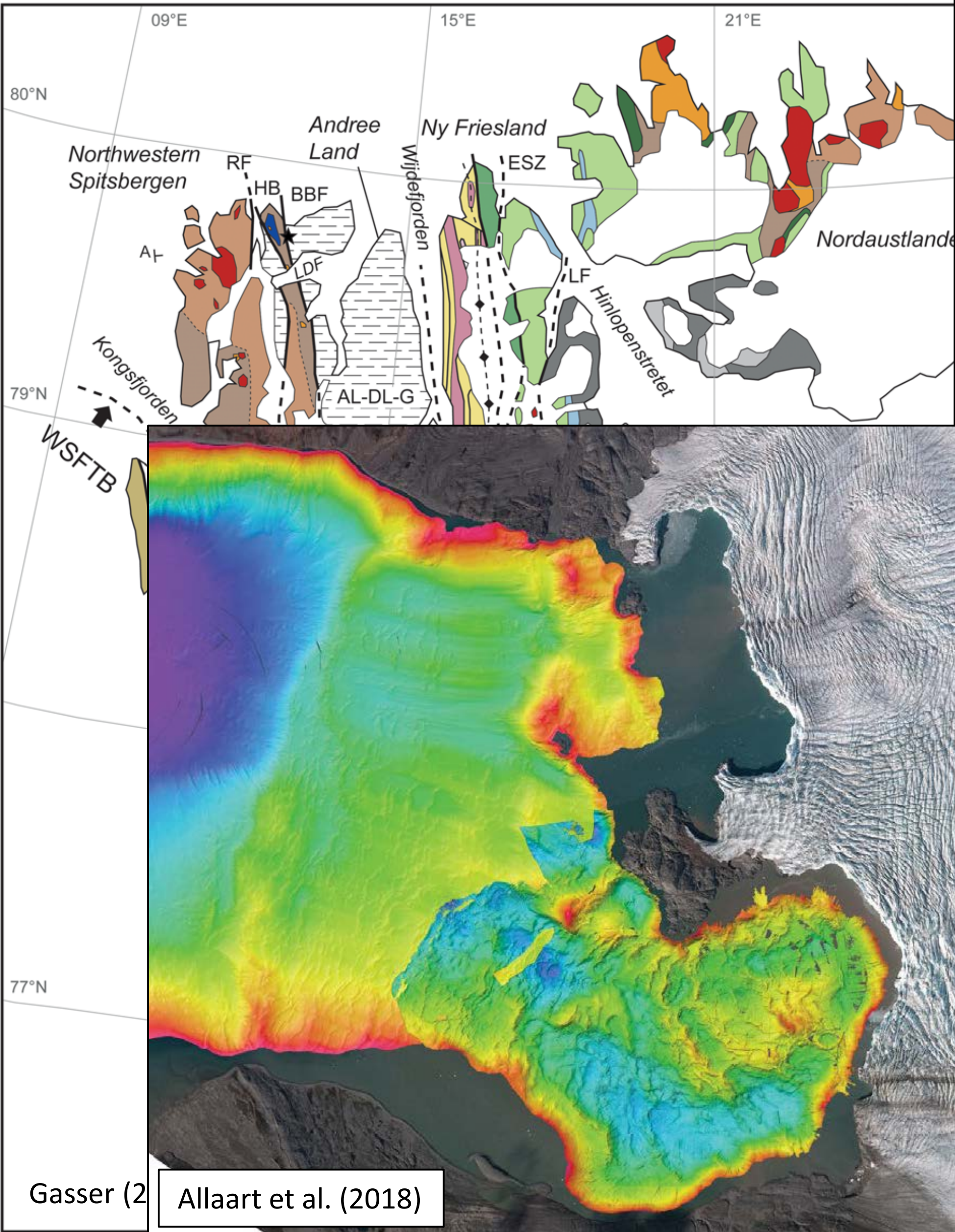

Gasser (2

Allaart et al. (2018)

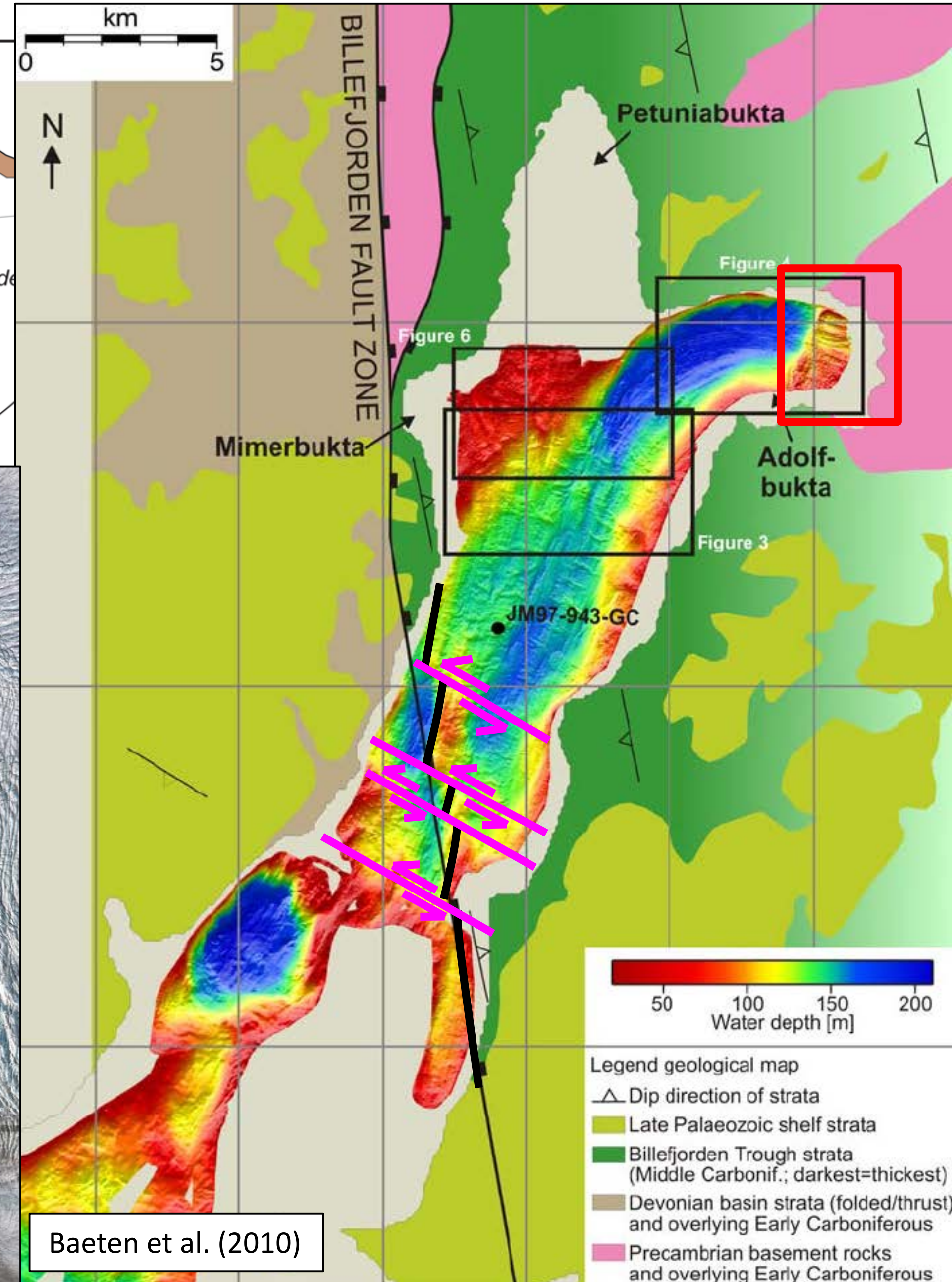

Baeten et al. (2010)

2 Bathymetry data in Billefjorden show that the N–S-striking Billefjorden Fault Zone is left-laterally offset by WNW–ESE-striking fault-related escarpments.

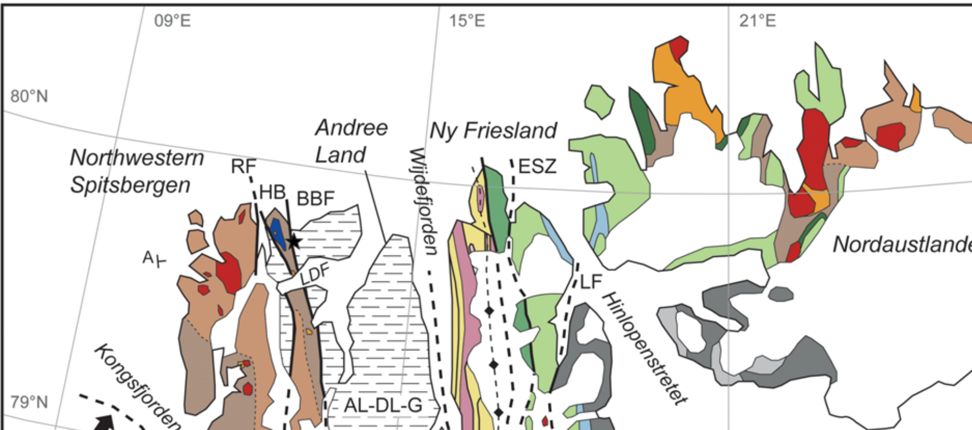

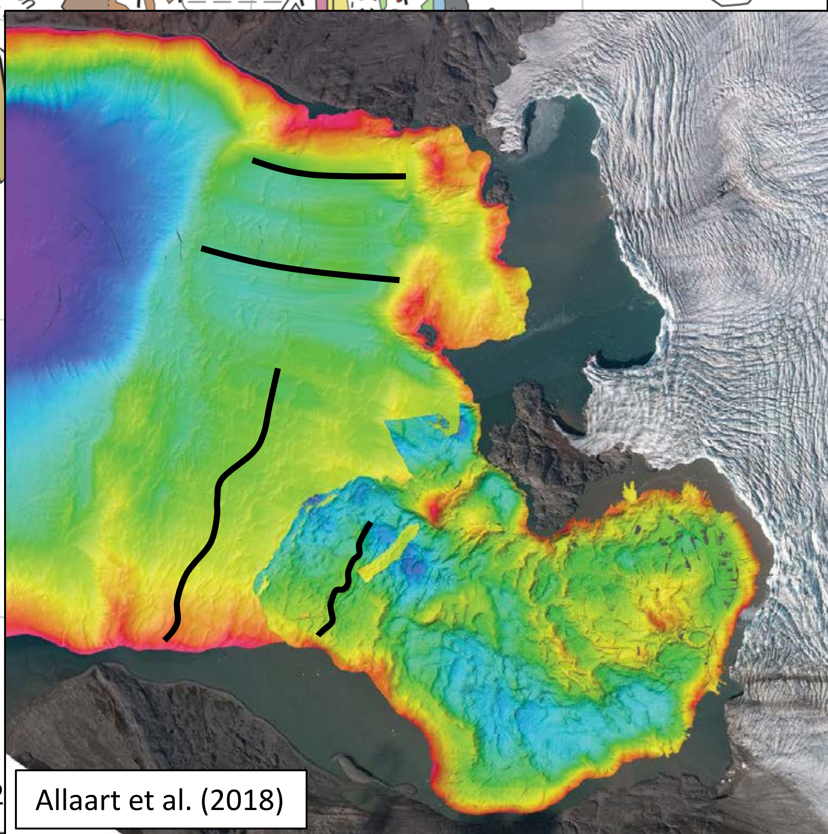

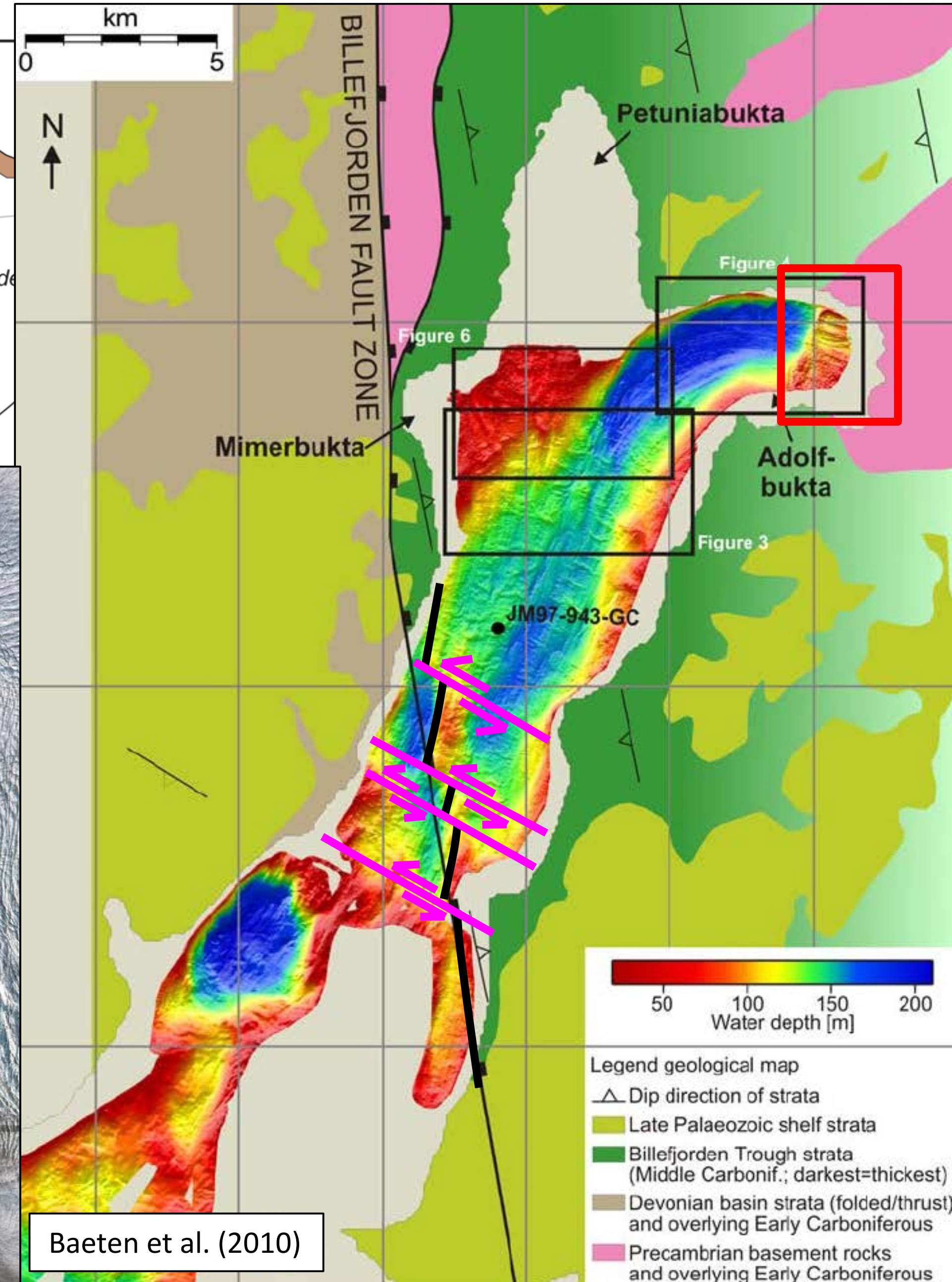

2 **Bathymetry data in Billefjorden show that the N–S-striking Billefjorden Fault Zone is left-laterally offset by WNW–ESE-striking fault-related escarpments.**

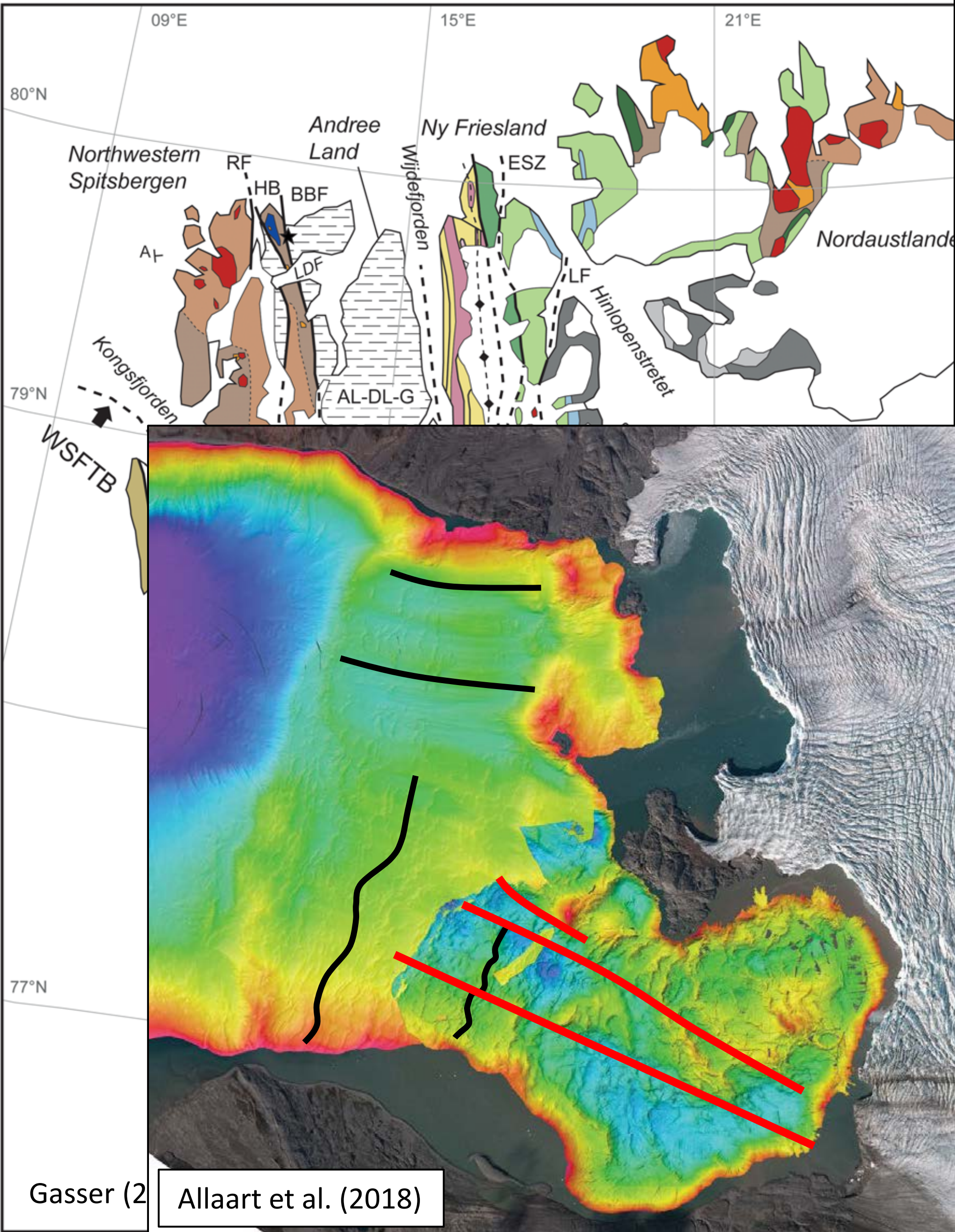

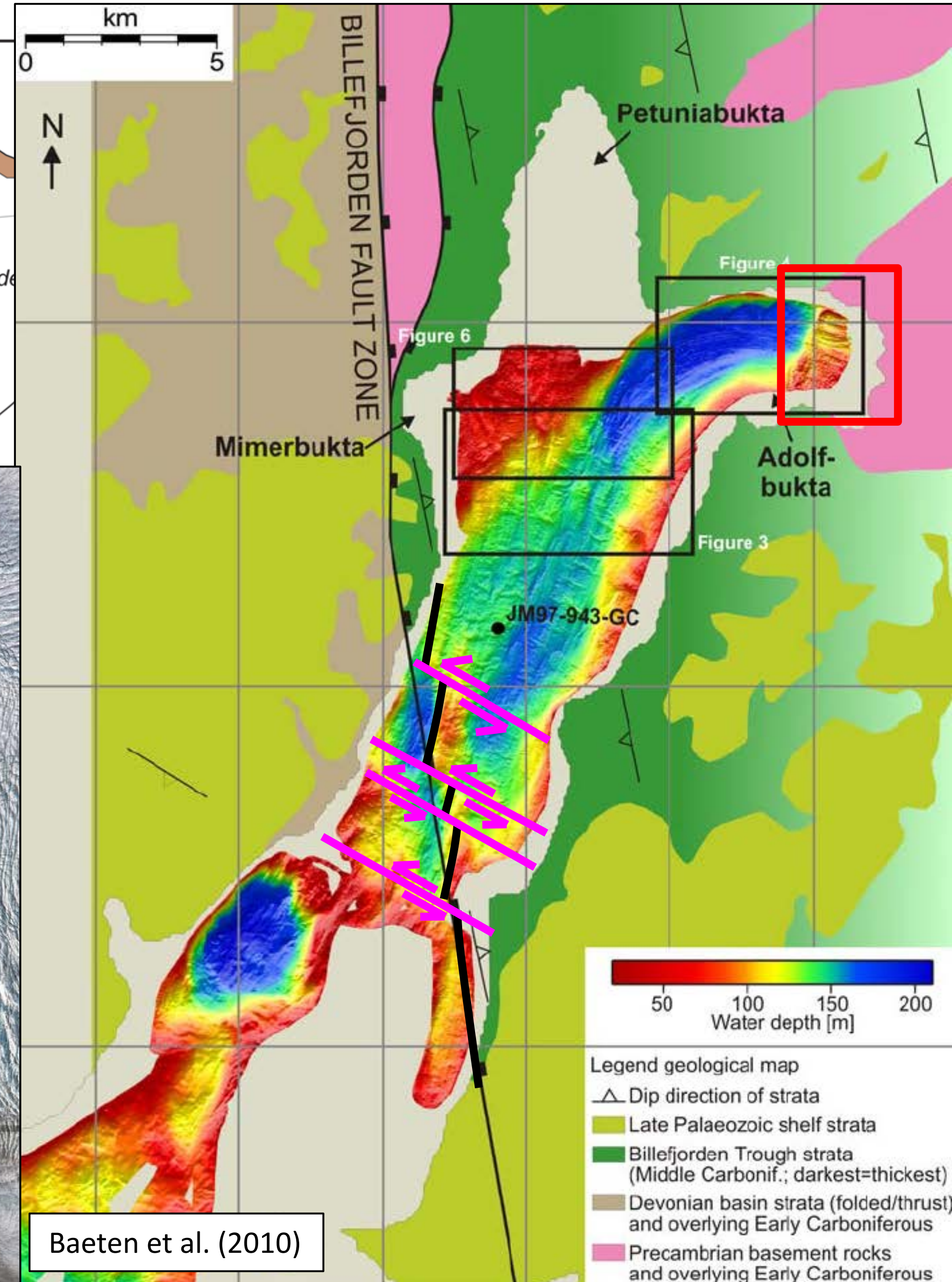

2 Bathymetry data in Billefjorden show that the N–S-striking Billefjorden Fault Zone is left-laterally offset by WNW–ESE-striking fault-related escarpments.

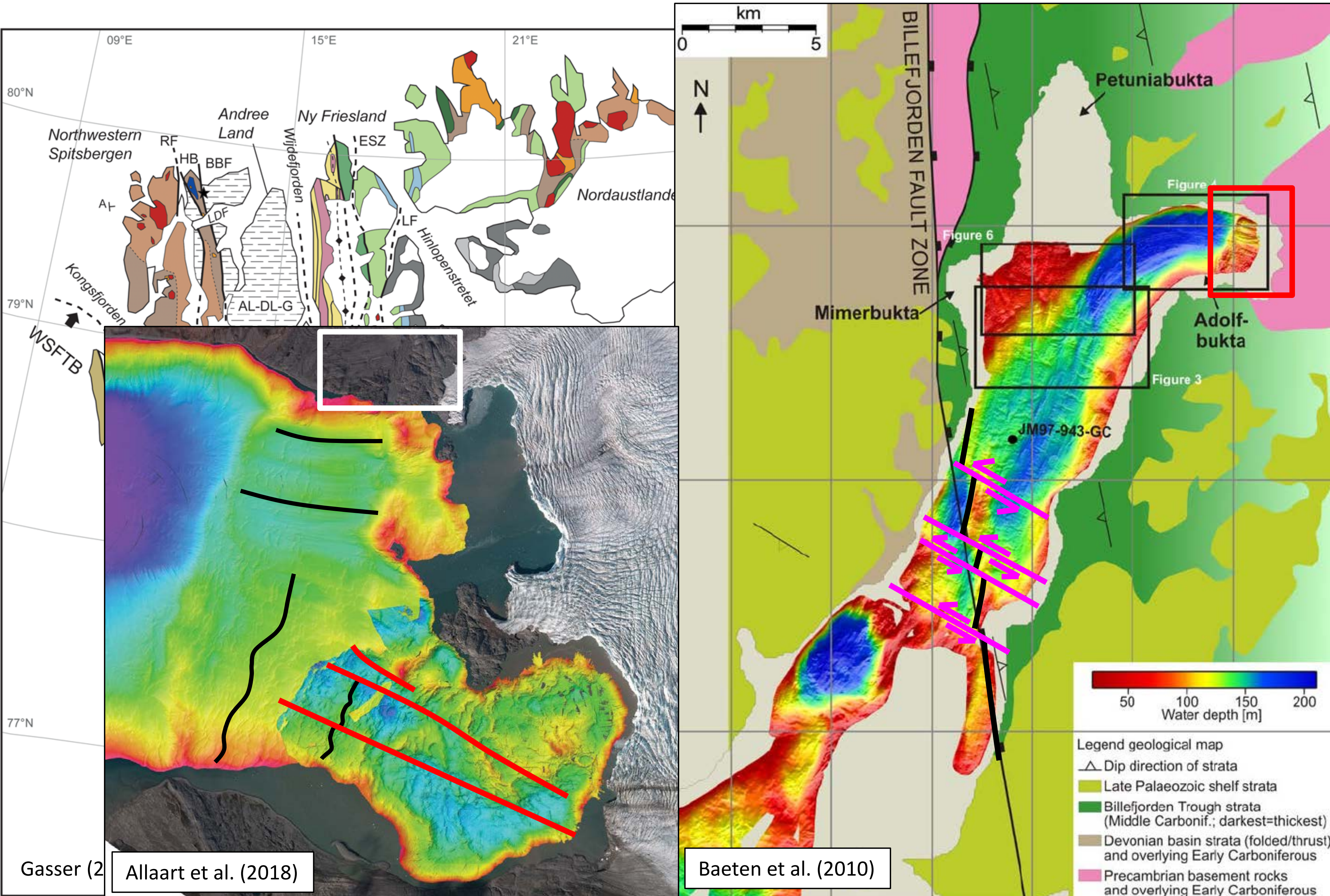

2 Bathymetry data in Billefjorden show that the N–S-striking Billefjorden Fault Zone is left-laterally offset by WNW–ESE-striking fault-related escarpments.

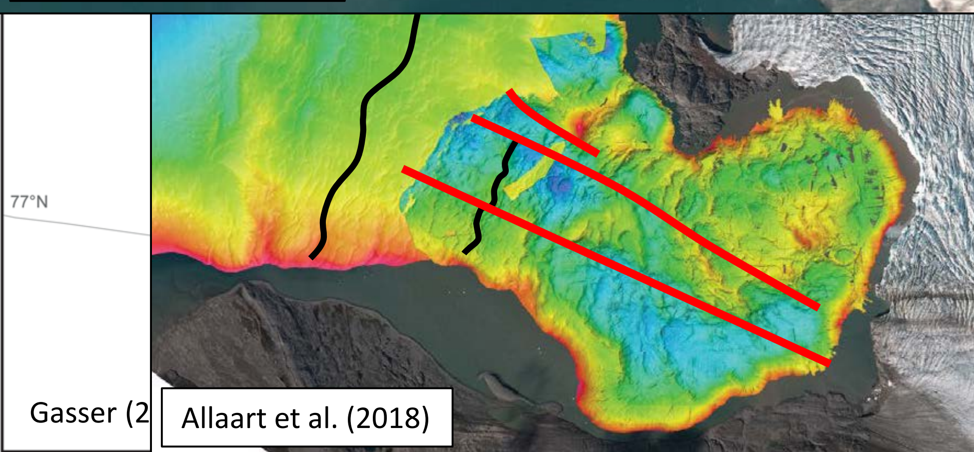

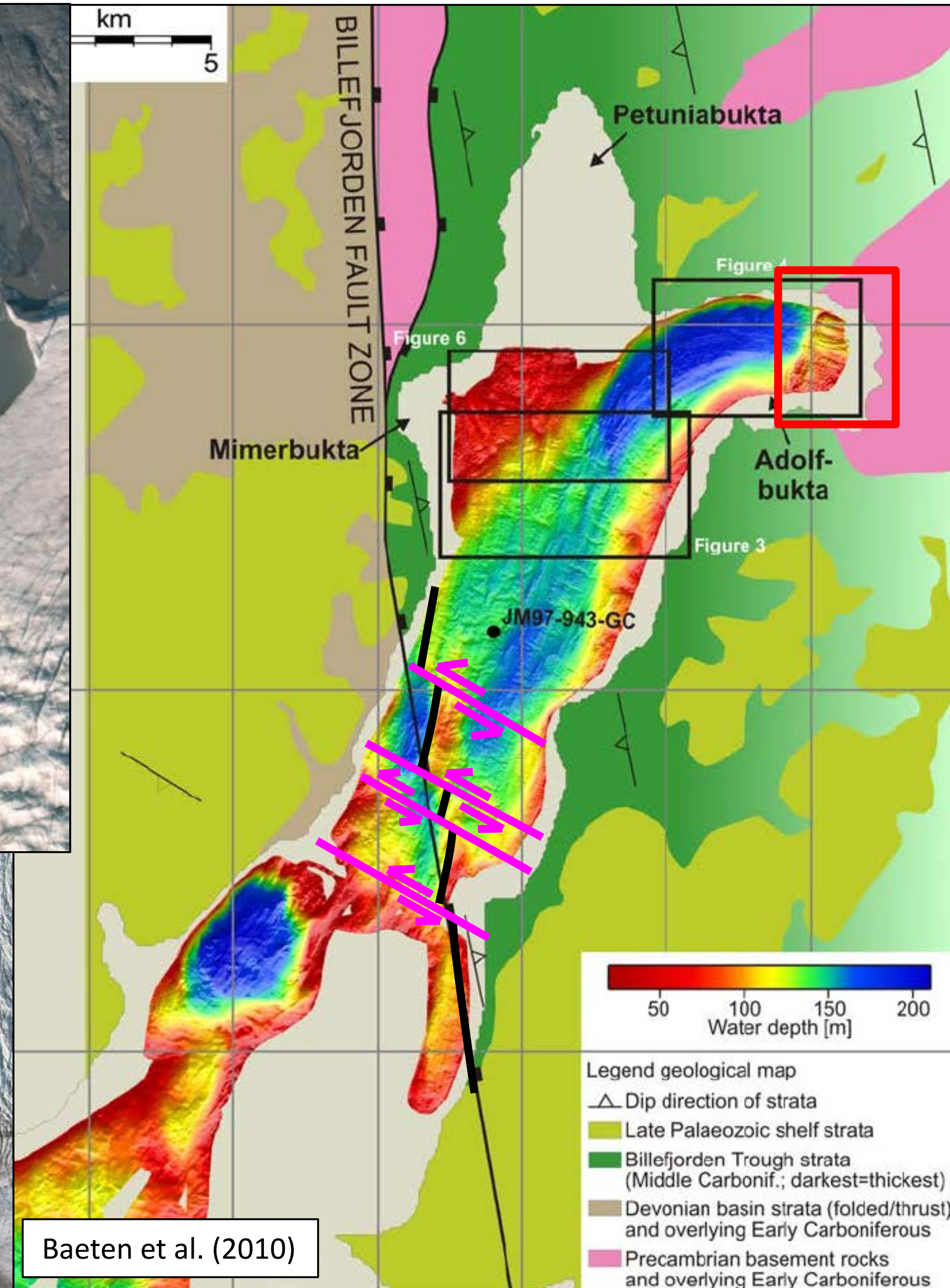

2 **Bathymetry data in Billefjorden show that the N–S-striking Billefjorden Fault Zone is left-laterally offset by WNW–ESE-striking fault-related escarpments.**

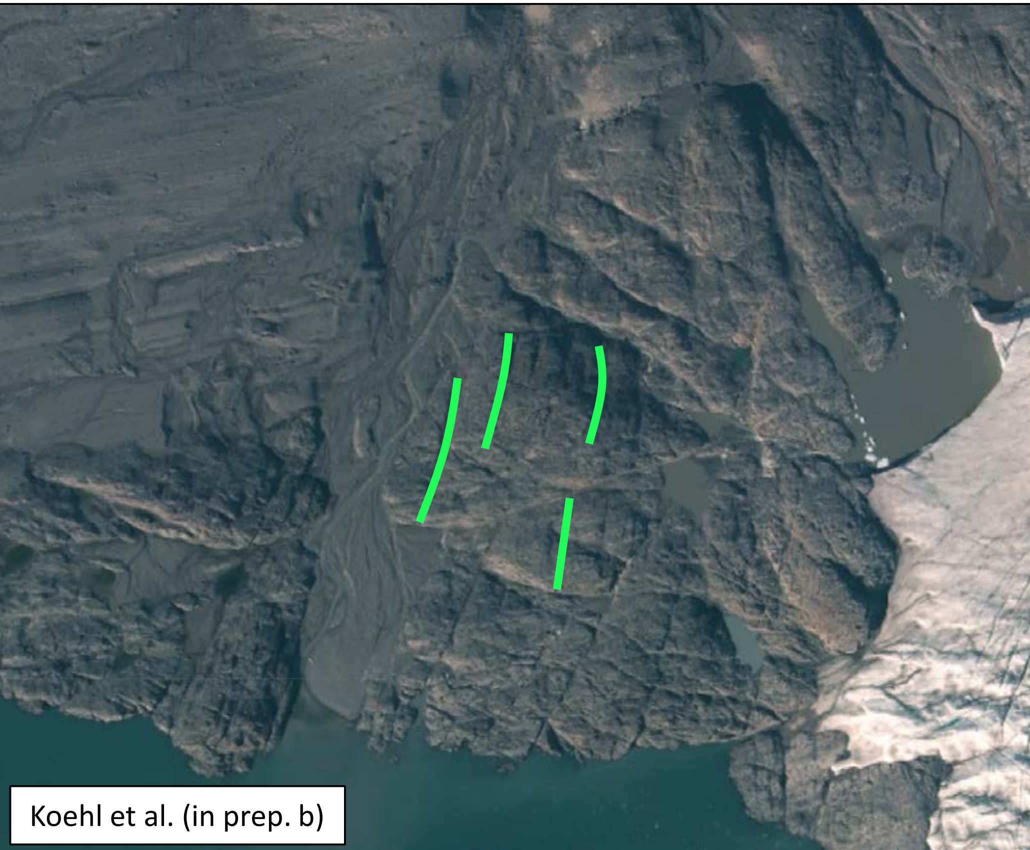

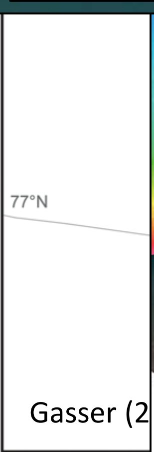

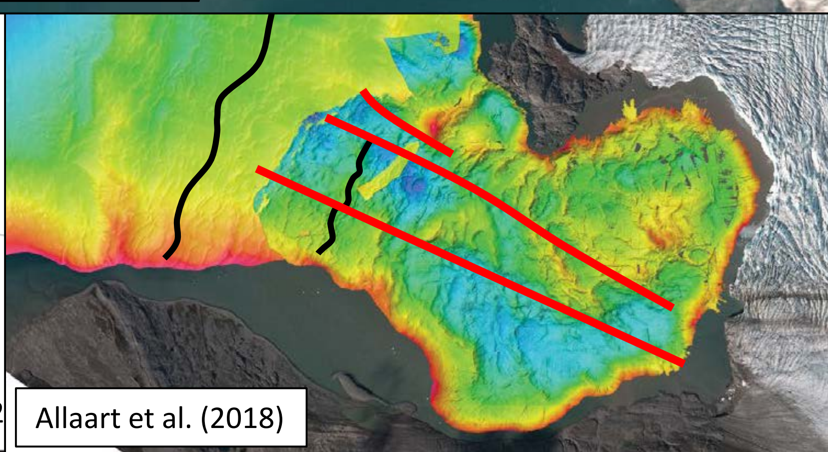

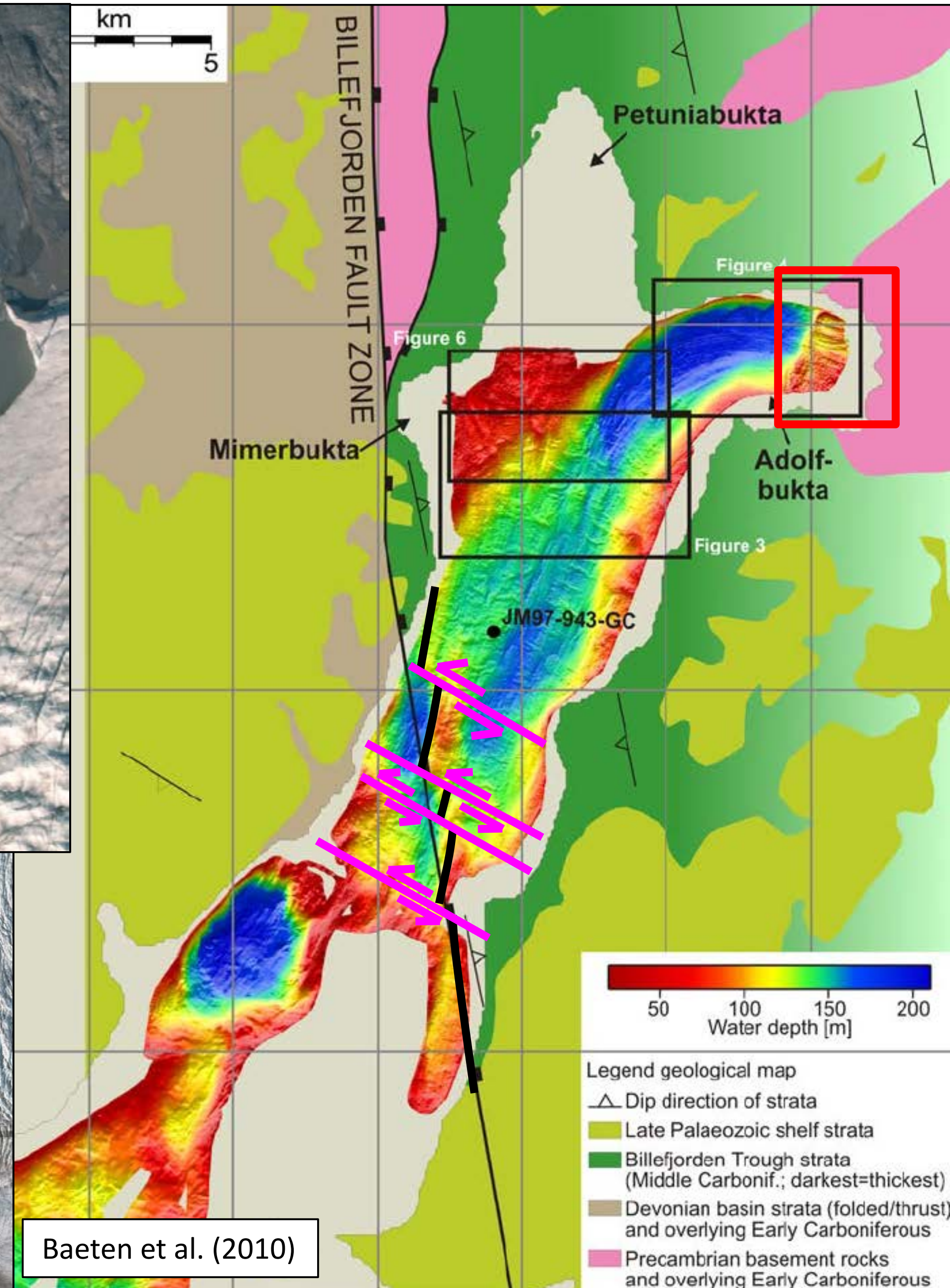

2 Bathymetry data in Billefjorden show that the N–S-striking Billefjorden Fault Zone is left-laterally offset by WNW–ESE-striking fault-related escarpments.

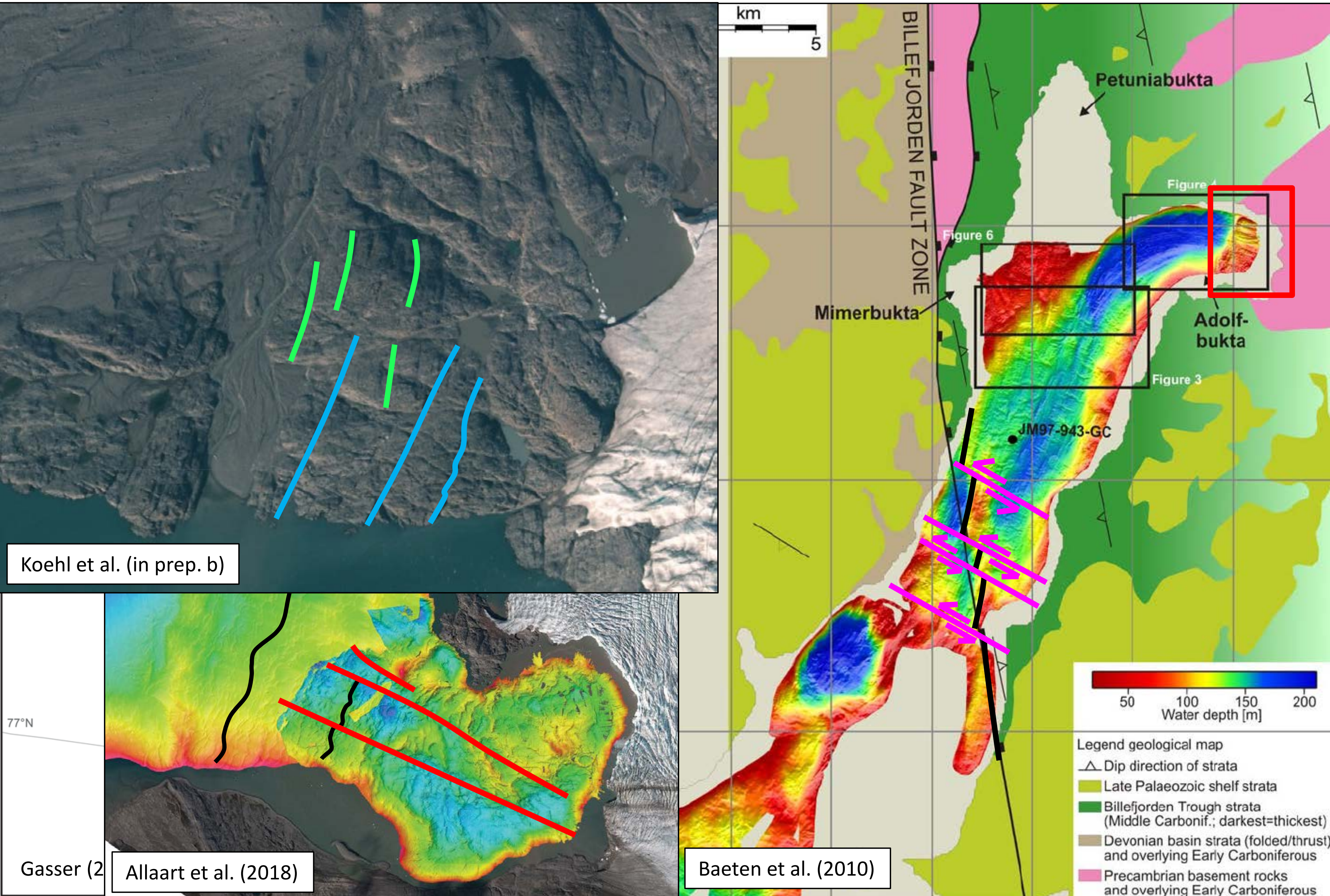

2 Bathymetry data in Billefjorden show that the N–S-striking Billefjorden Fault Zone is left-laterally offset by WNW–ESE-striking fault-related escarpments.

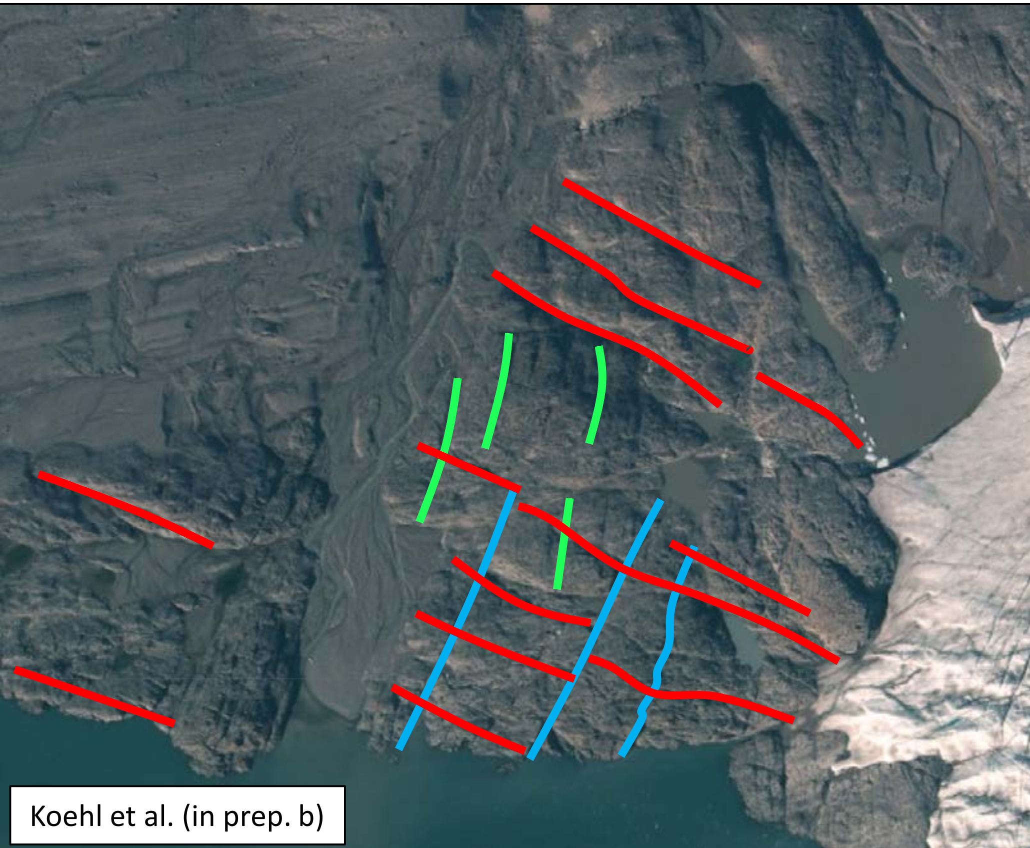

Koehl et al. (in prep. b)

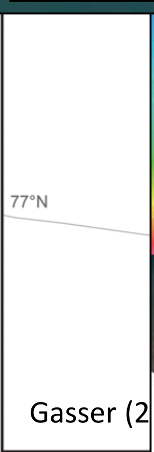

Gasser (2

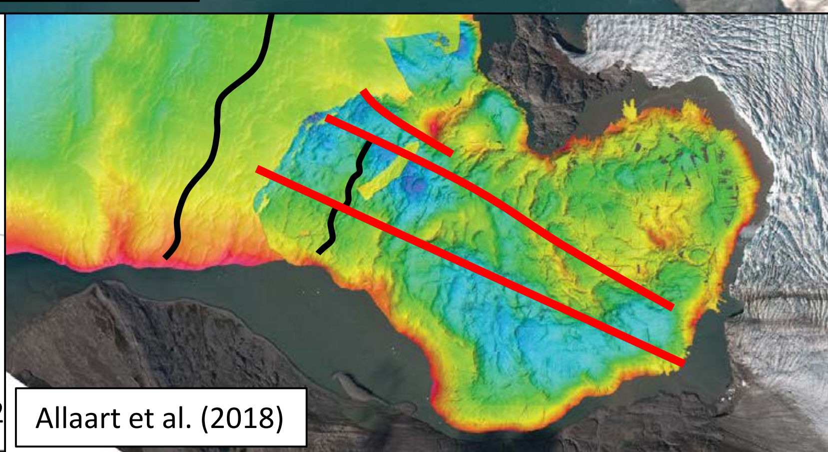

Allaart et al. (2018)

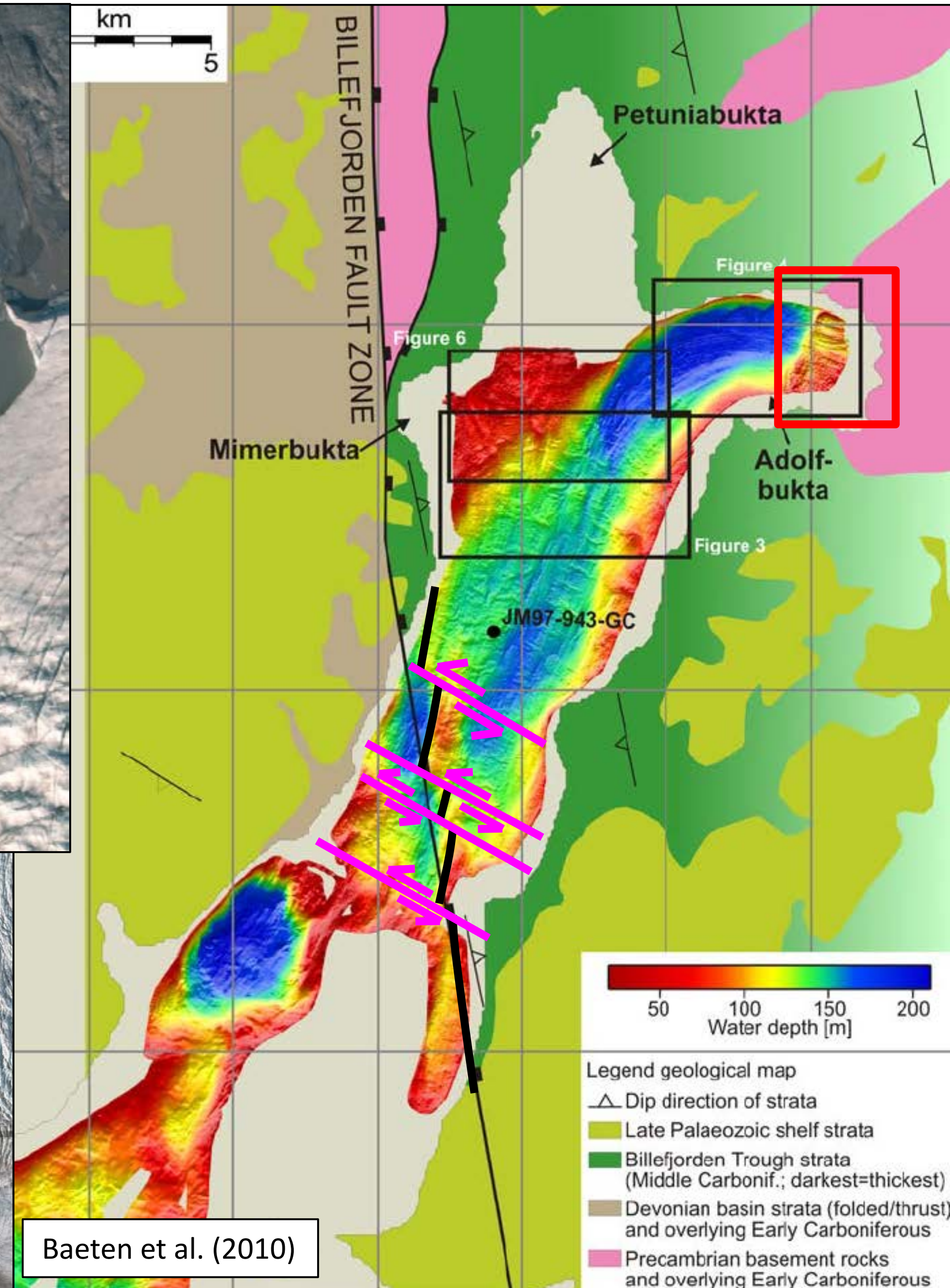

Baeten et al. (2010)

2 **Bathymetry data in Billefjorden show that the N–S-striking Billefjorden Fault Zone is left-laterally offset by WNW–ESE-striking fault-related escarpments.**

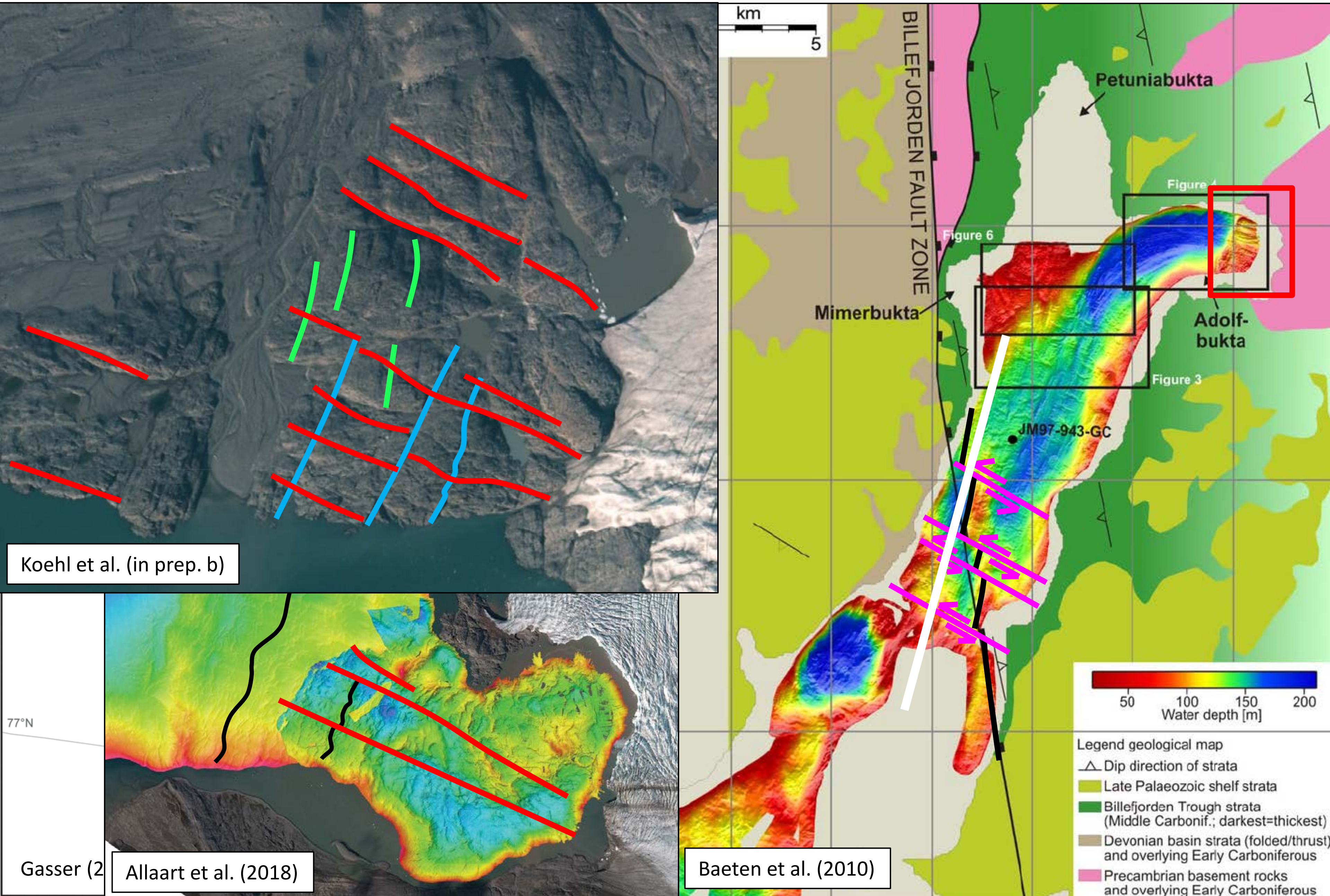

2 **Seismic data show that the WNW–ESE-striking faults that offset the Billefjorden Fault Zone correspond to reactivated Devonian normal faults merging into basement fabrics.**

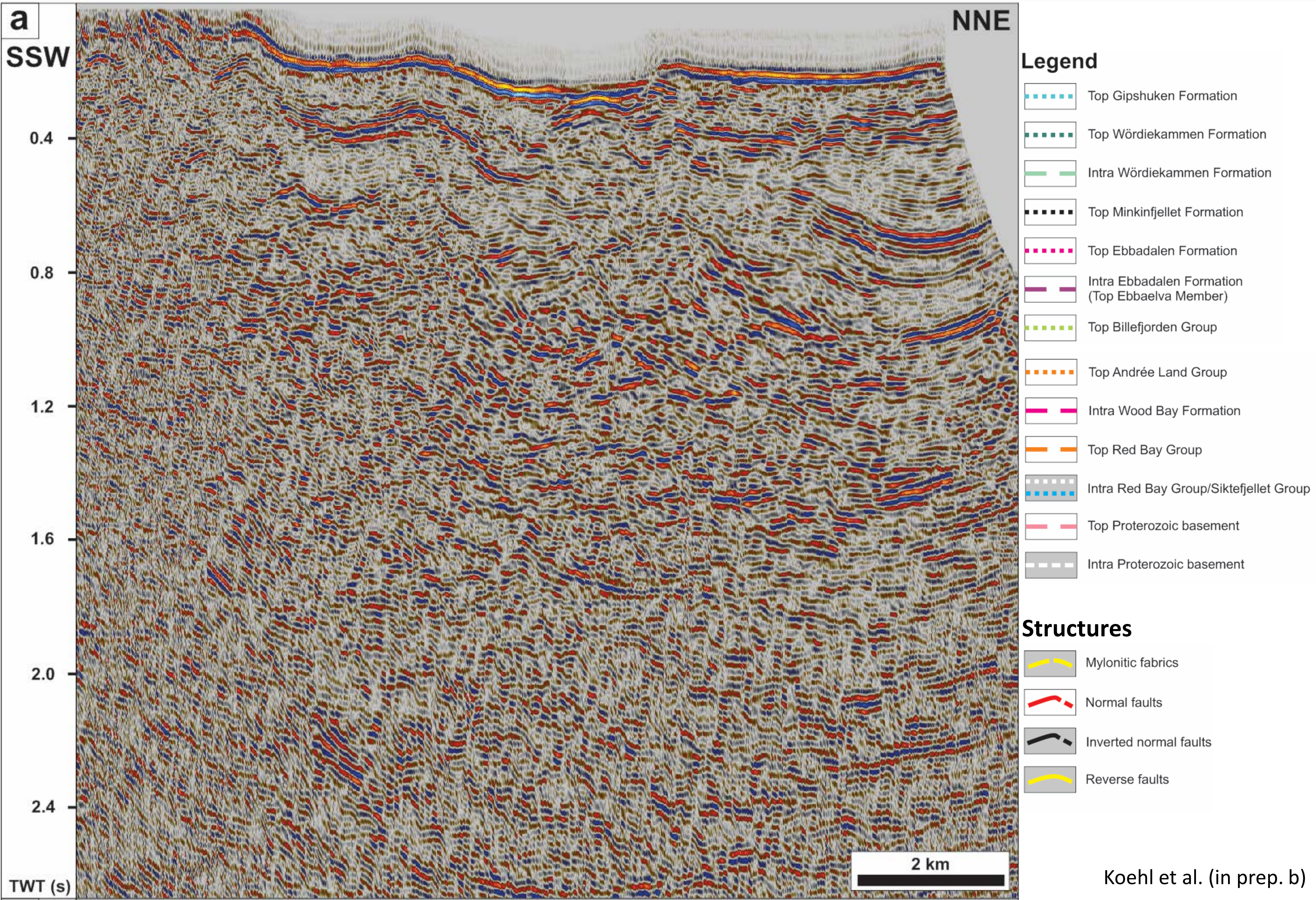

Koehl et al. (in prep. b)

2 **Seismic data show that the WNW–ESE-striking faults that offset the Billefjorden Fault Zone correspond to reactivated Devonian normal faults merging into basement fabrics.**

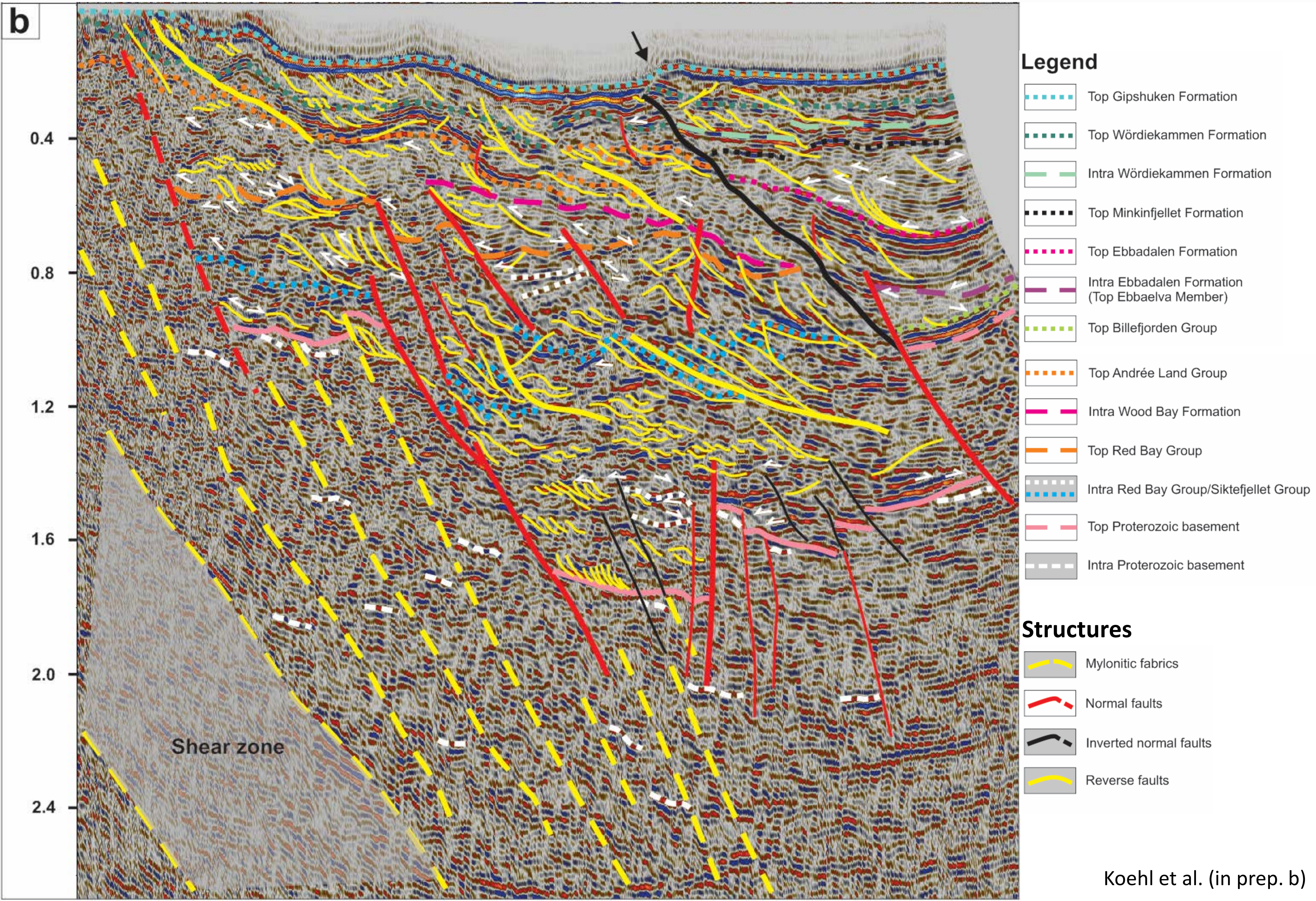

Koehl et al. (in prep. b)

2

Bathymetry data in Kongsfjorden show that WNW–ESE-trending fault-related escarpments offset a N–S-striking Cenozoic fault by 4.5 km left-laterally.

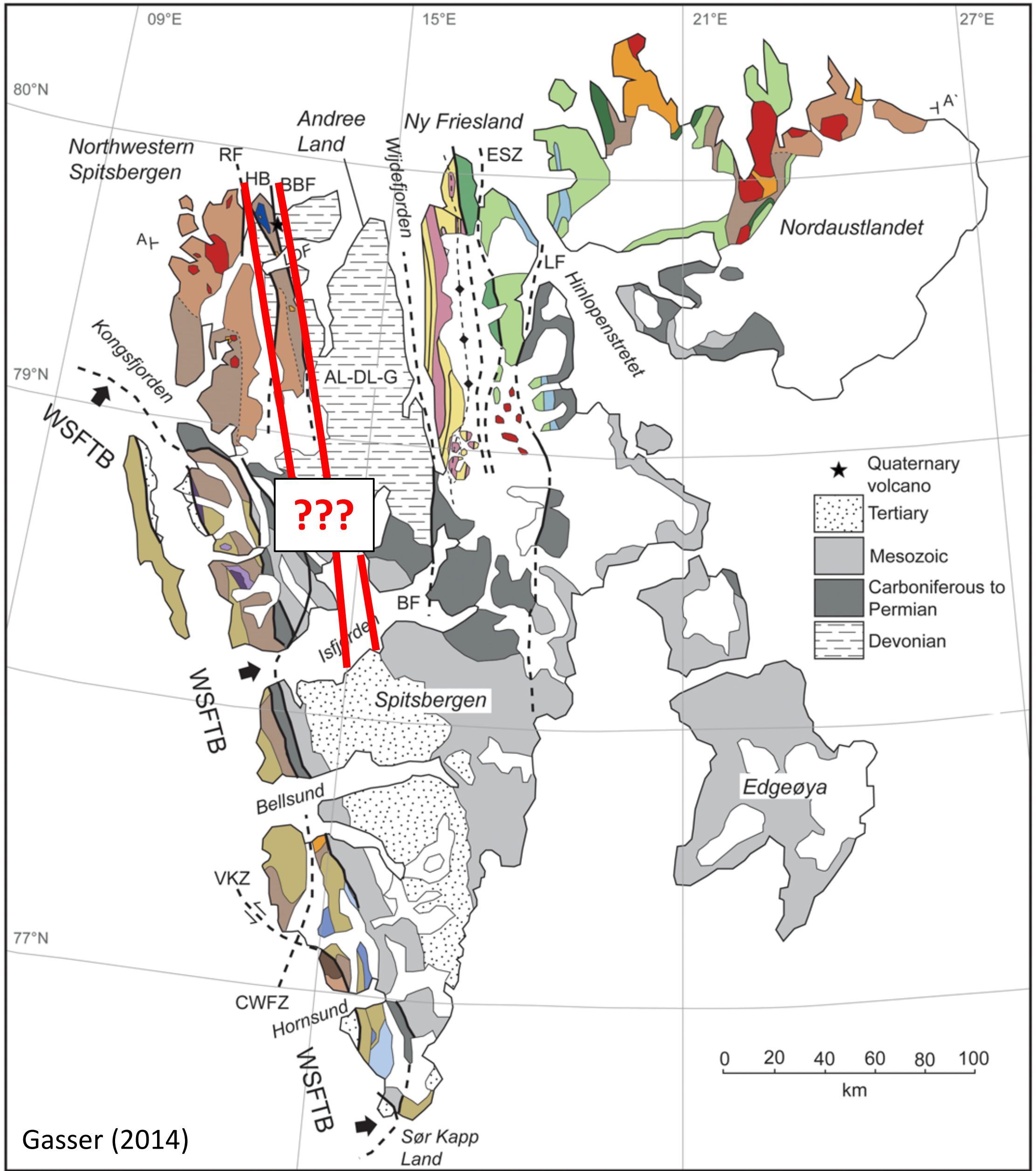

2

Bathymetry data in Kongsfjorden show that WNW–ESE-trending fault-related escarpments offset a N–S-striking Cenozoic fault by 4.5 km left-laterally.

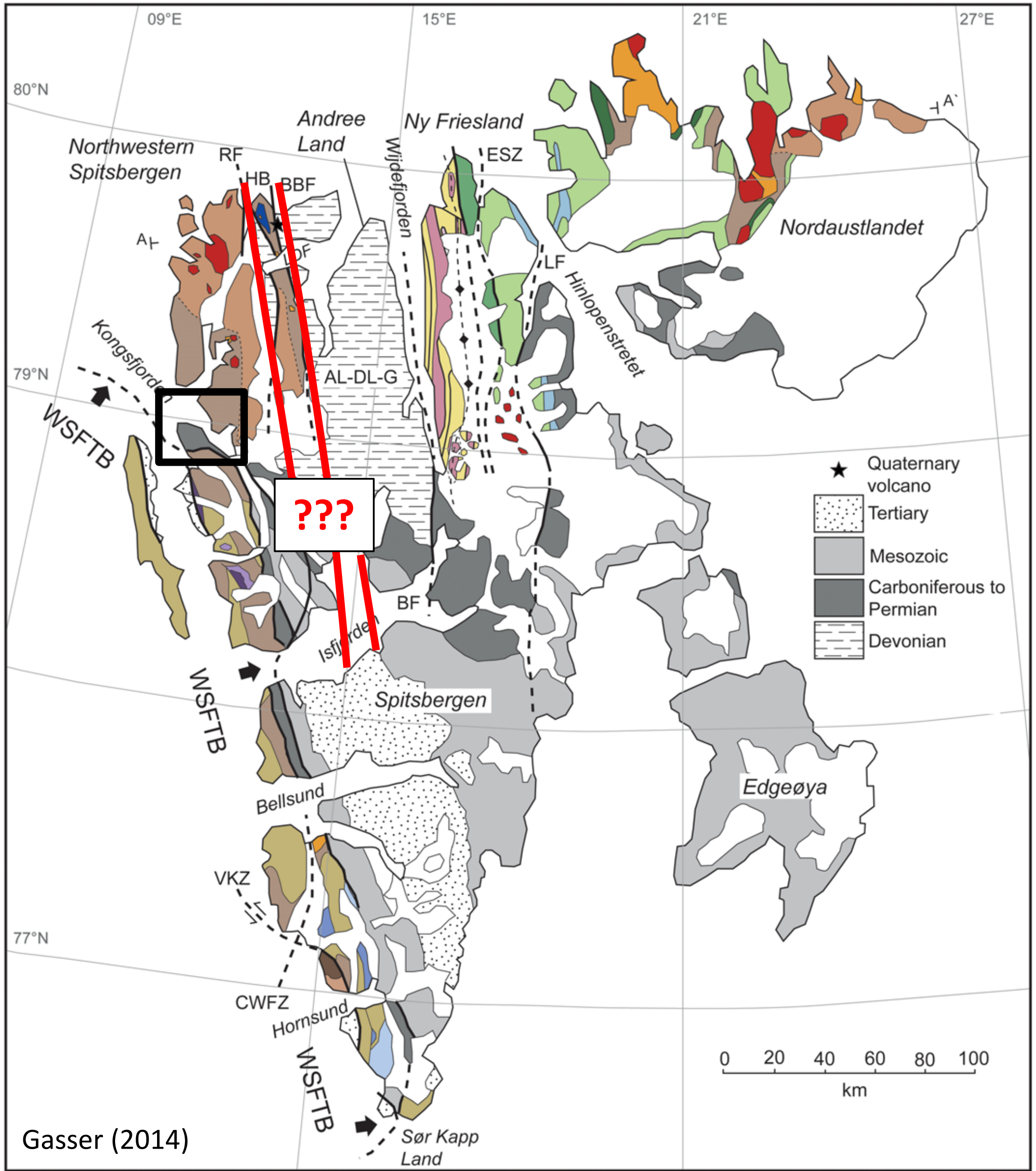

2

Bathymetry data in Kongsfjorden show that WNW–ESE-trending fault-related escarpments offset a N–S-striking Cenozoic fault by 4.5 km left-laterally.

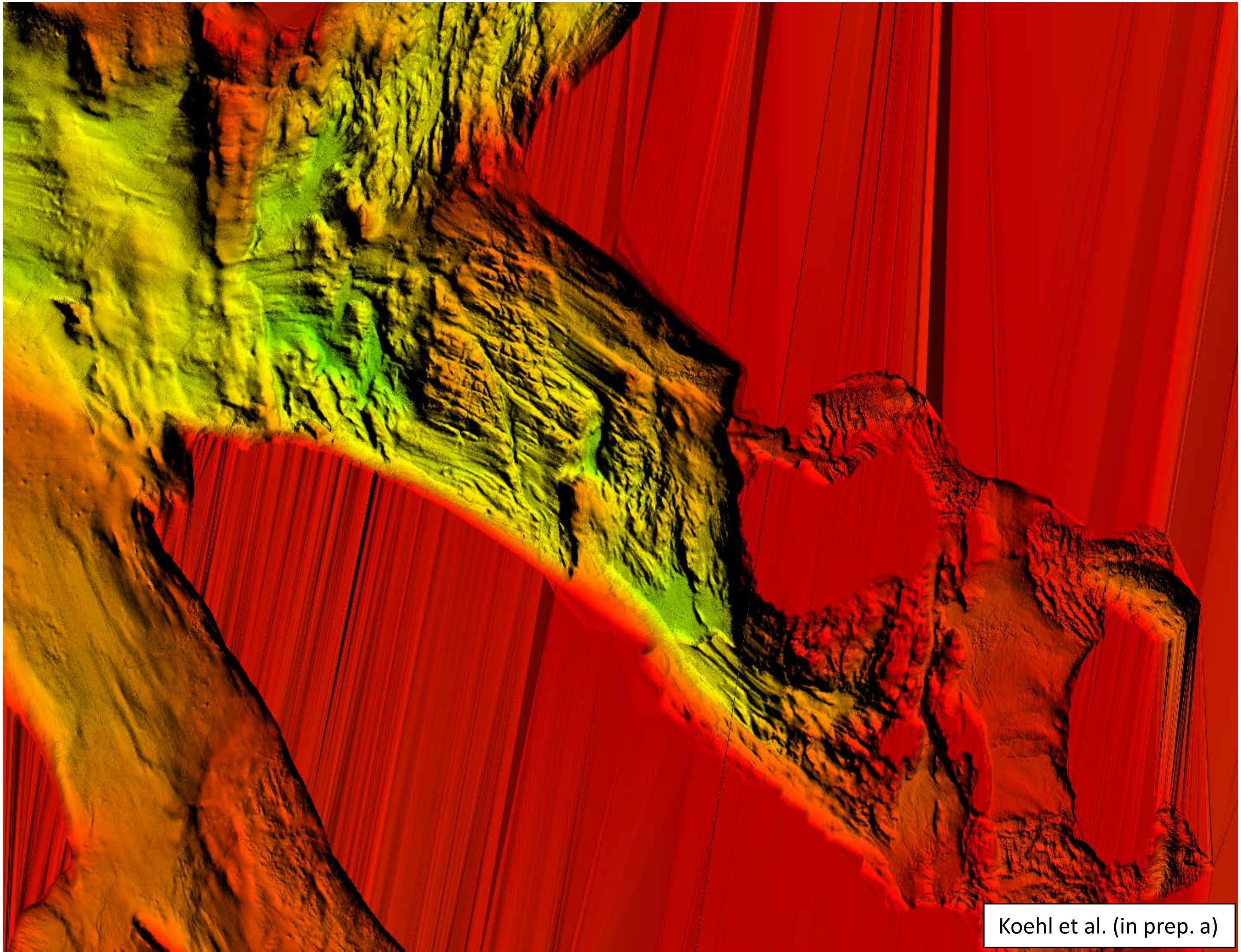

Koehl et al. (in prep. a)

2 **Bathymetry data in Kongsfjorden show that WNW–ESE-trending fault-related escarpments offset a N–S-striking Cenozoic fault by 4.5 km left-laterally.**

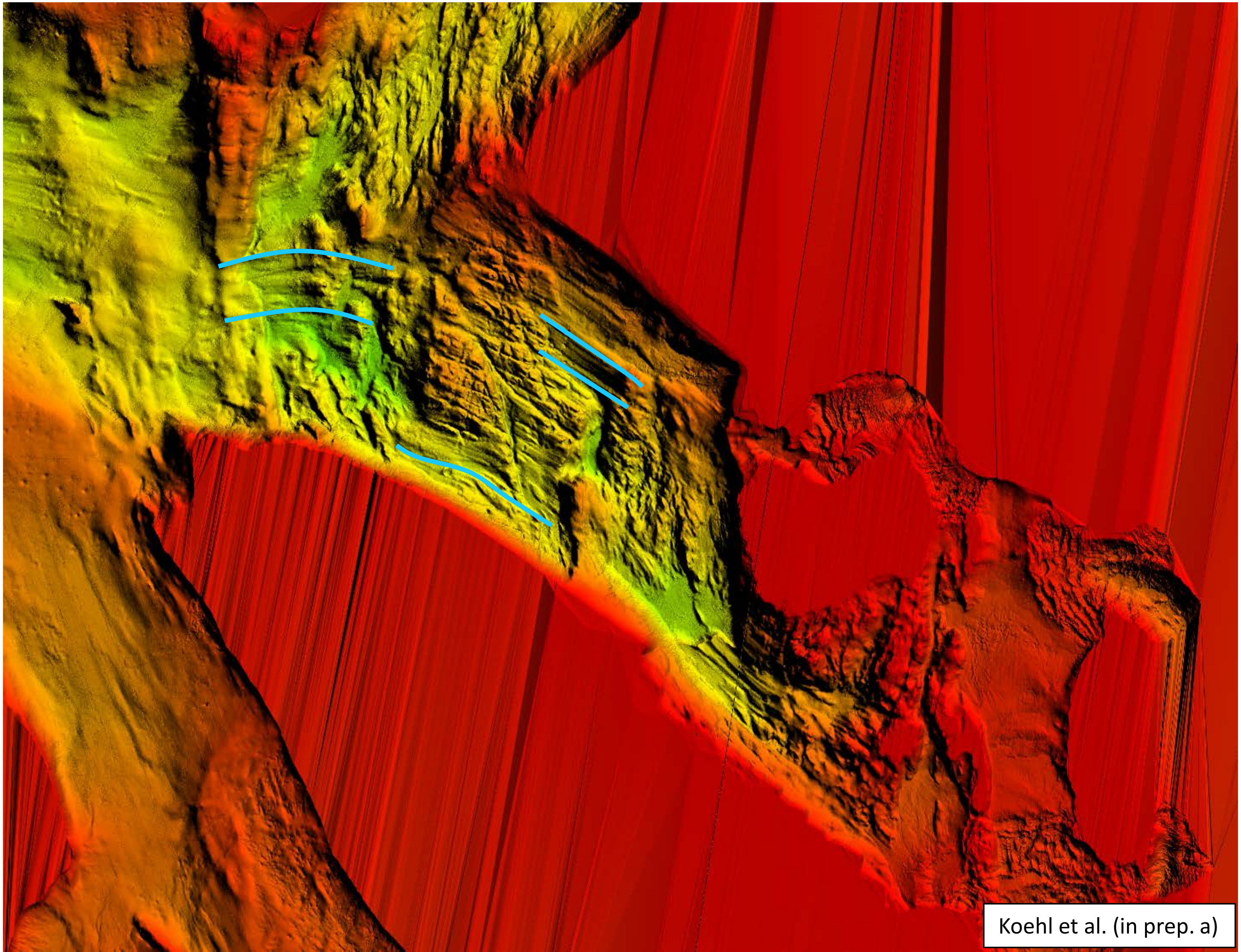

Koehl et al. (in prep. a)

2 **Bathymetry data in Kongsfjorden show that WNW–ESE-trending fault-related escarpments offset a N–S-striking Cenozoic fault by 4.5 km left-laterally.**

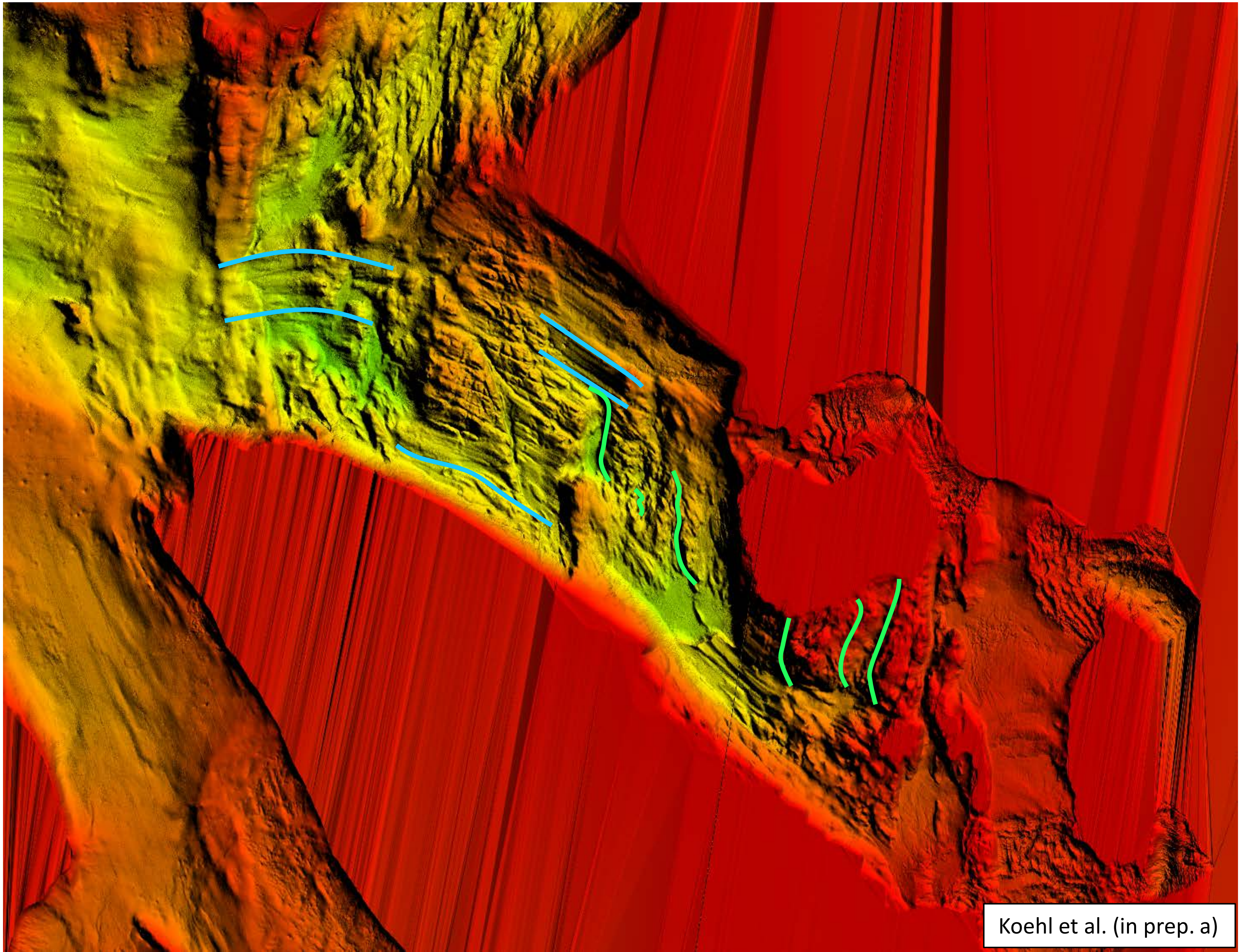

2 **Bathymetry data in Kongsfjorden show that WNW–ESE-trending fault-related escarpments offset a N–S-striking Cenozoic fault by 4.5 km left-laterally.**

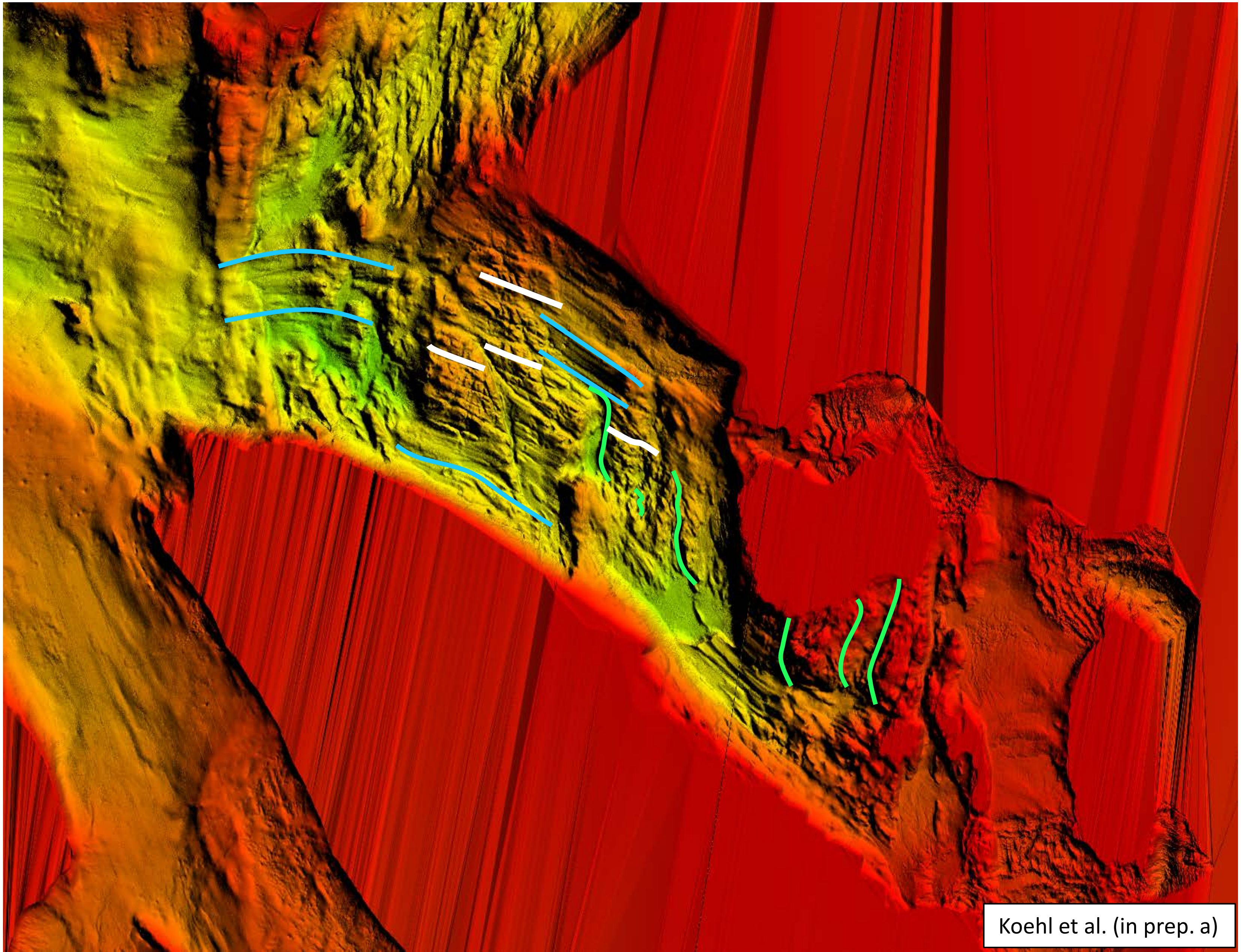

2 **Bathymetry data in Kongsfjorden show that WNW–ESE-trending fault-related escarpments offset a N–S-striking Cenozoic fault by 4.5 km left-laterally.**

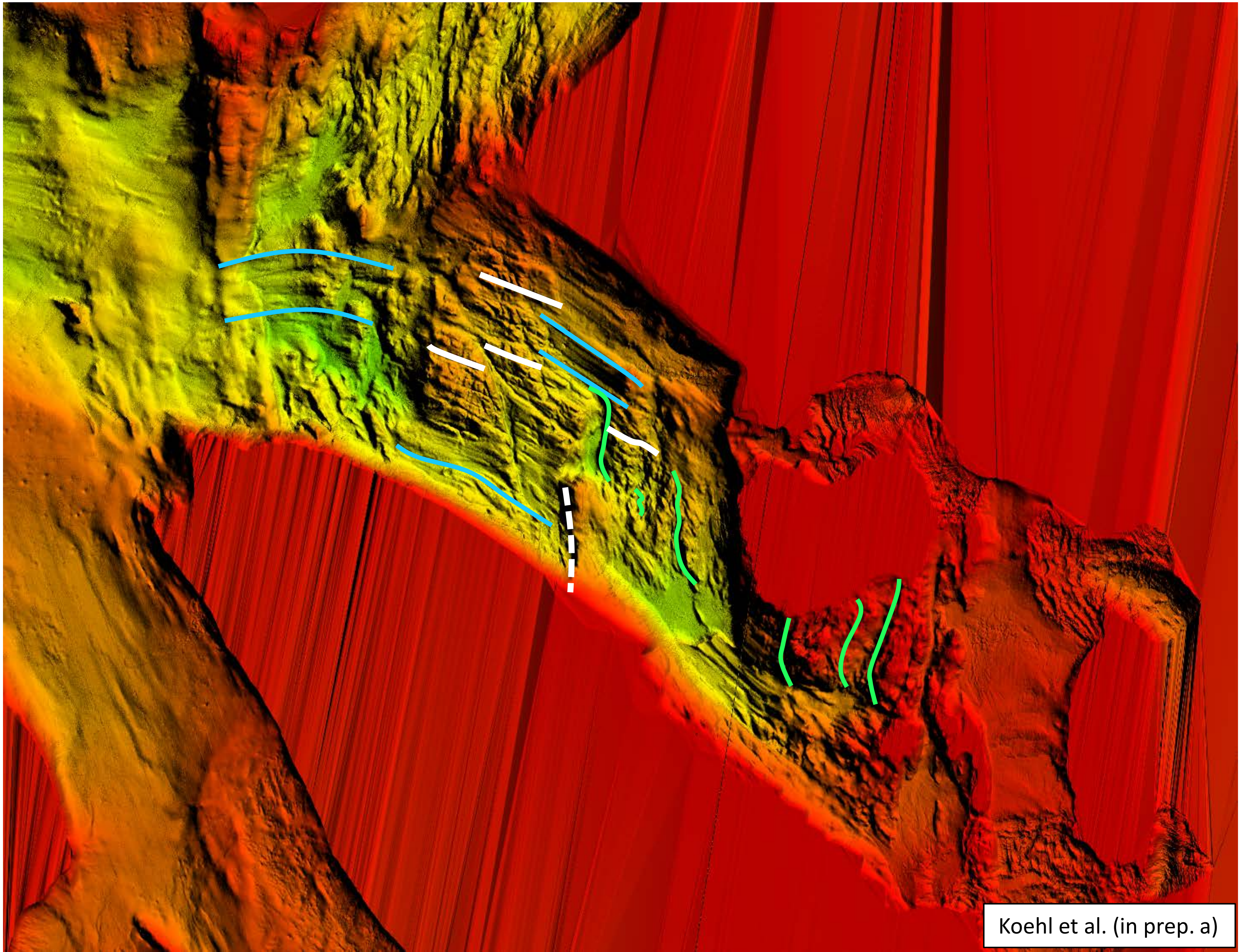

Koehl et al. (in prep. a)

2 **Bathymetry data in Kongsfjorden show that WNW–ESE-trending fault-related escarpments offset a N–S-striking Cenozoic fault by 4.5 km left-laterally.**

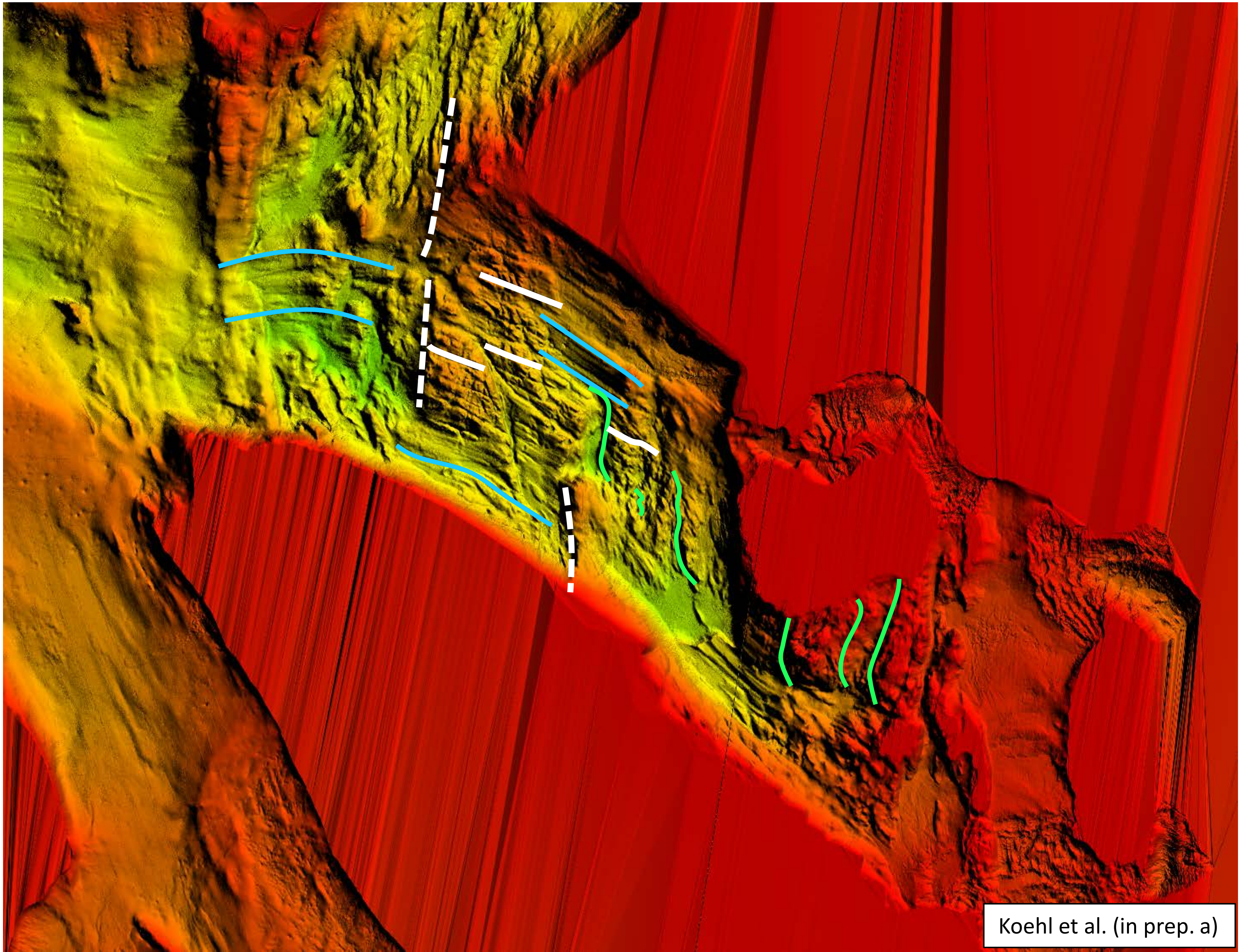

2 **Bathymetry data in Kongsfjorden show that WNW–ESE-trending fault-related escarpments offset a N–S-striking Cenozoic fault by 4.5 km left-laterally.**

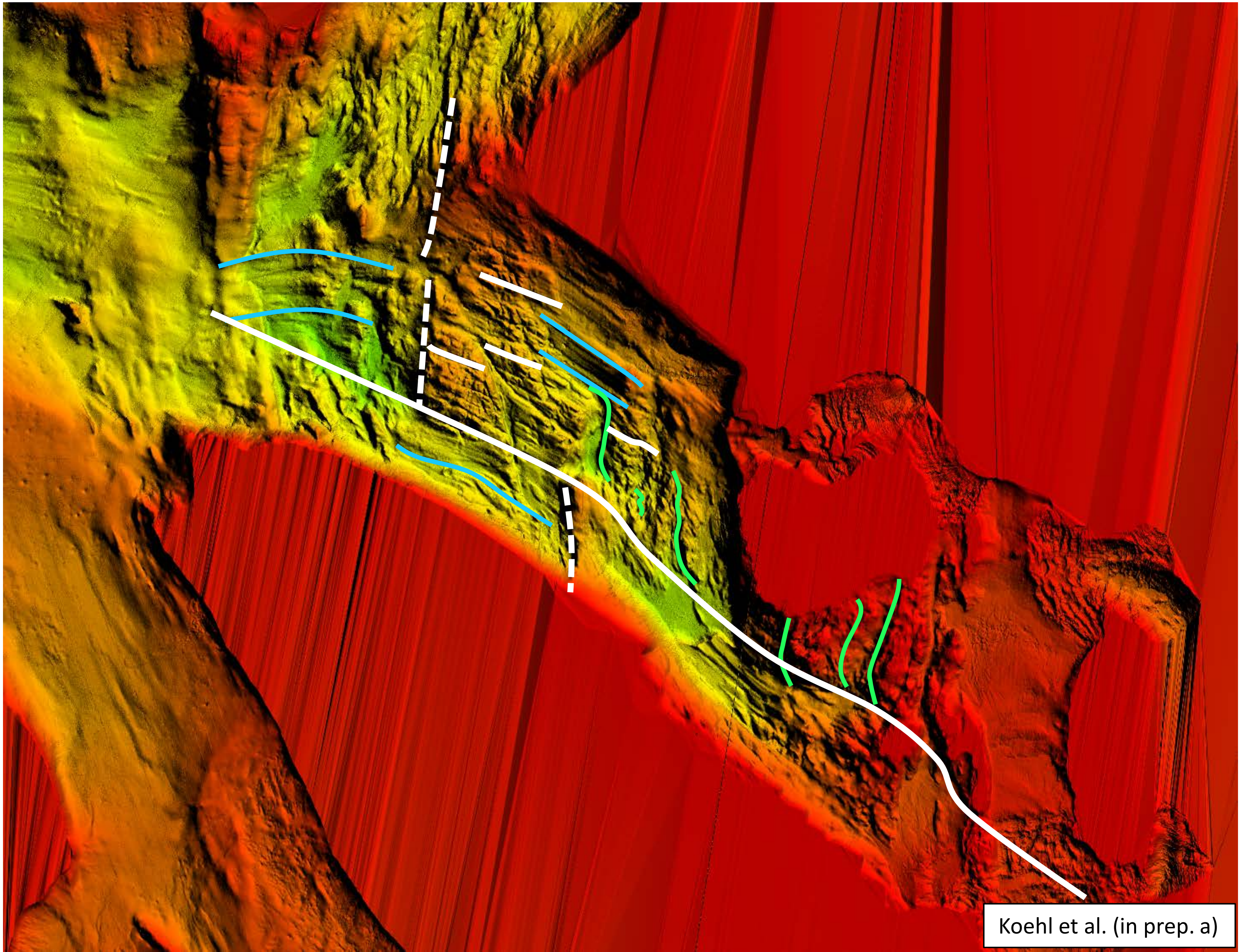

2

Bathymetry data in Kongsfjorden show that WNW–ESE-trending fault-related escarpments offset a N–S-striking Cenozoic fault by 4.5 km left-laterally.

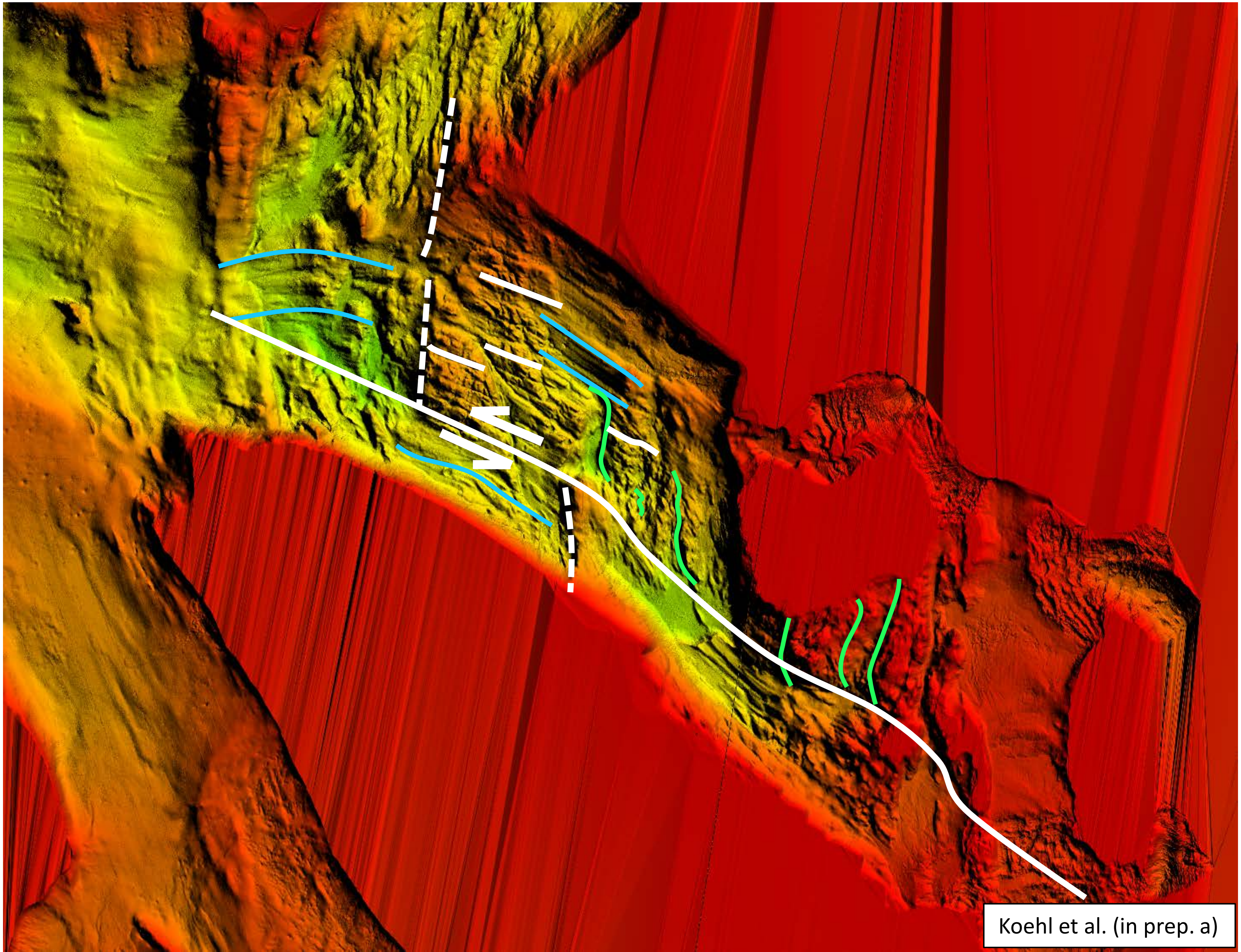

Koehl et al. (in prep. a)

2 **On the 29th of March 2016, an earthquake coinciding with the location of the WNW–ESE-striking Timanian thrust struck near the southwestern coast of Edgeøya.**

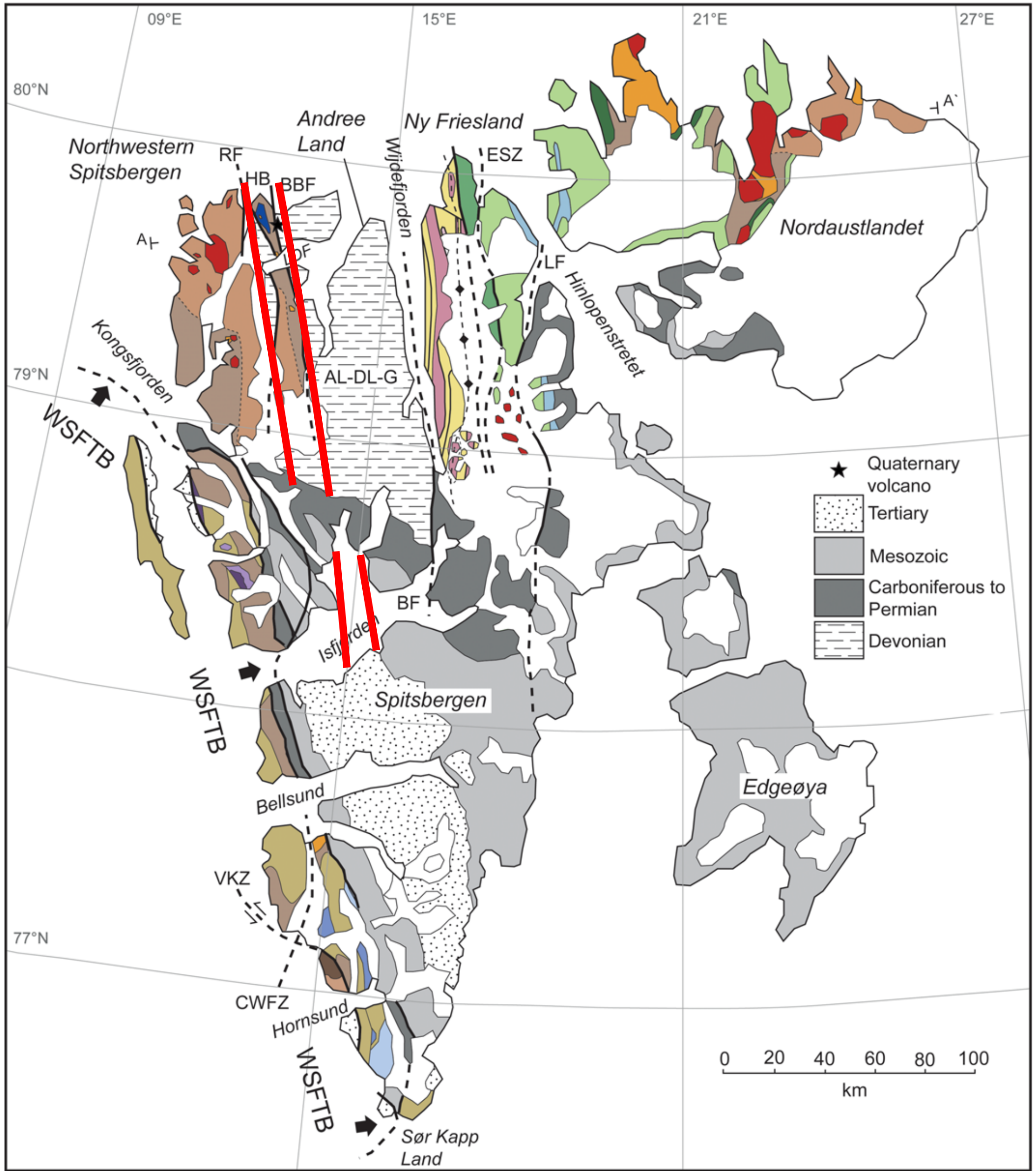

Gasser (2014)

2 **On the 29th of March 2016, an earthquake coinciding with the location of the WNW–ESE-striking Timanian thrust struck near the southwestern coast of Edgeøya.**

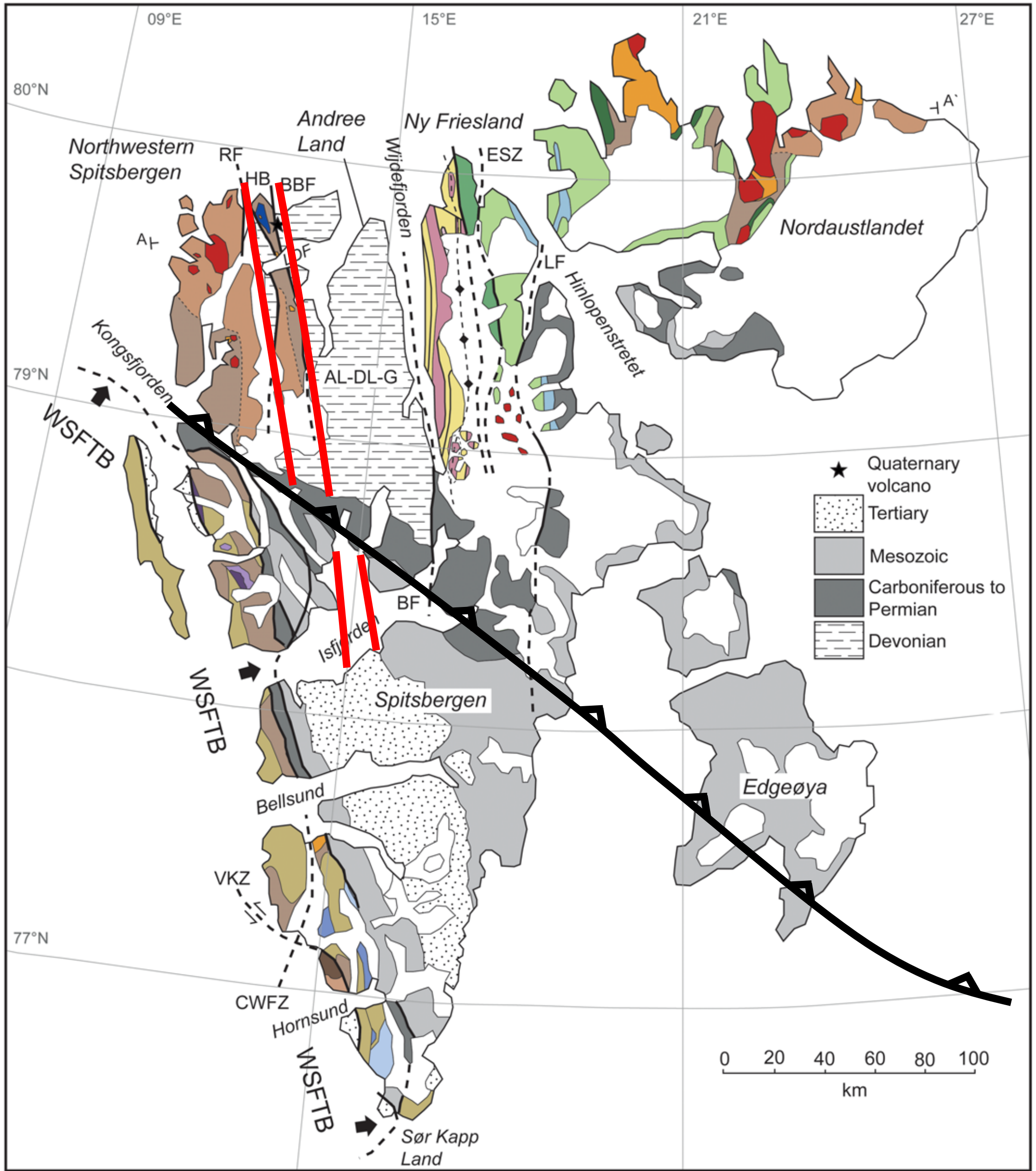

Gasser (2014)

2 **On the 29th of March 2016, an earthquake coinciding with the location of the WNW–ESE-striking Timanian thrust struck near the southwestern coast of Edgeøya.**

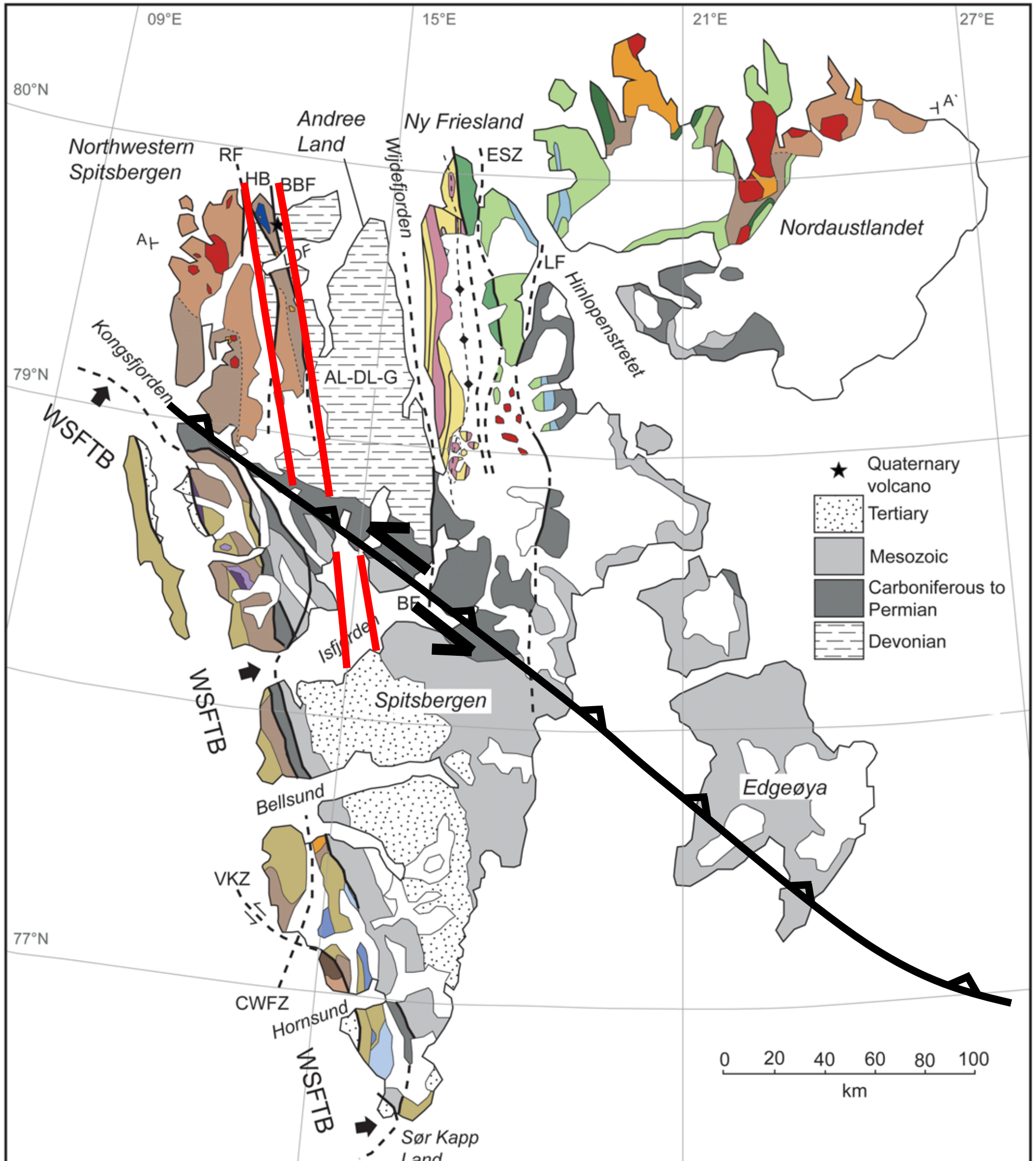

Gasser (2014)

2 **On the 29th of March 2016, an earthquake coinciding with the location of the WNW–ESE-striking Timanian thrust struck near the southwestern coast of Edgeøya.**

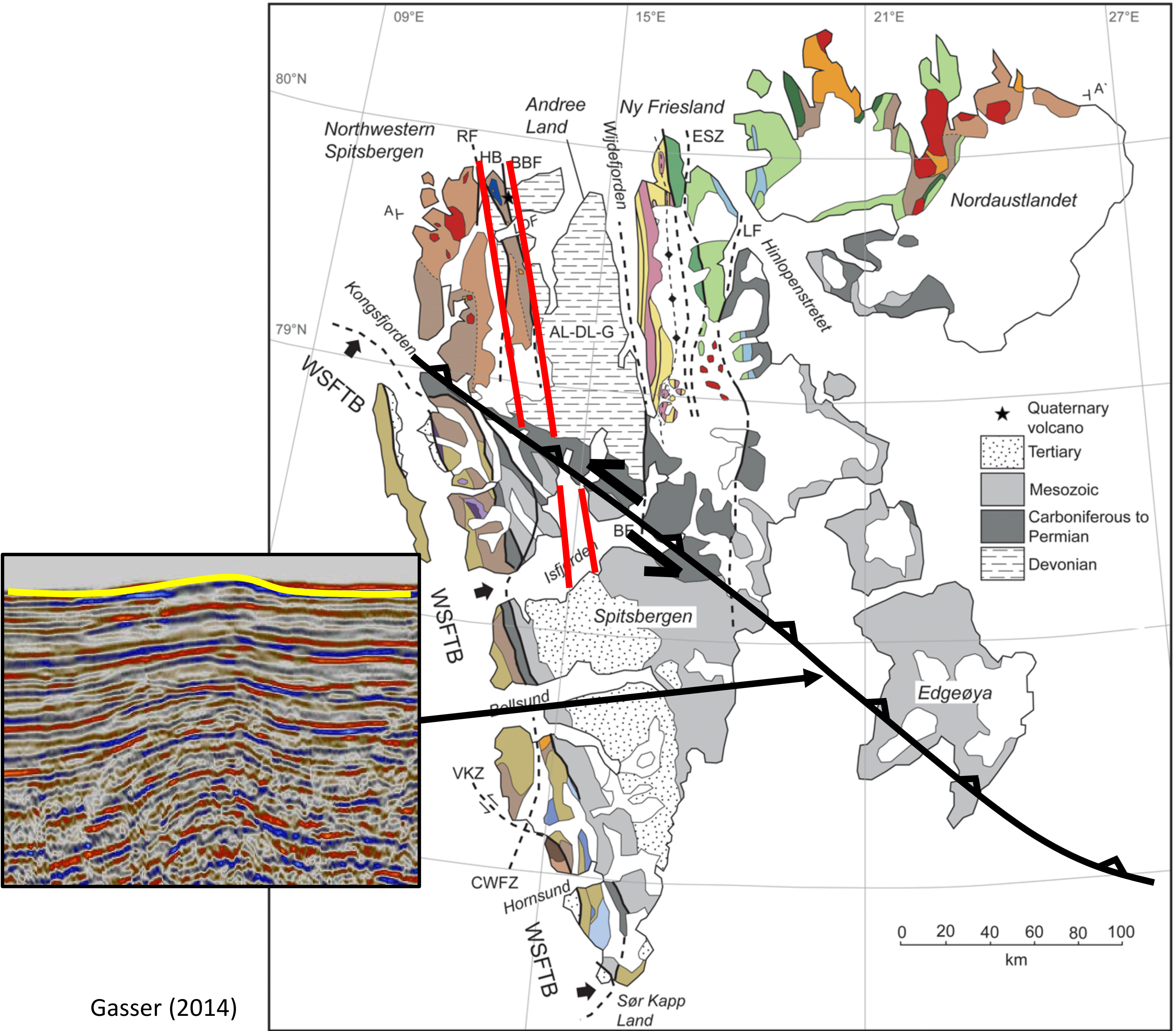

Gasser (2014)

2 **On the 29th of March 2016, an earthquake coinciding with the location of the WNW–ESE-striking Timanian thrust struck near the southwestern coast of Edgeøya.**

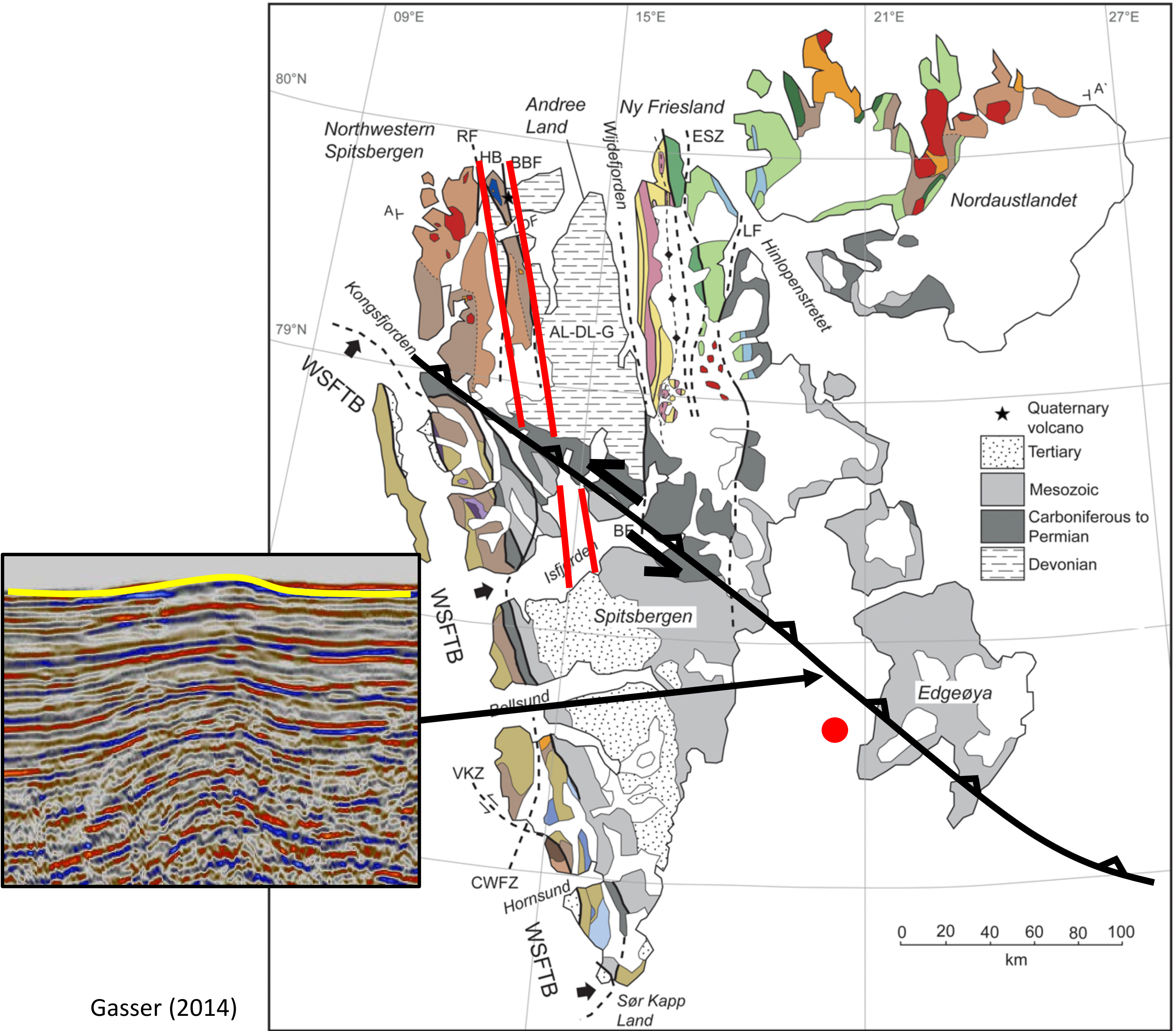

Gasser (2014)

2 On the 29th of March 2016, an earthquake coinciding with the location of the WNW–ESE-striking Timanian thrust struck near the southwestern coast of Edgeøya.

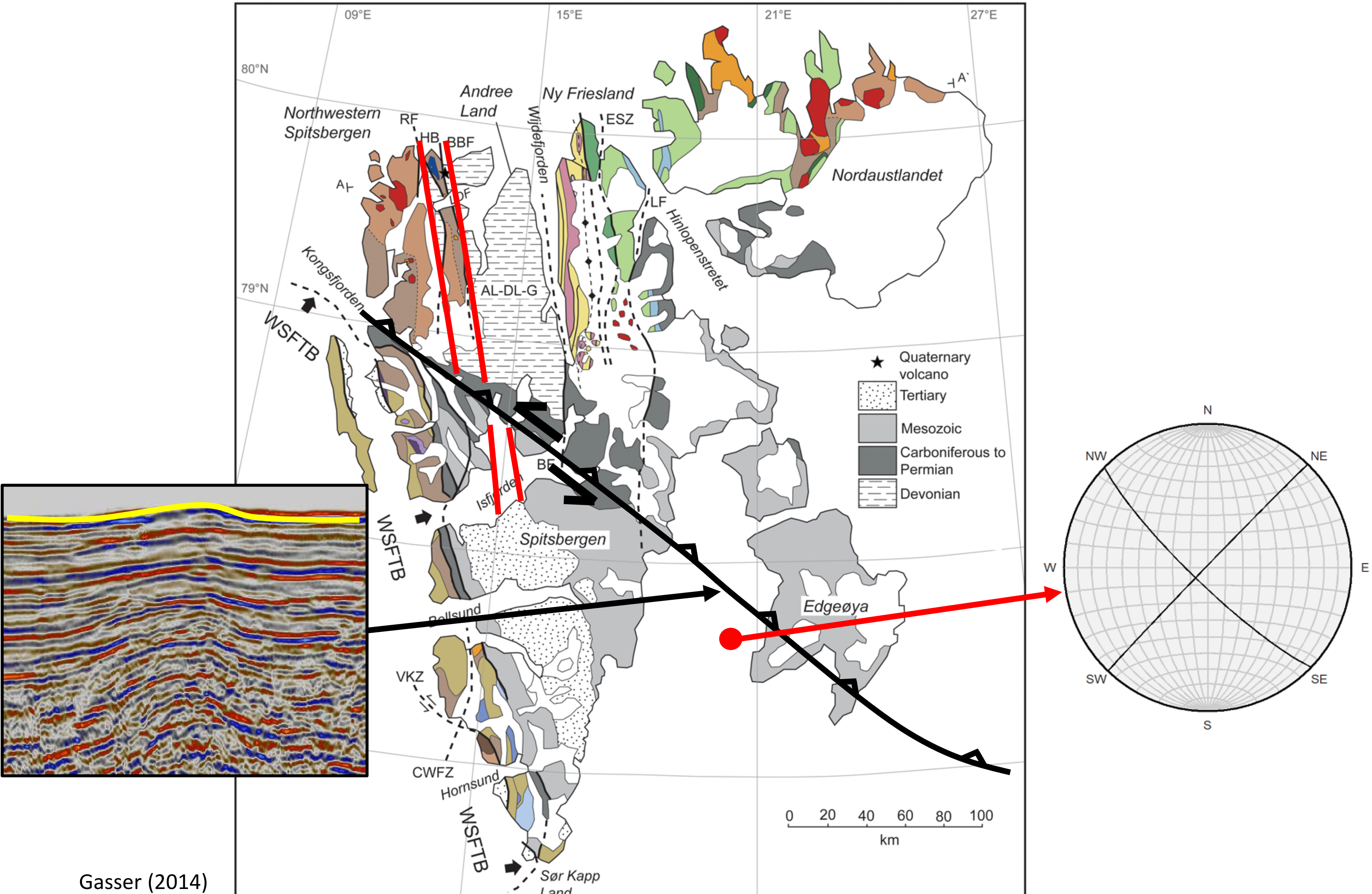

Gasser (2014)

2 **On the 29th of March 2016, an earthquake coinciding with the location of the WNW–ESE-striking Timanian thrust struck near the southwestern coast of Edgeøya.**

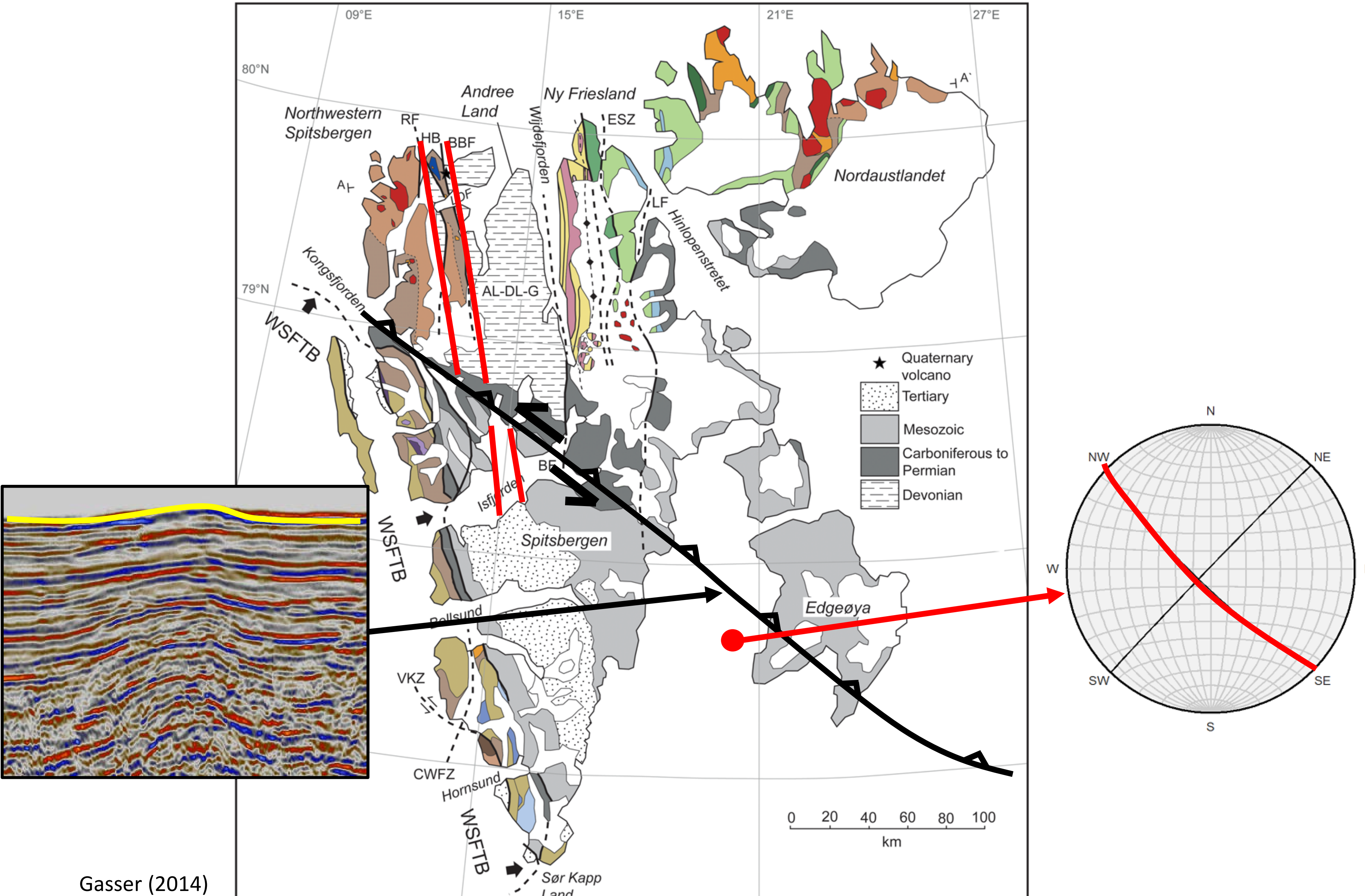

Gasser (2014)

2 Tilt-derivative aeromagnetic data suggest that N–S-trending Greenvillian, Caledonian and Devonian basement ridges are crosscut by WNW–ESE-striking faults.

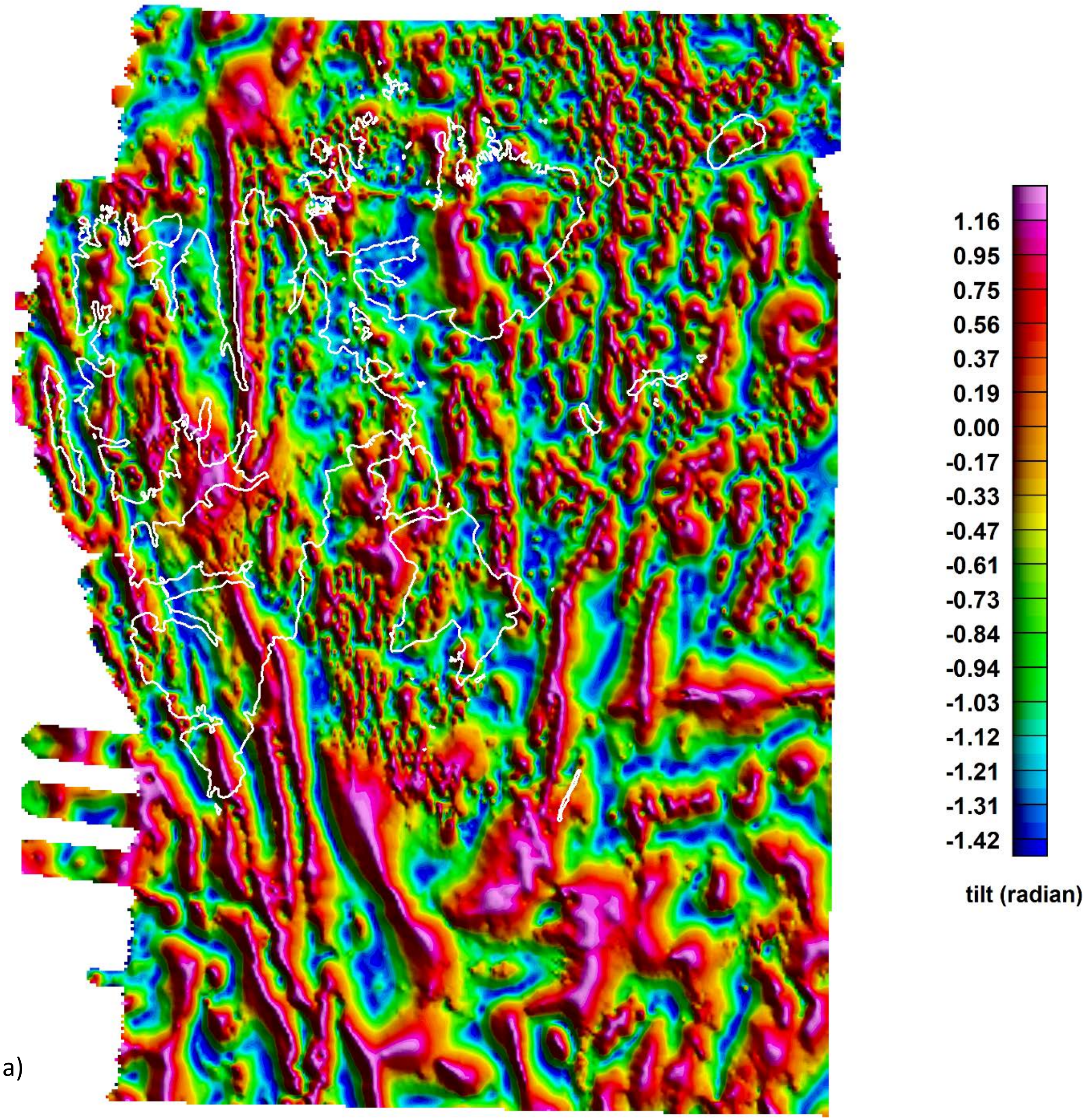

Koehl et al. (in prep. a)

2

Tilt-derivative aeromagnetic data suggest that N–S-trending Greenvillian, Caledonian and Devonian basement ridges are crosscut by WNW–ESE-striking faults.

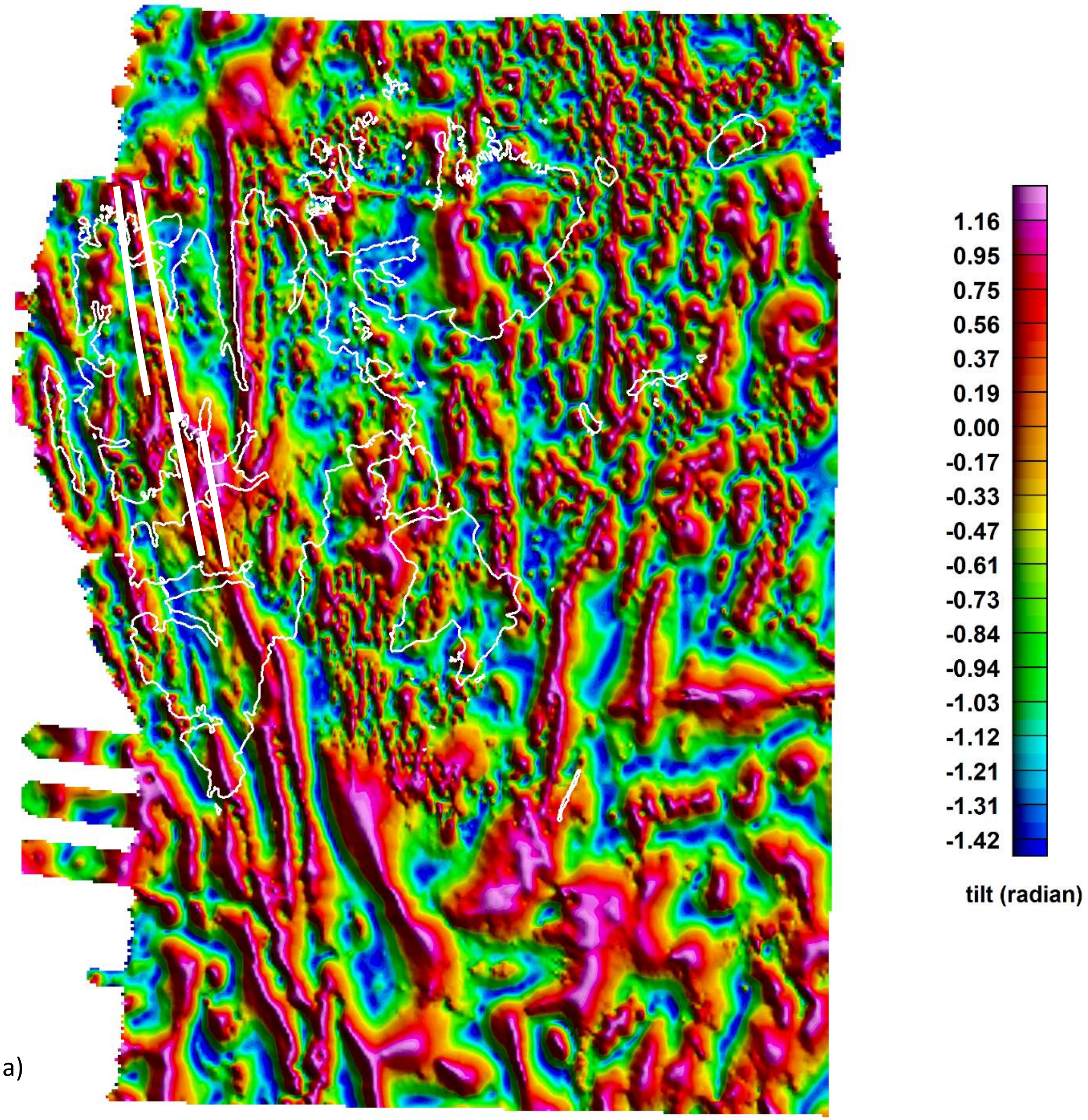

Koehl et al. (in prep. a)

2 **Tilt-derivative aeromagnetic data suggest that N–S-trending Greenvillian, Caledonian and Devonian basement ridges are crosscut by WNW–ESE-striking faults.**

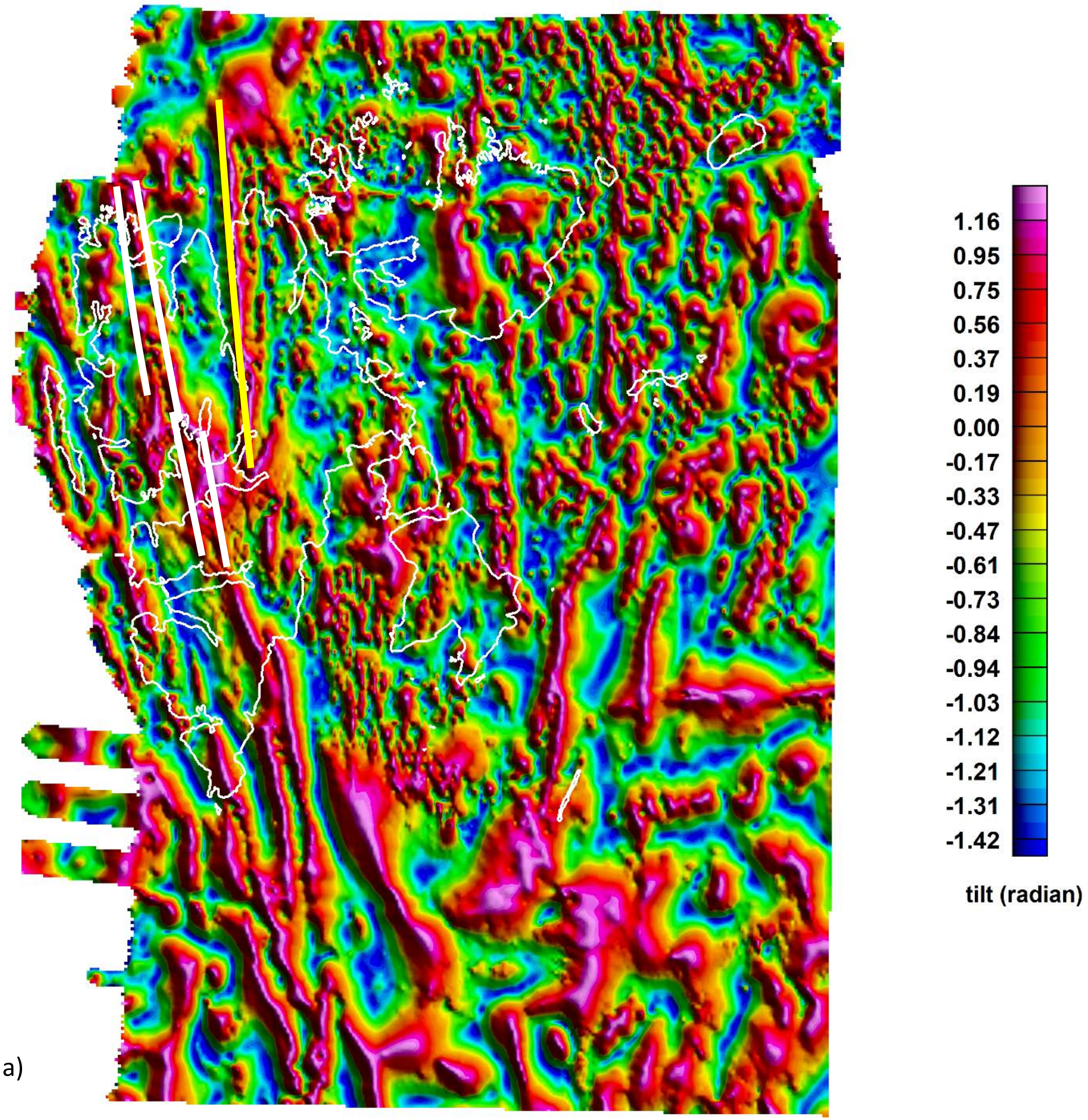

Koehl et al. (in prep. a)

2 **Tilt-derivative aeromagnetic data suggest that N–S-trending Greenvillian, Caledonian and Devonian basement ridges are crosscut by WNW–ESE-striking faults.**

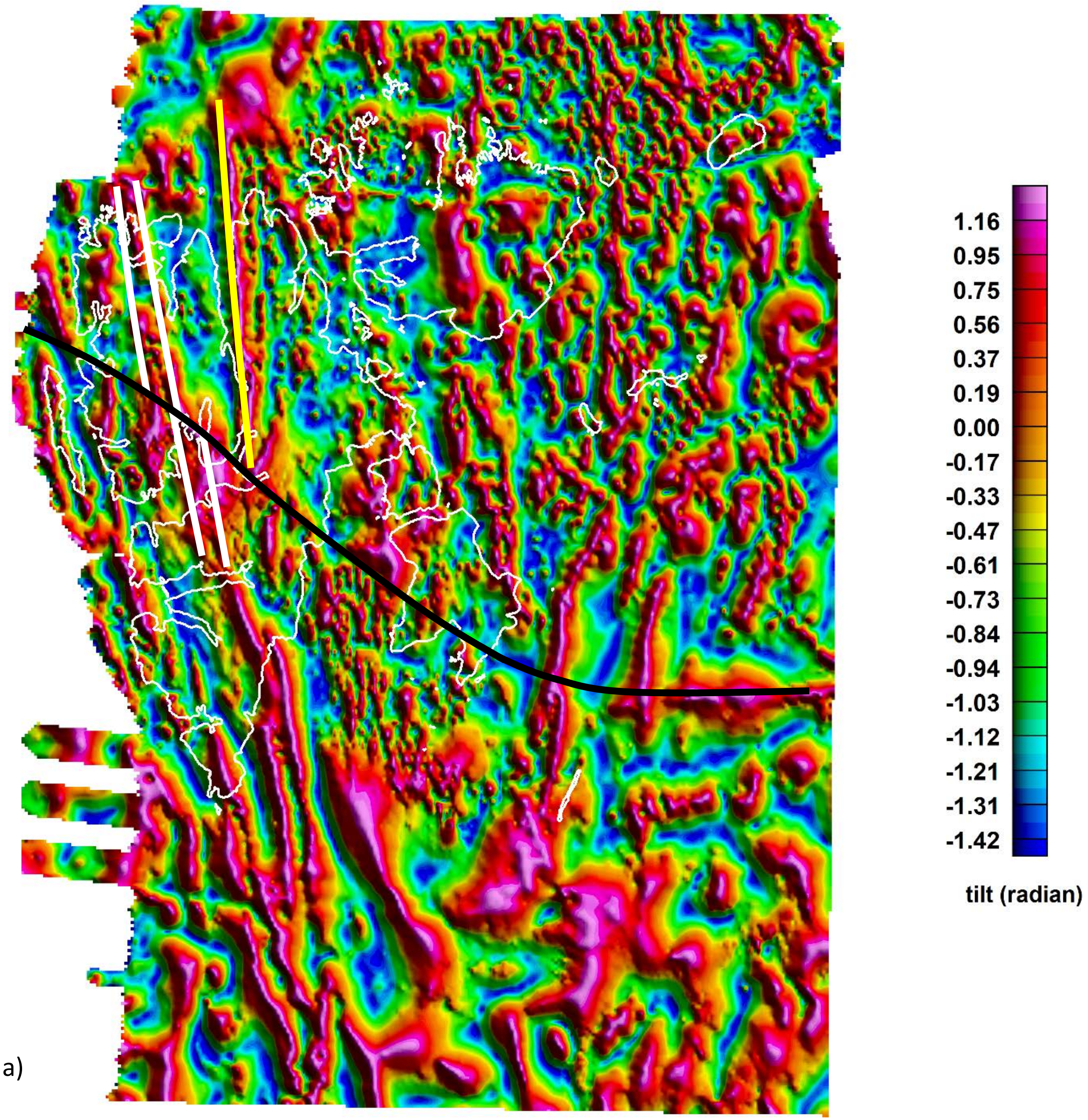

Koehl et al. (in prep. a)

2 **Tilt-derivative aeromagnetic data suggest that N–S-trending Greenvillian, Caledonian and Devonian basement ridges are crosscut by WNW–ESE-striking faults.**

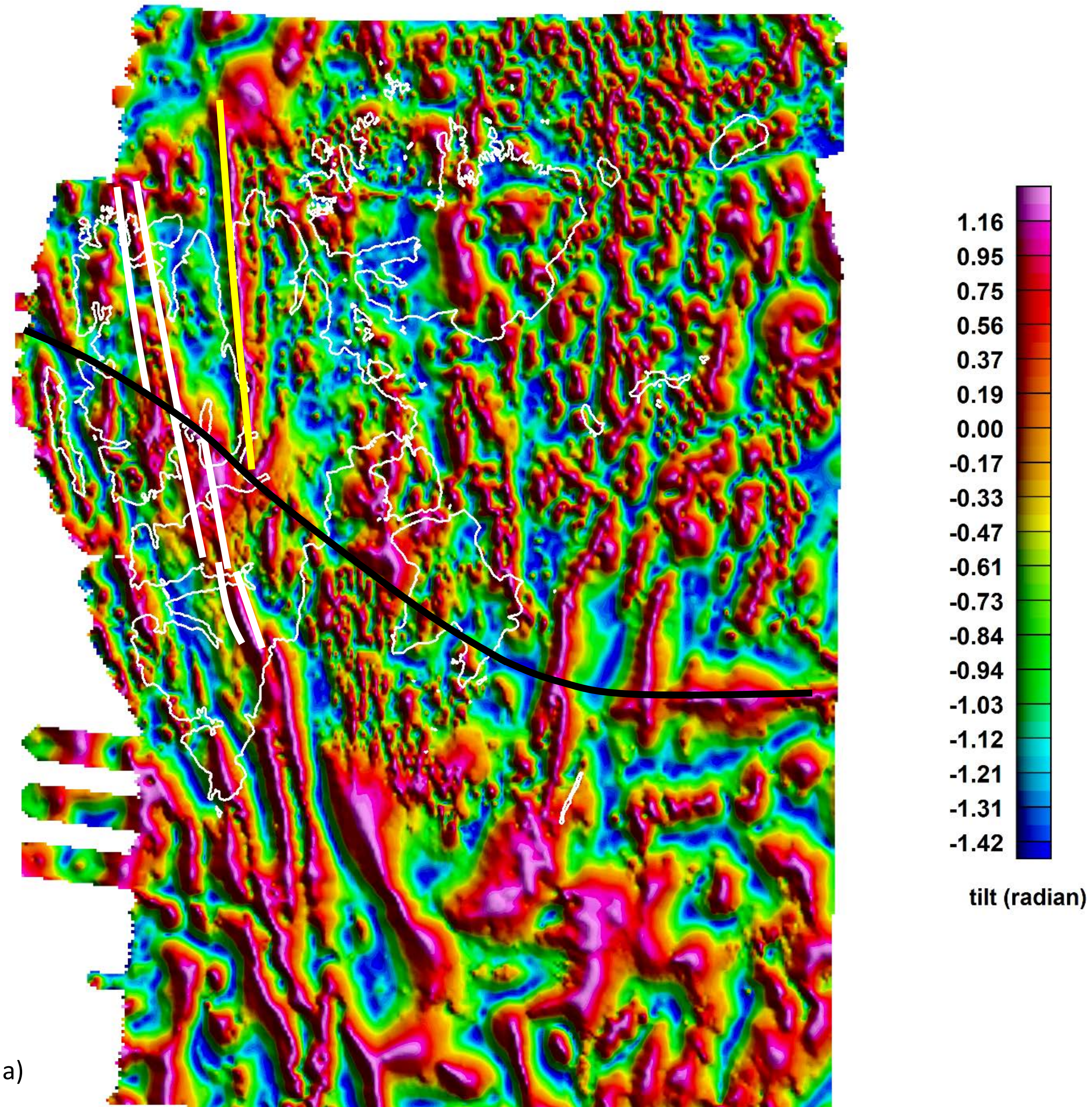

Koehl et al. (in prep. a)

2 Tilt-derivative aeromagnetic data suggest that N–S-trending Greenvillian, Caledonian and Devonian basement ridges are crosscut by WNW–ESE-striking faults.

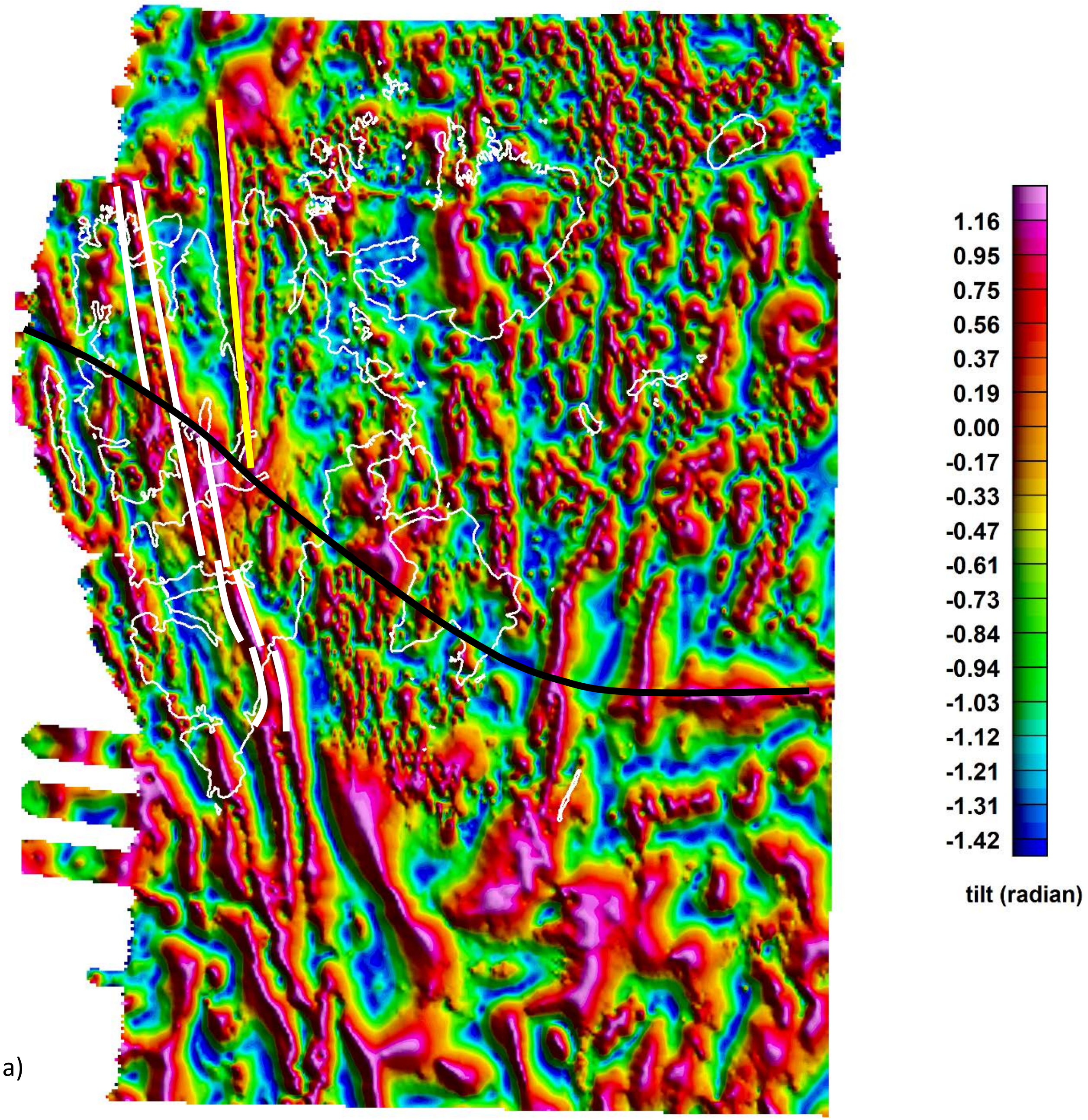

Koehl et al. (in prep. a)

2 **Tilt-derivative aeromagnetic data suggest that N–S-trending Greenvillian, Caledonian and Devonian basement ridges are crosscut by WNW–ESE-striking faults.**

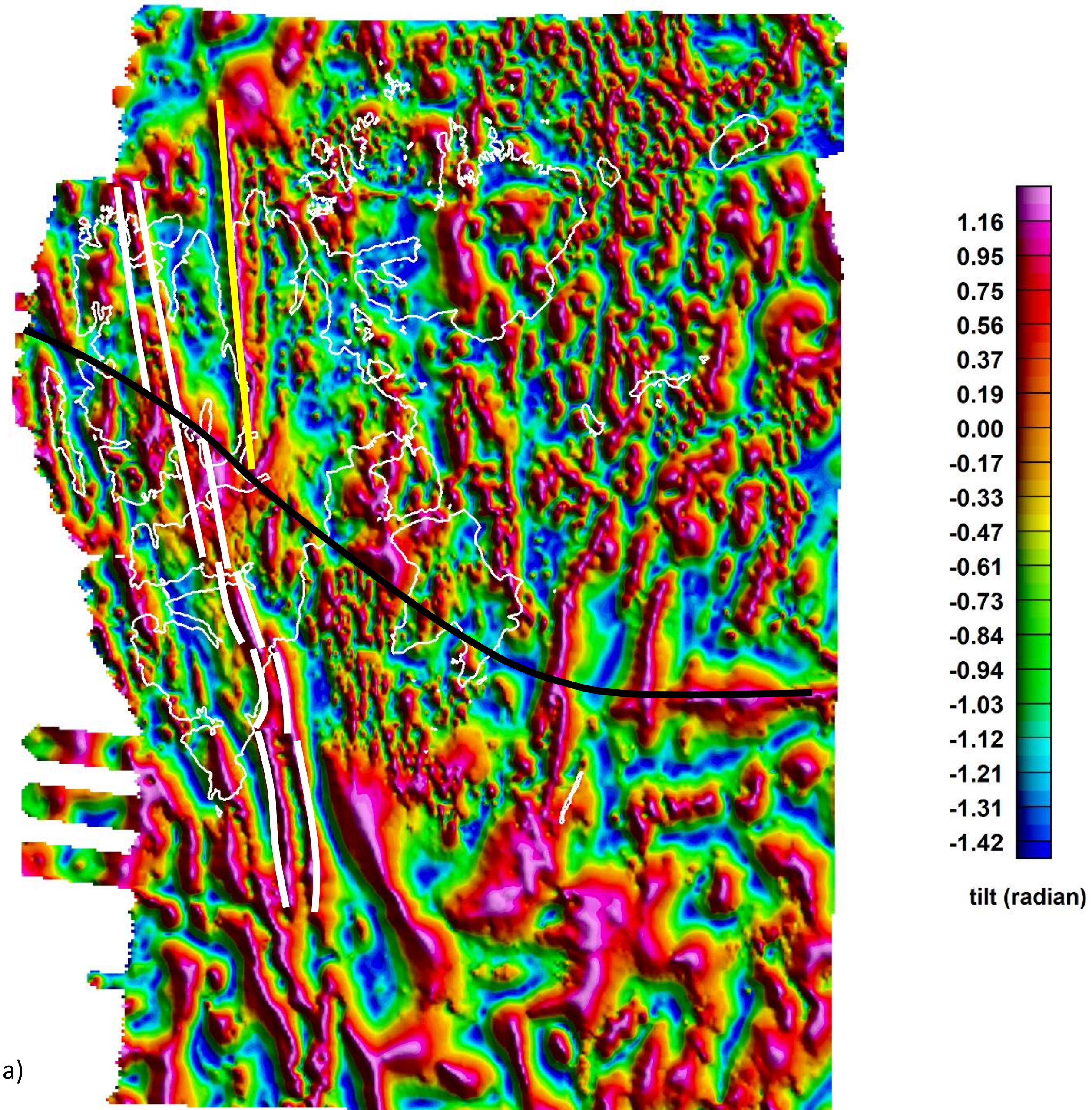

Koehl et al. (in prep. a)

2

Tilt-derivative aeromagnetic data suggest that N–S-trending Greenvillian, Caledonian and Devonian basement ridges are crosscut by WNW–ESE-striking faults.

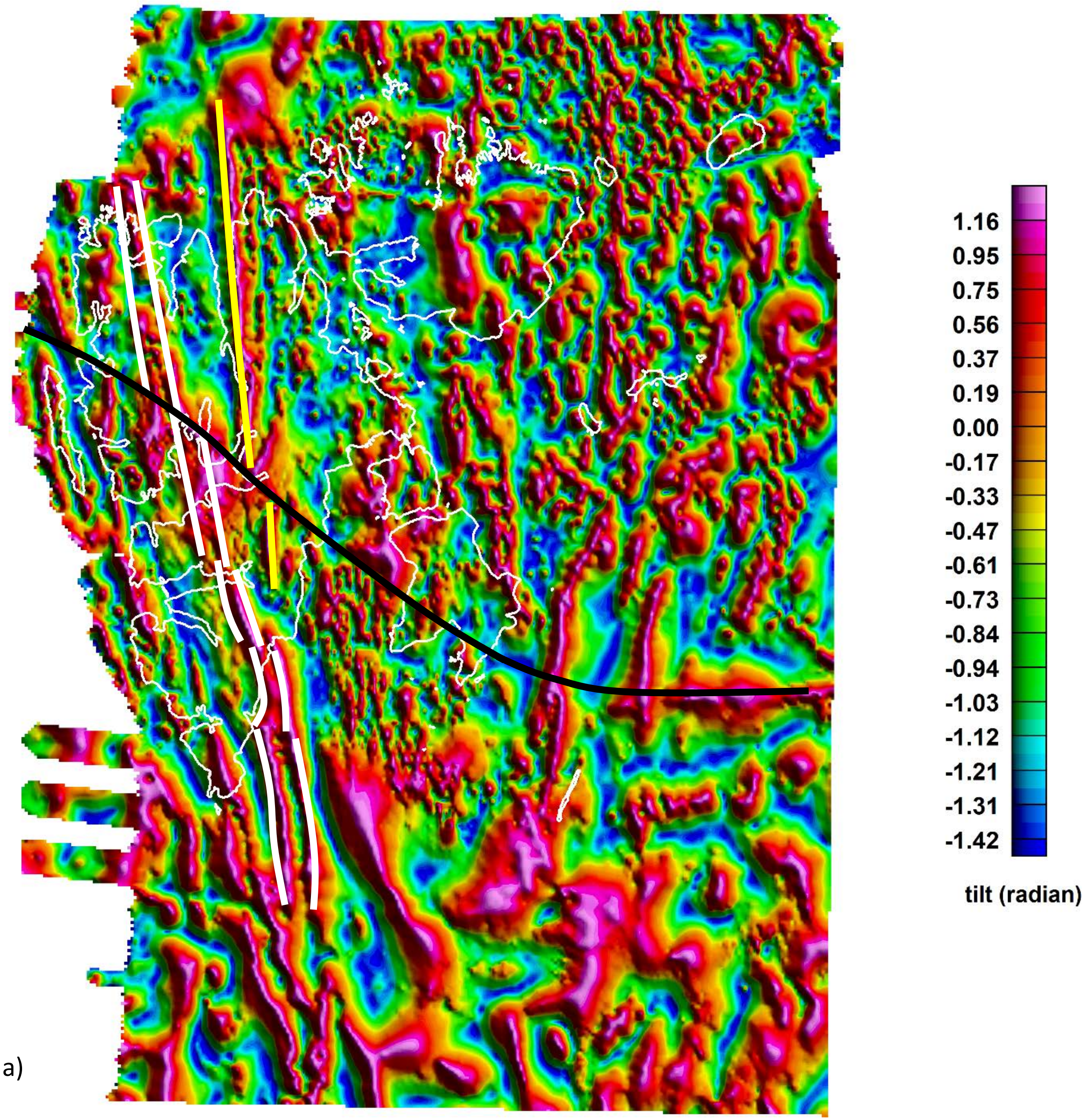

Koehl et al. (in prep. a)

2

Tilt-derivative aeromagnetic data suggest that N–S-trending Greenvillian, Caledonian and Devonian basement ridges are crosscut by WNW–ESE-striking faults.

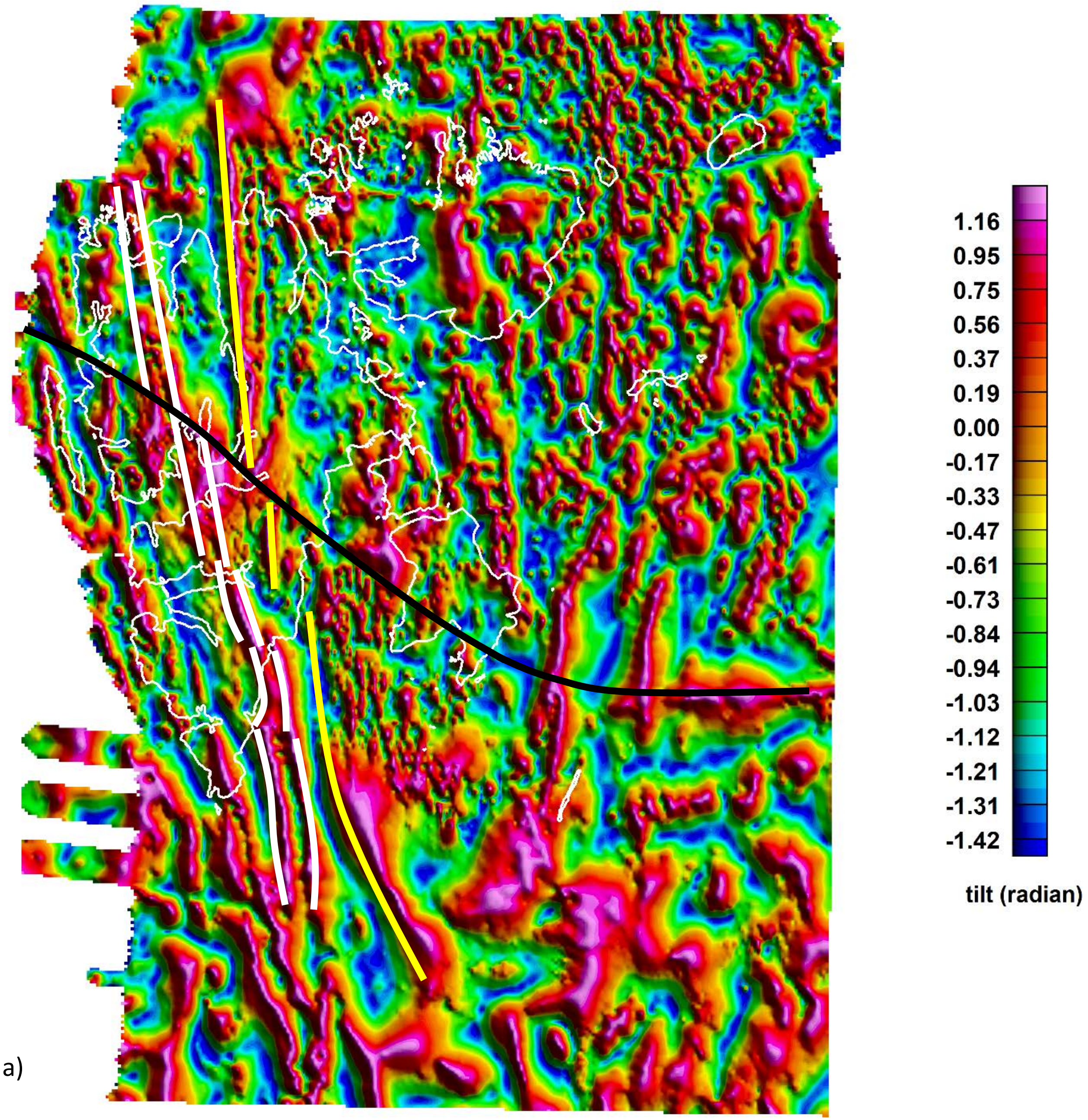

Koehl et al. (in prep. a)

2 **Tilt-derivative aeromagnetic data suggest that N–S-trending Greenvillian, Caledonian and Devonian basement ridges are crosscut by WNW–ESE-striking faults.**

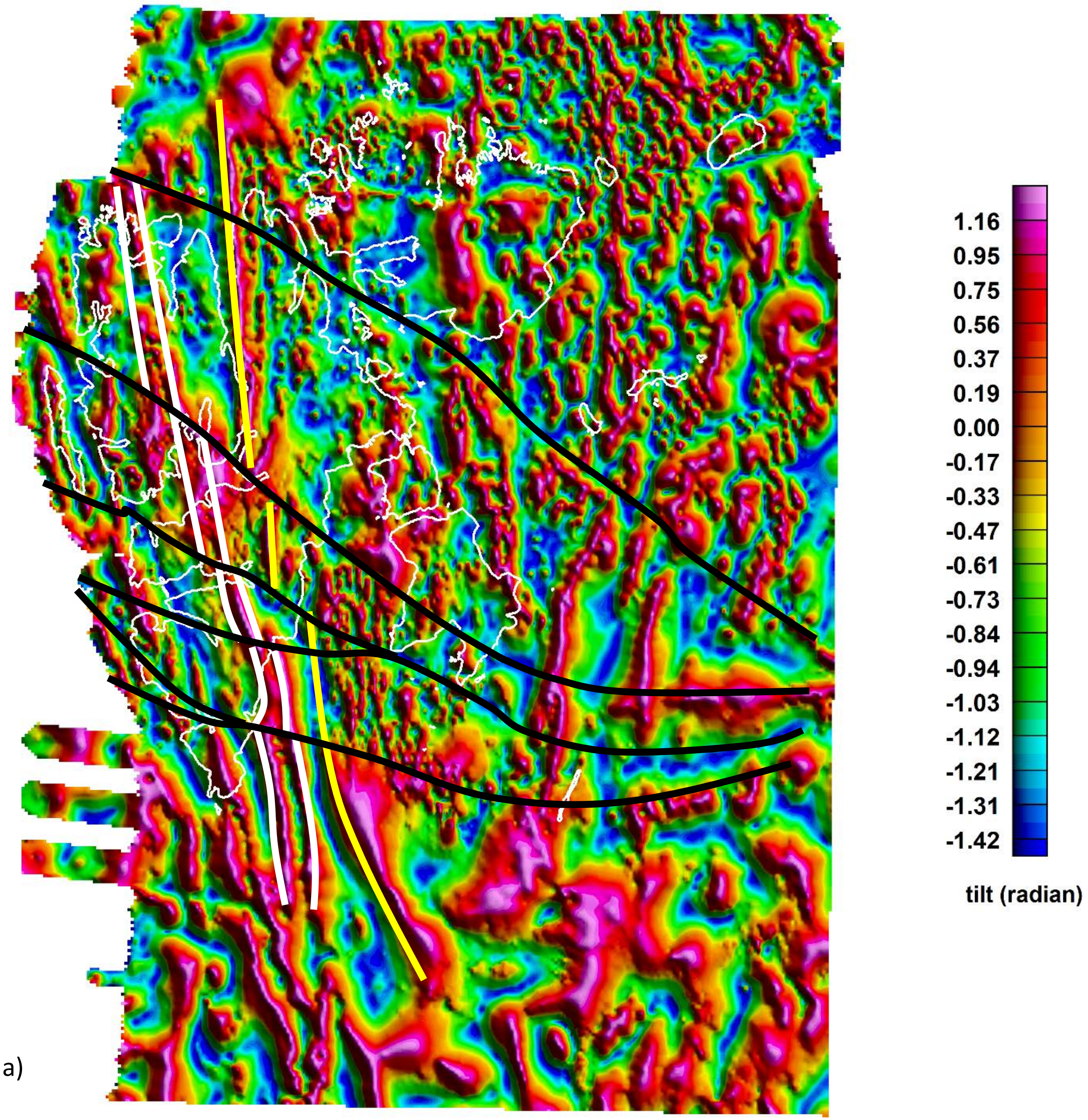

Koehl et al. (in prep. a)

2

Tilt-derivative aeromagnetic data suggest that N–S-trending Greenvillian, Caledonian and Devonian basement ridges are crosscut by WNW–ESE-striking faults.

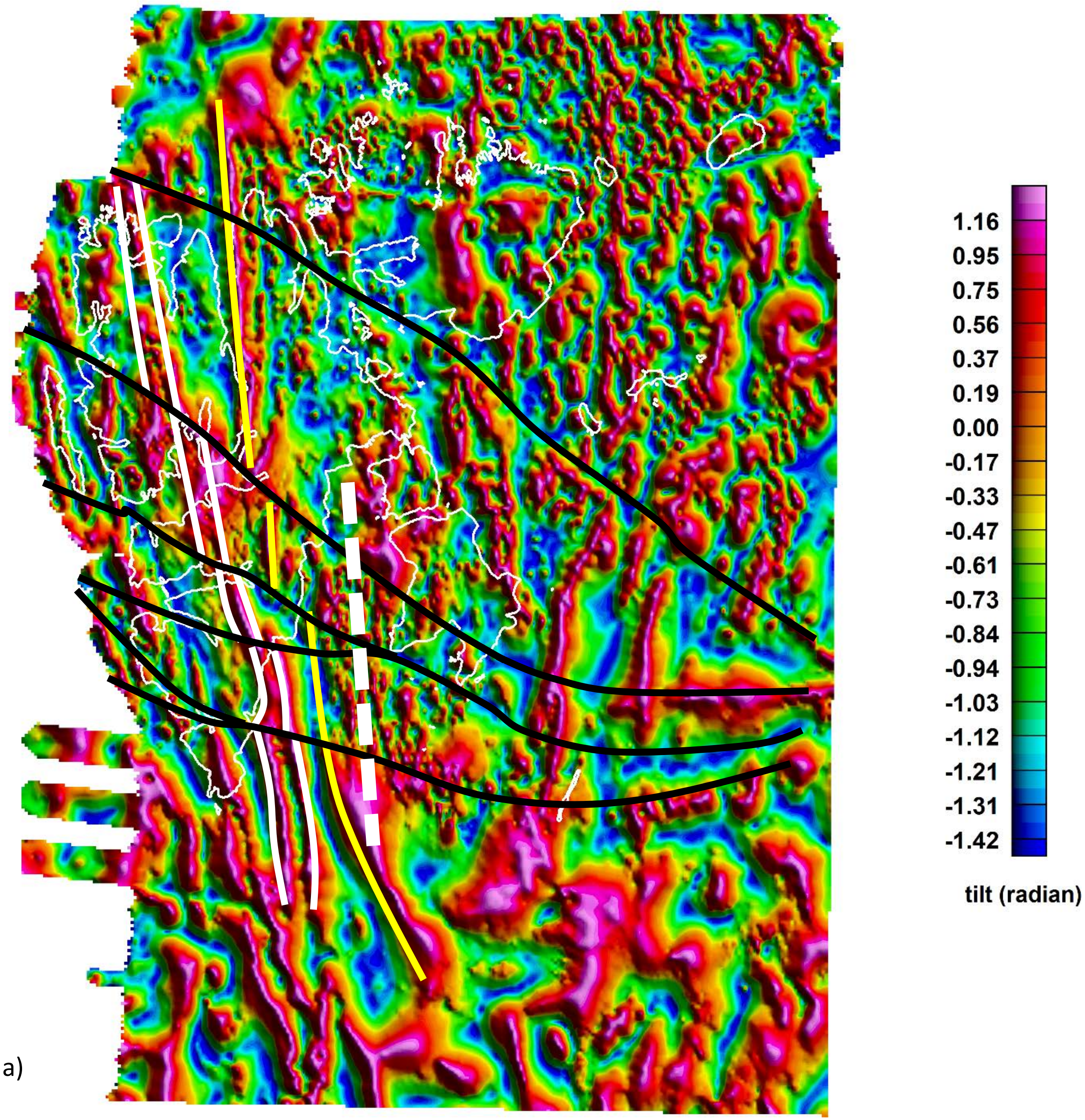

Koehl et al. (in prep. a)

2 **Seismic data in Storfjorden show a series of SSW-verging Timanian thrust systems.**

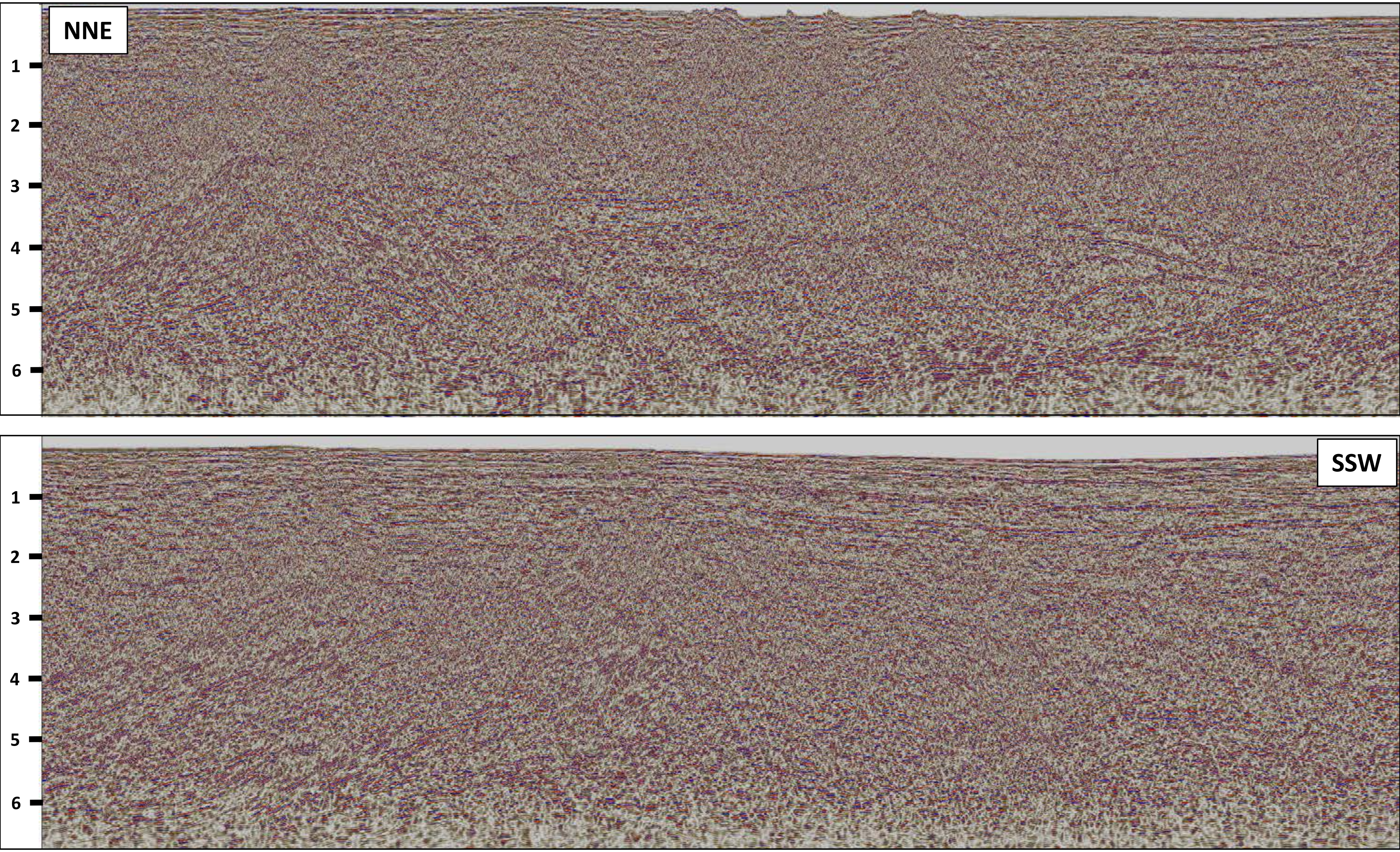

Koehl et al. (in prep. c)

2 **Seismic data in Storfjorden show a series of SSW-verging Timanian thrust systems.**

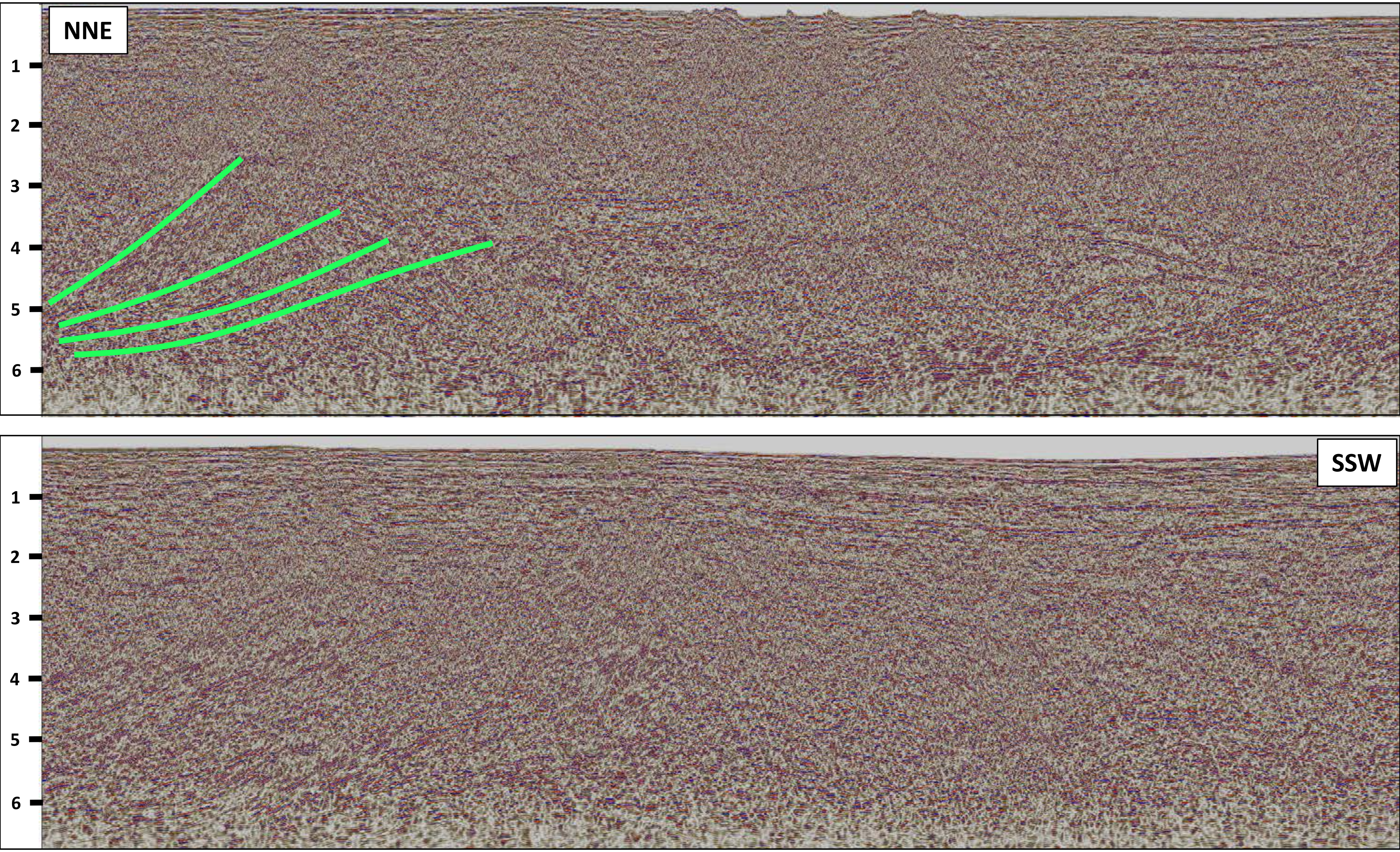

Koehl et al. (in prep. c)

2 Seismic data in Storfjorden show a series of SSW-verging Timanian thrust systems.

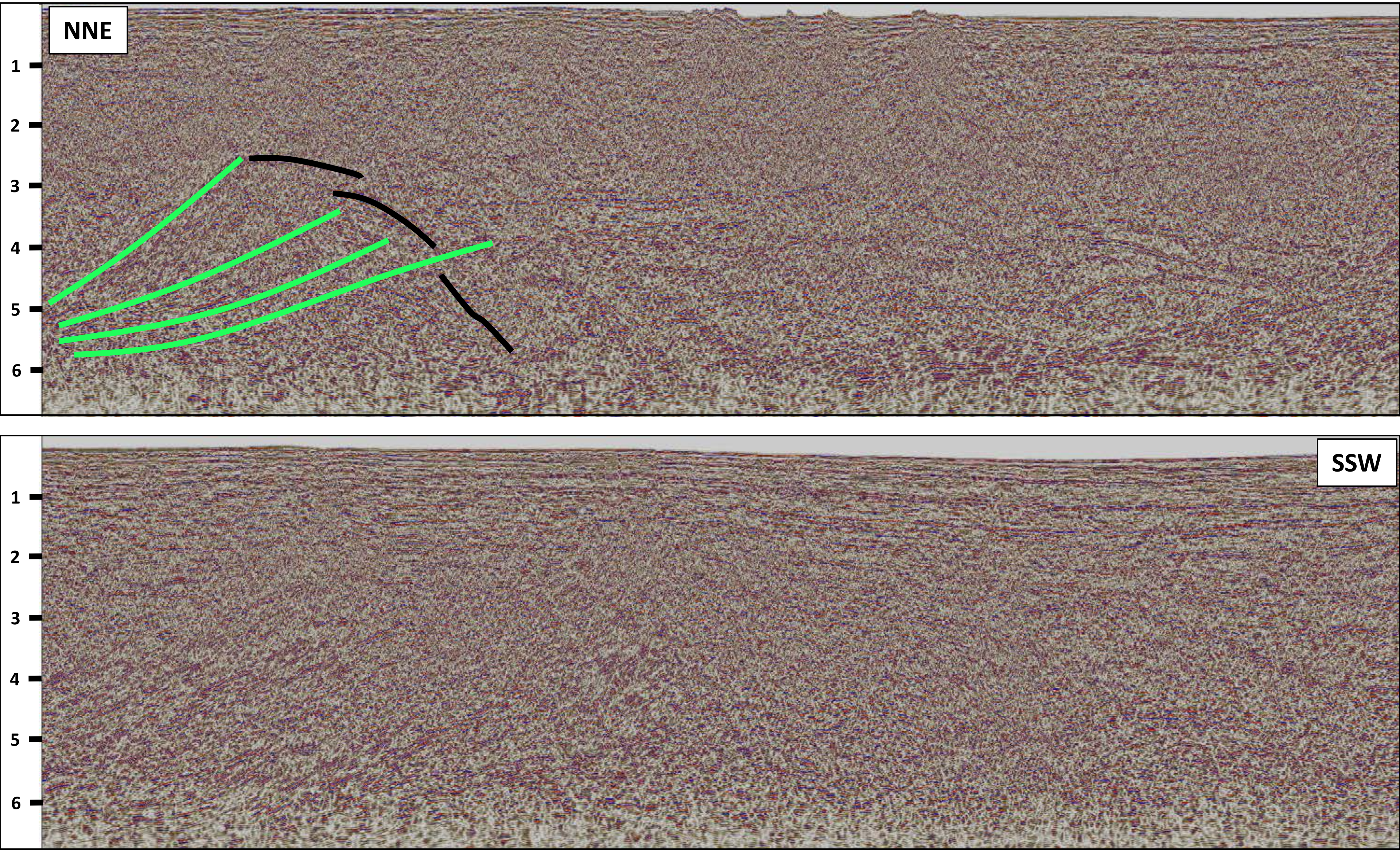

Koehl et al. (in prep. c)

2 Seismic data in Storfjorden show a series of SSW-verging Timanian thrust systems.

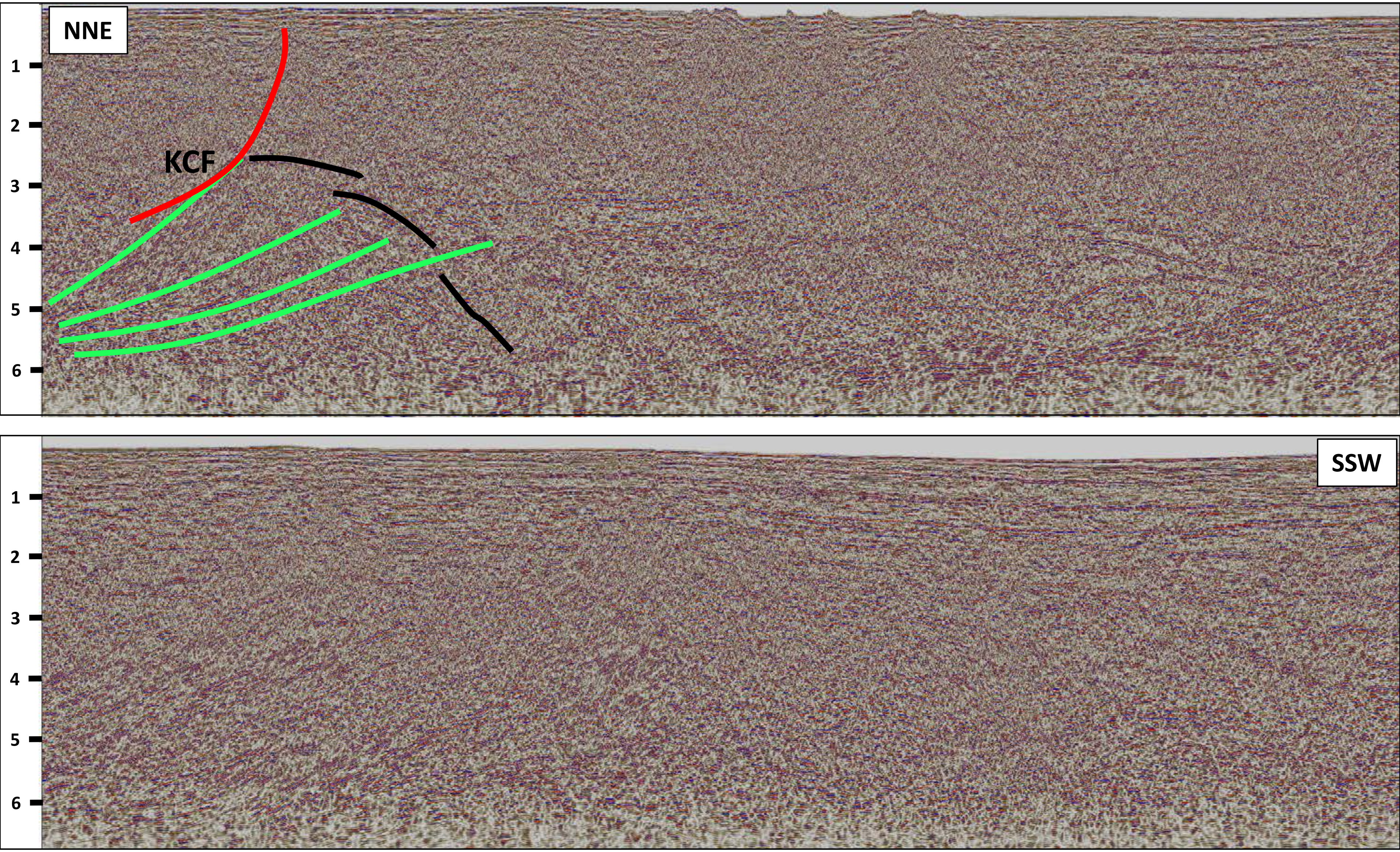

Koehl et al. (in prep. c)

2 **Seismic data in Storfjorden show a series of SSW-verging Timanian thrust systems.**

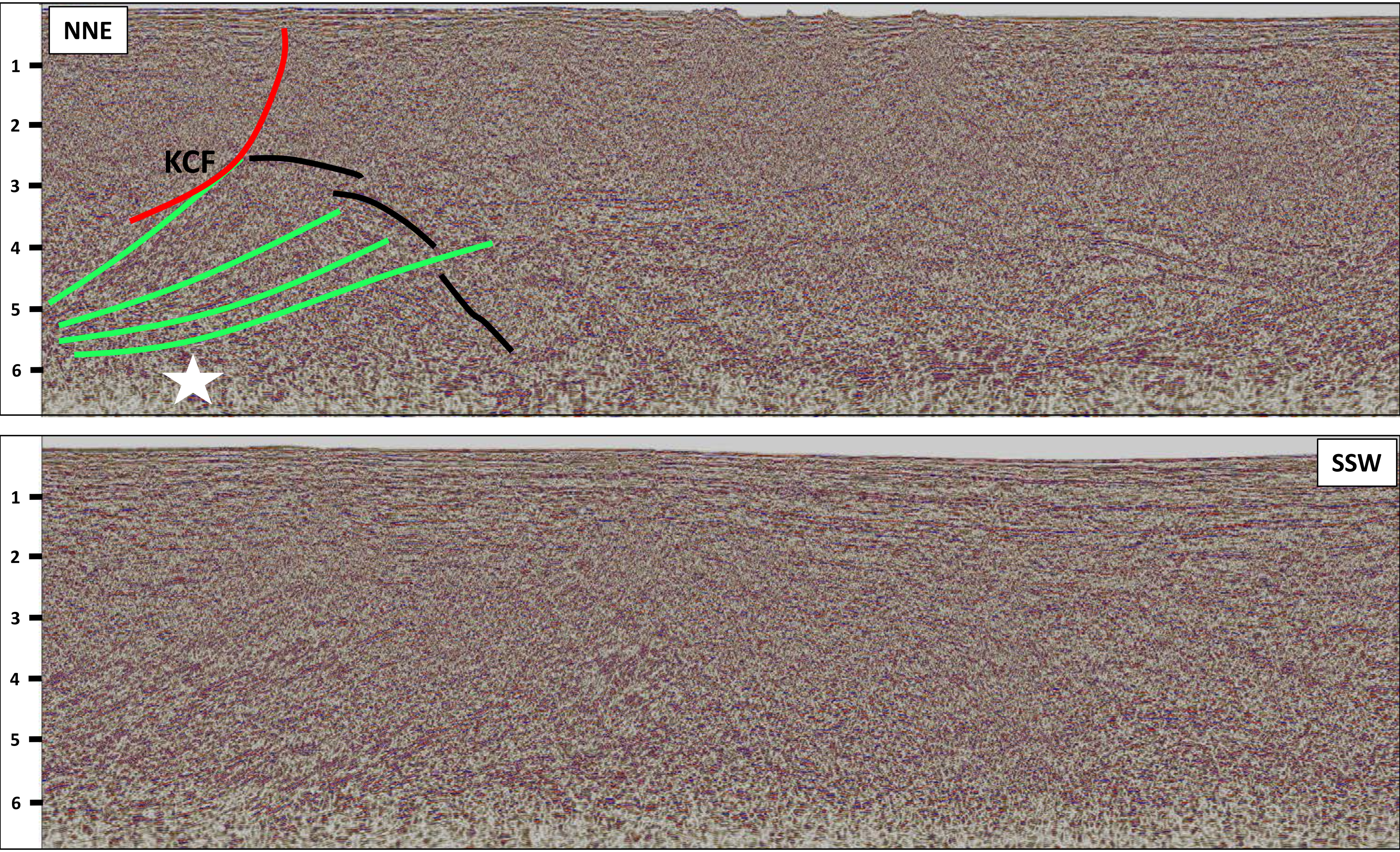

Koehl et al. (in prep. c)

2 Seismic data in Storfjorden show a series of SSW-verging Timanian thrust systems.

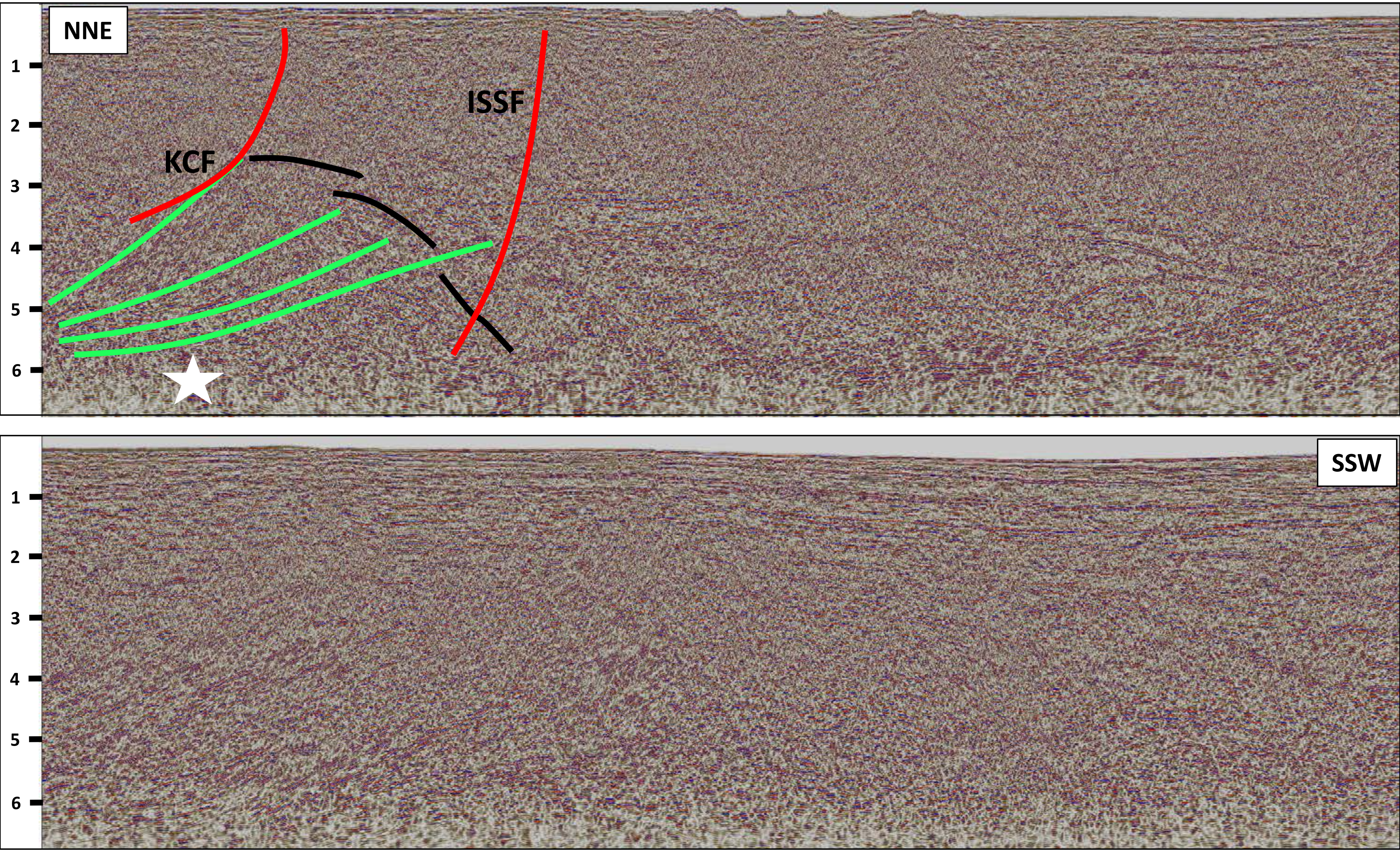

Koehl et al. (in prep. c)

2

Seismic data in Storfjorden show a series of SSW-verging Timanian thrust systems.

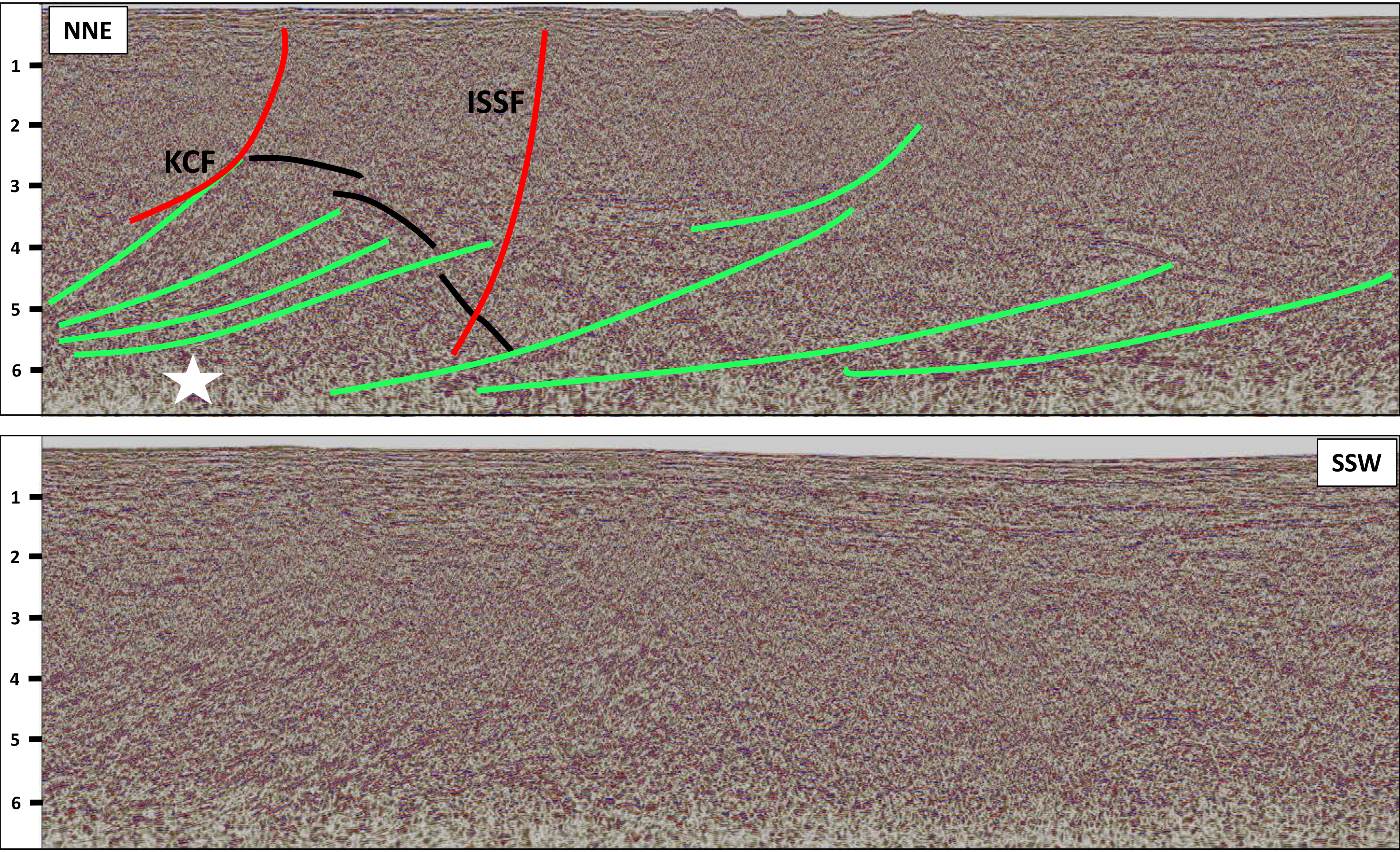

Koehl et al. (in prep. c)

2 Seismic data in Storfjorden show a series of SSW-verging Timanian thrust systems.

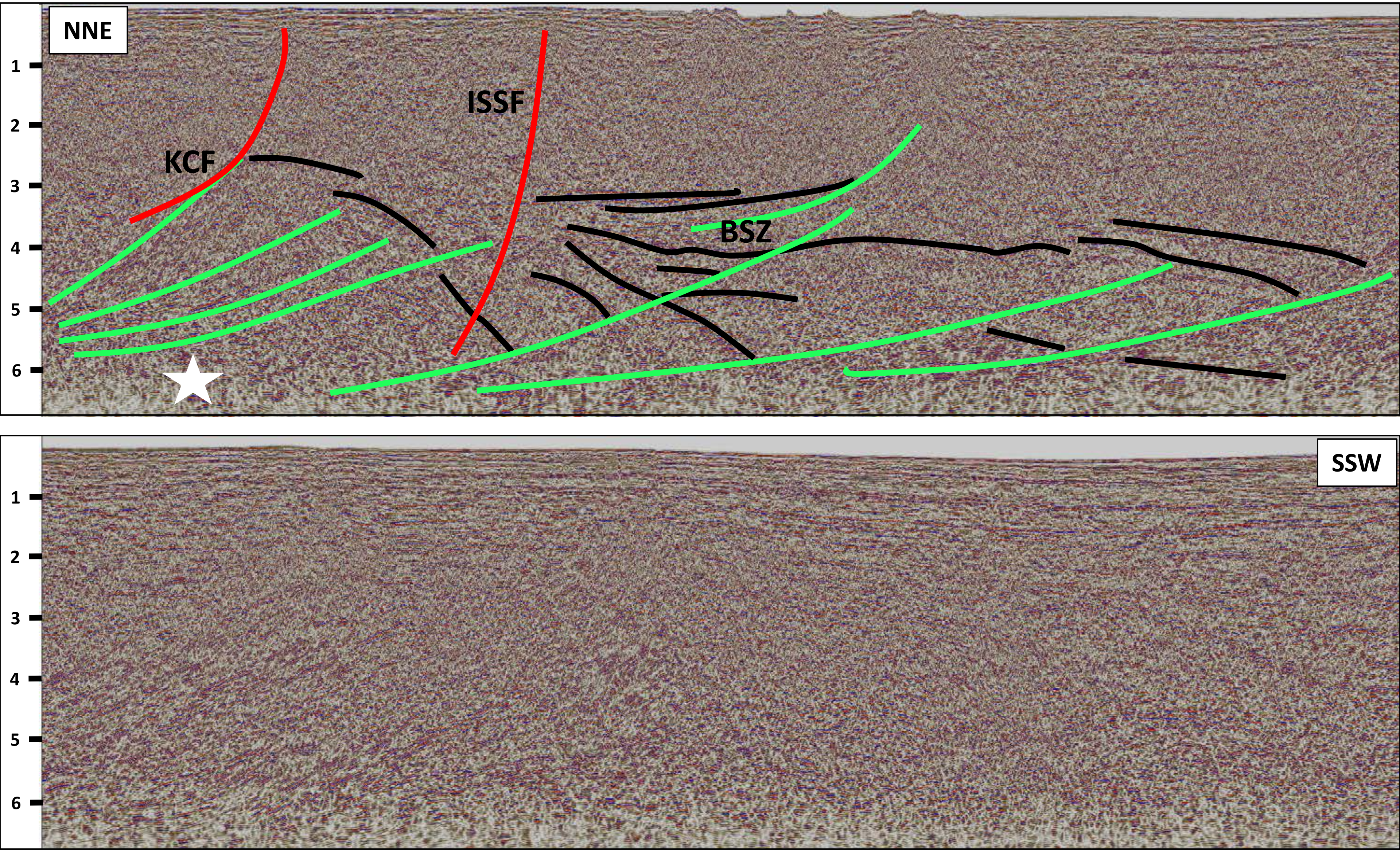

Koehl et al. (in prep. c)

2 Seismic data in Storfjorden show a series of SSW-verging Timanian thrust systems.

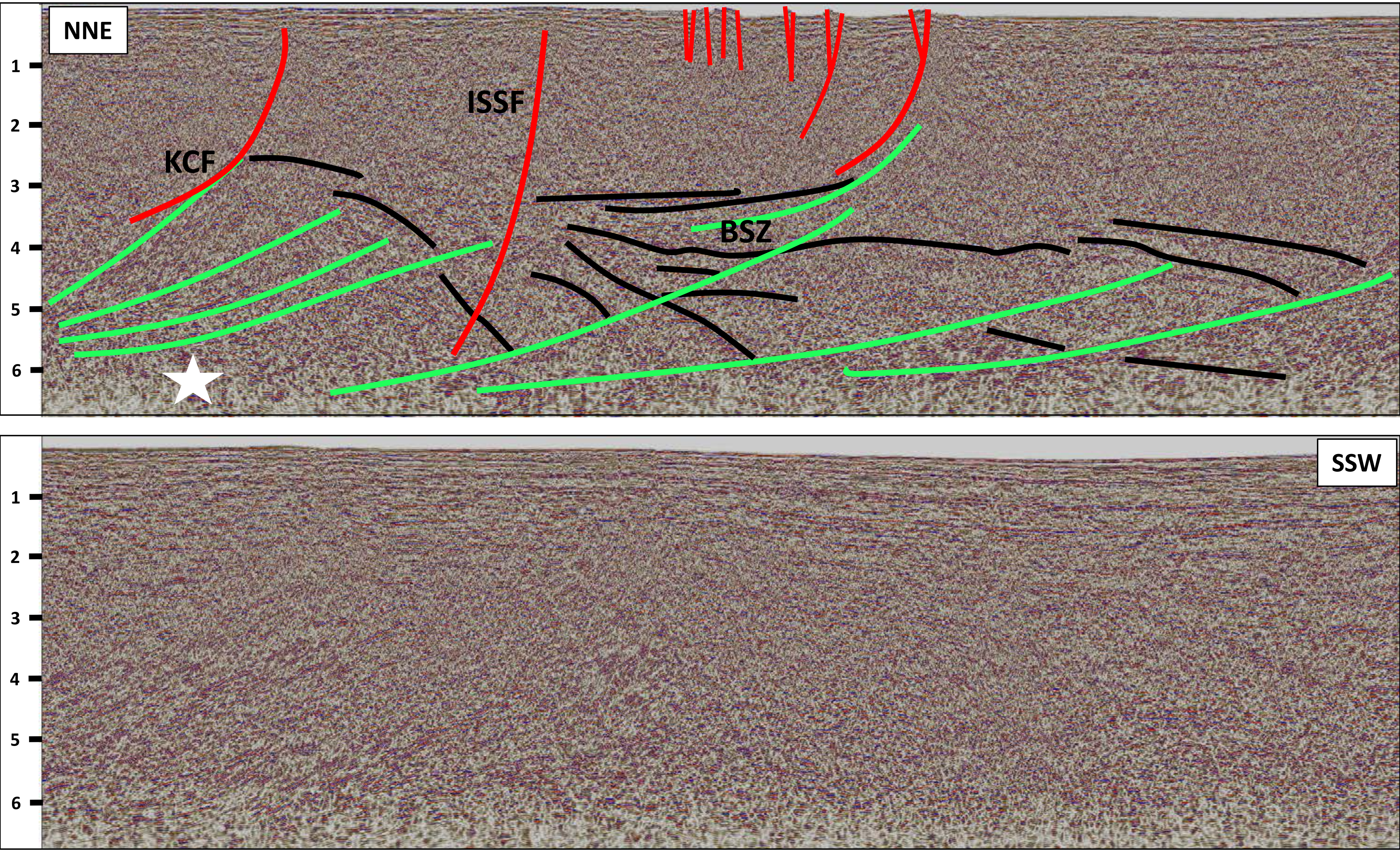

Koehl et al. (in prep. c)

2 Seismic data in Storfjorden show a series of SSW-verging Timanian thrust systems.

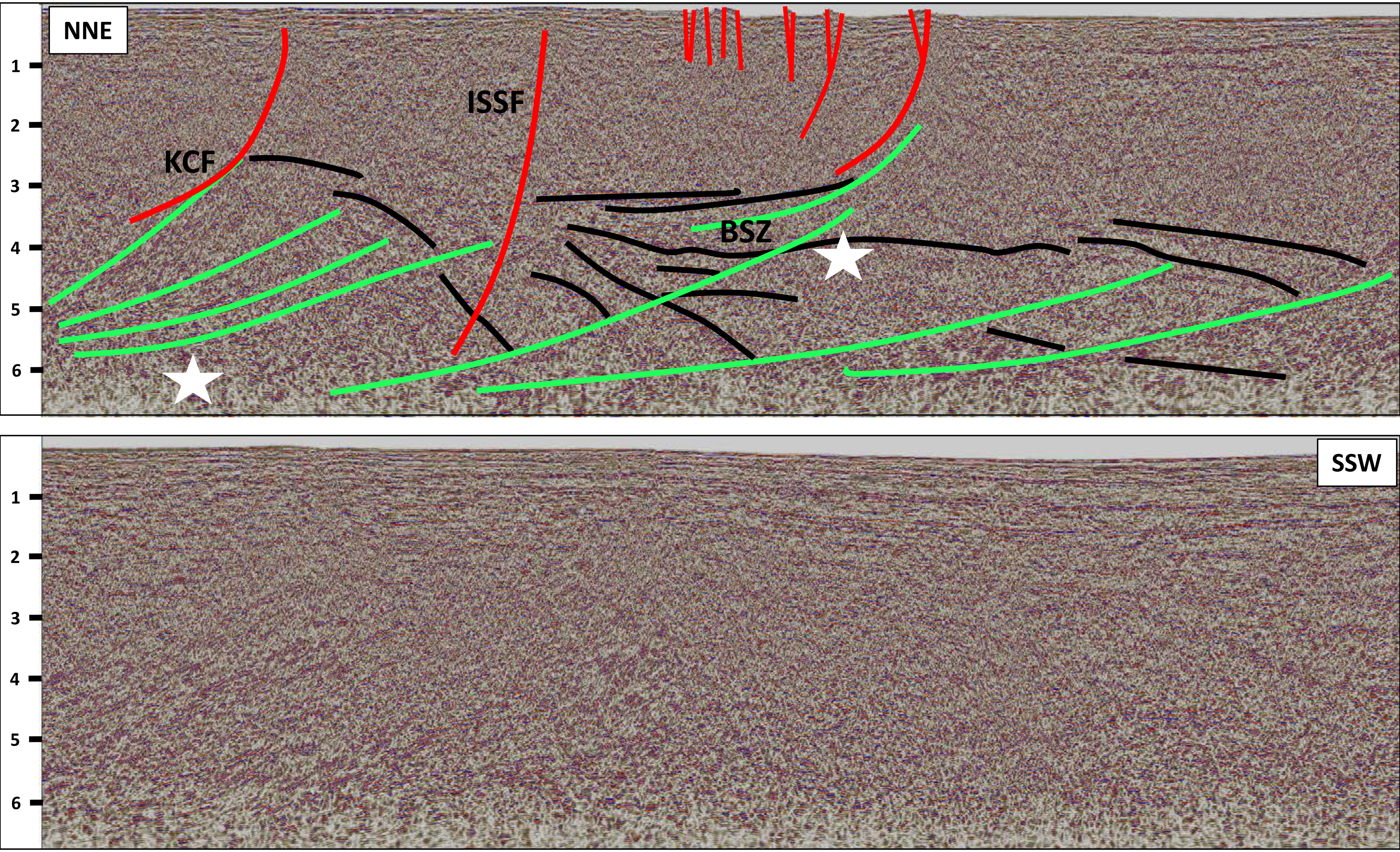

Koehl et al. (in prep. c)

2 Seismic data in Storfjorden show a series of SSW-verging Timanian thrust systems.

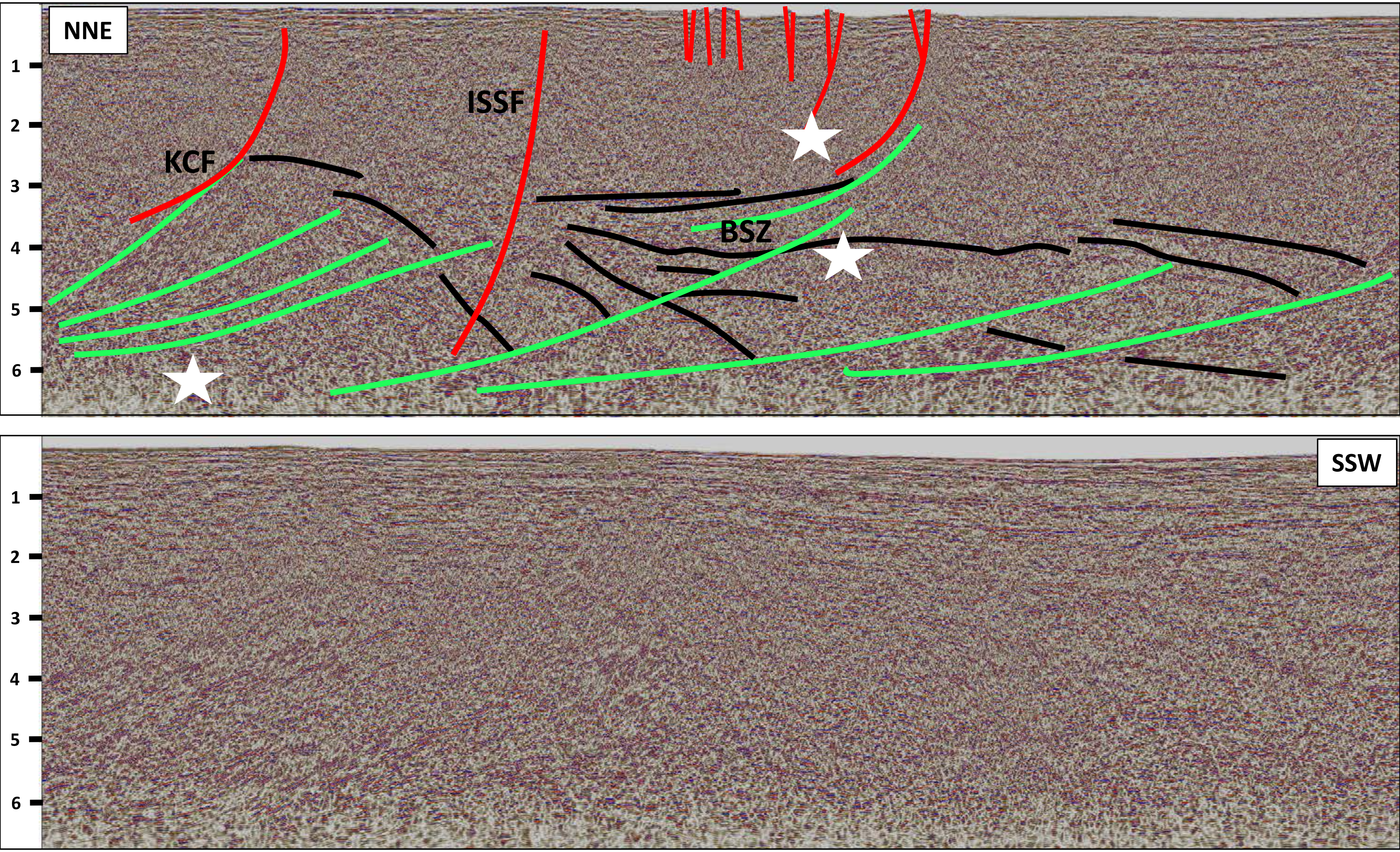

Koehl et al. (in prep. c)

2 **Seismic data in Storfjorden show a series of SSW-verging Timanian thrust systems.**

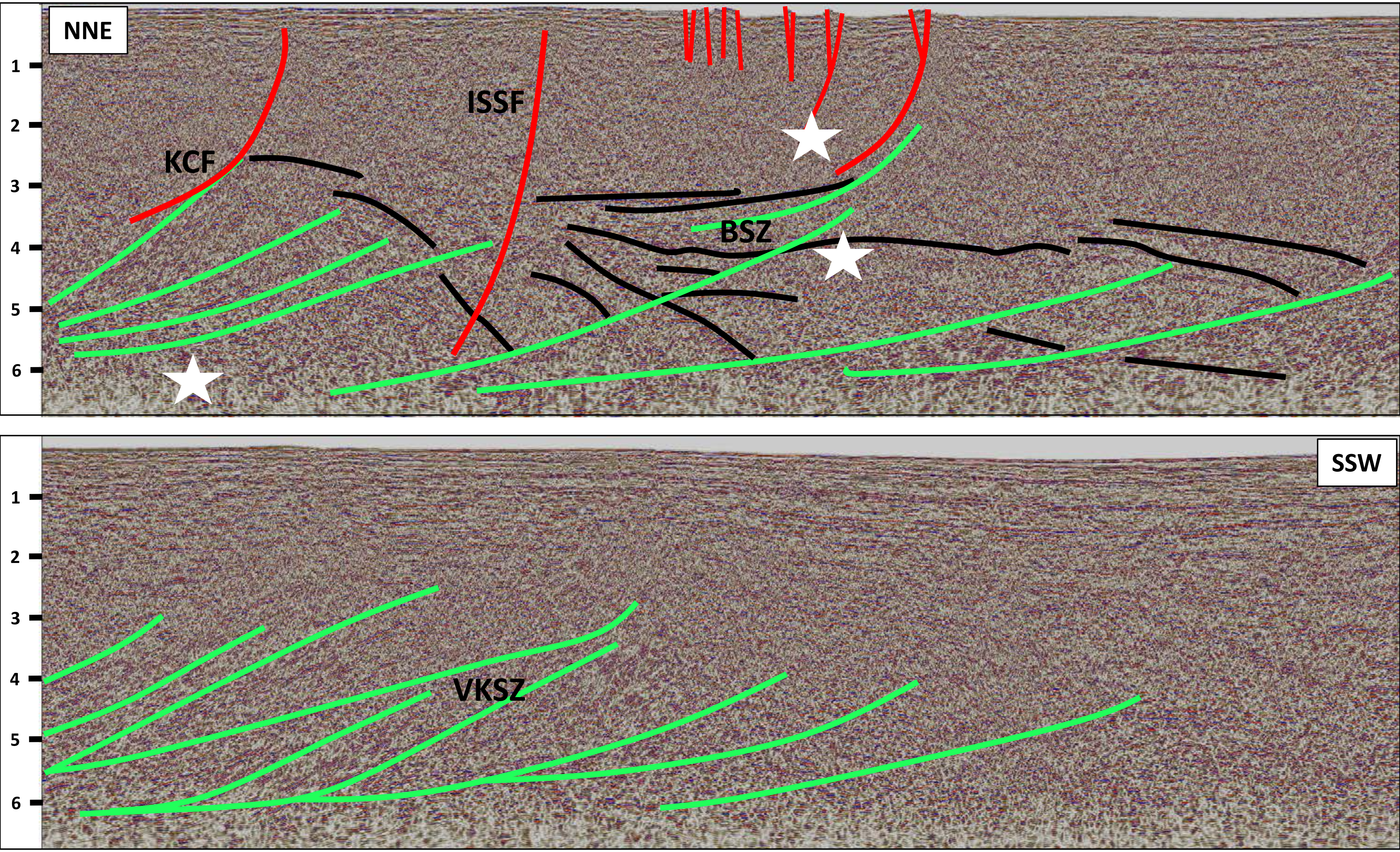

Koehl et al. (in prep. c)

2 **Seismic data in Storfjorden show a series of SSW-verging Timanian thrust systems.**

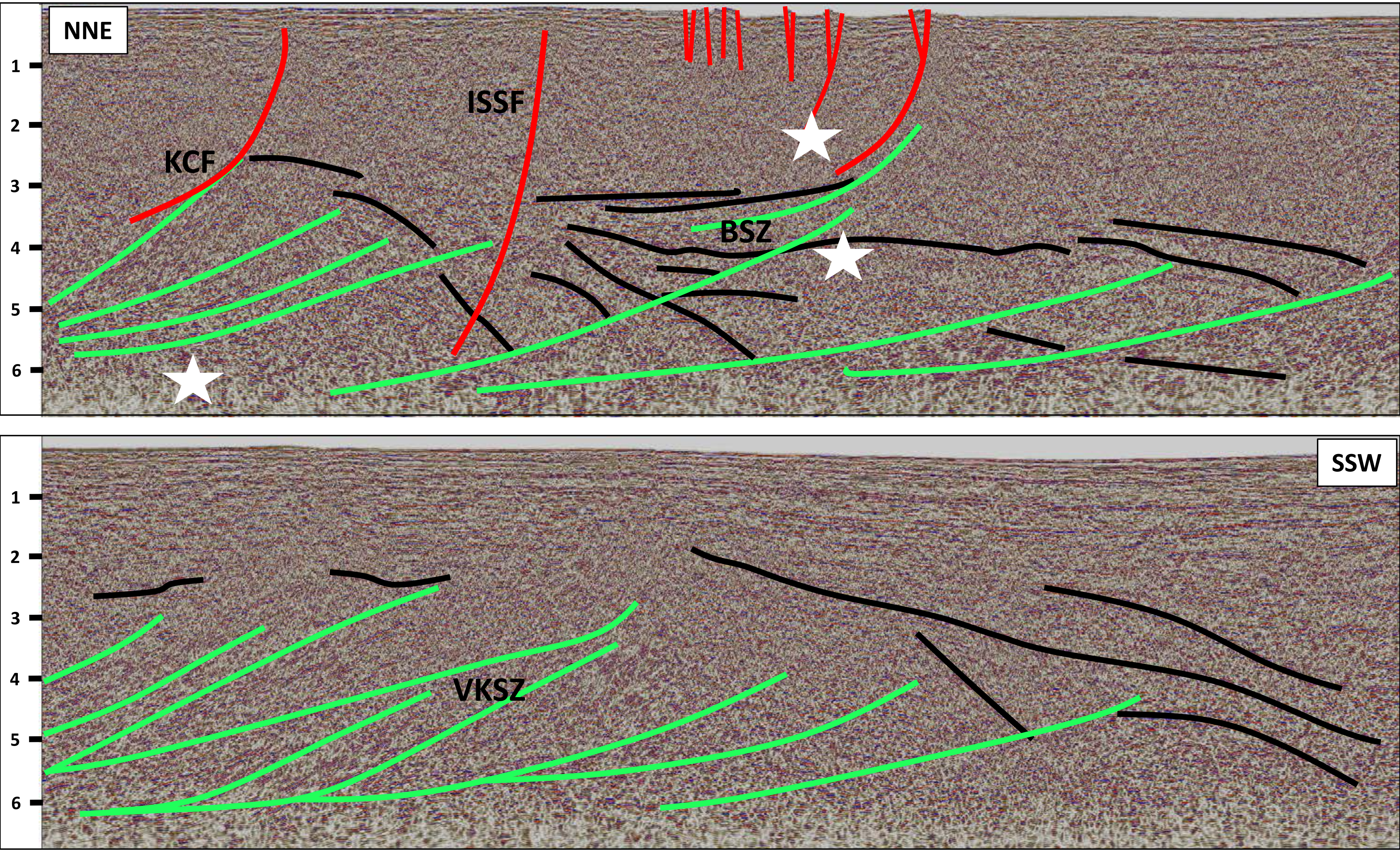

Koehl et al. (in prep. c)

2 Seismic data in Storfjorden show a series of SSW-verging Timanian thrust systems.

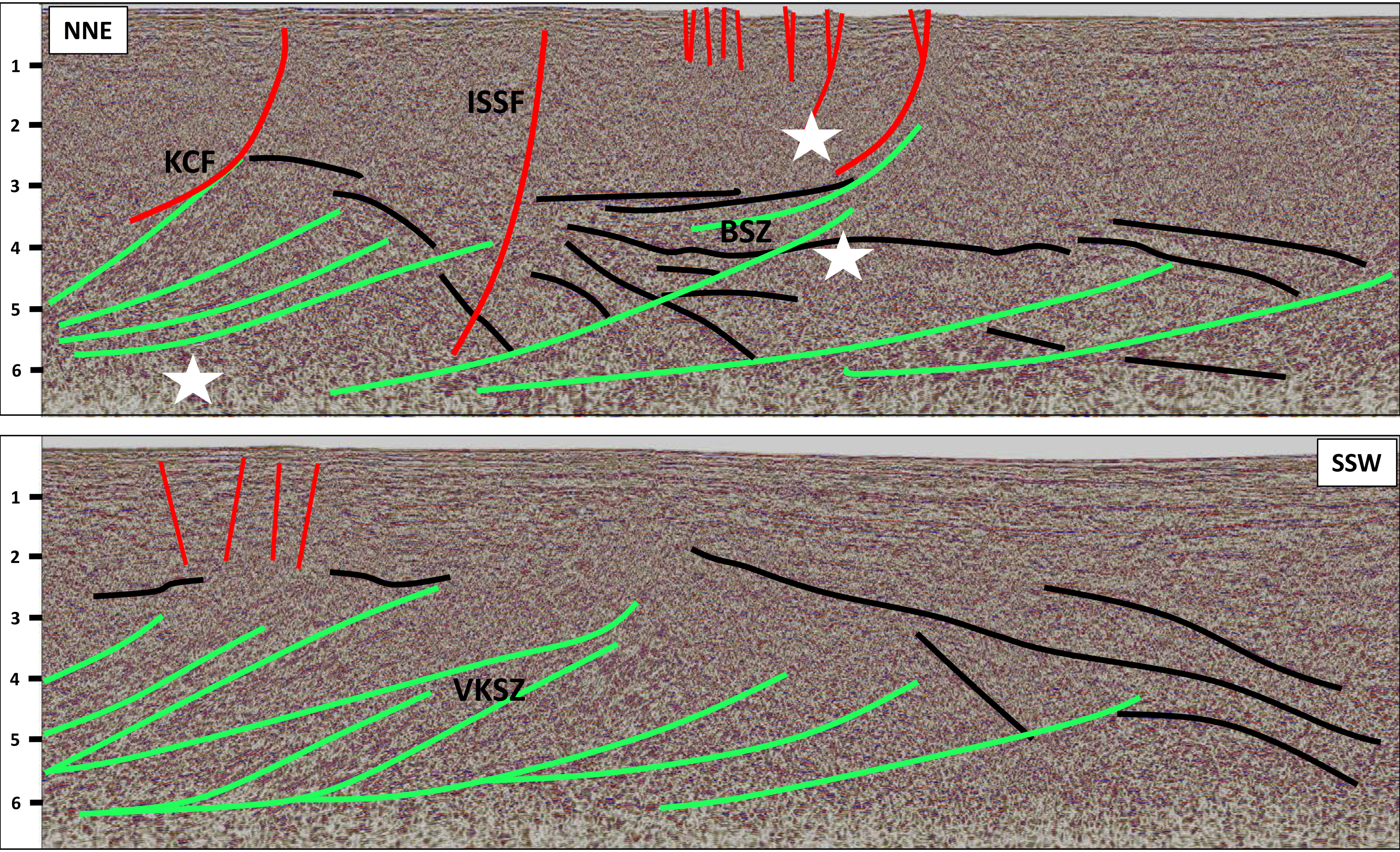

Koehl et al. (in prep. c)

2

North of Bjørnøya, potential NNE-verging Timanian thrusts were reactivated/overprinted during Devonian–Carboniferous extension, early Cenozoic deformation and at present day.

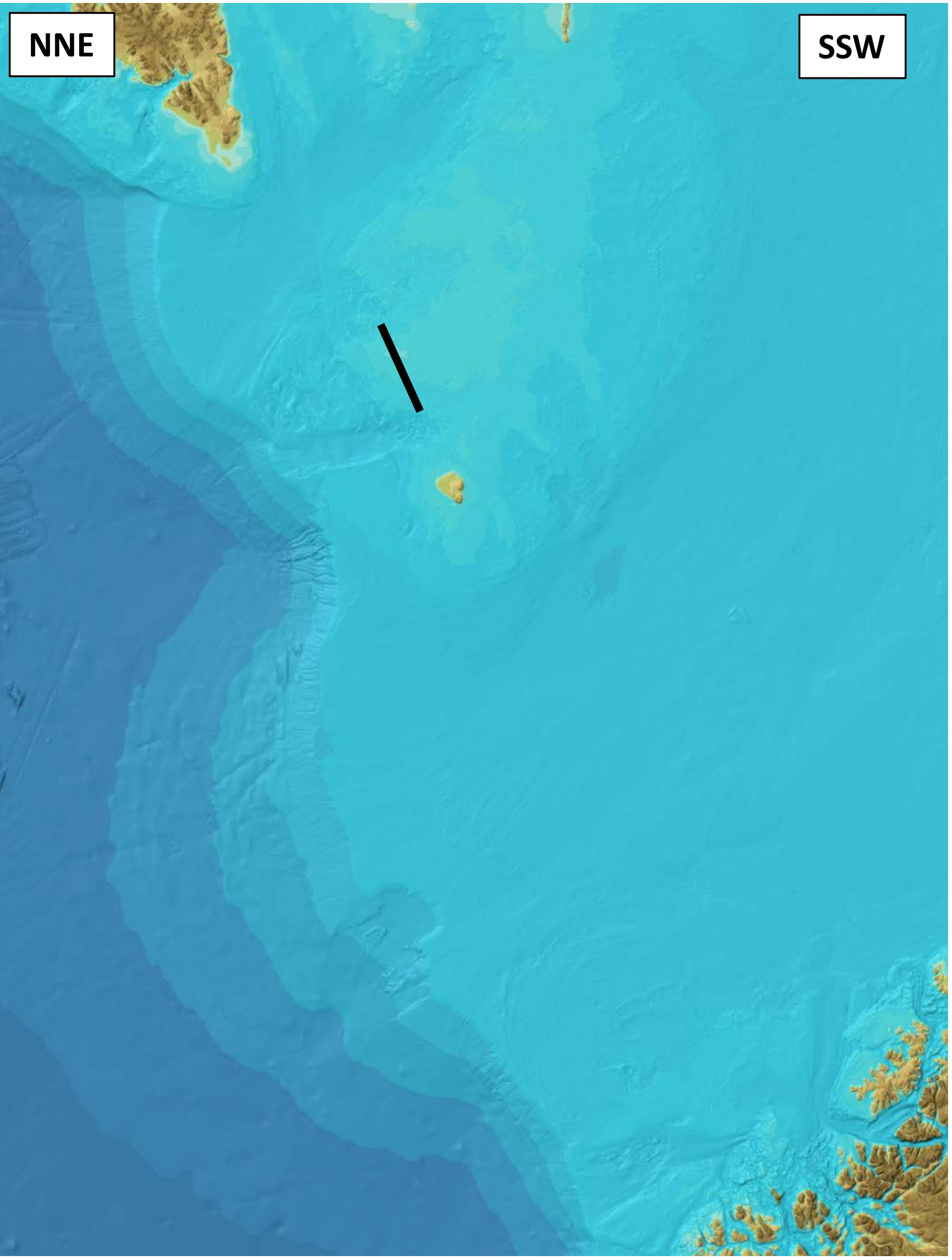

Koehl (in prep.)

2 **North of Bjørnøya, potential NNE-verging Timanian thrusts were reactivated/overprinted during Devonian–Carboniferous extension, early Cenozoic deformation and at present day.**

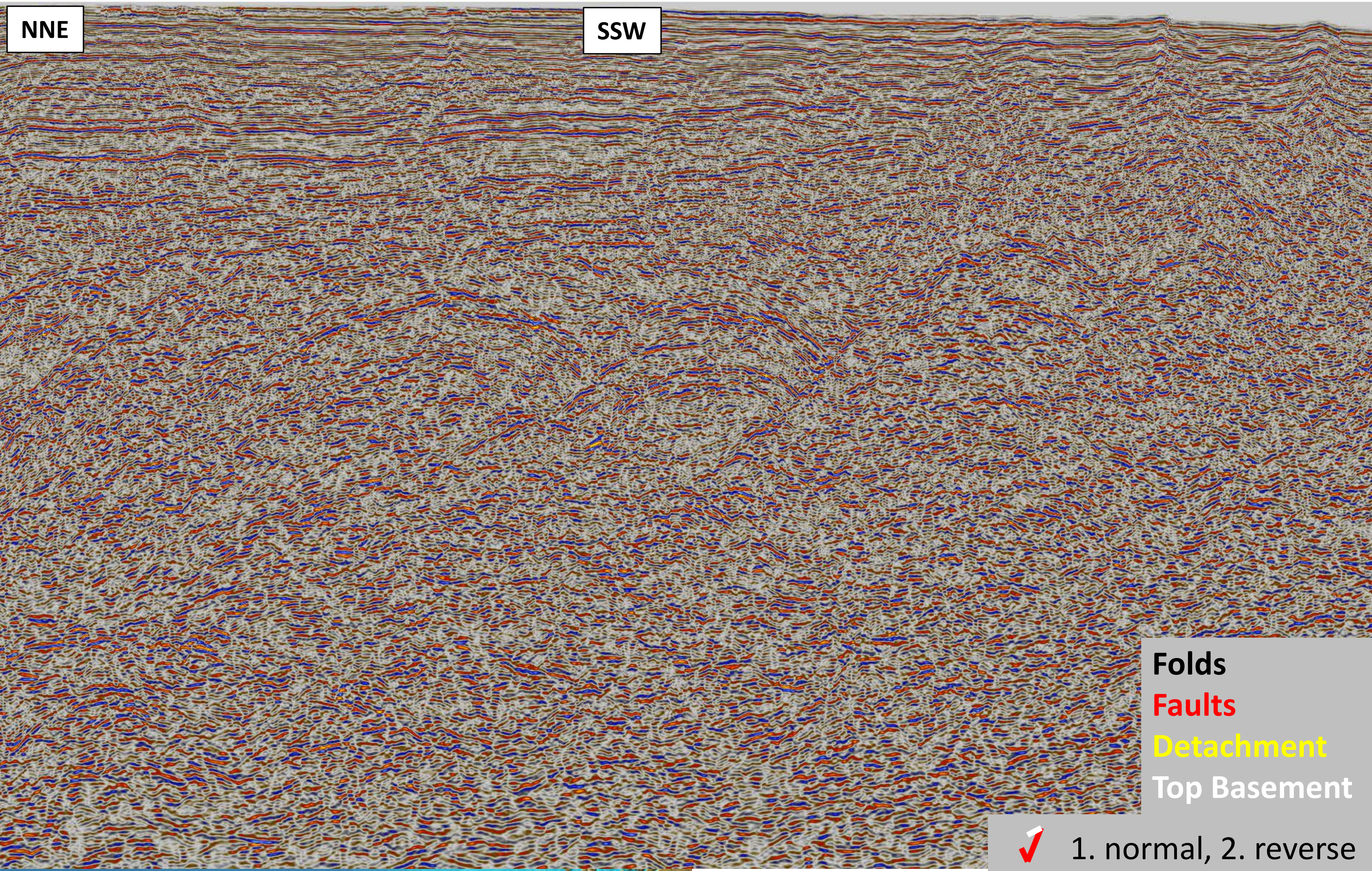

Koehl (in prep.)

2 **North of Bjørnøya, potential NNE-verging Timanian thrusts were reactivated/overprinted during Devonian–Carboniferous extension, early Cenozoic deformation and at present day.**

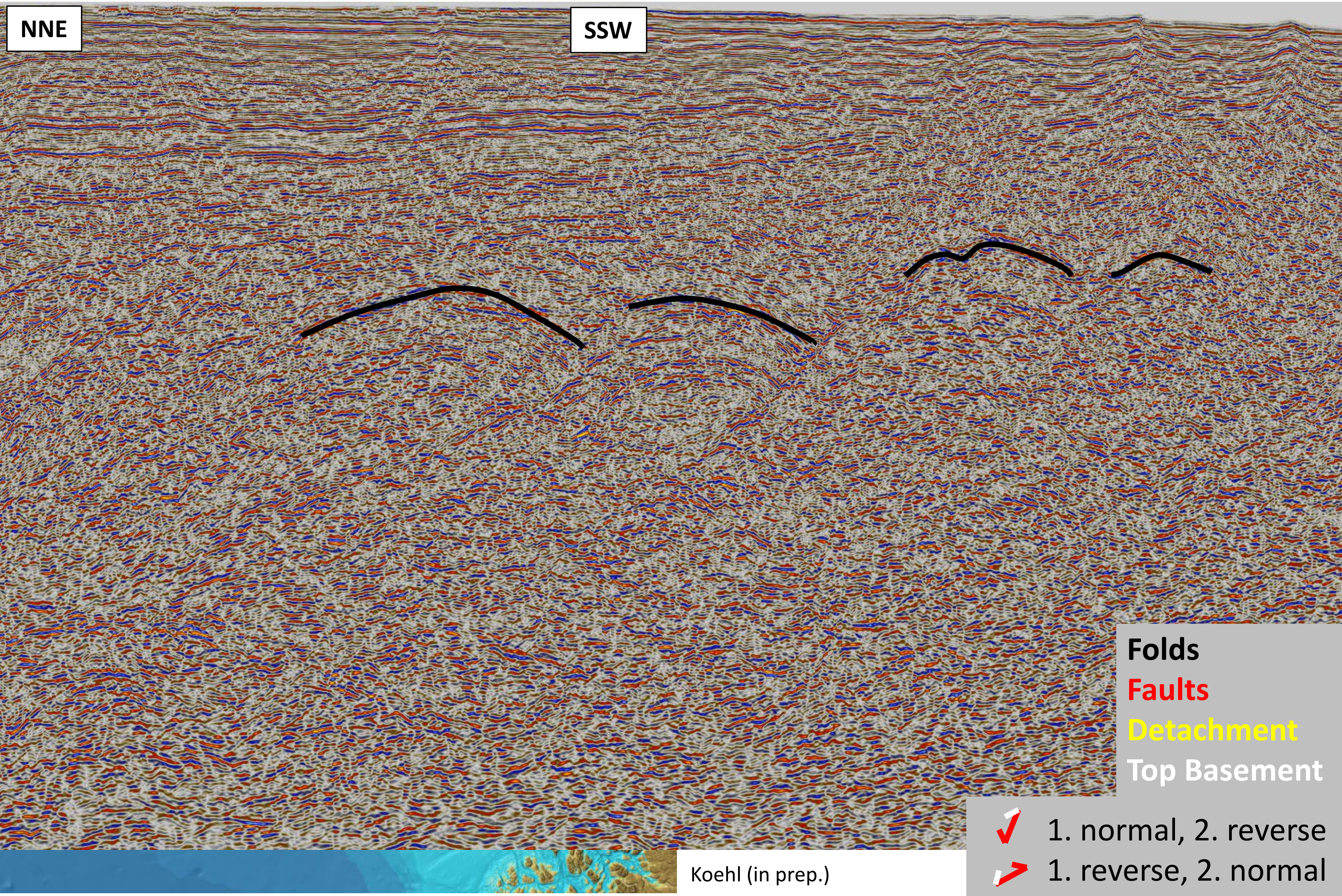

2 **North of Bjørnøya, potential NNE-verging Timanian thrusts were reactivated/overprinted during Devonian–Carboniferous extension, early Cenozoic deformation and at present day.**

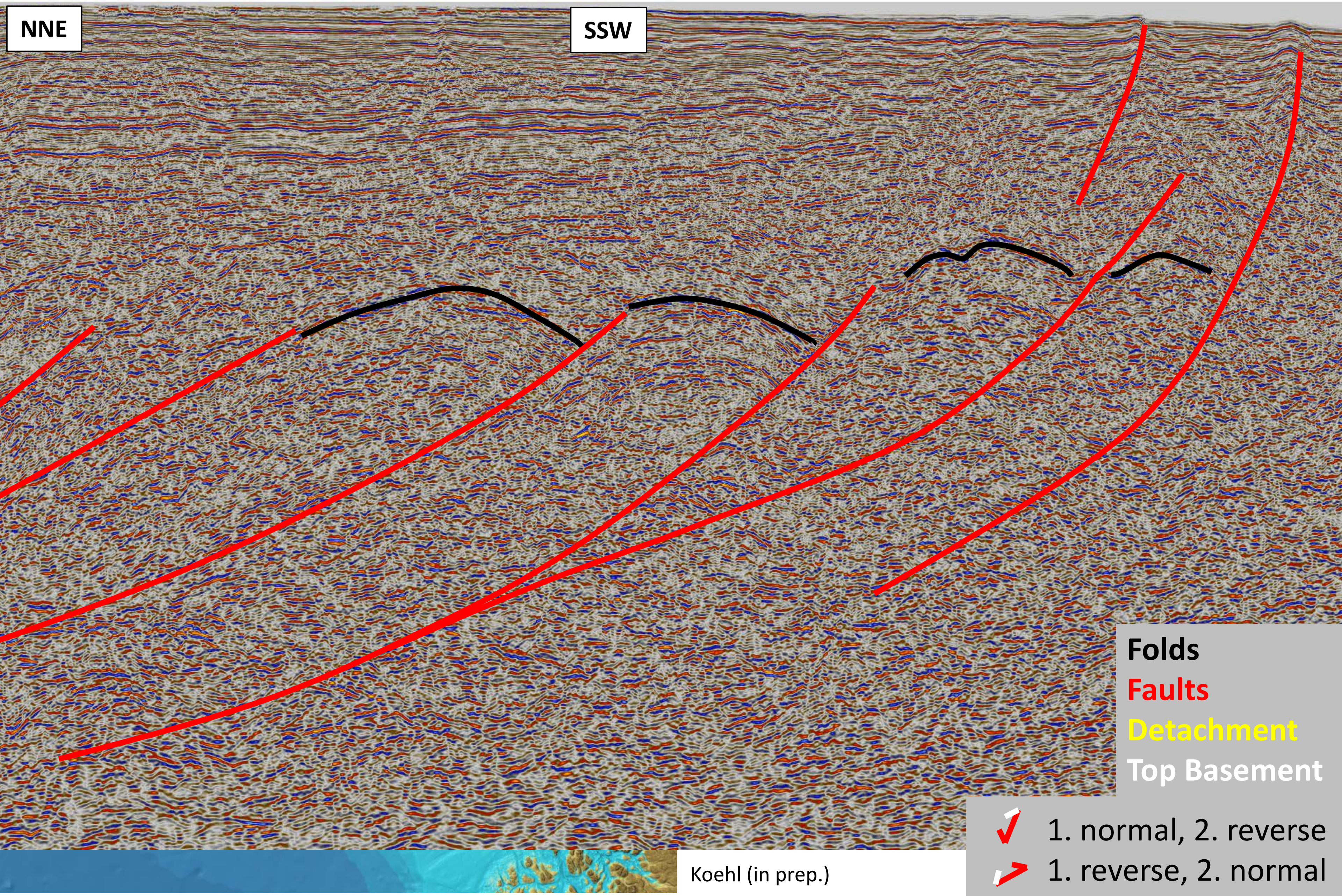

2

North of Bjørnøya, potential NNE-verging Timanian thrusts were reactivated/overprinted during Devonian–Carboniferous extension, early Cenozoic deformation and at present day.

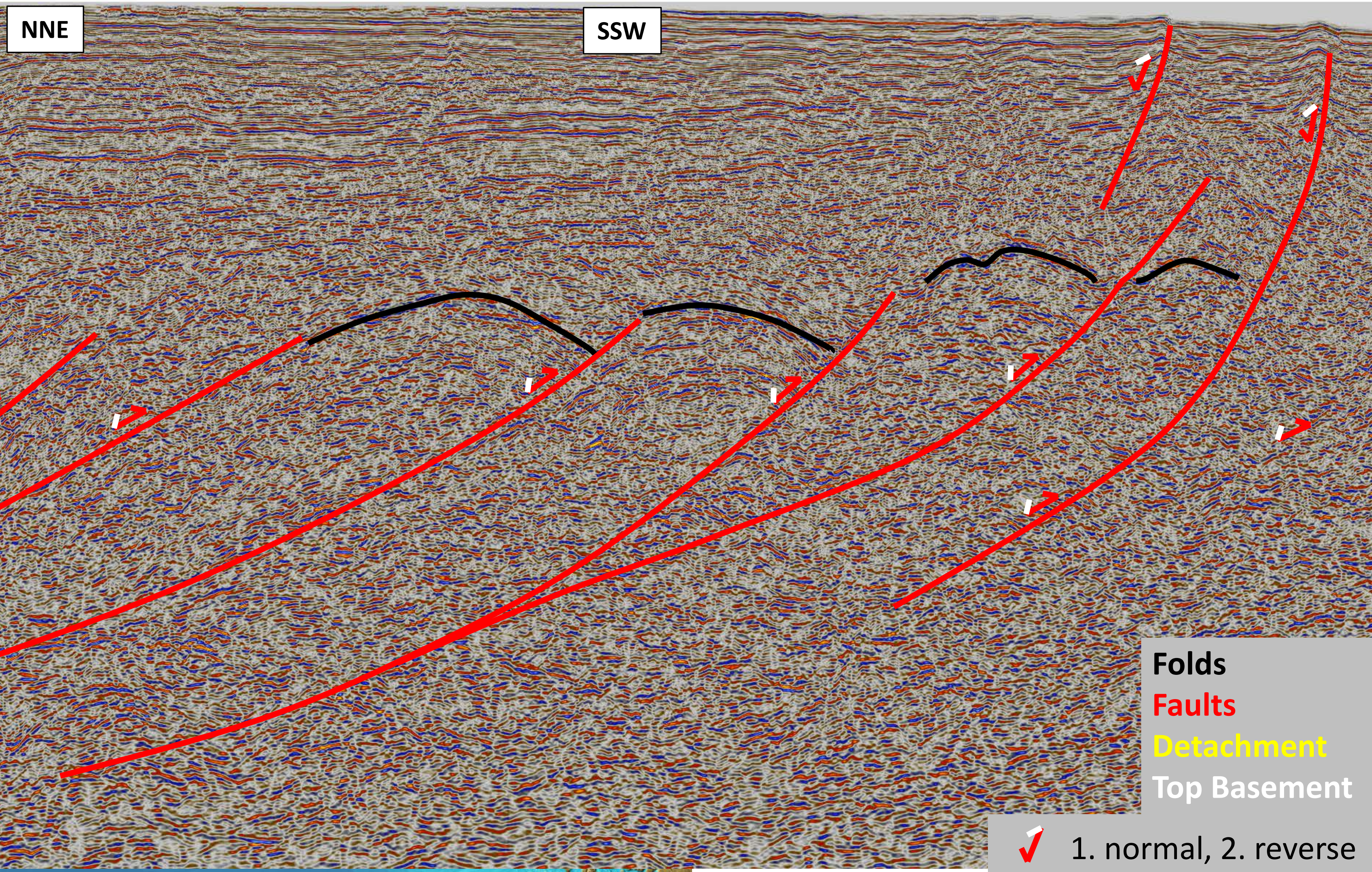

Koehl (in prep.)

2

North of Bjørnøya, potential NNE-verging Timanian thrusts were reactivated/overprinted during Devonian–Carboniferous extension, early Cenozoic deformation and at present day.

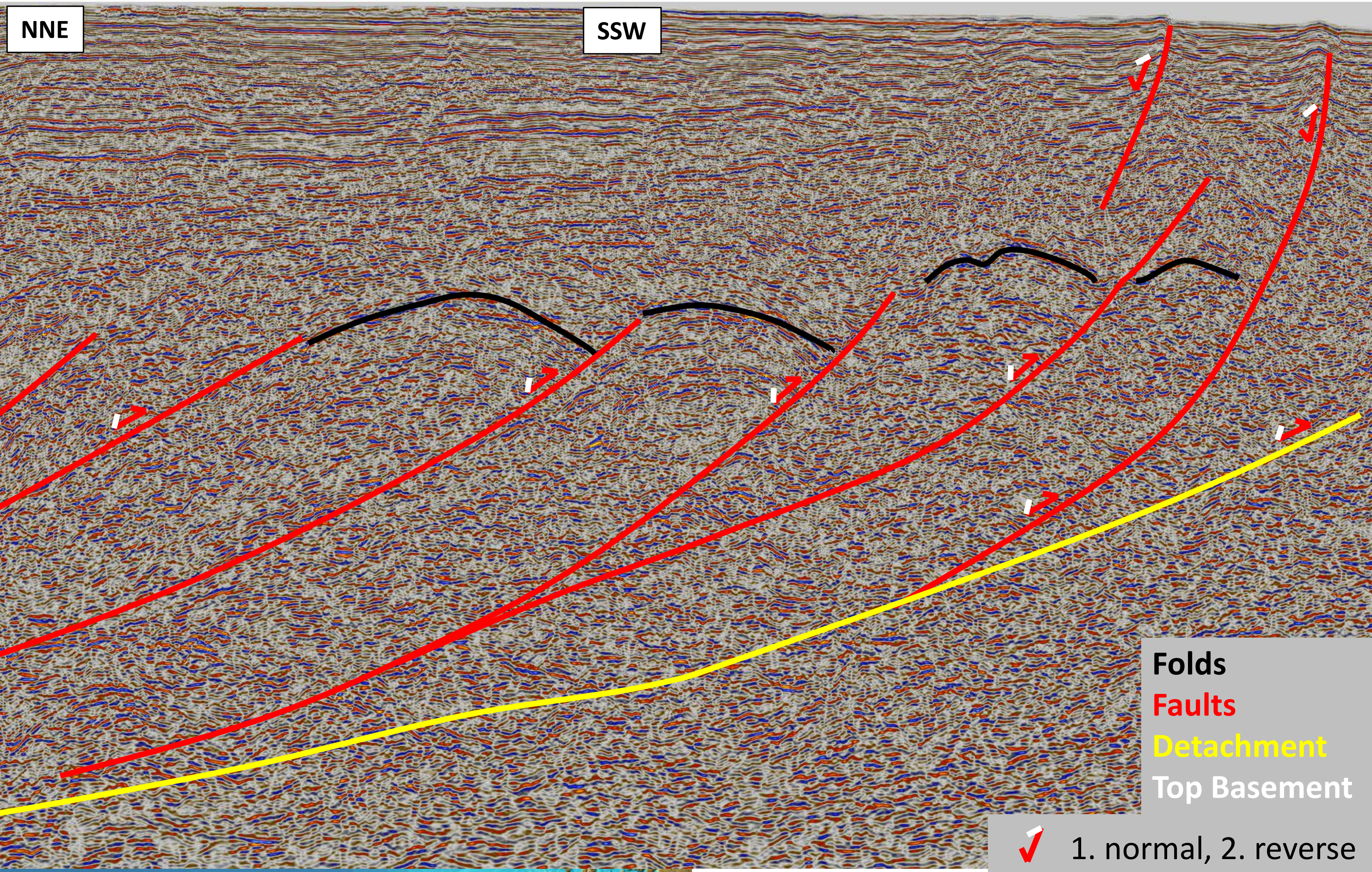

Koehl (in prep.)

2 **North of Bjørnøya, potential NNE-verging Timanian thrusts were reactivated/overprinted during Devonian–Carboniferous extension, early Cenozoic deformation and at present day.**

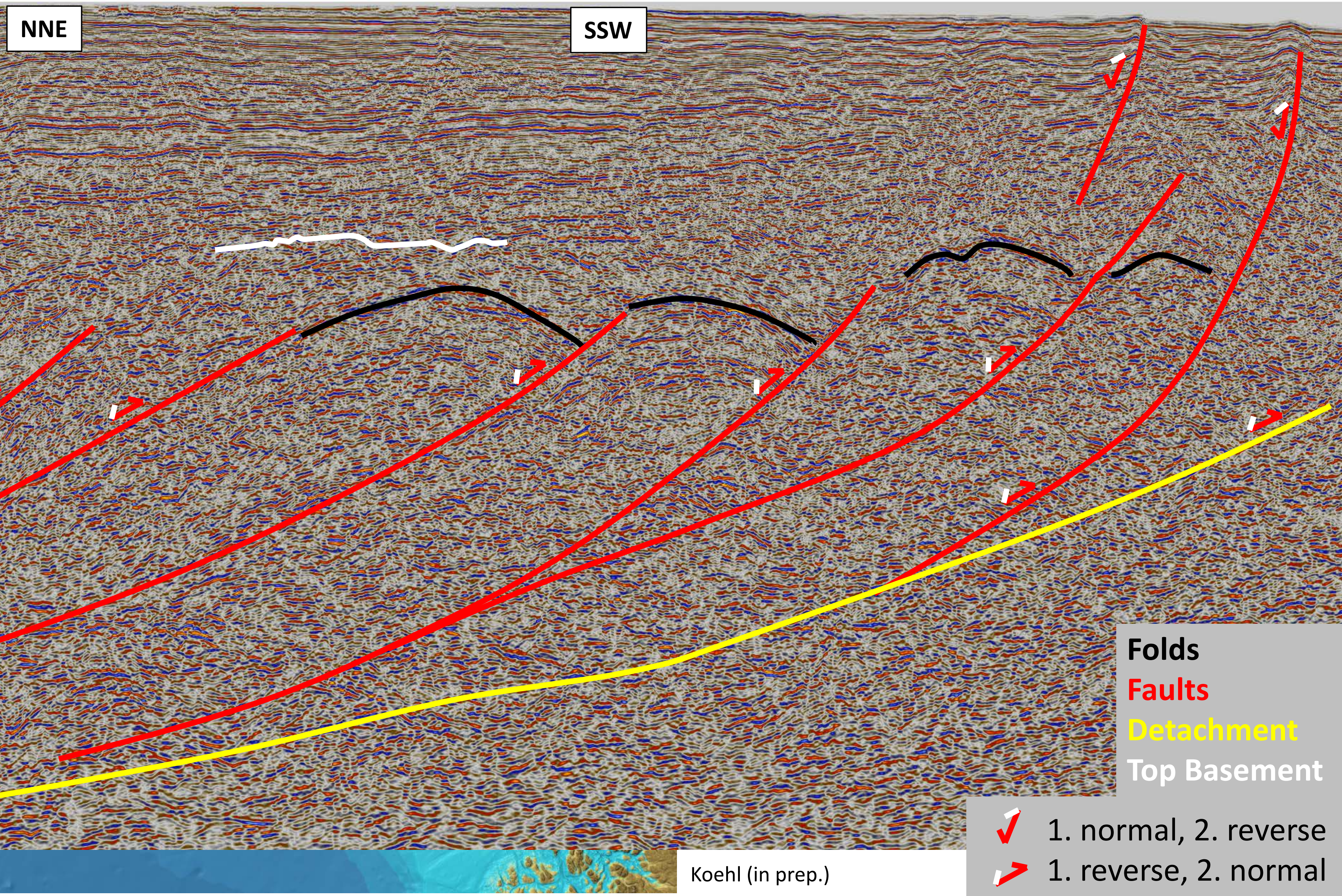

2 **North of Bjørnøya, potential NNE-verging Timanian thrusts were reactivated/overprinted during Devonian–Carboniferous extension, early Cenozoic deformation and at present day.**

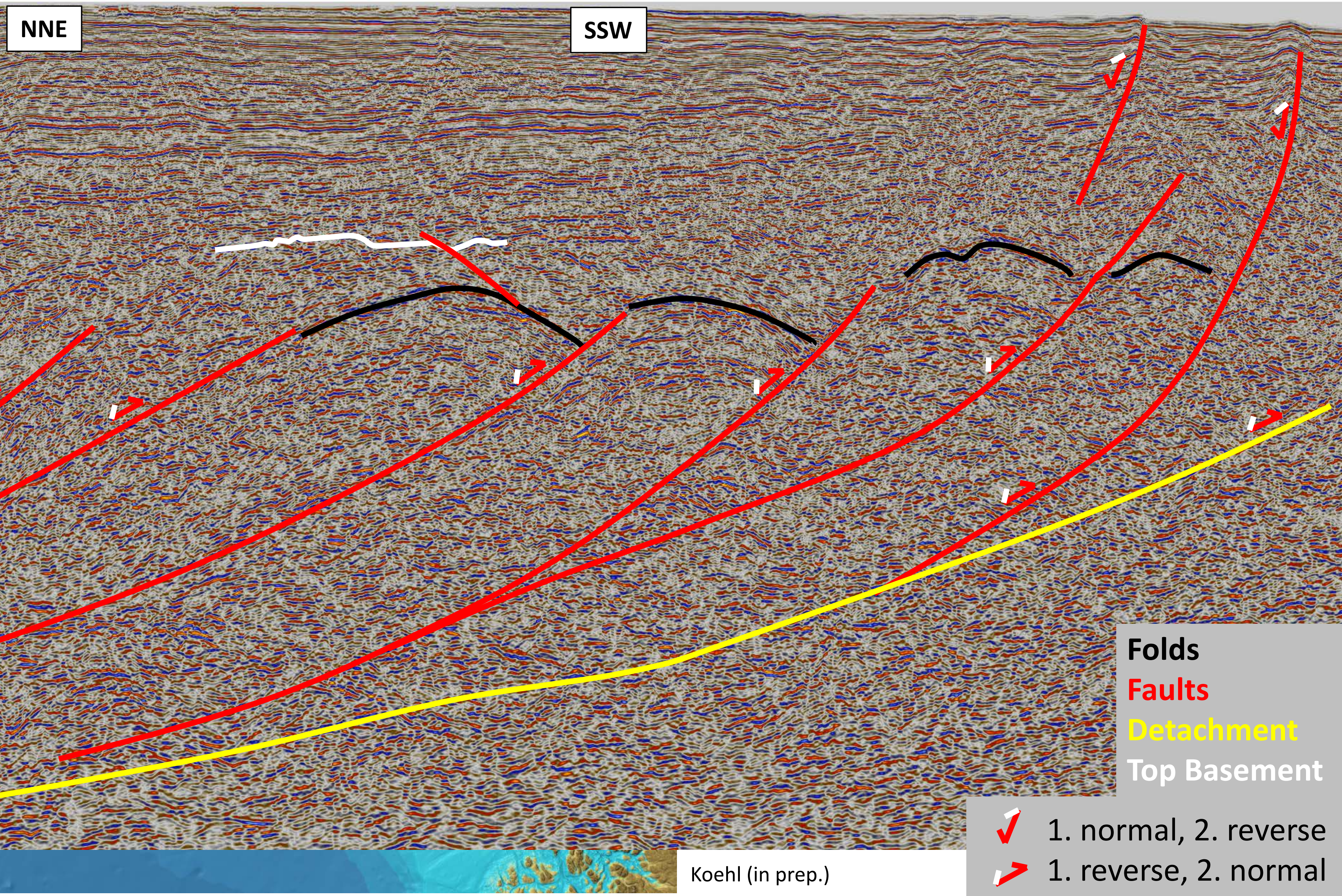

Koehl (in prep.)

2 North of Bjørnøya, potential NNE-verging Timanian thrusts were reactivated/overprinted during Devonian–Carboniferous extension, early Cenozoic deformation and at present day.

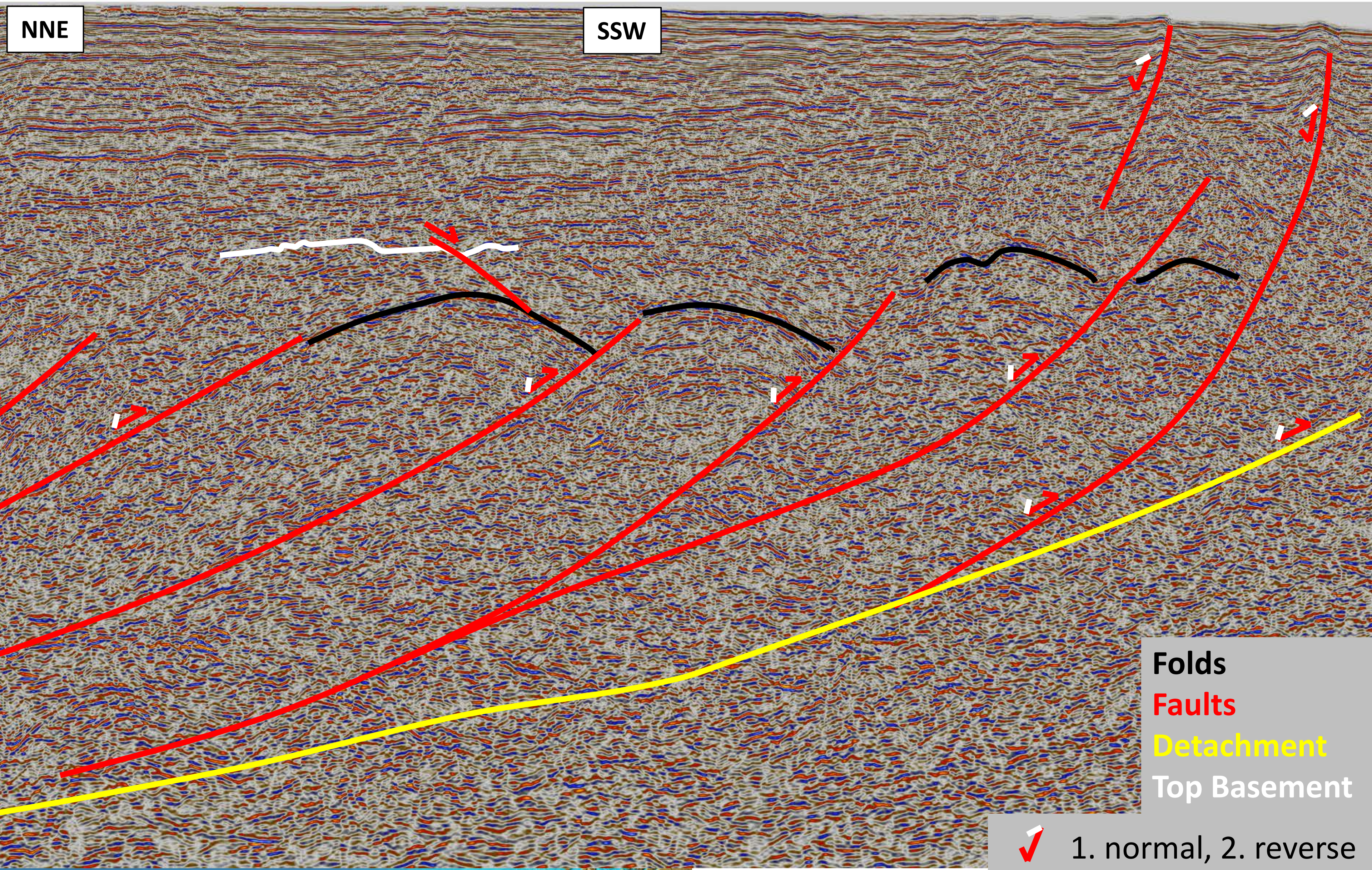

Koehl (in prep.)

2 North of Bjørnøya, potential NNE-verging Timanian thrusts were reactivated/overprinted during Devonian–Carboniferous extension, early Cenozoic deformation and at present day.

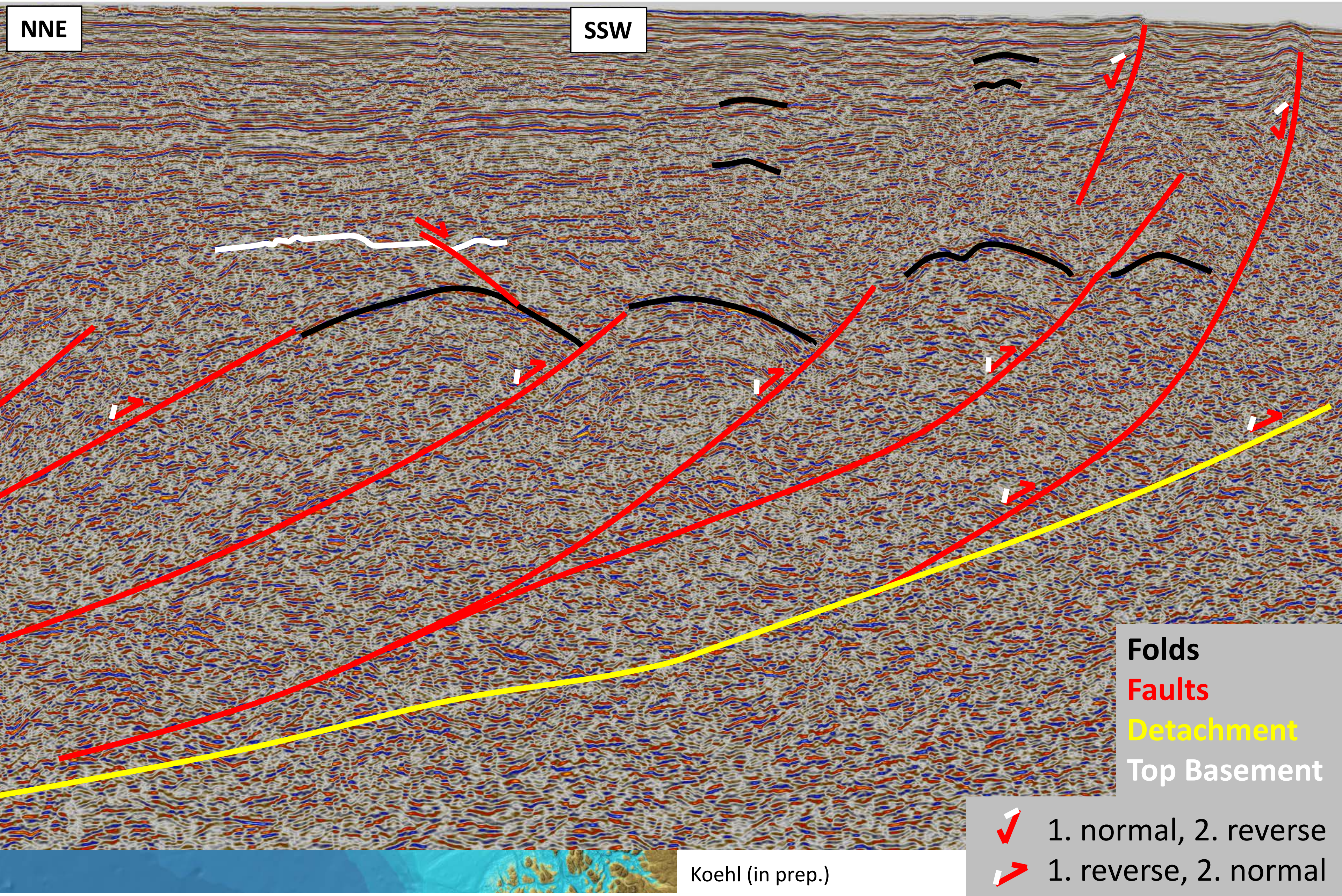

Koehl (in prep.)

2 **North of Bjørnøya, potential NNE-verging Timanian thrusts were reactivated/overprinted during Devonian–Carboniferous extension, early Cenozoic deformation and at present day.**

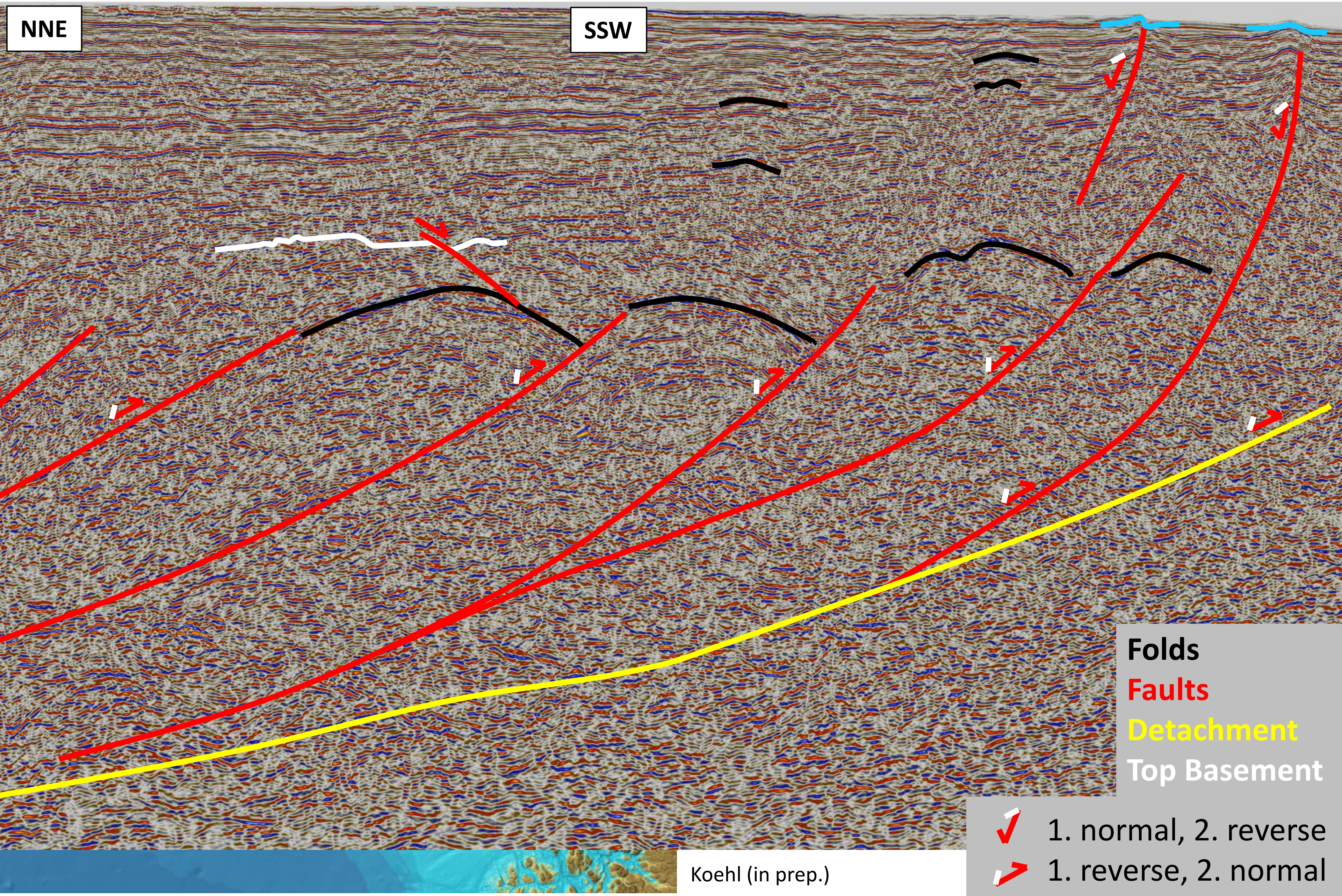

Koehl (in prep.)

3

The Mid-Ocean Ridge is segmented by major transform faults that strike parallel to Timanian faults and topographic highs of continental origin (e.g., Hovgård Ridge).

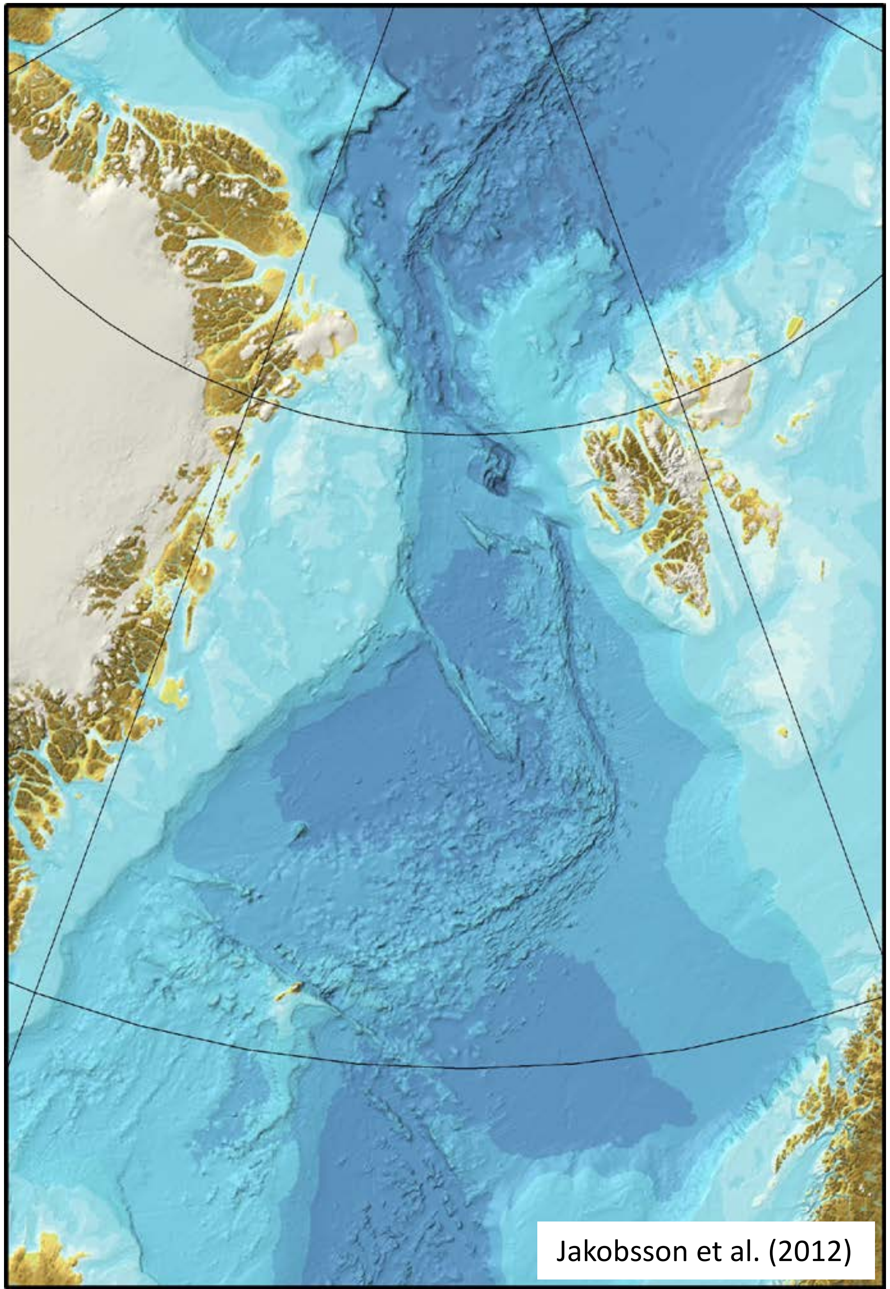

3

The Mid-Ocean Ridge is segmented by major transform faults that strike parallel to Timanian faults and topographic highs of continental origin (e.g., Hovgård Ridge).

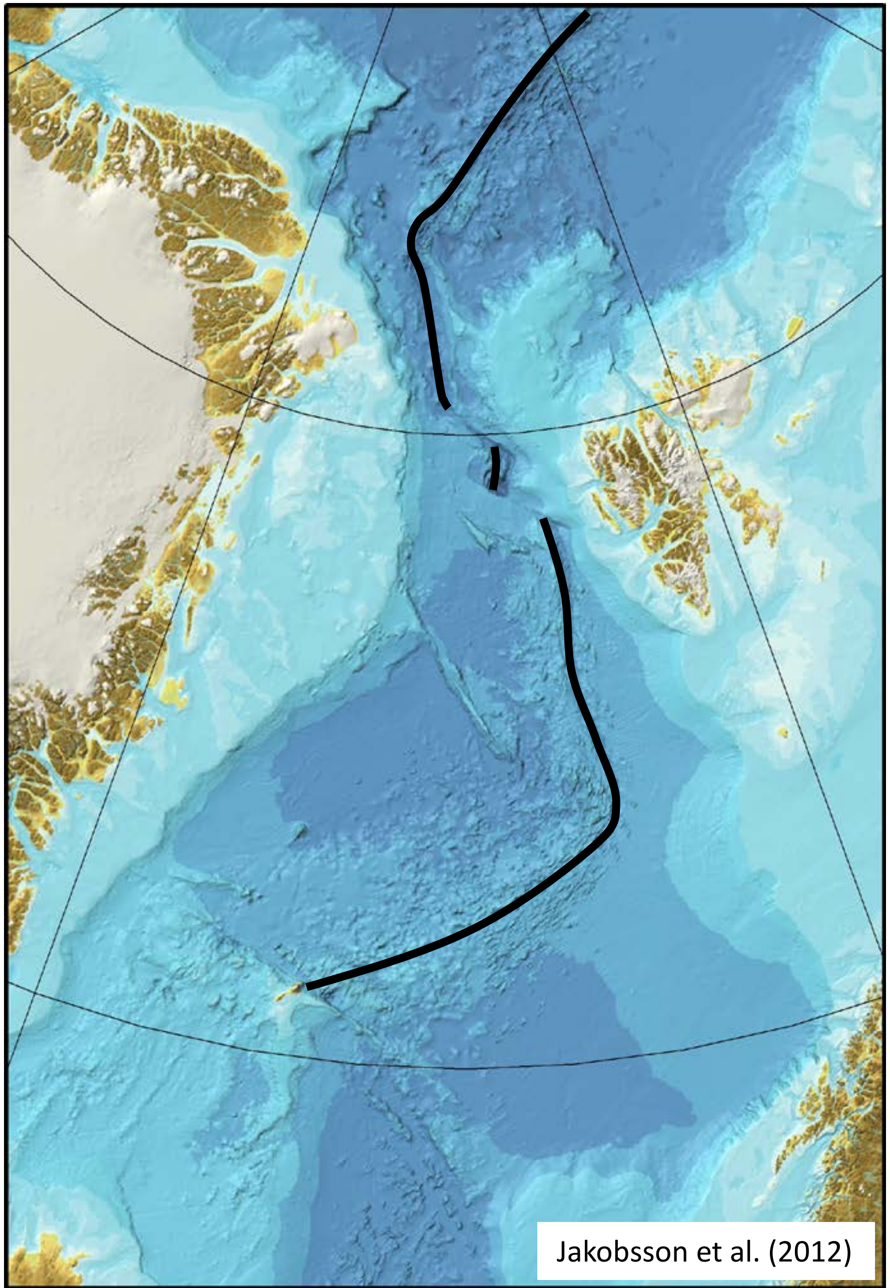

3

The Mid-Ocean Ridge is segmented by major transform faults that strike parallel to Timanian faults and topographic highs of continental origin (e.g., Hovgård Ridge).

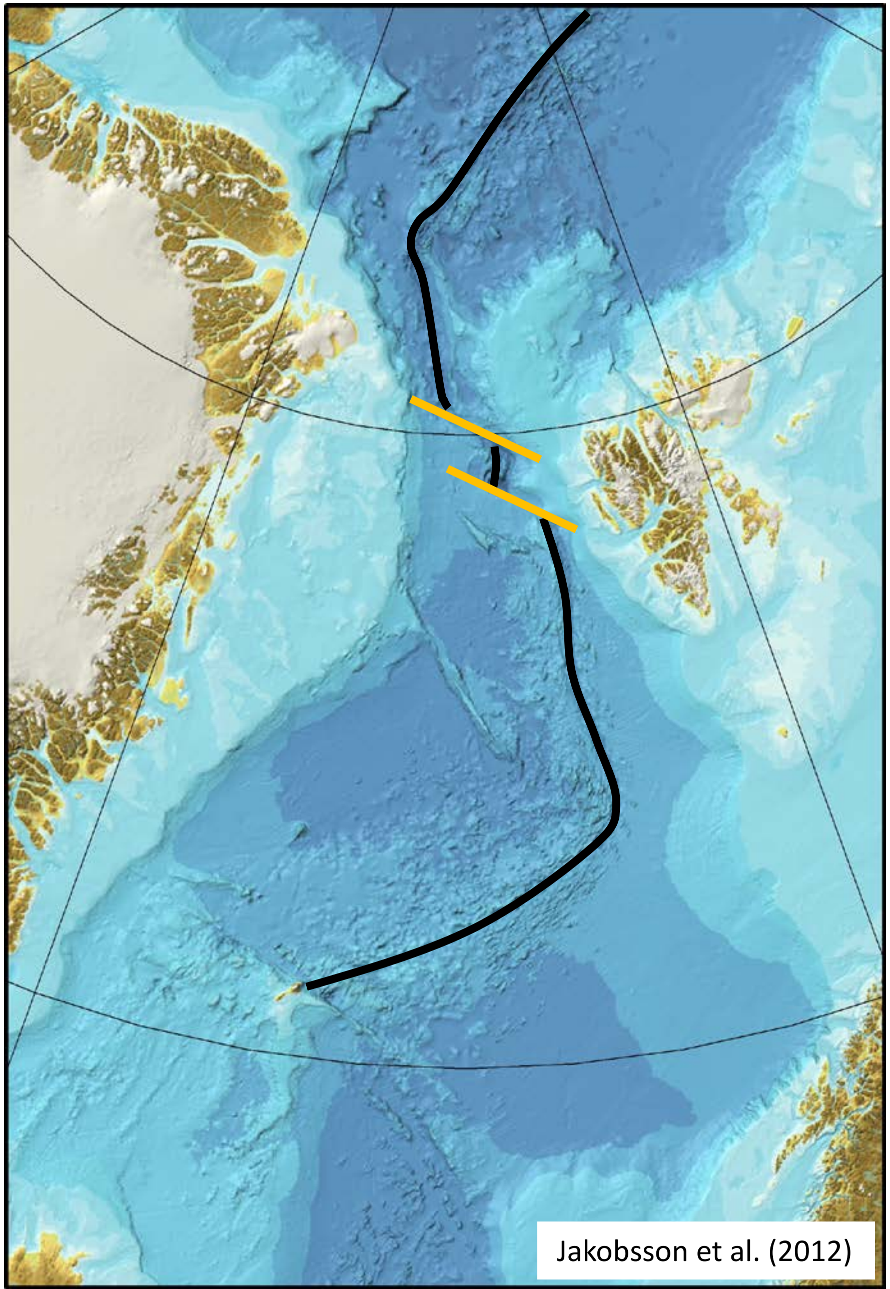

3

The Mid-Ocean Ridge is segmented by major transform faults that strike parallel to Timanian faults and topographic highs of continental origin (e.g., Hovgård Ridge).

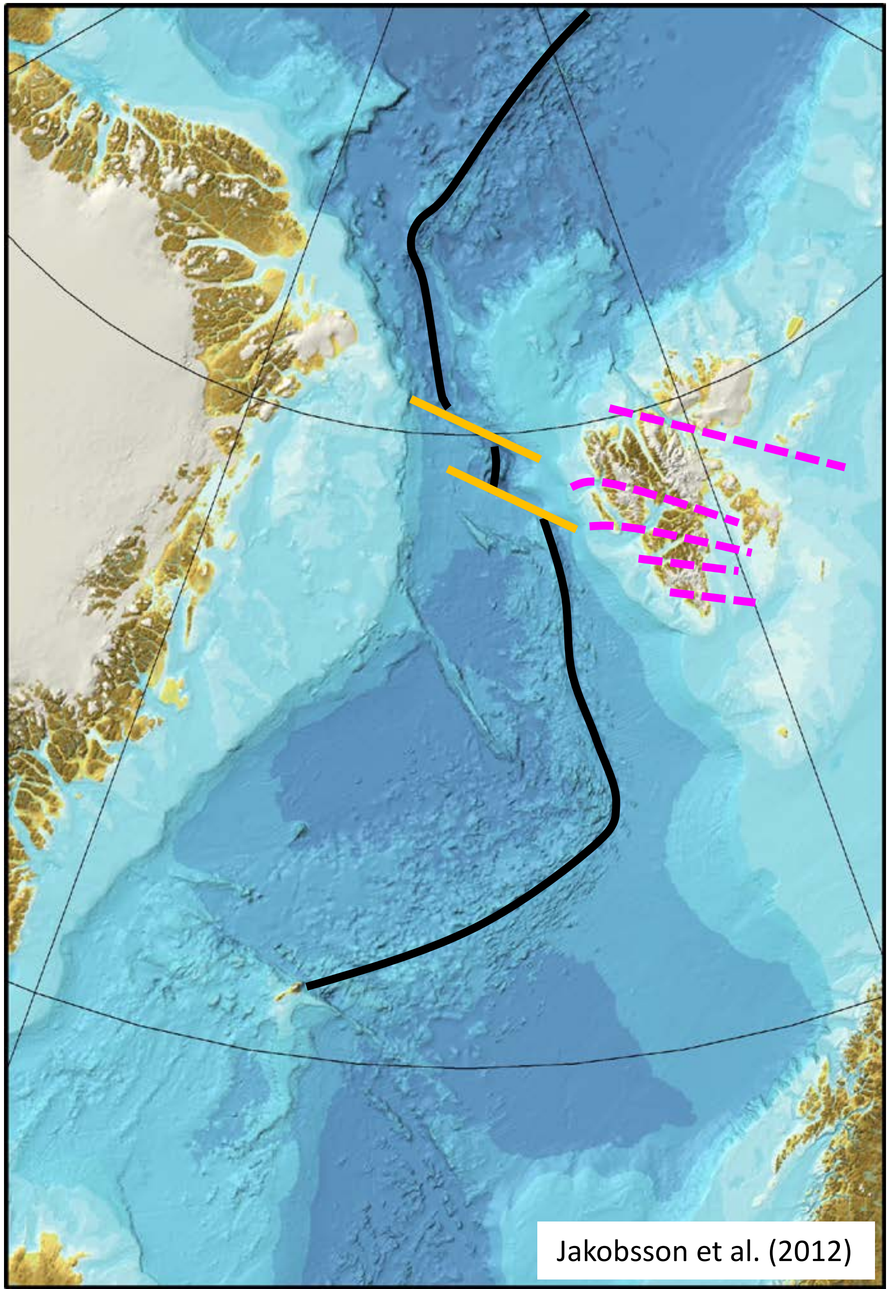

3

The Mid-Ocean Ridge is segmented by major transform faults that strike parallel to Timanian faults and topographic highs of continental origin (e.g., Hovgård Ridge).

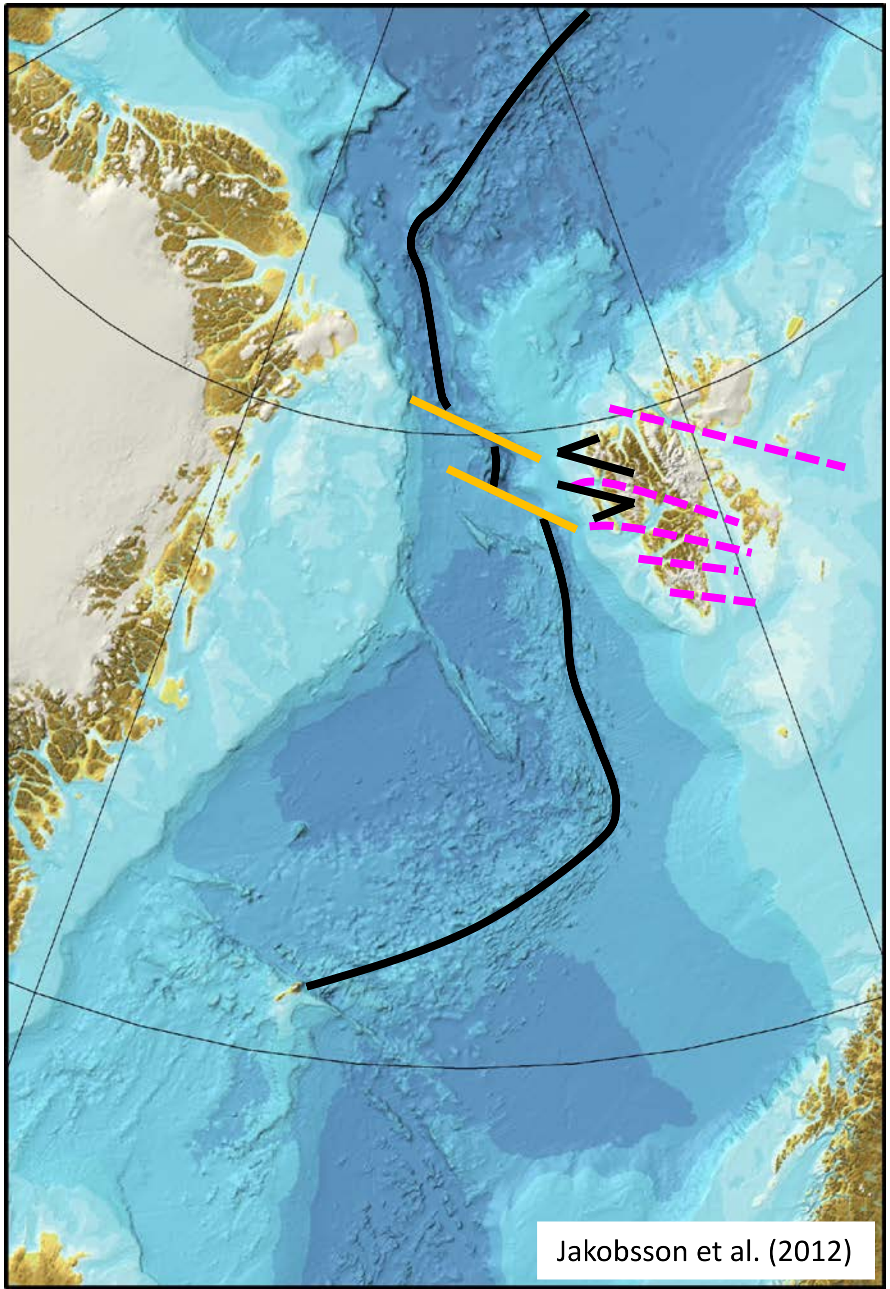

Jakobsson et al. (2012)

3

The Mid-Ocean Ridge is segmented by major transform faults that strike parallel to Timanian faults and topographic highs of continental origin (e.g., Hovgård Ridge).

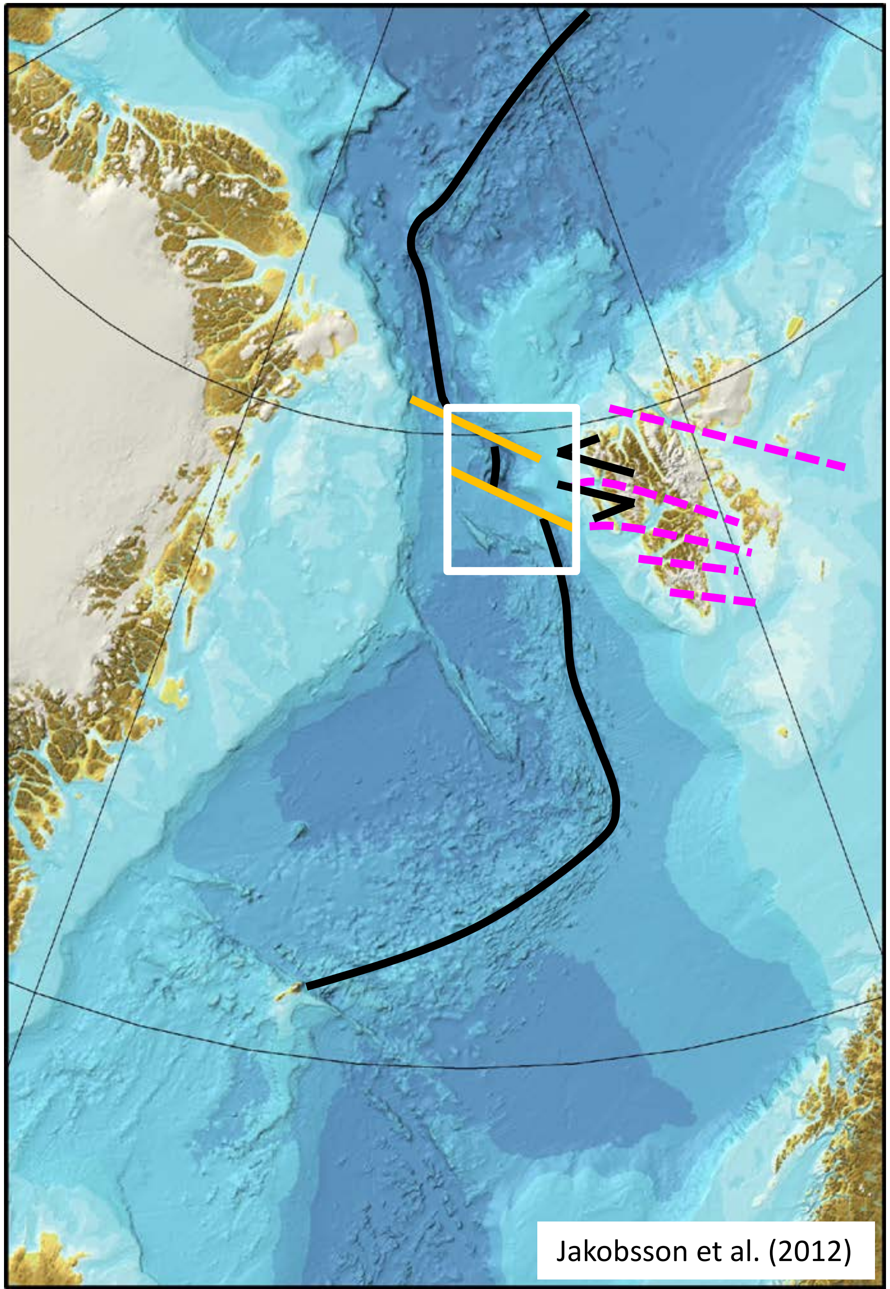

3

The Mid-Ocean Ridge is segmented by major transform faults that strike parallel to Timanian faults and topographic highs of continental origin (e.g., Hovgård Ridge).

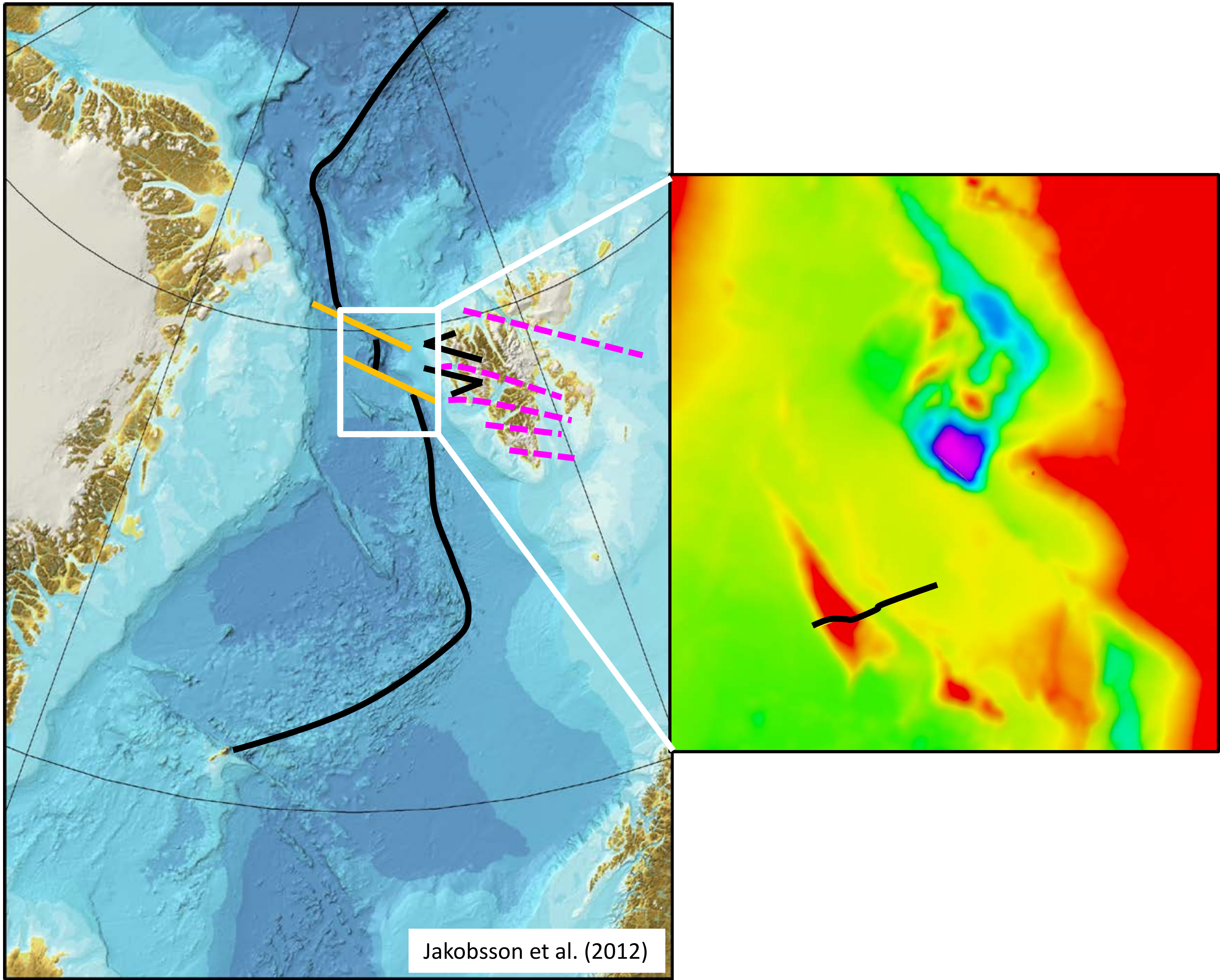

3 **The Hovgård Ridge may represent the western continuation of a Timanian thrust that was ripped off Svalbard during the breakup of the North Atlantic Ocean.**

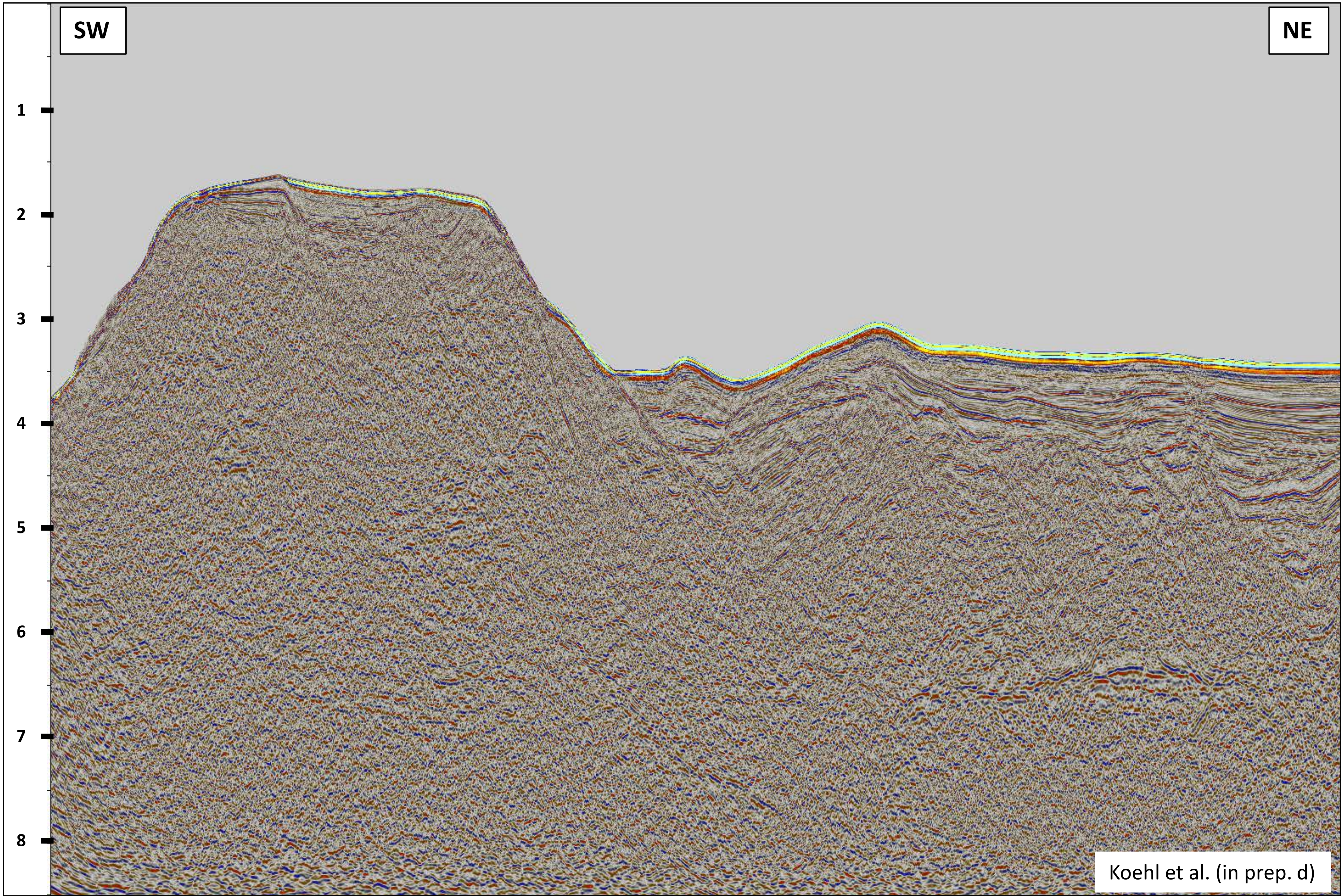

3 The Hovgård Ridge may represent the western continuation of a Timanian thrust that was ripped off Svalbard during the breakup of the North Atlantic Ocean.

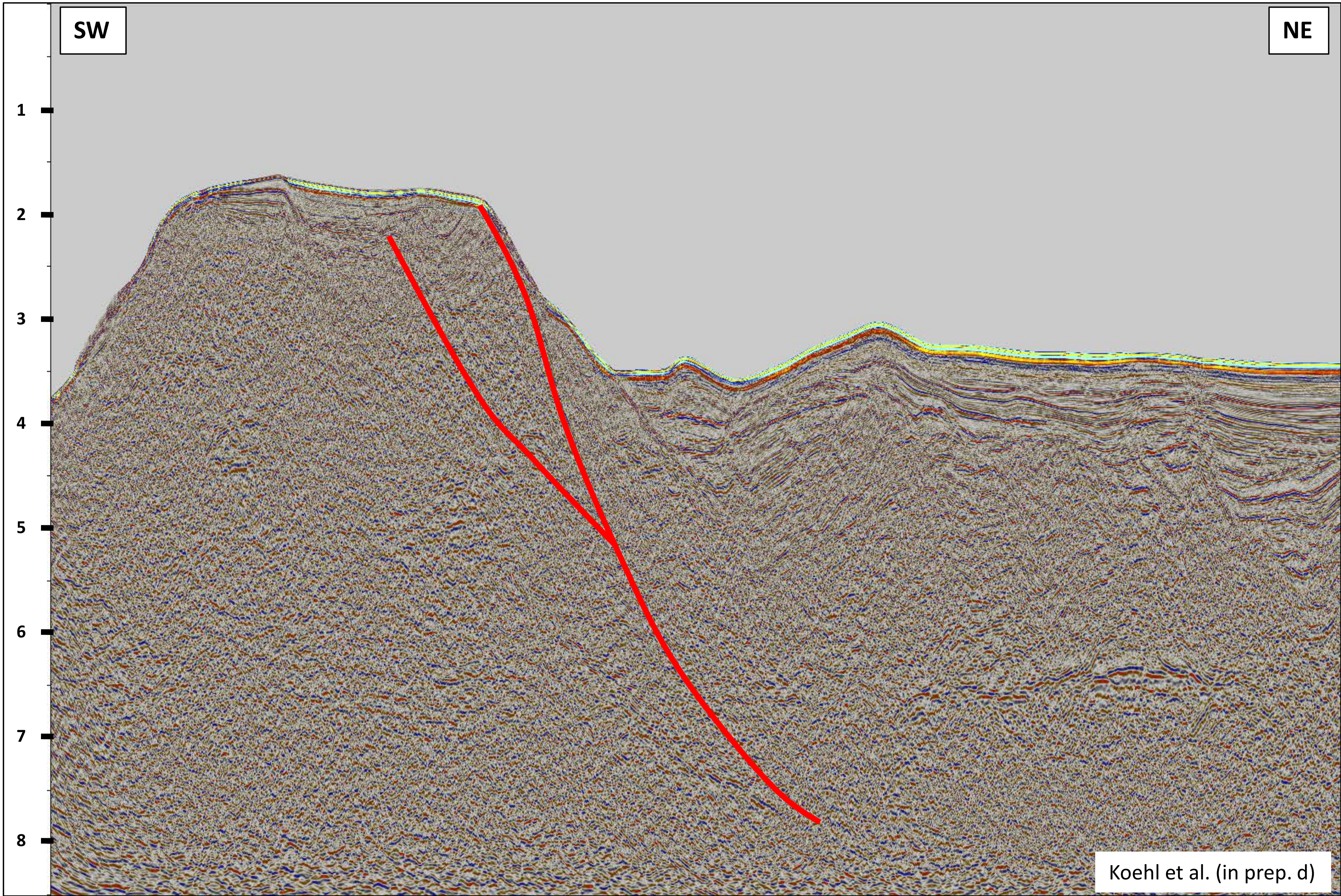

3

The Hovgård Ridge may represent the western continuation of a Timanian thrust that was ripped off Svalbard during the breakup of the North Atlantic Ocean.

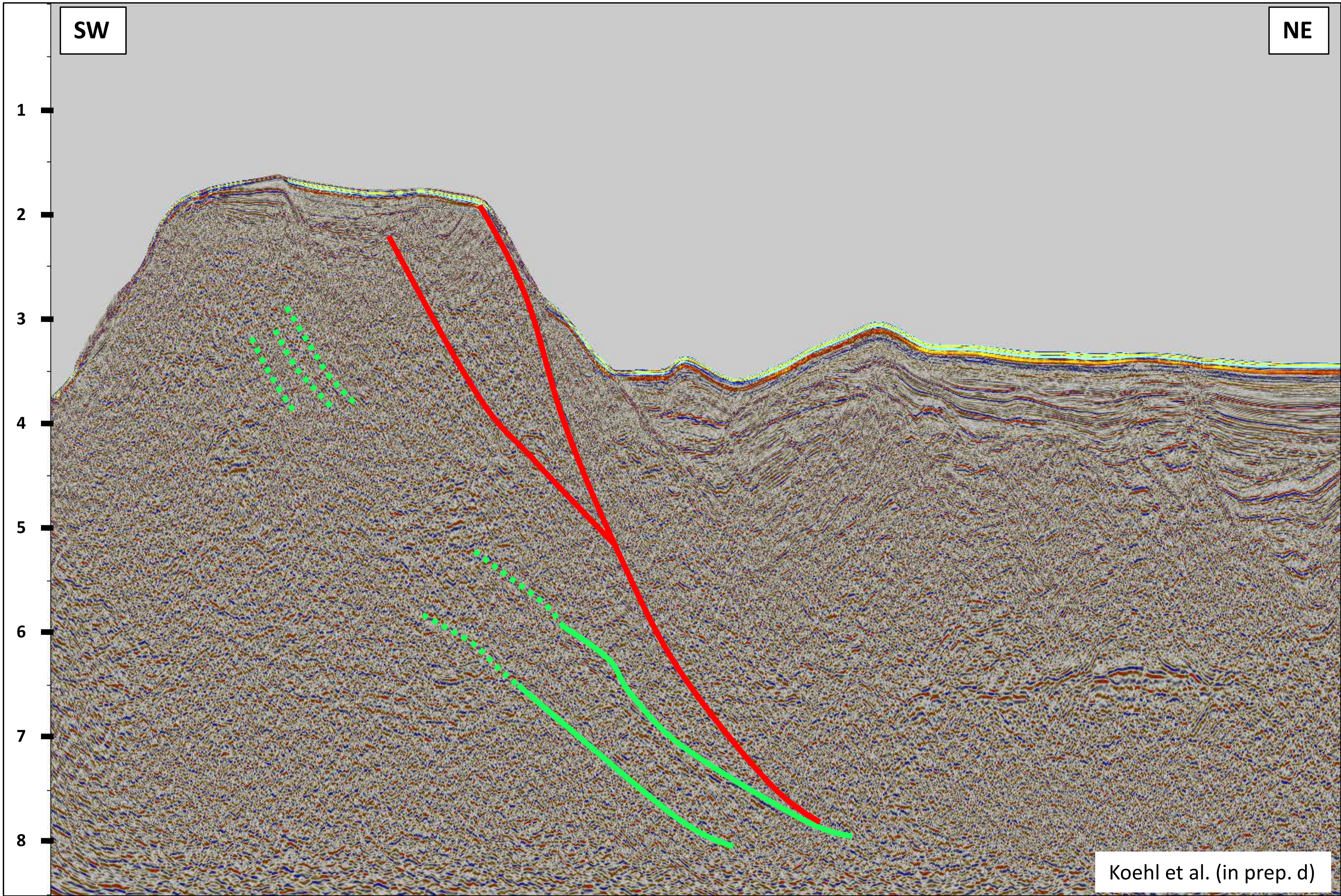

3 **The Hovgård Ridge may represent the western continuation of a Timanian thrust that was ripped off Svalbard during the breakup of the North Atlantic Ocean.**

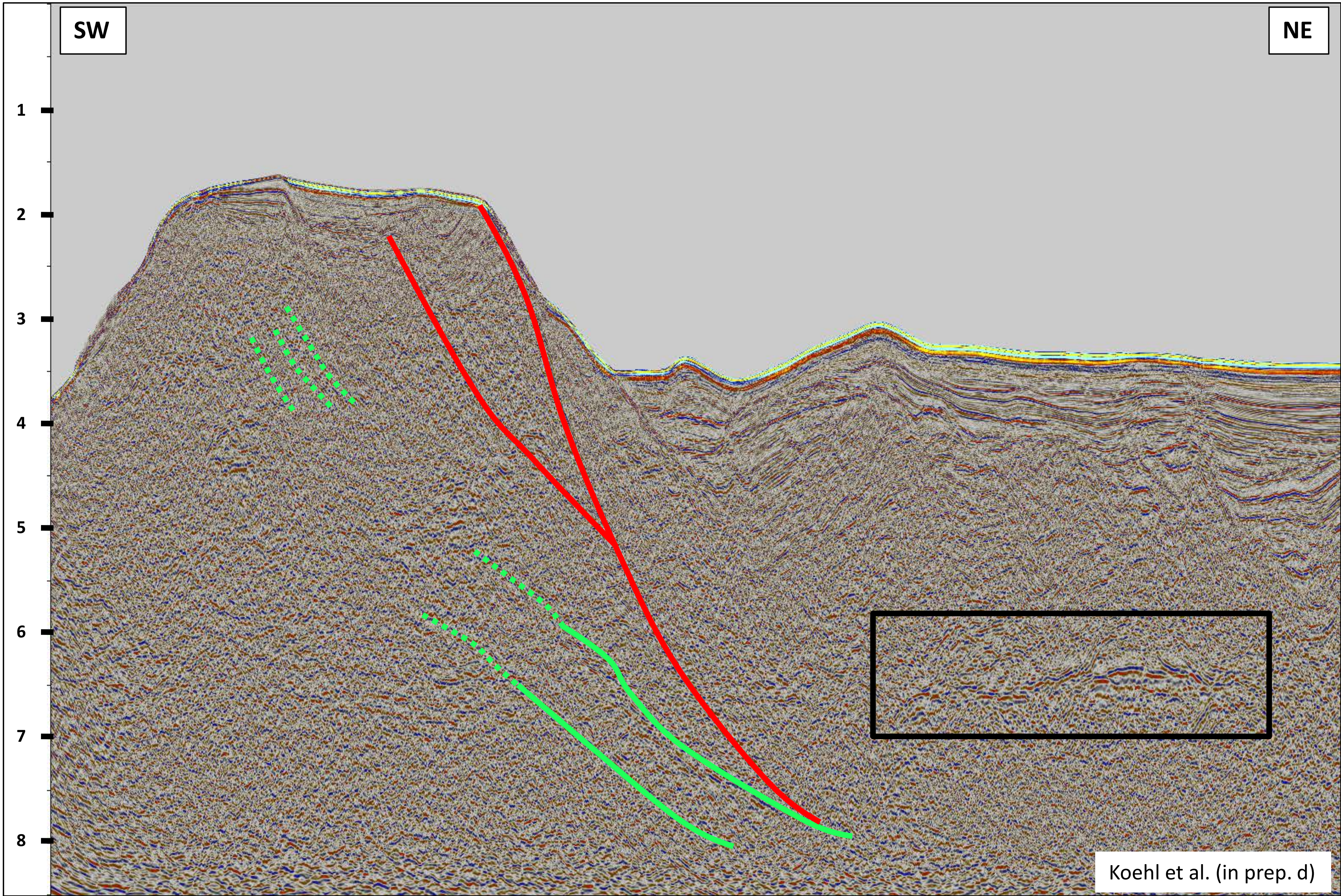

3

Gas flares and leakage along the crest of the Vestnesa Ridge are most likely related to gas hydrate destabilization.

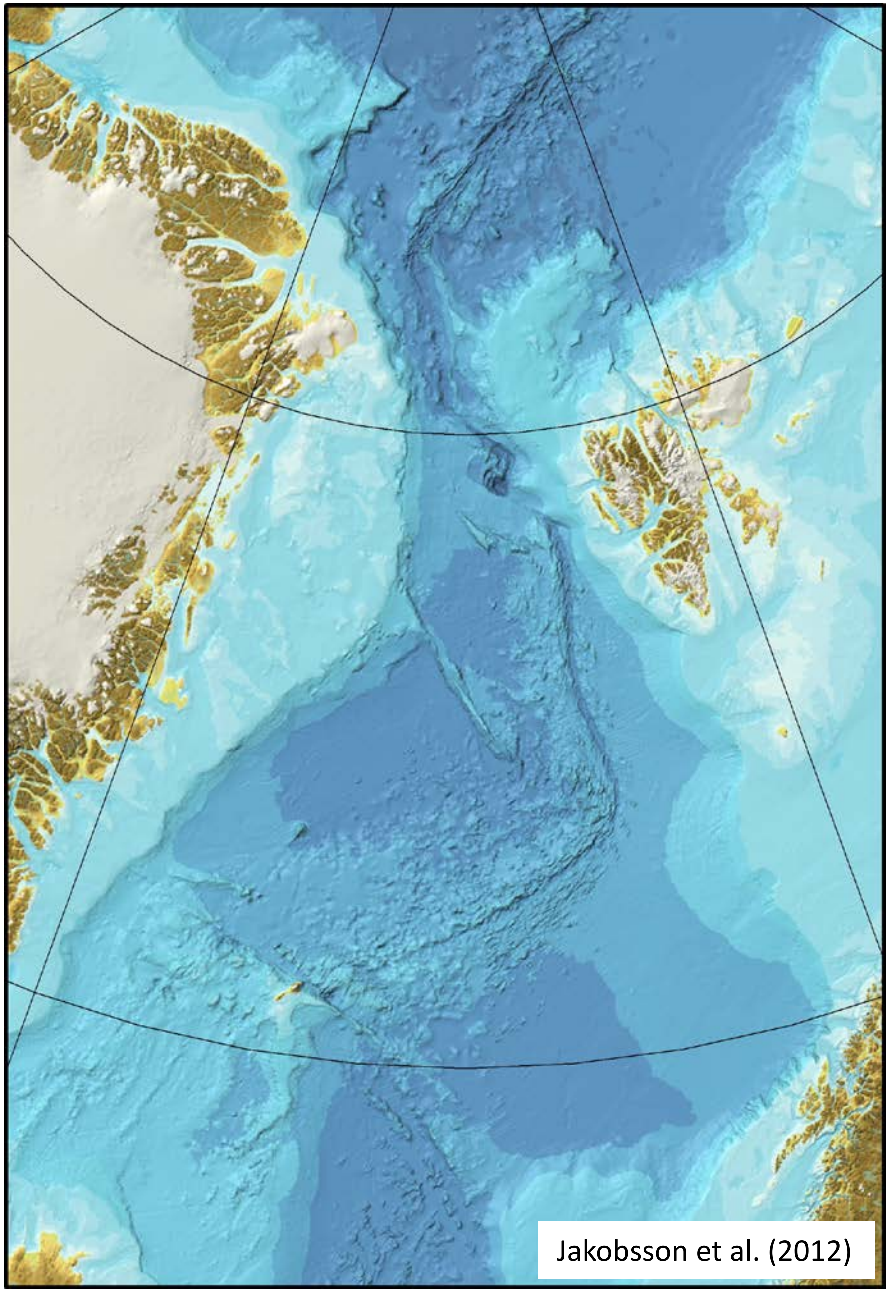

Jakobsson et al. (2012)

3 **Gas flares and leakage along the crest of the Vestnesa Ridge are most likely related to gas hydrate destabilization.**

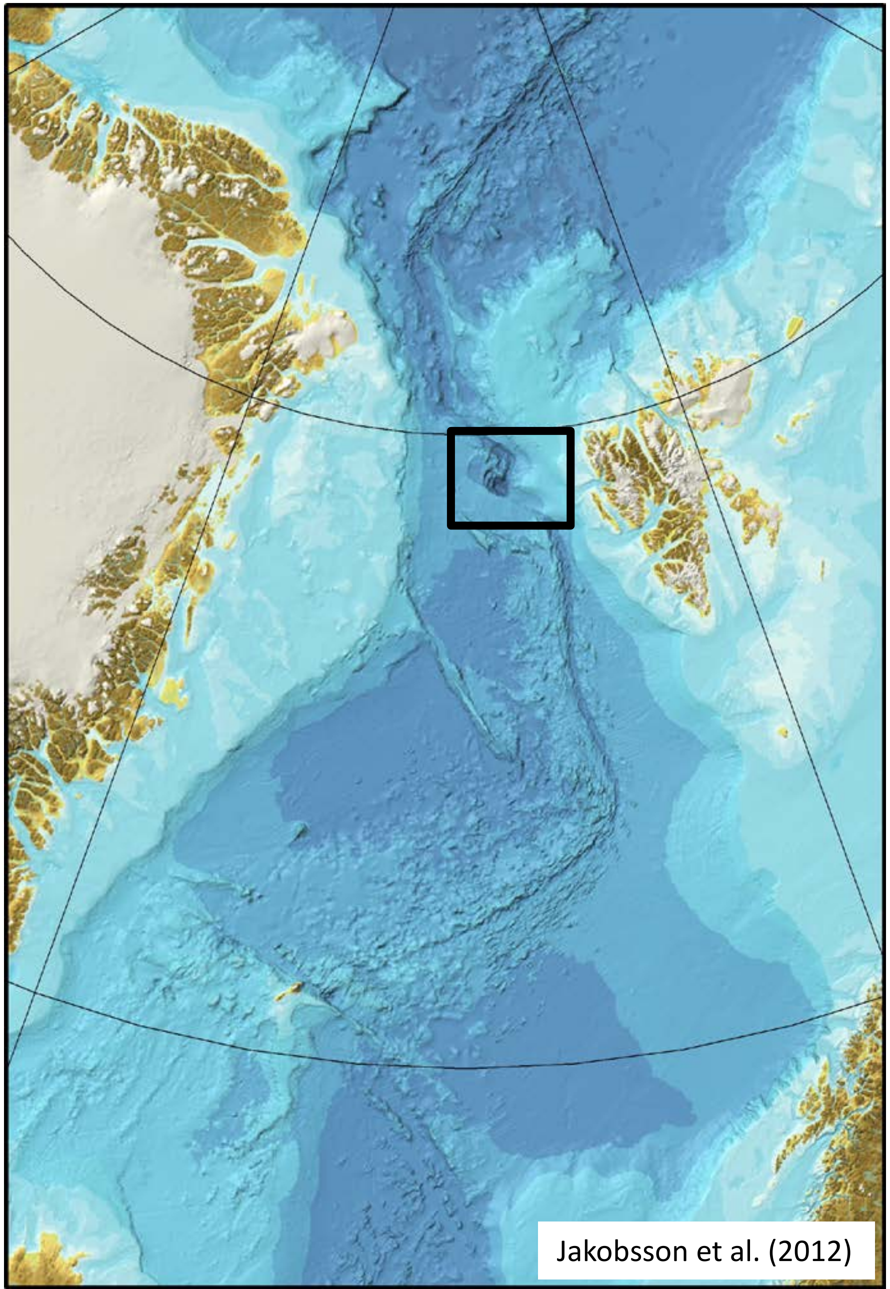

3 **Gas flares and leakage along the crest of the Vestnesa Ridge are most likely related to gas hydrate destabilization.**

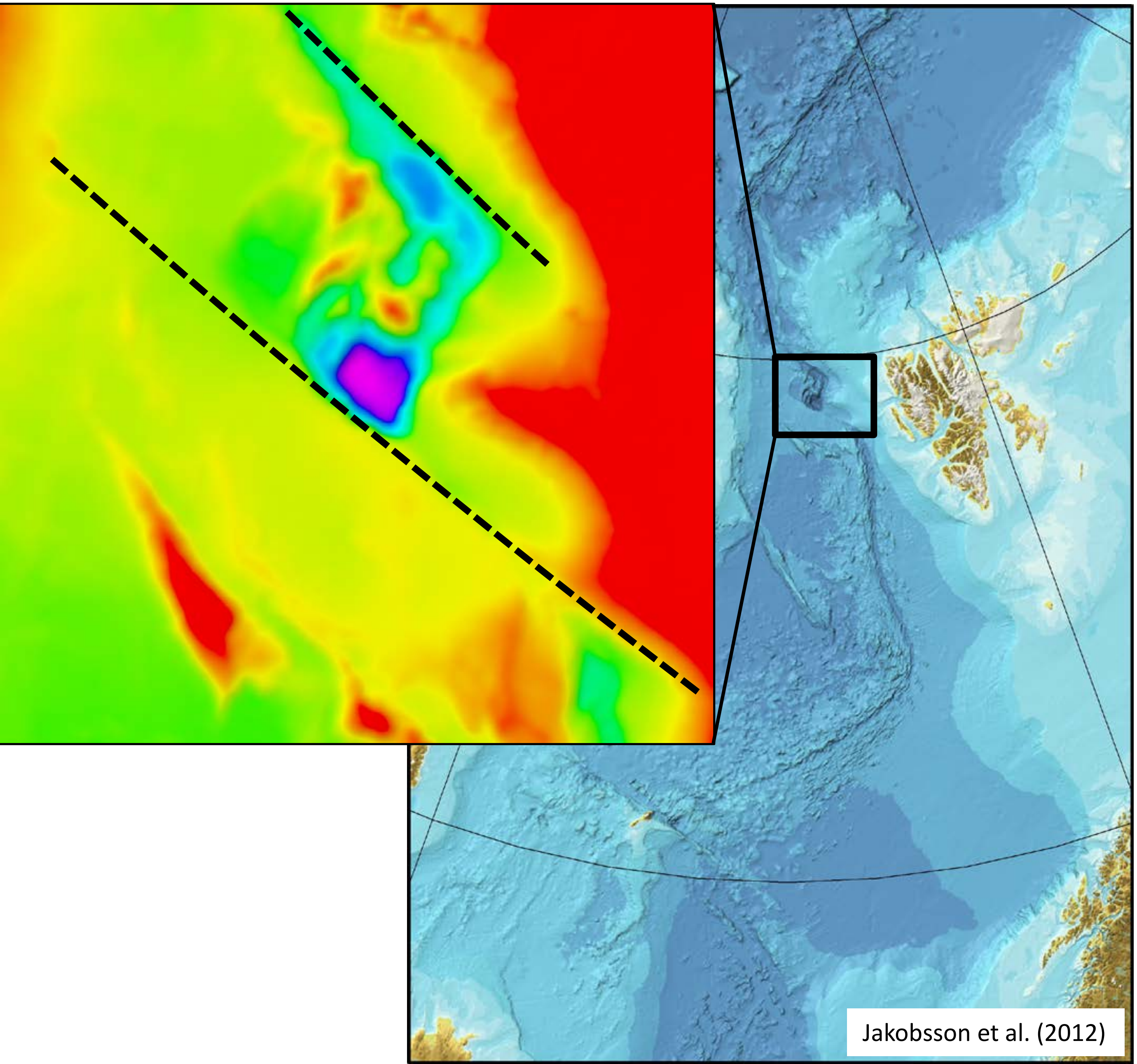

3

Gas flares and leakage along the crest of the Vestnesa Ridge are most likely related to gas hydrate destabilization.

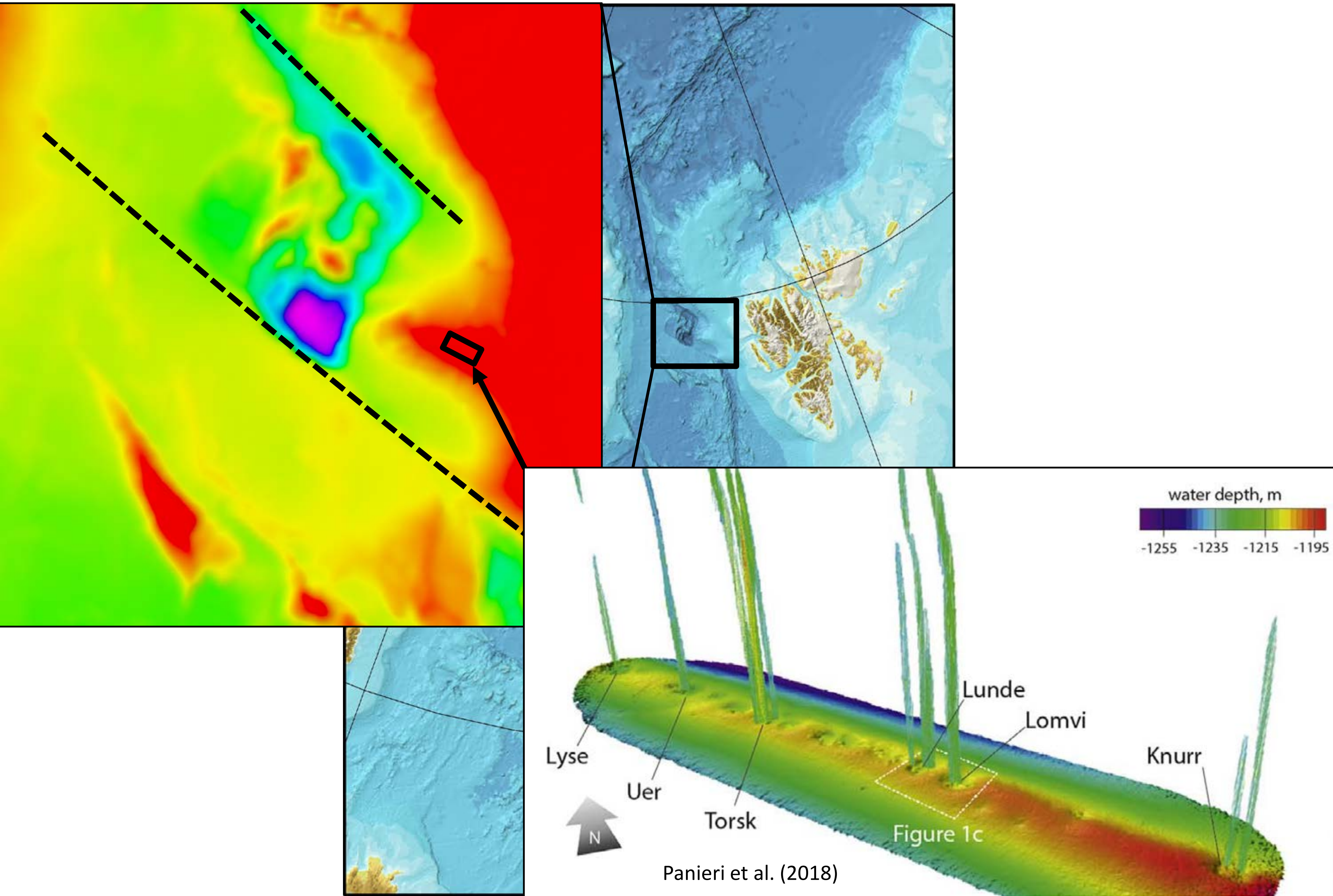

3 **Gas flares and leakage along the crest of the Vestnesa Ridge are most likely related to gas hydrate destabilization.**

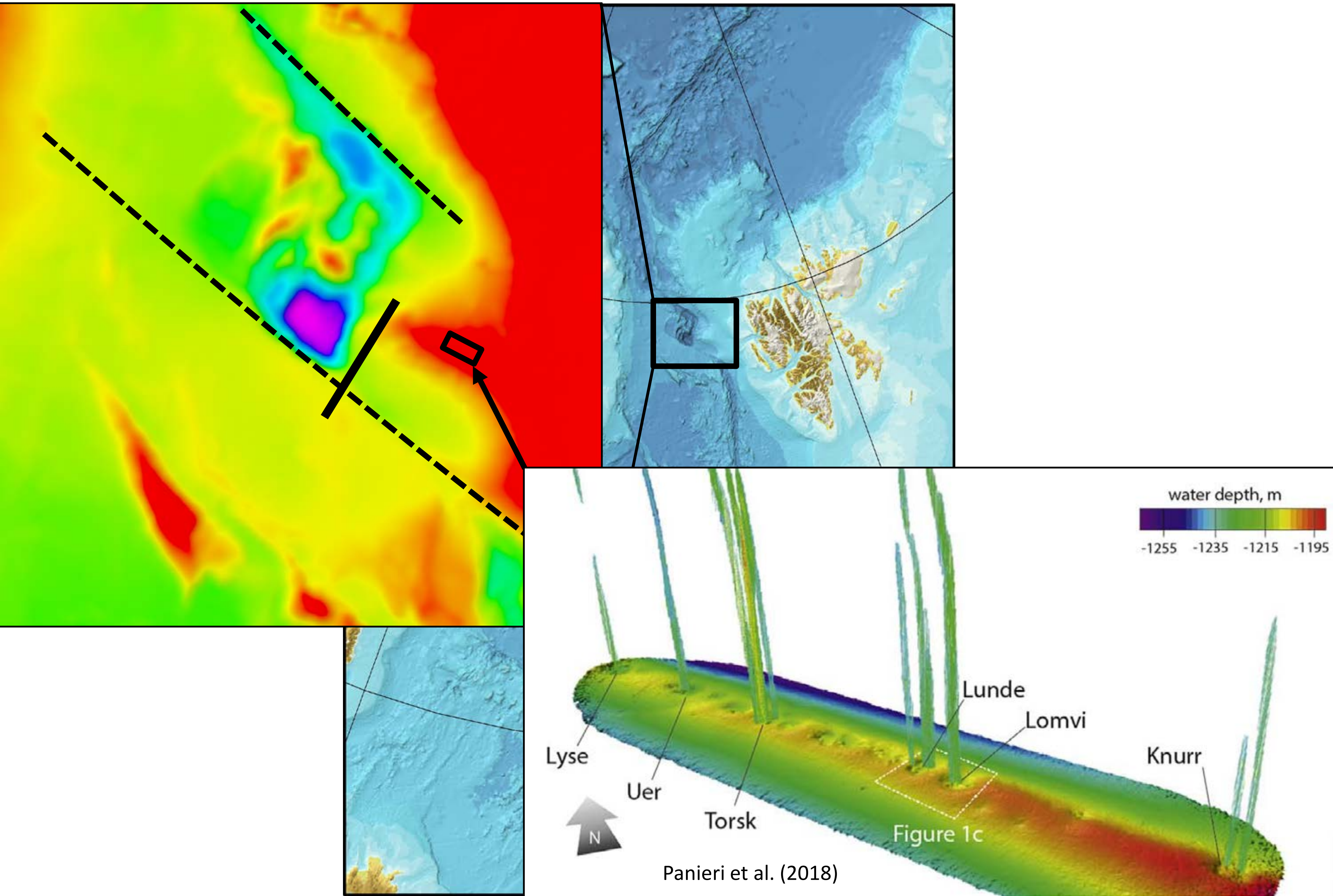

Panieri et al. (2018)

3 **The Vestnesa Ridge may represent relict Timanian basement, which may have controlled the formation of an oceanic core complex, resulting in fracturing of gas hydrates.**

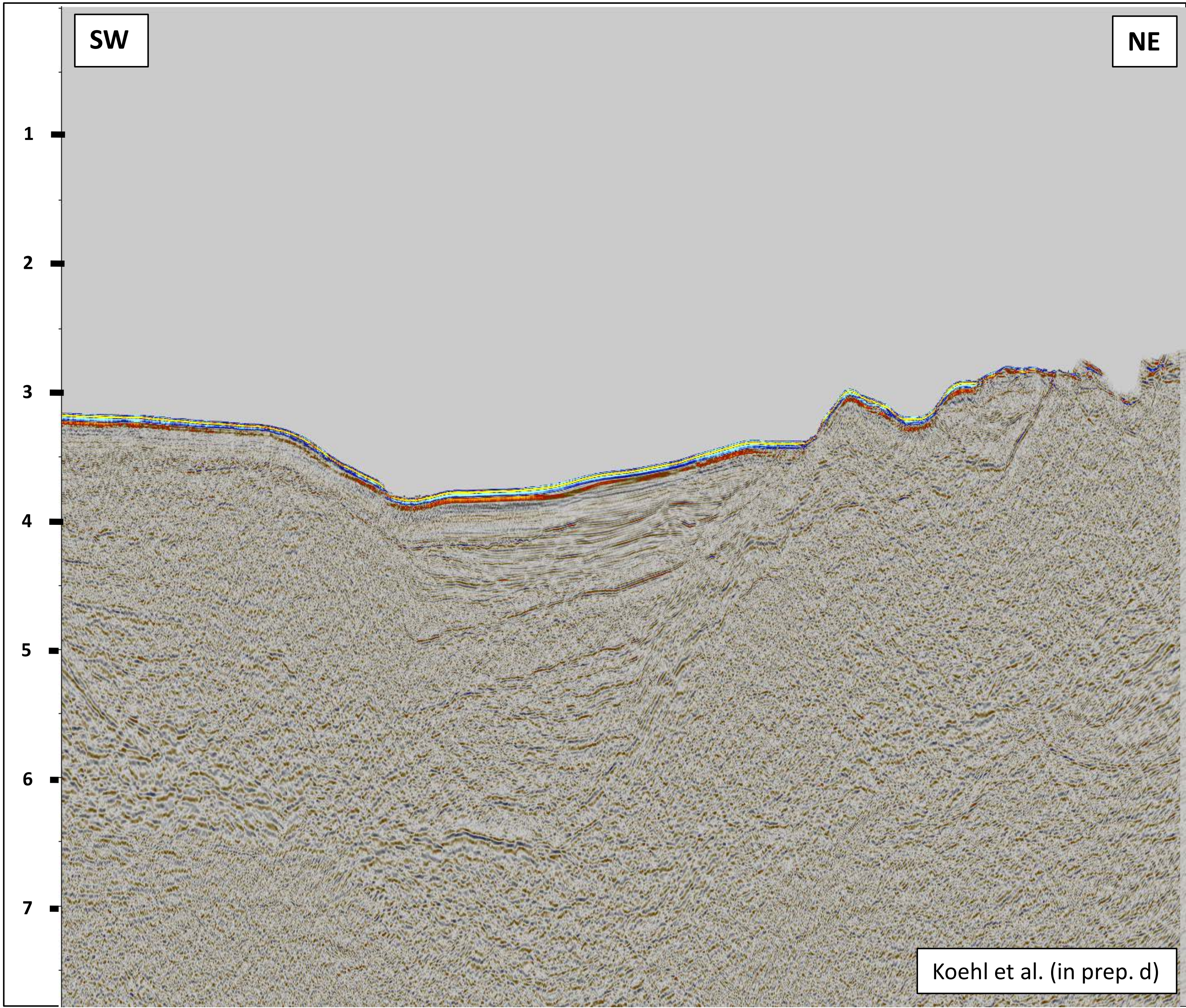

3

The Vestnesa Ridge may represent relict Timanian basement, which may have controlled the formation of an oceanic core complex, resulting in fracturing of gas hydrates.

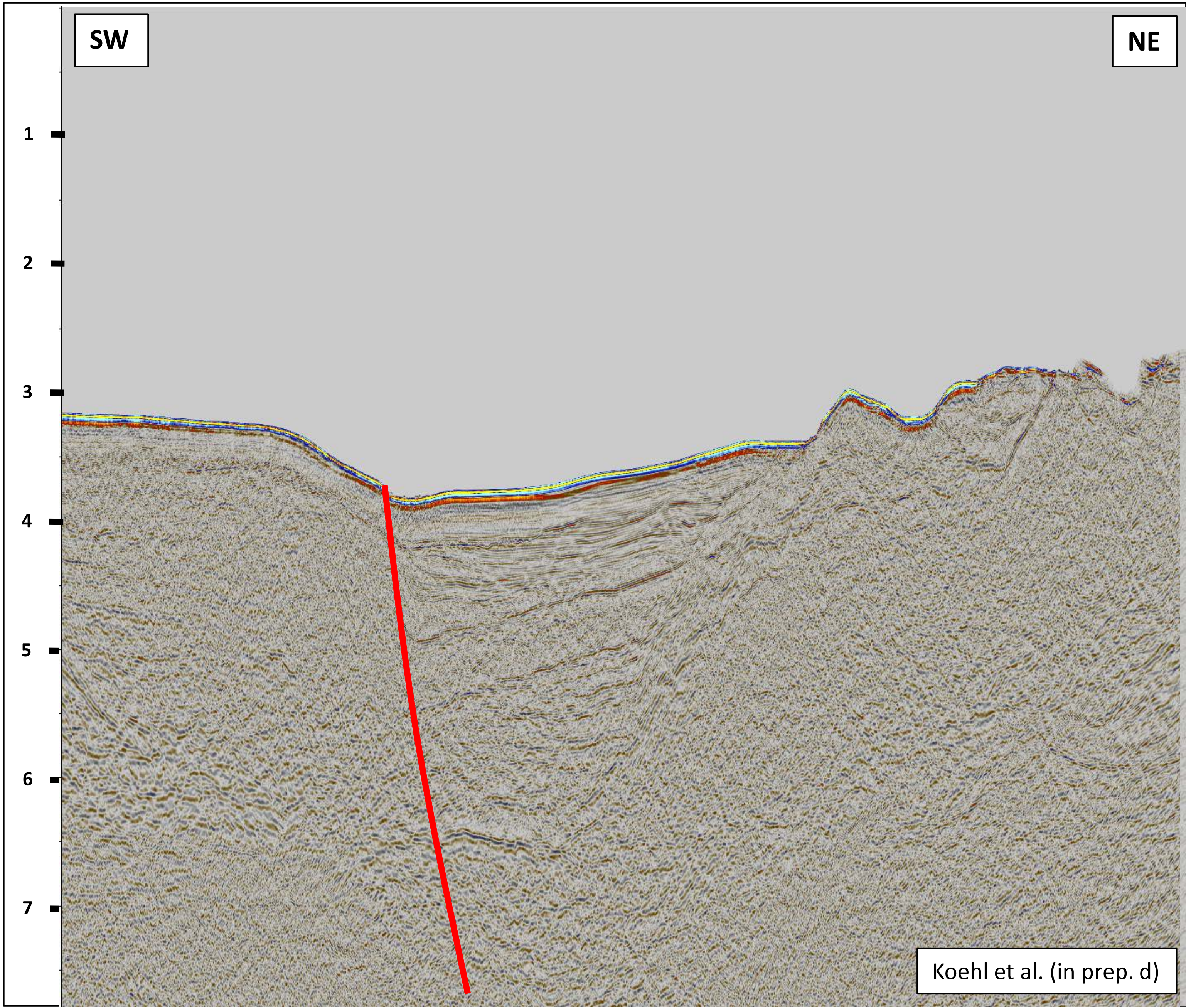

3

The Vestnesa Ridge may represent relict Timanian basement, which may have controlled the formation of an oceanic core complex, resulting in fracturing of gas hydrates.

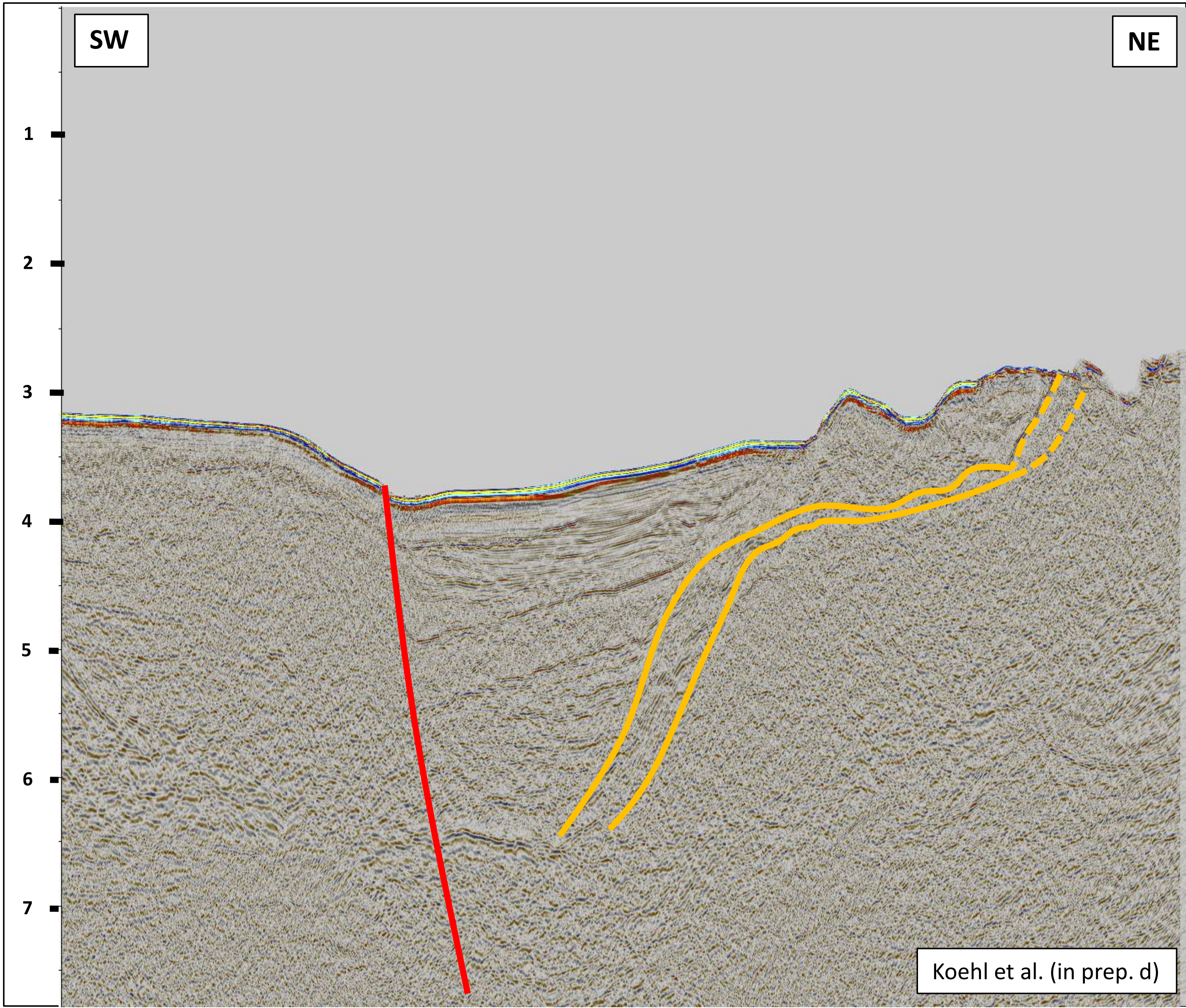

3

The Vestnesa Ridge may represent relict Timanian basement, which may have controlled the formation of an oceanic core complex, resulting in fracturing of gas hydrates.

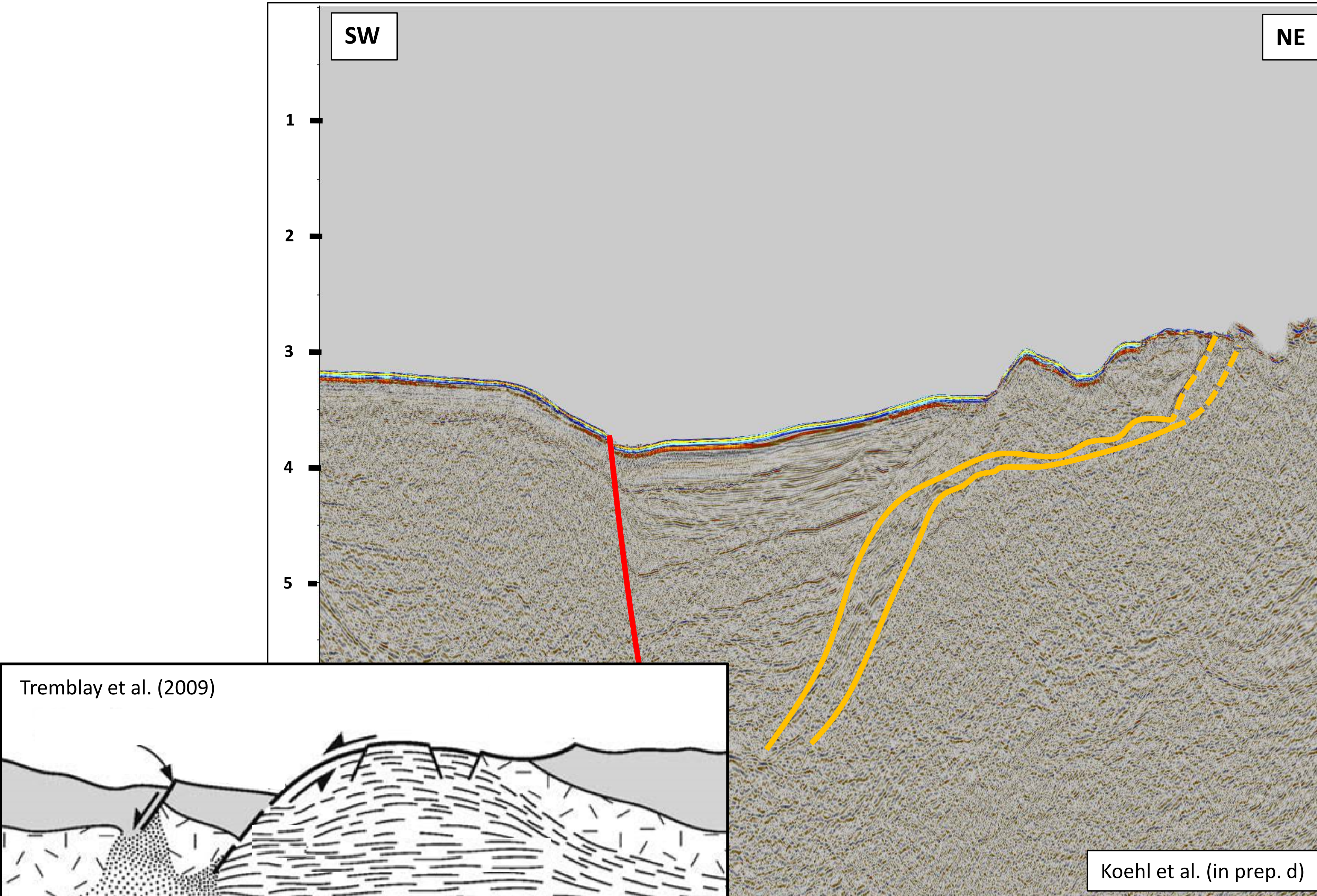

3 **The Vestnesa Ridge may represent relict Timanian basement, which may have controlled the formation of an oceanic core complex, resulting in fracturing of gas hydrates.**

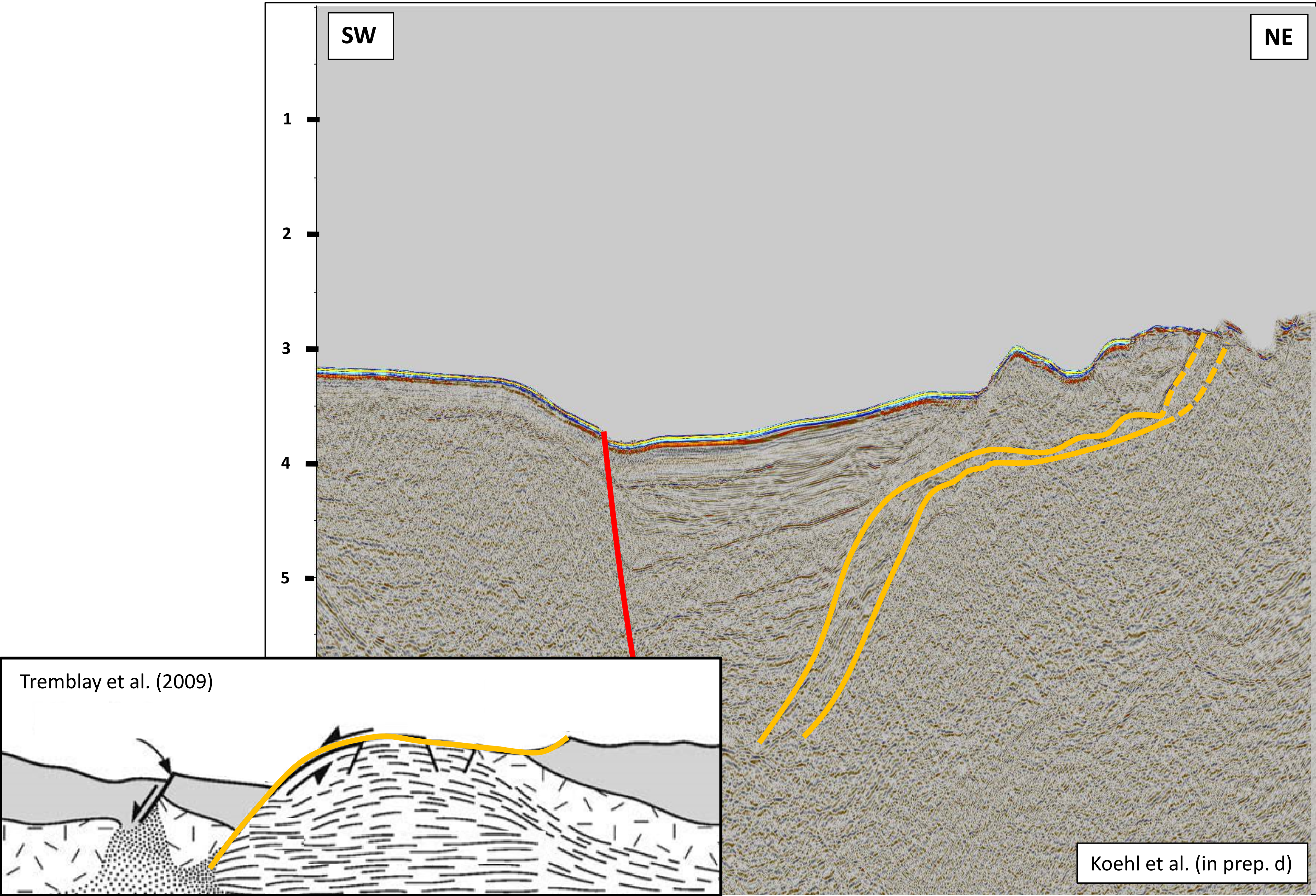

3 The Vestnesa Ridge may represent relict Timanian basement, which may have controlled the formation of an oceanic core complex, resulting in fracturing of gas hydrates.

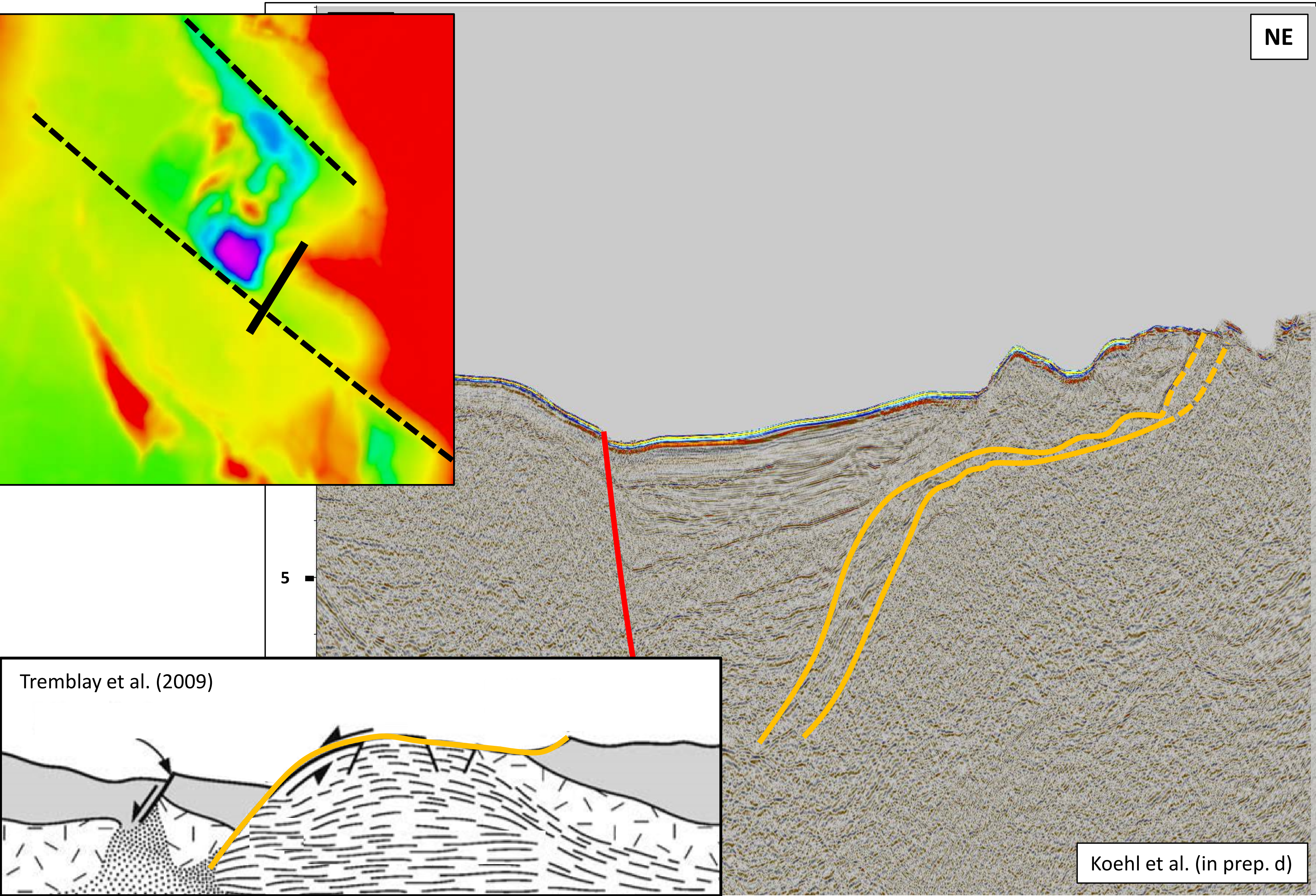

3 **The Vestnesa Ridge may represent relict Timanian basement, which may have controlled the formation of an oceanic core complex, resulting in fracturing of gas hydrates.**

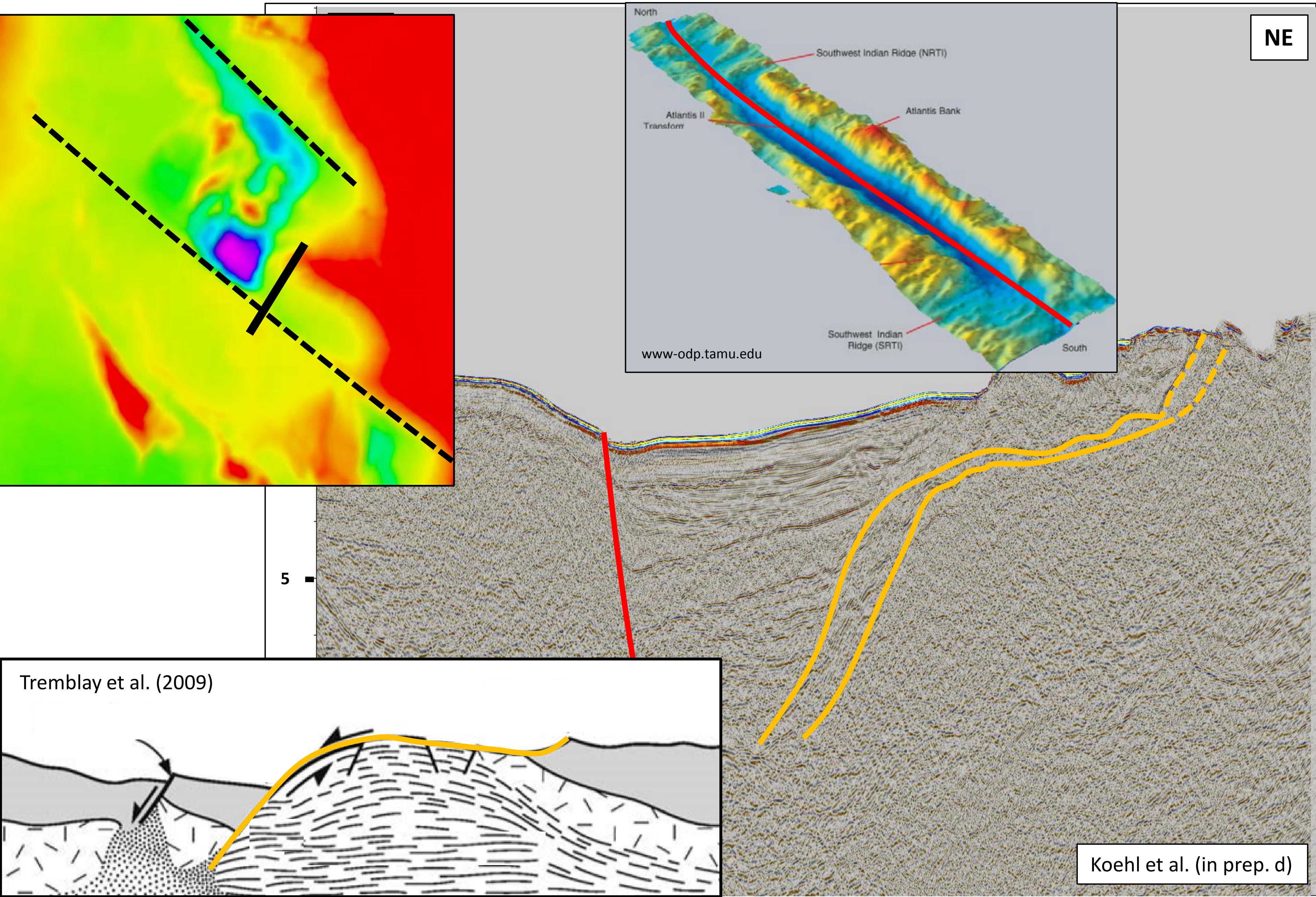

3

The Vestnesa Ridge may represent relict Timanian basement, which may have controlled the formation of an oceanic core complex, resulting in fracturing of gas hydrates.

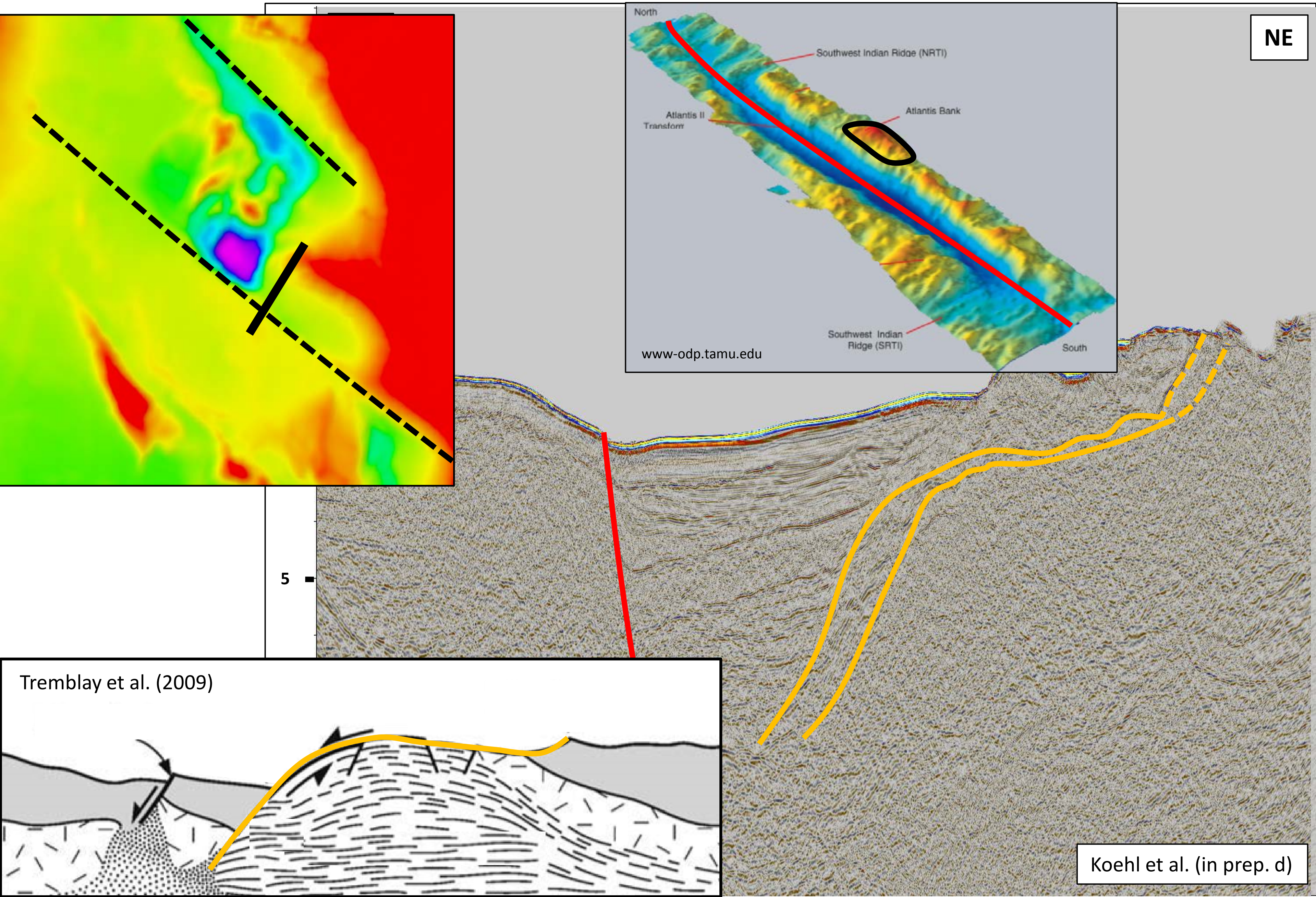

3 **The Vestnesa Ridge may represent relict Timanian basement, which may have controlled the formation of an oceanic core complex, resulting in fracturing of gas hydrates.**

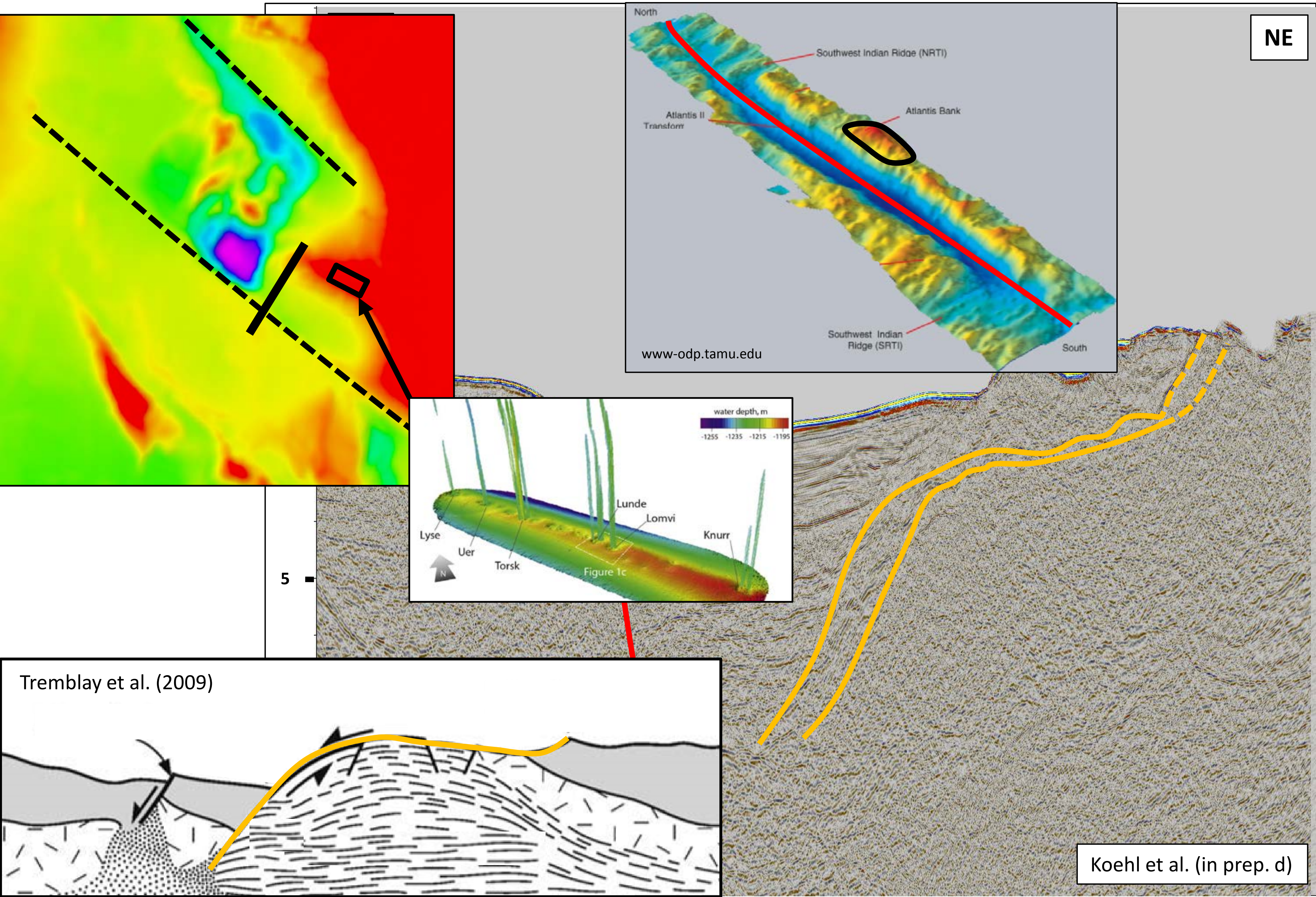

3

The Knipovich and Molloy ridges likely formed along oblique Caledonian weakness zones, while major transforms formed subparallel to Neoproterozoic (Timanian?) thrusts.

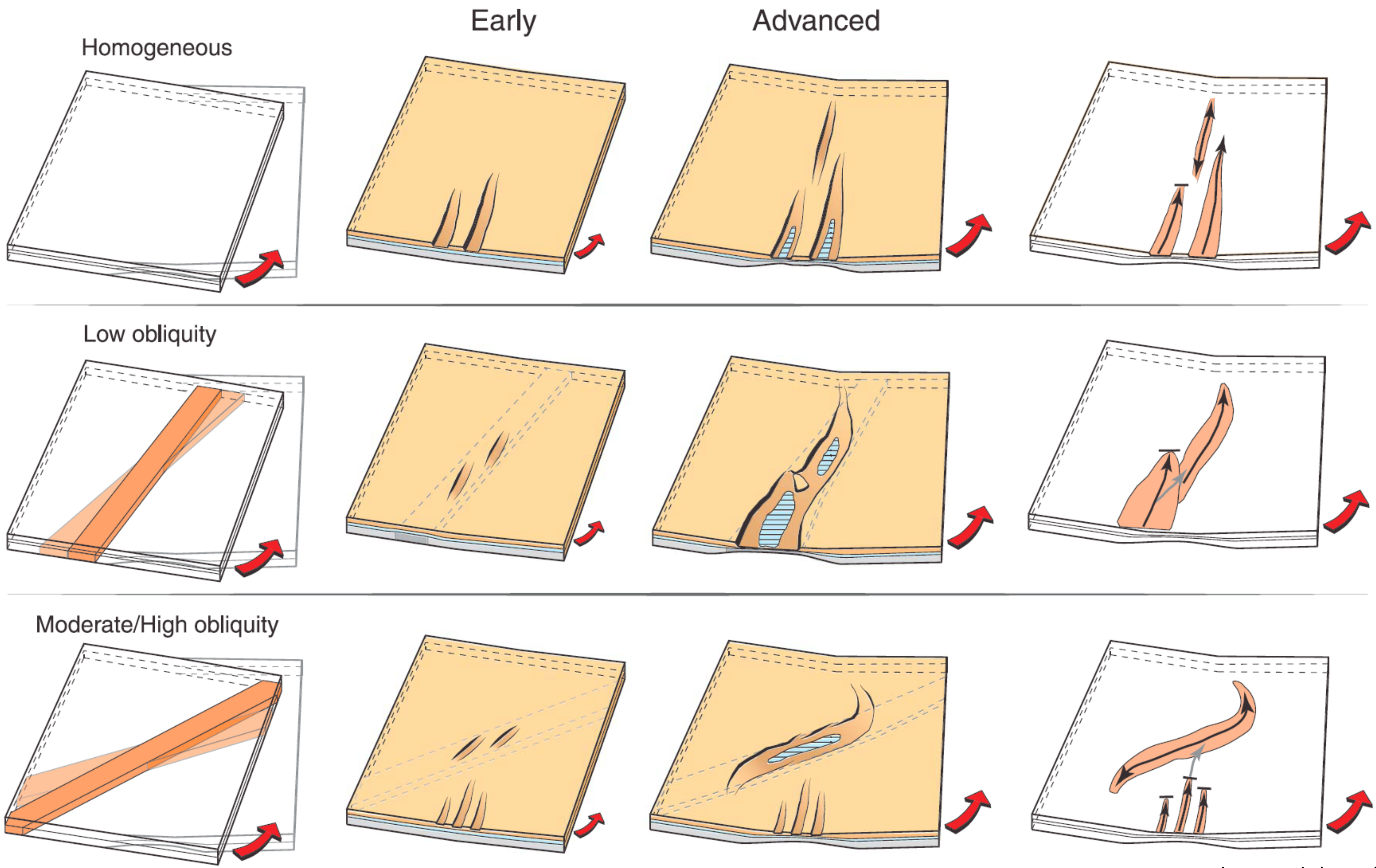

Molnar et al. (2017)

3

The Knipovich and Molloy ridges likely formed along oblique Caledonian weakness zones, while major transforms formed subparallel to Neoproterozoic (Timanian?) thrusts.

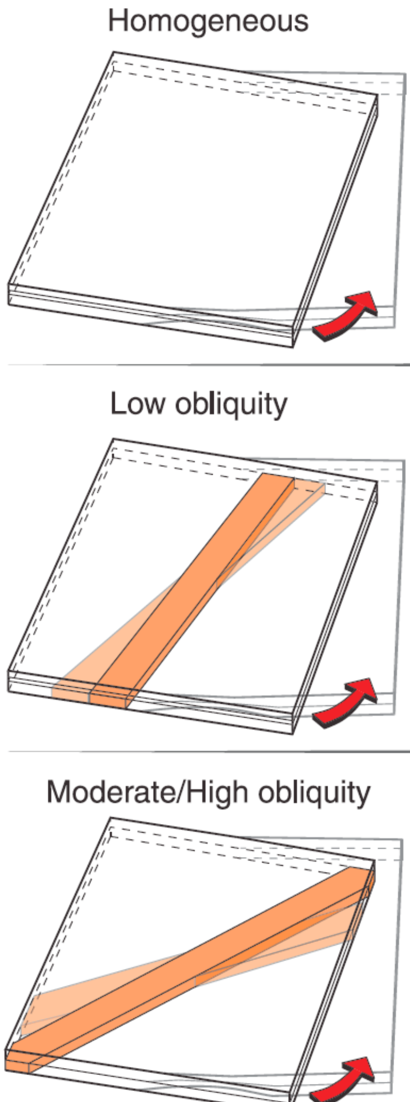

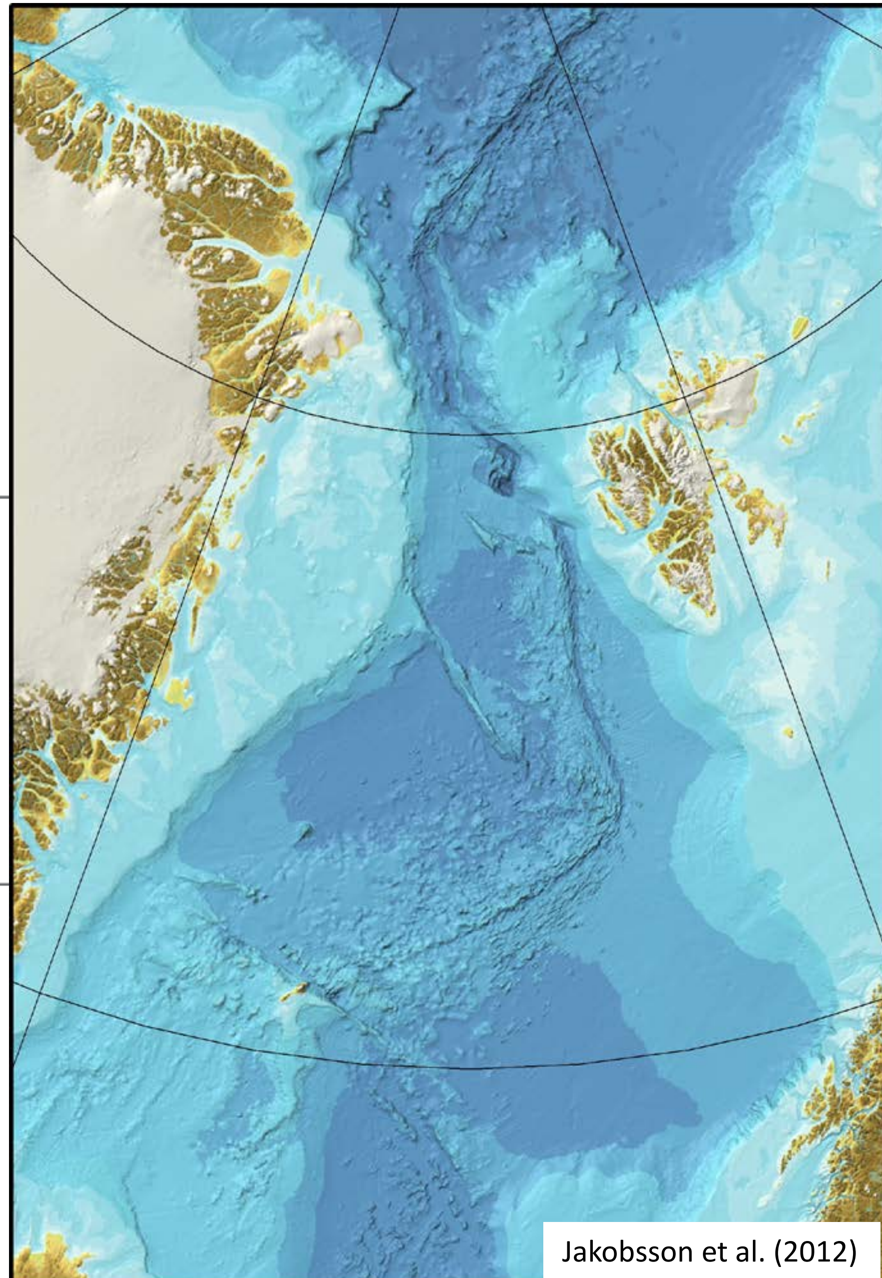

Jakobsson et al. (2012)

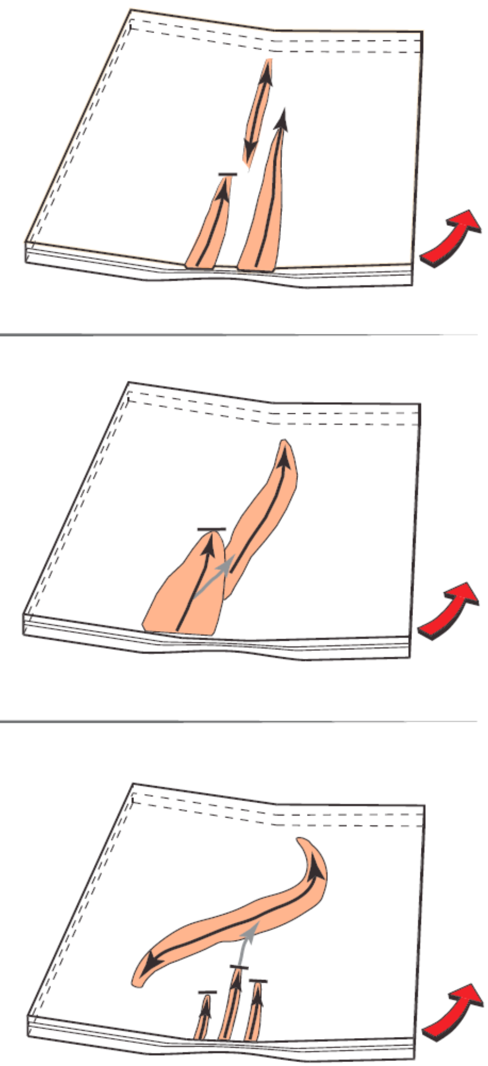

Molnar et al. (2017)

3

The Knipovich and Molloy ridges likely formed along oblique Caledonian weakness zones, while major transforms formed subparallel to Neoproterozoic (Timanian?) thrusts.

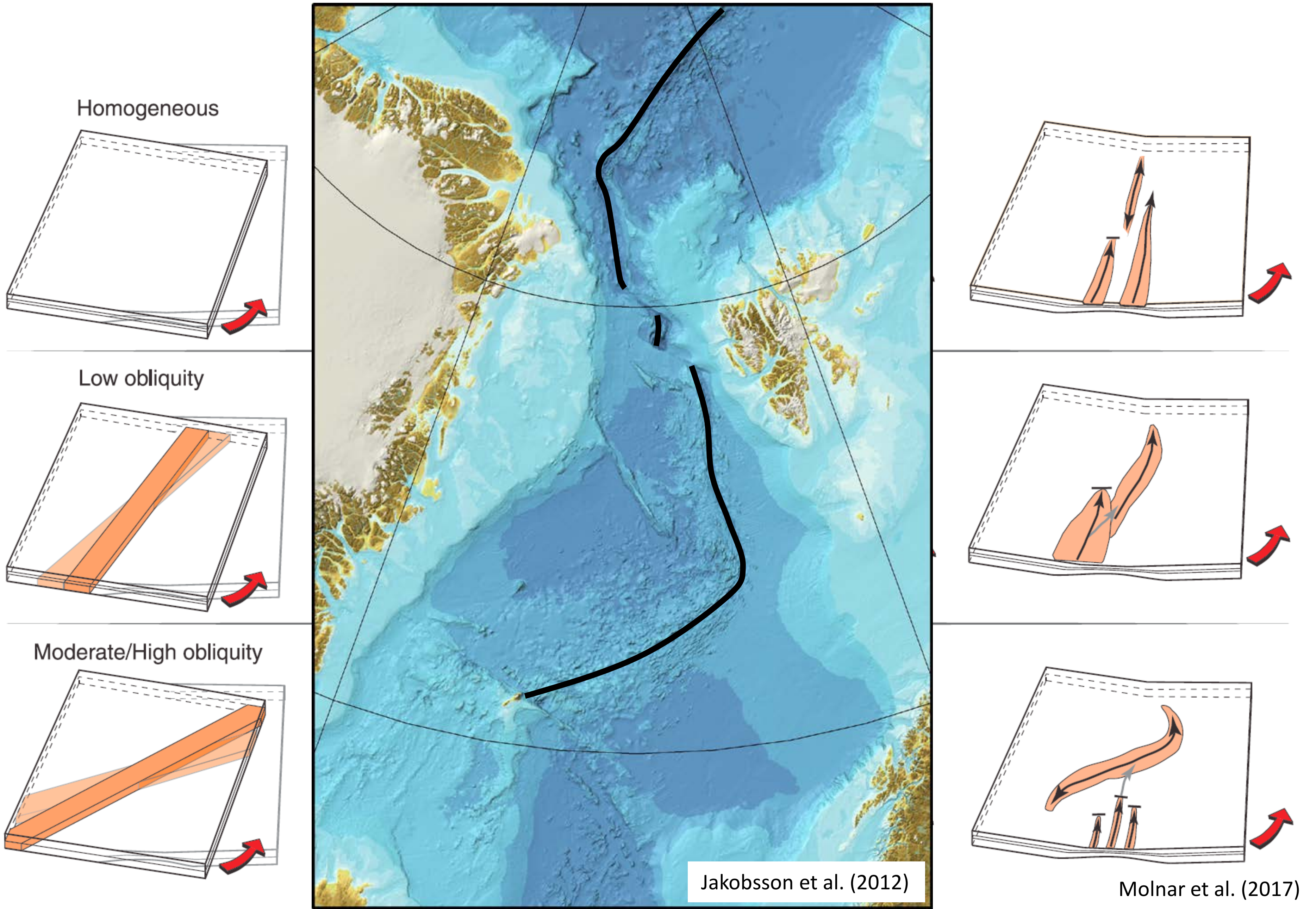

3 **The Knipovich and Molloy ridges likely formed along oblique Caledonian weakness zones, while major transforms formed subparallel to Neoproterozoic (Timanian?) thrusts.**

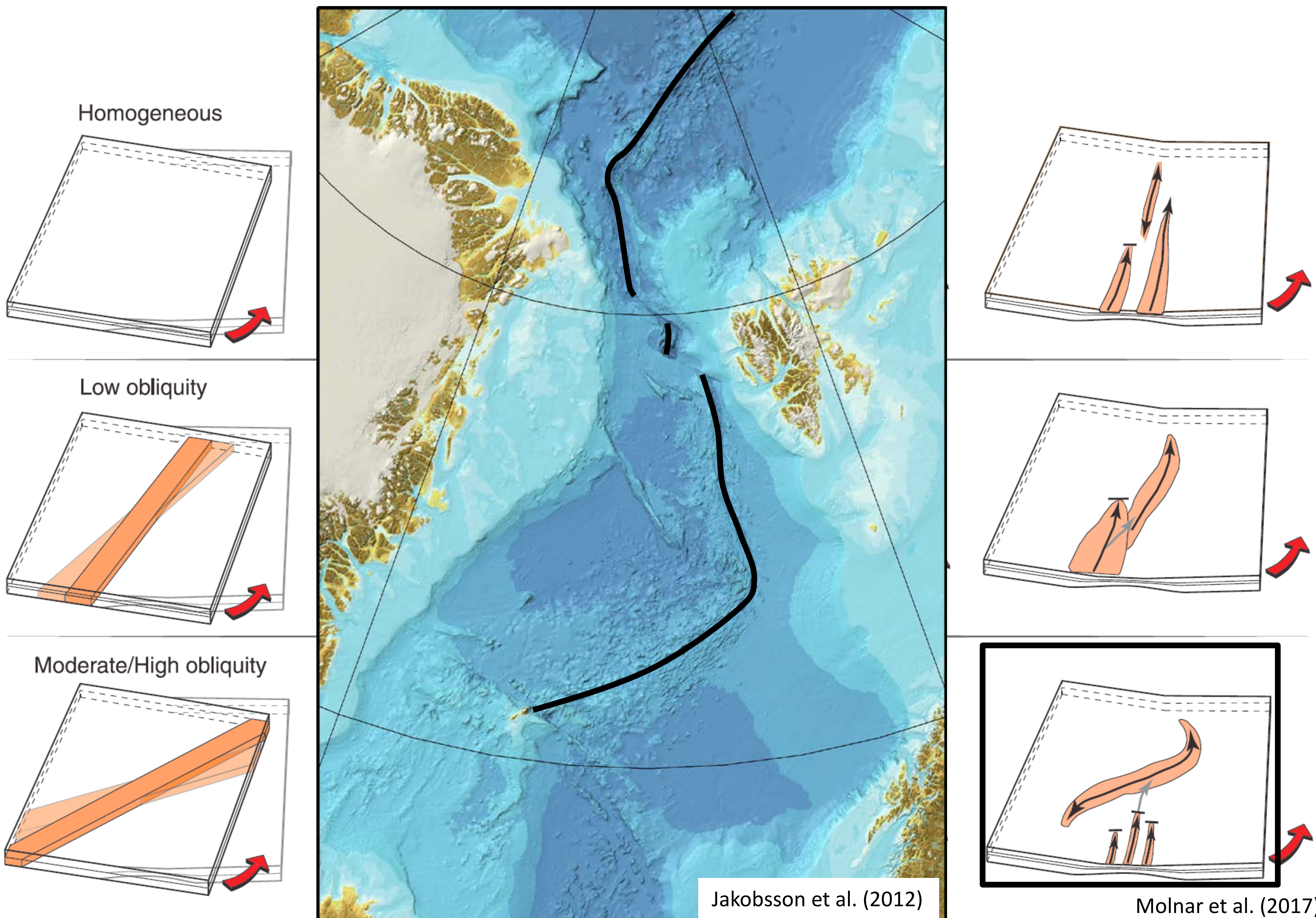

3

The Knipovich and Molloy ridges likely formed along oblique Caledonian weakness zones, while major transforms formed subparallel to Neoproterozoic (Timanian?) thrusts.

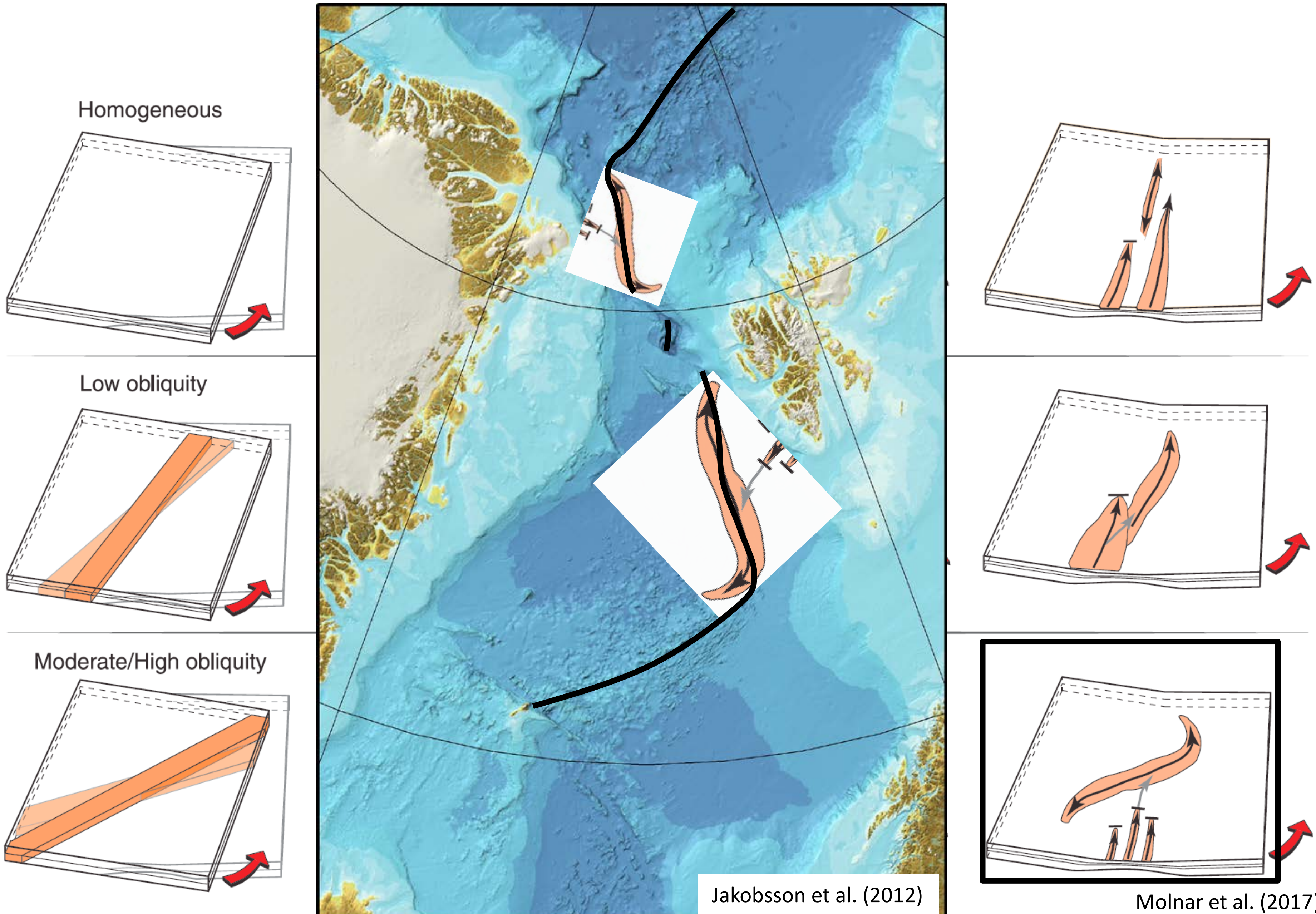

3

The Knipovich and Molloy ridges likely formed along oblique Caledonian weakness zones, while major transforms formed subparallel to Neoproterozoic (Timanian?) thrusts.

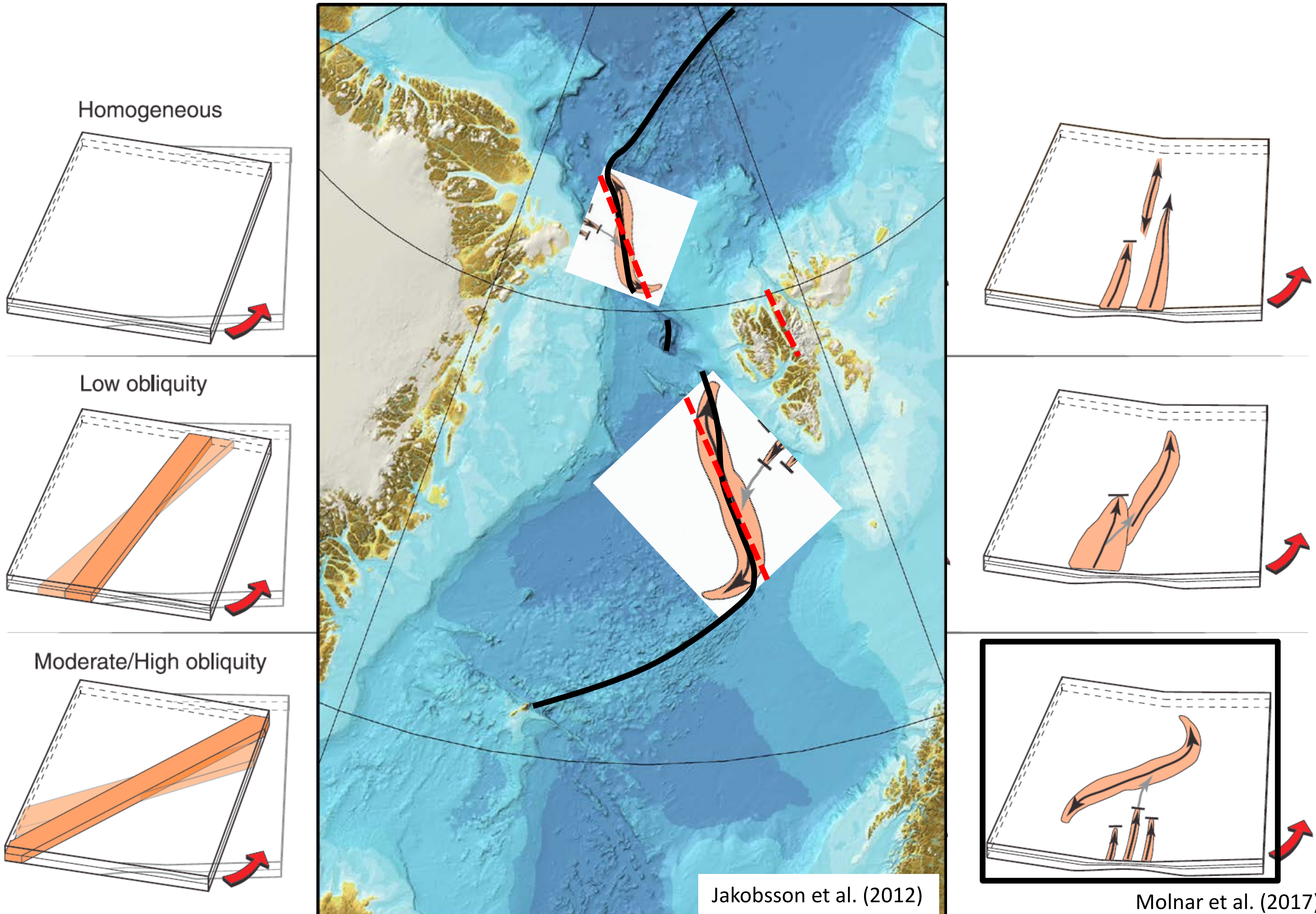

Molnar et al. (2017)

The Knipovich and Molloy ridges likely formed along oblique Caledonian weakness zones, while major transforms formed subparallel to Neoproterozoic (Timanian?) thrusts.

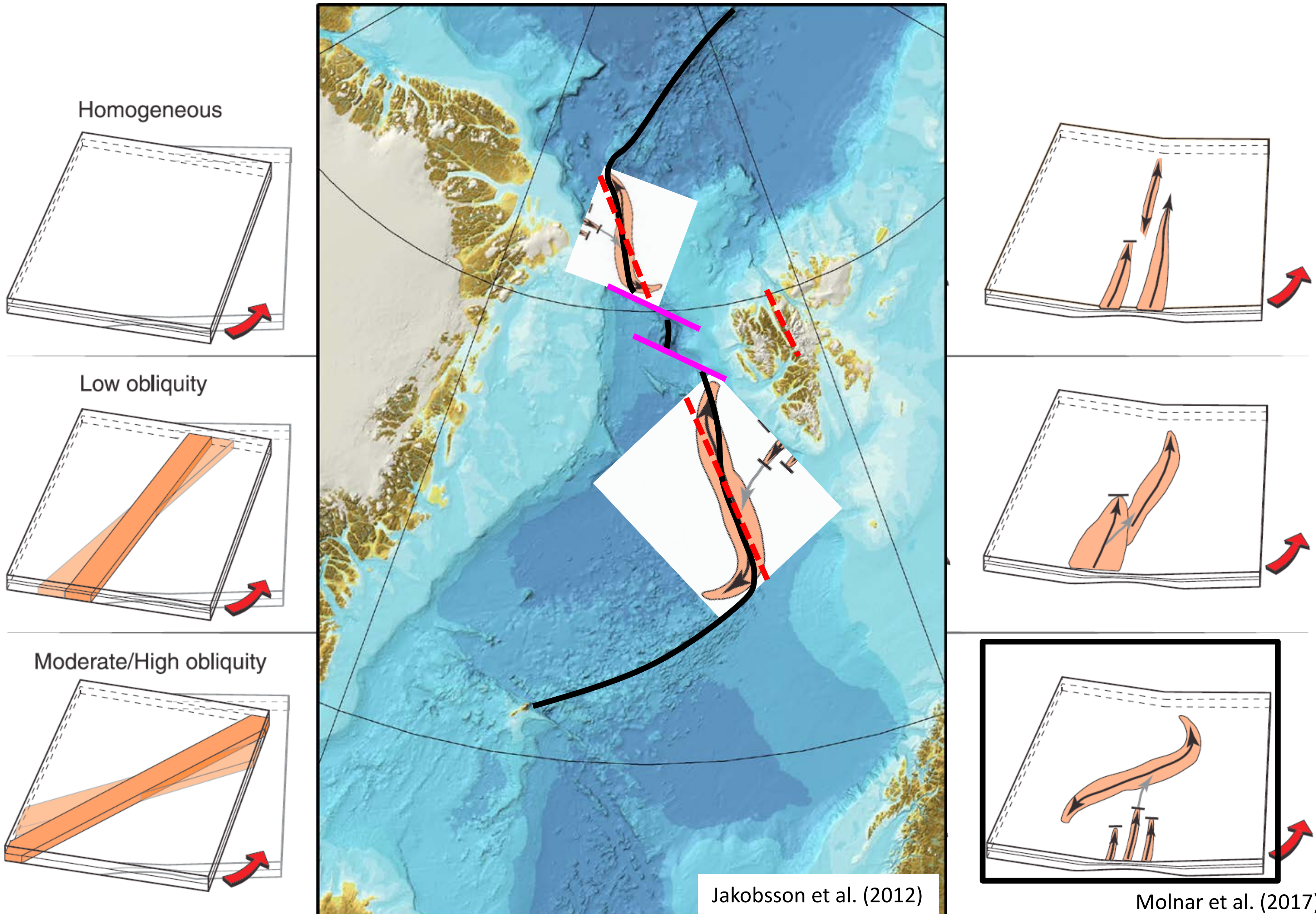

3 **The Knipovich and Molloy ridges likely formed along oblique Caledonian weakness zones, while major transforms formed subparallel to Neoproterozoic (Timanian?) thrusts.**

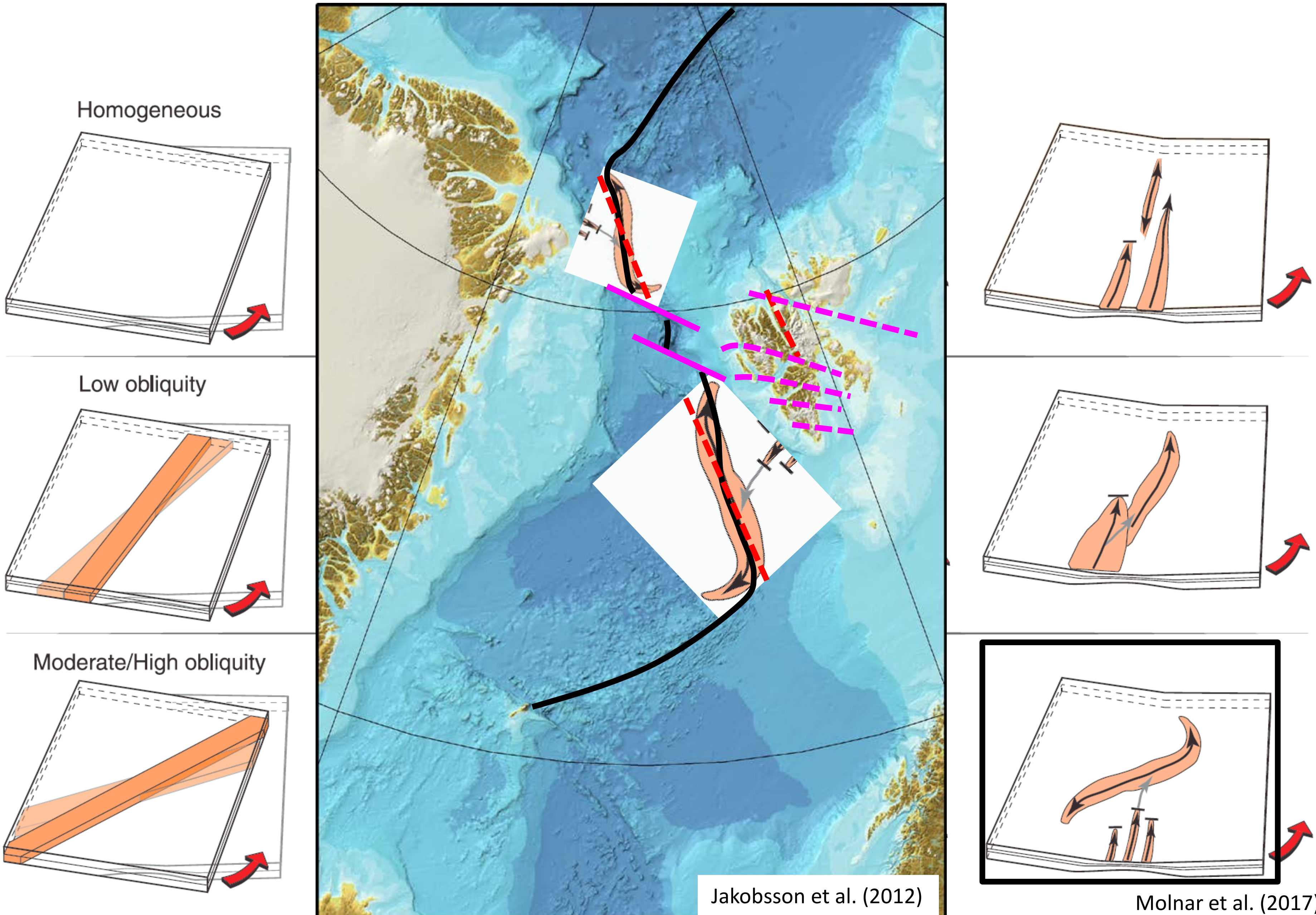

3

The Knipovich and Molloy ridges likely formed along oblique Caledonian weakness zones, while major transforms formed subparallel to Neoproterozoic (Timanian?) thrusts.

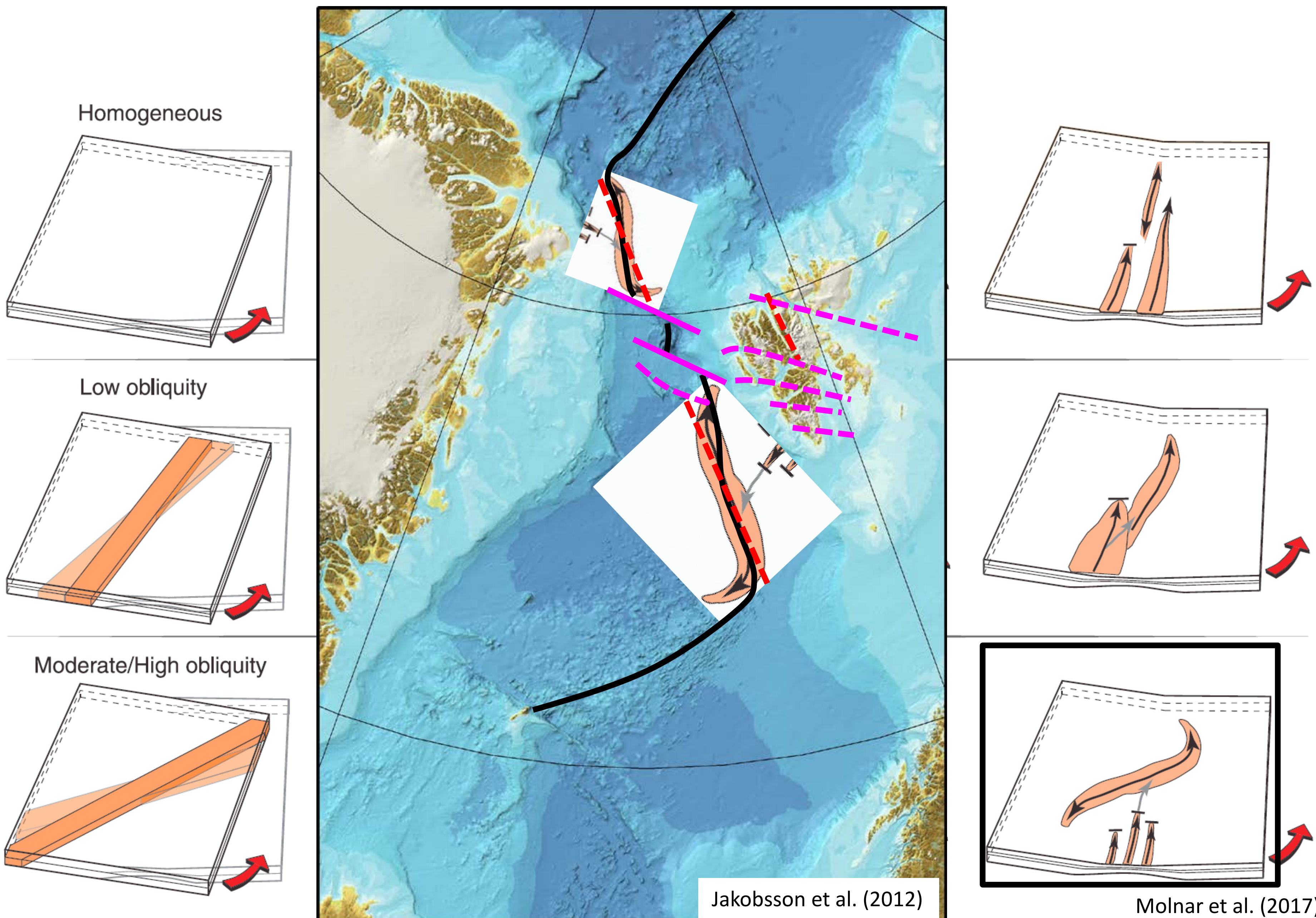

3

The Knipovich and Molloy ridges likely formed along oblique Caledonian weakness zones, while major transforms formed subparallel to Neoproterozoic (Timanian?) thrusts.

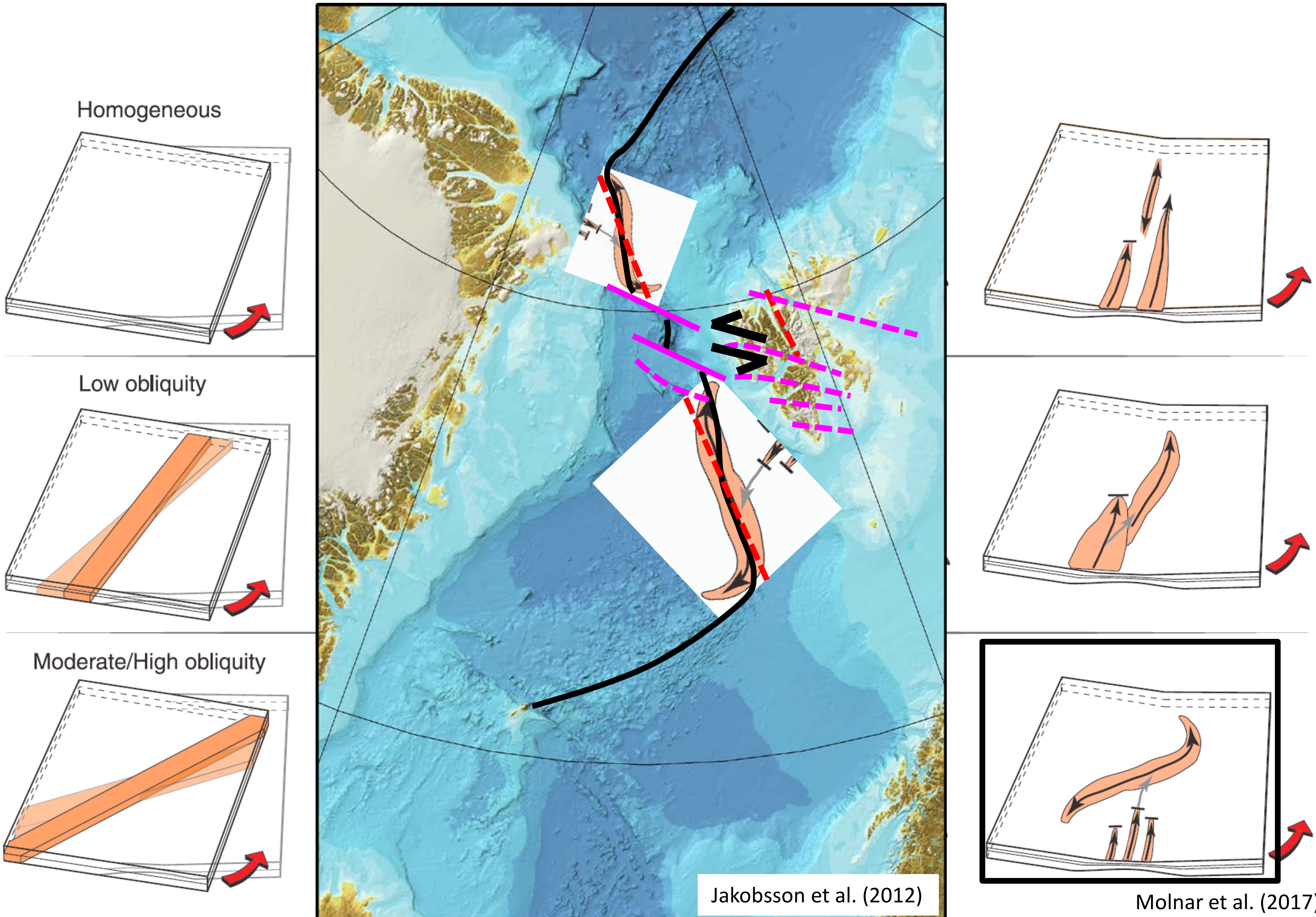

3

The Knipovich and Molloy ridges likely formed along oblique Caledonian weakness zones, while major transforms formed subparallel to Neoproterozoic (Timanian?) thrusts.

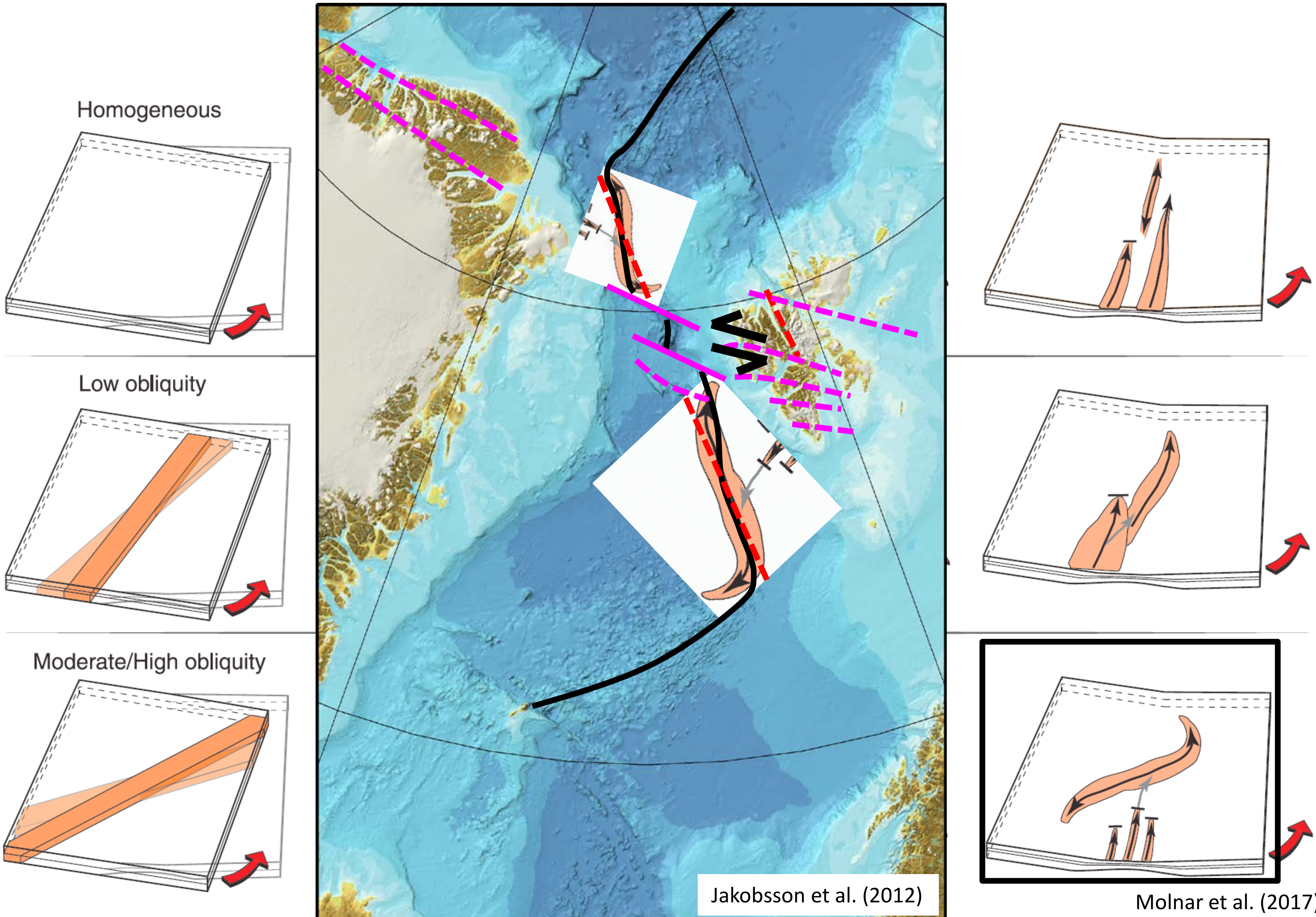

3

The Knipovich and Molloy ridges likely formed along oblique Caledonian weakness zones, while major transforms formed subparallel to Neoproterozoic (Timanian?) thrusts.

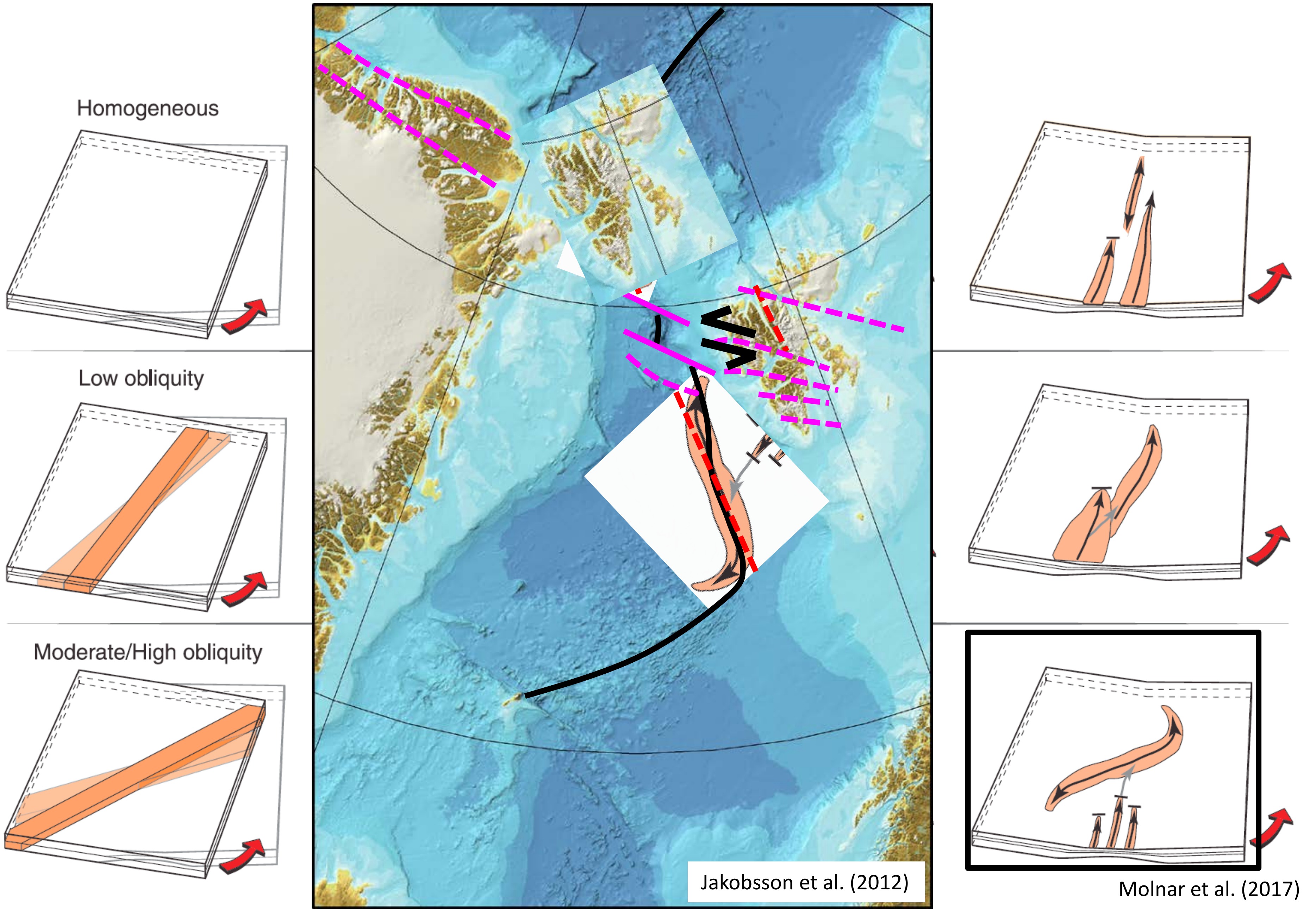

3 **Earliest Mississippian amphibolite facies metamorphism and down-west kinematics in western Svalbard may be related to core complex exhumation.**

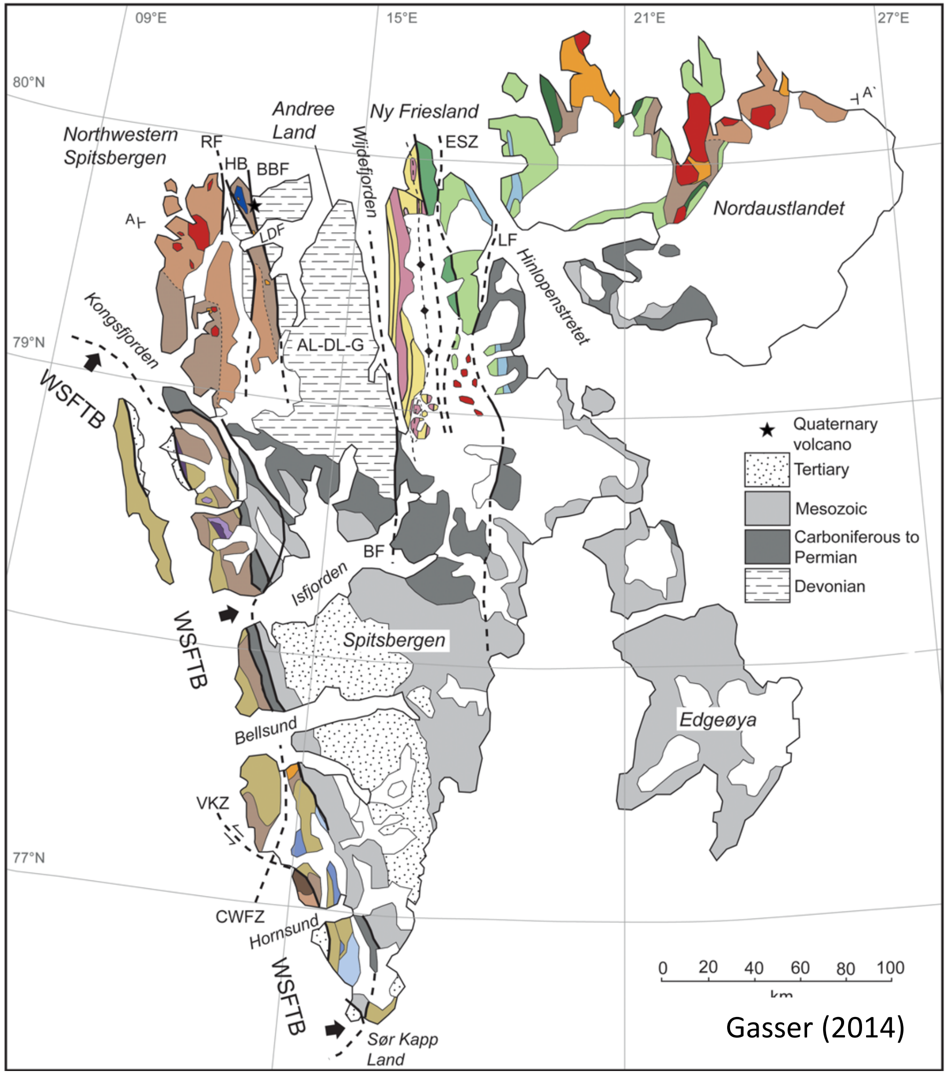

3

Earliest Mississippian amphibolite facies metamorphism and down-west kinematics in western Svalbard may be related to core complex exhumation.

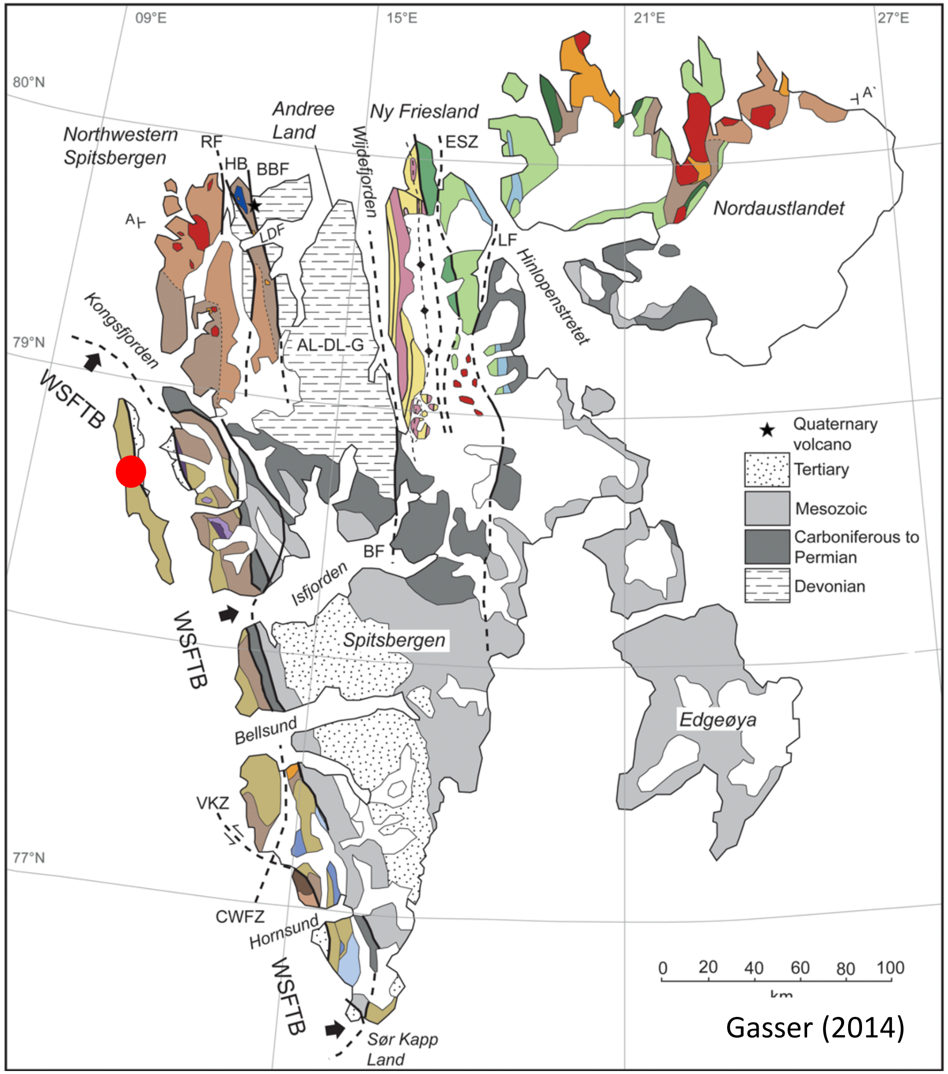

Gasser (2014)

3

Earliest Mississippian amphibolite facies metamorphism and down-west kinematics in western Svalbard may be related to core complex exhumation.

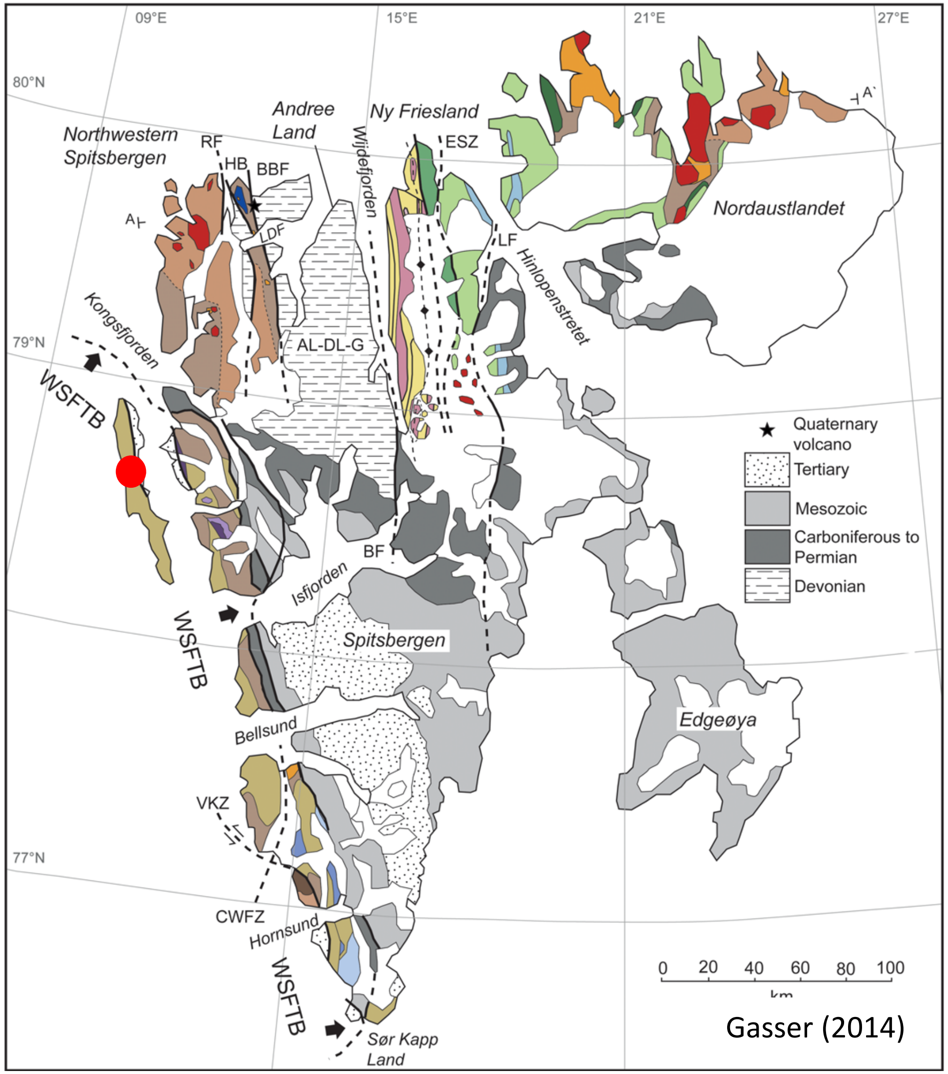

3 Earliest Mississippian amphibolite facies metamorphism and down-west kinematics in western Svalbard may be related to core complex exhumation.

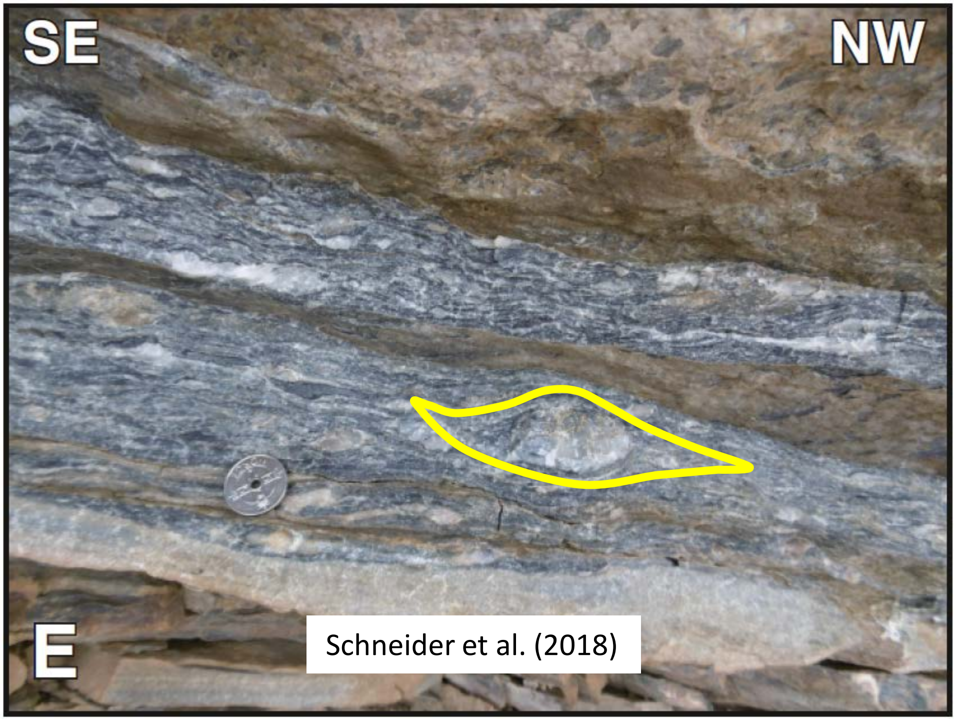

Schneider et al. (2018)

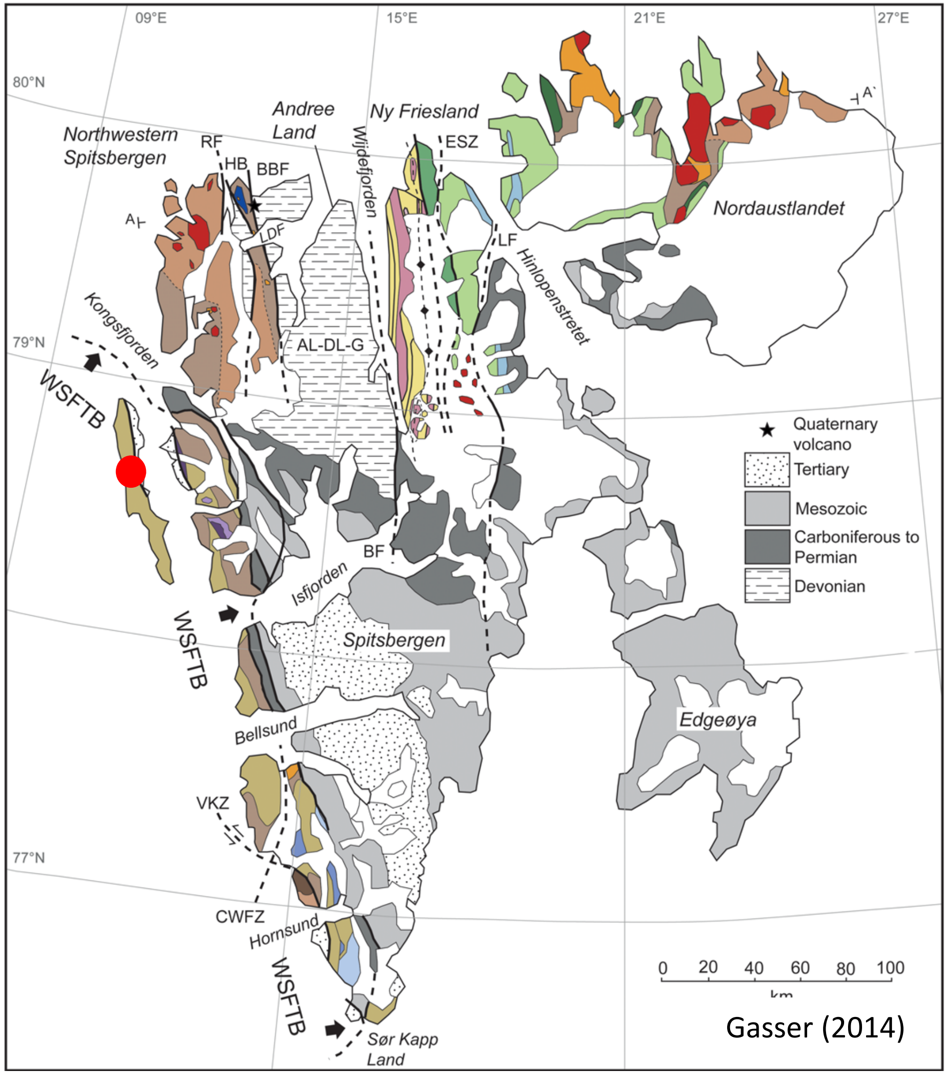

Gasser (2014)

3

Earliest Mississippian amphibolite facies metamorphism and down-west kinematics in western Svalbard may be related to core complex exhumation.

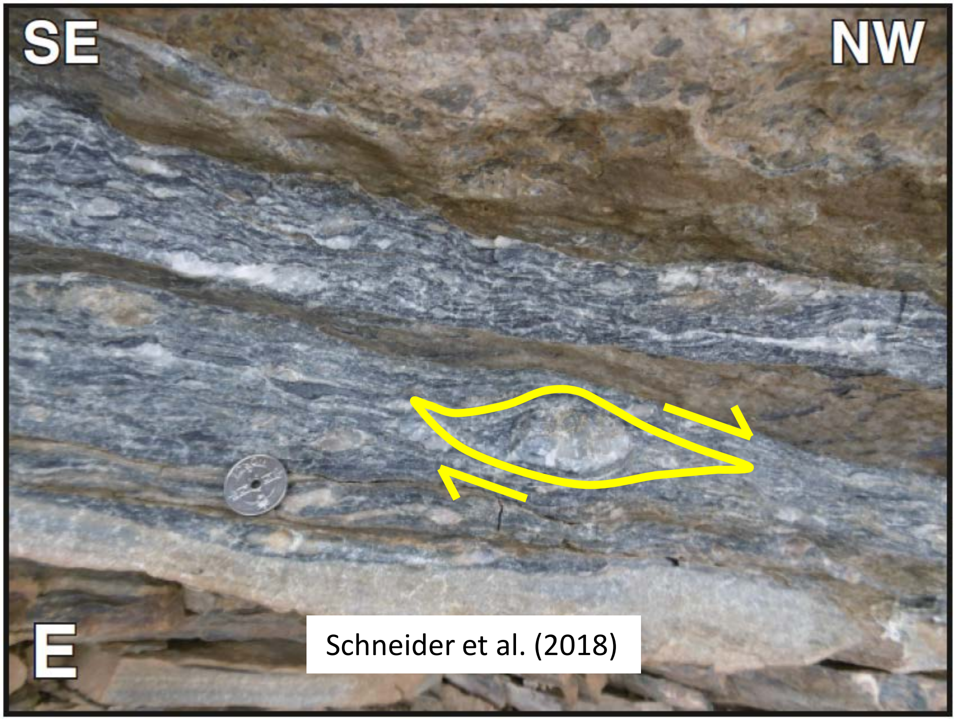

Schneider et al. (2018)

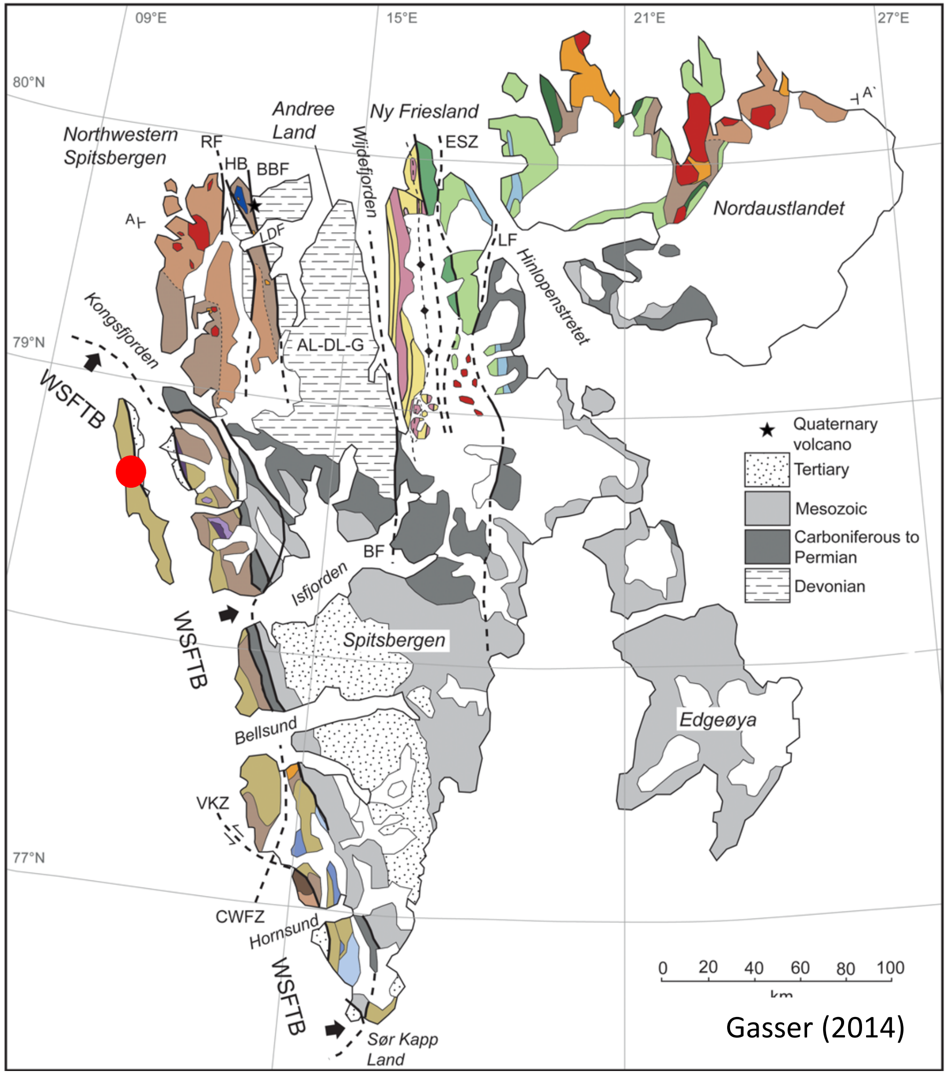

Gasser (2014)

3 Earliest Mississippian amphibolite facies metamorphism and down-west kinematics in western Svalbard may be related to core complex exhumation.

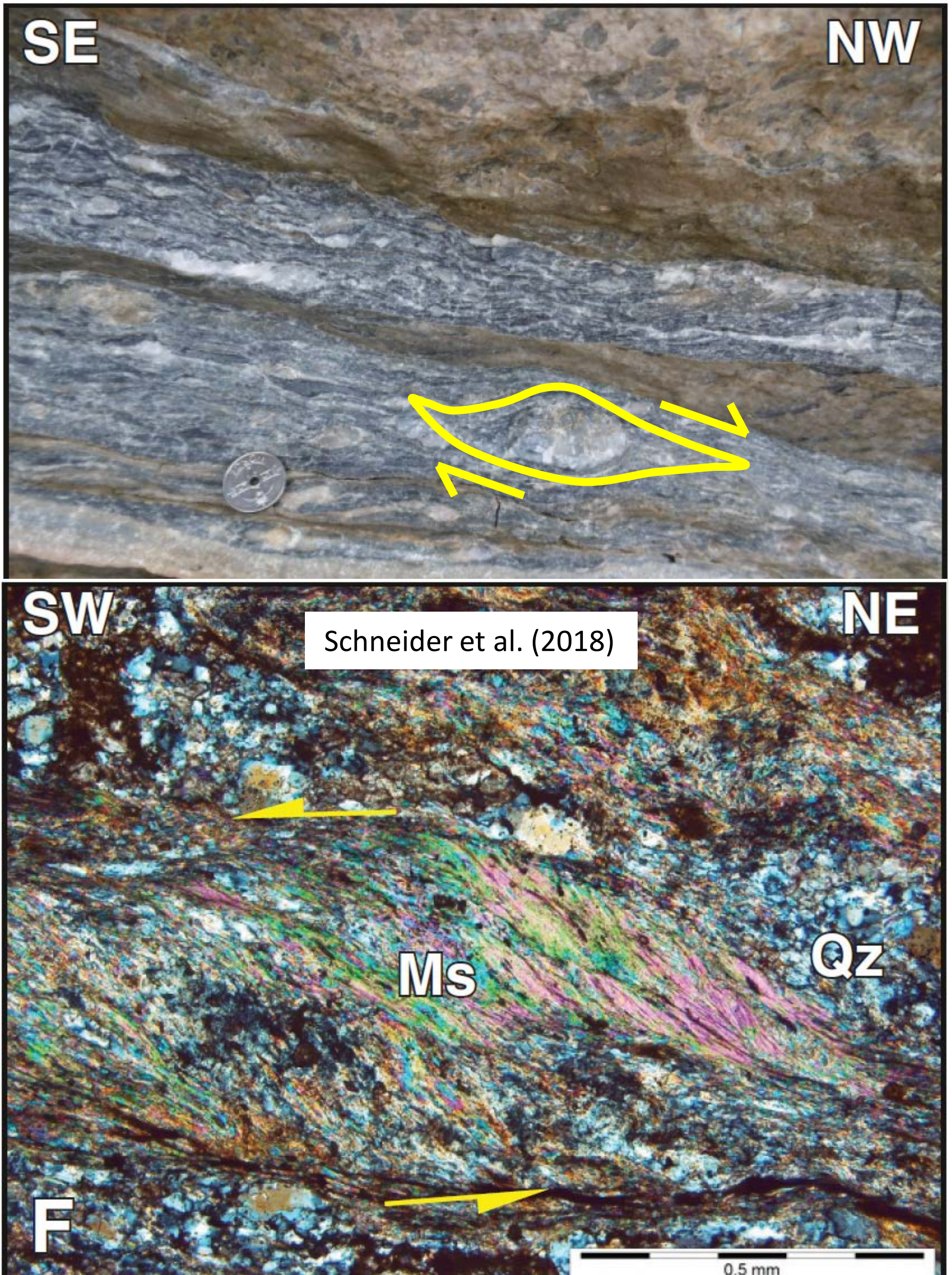

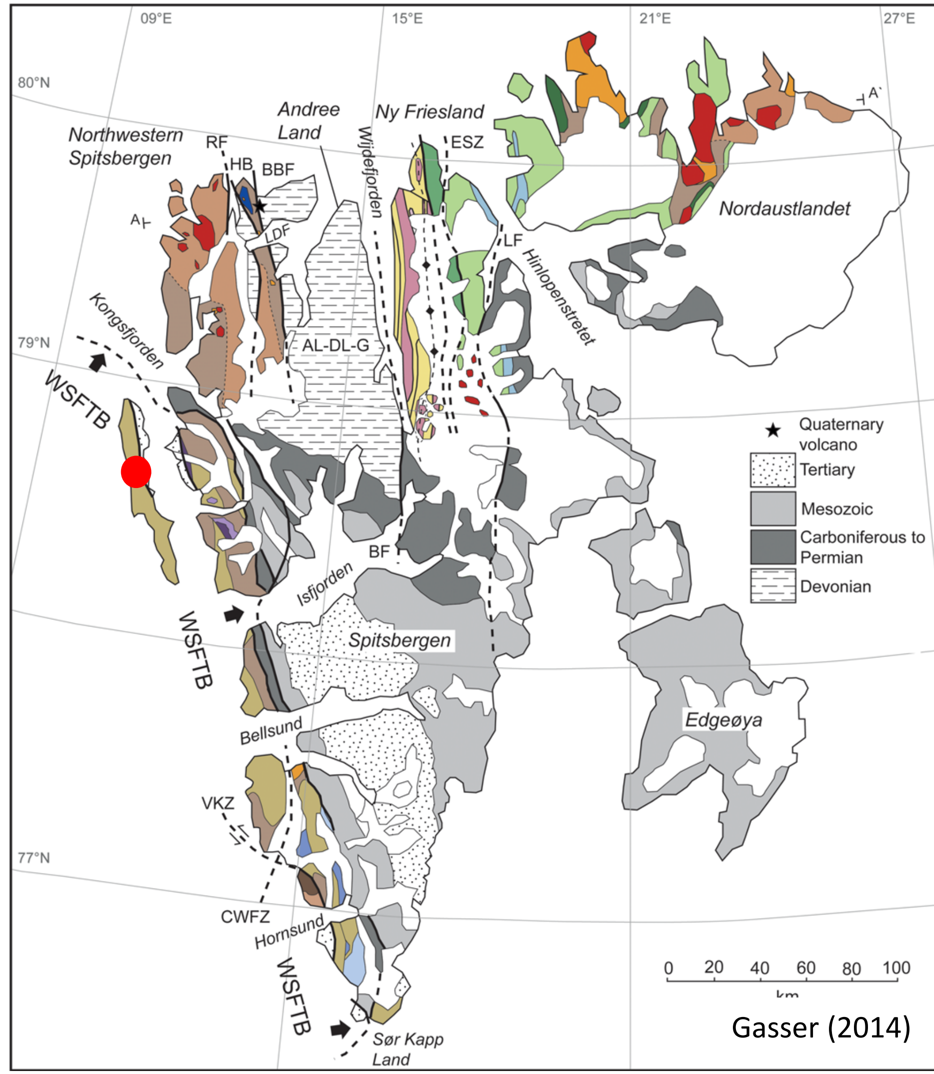

3 Earliest Mississippian amphibolite facies metamorphism and down-west kinematics in western Svalbard may be related to core complex exhumation.

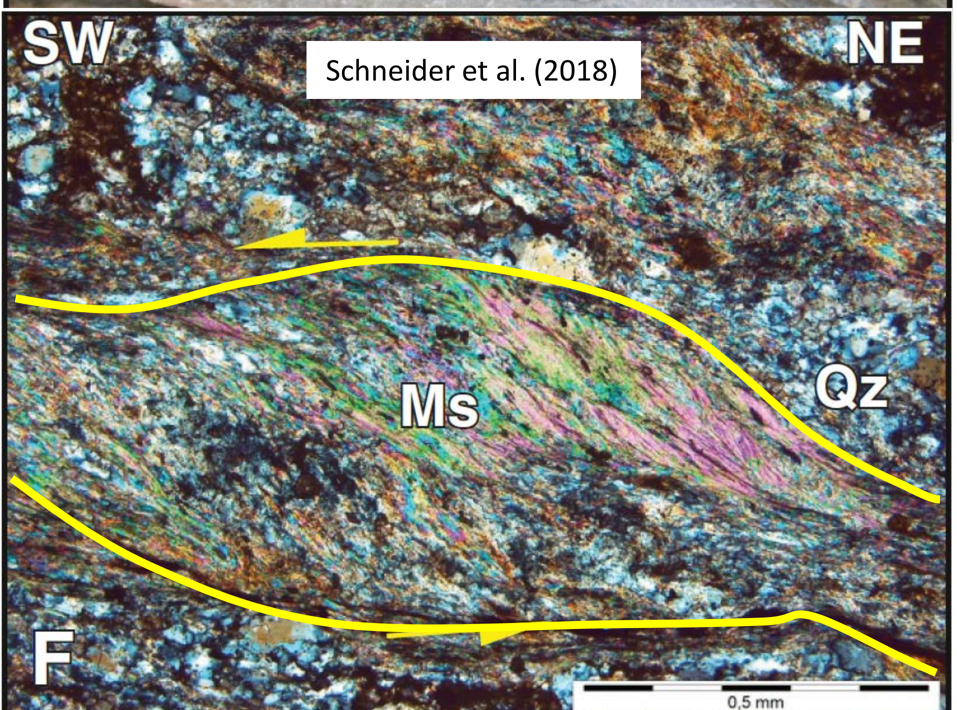

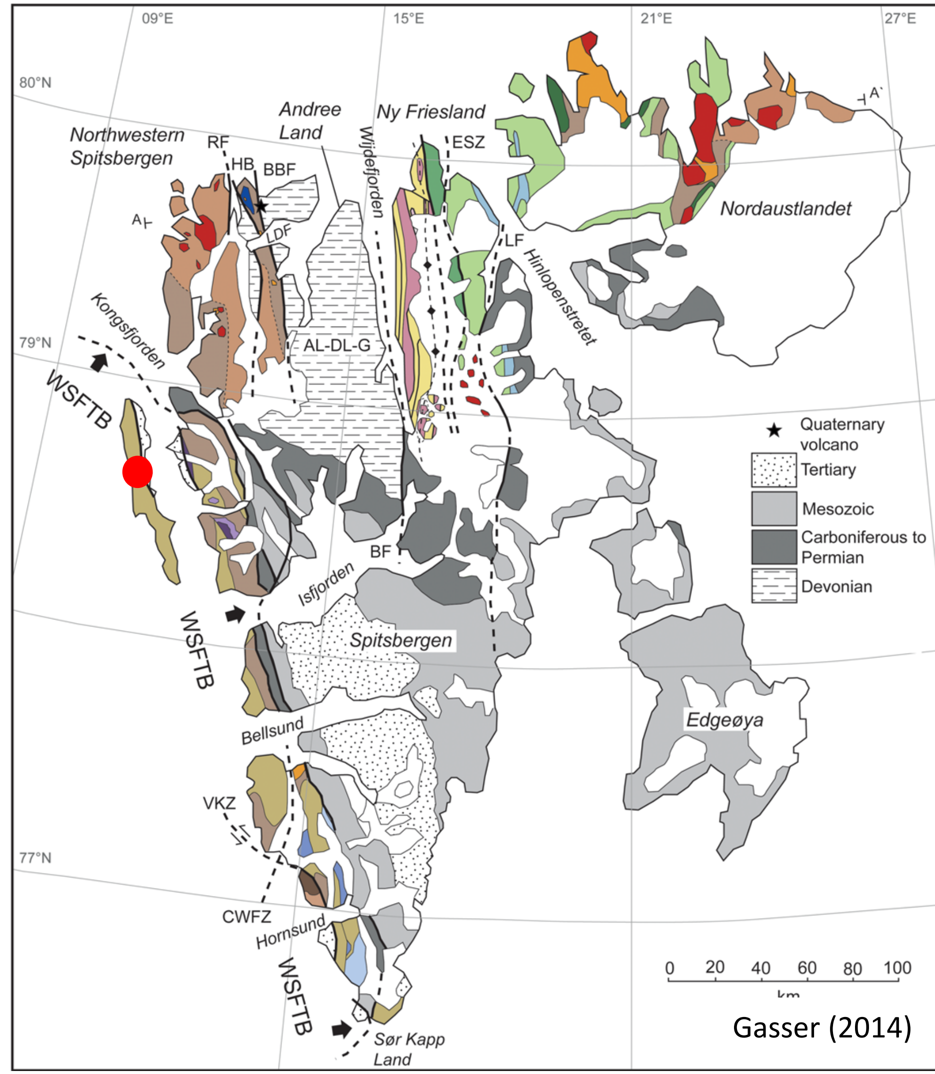

3 **Earliest Mississippian amphibolite facies metamorphism and down-west kinematics in western Svalbard may be related to core complex exhumation.**

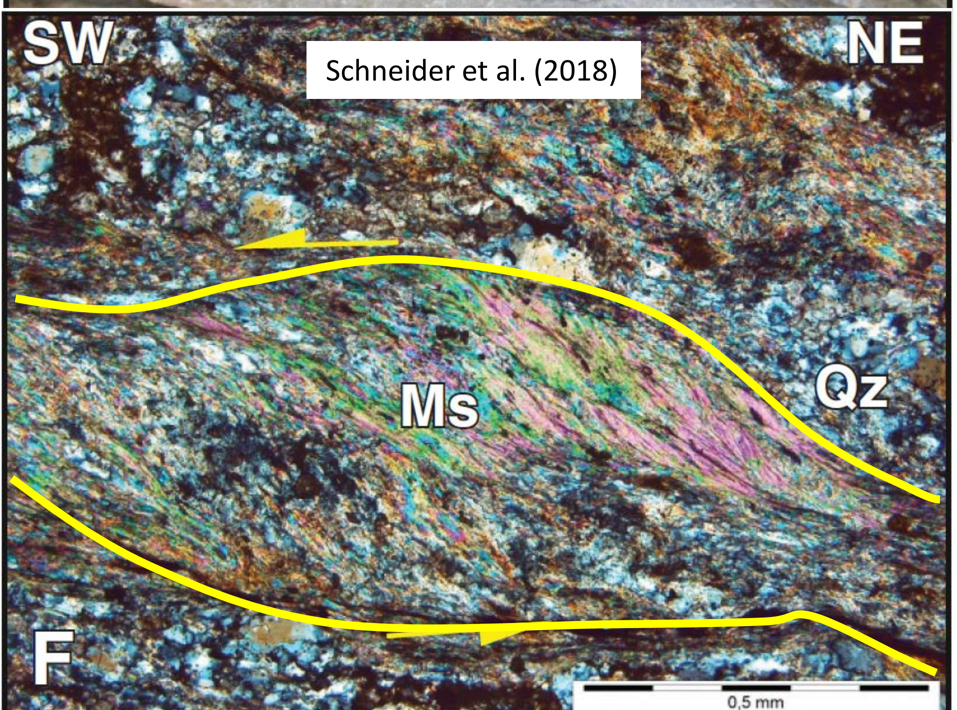

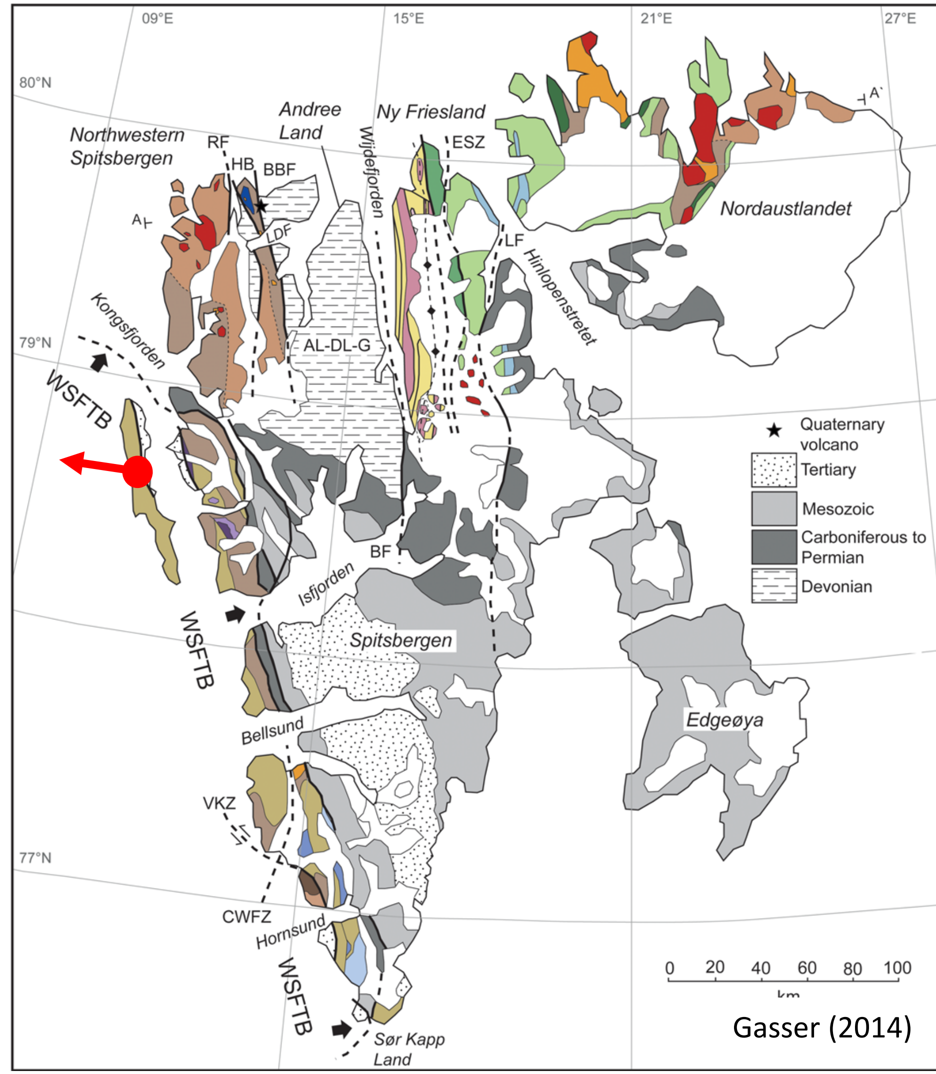

3

Earliest Mississippian amphibolite facies metamorphism and down-west kinematics in western Svalbard may be related to core complex exhumation.

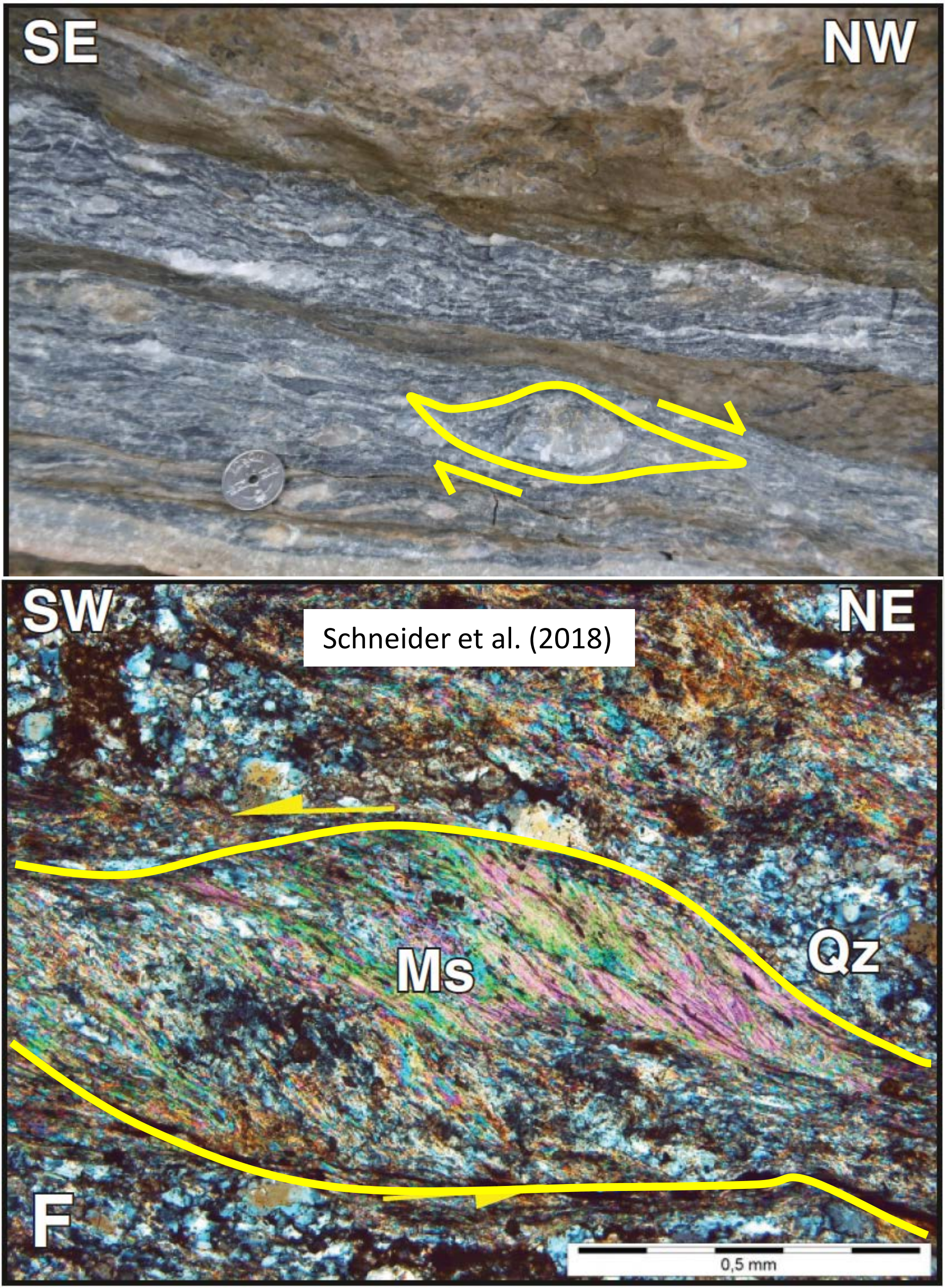

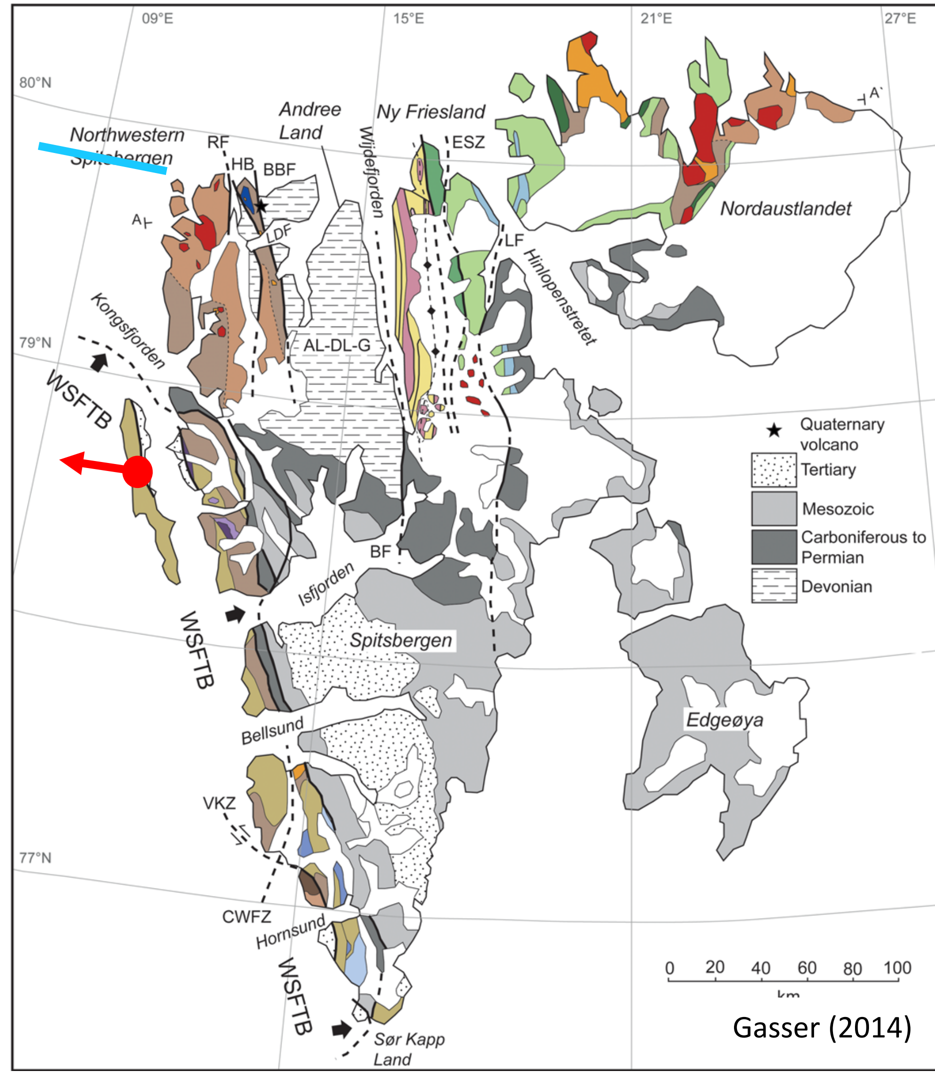

3 Basement ridges northwest/west of Spitsbergen may have exhumed as metamorphic core complexes and represent the northern continuation of Prins Karls Forland basement rocks.

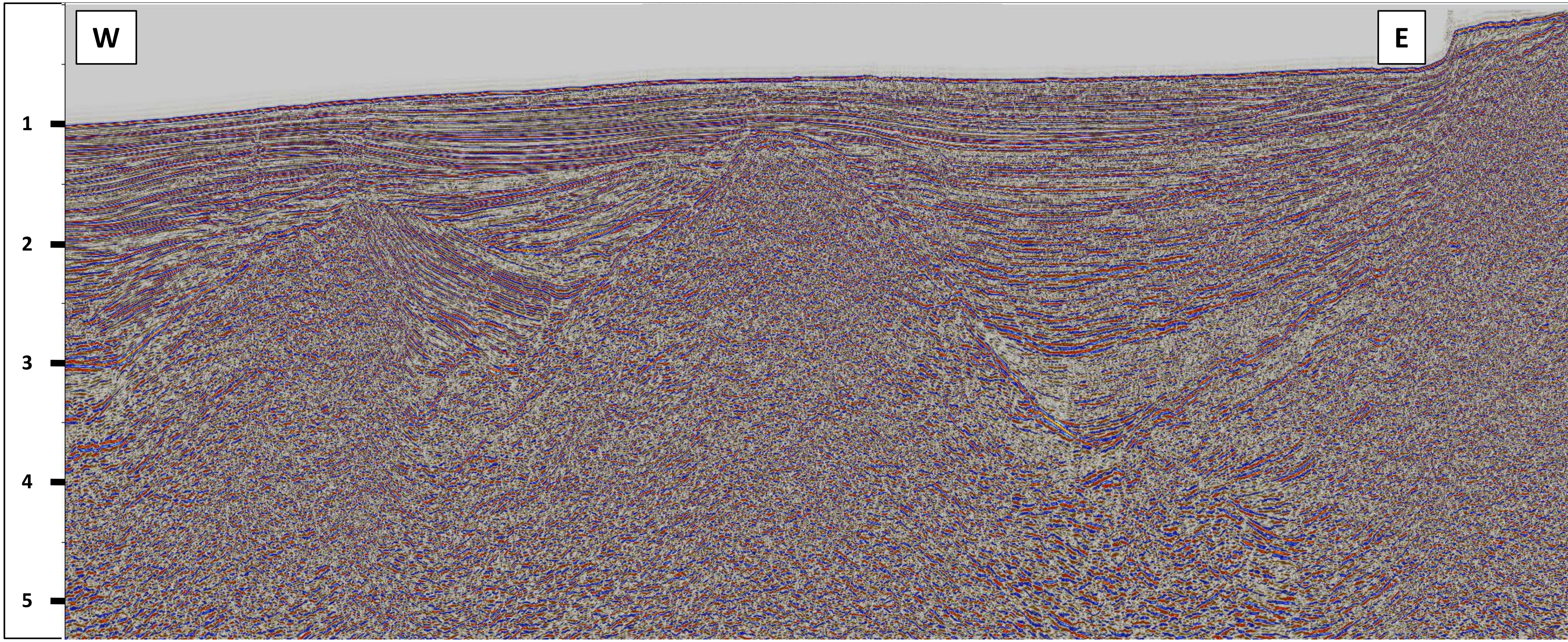

Koehl et al. (in prep. a)

3 **Basement ridges northwest/west of Spitsbergen may have exhumed as metamorphic core complexes and represent the northern continuation of Prins Karls Forland basement rocks.**

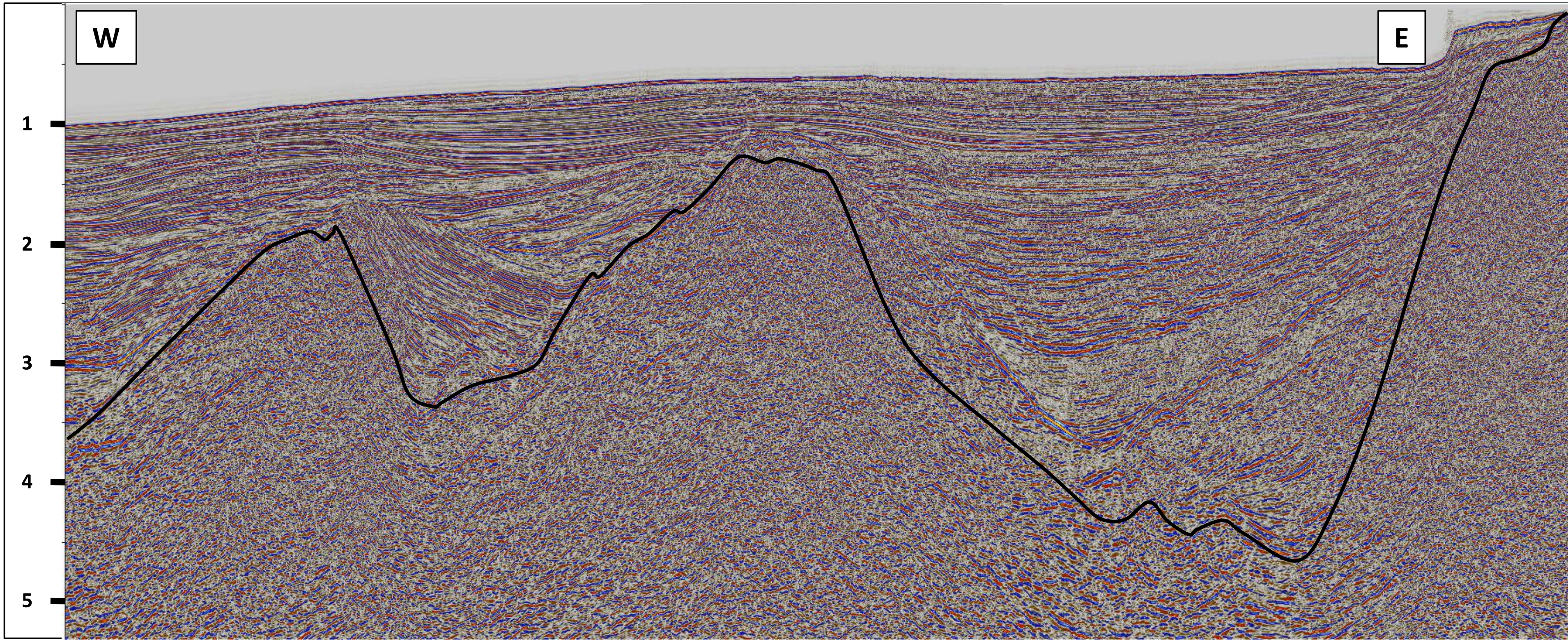

Koehl et al. (in prep. a)

3

Basement ridges northwest/west of Spitsbergen may have exhumed as metamorphic core complexes and represent the northern continuation of Prins Karls Forland basement rocks.

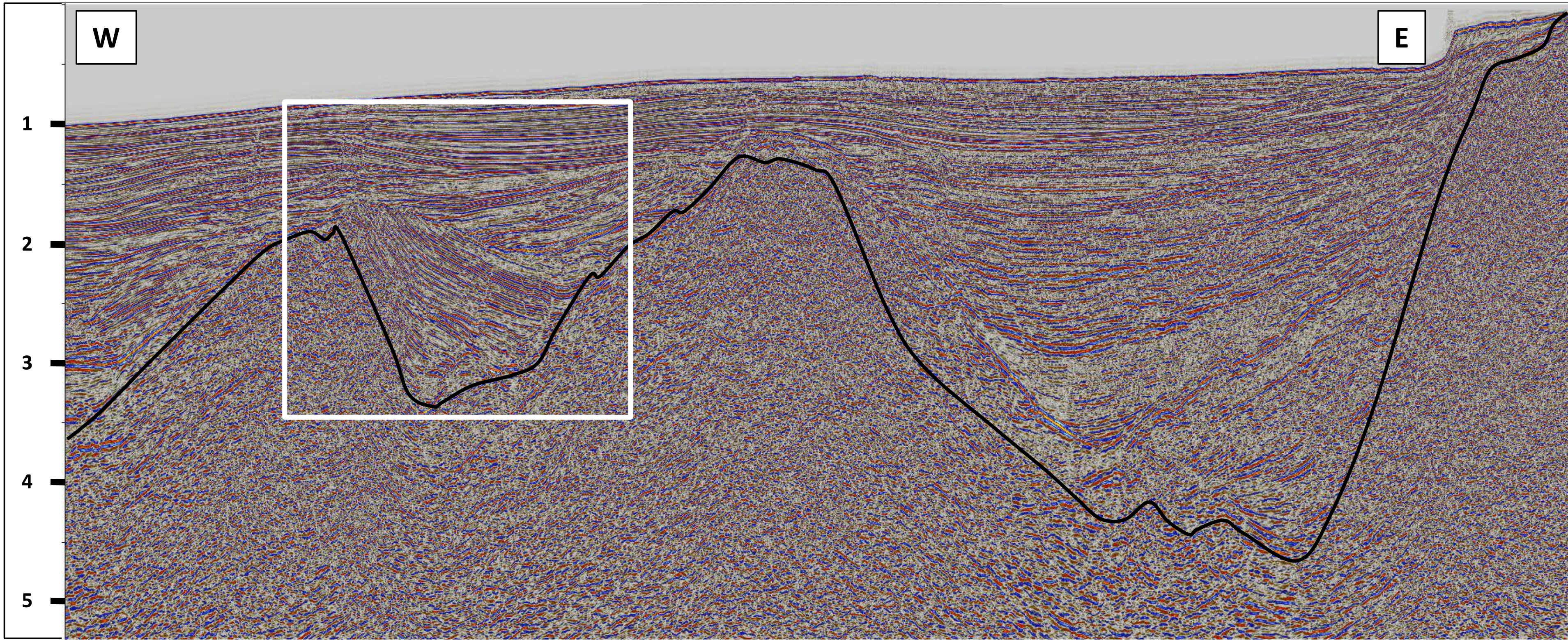

Koehl et al. (in prep. a)

3 **Basement ridges northwest/west of Spitsbergen may have exhumed as metamorphic core complexes and represent the northern continuation of Prins Karls Forland basement rocks.**

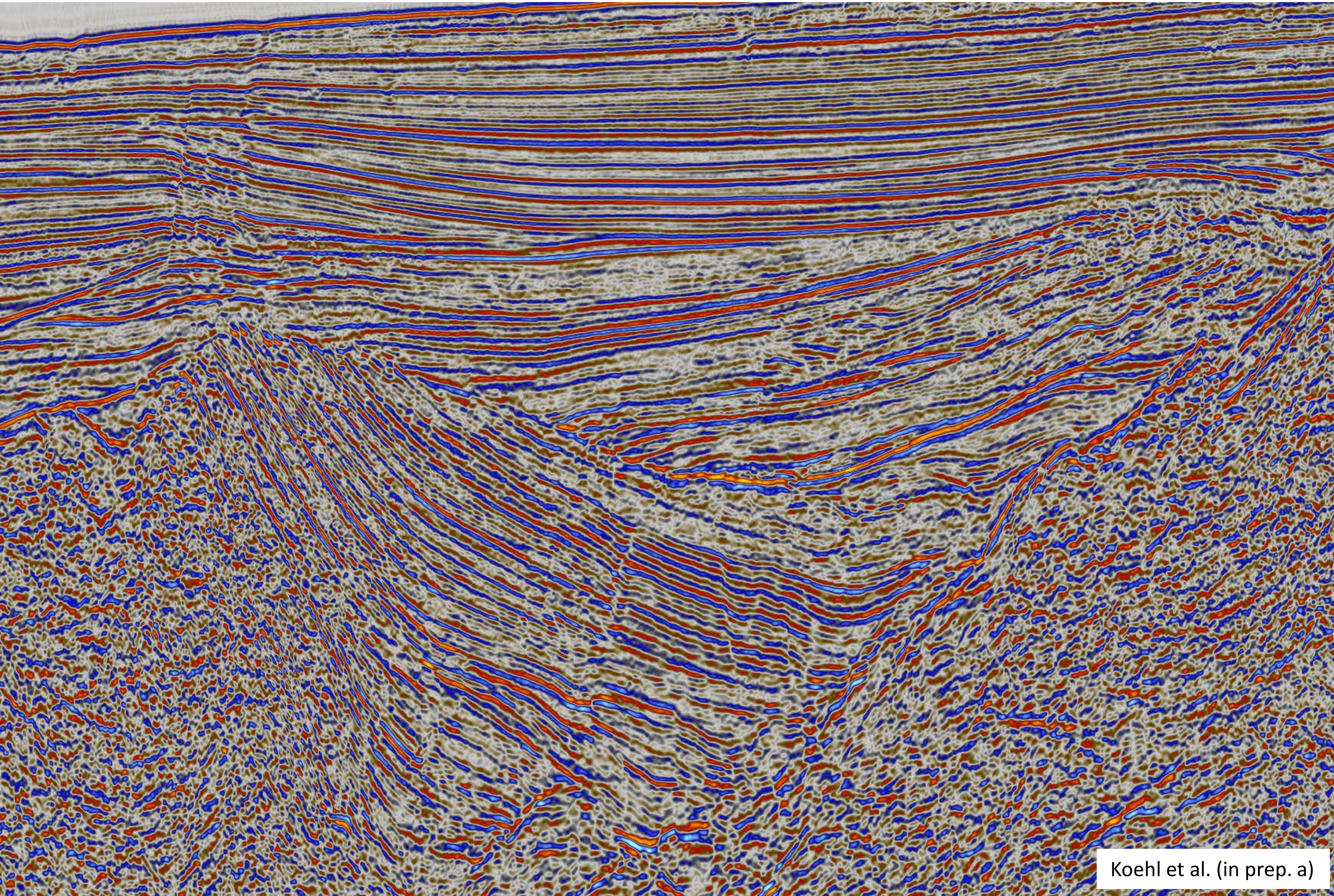

Koehl et al. (in prep. a)

3 **Basement ridges northwest/west of Spitsbergen may have exhumed as metamorphic core complexes and represent the northern continuation of Prins Karls Forland basement rocks.**

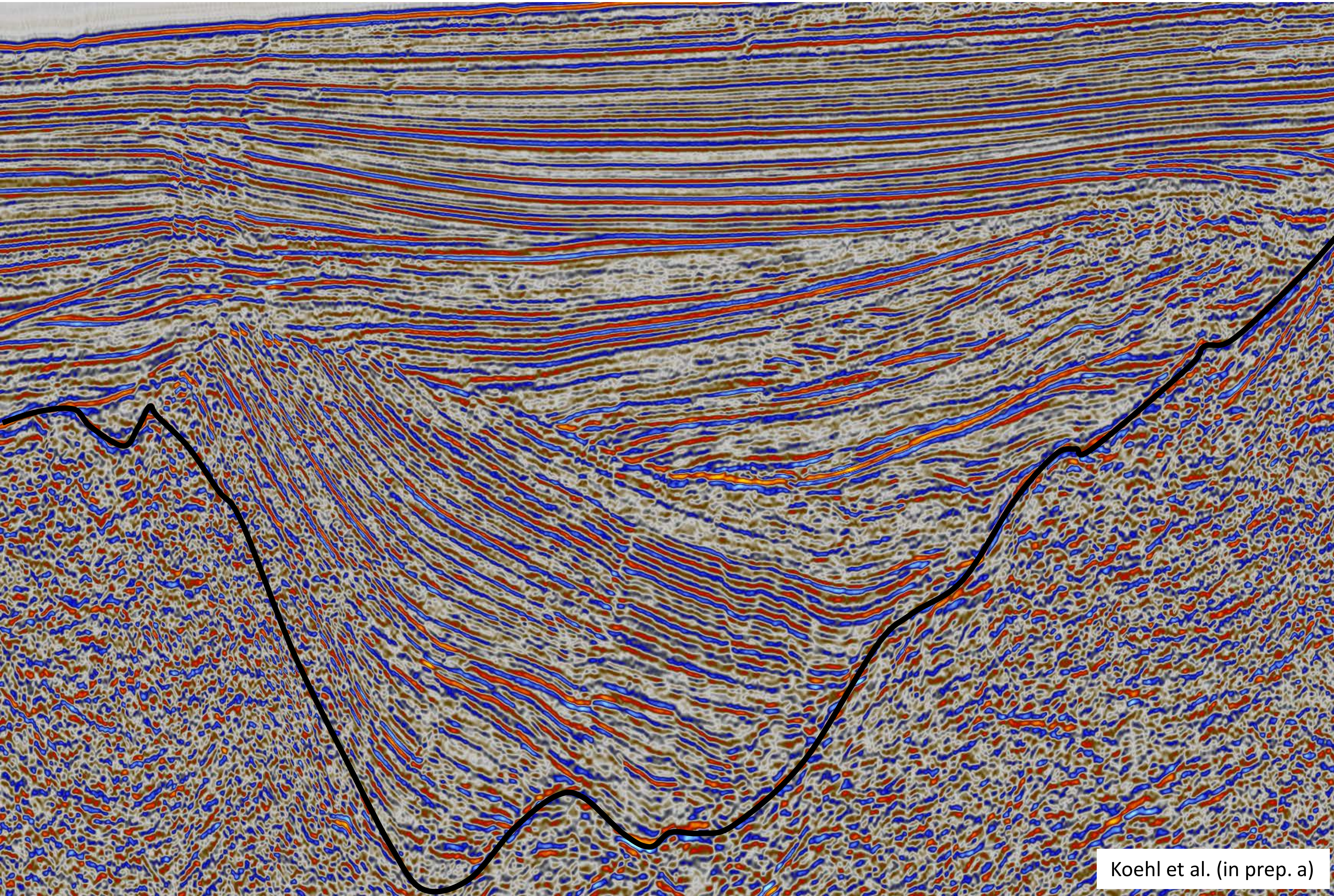

3

Basement ridges northwest/west of Spitsbergen may have exhumed as metamorphic core complexes and represent the northern continuation of Prins Karls Forland basement rocks.

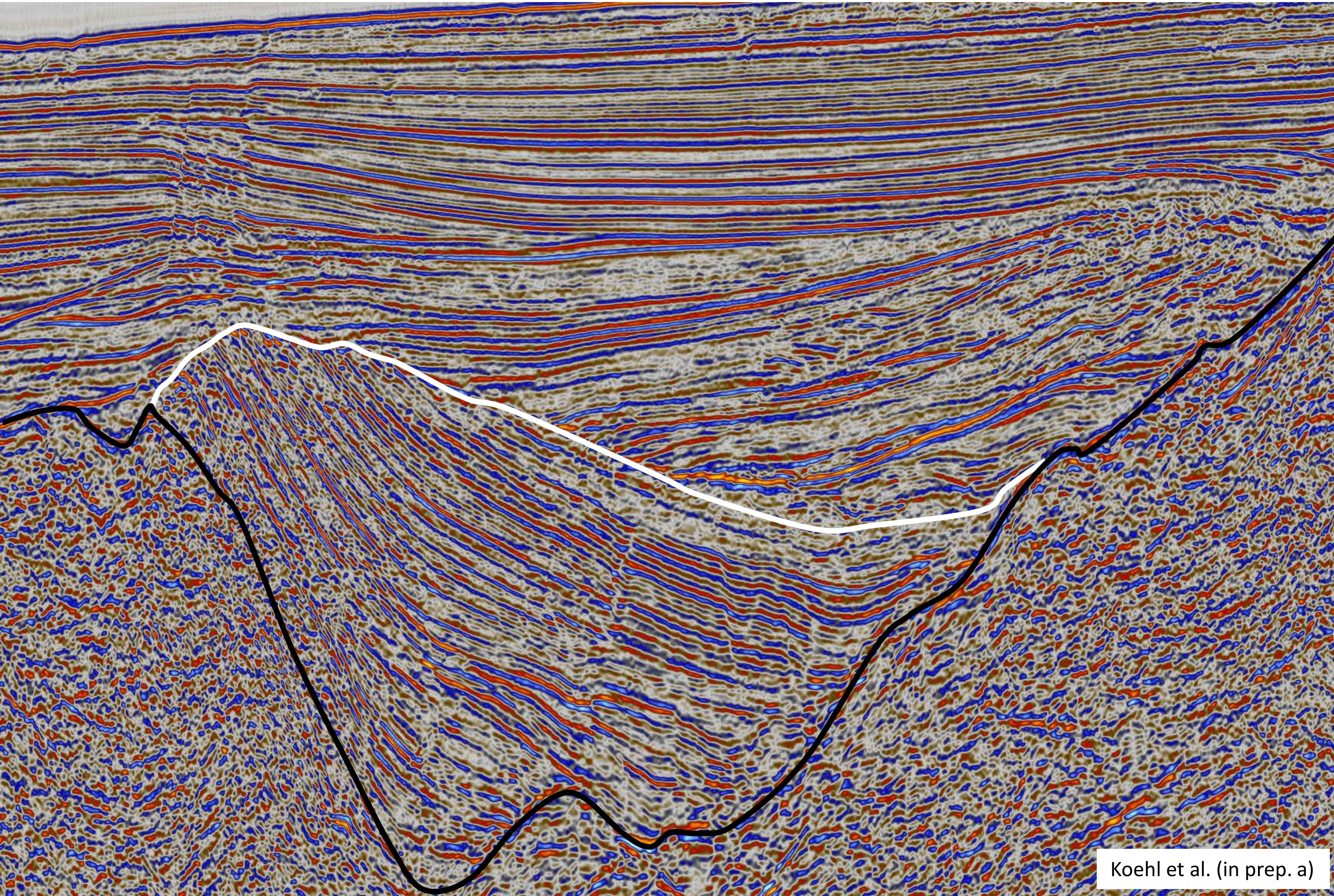

3 **Basement ridges northwest/west of Spitsbergen may have exhumed as metamorphic core complexes and represent the northern continuation of Prins Karls Forland basement rocks.**

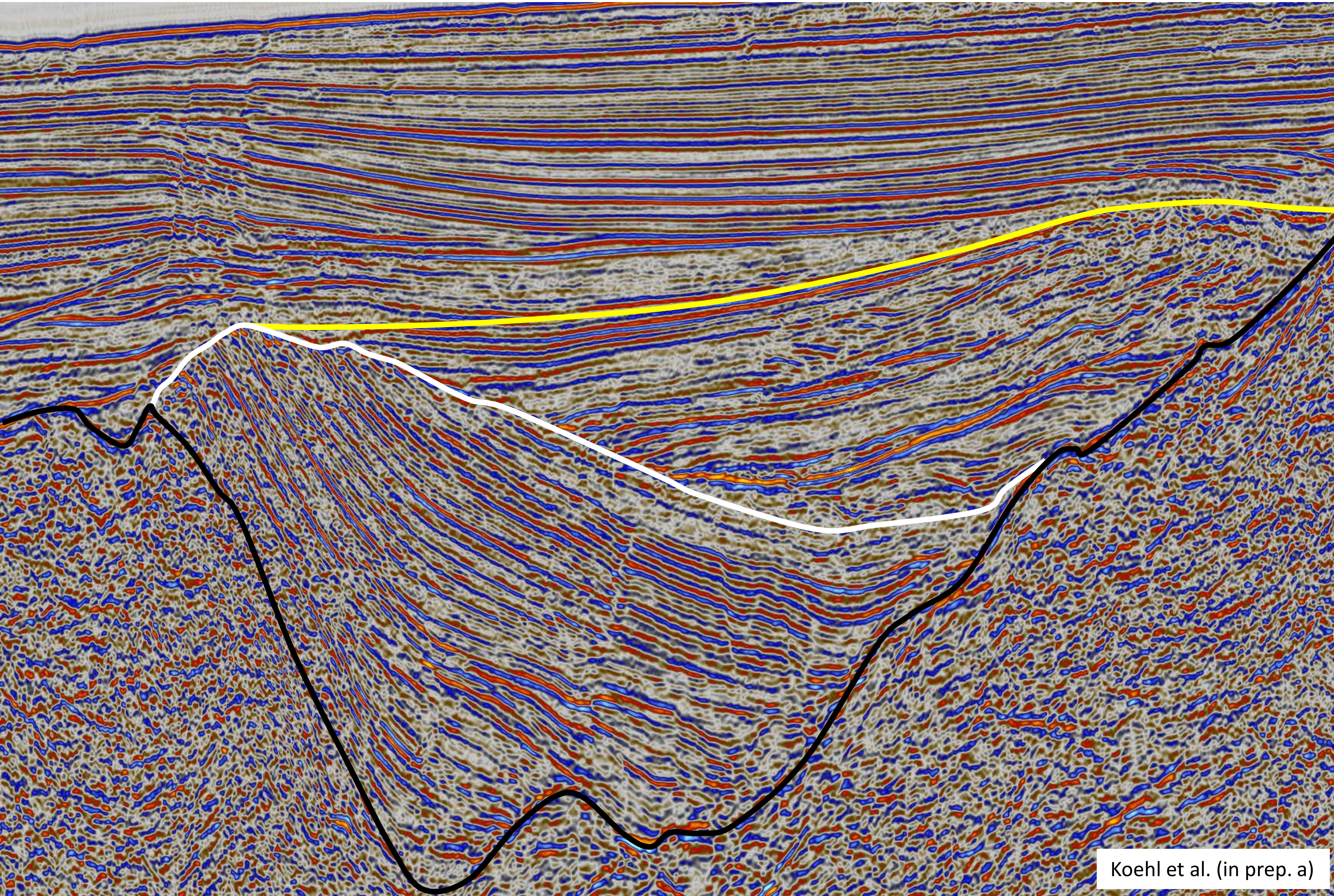

3

Basement ridges northwest/west of Spitsbergen may have exhumed as metamorphic core complexes and represent the northern continuation of Prins Karls Forland basement rocks.

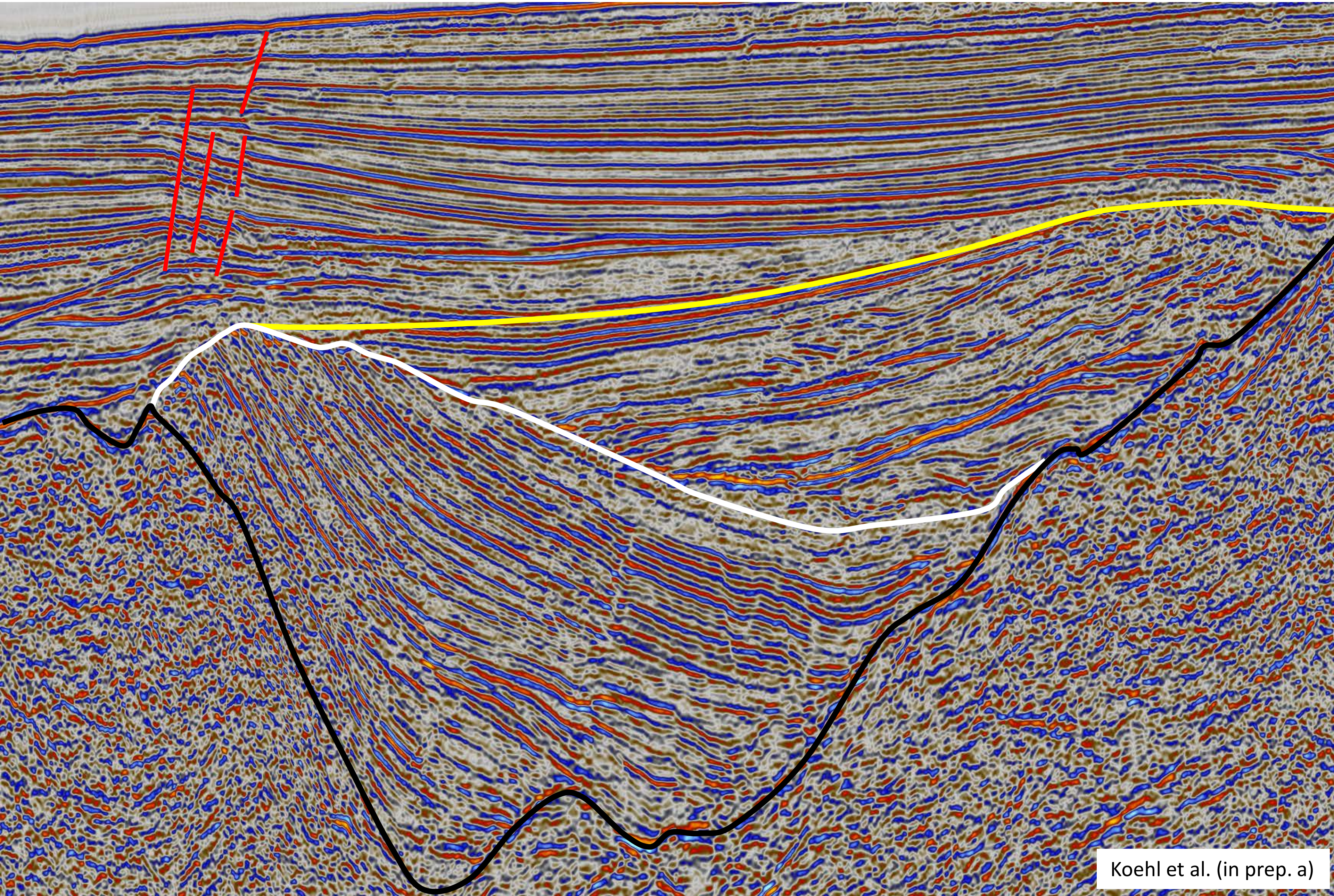

3 **Basement ridges northwest/west of Spitsbergen may have exhumed as metamorphic core complexes and represent the northern continuation of Prins Karls Forland basement rocks.**

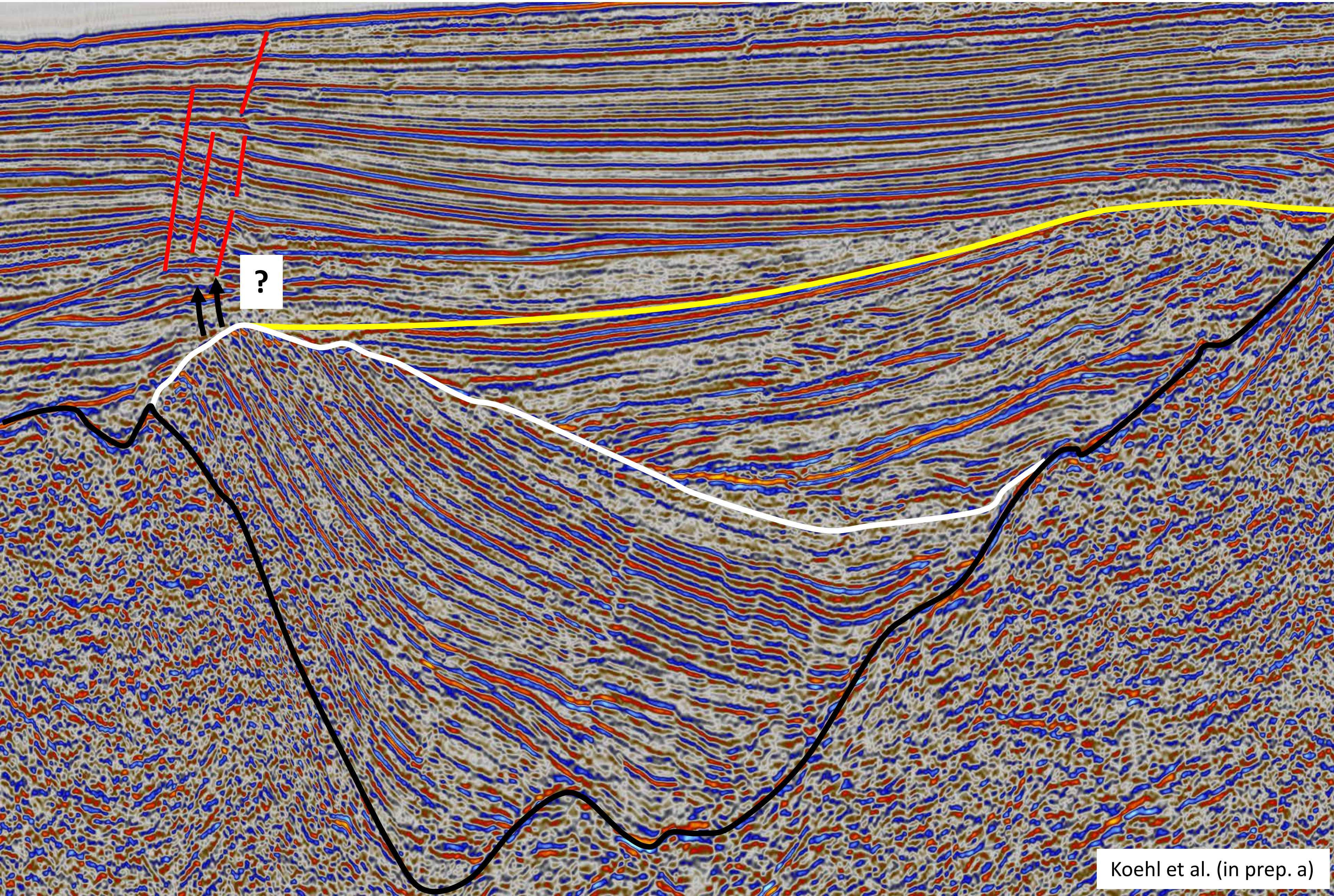

3

WNW–ESE-striking Timanian and transform faults may, alone, have accommodated the movement of Svalbard from next to Greenland to its present position, c. 400 km away.

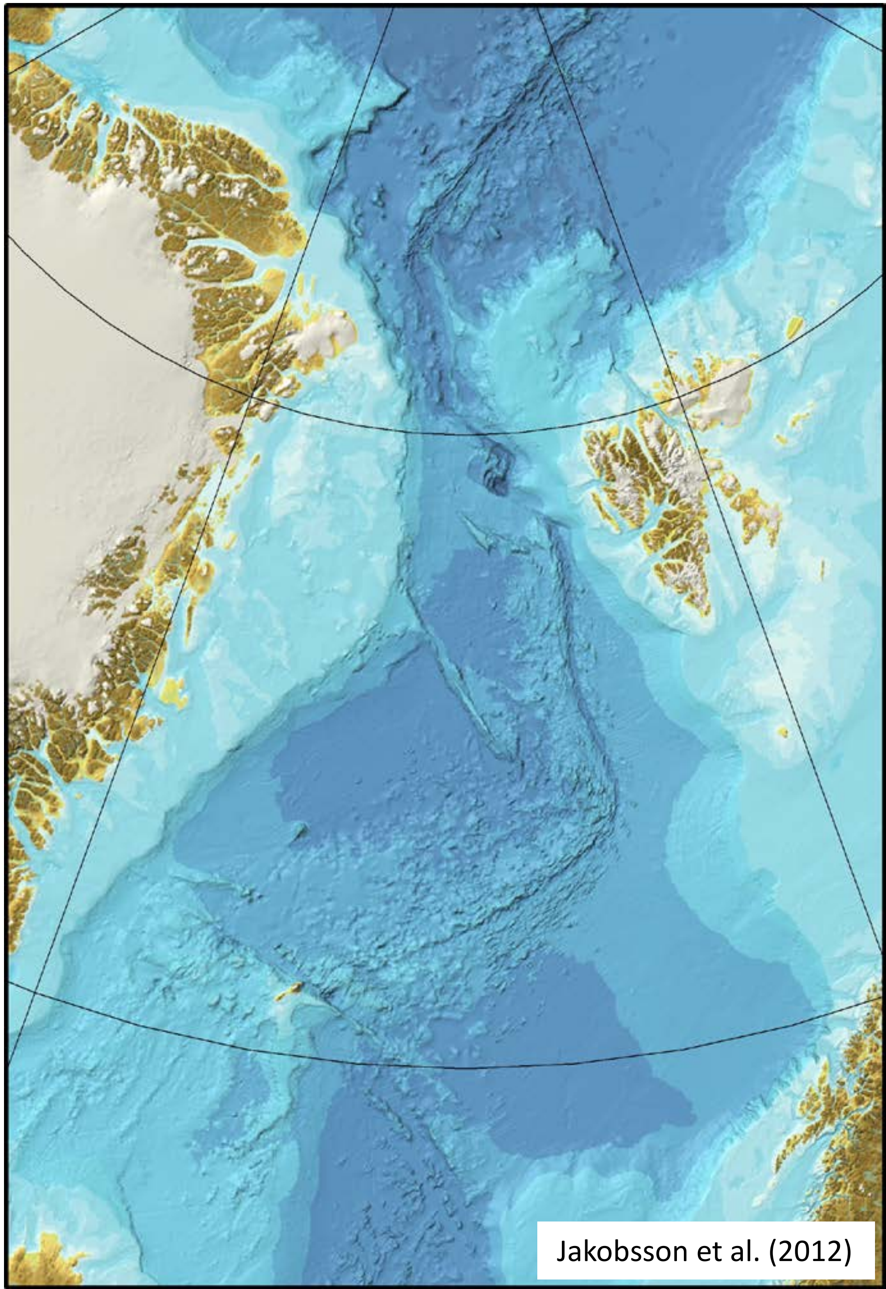

3

WNW–ESE-striking Timanian and transform faults may, alone, have accommodated the movement of Svalbard from next to Greenland to its present position, c. 400 km away.

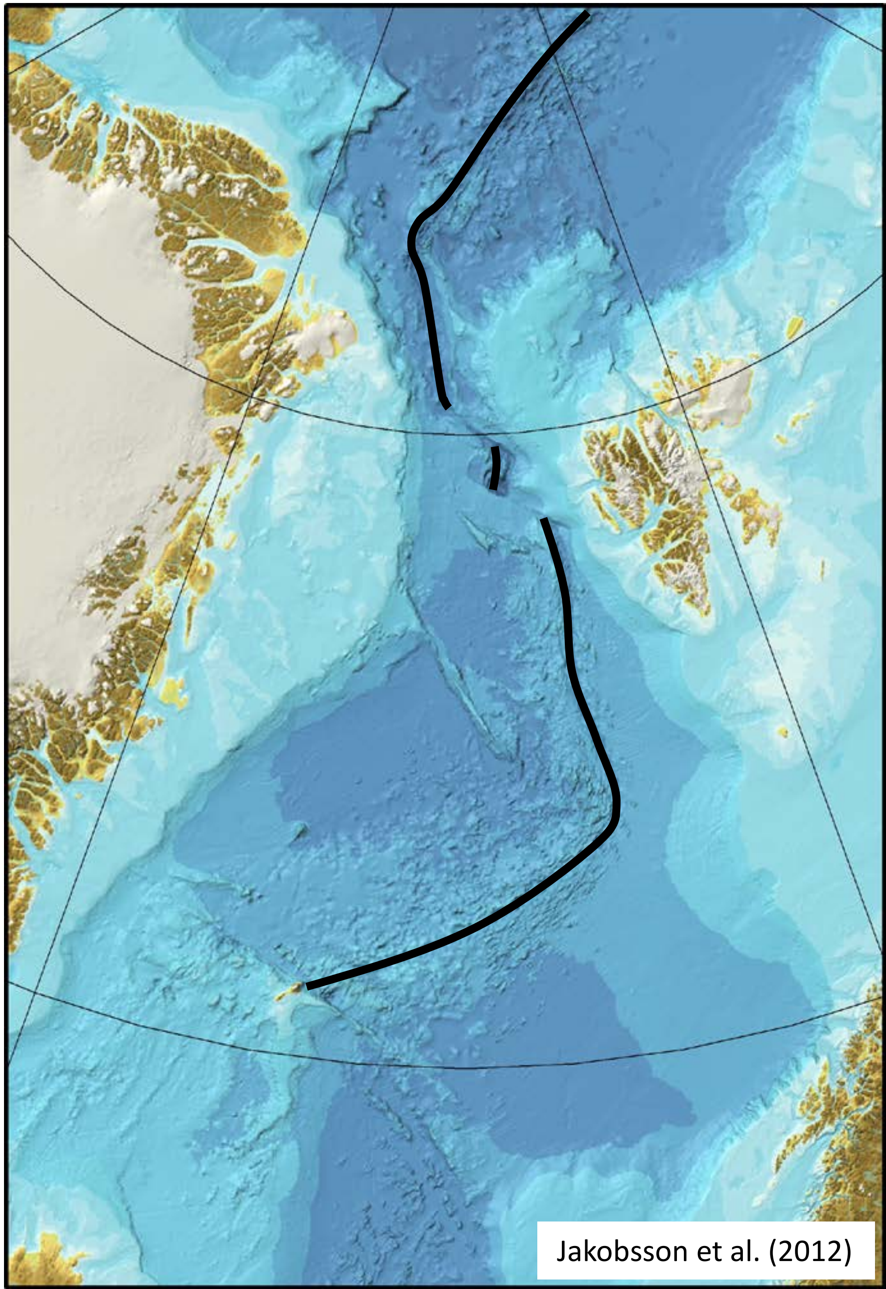

Jakobsson et al. (2012)

3

WNW–ESE-striking Timanian and transform faults may, alone, have accommodated the movement of Svalbard from next to Greenland to its present position, c. 400 km away.

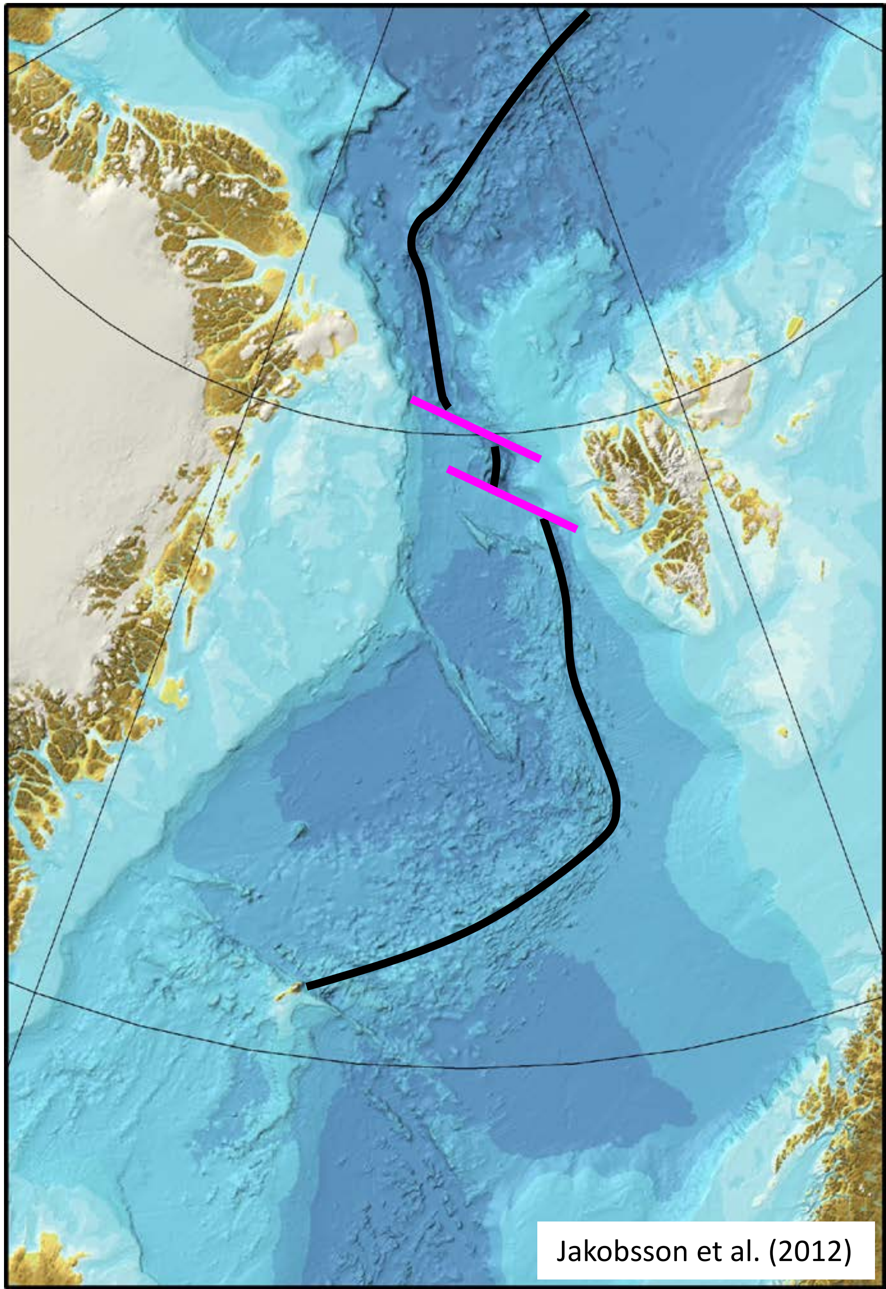

3 **WNW–ESE-striking Timanian and transform faults may, alone, have accommodated the movement of Svalbard from next to Greenland to its present position, c. 400 km away.**

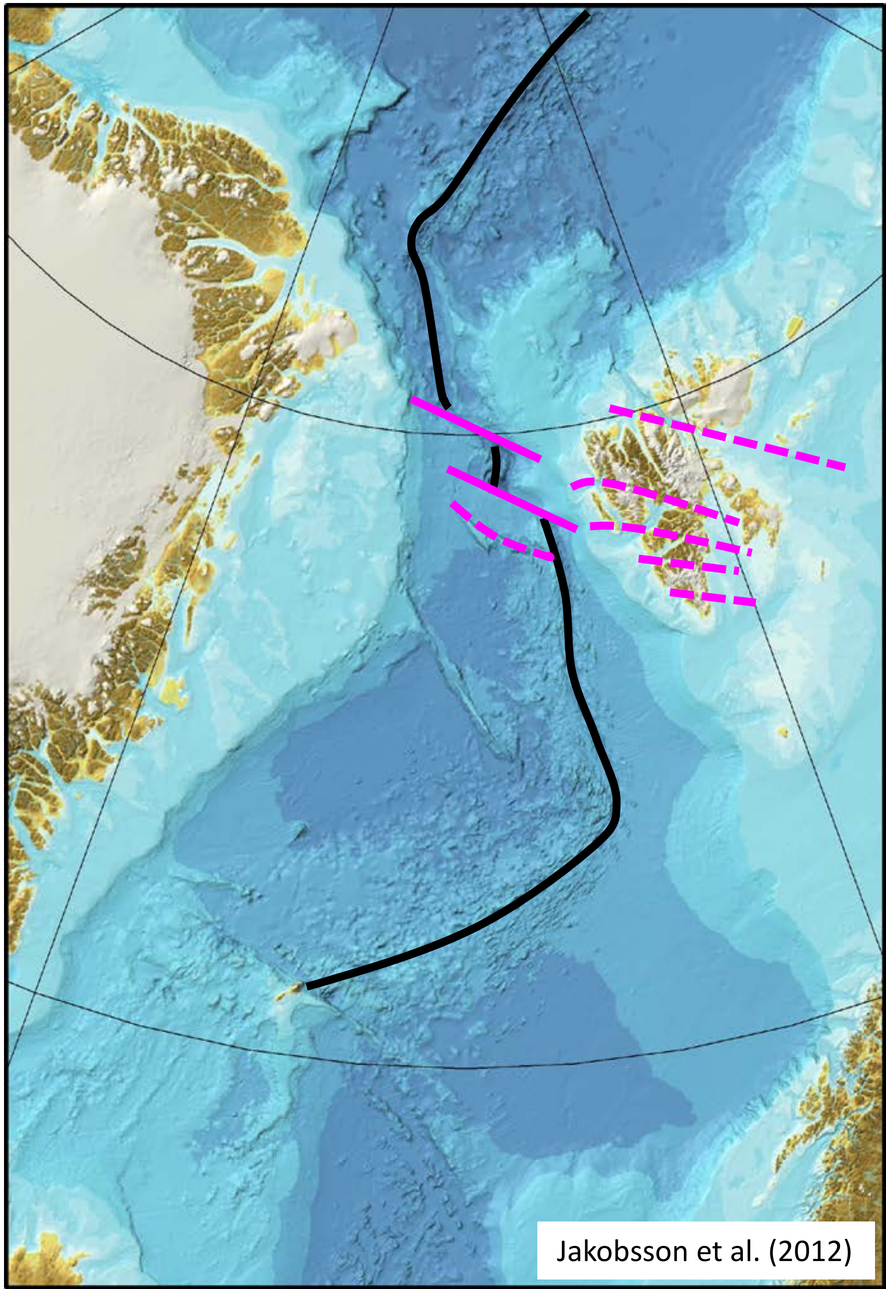

3 WNW–ESE-striking Timanian and transform faults may, alone, have accommodated the movement of Svalbard from next to Greenland to its present position, c. 400 km away.

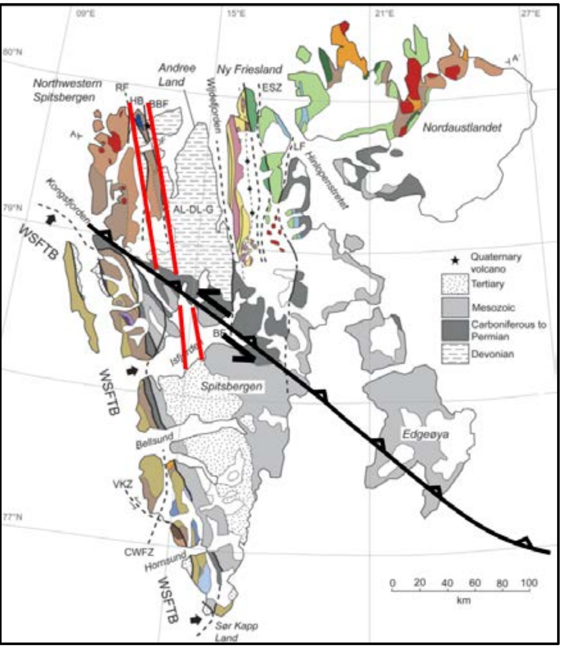

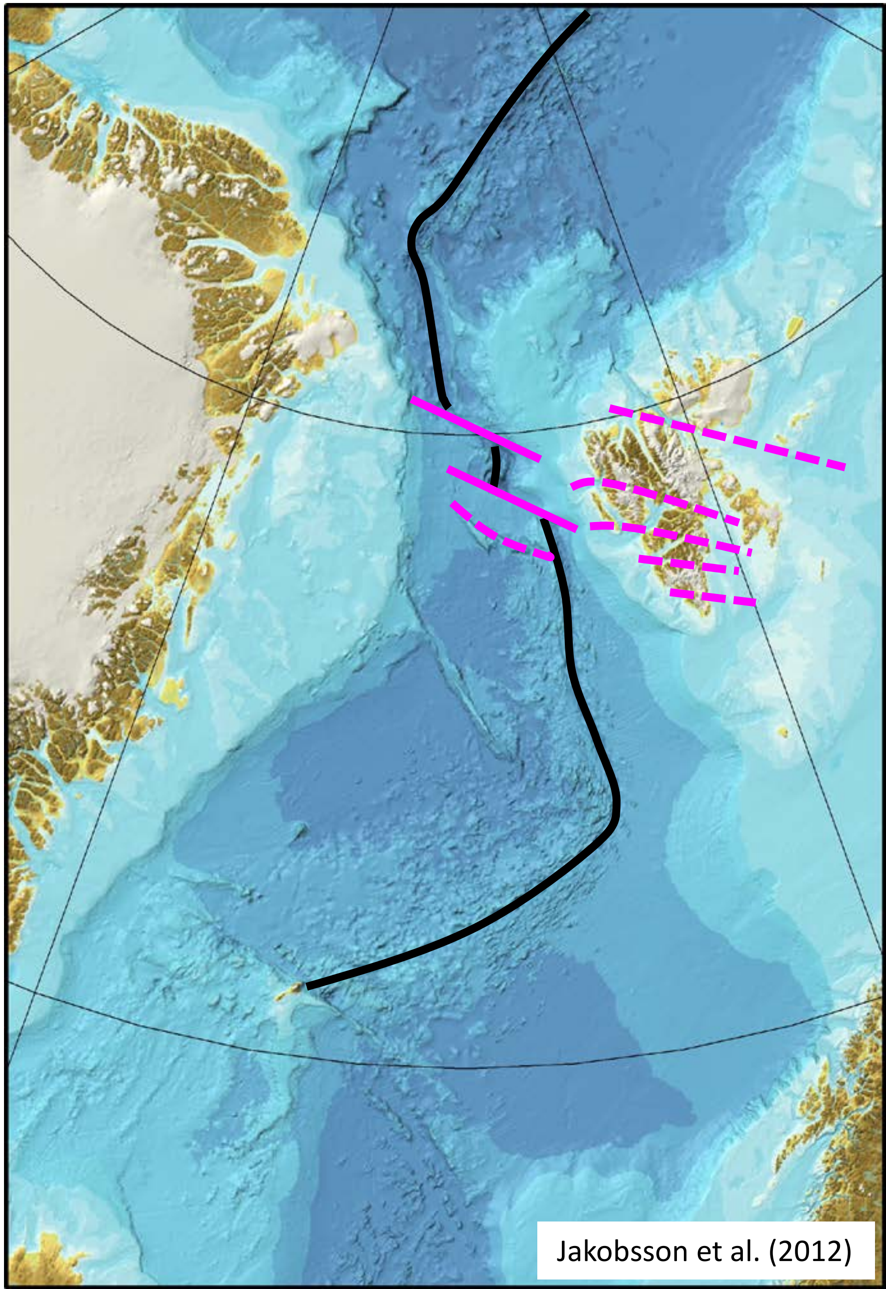

3

WNW–ESE-striking Timanian and transform faults may, alone, have accommodated the movement of Svalbard from next to Greenland to its present position, c. 400 km away.

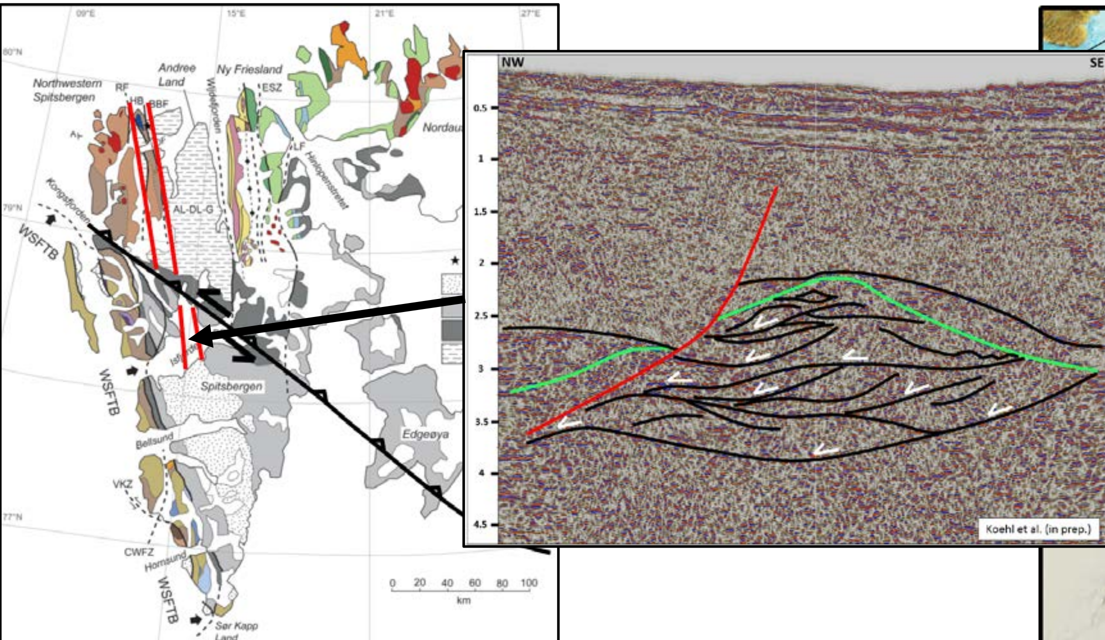

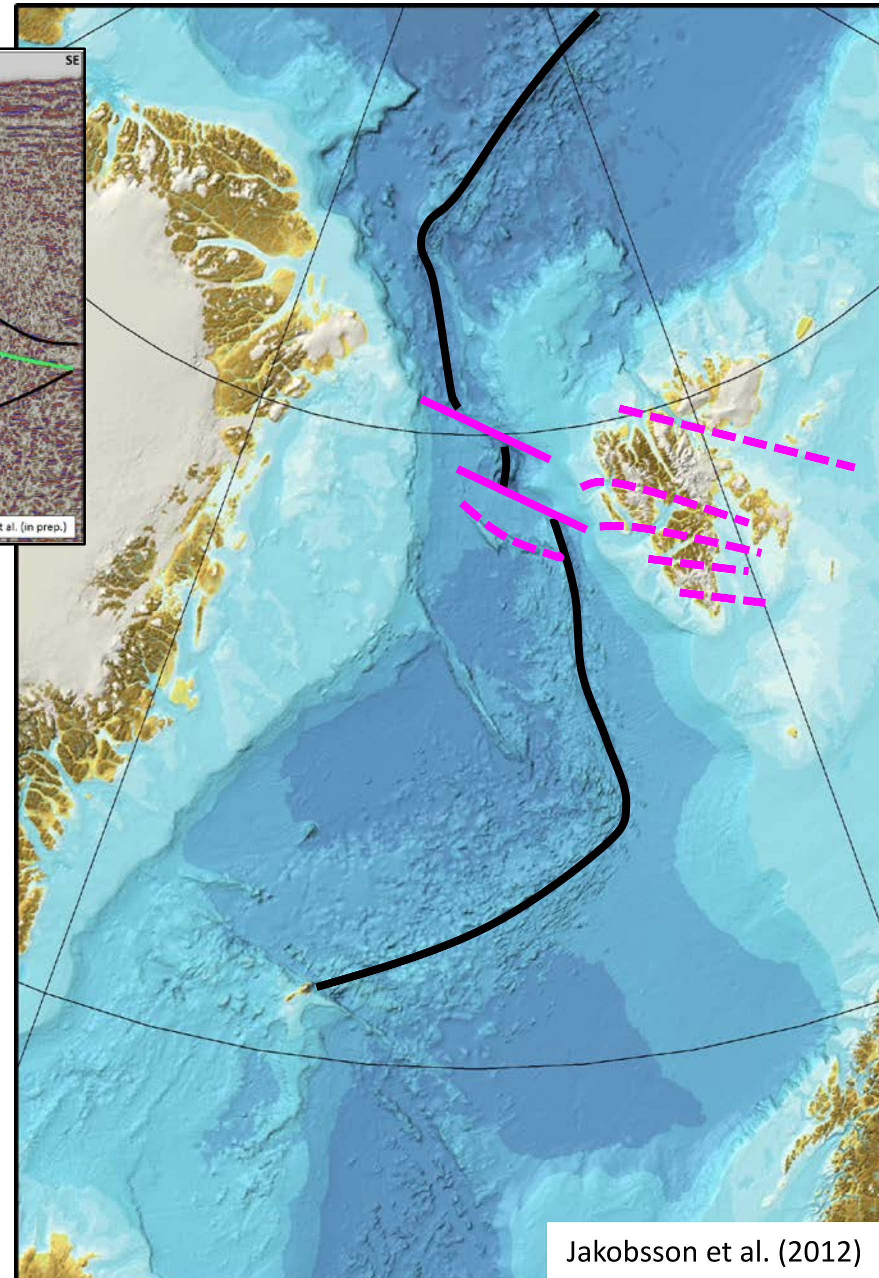

3

WNW–ESE-striking Timanian and transform faults may, alone, have accommodated the movement of Svalbard from next to Greenland to its present position, c. 400 km away.

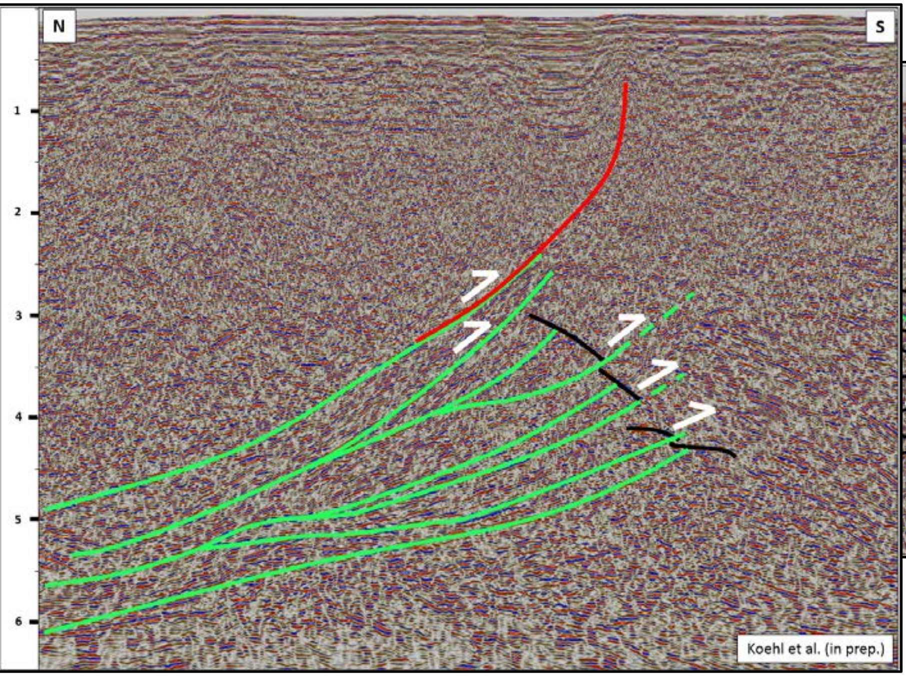

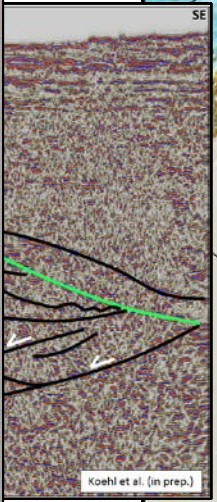

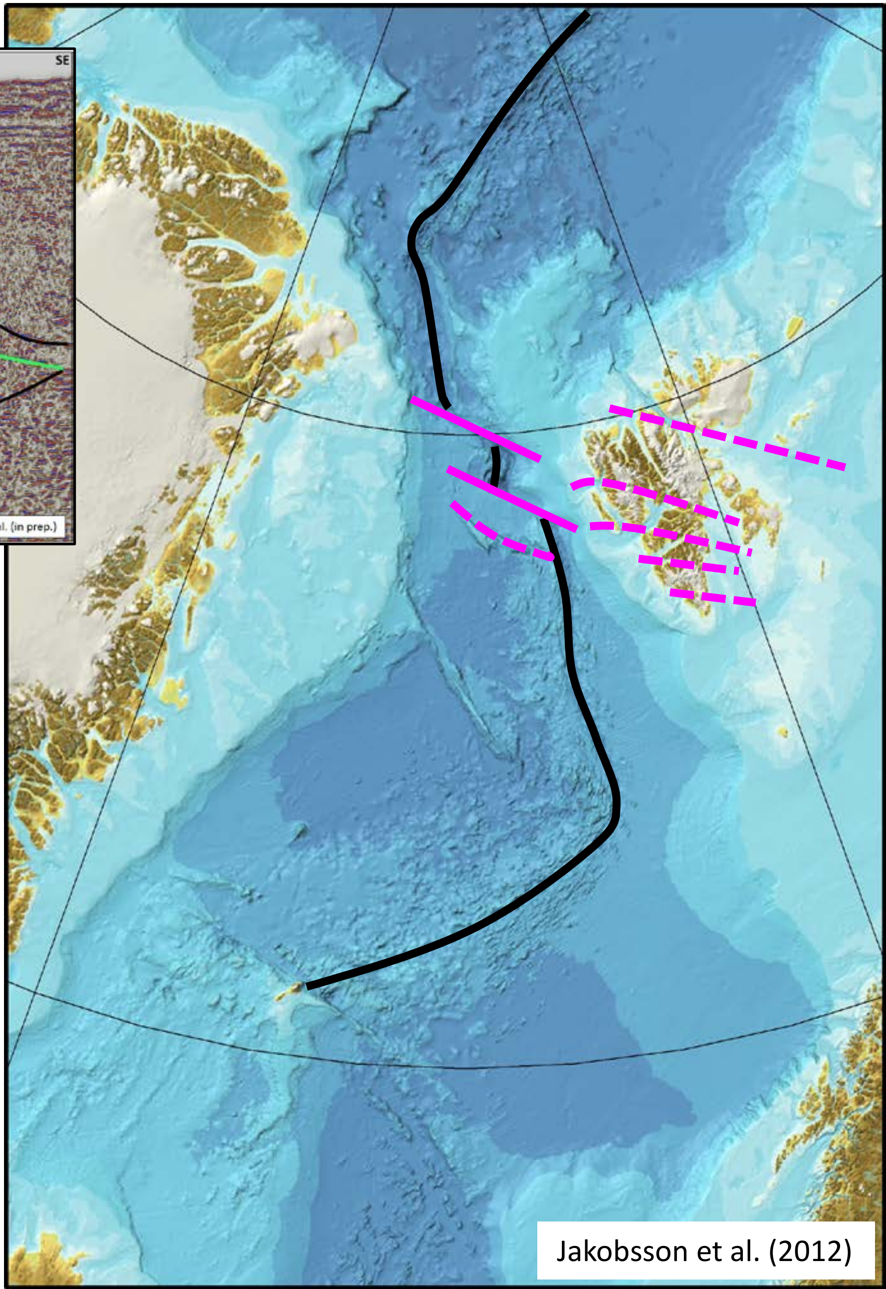

3

WNW–ESE-striking Timanian and transform faults may, alone, have accommodated the movement of Svalbard from next to Greenland to its present position, c. 400 km away.

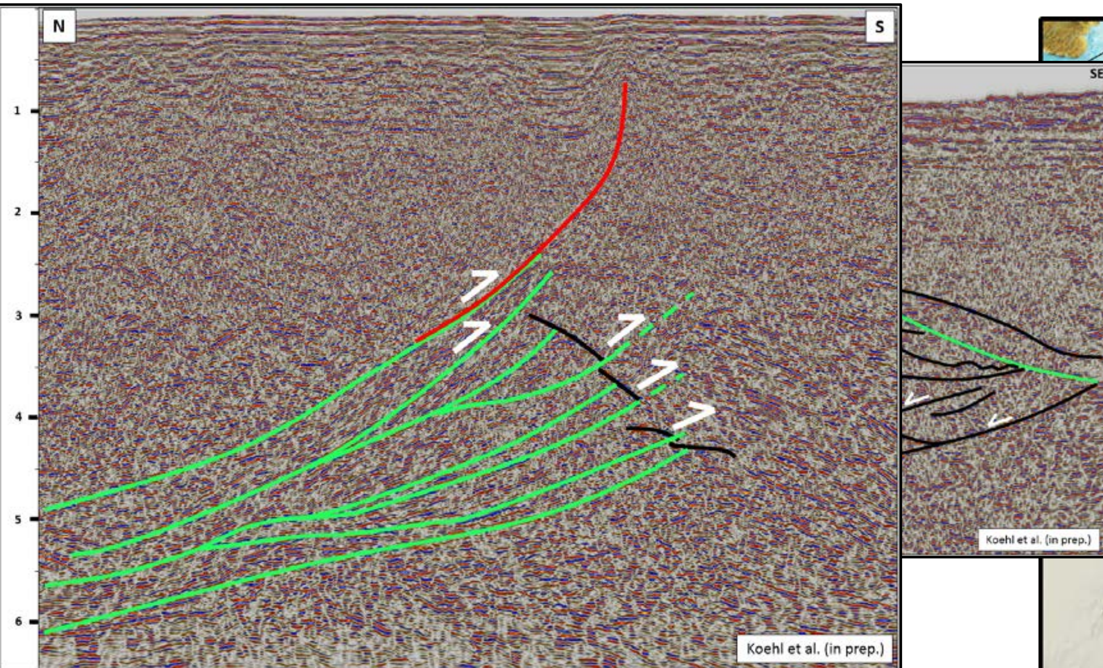

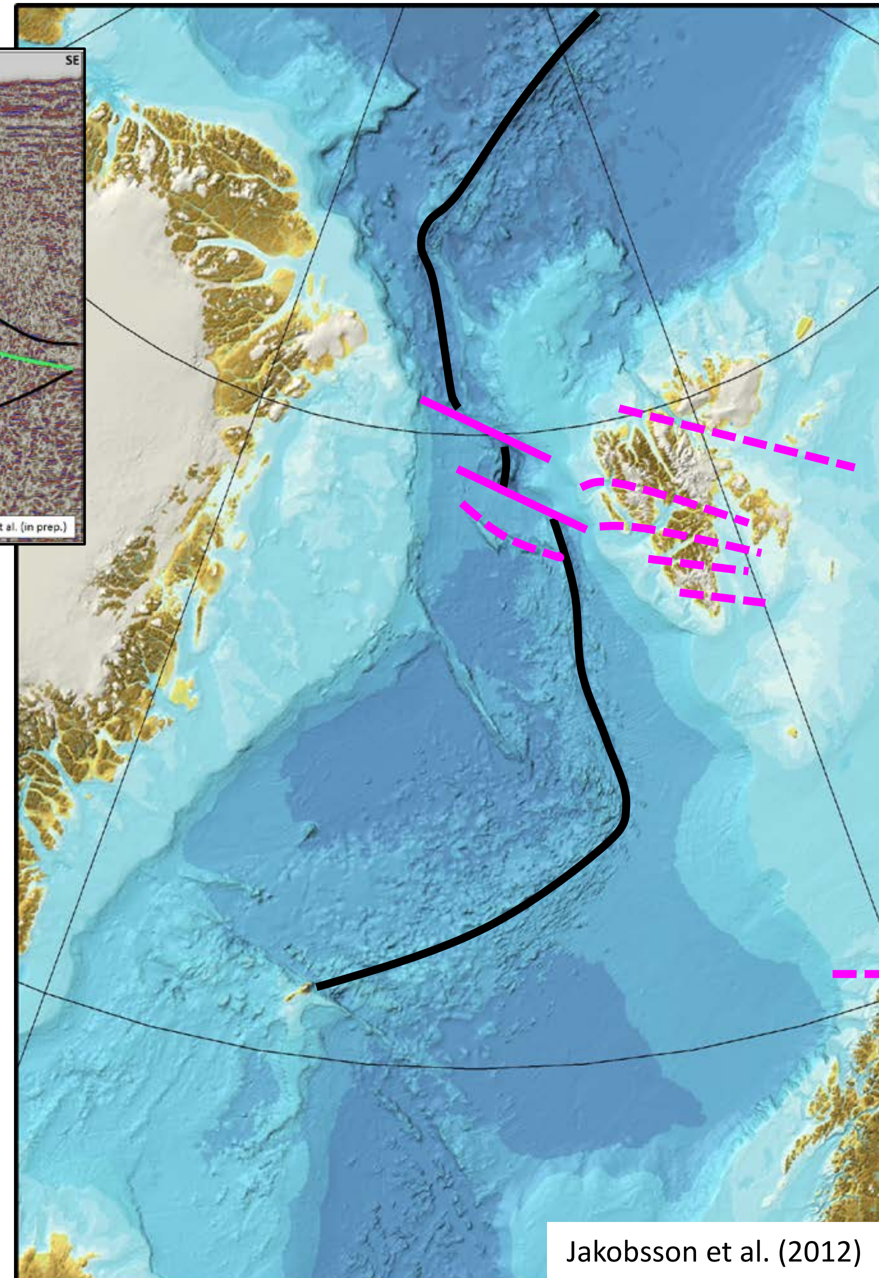

3 **WNW–ESE-striking Timanian and transform faults may, alone, have accommodated the movement of Svalbard from next to Greenland to its present position, c. 400 km away.**

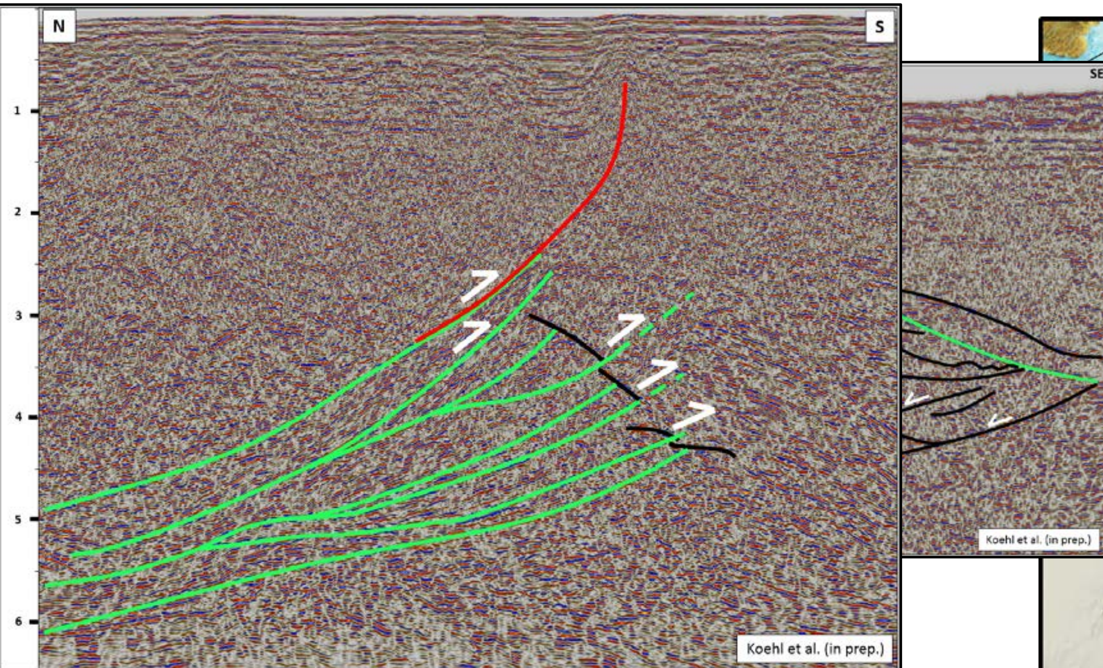

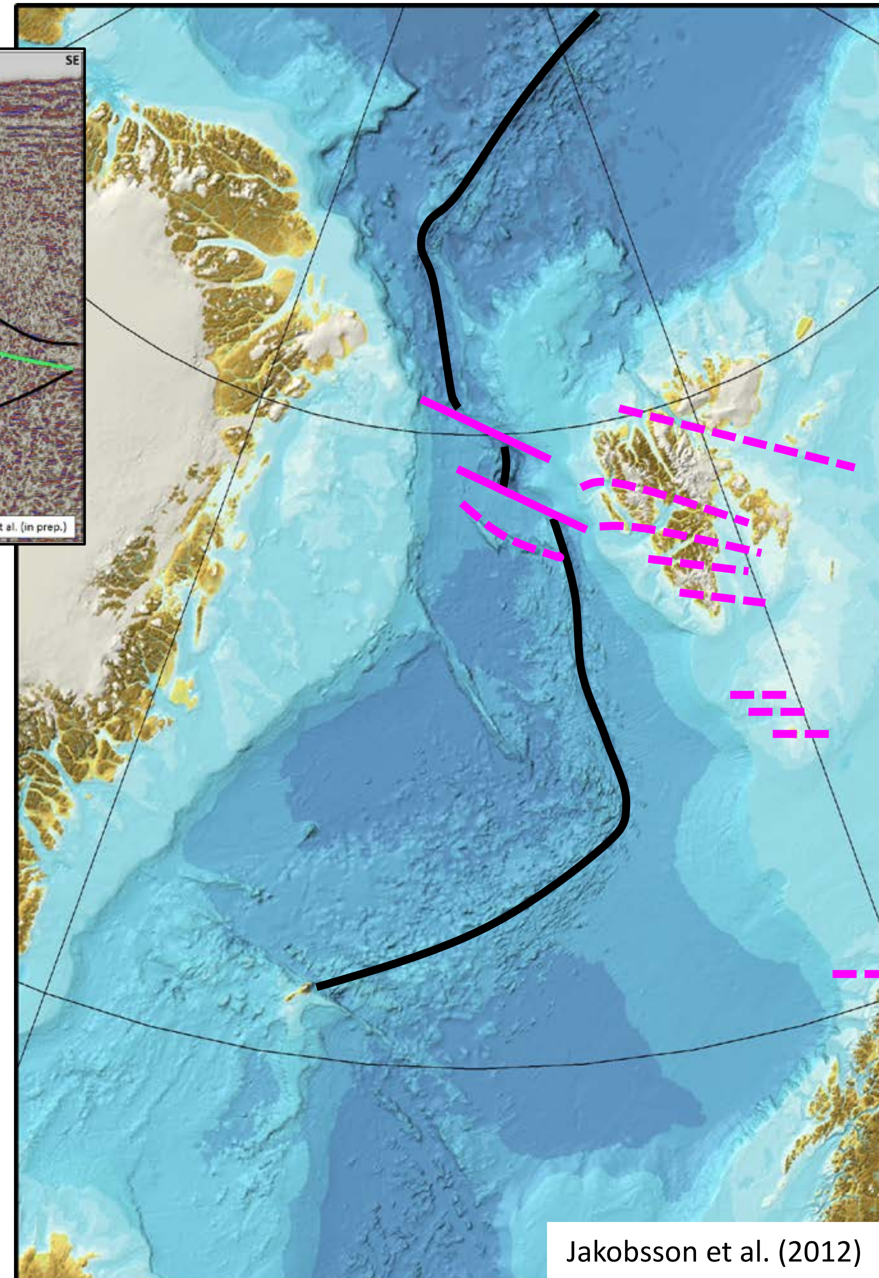

3 WNW–ESE-striking Timanian and transform faults may, alone, have accommodated the movement of Svalbard from next to Greenland to its present position, c. 400 km away.

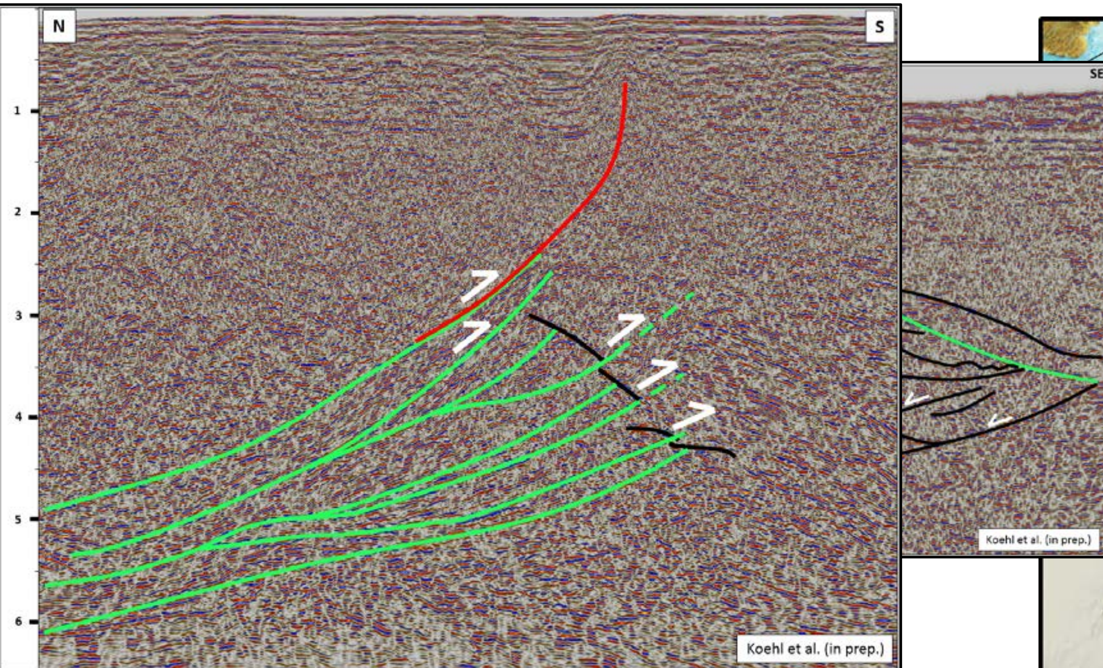

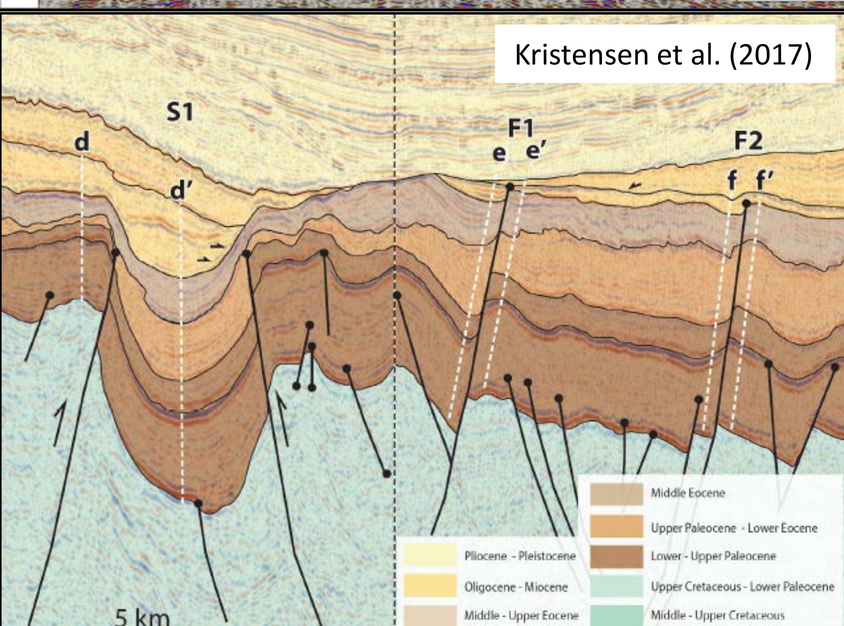

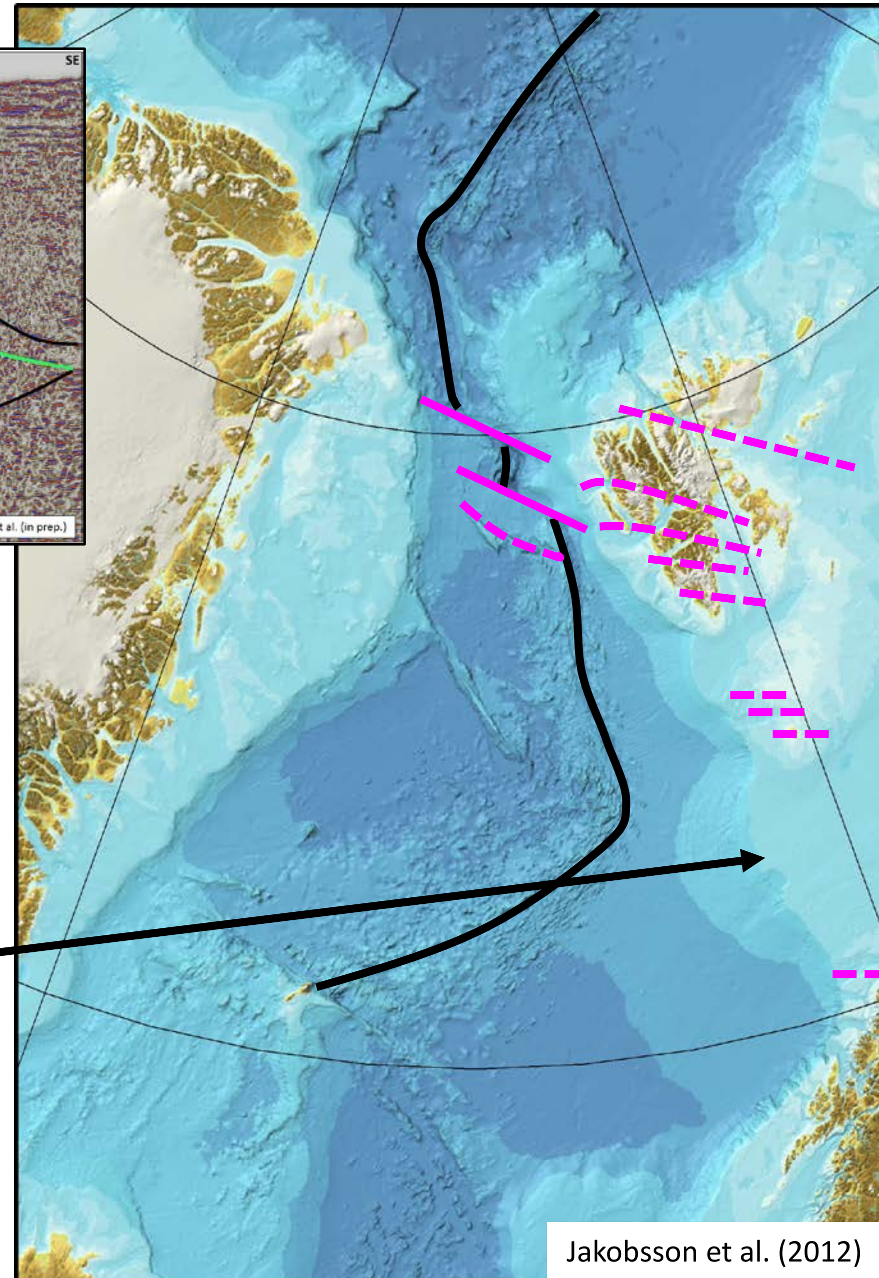

3 **WNW–ESE-striking Timanian and transform faults may, alone, have accommodated the movement of Svalbard from next to Greenland to its present position, c. 400 km away.**

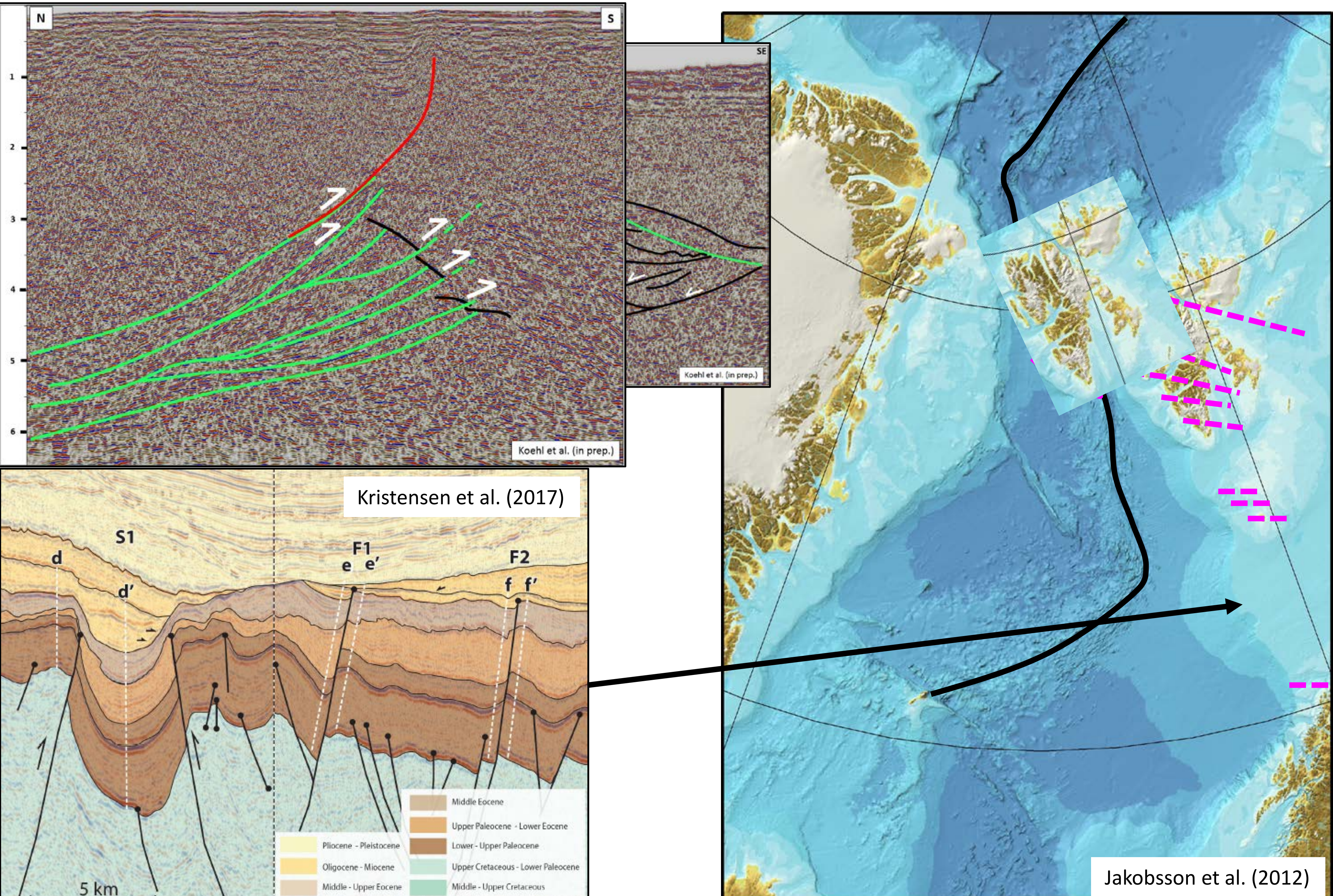

3

WNW–ESE-striking Timanian and transform faults may, alone, have accommodated the movement of Svalbard from next to Greenland to its present position, c. 400 km away.

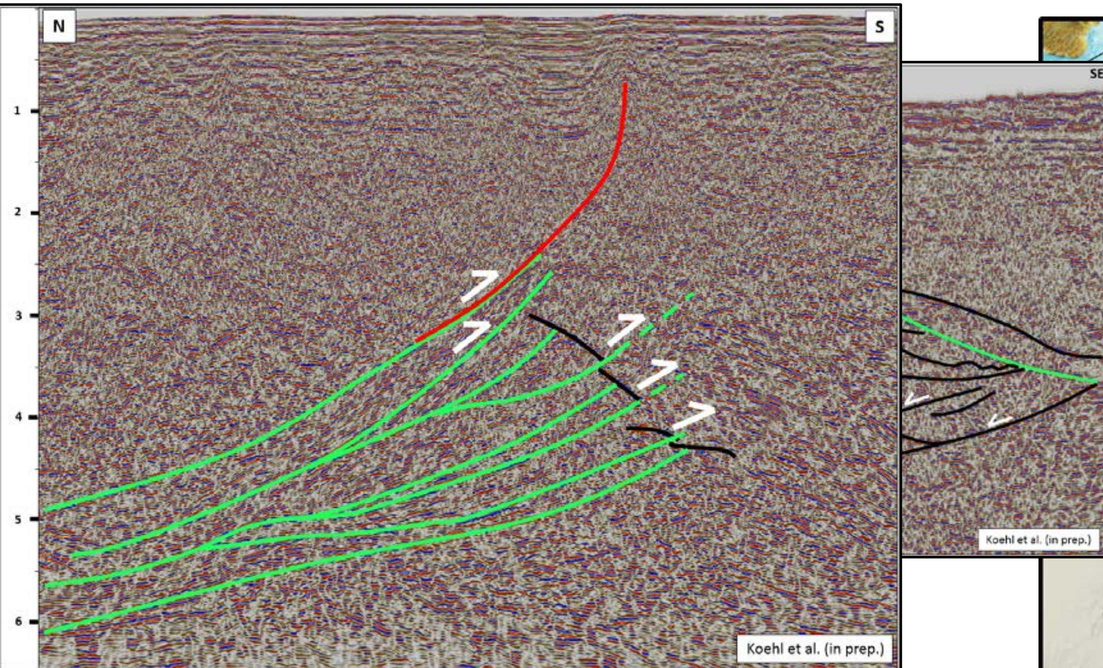

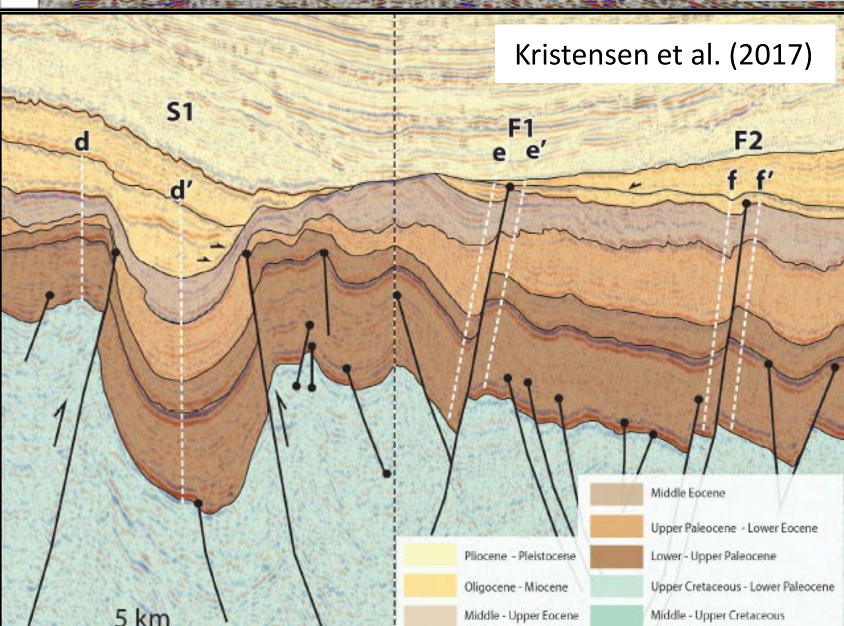

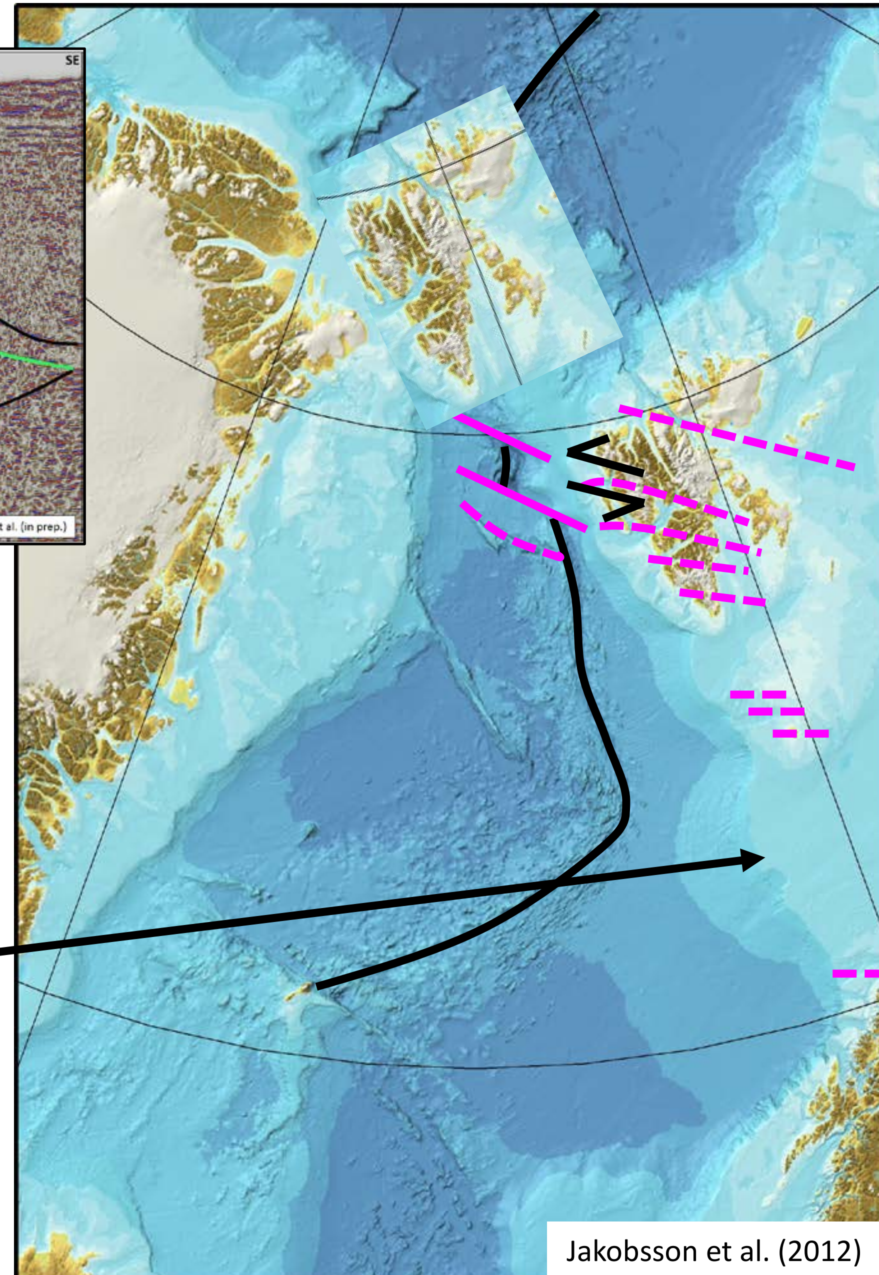

3

Hundreds-of-kilometer dextral displacement along N–S-striking faults (e.g., De Geer Zone) is not required to explain Svalbard's (c. 400 km) southward motion in the Cenozoic.

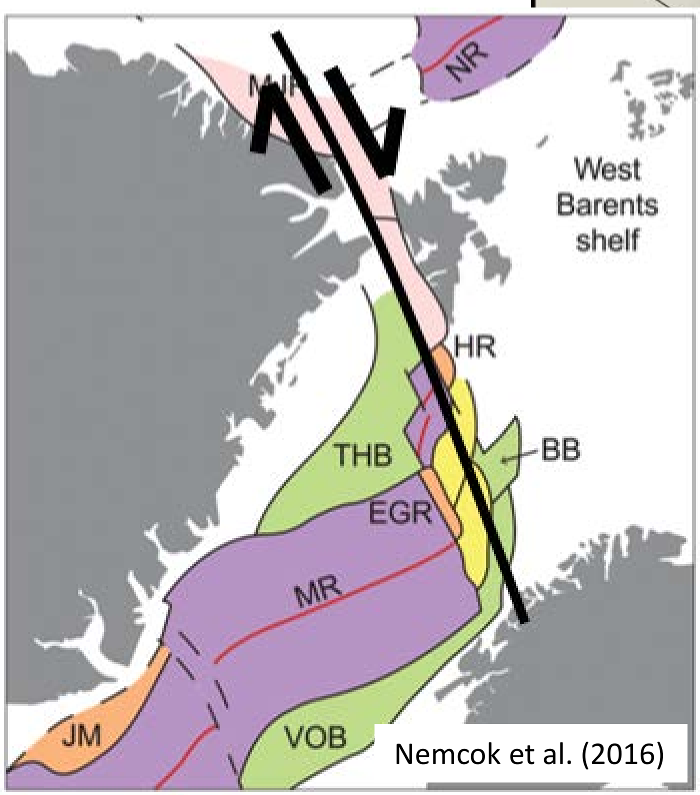

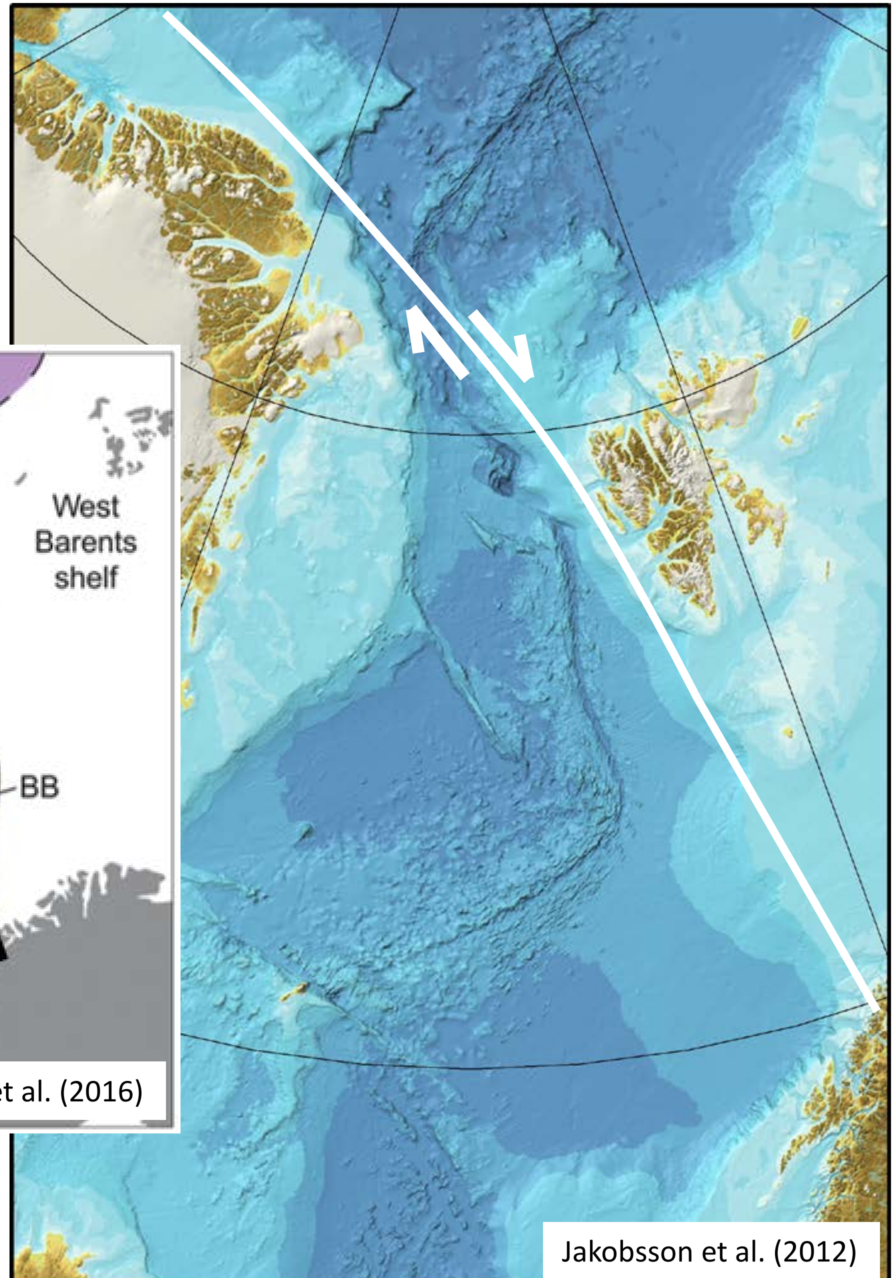

3

Hundreds-of-kilometer dextral displacement along N–S-striking faults (e.g., De Geer Zone) is not required to explain Svalbard's (c. 400 km) southward motion in the Cenozoic.

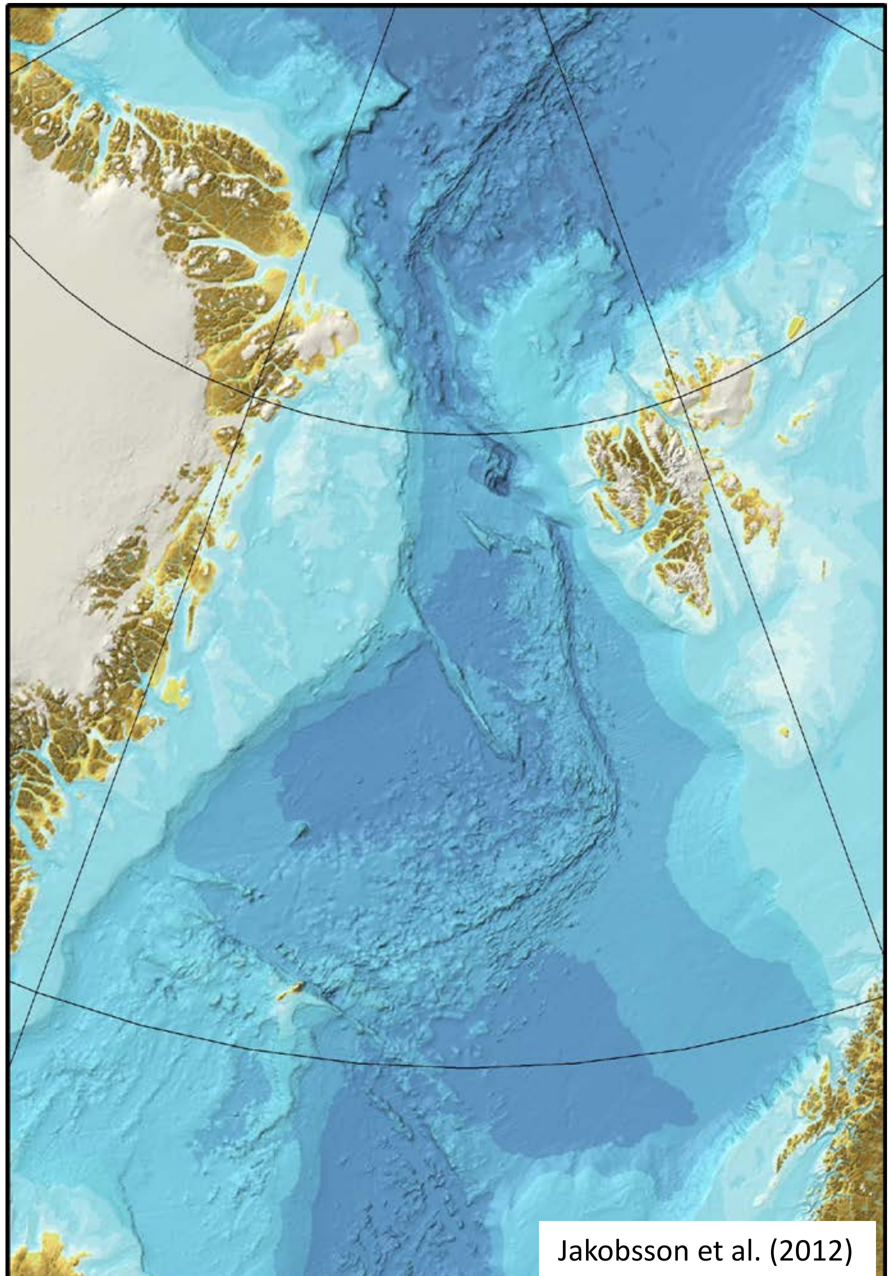

3

Hundreds-of-kilometer dextral displacement along N–S-striking faults (e.g., De Geer Zone) is not required to explain Svalbard's (c. 400 km) southward motion in the Cenozoic.

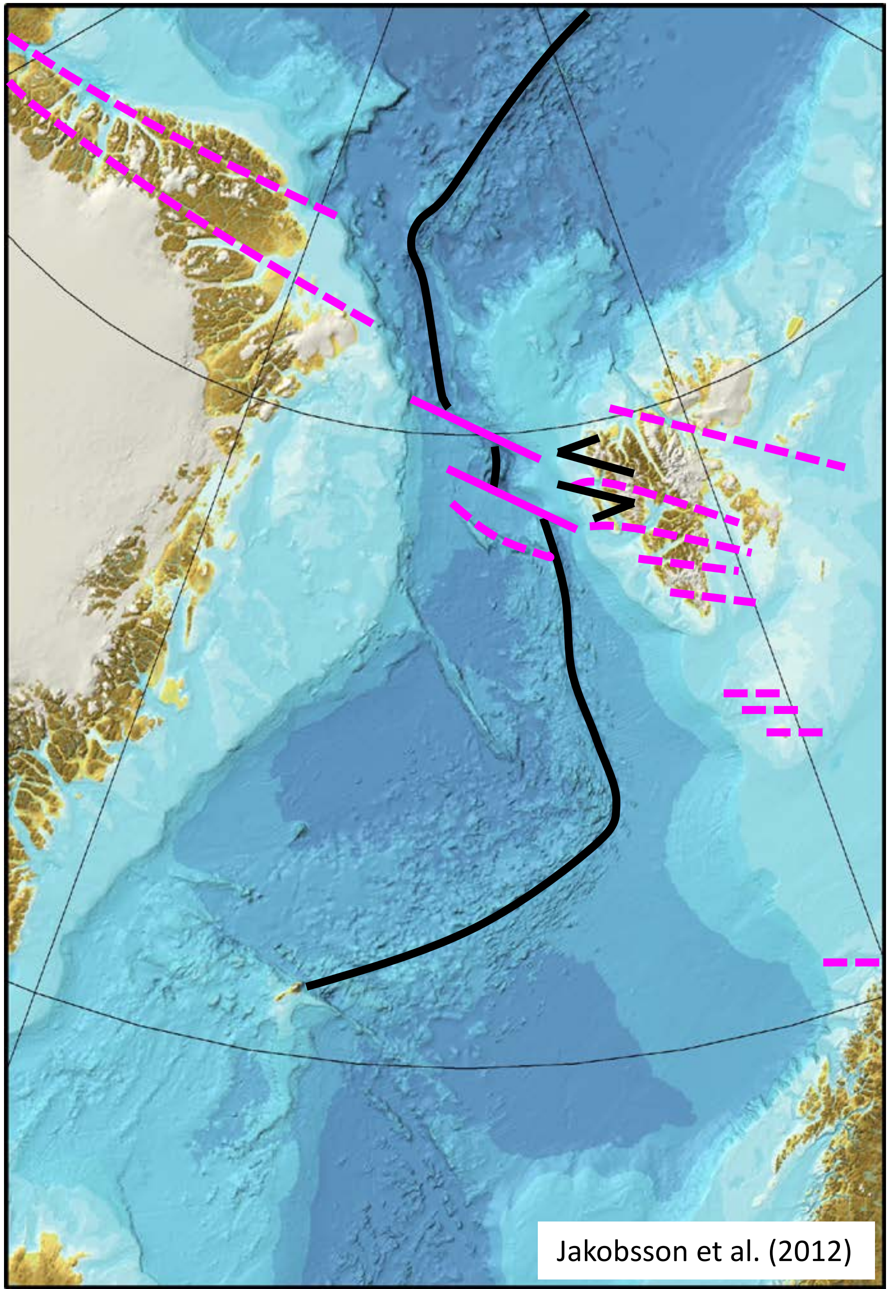

3

Hundreds-of-kilometer dextral displacement along N–S-striking faults (e.g., De Geer Zone) is not required to explain Svalbard's (c. 400 km) southward motion in the Cenozoic.

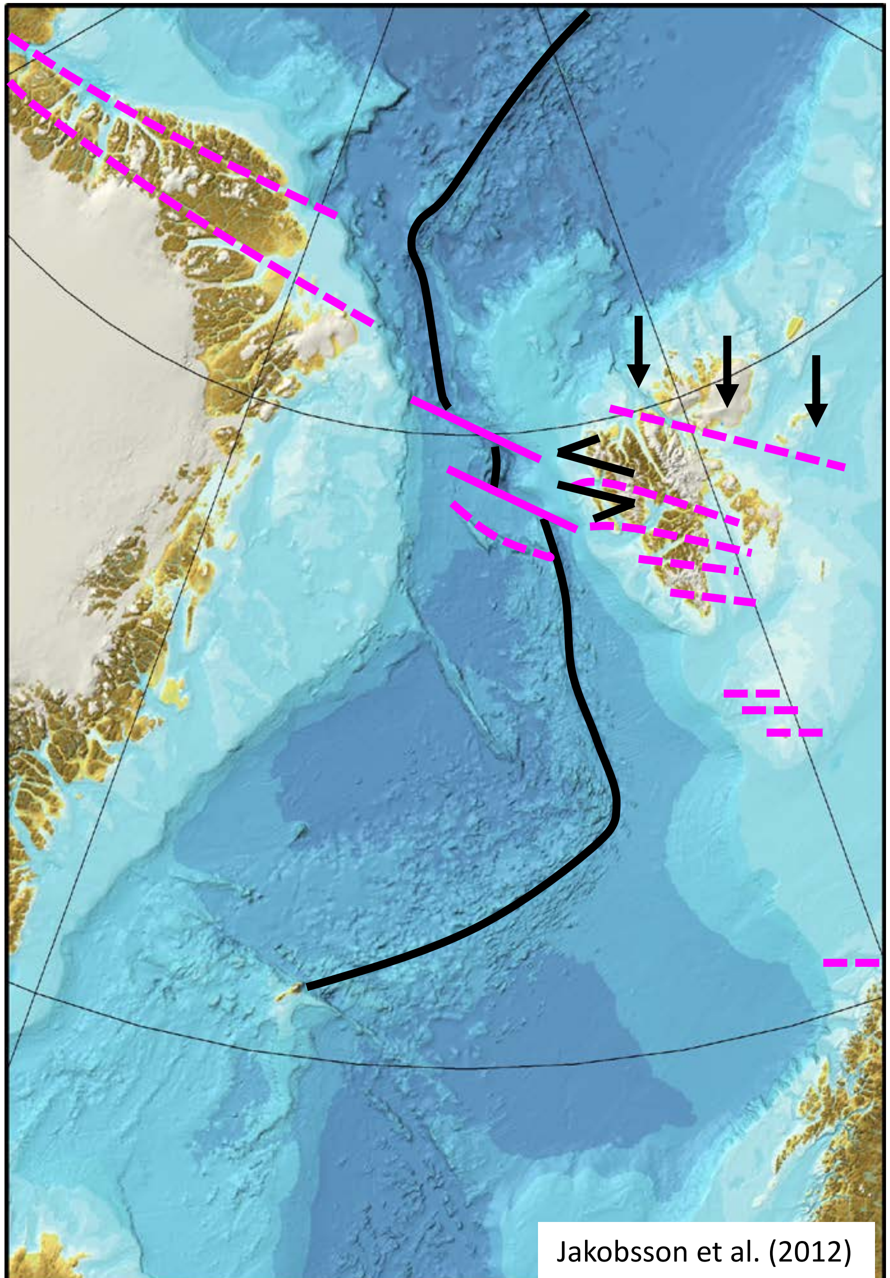

3

Svalbard's three basement terranes were already accreted in the late Neoproterozoic, thus suggesting that Arctic tectonic plates have been much more stable than expected.

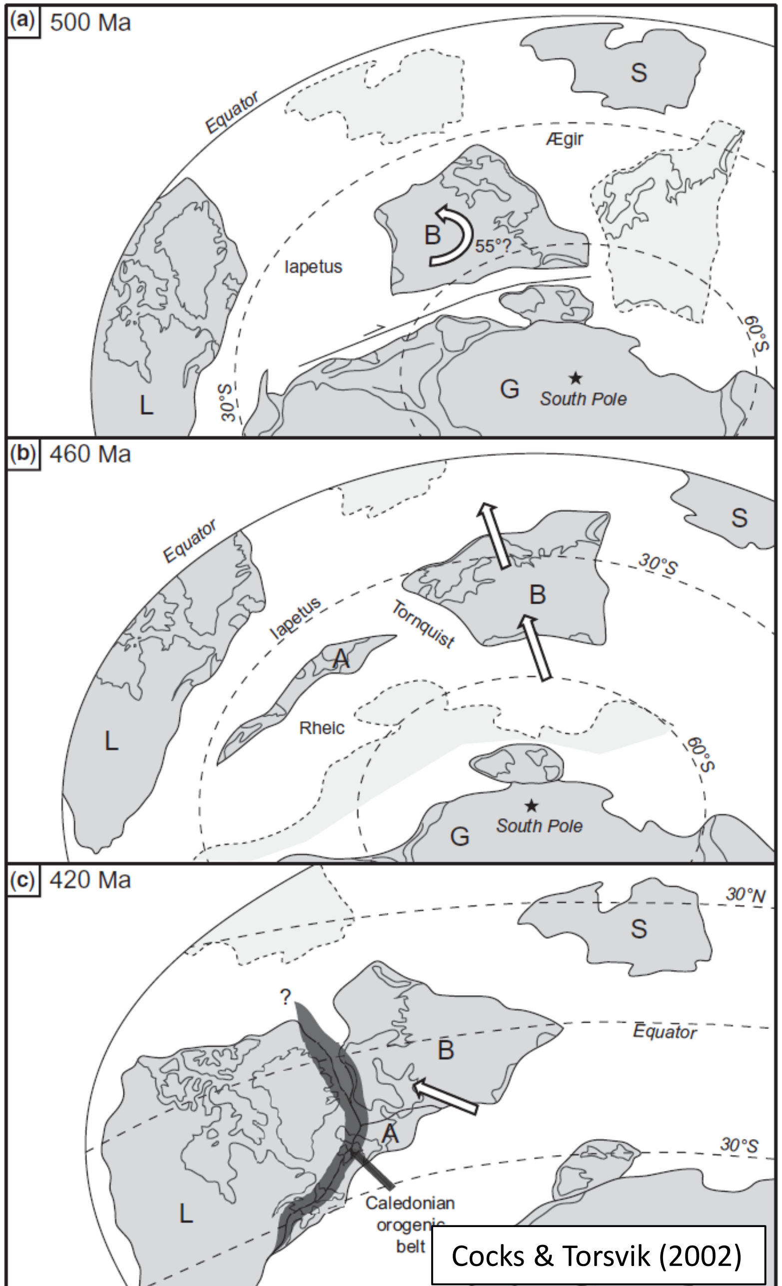

Cocks & Torsvik (2002)

3

Svalbard's three basement terranes were already accreted in the late Neoproterozoic, thus suggesting that Arctic tectonic plates have been much more stable than expected.

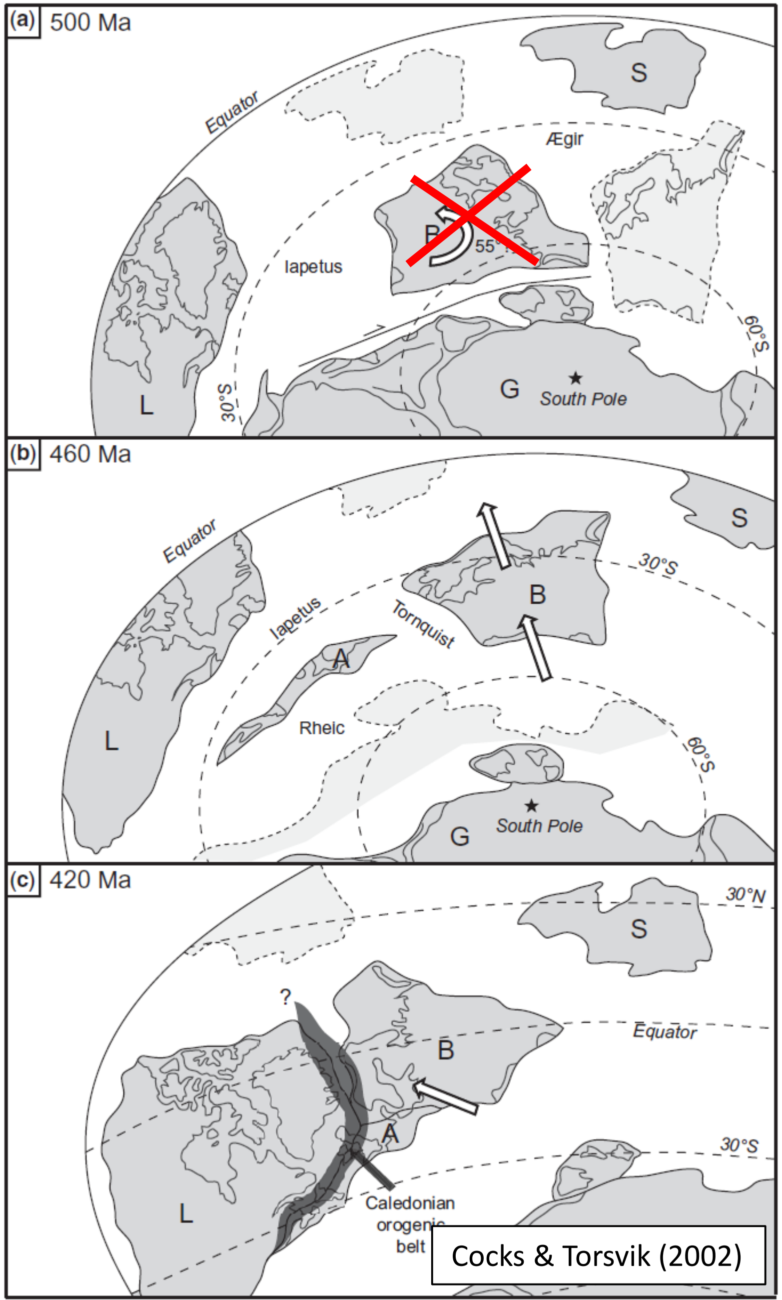

Cocks & Torsvik (2002)

3

Svalbard's three basement terranes were already accreted in the late Neoproterozoic, thus suggesting that Arctic tectonic plates have been much more stable than expected.

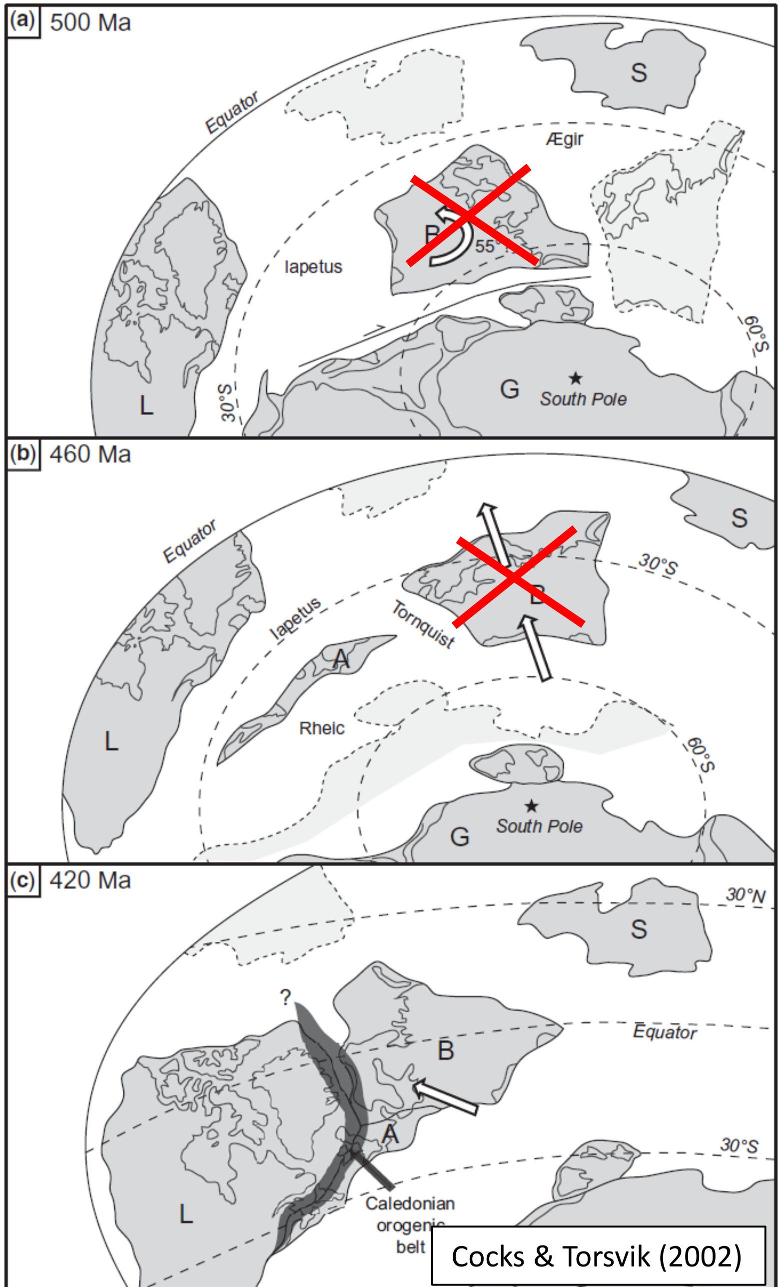

Cocks & Torsvik (2002)

3

Svalbard's three basement terranes were already accreted in the late Neoproterozoic, thus suggesting that Arctic tectonic plates have been much more stable than expected.

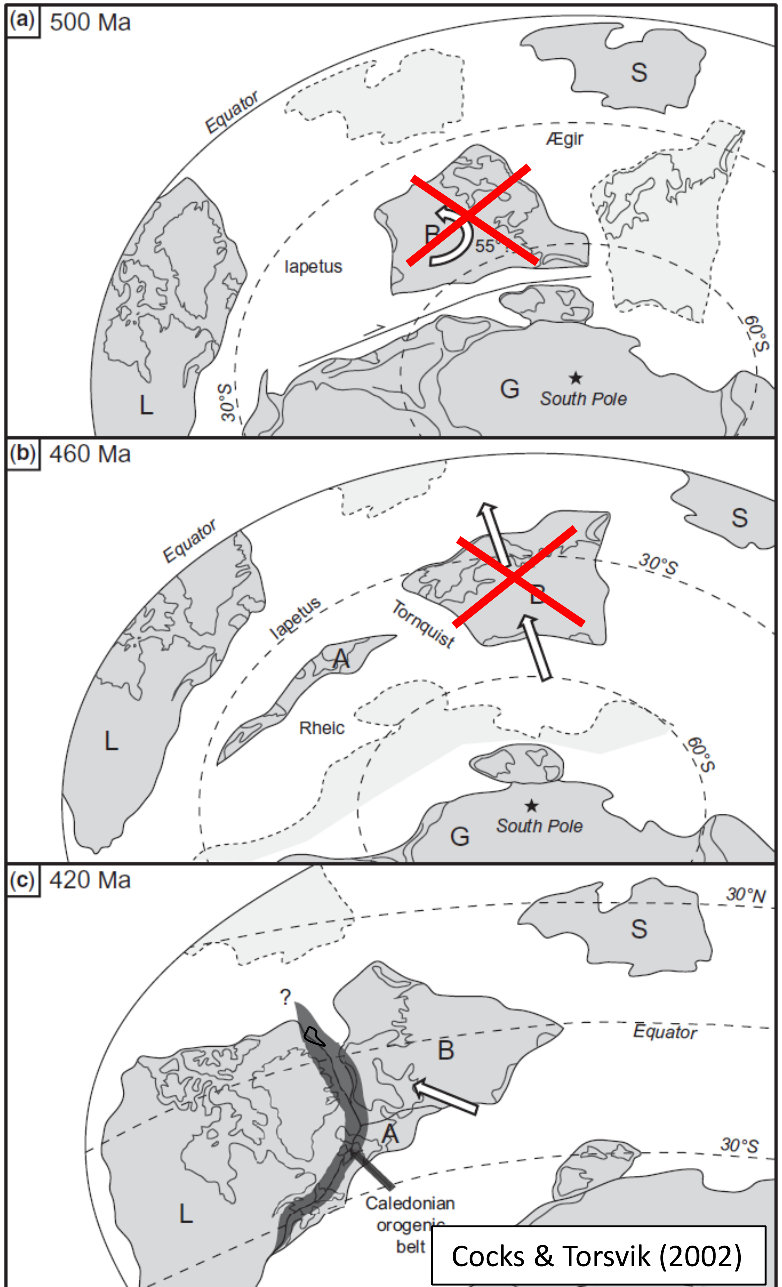

Cocks & Torsvik (2002)

3

Svalbard's three basement terranes were already accreted in the late Neoproterozoic, thus suggesting that Arctic tectonic plates have been much more stable than expected.

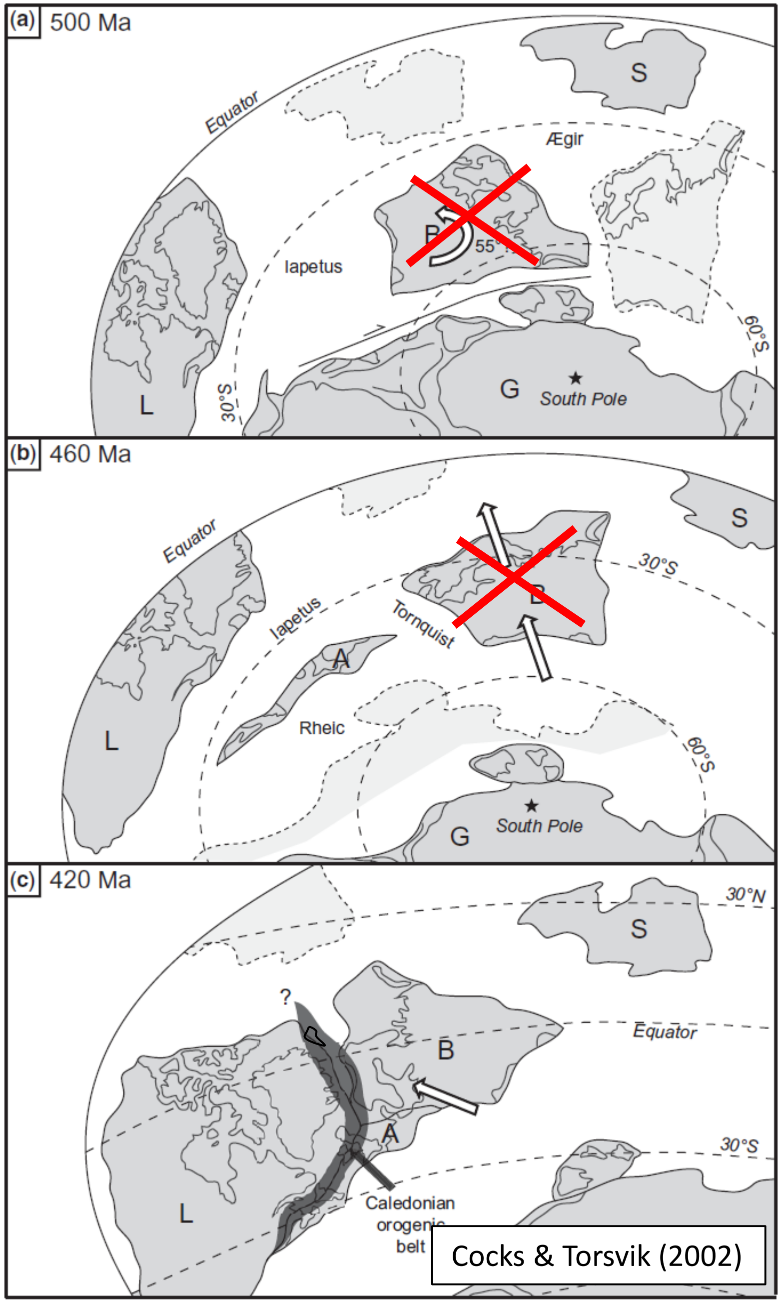

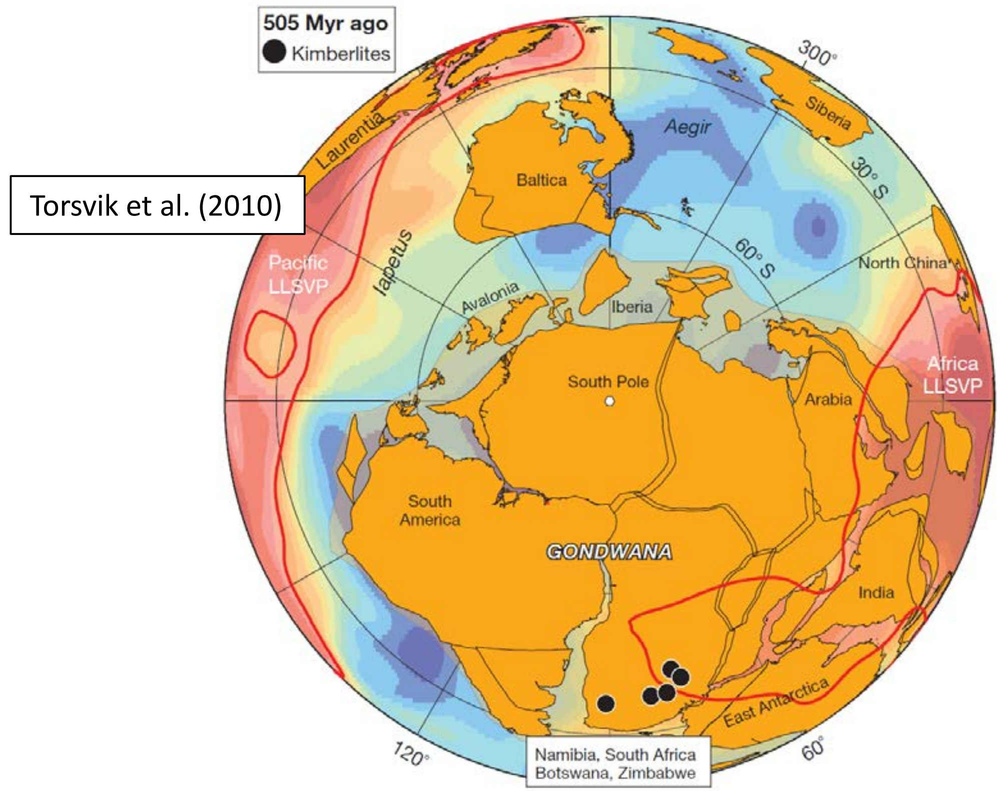

3 **Svalbard’s three basement terranes were already accreted in the late Neoproterozoic, thus suggesting that Arctic tectonic plates have been much more stable than expected.**

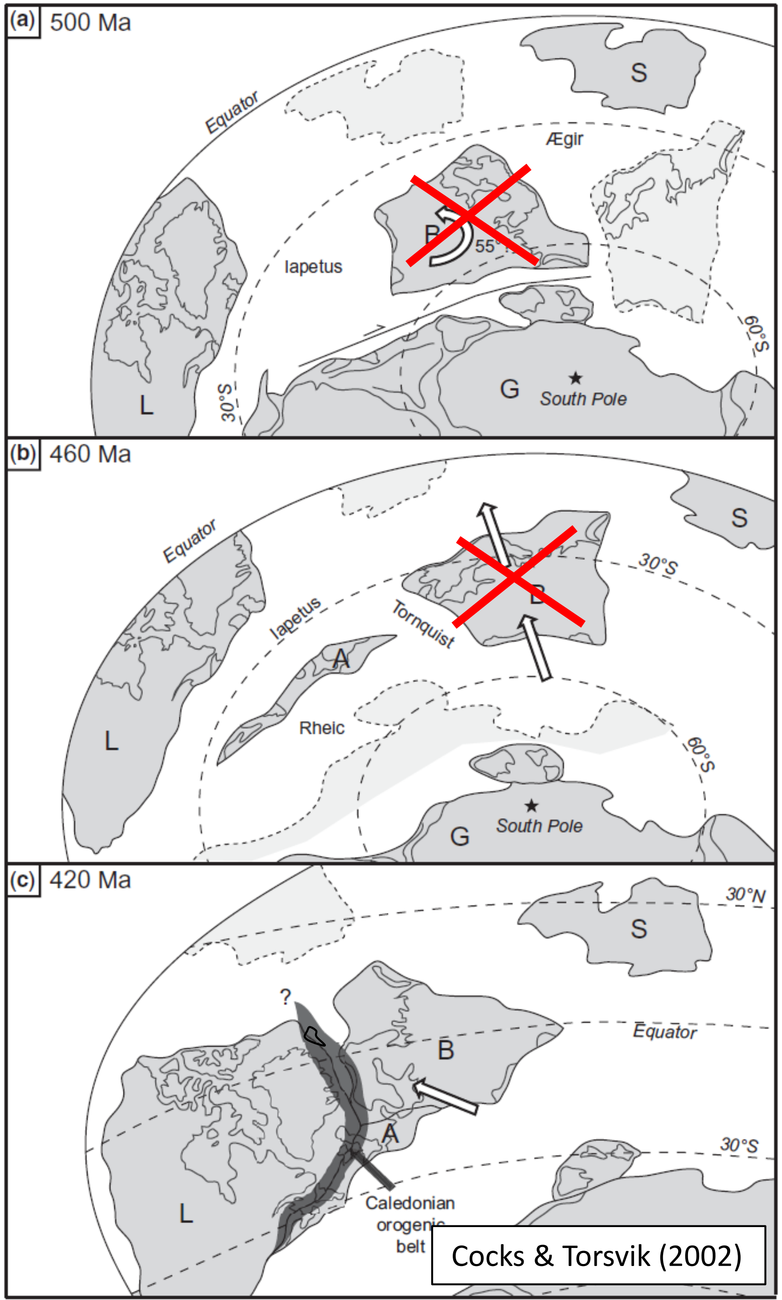

Cocks & Torsvik (2002)

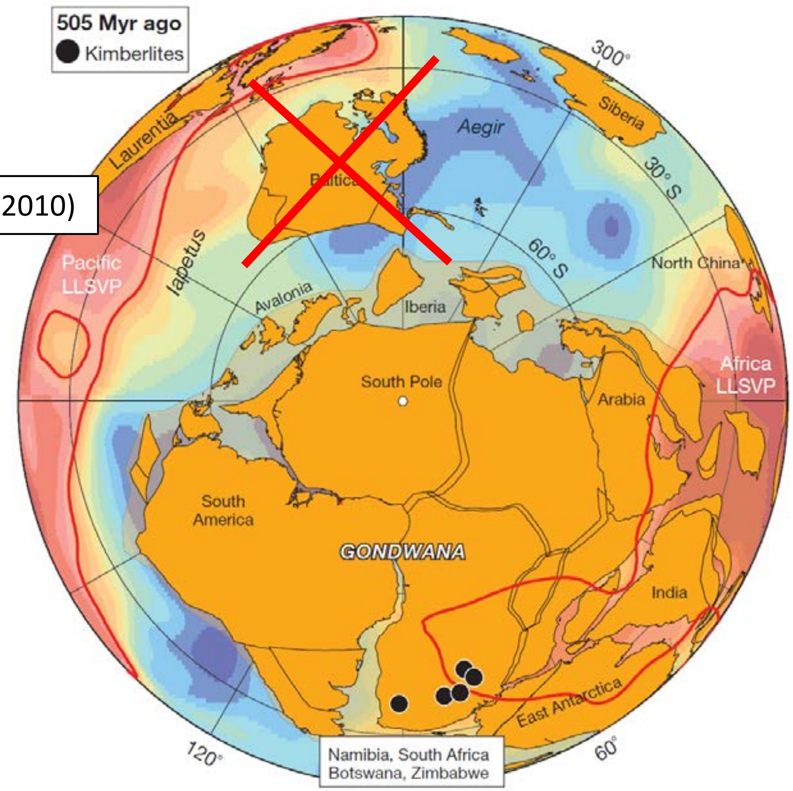

Torsvik et al. (2010)

3

Svalbard's three basement terranes were already accreted in the late Neoproterozoic, thus suggesting that Arctic tectonic plates have been much more stable than expected.

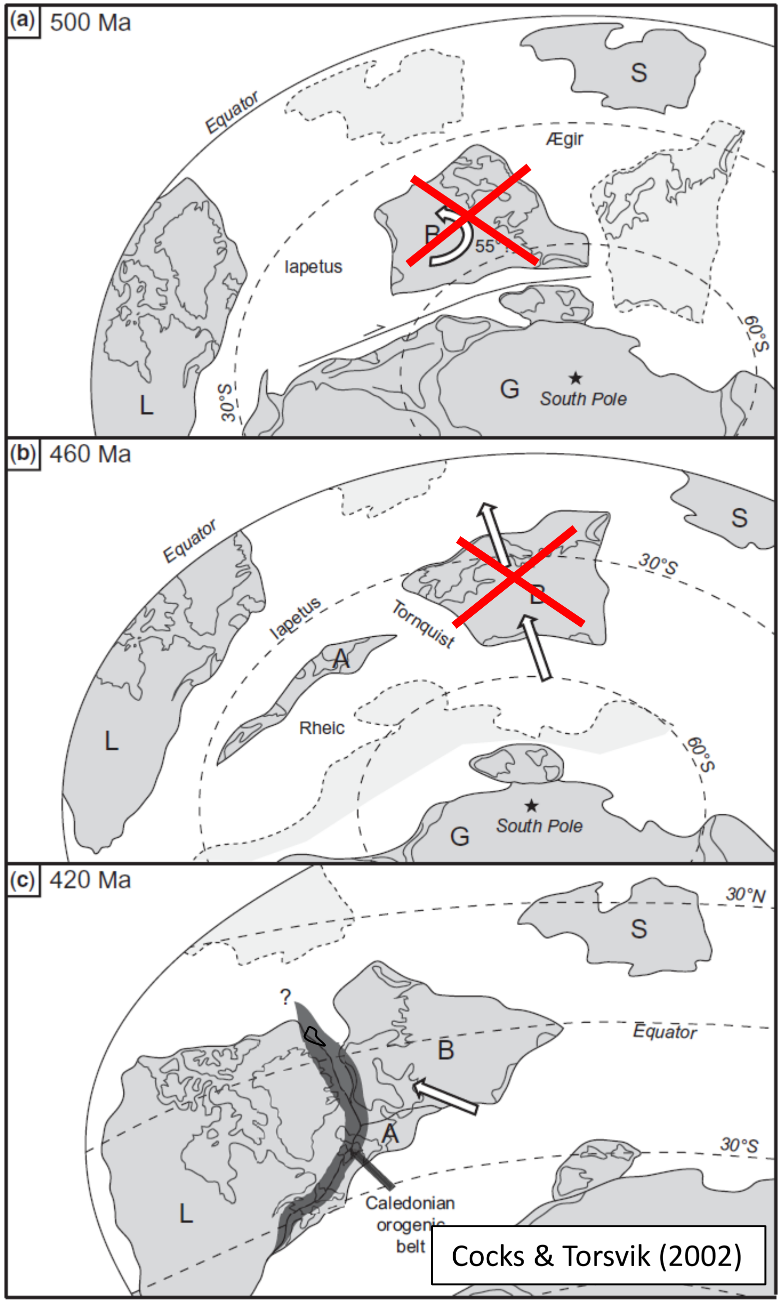

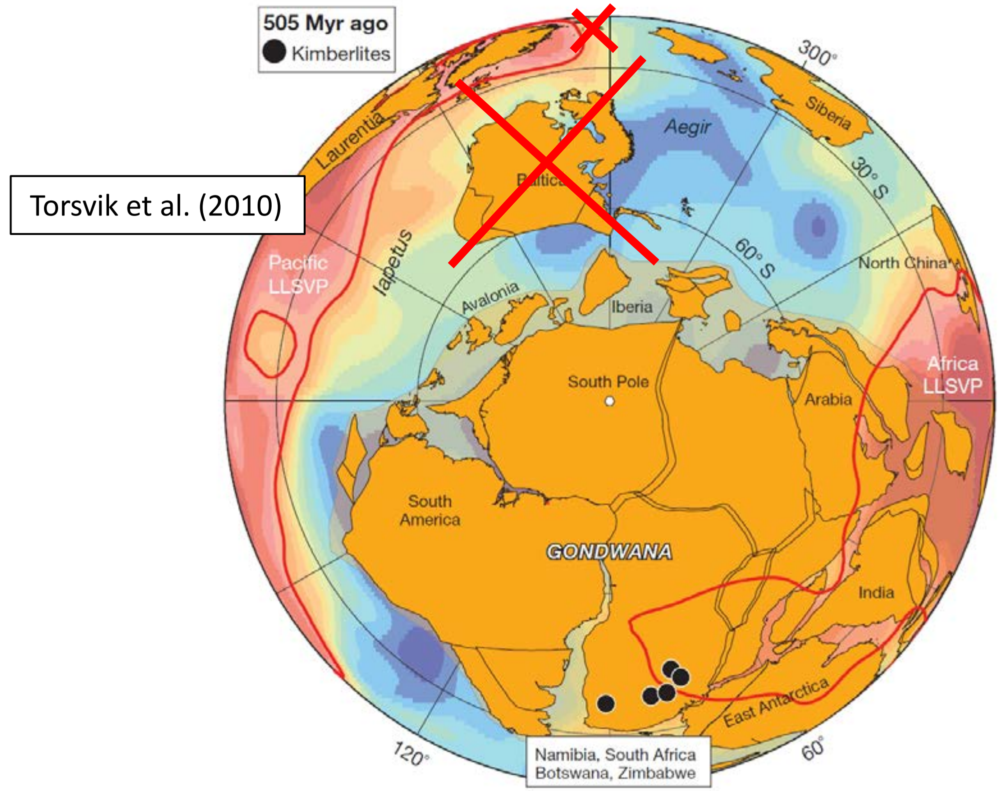

3 **Svalbard's three basement terranes were already accreted in the late Neoproterozoic, thus suggesting that Arctic tectonic plates have been much more stable than expected.**

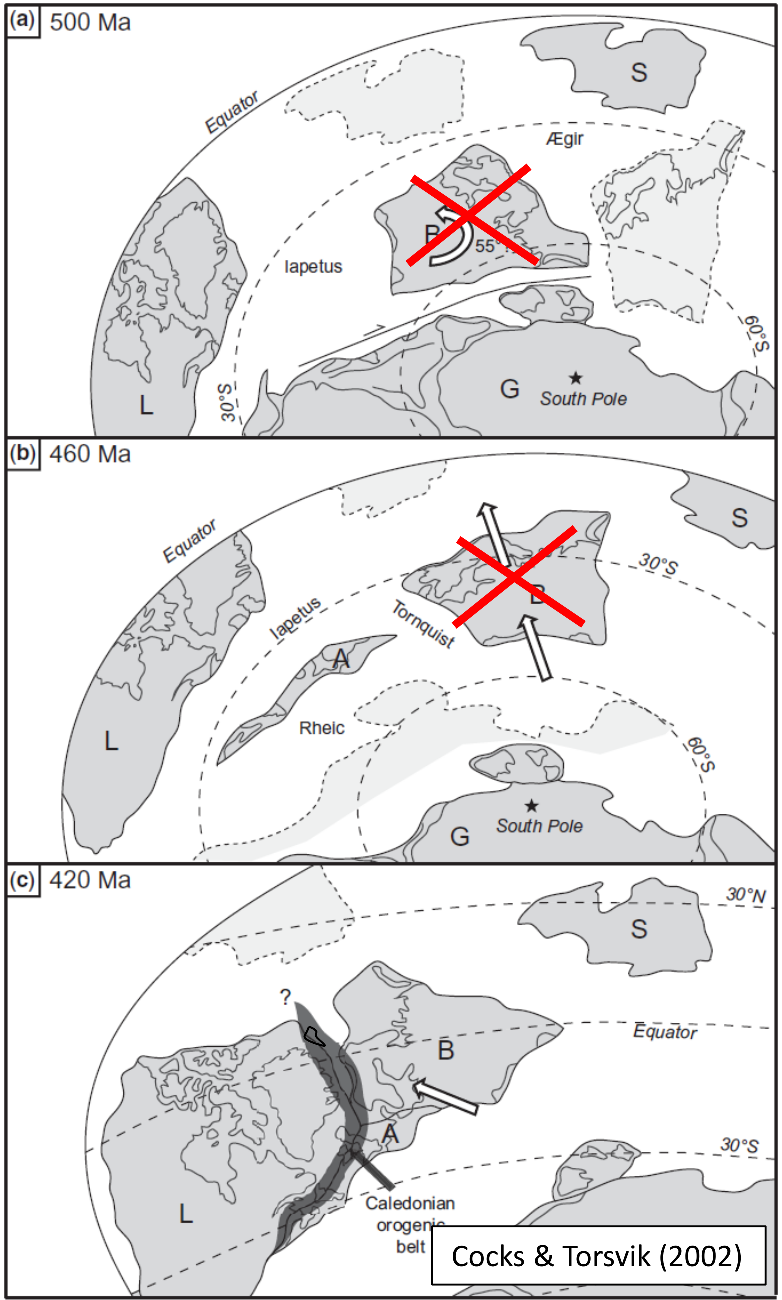

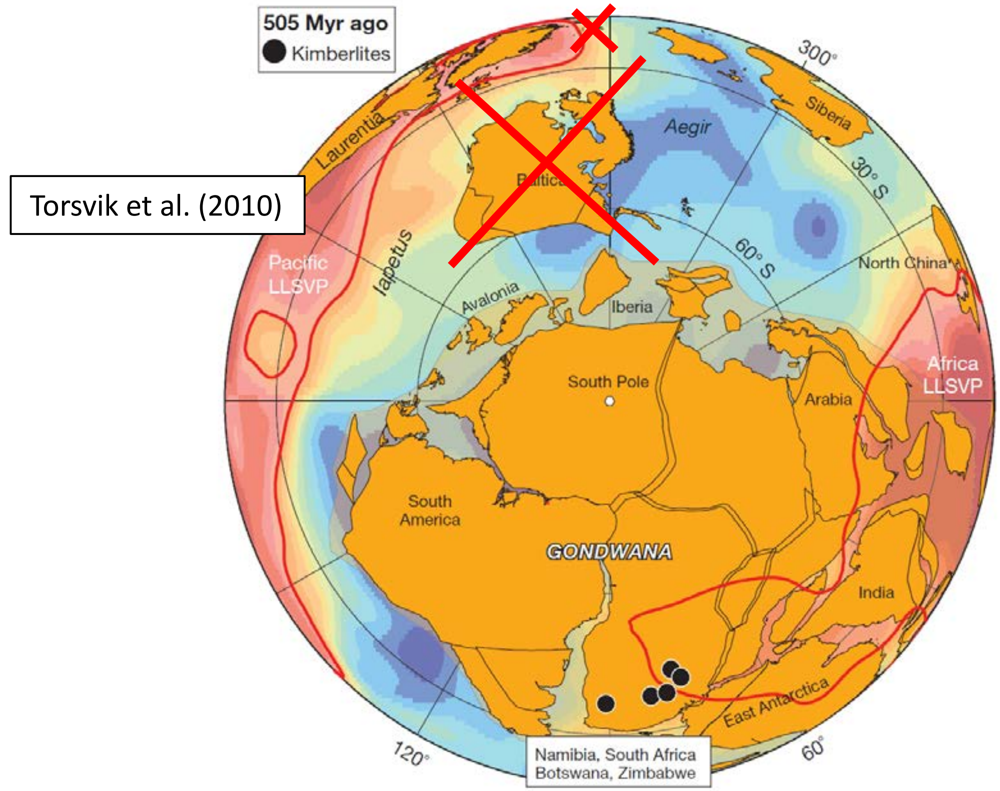

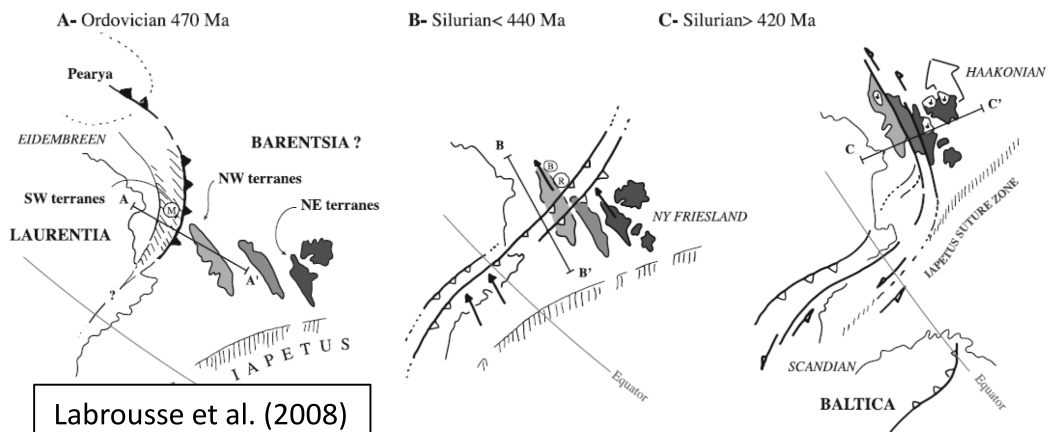

3

Svalbard's three basement terranes were already accreted in the late Neoproterozoic, thus suggesting that Arctic tectonic plates have been much more stable than expected.

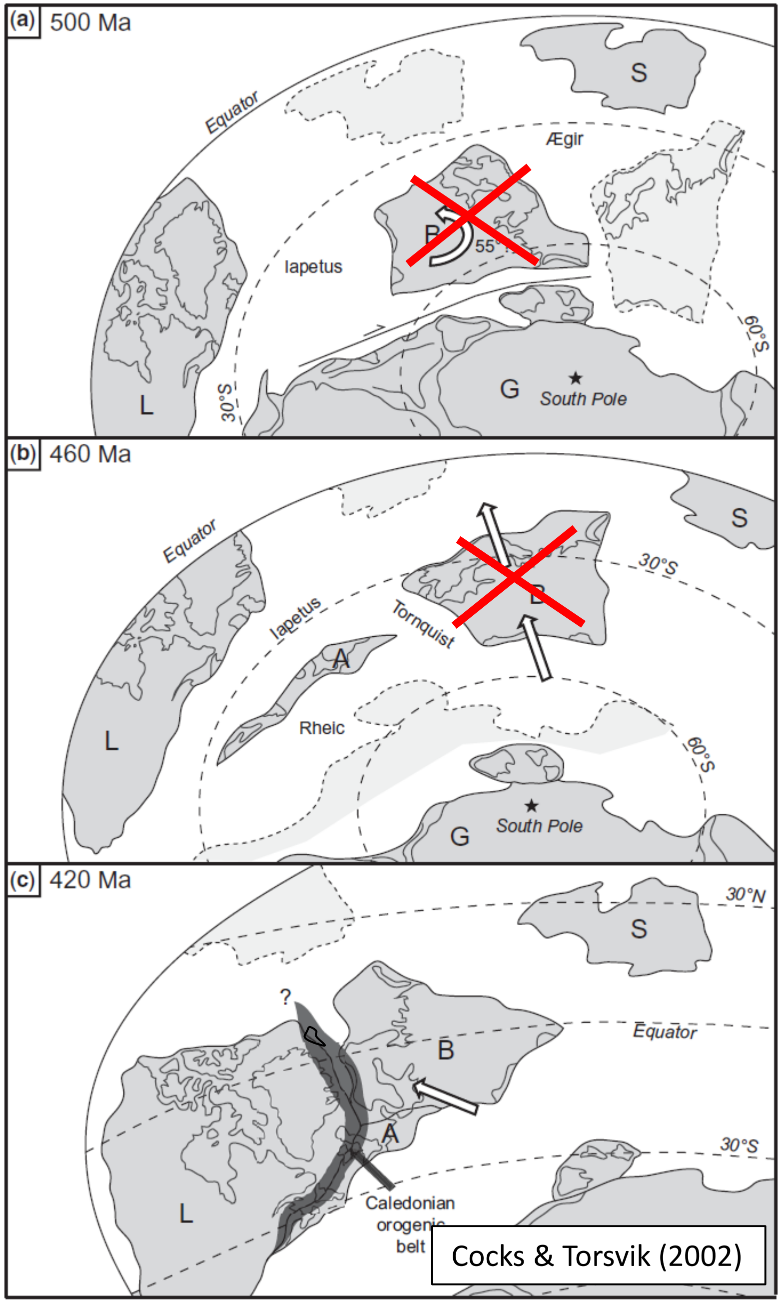

Torsvik et al. (2010)

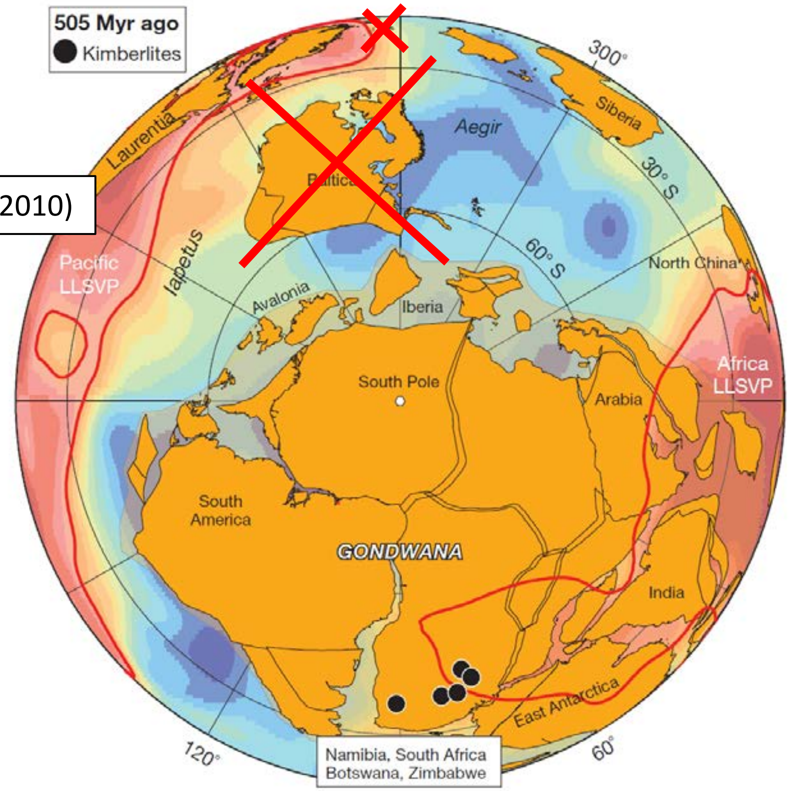

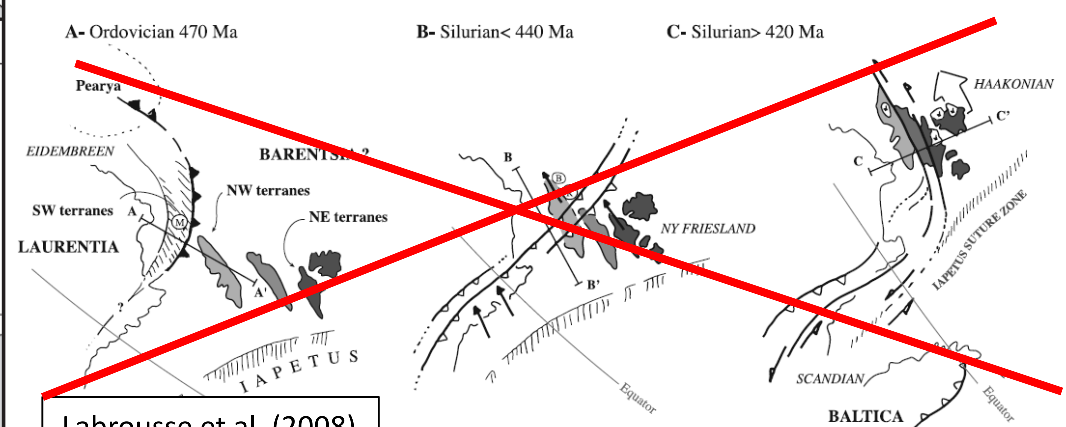

Labrousse et al. (2008)

3 **Svalbard's three basement terranes were already accreted in the late Neoproterozoic, thus suggesting that Arctic tectonic plates have been much more stable than expected.**

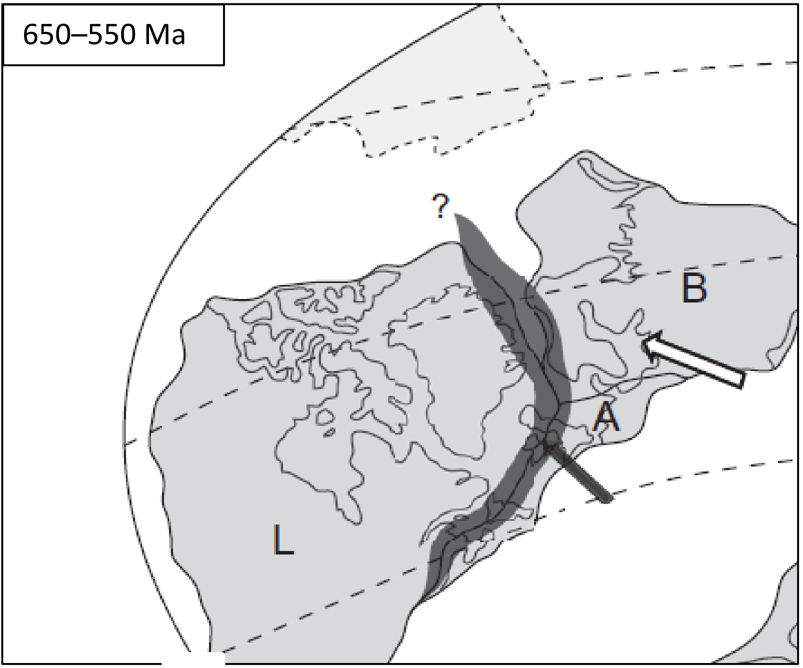

Modified after Cocks & Torsvik (2002)

3

Svalbard's three basement terranes were already accreted in the late Neoproterozoic, thus suggesting that Arctic tectonic plates have been much more stable than expected.

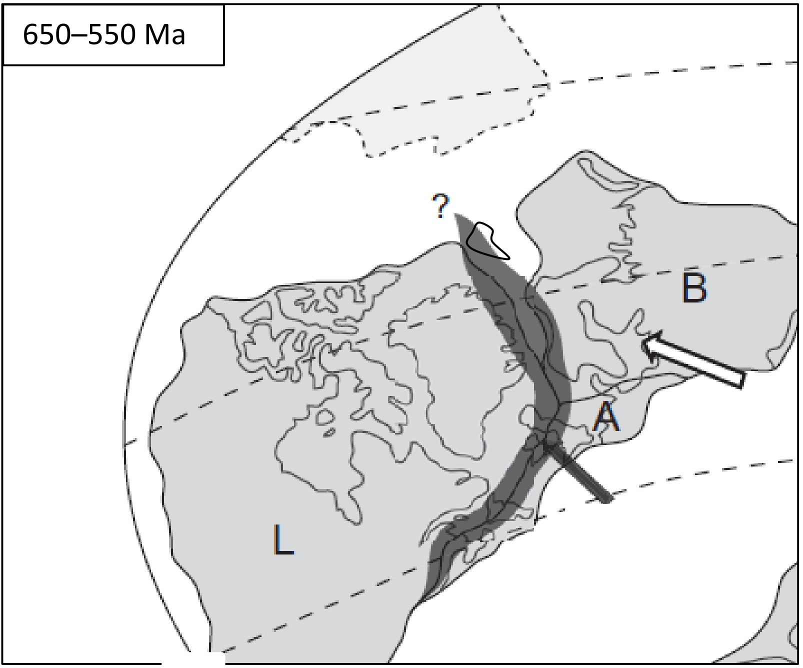

Modified after Cocks & Torsvik (2002)

3 **Svalbard's three basement terranes were already accreted in the late Neoproterozoic, thus suggesting that Arctic tectonic plates have been much more stable than expected.**

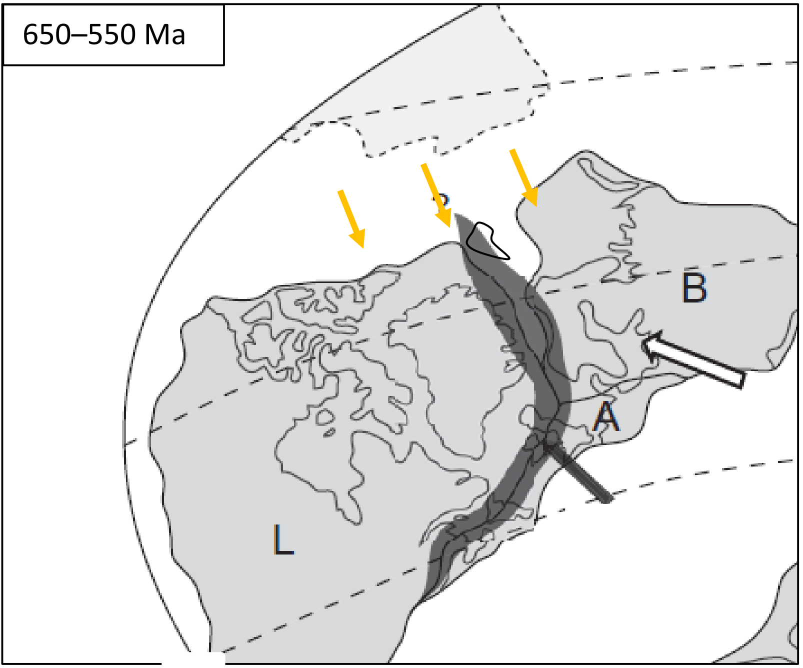

Modified after Cocks & Torsvik (2002)

3 **Svalbard's three basement terranes were already accreted in the late Neoproterozoic, thus suggesting that Arctic tectonic plates have been much more stable than expected.**

650–550 Ma

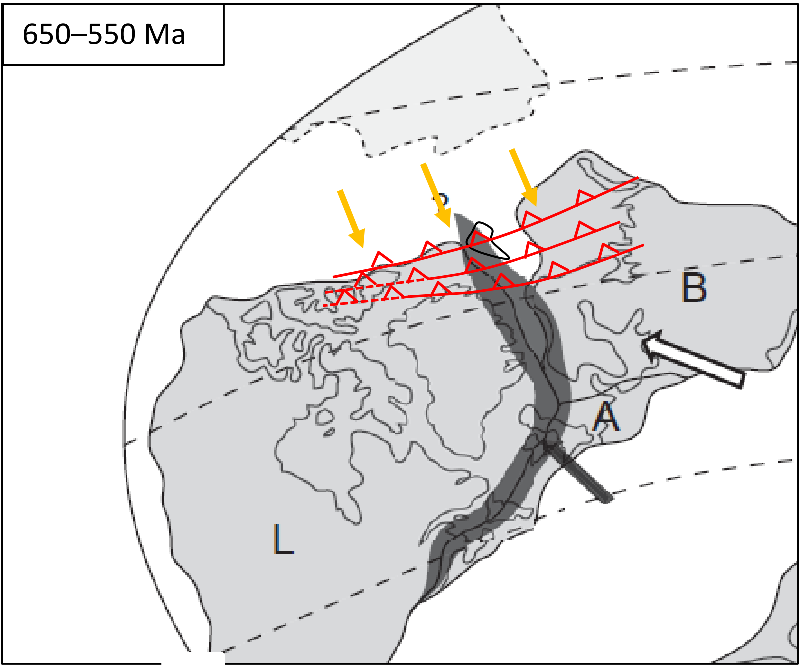

Modified after Cocks & Torsvik (2002)

3

Svalbard's three basement terranes were already accreted in the late Neoproterozoic, thus suggesting that Arctic tectonic plates have been much more stable than expected.

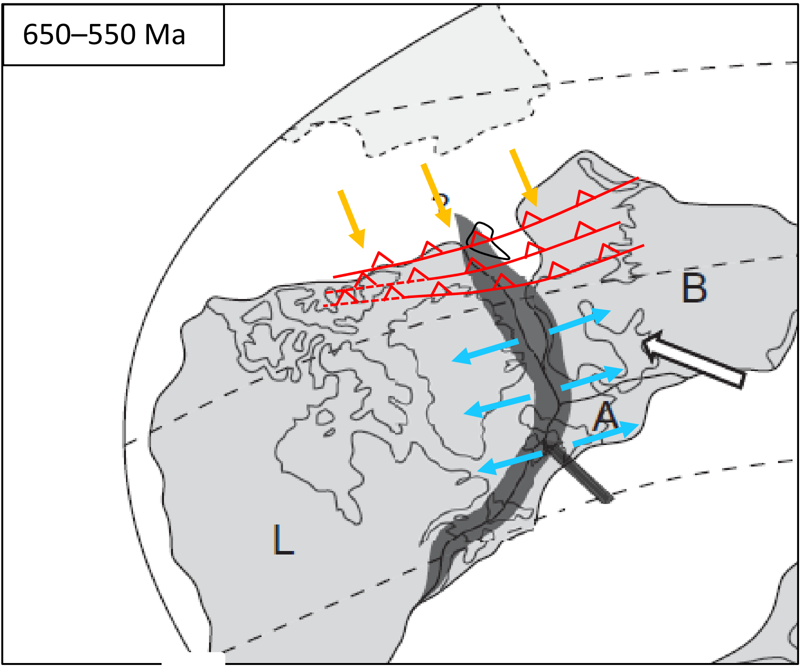

Modified after Cocks & Torsvik (2002)

3

Svalbard's three basement terranes were already accreted in the late Neoproterozoic, thus suggesting that Arctic tectonic plates have been much more stable than expected.

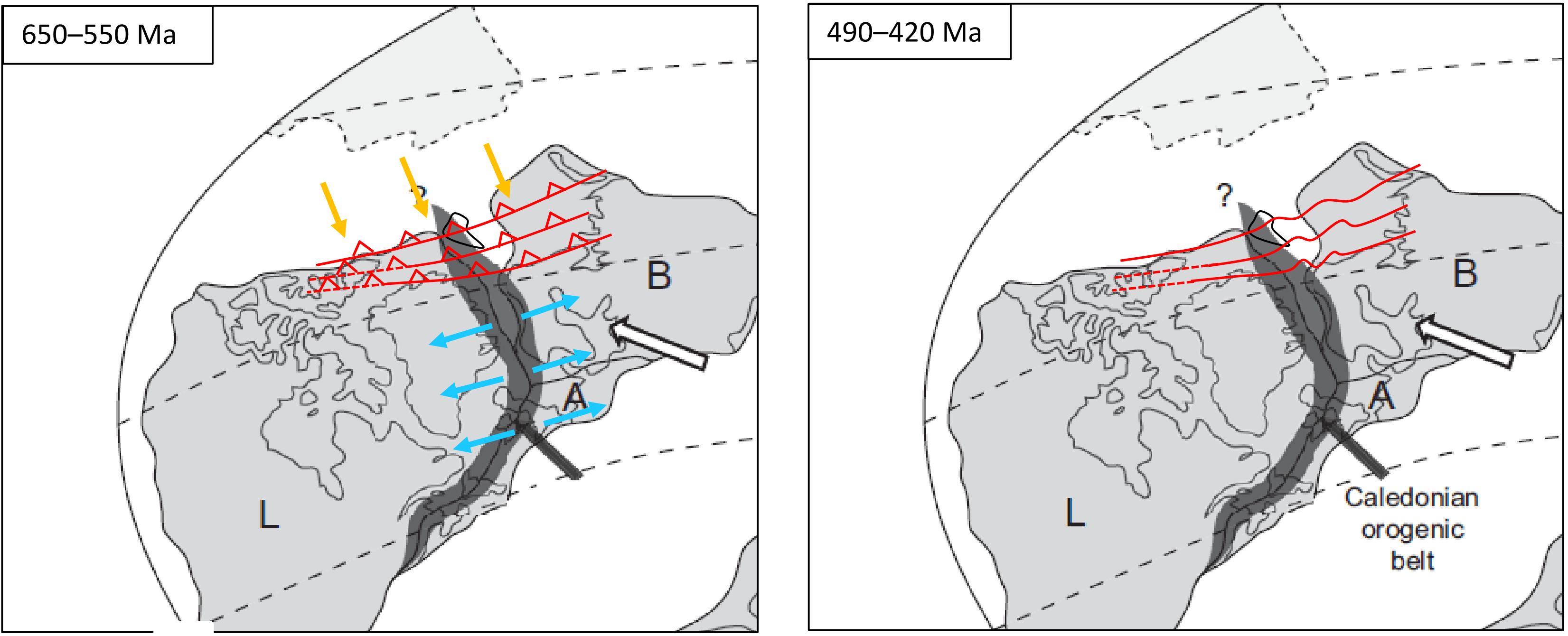

Modified after Cocks & Torsvik (2002)

3

Svalbard's three basement terranes were already accreted in the late Neoproterozoic, thus suggesting that Arctic tectonic plates have been much more stable than expected.

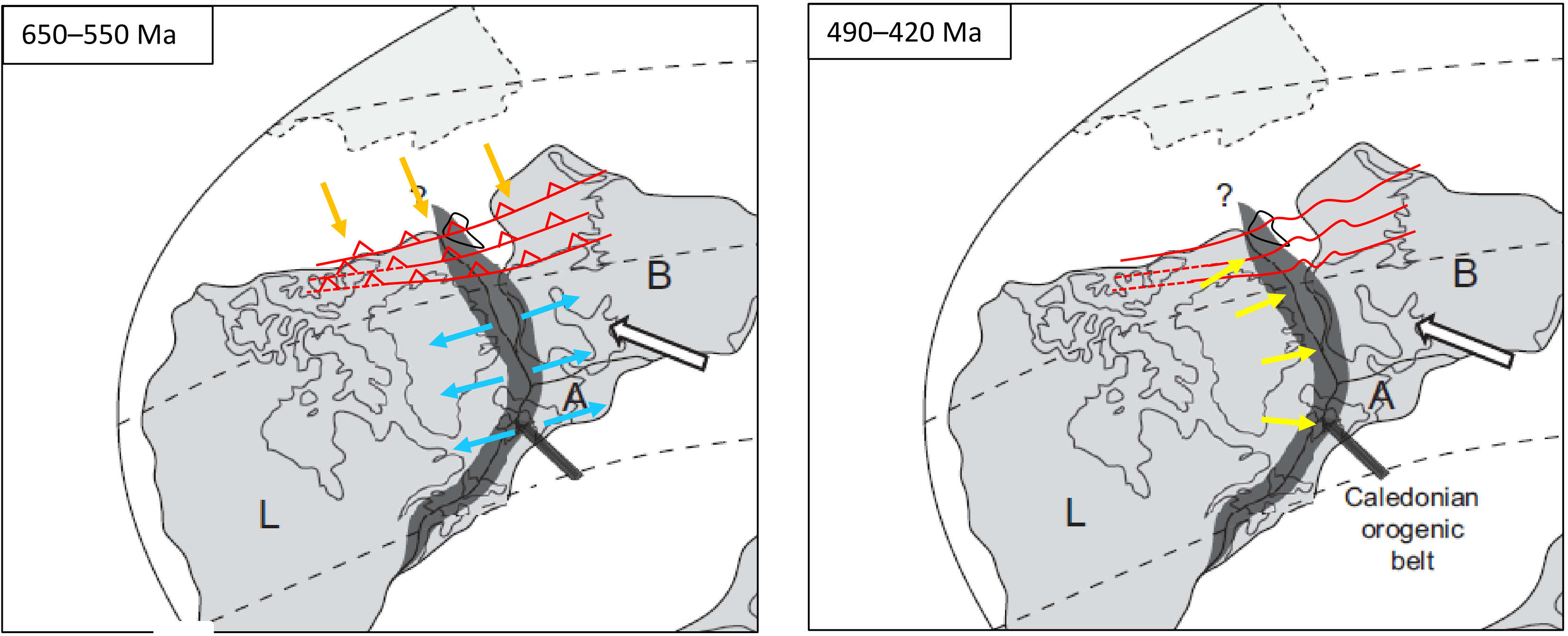

Modified after Cocks & Torsvik (2002)

3 **Svalbard's three basement terranes were already accreted in the late Neoproterozoic, thus suggesting that Arctic tectonic plates have been much more stable than expected.**

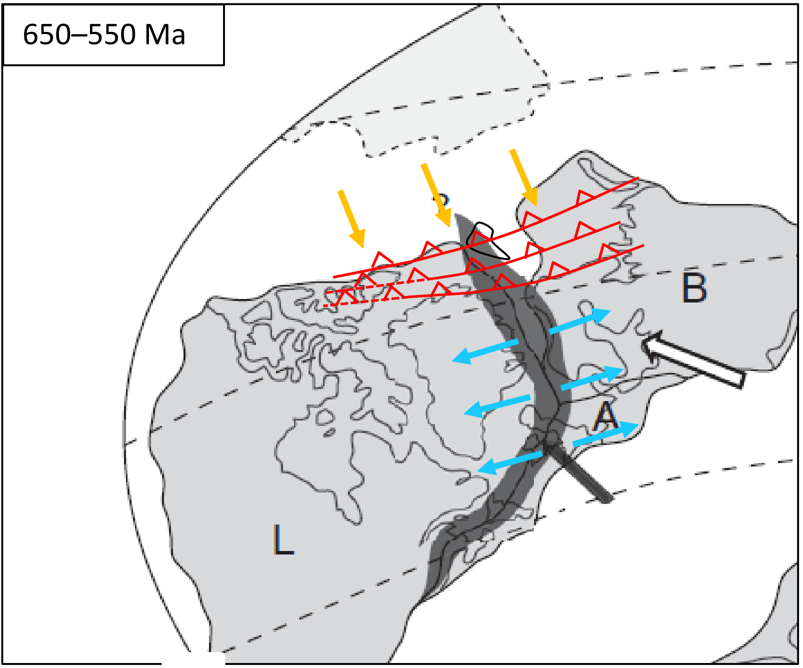

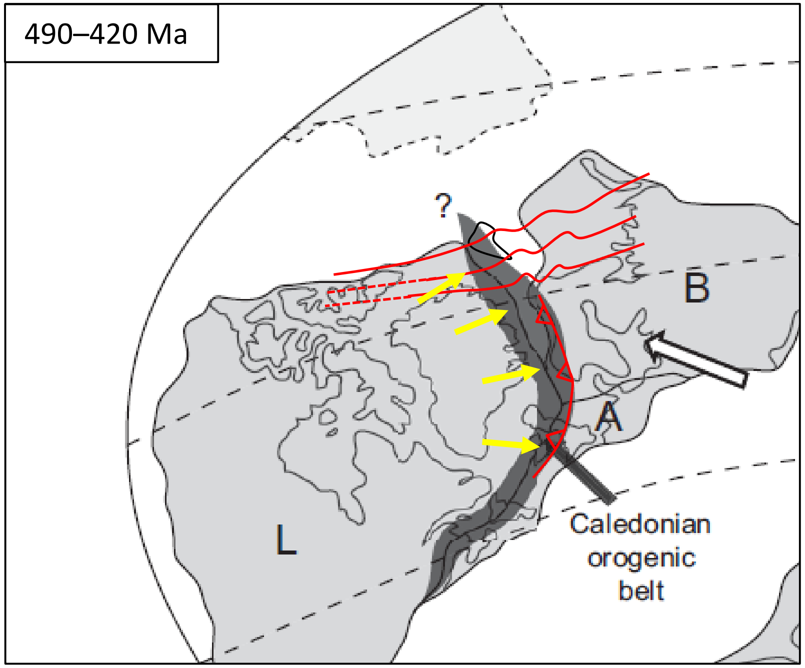

Modified after Cocks & Torsvik (2002)

3 Svalbard's three basement terranes were already accreted in the late Neoproterozoic, thus suggesting that Arctic tectonic plates have been much more stable than expected.

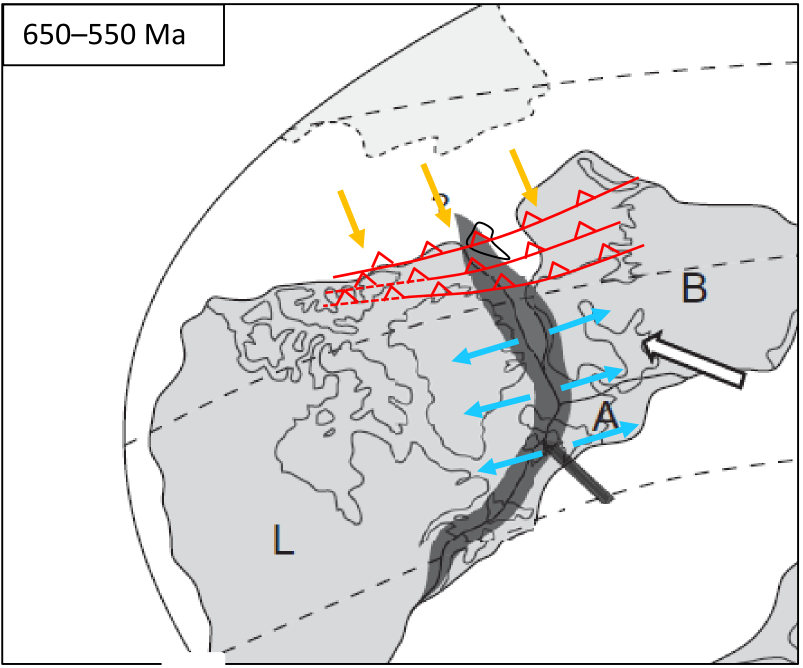

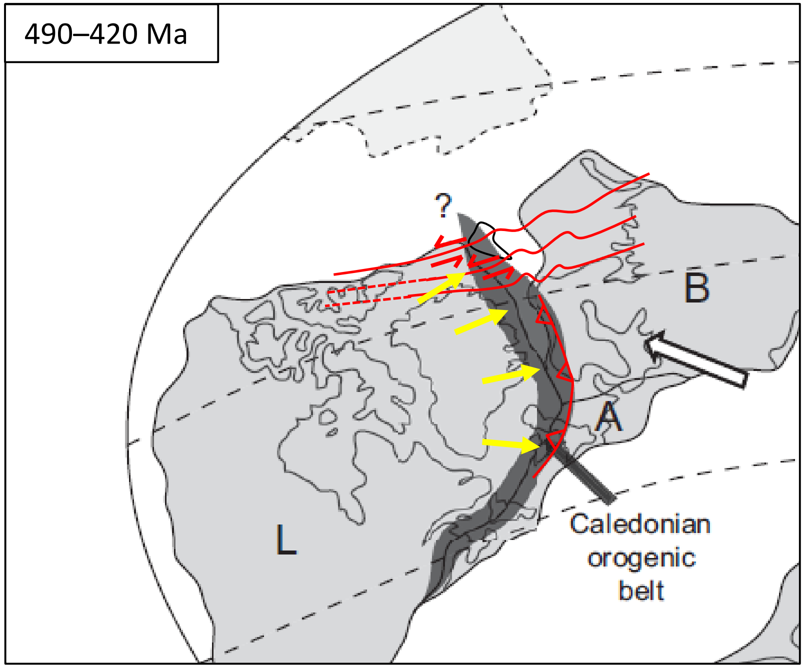

Modified after Cocks & Torsvik (2002)

3 Svalbard's three basement terranes were already accreted in the late Neoproterozoic, thus suggesting that Arctic tectonic plates have been much more stable than expected.

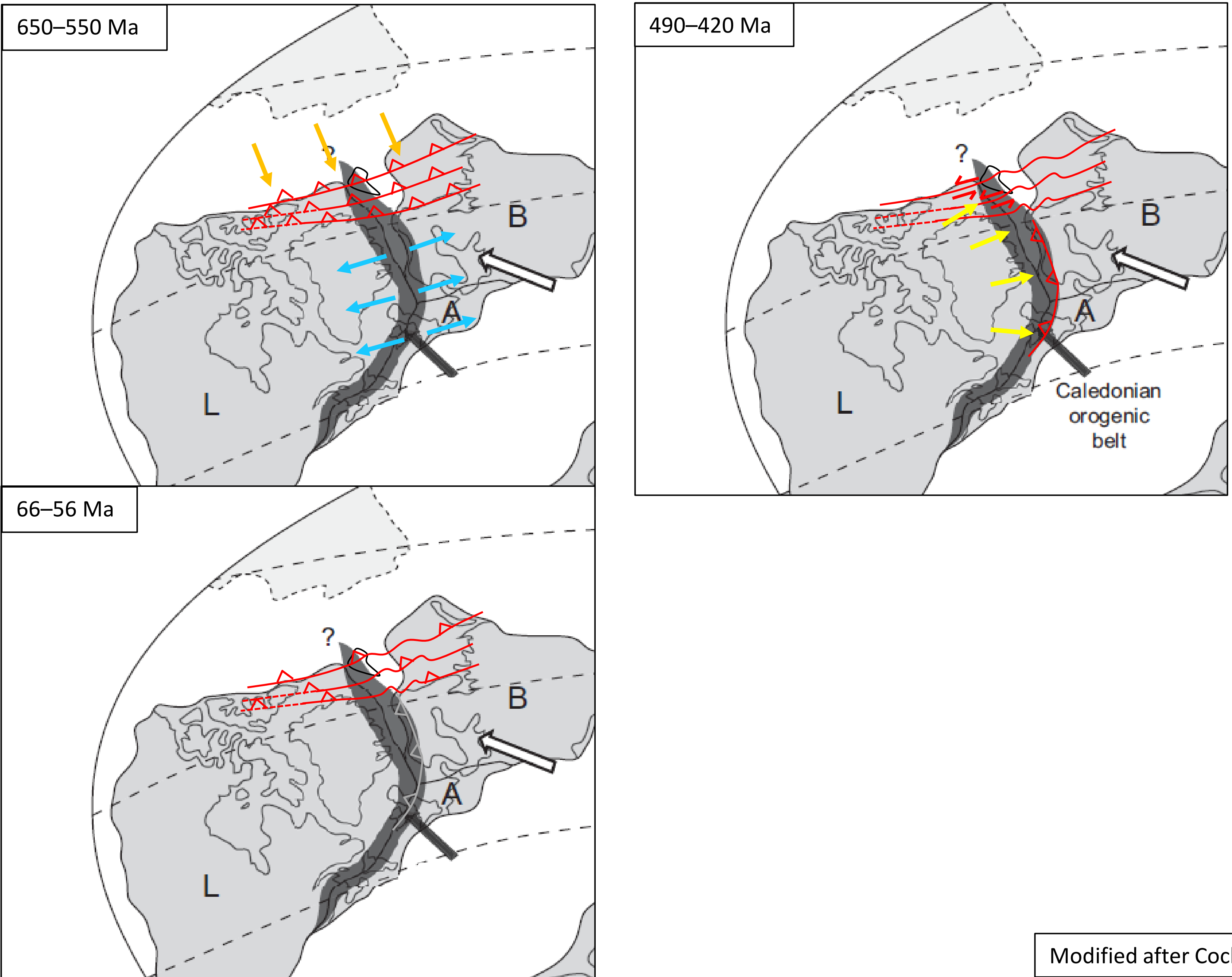

Modified after Cocks & Torsvik (2002)

3 **Svalbard's three basement terranes were already accreted in the late Neoproterozoic, thus suggesting that Arctic tectonic plates have been much more stable than expected.**

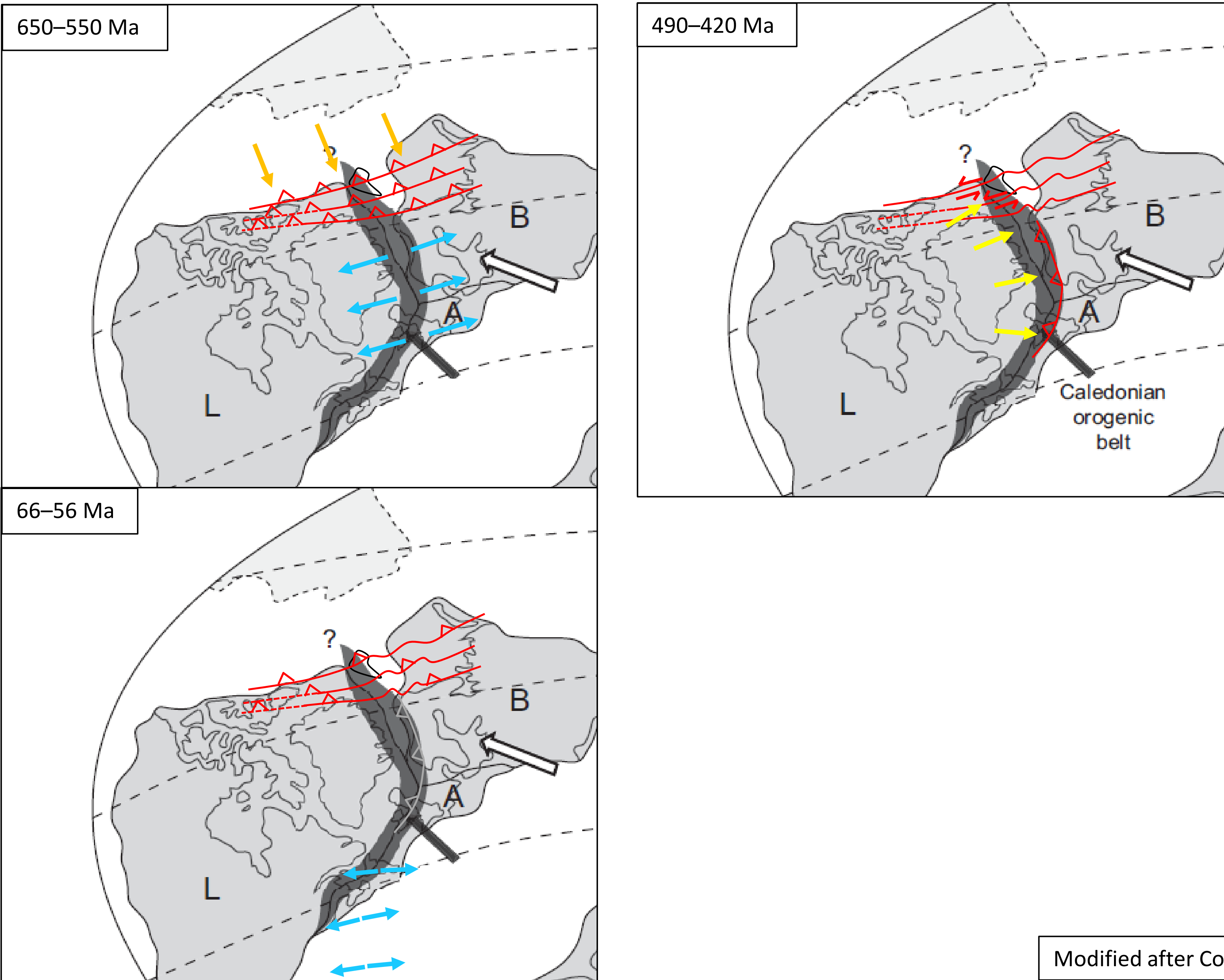

Modified after Cocks & Torsvik (2002)

3 Svalbard’s three basement terranes were already accreted in the late Neoproterozoic, thus suggesting that Arctic tectonic plates have been much more stable than expected.

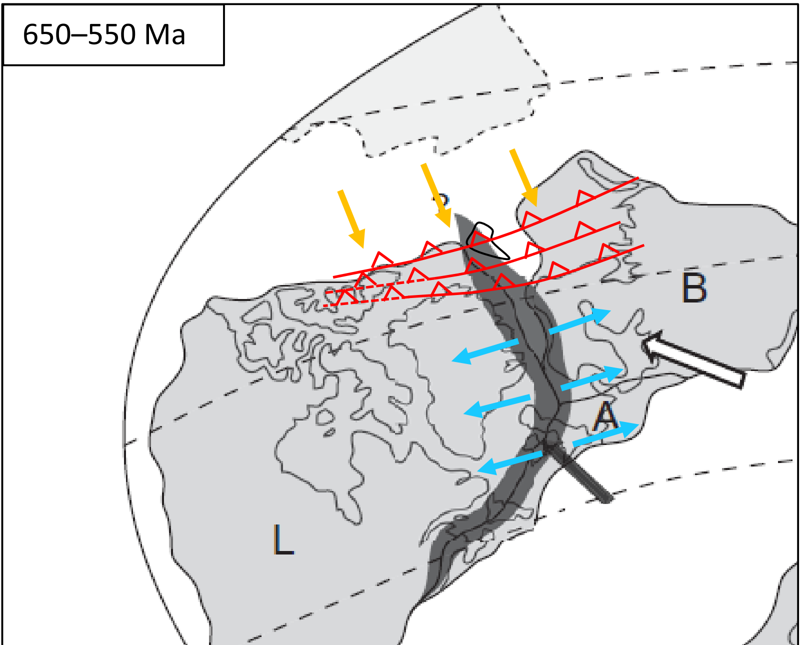

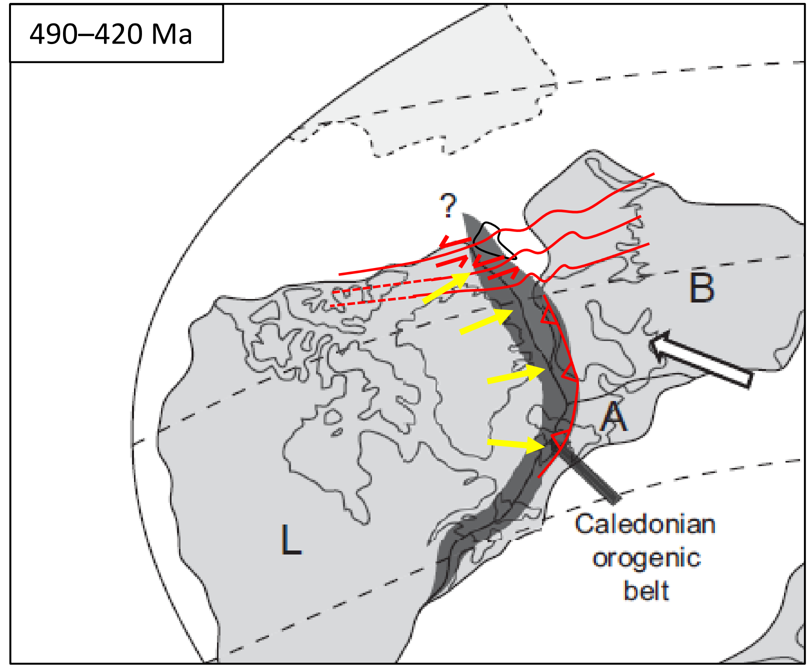

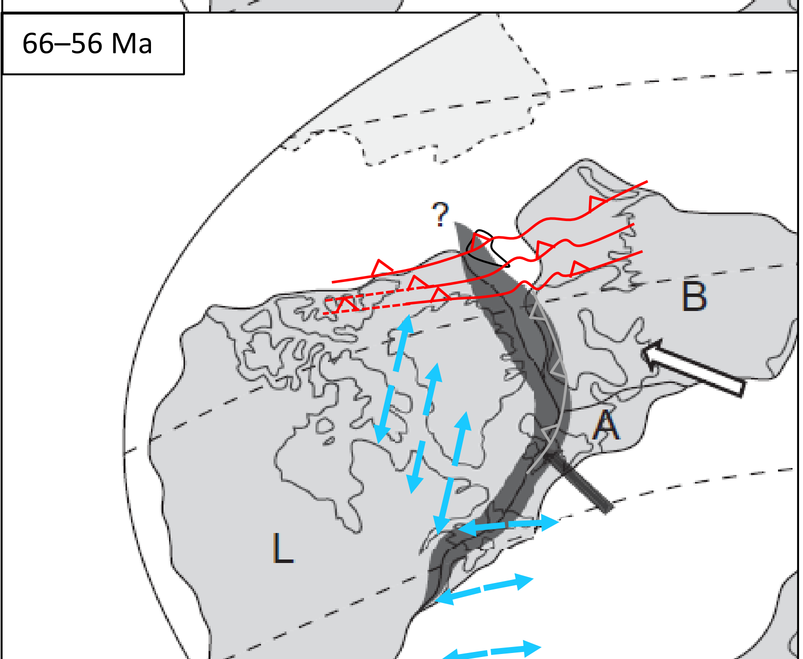

Modified after Cocks & Torsvik (2002)

3

Svalbard's three basement terranes were already accreted in the late Neoproterozoic, thus suggesting that Arctic tectonic plates have been much more stable than expected.

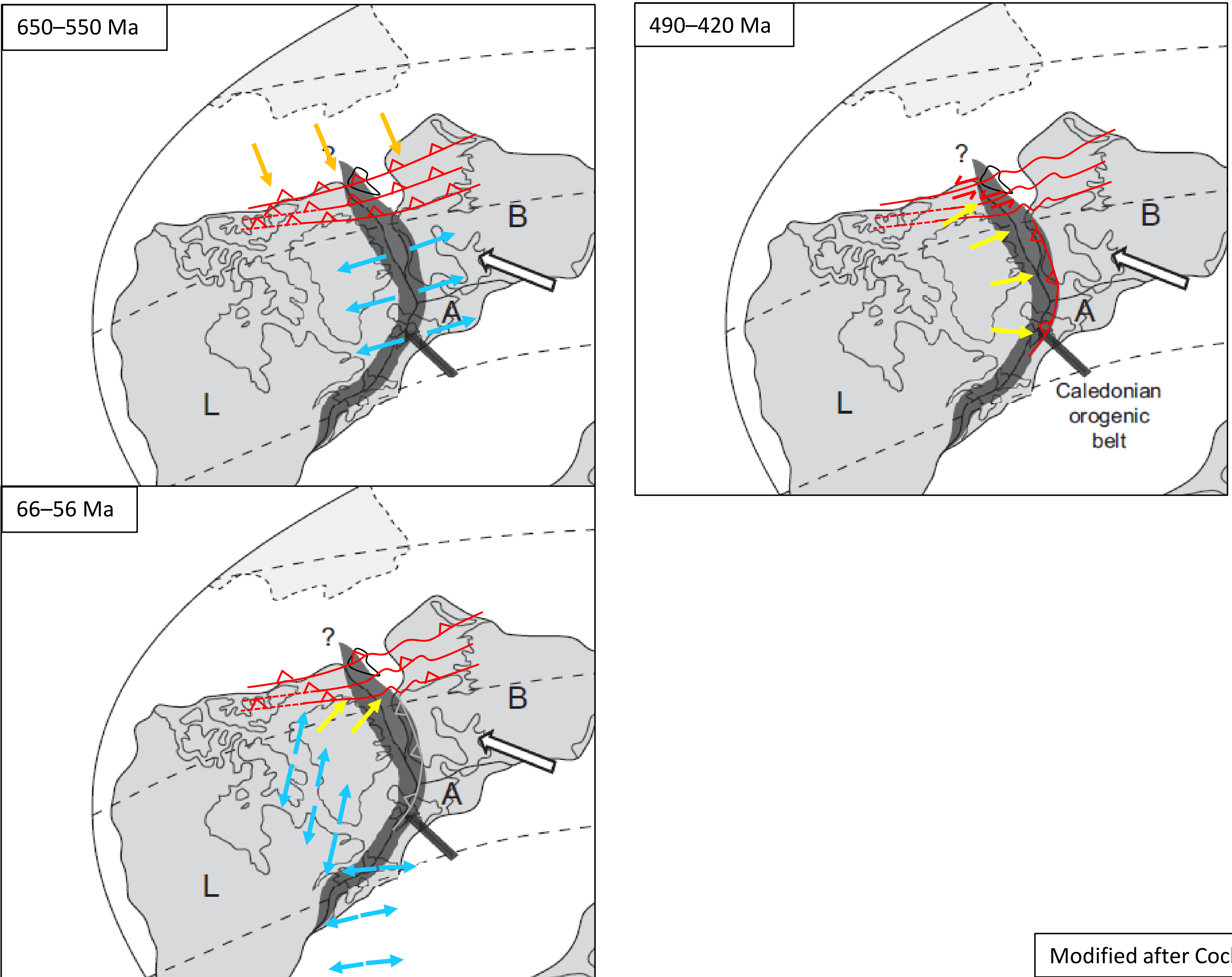

Modified after Cocks & Torsvik (2002)

3 **Svalbard's three basement terranes were already accreted in the late Neoproterozoic, thus suggesting that Arctic tectonic plates have been much more stable than expected.**

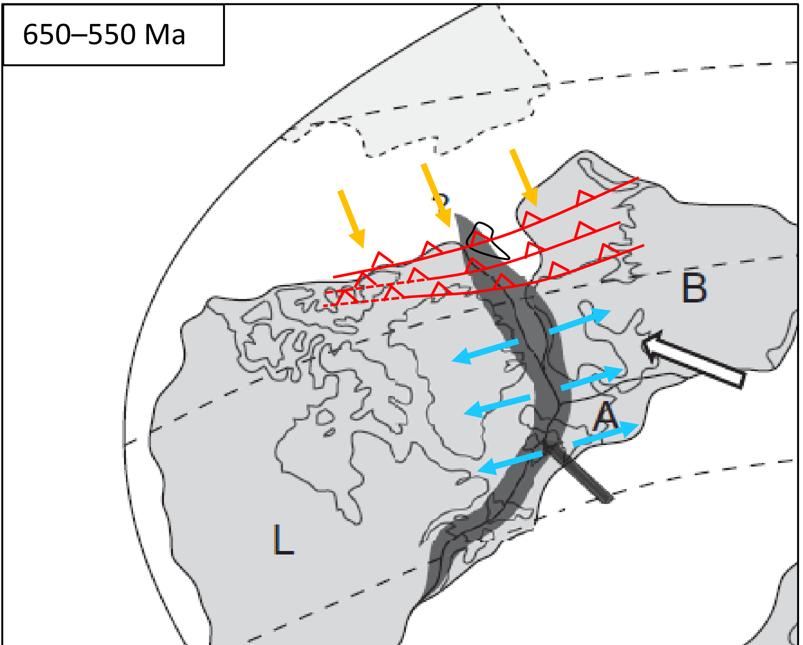

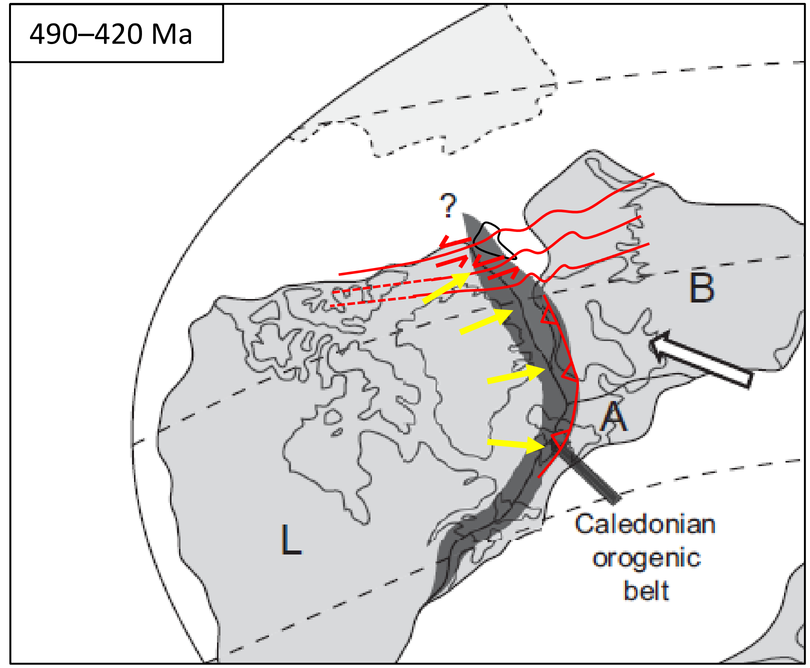

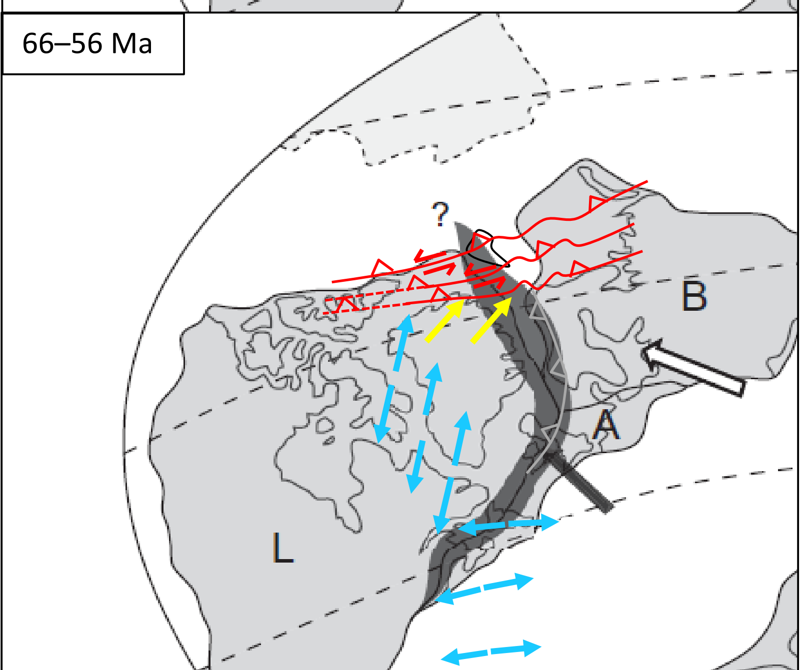

Modified after Cocks & Torsvik (2002)

3 **Svalbard's three basement terranes were already accreted in the late Neoproterozoic, thus suggesting that Arctic tectonic plates have been much more stable than expected.**

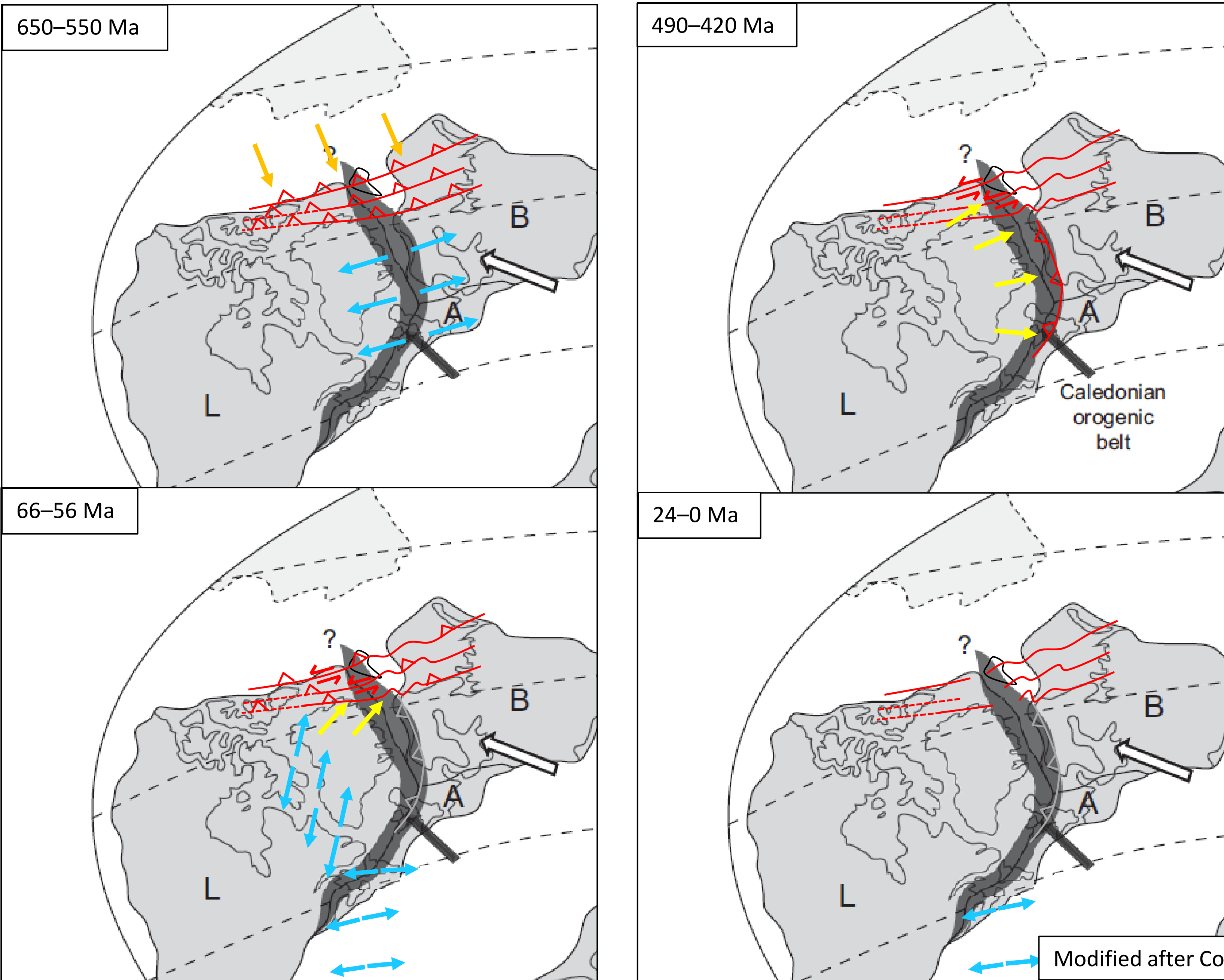

Modified after Cocks & Torsvik (2002)

3 **Svalbard's three basement terranes were already accreted in the late Neoproterozoic, thus suggesting that Arctic tectonic plates have been much more stable than expected.**

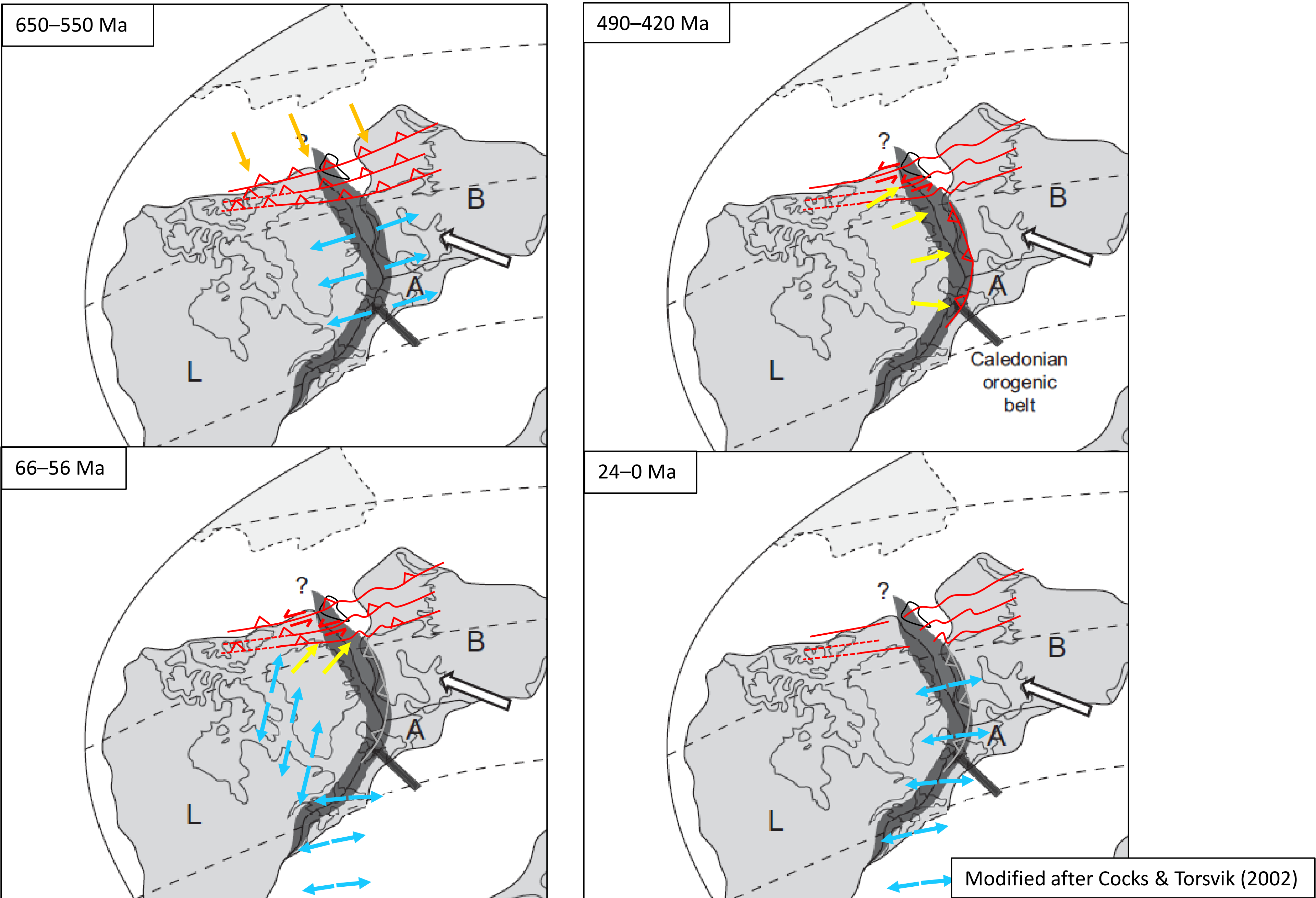

Modified after Cocks & Torsvik (2002)

3

Svalbard's three basement terranes were already accreted in the late Neoproterozoic, thus suggesting that Arctic tectonic plates have been much more stable than expected.

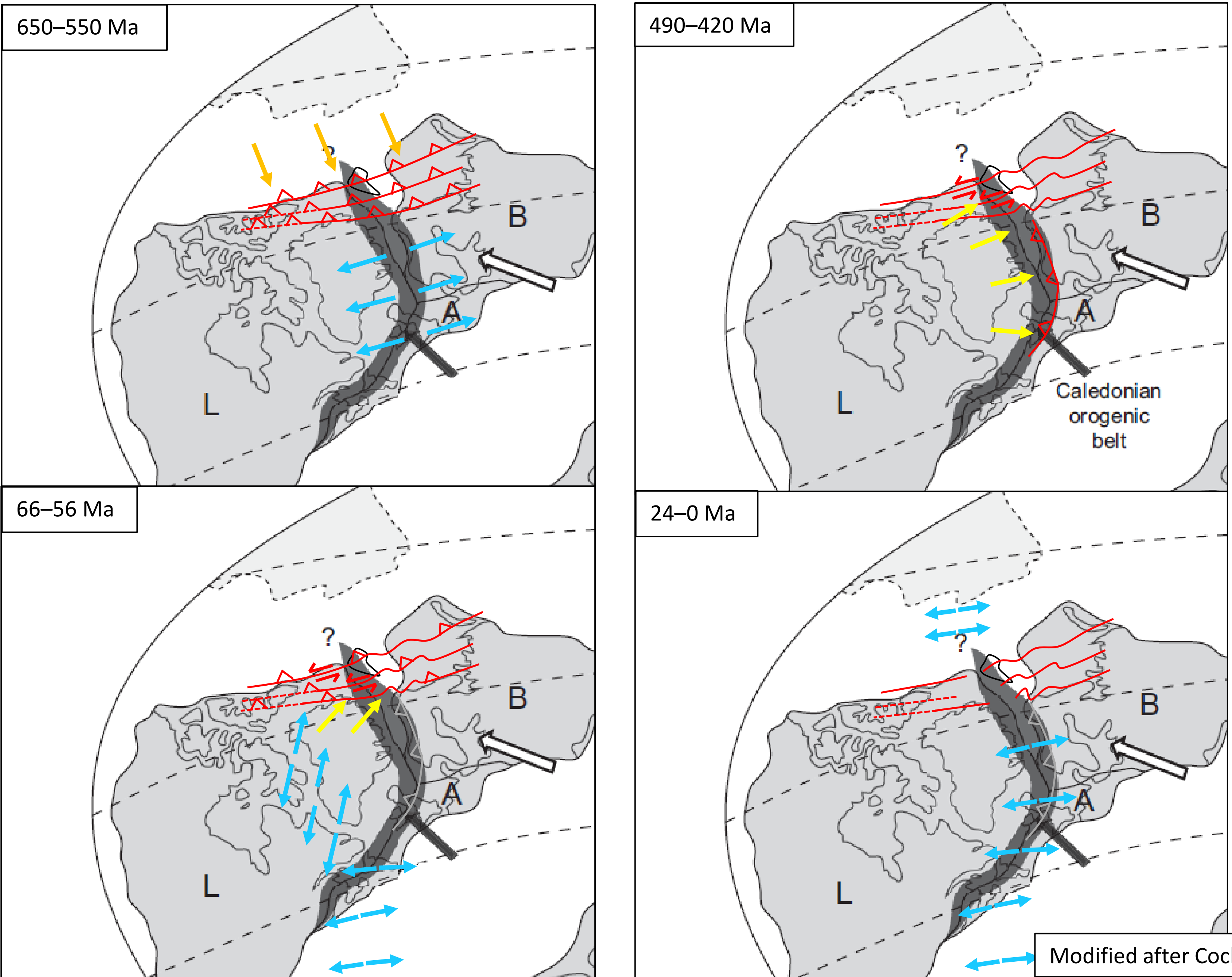

Modified after Cocks & Torsvik (2002)

3 **Svalbard's three basement terranes were already accreted in the late Neoproterozoic, thus suggesting that Arctic tectonic plates have been much more stable than expected.**

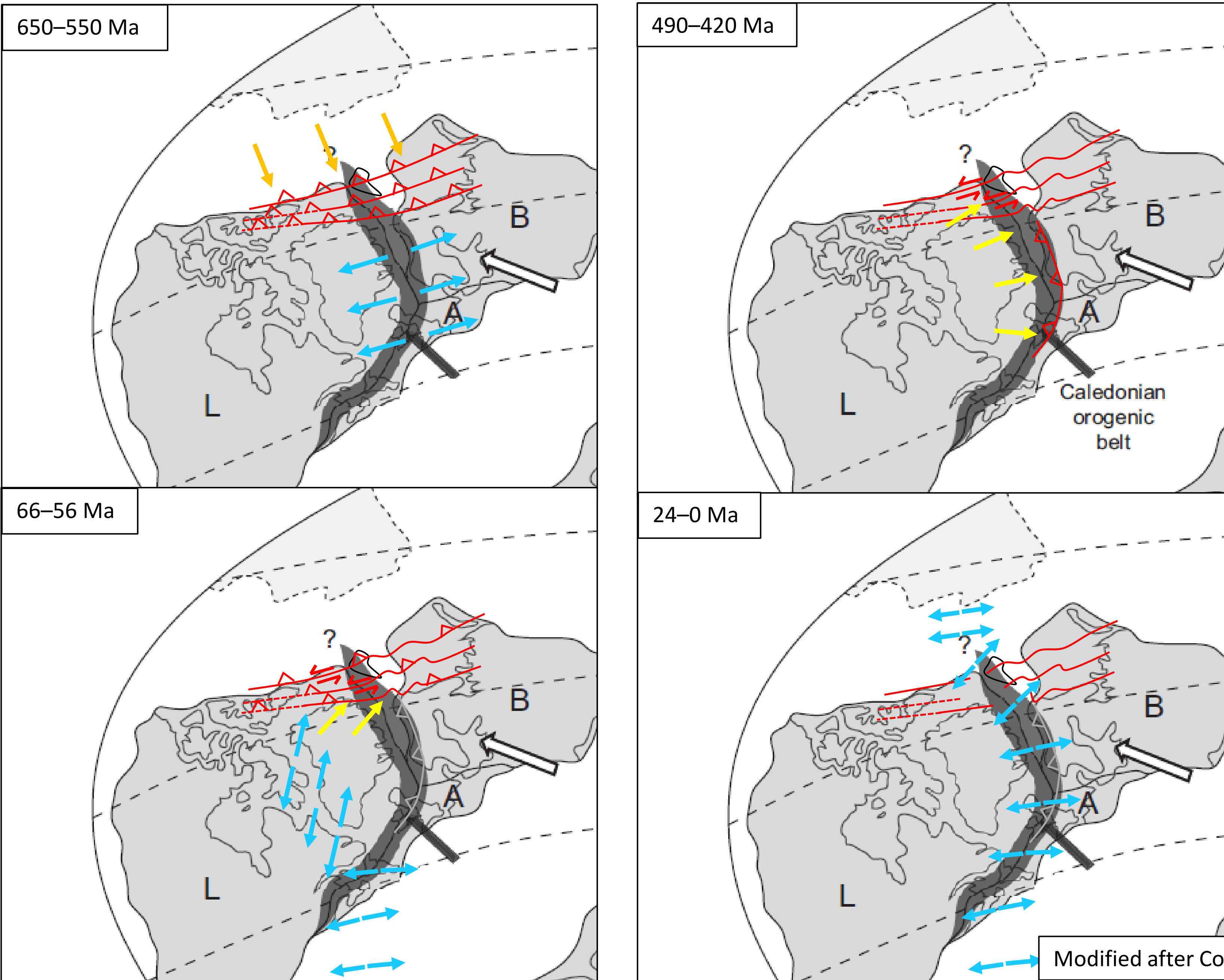

Modified after Cocks & Torsvik (2002)

3 **Svalbard's three basement terranes were already accreted in the late Neoproterozoic, thus suggesting that Arctic tectonic plates have been much more stable than expected.**

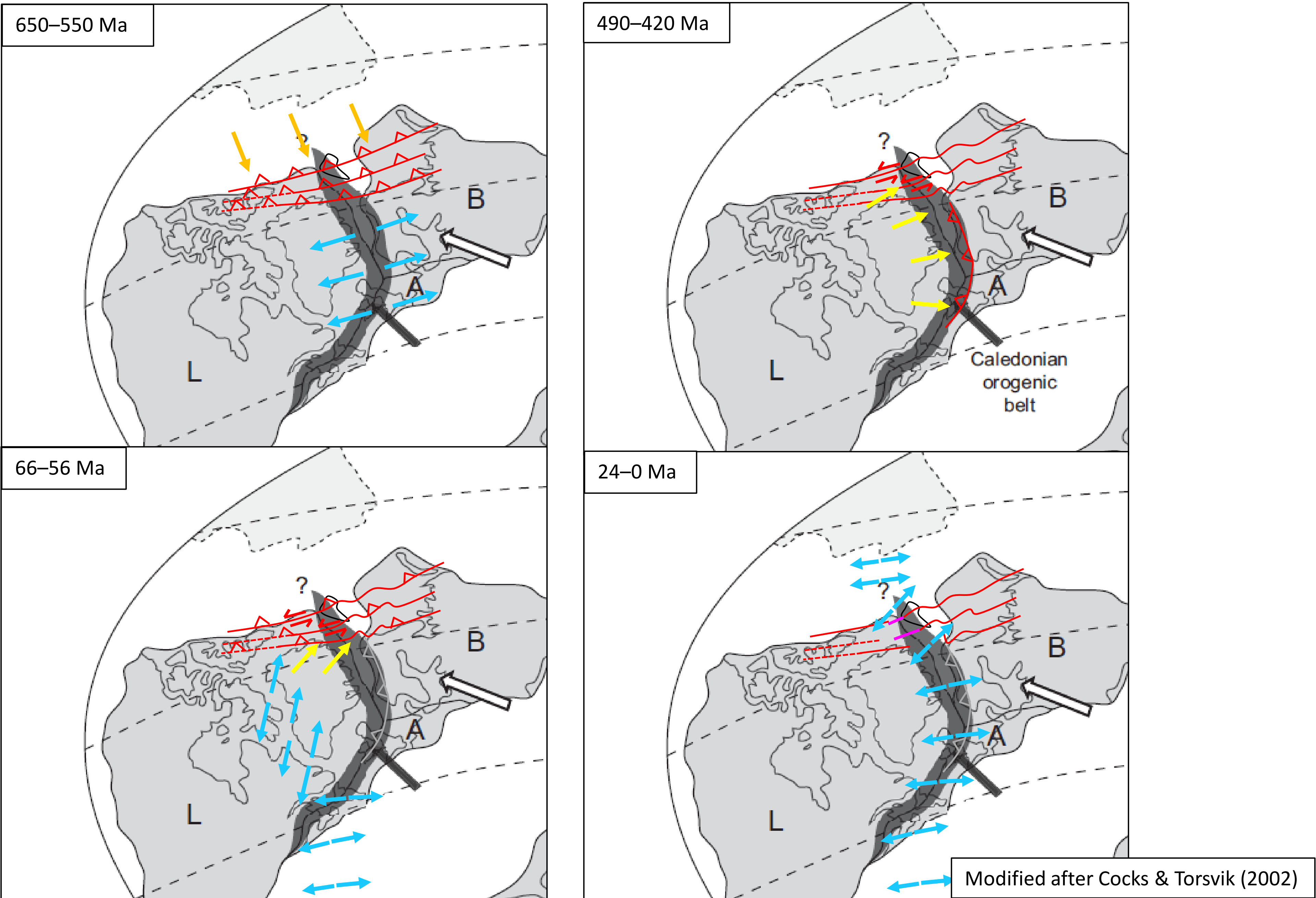

3 **Svalbard's three basement terranes were already accreted in the late Neoproterozoic, thus suggesting that Arctic tectonic plates have been much more stable than expected.**

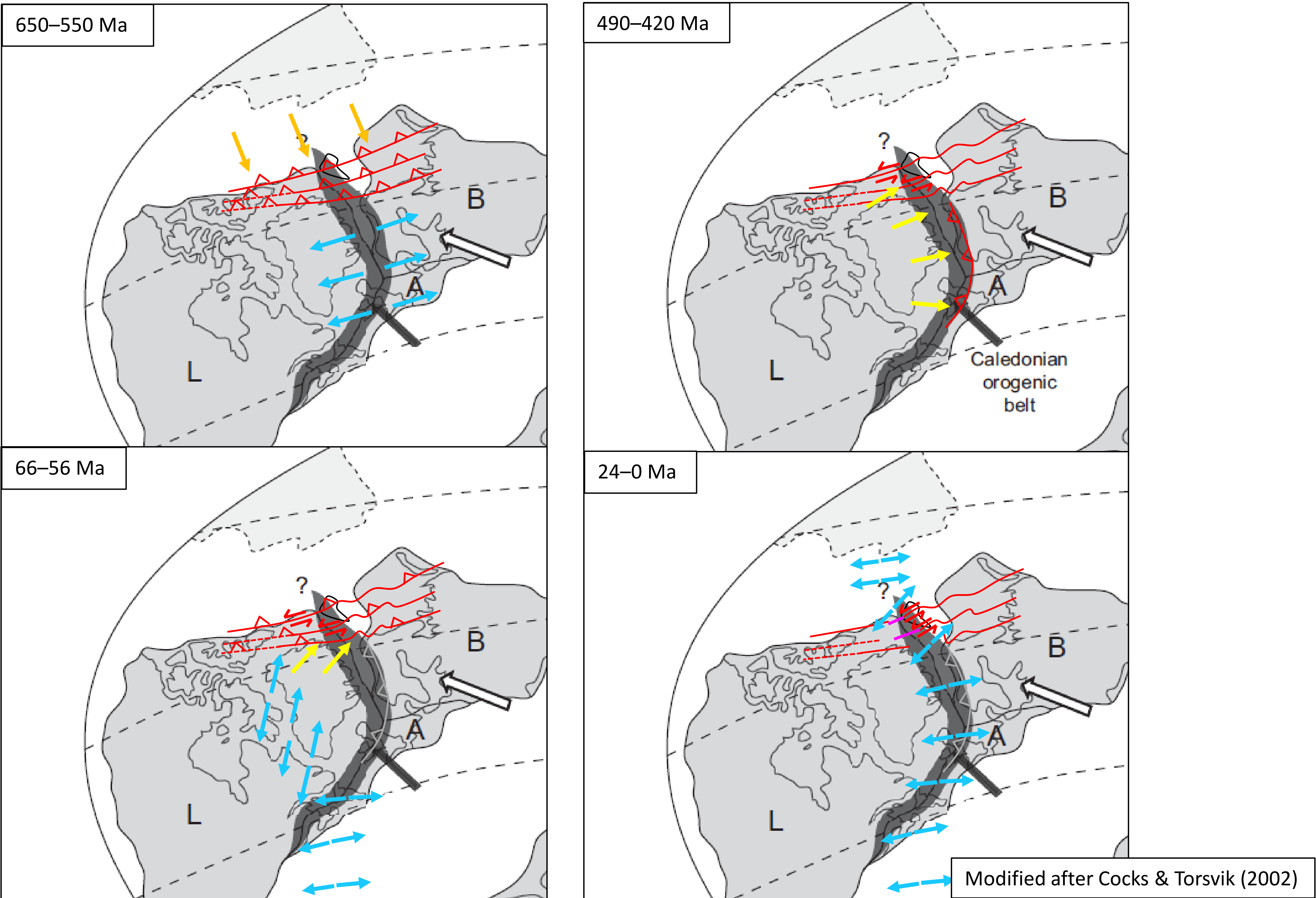

Modified after Cocks & Torsvik (2002)

Conclusion

Timanian faults reactivated during Caledonian and Eurekan deformation, and Devonian–Carboniferous and late Cenozoic extension, localizing the formation of faults, basins, oceanic core complexes, transform faults, and breakup in the NE Atlantic.

Conclusion

Timanian faults reactivated during Caledonian and Eurekan deformation, and Devonian–Carboniferous and late Cenozoic extension, localizing the formation of faults, basins, oceanic core complexes, transform faults, and breakup in the NE Atlantic.

1

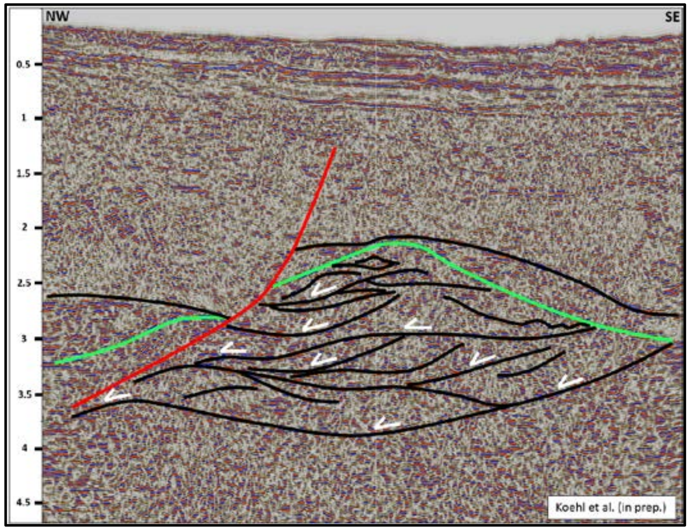

Conclusion

Timanian faults reactivated during Caledonian and Eurekan deformation, and Devonian–Carboniferous and late Cenozoic extension, localizing the formation of faults, basins, oceanic core complexes, transform faults, and breakup in the NE Atlantic.

1

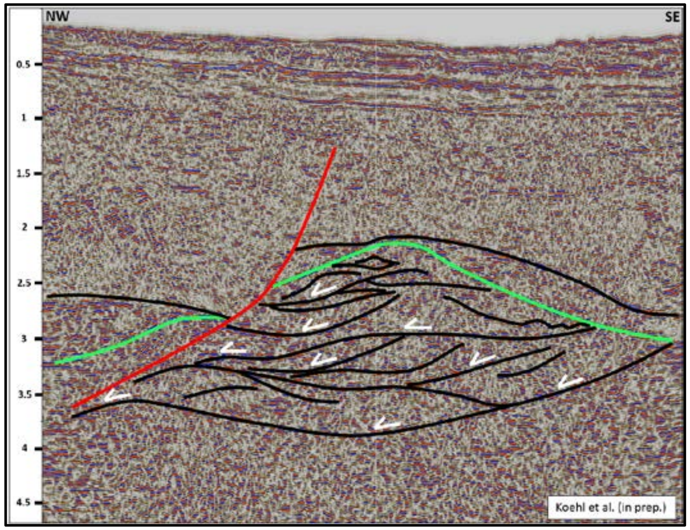

2

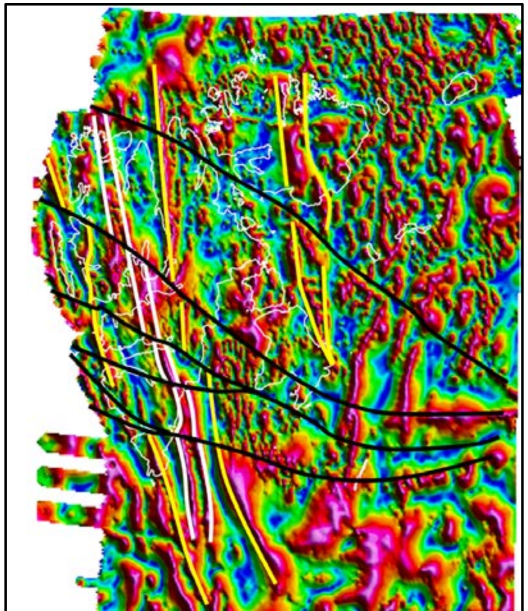

Conclusion

Timanian faults reactivated during Caledonian and Eurekan deformation, and Devonian–Carboniferous and late Cenozoic extension, localizing the formation of faults, basins, oceanic core complexes, transform faults, and breakup in the NE Atlantic.

1

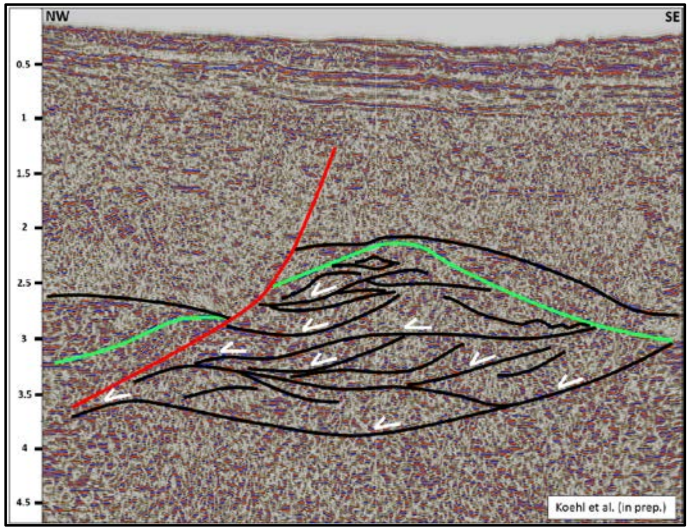

2

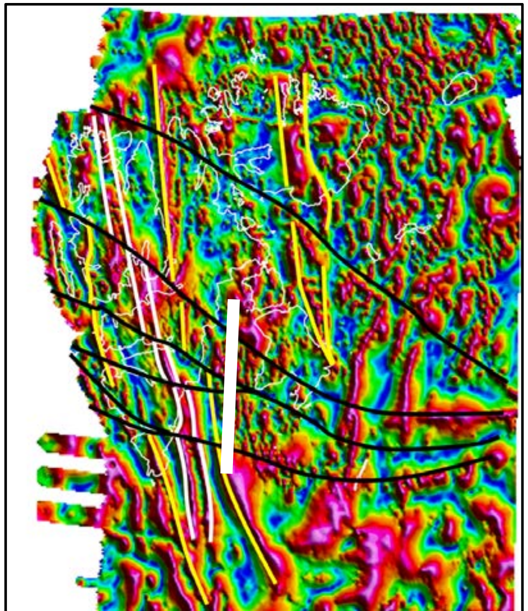

Conclusion

Timanian faults reactivated during Caledonian and Eurekan deformation, and Devonian–Carboniferous and late Cenozoic extension, localizing the formation of faults, basins, oceanic core complexes, transform faults, and breakup in the NE Atlantic.

1

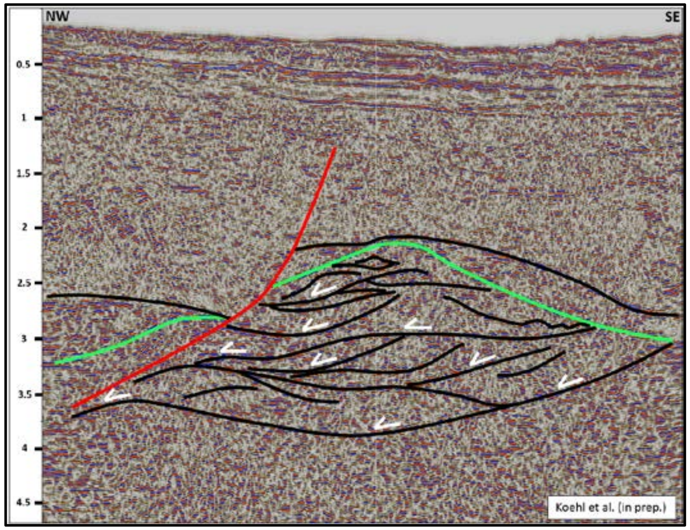

2

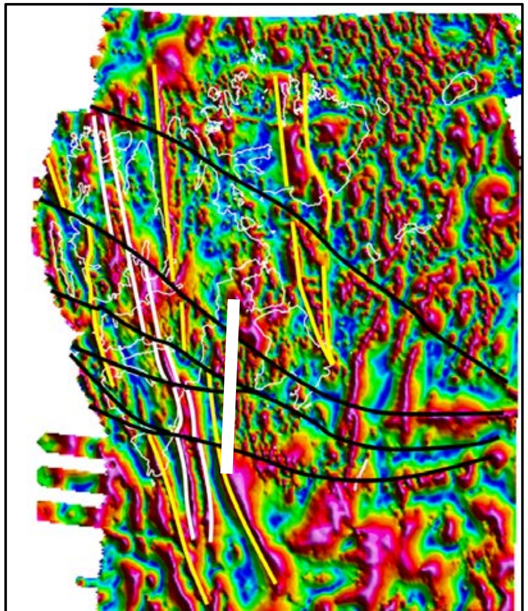

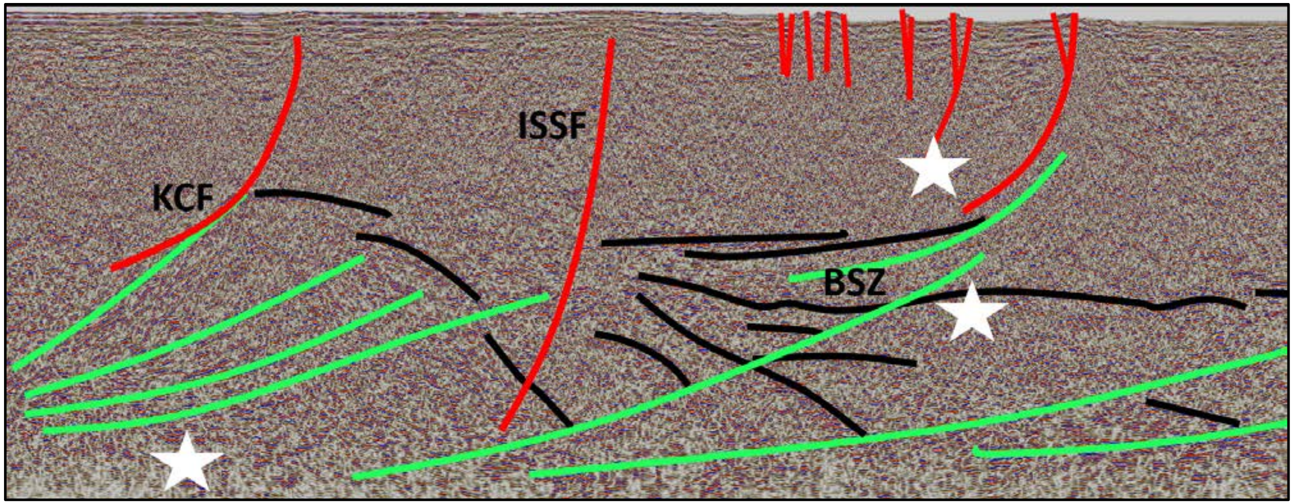

Conclusion

Timanian faults reactivated during Caledonian and Eurekan deformation, and Devonian–Carboniferous and late Cenozoic extension, localizing the formation of faults, basins, oceanic core complexes, transform faults, and breakup in the NE Atlantic.

1

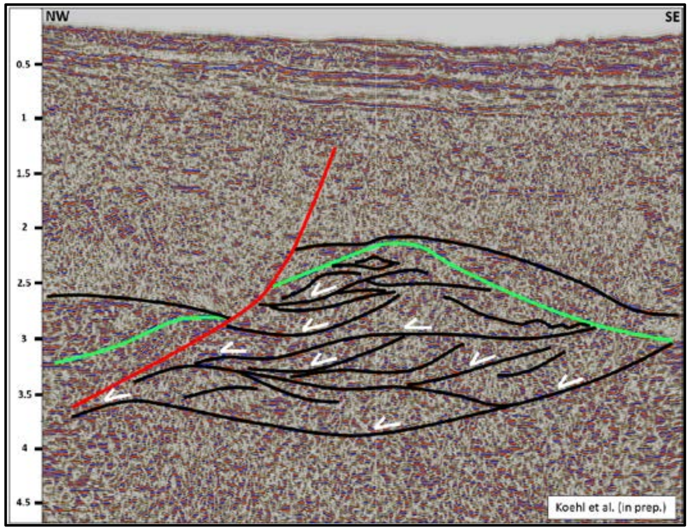

3

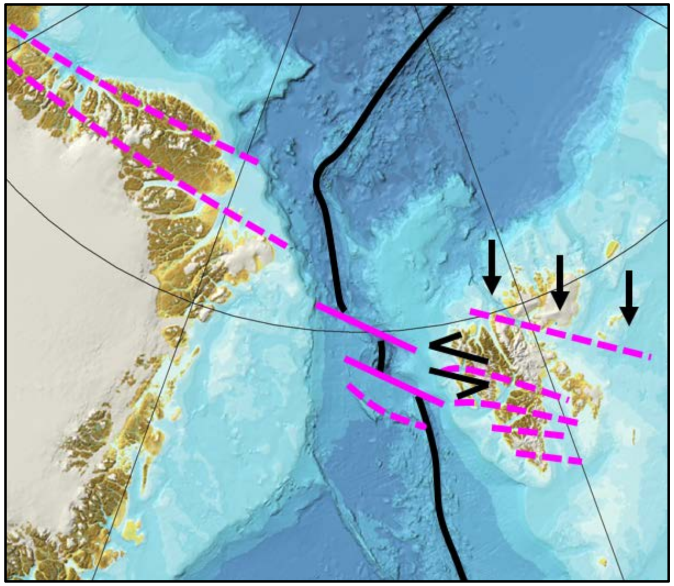

2

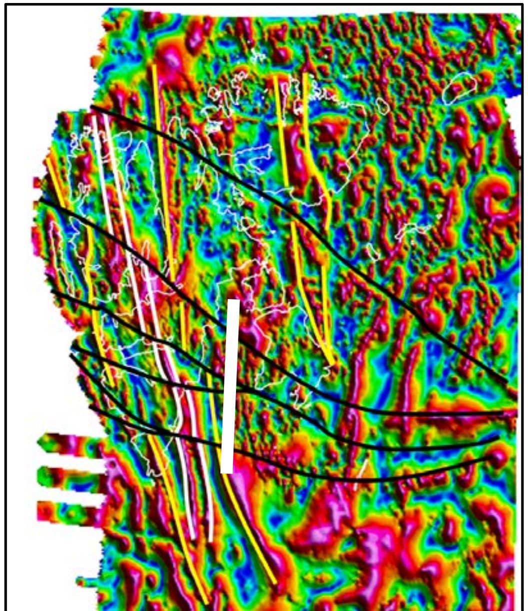

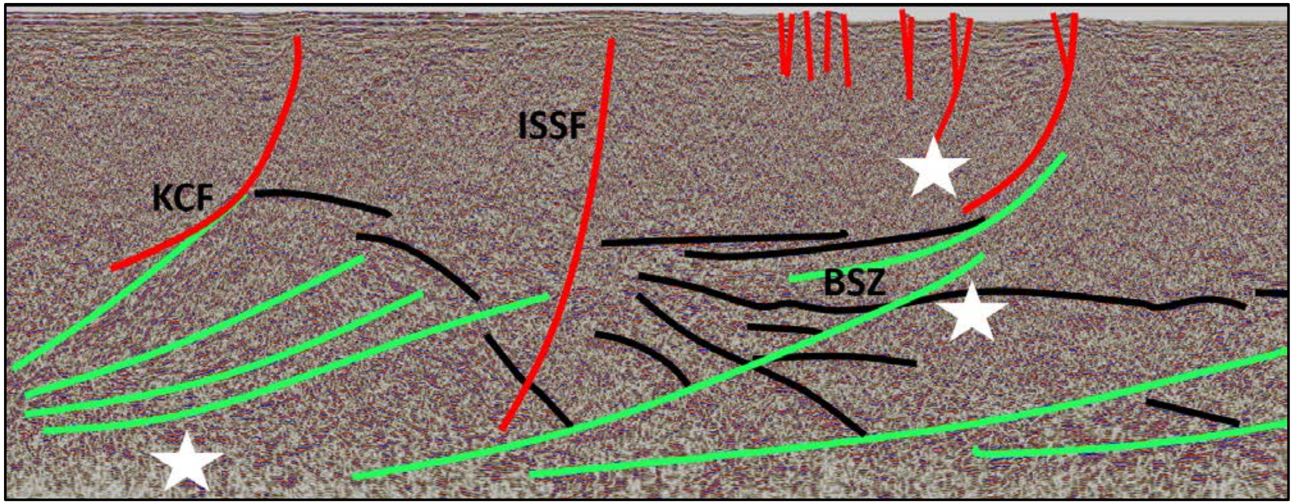

Conclusion

Timanian faults reactivated during Caledonian and Eurekan deformation, and Devonian–Carboniferous and late Cenozoic extension, localizing the formation of faults, basins, oceanic core complexes, transform faults, and breakup in the NE Atlantic.

1

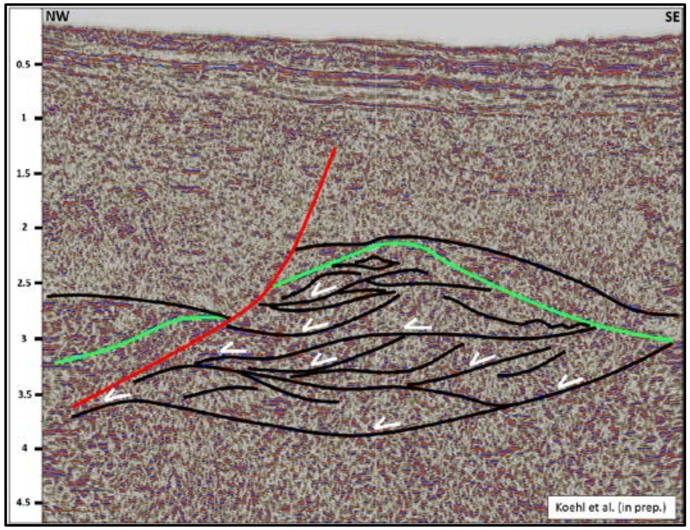

2

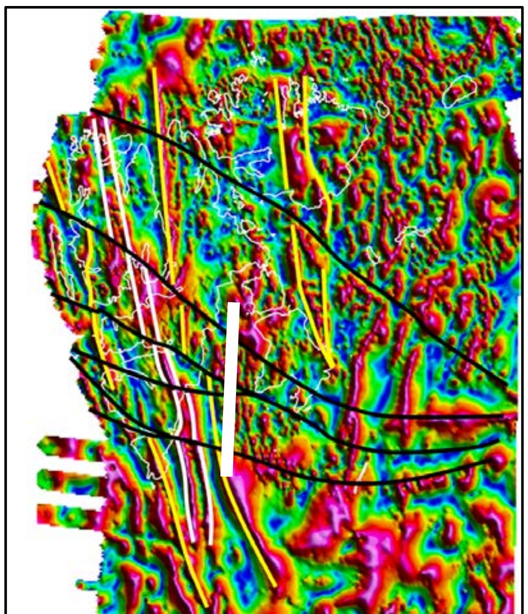

3

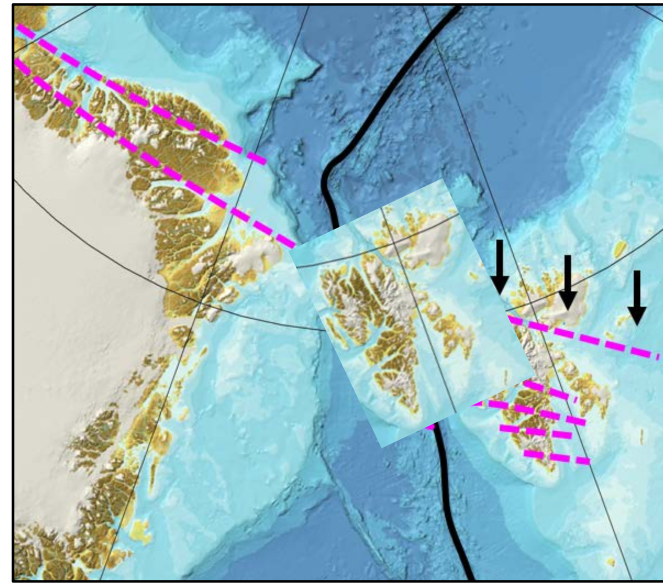

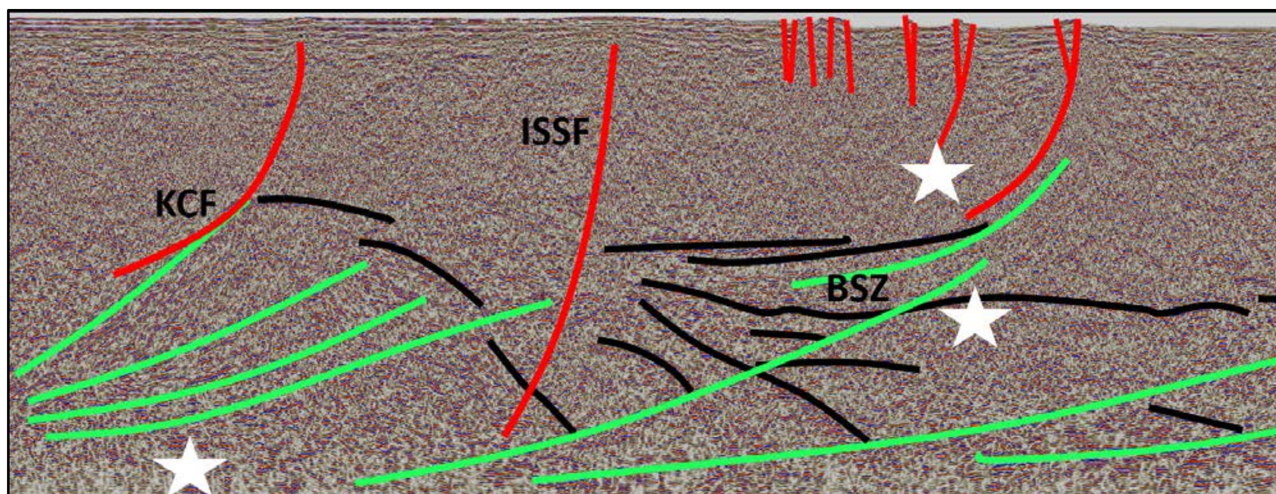

Conclusion

Timanian faults reactivated during Caledonian and Eurekan deformation, and Devonian–Carboniferous and late Cenozoic extension, localizing the formation of faults, basins, oceanic core complexes, transform faults, and breakup in the NE Atlantic.

1

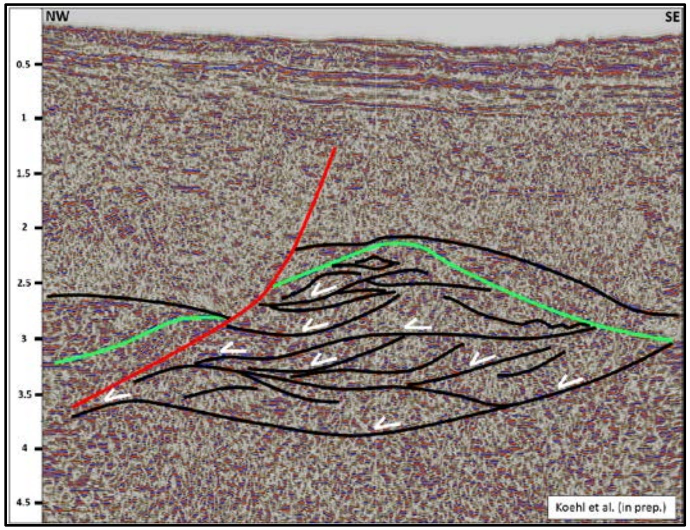

2

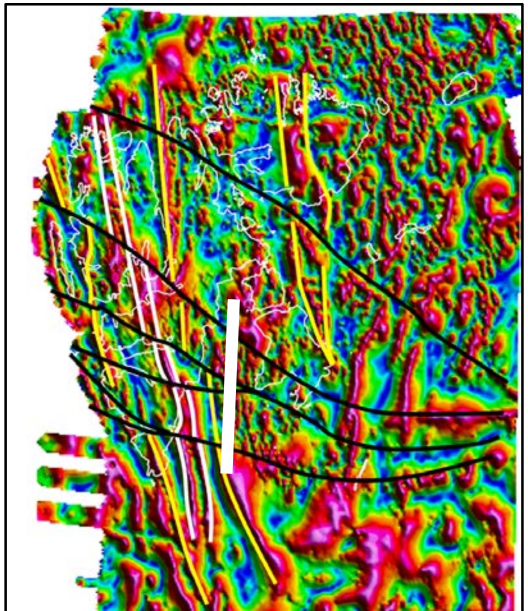

3

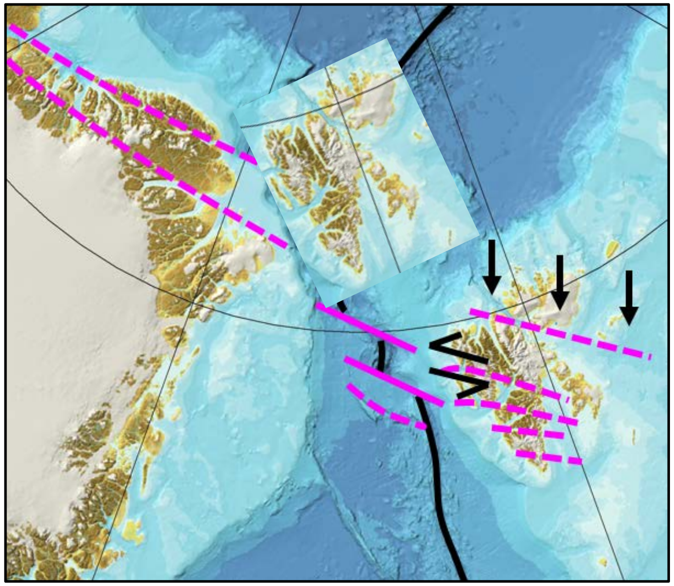

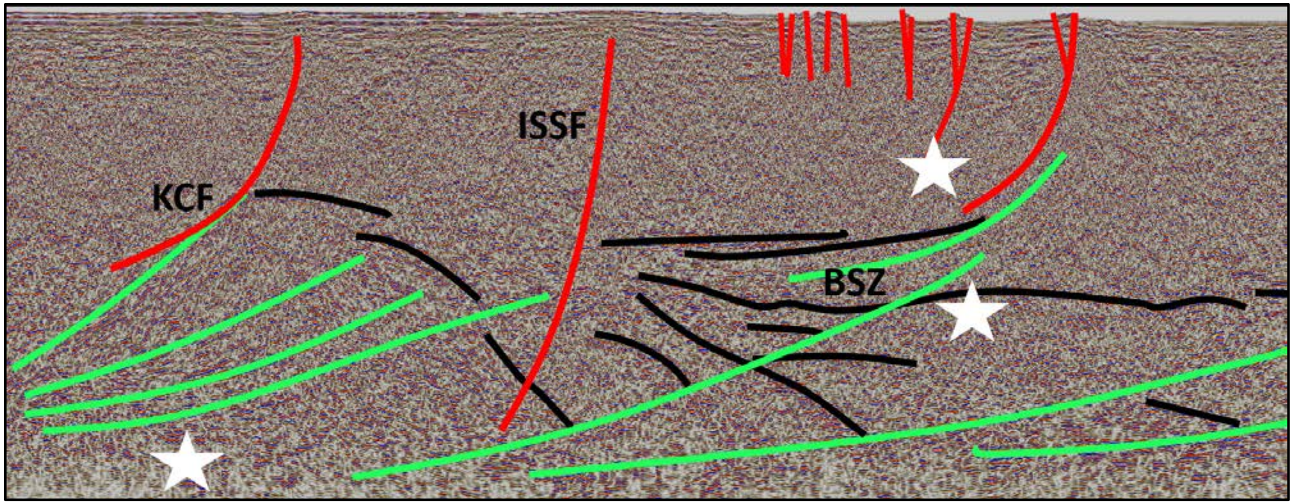

Conclusion

Timanian faults reactivated during Caledonian and Eurekan deformation, and Devonian–Carboniferous and late Cenozoic extension, localizing the formation of faults, basins, oceanic core complexes, transform faults, and breakup in the NE Atlantic.

1

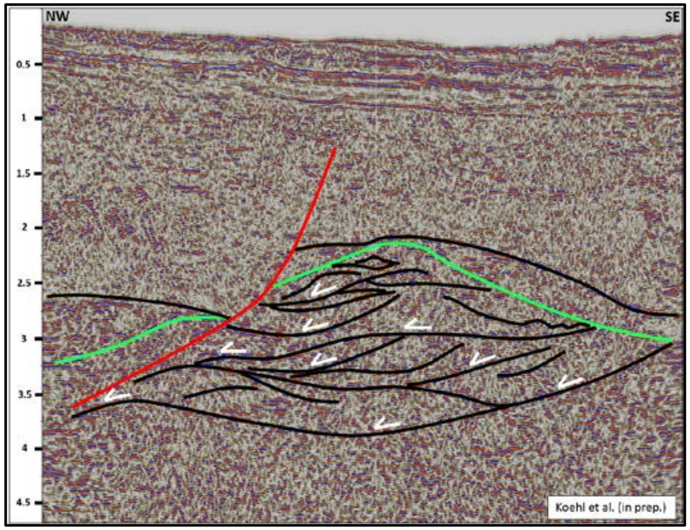

2

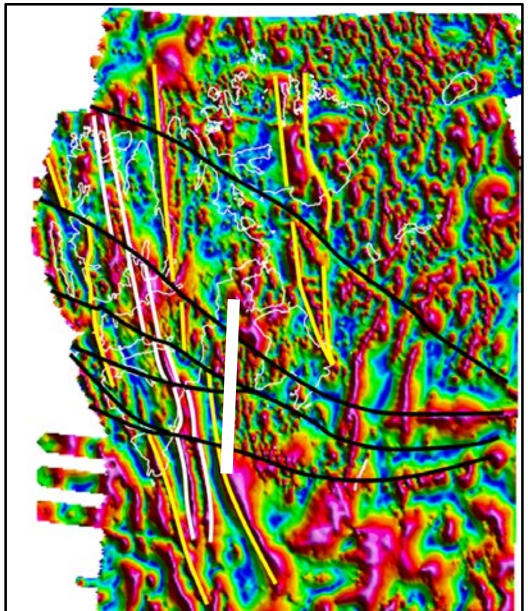

3